Advances in Experimental Medicine and Biology 1064

Insup Noh *Editor*

Biomimetic Medical Materials

From Nanotechnology to 3D Bioprinting

Springer

Advances in Experimental Medicine and Biology

Volume 1064

More information about this series at http://www.springer.com/series/5584

Insup Noh
Editor

Biomimetic Medical Materials

From Nanotechnology to 3D Bioprinting

Springer

Editor
Insup Noh
Seoul National University of Science and Technology
Seoul, South Korea

ISSN 0065-2598 ISSN 2214-8019 (electronic)
Advances in Experimental Medicine and Biology
ISBN 978-981-13-0444-6 ISBN 978-981-13-0445-3 (eBook)
https://doi.org/10.1007/978-981-13-0445-3

Library of Congress Control Number: 2018951426

This Springer imprint is published by the registered company Springer Nature Singapore Pte Ltd.
The registered company address is: 152 Beach Road, #21-01/04 Gateway East, Singapore 189721, Singapore

Preface

Biomimetics is an imitation of the structures, properties, models, and compounds of nature to solve complex human difficulties. Biomimetics has been recognized as an important mission in science and engineering for a long time. Recently, it has emerged as a new technology inspired by material science and engineering as well as pure sciences such as chemistry and biology at different levels from macro- to nanotechnology for diverse applications such as medical science, aerospace, automobile, and so on. Taking inspiration from natural phenomena such as the structures and behaviors of birds, reptile, and shark skin, self-healing abilities in tissues and proteins in the human body, the hydrophobic surface structure of lotus leaf, as well as the self-assembly of proteins and deoxyribonucleic acid, scientists and engineers are continuously working and thinking about how to mimic and transform the natural resources/synthetic materials for the use in our daily life. This field is rapidly progressing through the developments in macro-, micro-, and nanotechnology. Especially, nanotechnology has helped us to understand the interaction between cell and material surfaces, cell-cell interactions, protein-protein interactions, as well as cell-extracellular matrix in human tissues. As an example, the biomimicking of natural structures of medical devices using nanotechnology and adhesiveness are inspired from Gekkota's nanomorphologies due to physical interactions, and murine muscle's underwater adhesion, caused by adhesive proteins such as 3,4-dihydroxyphenylalanin (DOPA). Currently, by developing and converging micro-, nano-, and 3D bioprinting technology, the patient's specific and complex tissues/organs are designed and fabricated for the applications in tissue engineering and regenerative medicine. Further to improve these technologies, involvement of multidisciplinary scientific understanding of physical, chemical, compositional, and biological properties and morphologies of tissues and organs is required with the convergence of basic sciences, engineering, as well as clinical aspects.

This book provides the overviews of biomimetic medical materials which cover the significance of terminology, diverse fabrication methods, and technologies ranging from micro-nano to macroscopic 3D printing for development of functional biomimetic medical materials. While nanotechnology is to understand the basic sciences of biomimetics of biomolecular structures, drug delivery, biosensors, tissue regeneration, and

functional biomaterials, 3D printing technology is to develop micro- and macroscale biomimetic materials in engineering aspects. This book also depicts specific fundamental characteristics required for a biomaterial to be a model biomimetic material, targeting diverse applications in biomedical and tissue engineering. This book basically outlines the current status of biomimetic medical materials used in tissue engineering and regenerative medicine, nano-biotechnology-based drug/protein delivery, bioimaging, biosensing, and 3D bioprinting technology. It also illustrates the effect of functionalization of a biomaterial through chemical and biological approaches toward different applications. This book describes not only the key properties and potential applications of the biomimetic materials but also the way of product commercialization by protecting and utilizing the intellectual properties of the materials and technologies.

I believe that my book will be read by the majority of people working in this area of research, and they will be benefited from the in-depth explanations in the book.

I sincerely express my thanks to the authors for their contributions to valuable chapters and to my lab members, Dr. Dipankar Das, Dr. Janarthanan Gopinathan, Ms. Sumi Bang, and Eunha Choi, for their contributions toward research and editing manuscripts. I appreciate our publisher, Dr. Sue Lee, for the publication of the book. Finally, I would like to give my special appreciation to my family, Youngmee, April, John, and Claire Noh, as well as my mother Whoazha Lee for their continuous support, encouragement, and love throughout my family and research life. I would also like to thank lifetime mentors, Professor Jeffrey A. Hubbell in the Institute of Molecular Engineering at the University of Chicago and Professor Elazer R. Edelman in the Medical Engineering and Science at the Massachusetts Institute of Technology, at Harvard Medical School, and at Brigham and Women's Hospital, USA. This work was supported by the National Research Foundation of Korea (NRF) Grant (2015R1A2A1A10054592).

Seoul, South Korea Insup Noh

Contents

Part I

Introduction

Overviews of Biomimetic Medical Materials

1

Dipankar Das and Insup Noh

1.1 General Introduction

The term 'biomimetics' was coined by renowned American biophysicist Otto Herbert Schmitt in the 1950s (Julian et al. 2006). Biomimetics originates from the Greek words 'bios' and 'mimesis' which mean "life" and "to imitate," respectively (Bar-Cohen 2006). Scientist Janine Benyus defined 'Biomimicry' in her book 'Biomimicry: Innovation Inspired by Nature' as an "innovative science that observes nature's models and formerly duplicates or takes inspiration from those designs and procedures to solve human problems" (Benyus 1997; Bello et al. 2013). Benyus suggests that by treating nature as a 'model, measure and mentor,' biomimicry can offer advantages relating to 'leading edge opportunities' (Benyus 1997). One important example of biomimicry can be observed in the field of medical materials. Biomimetic medical materials are biocompatible and/or biodegradable materials designed by careful observation of nature's models and then developed by imitating natural architectures and methods for use in the medical industry (e.g., biosensing, tissue engineering and regenerative medicine, biosignals and drug/protein delivery) (Fig. 1.1). The method involves the development of composite materials that mimic the characteristics and/or structures of diverse materials found in nature. Examples of natural structures serving as inspiration include the honeycomb organization of a beehive, the fibrous structure of wood, spider webs, nacre, bone, hedgehog quills, and so on (Bello et al. 2013). The rapid development of biomaterials for medical applications is emerging as a promising interdisciplinary research field between materials science and biology. Advances in the biomedical field create an ever-increasing demand for novel biomaterials with precise and definite host interactions (Bello et al. 2013; Eggermont 2008; Nagarajan 2008), and recent progress within materials research encourages further inquiry into how to best emulate the structures of natural materials in biomimetic materials (Bello et al. 2013; Erik and Stephen 2002; Hengstenberg et al. 2001). The emerging field of biomimetics deals with new technologies generated from biologically stimulated engineering at nano- to macro- levels and 3D-bioprinting. Improved understandings of biological functions and human anatomy are critical to achieving more varied and efficient biomedical applications through the development of: (1) more effective biomimetic materials and (2) approaches to best leverage advanced technologies.

This book focuses on the development of diverse biomimetic medical materials with intellectual properties for biomedical applications. It contains eight sections: (1) introduction,

D. Das · I. Noh (✉)
Department of Chemical and Biomolecular Engineering, Seoul National University of Science and Technology, Seoul, South Korea

Convergence Institute of Biomedical Engineering and Biomaterials, Seoul National University of Science and Technology, Seoul, South Korea
e-mail: insup@seoultech.ac.kr

I. Noh (ed.), *Biomimetic Medical Materials*, Advances in Experimental Medicine and Biology 1064,
https://doi.org/10.1007/978-981-13-0445-3_1

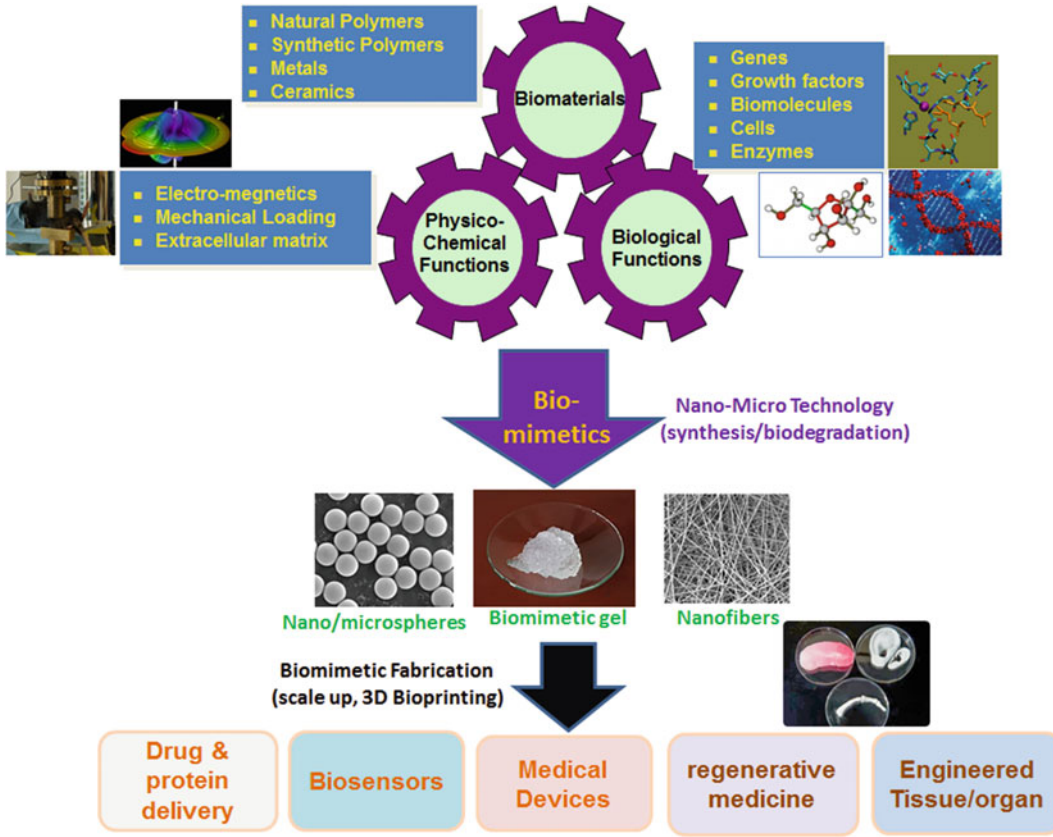

Fig. 1.1 Overview of biomimetic medical materials

(2) nanomaterials as emerging biomimetic materials, (3) biomimetic materials in tissue engineering, (4) biomimetic materials and stem cell, (5) 3-D bioprinting materials, (6) immune responses of biomaterials, (7) functional biomaterials, and (8) intellectual properties of biomimetic materials. This chapter provides a general overview of important developments in the field of biomimetic medical materials (e.g., key properties and potential applications). Chapters 2, 3, 4, 5, 6, 7, and 8 provide more details and the current statuses of individual topics.

1.2 Nanomaterials: A Promising Class of Biomimetic Medical Materials

Progress made in the fields of nanoscience and nanotechnology have directly led to advancements of functional materials with biomedical applications. Examples of important nanomaterials include graphene, carbon nanotubes, fullerenes, polymeric nanoparticles, nanogels, metal organic nanomaterials, and supramolecular nanostructures (Bhattacharya et al. 2014). The distinctive physico-chemical properties (e.g., size, shape, surface charge and chemical composition) drive their potential utility in sensors, protein cages, drug delivery, bioimaging, tissue engineering, and so on (Bhattacharya et al. 2014). The remarkable variety of potential roles for biomimetic nanomaterials arises from the observation that humans are fabricated by nanoscale interactions, specifically the efficient self-assembly of biological molecules (Bhattacharya et al. 2014). Recent noteworthy advancements in the field of biomimetic materials include organs-on-chips, smart robotic devices, nanomaterials for tissue

engineering and orthopaedic implants (Bhattacharya et al. 2014).

1.2.1 Protein Cages

Protein cages are artificial, symmetrical, multifunctional constructions with three discrete interfaces (Fig. 1.2): (1) interior, (2) exterior, and (3) intra-subunit (Uchida et al. 2007; Chen et al. 2012). These subunits can be chemically and genetically tailored to generate distinct cages best designed for a specific biomedical application (Bhattacharya et al. 2014; Uchida et al. 2007; Chen et al. 2012). The most common protein cage applications involve DNA assays, biomineralization, immunoassay, sequestration, and the delivery of drugs and nucleic acids (Bhattacharya et al. 2014). Huard et al. developed the reverse metal-templated interface redesign (rMeTIR) method which converts a natural protein–protein interface into one that selectively responds to a metal ion (Harrison and Arosio 1996).

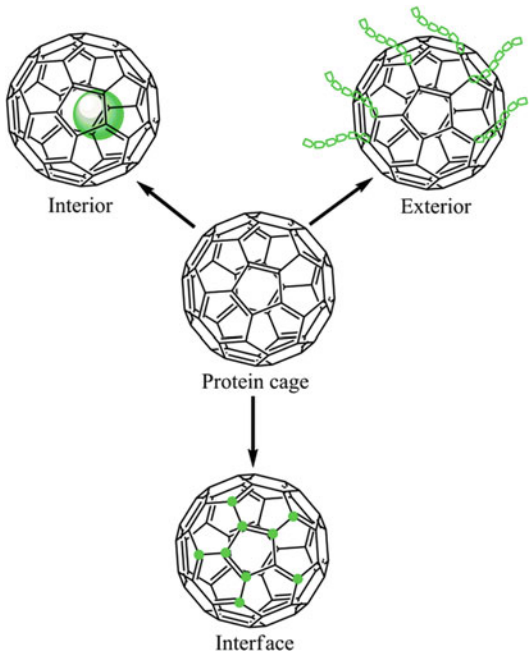

Fig. 1.2 Schematic representation of interfaces in a protein cage available for chemical or genetic modification

They employed this method to the self-assembly of ferritin protein cage bound by divalent copper metal. In this case, copper acts as a structural template for ferritin assembly like RNA sequences that serve as the template for viral capsid formation (Bhattacharya et al. 2014). This process helps to mimic the structure, stability and modifications of isolated ferritin occurring under physiological conditions (Bhattacharya et al. 2014). The most common protein cage applications involve DNA assays, biomineralization, immunoassay, sequestration, and the delivery of drugs and nucleic acids (Bhattacharya et al. 2014). Huard et al. developed the reverse metal-templated interface redesign (rMeTIR) method which converts a natural protein–protein interface into one that selectively responds to a metal ion (Harrison and Arosio 1996). They employed this method to the self-assembly of ferritin protein cage bound by divalent copper metal. In this case, copper acts as a structural template for ferritin assembly like RNA sequences that serve as the template for viral capsid formation (Bhattacharya et al. 2014). This process helps to mimic the structure, stability and modifications of isolated ferritin occurring under physiological conditions (Bhattacharya et al. 2014).

1.2.1.1 Application of Protein Cage Towards Nanomedicine

Protein-based nanomedicine systems are attractive for drug delivery because of their biocompatibility, biodegradability and low toxicity (Bhattacharya et al. 2014; Suchi et al. 2009). The subunits of the same protein or a mixture of proteins self-assemble and form cage-like structures. Drugs can be loaded into the void within the protein cage and then selectively delivered to target cells (Bhattacharya et al. 2014). Cage sizes are consistent and facilitate the loading of comparatively even amounts of drugs (Tang et al. 2011; MaHam et al. 2009). Ferritin- or apoferritin-based protein cages are naturally derived, physiologically stable and used as biocompatible drug delivery systems. The removal of iron atoms from ferritin forms apoferritin (Mazur et al. 1950; Nakamura and Konno 1954). At pH 2, the 24 subunits of ferritin/

apoferritin can dissociate and when the pH of the solution is gradually increased, it restructures into an integral shell structure at neutral and basic pH (Aime et al. 2002). The dissociation–reassembly characteristics of ferritin/apoferritin facilitates the encapsulation of small drugs and biomarkers (Turyanska et al. 2009; Zhang et al. 2011a, b. c). Maeda et al. reported apoferritin as a tumor-targeted drug delivery system. The difference in pHs of the tumor cells and pH-responsive property of apoferritin make it a promising carrier to load and deliver drugs to cancer cells. They loaded daunomycin—a drug normally used to treat acute myeloid leukaemia and acute lymphocytic leukaemia diseases—into apoferritin (Maeda et al. 1999). Fan et al. demonstrated that magnetoferritin nanoparticles could be employed to target and visualize tumour tissues without any targeting ligands or contrast agents (Fan et al. 2012). For this purpose, they incorporated iron oxide nanoparticles into human heavy-chain ferritin (HFn) protein shells, which can bind target tumour cells (Maeda et al. 1999). The iron oxide core catalyses the oxidation of peroxidase in the presence of hydrogen peroxide to yield a colour reaction which is used to visualize tumour tissues (Bhattacharya et al. 2014; Maeda et al. 1999). They studied 474 clinical samples from patients with nine types of cancers and proved that the magnetoferritin nanoparticles can discriminate cancerous cells from normal cells with a sensitivity of 98% and specificity of 95% (Bhattacharya et al. 2014; Maeda et al. 1999). Zhen et al. reported that RGD-modified ferritin is an efficient carrier of doxorubicin for tumor-targeted delivery (Zhen et al. 2013). They loaded doxorubicin onto RGD-modified apoferritin nanocages with high efficiency (up to 73.49 wt %) after being pre-complexed with Cu(II) (Zhen et al. 2013). The doxorubicin-loaded ferritin nanocages exhibited longer circulation half-life, higher tumor uptake, improved tumor growth inhibition, and less cardiotoxicity than free doxorubicin on U87MG subcutaneous tumor models (Zhen et al. 2013). Lin et al. described several multifunctional ferritin nanocages with defined control of their composition (Lin et al. 2011). They performed *in vitro* and *in vivo* studies to assess their possible suitability as multi-modal imaging probes. An excellent tumour targeting efficiency was observed and attributed to the EPR effect and biovector-mediated targeting (Lin et al. 2011).

1.2.1.2 Protein Cage Nanomaterials for DNA Assays and Immunoassays

Protein cages also act as templates to prepare monodispersed nanoparticles for protein assays. In these methods, the protein cage has diverse roles: (1) it offers a precise environment and conditions for the development of highly monodispersed nanoparticles, (2) it inhibits aggregation of the designed nanoparticles, and (3) in several cases, it prompts a mineralization reaction (Bode et al. 2011; Scuderi et al. 1986). For example, the Liu group developed different marker-loaded apoferritin nanoparticle labels for highly sensitive electrochemical immunoassays of protein biomarkers and DNA assays (Liu and Lin 2007; Liu et al. 2006a, b). Apoferritin-templated synthesis of cadmium phosphate nanoparticle labels for electrochemical immunoassay of tumour necrosis factor-α (TNF-α) protein biomarker was performed by Liu et al., where sharp cadmium signals were observed with low concentrations of TNF-α (i.e., from 0.01 to 10 ng/mL) (Scuderi et al. 1986 (Bhattacharya et al. 2014). The response achieved with a TNF-α target concentration of 10 pg/mL specifies a detection limit of about 2 pg/mL. The low detection is equivalent to the values acquired by means of a common immunological assay, like the enzyme-linked immunosorbent assay (40 pg/mL) (Bhattacharya et al. 2014). Jaaskelainen et al. developed a method of fabricating modified nanoparticles using human ferritin as a labelling agent for a bioaffinity assay (Sharma et al. 2017). A single chain antibody Fv fragment (scFv) was employed as the binding substrate and Eu^{3+} ions as the label. They claimed that the synthesized nanoparticles rapidly bound antigens, and that the process is inexpensive and ecologically sustainable, thus making the system highly beneficial, specifically in large-scale applications (Bhattacharya et al. 2014).

1.2.1.3 Synthetic Dendrimers as Alternative Protein Cages

Dendrimers are unimolecular, three-dimensional, highly branched monodispersed macromolecules (Sharma et al. 2017). The term 'dendrimer' initiated from the Greek word 'dendrons' which means tree or branches, and the word 'meros' means parts (Sharma et al. 2017; Tomalia et al. 1990). The availability of various exterior functional groups and tunable surface engineering empower the modifications of the dendrimer for gene and drug delivery. The distinctive properties of dendrimers (e.g., monodispersity, flexible surface functionality and internal holes), make them model gene and drug delivery carriers. The important properties of dendrimers which aids their use in drug delivery include rapid uptake by cells, presence of large numbers of different functional groups (e.g., hydroxyl, amine, and carboxylic acid), and their capability to conjugate comparatively higher-molecular-weight drugs at a higher percentage (Sharma et al. 2017). Among various dendrimers, poly(amido amine) (PAMAM) dendrimers are especially promising and have a topology similar to biomacromolecules, mimicking globular proteins (Bhattacharya et al. 2014). Dendrimers are more robust for biomedical applications than proteins, because: (1) globular proteins are vulnerable to denaturation by pH, temperature, and light due to their bent structures containing linear polypeptides units, (2) the interiors of protein are heavily packed and their surfaces are more heterogeneous. While, the globular character of dendrimers is covalently linked and their homogeneous surfaces with precise interiors give a structural reliability for specific biological functions (Bhattacharya et al. 2014). Dendrimer-encapsulated gold nanoparticles as carriers of thiolated anti-cancer drugs were reported by Wang et al., where dendrimer-encapsulated drugs exhibited significantly lower cytotoxicity compared with free anti-cancer drugs (Wang et al. 2013a, b, c, d). Dendrimer-encapsulated gold nanoparticles have been used to covalently immobilize a monoclonal electrochemical carcinoembryonic antigen for highly responsive immune-sensing (Jeong et al. 2013). Dendrimer-encapsulated Pt nanoparticles have also been employed as protein mimics that displayed similar catalytic action to catalase, an enzyme which removes excessive reactive oxygen species (ROS) in normal cells (Wang et al. 2013a, b, c, d). The generation 9 PAMAM dendrimers also provide distinctive benefits to fabricate artificial enzymes (Bhattacharya et al. 2014). Both dendrimers and protein cages have also been utilized as magnetic resonance imaging (MRI) contrast materials with high relaxivity of water protons (Helms and Meijer 2006; Aime et al. 2002).

1.2.2 Medical Applications of Graphene-Based Biomaterials

Graphene is a single-layer two-dimensional structured nanomaterial (Yang et al. 2013a, b). Recently, graphene-based materials received profound interest in physical, chemical and biomedical fields (Fig. 1.3) because of their distinctive physicochemical properties (e.g., high surface area (2630 m2/g) (Zhu et al. 2010), strong mechanical strength (~1100 GPa) (An et al. 2011), outstanding electrical conductivity (1738 siemens/m) (Weiss et al. 2012), consummate thermal conductivity (5000 W/m/K) (Balandin et al. 2008), and ease of modification (Georgakilas

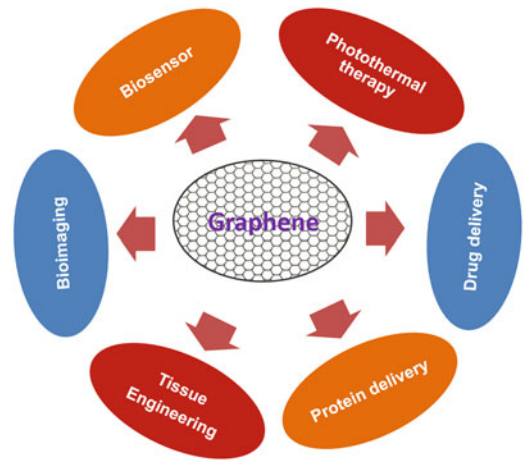

Fig. 1.3 Schematic representation of potential biomedical applications of graphene

et al. 2012; Huang et al. 2012). Graphene-based materials exhibit excellent electrochemical and optical properties, with the ability to adsorb several aromatic biomolecules via π– π stacking interaction and/or electrostatic interaction, which make them excellent candidates for bio-sensing and drug delivery (Yang et al. 2013a, b).

1.2.2.1 Graphene-Based Biosensors for Biomolecule Detection

Graphene-based materials have been used to build several biosensors which work through optical and electrochemical signalling mechanisms (Liu et al. 2012). The powerful electrochemical properties of graphene create a favorable electrode substrate to improve biomolecule detection (Yang et al. 2013a, b). Zhou et al. designed graphene-based electrodes to detect H_2O_2, which exhibited higher rate of electron transfer than graphite-based and bare electrodes. The result suggest that these materials can be used as highly sensitive electrochemical sensors (Zhou et al. 2009). It has also been noted that N-doped graphene (N-graphene) shows enhanced electrocatalytic activity toward H_2O_2 reduction compared with graphene (Shao et al. 2010). The H_2O_2 release from living cells was also detected by N-graphene (Wu et al. 2012). Numerous graphene-based glucose biosensors have been developed and may be useful for the diagnosis and treatment of diabetes. Thermally split graphene was used to design a glucose oxidase-graphene chitosan nanocomposite modified electrode by Kang et al., where the electrode showed a broader linear range of glucose sensitivity and a detection limit of 0.02 mM (Kang et al. 2009). Shan et al. developed a graphene-based glucose biosensor on the modified electrode through electrostatic interaction with poly(vinyl pyrrolidone)-protected graphene and negatively charged glucose oxidase (Shan et al. 2009). Wang et al. showed that nitrogen doped-graphene displayed high sensitivity and selectivity for glucose biosensing (Wang et al. 2010a, b). The high sensitivity of graphene-based materials towards glucose suggests that graphene is a potentially promising material for biosensors (Yang et al. 2013a, b).

Graphene-based materials have been used to detect dopamine, a monoamine neurotransmitter and hormone usually dispersed in the central nervous system of mammals (Yang et al. 2013a, b). Changes in dopamine concentrations are connected with human health issue, and fast and sensitive detection of dopamine is sometimes critical. Wang et al. reported a graphene-based electrode for selective determination of dopamine (Wang et al. 2009). Because of the presence of phenyl ring, dopamine adsorbs on the electrode surface via the pi–pi stacking interaction with graphene (Wang et al. 2009).

1.2.2.2 Graphene-Based Bioimaging Materials

Graphene-based materials, specially graphene oxide (GO), have been used for biological imaging due to excellent cellular uptake, biocompatibility, ease of chemical modifications and typical optical properties. To visualize adenosine-5′-triphosphate (ATP) and guanosine-5′-triphosphate (GTP) in living cells, an aptamer-carboxyfluorescein/graphene oxide nanosheet nano-complex was developed (Wang et al. 2013a, b, c, d) and tested in JB6 cells (Wang et al. 2010a, b) and a human breast cancer cell MCF-7 (Wang et al. 2013a, b, c, d), where graphene does not affect the fluorescence property of the complex.

Different, coloured (e.g., blue, green and yellow) graphene quantum dots have been developed by changing the reaction temperature (Yang et al. 2013a, b). Tetsuka et al. and Pan et al. prepared blue fluorescent graphene quantum dots from cutting graphene sheets by a hydrothermal process (Tetsuka et al. 2012; Pan et al. 2010). Zhang et al. fabricated yellow-photoluminescent graphene quantum dots using an electrochemical method (Zhang et al. 2012). Peng et al. prepared graphene quantum dots from carbon fibres using the acid treatment and chemical exfoliation process (Peng et al. 2012). All the prepared quantum dots are associated with high solubility, excellent biocompatibility, and favorable optical properties, and hence can be used directly for intracellular imaging without any surface treatment or modification (Zhang et al. 2012; Peng et al. 2012; Wu et al. 2013; Zhu et al. 2011).

1.2.2.3 Graphene-Based Drug/Gene Delivery Materials

The ultrahigh surface area (2630 m^2/g) and presence of large numbers of SP^2 hybridized carbon make graphene a more suitable and competent drug carrier than other nanomaterials (Yang et al. 2013a, b). For instance, Dai's group reported loading of anticancer drugs SN38 (Liu et al. 2008) and doxorubicin (Sun et al. 2008) onto nano-graphene oxide, which occurred due to physisorption through π-π stacking interaction. Zhang et al. described controlled loading of mixed anticancer drugs (doxorubicin and camptothecin) onto the folic acid-conjugated nano-graphene oxide through π–π stacking and hydrophobic interactions. They used it for the targeted delivery to MCF-7 cells. Results established that folic acid-conjugated nano-graphene oxide loaded with the two anticancer drugs showed very high cytotoxicity against target cells than that of a single drug-loaded graphene conjugate (Zhang et al. 2010).

Graphene-based materials are also used for gene delivery. For example, poly(ethylene imine) (PEI) and graphene oxide (GO) were covalently combined through an amidation process (Zhang et al. 2011a, b, c). The synthesized PEI-GO supported loading of siRNA by electrostatic adsorption and anticancer drug doxorubicin through π–π stacking. The loaded PEI-GO-siRNA and PEI-GO-DOX were transported into Hela cells. Because of the synergistic effect of reducing Bcl-2 protein activity (via Bcl-2-targeted siRNA) and preventing DNA and RNA production (via DOX), the anticancer efficiency was considerably increased (Zhang et al. 2011a, b, c).

1.2.2.4 Graphene-Based Photothermal Therapy Materials

Phototherapy is an approach taken for the treatment of many diseases. This method controls disease by specific light irradiation through two processes: (1) photothermal therapy, and (2) photodynamic therapy (Yang et al. 2013a, b). In case of photothermal therapy, an optical-absorbing agent capable of producing heat under light irradiation is required. Elevated temperatures facilitate the selective death of abnormal cells (Li et al. 2012). Owing to the strong optical adsorption in the near-infrared region, graphene gained significant attention in photothermal therapy. Zhang et al. synthesized DOX-loaded PEGylated nanographene oxide that can transport both the heat and drug to the tumorigenic area to assist chemotherapy as well as photothermal treatment (Zhang et al. 2011a, b, c). Yang et al. fabricated a nanocomposite probe using chemically reduced graphene oxide and iron oxide nanoparticle for tumor bioimaging and photothermal therapy (Yang et al. 2012). Hu et al. developed a nanocomposite of quantum-dot-tagged chemically reduced graphene oxide capable of cell/tumor bright fluorescence bioimaging and use as a photothermal therapy (Hu et al. 2013).

1.2.2.5 Graphene-Based Tissue Engineering Biomaterials

The functionalized graphene, specifically graphene oxide, serves as a complementary carbon nanomaterial to design scaffolds for tissue engineering due to its high mechanical strength, large surface area, and favorable electrical properties (Xie et al. 2013; Shin et al. 2011; Ramón-Azcón et al. 2013; Li et al. 2013; Geim and Novoselov 2007; Park and Ruoff 2009; Gao 2015). Wang et al. described that compared to a crosslinker, a small amount of graphene oxide dramatically improved the mechanical property of their prepared self-healing nanocomposite (Wang et al. 2013a, b, c, d). The effect of graphene on the proliferation of human mesenchymal stem cells (hMSCs) was studied by Nayak et al. and results showed that it did not hamper cell proliferation and specifically enhanced their differentiation into bone cells (Nayak et al. 2011). Shin et al. designed RGD peptide-graphene oxide-PLGA nanofiber mats to be used as scaffolds for vascular tissue engineering (Shin et al. 2017). It was observed that the physicochemical, thermal and mechanical properties of fabricated nanofiber mats are suitable for supporting cell growth and thus may serve as promising scaffolds for vascular tissue engineering (Shin et al. 2017).

1.2.3 Nanogel as an Effective Drug Delivery System

As a member of nano-size particulate materials, nanogels have potentially enormous significance for the drug delivery field. By definition, nanogels are three-dimensional, crosslinked swellable polymeric networks (smaller than 1000 nm) that, without dissolving into aqueous media, have high water-holding capacity (Oh et al. 2008; Soni et al. 2016). Gels with particle size ranges within 200 nm are efficient for targeted drug delivery. While these particles are mainly spherical, recent advances in synthetic approaches permit for the design of nanogels with different shapes (Rolland et al. 2005; Kersey et al. 2012). Nanogels are fabricated using physical or chemical crosslinking methods (Zhang et al. 2016). They possess combined characteristics of gels—a soft material which merges the properties of solids and fluids—and nanoparticles (Soni et al. 2016). Nanogels have the capacity of absorbing large amount of water or biological fluids principally due to its large surface-to-volume ratio and the presence of –OH, –COOH, –CONH–, $–CONH_2$, and $–SO_3H$ group in their polymer chains (Zhang et al. 2016). The biocompatible nature of the nanogels is attributed to the high water content and low surface tension (Zhang et al. 2016).

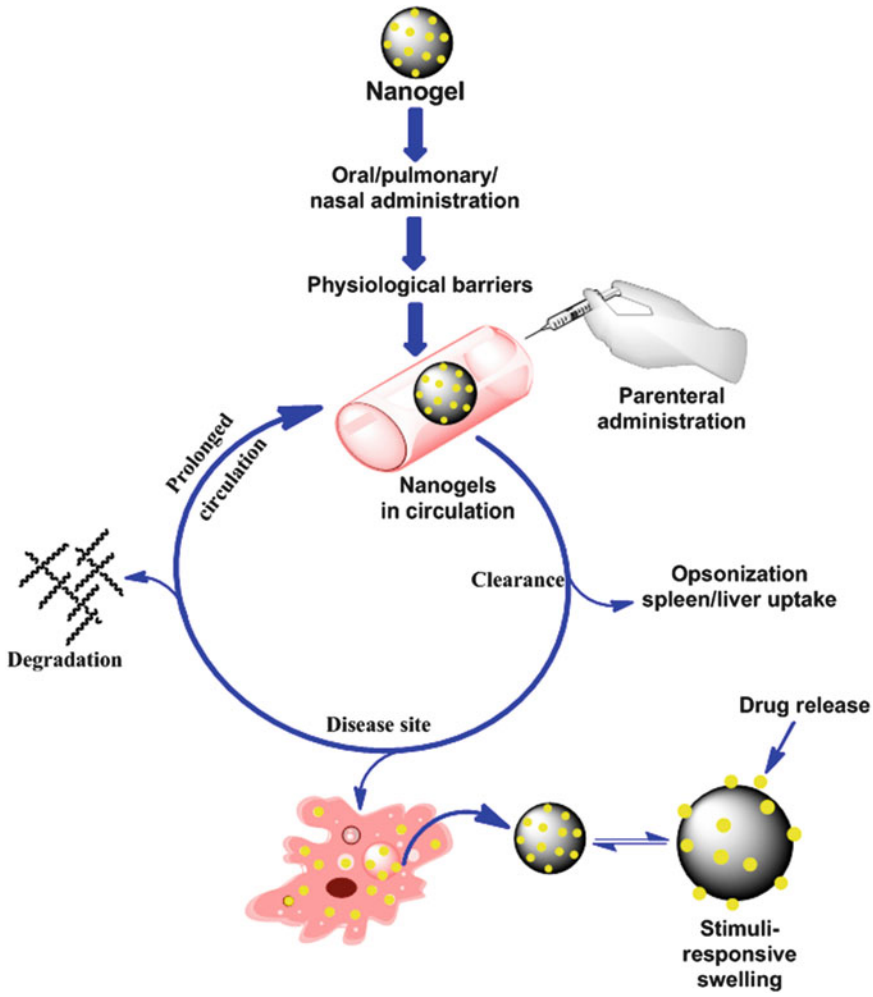

Fig. 1.4 *In vivo* behaviors of nanogel

The porous nature of nanogels contributes to the high loading efficiency of guest molecules and excellent swelling property which makes them suitable for controlled release systems (Fig. 1.4). Their features (e.g., size, charge, porosity, softness, and degradability) can be tuned by changing the chemical composition of the nanogels (Soni et al. 2016). Their flexibility permits for incorporation of different types of guest molecules (e.g., inorganic nanoparticles, proteins, drugs and DNA), without disturbing their gel-like behaviors (Chacko et al. 2012). These multi-functionalities and stabilities are not observed in other categories of nano particulates (Napier and DeSimone 2007) particularly the capacity to incorporate materials with different physical properties within the same carrier. Nanogels prevent the denaturation and degradation of loaded guest molecules (e.g., enzymes, drugs and genetic material), while the structural properties of nanogel macromolecular networks and sustained releases of bioactive molecules enhance the circulation half-lives of small drug molecules, and provide a suitable matrix for combination delivery of therapeutic molecules (Zhang et al. 2016). They can be specifically target sites of interest through conjugation with a targeting ligand or by passive targeting owing to their nano-scale size (Zhang et al. 2016).

1.3 Biomimetic Materials and Tissue Engineering

Tissue engineering is a process designed to repair diseased or damaged tissue by incorporating healthy cells (from the patient or a donor) into scaffold materials which serve as matrices for cell cultivation (Kolos and Ruys 2013). To construct biological tissues, three main components are essential: (1) scaffold materials, (2) cells, and (3) signals (Fig. 1.5). Biocompatibility, 3D-structure, distribution of interconnected pores to encourage vascularization, cell attachment and growth are primary attributes of a promising scaffold material (Kolos and Ruys 2013; Patterson et al. 2010). Scaffolds may be biodegradable or permanent. Biodegradation is

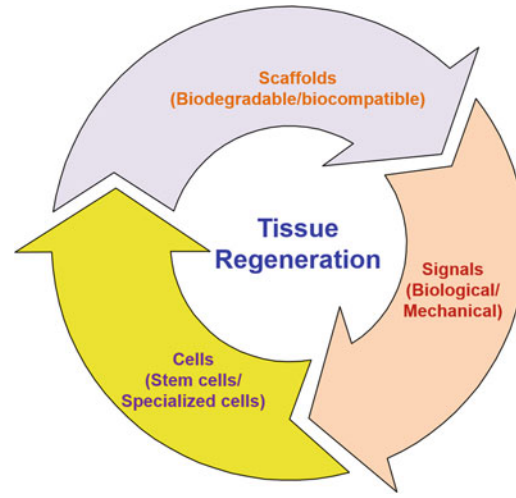

Fig. 1.5 Components for the engineering of tissues

ideal for tissue regeneration where host tissue can substitute the scaffold and that stress can be shifted gradually from the scaffold to the new tissue (Kolos and Ruys 2013). Cell signals can be tuned using differentiation factors or specific receptors (Kolos and Ruys 2013).

Biomimetic materials for tissue engineering mimic the important mechanical features of the organs, tissues and extracellular matrix (e.g., mechanical strength, softness, composition of extracellular matrix), and biological performance (e.g., adhesion, release and delivery of growth factors, and tissue-remodeling behaviors (Patterson et al. 2010). Different types of biomaterials (e.g., naturally occurring molecules, functionalized biomolecules, and synthetic chemical materials) have been used in tissue engineering.

1.3.1 Naturally Occurring Molecules

1.3.1.1 Collagen

Collagen, the most plentiful mammalian protein, is a triple helix primarily made up of glycine, proline and 4-hydroxyproline (Patterson et al. 2010). Collagens can be reconstructed into a fibrillar matrix or gel by changing the temperature or pH, however, reduced mechanical strength of collagen gel is a major concern for *in vivo*

applications (Patterson et al. 2010). Thus, several methods have been applied to improve the mechanical strength of collagen in applications such as hydrogels, hybrid gels, and hybrid scaffolds through chemical or physical combination with other biomaterials (Sheehy et al. 2018; Hatayama et al. 2017).

1.3.1.2 Glycosaminoglycans

Glycosaminoglycans (GAG) are long unbranched polysaccharides which can amplify the biomechanical and biochemical functions of ECM (Patterson et al. 2010). Most GAGs, with the exception of hyaluronic acid, are components of proteoglycans; hyaluronic acid does not remain covalently attached to a protein core, but rather is entangled within the extracellular space (Patterson et al. 2010). The anionic polymer supplies mechanical strength to the ECM by absorbing water, whereas, the GAG unit influences tissue organization through cell-surface receptor interactions (Toole 2004).

The natural source of hyaluronic acid is rooster comb, however, it can also be produced using *Streptococcus* bacterium. It forms a gel by absorbing large amounts of water, and due to its high molecular weight, loses its shapes very slowly. Through the carboxyl and hydroxyl functional groups of hyaluronic acid, several types of gels and scaffolds with tunable mechanical properties have been developed and applied to tissue engineering (Kutlusoy et al. 2017; Walimbe et al. 2017; Entekhabi et al. 2016; Chen et al. 2017; Fan et al. 2015).

1.3.1.3 Self-Assembling Polypeptides

Like proteins, peptides self-assemble and may form nanofibrillar gels through non-covalent intermolecular interactions (Branco and Schneider 2009). Numerous nanofibrillar gels and scaffolds were developed through self-assembly of peptides and used to deliver growth factors and impact the 3-D organization of cells (Zhang et al. 1995; Gelain et al. 2007; Schneider et al. 2008; Segers et al. 2007; Hsieh et al. 2006). These gels have been designed to form specific cell interactions, depending the availability of specific biofunctional ligands (Branco and Schneider 2009). To increase cell:tissue interactions, a laminin-derived peptide Ile-Lys-Val-Ala-Val-based scaffold was designed by Silva et al., where the encapsulated neural progenitor cells were perceived to differentiate into neurons (Silva et al. 2004).

An alternative polypeptide capable of forming hydrogels from Val-Pro-Gly-X-Gly penta-units (X is amino acid other than proline) is elastin-like-polypeptides. They are soluble in aqueous media, but become insoluble and aggregate at a critical temperature (Chilkoti et al. 2006). Elastin-like-polypeptides stimulate the preparation and preservation of cartilaginous matrix from captured chondrocytes and stem cells (Betre et al. 2006), while, for cell attachment, elastin-like-polypeptides have also been reformed with ECM ligands (Liu et al. 2004).

1.3.1.4 Synthetic Hydrogel Materials Mimicking Biological Functionality

Synthetic analogues of biomaterials may offer several advantages for tissue engineering, however, in some cases, viability may be affected by reaction or physiological conditions (Patterson et al. 2010). Importantly, the use of completely synthetic materials may reduce purification issues. One of the emerging materials which open a new door for tissue engineering is polymeric hydrogels which may be fully synthetic or modified biopolymers. Appropriate swelling characteristics are important to mimic the viscoelastic properties of natural ECM (Patterson et al. 2010). Cell-responsive hydrogels for use in tissue engineering can be prepared by using polysaccharides (e.g., alginate, starch, cellulose, chitosan, chitin, pectins, agar, dextran, gellan, pullulan, xanthan) (Bacakova et al. 2014) and synthetic polymers incorporating cell-responsive peptide domains (e.g., poly(ethylene glycol) (PEG), poly(hydroxyethyl methacrylate), poly (vinyl alcohol) (Patterson et al. 2010). Peptide-conjugated polymers may offer ECM-derived bimolecular signals (Patterson et al. 2010). RGD is an example of a peptide where conformation also has a great effect on cell adhesion. For example, the incorporation of cyclic RGD into photo-

crosslinked PEG-diacrylate hydrogels demonstrated improved endothelial cell adhesion compared with hydrogels containing linear peptides (Zhu et al. 2009).

Degradability is another crucial factor for the design and development of cell responsive biomaterials (Patterson et al. 2010). The degradation behaviour of the general hydrogel can be prompted by the incorporation of hydrolytically degradable moieties (e.g., poly(glycolic acid), poly(lactic acid), alginate, or hyaluronate) (Patterson et al. 2010). *In vivo*, ECM molecules are degraded enzymatically by cell-secreted proteases. Thus, cell-mediated control of degradation can be designed into synthetic hydrogels by combining protease substrates (Patterson et al. 2010). Again, degradation of photo-crosslinked PEG-caprolactone gels take place in the presence of lipase (Patterson et al. 2010). Furthermore, bio-functionalization will also afford signals essential to stimulate cell behaviours (Patterson et al. 2010). For these purposes, researchers are using single or multiple growth factors to recapitulate natural processes (Patterson et al. 2010).

1.4 Biomimetic Materials and Stem Cells

1.4.1 The Potential Roles of Stem Cells in Biomimetic Scaffold Formation

Stem cells have been renowned for their cell therapy potential because of their potential to self-renew via cell division and differentiation into diverse specialized cell types (Liao et al. 2008). The regeneration of diseased and damaged tissues using cell therapy is receiving significant interest because it may potentially extended human organ functionality, and lead to longer and healthier lives (Vunjak-Novakovic and Scadden 2011; Nassar et al. 2017). Recently, due to the lack of matching donor organs, tissues which are away from repair, or missing owing to surgical resection or inborn abnormalities are being substituted by transplantation (Vunjak-Novakovic and Scadden 2011). Current advances in stem cell biology and tissue engineering are allowing tissue engineers to instruct multipotent stem cells to differentiate into a proper phenotype at the right time and location to assist well-designed tissue structures (Vunjak-Novakovic and Scadden 2011). A proper combination of biology and engineering is required for creating biomimetic atmospheres appropriate for the development and regeneration of tissue *in vivo*. The presence of bioactive molecules capable of supplying chemical, physical and spatial signals in the scaffolds is indispensable to mimic natural tissue growth (Vunjak-Novakovic and Scadden 2011). In addition to that flexibility of stem cells, one vital characteristic for multiple-tissue engineering applications is the most promising source for this purpose.

Generally, stem cells are one of two types, (1) pluripotent stem cells, containing embryonic stem cells (ESCs) and induced pluripotent stem cells (iPSCs), and (2) multipotent adult stem cells (Fig. 1.6) (Lee et al. 2018). Shinya Yamanaka's group first discovered induced pluripotent stem cells (iPSCs) using the nuclear reprogramming of unipotent adult somatic cells (Takahashi and Yamanaka 2006; Rashid and Alexander 2013). These are a distinct group of stem cells, which retain pluripotency and the capacity for self-renewal (Takahashi and Yamanaka 2006; Rashid and Alexander 2013). Like embryonic stem cells, induced pluripotent stem cells are known for their ability to grow indefinitely in culture without the losing pluripotency and ability to differentiate into different somatic cells. Multipotent adult stem cells are seen in many tissues and organs (e.g., bone marrow, skin, and within the central nervous system) (Caplan 2007). Human mesenchymal stem cells (hMSCs) are a type of multipotent stem cells found in muscles, fats, and bone marrow) (Caplan 2007). The hMSCs of bone marrow are capable of differentiating into different tissue lineages, like osteoblasts (i.e., bone cells), adipocytes (i.e., fat cells), and chondrocytes (i.e., cartilage cells) (Pittenger et al.

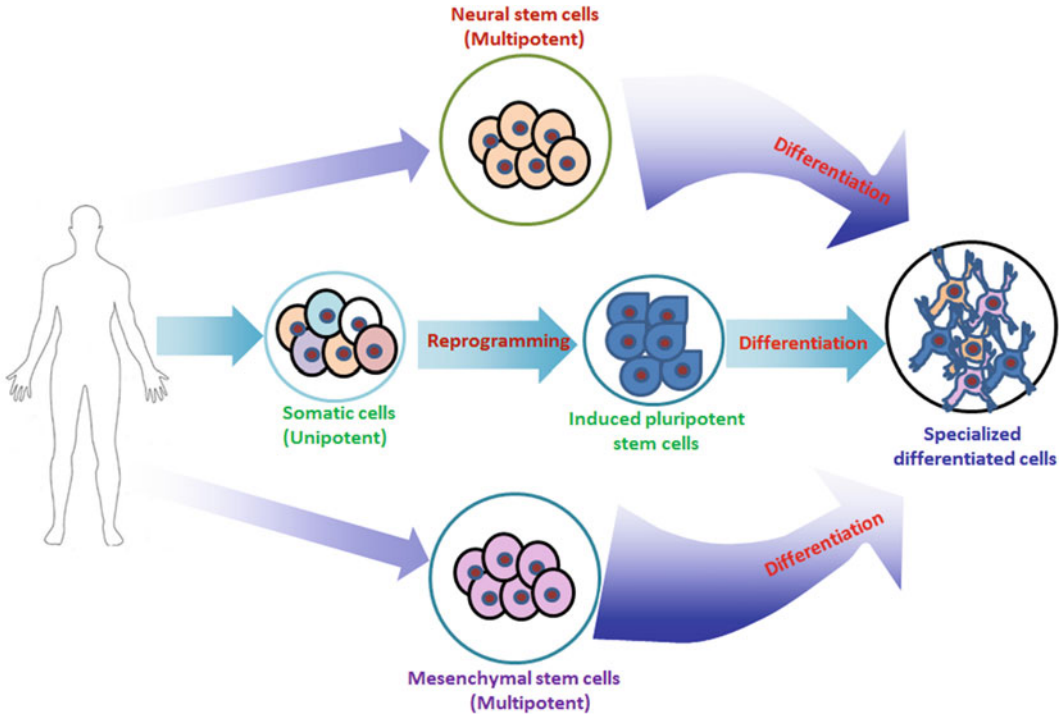

Fig. 1.6 Classification and processing of stem cells

1999). These hMSC-associated abilities support their potential as striking alternatives for musculoskeletal tissue regeneration.

1.4.1.1 Stem Cells Fate

For practical tissue engineering and regenerative medicine, morphological and physiological similarity is required between *in vivo* condition and converted stem cells and tissues. The reformations of these cells depend on various factors (e.g., cell-ECM interaction, concentration of growth factors, topography, elasticity, stiffness, and porosity of the ECM) (Lee et al. 2018). Generally, cell-secreted molecules (e.g., proteoglycans, collagen and elastin) in ECM have important roles for stem cell activities (Lee et al. 2018).

1.4.1.2 Polymeric Materials Impacting Stem Cell Fates

To reduce challenges associated with *in vivo* physiological cellular microenvironments and to control stem cell fate, advanced research is focusing on in the field of biomaterials science and engineering (e.g., manipulation of biomaterial's composition, stiffness, surface topography, and porosity) (Lee et al. 2018). In this regard, polymeric hydrogels have been employed to mimic the physiological microenvironments of stem cells (Hoffman 2012) due to the available of compatible space for cellular adhesion, proliferation and its mechanical properties (Hoffman 2012). Hydrogels made from natural products (e.g., collagen, silk protein, hyaluronic acid, cellulose or chitosan) have been extensively used to arrange stem cells and improve embryonic body differentiation (Lee et al. 2018). Besides, synthetic polymers [e.g., poly(ethylene glycol), poly(lactic acid), and poly(lactic-co-glycolic acid)] have been used for the *in vitro* and *in vivo* stimulation of stem cell differentiation by incorporating bioactive signals (Lee et al. 2018).

1.4.1.3 Nanomaterials for Stem Cells Fate

As nanotechnology and material sciences progress, various nanomaterials (eg, 0-D nanoparticles, 1-D nanotubes, 2-D nanosheets, and 3-D nanofoams) have been developed to mimic natural cellular environments to optimize stem cell control (Lee et al. 2018). Nano-architectured scaffolds have been designed to improve cellular attachment and enhance the modification of overall cellular shapes and alignments (Lee et al. 2018). Moreover, nanomaterials should ideally play an important role leading to improved mechanical properties and electrical conductivity of the scaffolds (Lee et al. 2018). Typically, 0-D nanoparticles are used to design differently patterned topographies to mimic natural ECMs and to enhance cellular attachment for cell-ECM interactions (Hou et al. 2013). By controlling surface charges and hydrophobicity of nanoparticles, they can be used in protein targeting and binding, which will be beneficial for stem cell applications (Lee et al. 2018). Again, the uses of 1-D carbon nanotubes and 2-D graphene nanosheets, and graphene oxide are broadly used for the improvement of properties of synthetic tissue engineering scaffolds because of their excellent electrical conductivity and strong mechanical strengths, and particularly accelerating stem cell proliferation and differentiation ability of carbon nanotubes (Lee et al. 2018).

1.5 3-D Bioprinting Materials

In spite of advances in tissue engineering, demand for substitute fabrication methods to build up complex tissues and organs is increasing due to limited controlling power of conventional techniques including porogen-leaching, electrospinning, and injection molding on scaffold architectures, composition, pore shape, size, and distribution (Ji and Guvendiren 2017; Murphy and Atala 2014; Groen et al. 2016; Shafiee and Atala 2016). 3D bioprinting provides immense prospective to construct highly multifaceted designs with precise control of structures, mechanics, and biological characteristics (Ji and Guvendiren 2017). Owing to diverse advantages (e.g., computer-supported patient-specific design, controlled manufacture, superior structural complexity, and high-efficiency), 3-D printing is a striking technology to make scaffolds, devices, and tissue models for biomedical applications (Ji and Guvendiren 2017; Guvendiren et al. 2016). 3D bioprinting processes involve fabrication of scaffolds or devices in a layer-by-layer approach using living cells into a tissue construct with or without a carrier (Cui et al. 2017; Shafiee and Atala 2016). The biomaterial used for cellular bioprinting is called bioink. Cell-loaded hydrogels, decellulerized ECM-based solutions, and cell suspensions are the most commonly used bioinks (Ji and Guvendiren 2017; Chen et al. 2016; Gu et al. 2016).

1.5.1 Essential Properties of Bioinks

A model bioink material should contain several key characteristics of biomaterials and functions (e.g., printability, mechanics, shape stability, functionalizability, biocompatibility, bioactivity, cytocompatibility, and degradability) (Ji and Guvendiren 2017). Printability includes two branches: (1) processability of the bioink, and (2) reliability of mechanical strength of the printed 3D construction after printing (Ji and Guvendiren 2017). Viscosity is a vital bioink factor affecting printability and cell-encapsulation efficiency. Highly viscous polymer solutions do not flow easily and thus cannot hold their shapes for a long time after printing. However, for regular printing through direct ink writing method, high pressure is required. Generally, for inkjet or droplet-based bioprinters, the bioink viscosity value is near to 10 mPa·s (Gudapati et al. 2016; Ozbolat et al. 2017), the viscosity of bioinks for extrusion-based direct ink writing bioprinting ranges from 6–30$\times$ 10^7 mPa·s (Ozbolat et al. 2017), and in case of laser-assisted bioprinting, the bioink viscosity ranges from 1–300 mPa·s (Hölzl et al. 2016). The whole

mechanics, (i.e., attainable stiffness), is significant to produce self-supporting structures and to control and direct cellular behaviors (Ji and Guvendiren 2017). Degradation is noteworthy to progressively replacing the construct with their regenerated ECM *in vivo* by cells. Functionalizability is requisite to incorporate biological signals, specifically, bioactivity, to direct cellular behavior (e.g., migration, adhesion and differentiation) (Ji and Guvendiren 2017). Furthermore, biocompatibility, cytocompatibility, and high cell viability are fundamental for the ink materials (Kim et al. 2016; Park et al. 2016; Jung et al. 2017).

1.5.2 Currently Available Bioinks

Cell-loaded hydrogels, decellularized ECM-based solutions, and cell suspensions are regularly used as bioinks for tissue and organ printing (Ji and Guvendiren 2017). Cell-loaded hydrogels are remarkable because of their tunable characteristics and their ability to recapitulate the cellular microenvironment (Ji and Guvendiren 2017). ECM-based bioink/decellulerized tissue inks are attractive because of their intrinsic bioactivity and easiness of making printable bioink (Ji and Guvendiren 2017). Cell suspension inks are used to generate scaffold-free biological constructs using cell aggregates (Ji and Guvendiren 2017).

1.5.2.1 Cell-Loaded Hydrogels

Cell-loaded hydrogels are typically used as bioinks for extrusion-based, droplet-based (inkjet), and laser-based bioprinting methods to construct scaffolds or organs. Generally, these bioinks are natural hydrogels derived from biopolymers (e.g., agarose, chitosan, alginate, hyaluronate, collagen, fibrin, and gelatin). Additionally, synthetic hydrogels (e.g., pluronic (poloxamer) and PEG) are also used. Except agarose and alginate, biopolymer-based hydrogels have inherent bioactivity and exhibit structural similarity to ECM (Ji and Guvendiren 2017). Compared to natural hydrogels, synthetic hydrogels have more advantageous mechanical properties, but they do not endorse cellular function, thus additional functionalization is required to tether bioactive cues into synthetic hydrogels. Sometimes, the mechanical properties and/or bioactivity can also be modified by embedding nanoparticles into bioink formulation (Ribeiro et al. 2015). Crosslinking is one of the best techniques for bioink preparation using polymeric materials. Two types of crosslinking process exist, (1) physical crosslinking, and (2) chemical crosslinking. Physical crosslinking deals with hydrophobic interactions, hydrogen bonding, and ionic interactions. Chemical crosslinking involves formation of covalent bonds through radical polymerization, enzymatic reaction or Michael-type addition reaction. Chemically crosslinked hydrogels are mechanically stronger than physically crosslinked gels, which is mainly significant for the stem cell behavior including differentiation (Ji and Guvendiren 2017). A stable crosslinked gel of acrylated pluronic has been prepared after printing using UV light by Müller et al. (Müller et al. 2015). Two PEG derivatives (e.g., PEG-diacrylate and PEG-methacrylate) are used as proper polymers for extrusion-based, laser-based, droplet-based printing systems (Wüst et al. 2015). Basically, PEG is hydrophilic, but not adhesive to proteins and cells. For this reason, the addition of natural polymers or functionalization with biochemical cues is required to make it suitable for biological application. Hong et al. synthesized 3D printing of tough and biocompatible, cell-laden PEG–alginate–nanoclay hydrogels infused with collagen (Hong et al. 2015). Alginate is also used to prepare bioinks for inkjet and extrusion-based printing process. In case of inkjet printing, calcium chloride is sprayed onto the solution of alginic acid (Boland et al. 2007). For extrusion-based printing, a viscous solution of alginate is first printed and then the printed designs are exposed to $CaCl_2$ solution to make a stable shape after ionic crosslinking (Ji and Guvendiren 2017). Alginate is not cell-adhesive, therefore, natural polymers like gelatin or fibrinogen are incorporated into the matrix to induce cell adhesiveness and biological activity (Lim

et al. 2016; Pan et al. 2016). Among all biopolymers, hyaluronic acid and gelatin have been widely employed for the preparation of functionalized polymers for 3D-bioprinting applications. For instance, methacrylated gelatin are used for the preparation of hydrogels through radical polymerization for 3D-bioprinting (Loessner et al. 2016; Lim et al. 2016]. Hyaluronate-based hydrogels have also been developed and used for 3D-bioprinting technology by many research groups (Highley et al. 2015; Ouyang et al. 2016). Recently, self-assembled peptides (Raphael et al. 2017), and polypeptide–DNA hydrogels (Li et al. 2015) have been used as other promising materials for bioinks fabrication.

1.5.2.2 Cell Suspension Bioinks

Bioprinting of scaffold-free constructs exploits cell aggregates by forming cellular spheroids as bioinks (Jakab et al. 2010; Christensen et al. 2015). This procedure relies on tissue liquidity and fusion, that permit cells self-assembly of cells and fuse owing to cell–cell interactions (Ji and Guvendiren 2017). Organovo Inc. is a typical medical research company that fabricated liver models through extrusion-based printing technique with high density bioinks using parenchymal cells/non-parenchymal cells (Nguyen et al. 2016). Again, by combining bioprinting and microcarrier technology, Tan et al. proliferated cells on poly(D,L-lactic-co-glycolic acid) porous microspheres and then performed printing (Tan et al. 2016).

1.5.2.3 Decellularized ECM-Based Bioinks

This type of bioink is prepared by: (1) tissue decellularization, (2) ECM drying (to generate a powder) and (3) dissolving the powder in a cell friendly buffer solution (Ji and Guvendiren 2017). A carrier polymer could be employed to enhance solubility, viscosity, or to induce post-crosslinking of the bioink (Ji and Guvendiren 2017). Even though this method offers a novel solution for bioink preparation, the decellularization procedure involves numerous steps (e.g., accurate quantification of the DNA and the ECM components), which make it expensive. Using this method, decellularized ECM-based bioinks supported by PCL has been printed to form 3D constructs (Pati et al. 2014). Printing of vitamin B_2-induced decellularized ECM-based covalent crosslink gel has been recently reported by Jang et al. (Jang et al. 2016; Jang et al. 2017).

1.6 Immune Responses of Biomaterials

The immune system is conventionally considered from the standpoint of protecting against bacterial or viral infections (Gardner et al. 2013). The compatibility of biomaterials is important to their structural and genetic functions in biomedical applications (Chung et al. 2017). However, biomaterial implants can also illicit immune responses (Gardner et al. 2013). These immune responses are adjudicated by different molecular cues (e.g., antibodies, cytokines, and cell types, such as macrophages, neutrophils, natural killer cells, neutrophils, T-cells, B-cells, T-cells, and dendritic cells) (Gardner et al. 2013). Normally, these molecular signals direct the production of fibrous capsule around implants, thus protecting the body from these foreign materials (Gardner et al. 2013; Chung et al. 2017).

The effect of the biological scaffolds on the immune system is a crucial feature responsible for the constructive regenerative results. Many mechanisms have been proposed for this response (e.g., the breakdown of ECM can expose multiple secret domains that govern many cell functionalities like invasion, migration, adhesion and differentiation) (Chung et al. 2017). Again, T helper cells coordinate the phenotypic and functional changes of macrophages to regenerative ability (Chung et al. 2017). On the basis of *in vitro* responses to different cytokines, macrophages have two functional phenotypes, M1 (pro-inflammatory) and M2 (pro-healing) (Chung et al. 2017). From the viewpoint of immunomodulatory biomaterials, the ECM renovation process could be an excellent approach to improve regeneration. ECM remodelling is like

tissue homeostasis, and has precise effects on wound healing (Chung et al. 2017). Because of the collagen synthesis and breakdown capacity, and as a part of ECM, fibroblasts are main agents in this process. The interaction between fibroblast and immune cells is related to wound closing and tissue regeneration (Chung et al. 2017). Actually, during the wound repairing process, macrophages favour the anti-inflammatory phenotype, and discharge vascular endothelial growth factor (VEGF) and transforming growth factor (TGF)-β (Chung et al. 2017). These elements act as intercellular communication signals leading to the proliferation and growth of fibroblast during the wound remodelling process (Chung et al. 2017). Therefore, understanding the crosstalk between fibroblasts and immune cells may empower the design of biomaterials that can control the healing response and regeneration ability (Chung et al. 2017). Synthetic biomaterials have been fabricated in plastics and fabrics, and used for biomedical applications ranging from artificial articulating joints to vascular grafts (Chung et al. 2017). While non-degradable synthetic materials also employed in commercial tissue engineering, synthetic degradable polymers, like polyesters, were used as tissue engineering scaffolds to afford a biocompatible cellular environment which degrades as tissue forms (Chung et al. 2017). However, biological signals including proteins, peptides, small molecules, and carbohydrates could be embedded to improve cell function and tissue development. The biocompatibility of the synthetic implants involved escaping the foreign body response (FBR), fibrotic encapsulation, and toxicity of degradation products (Chung et al. 2017). The FBR was naturally characterized through the arrival and fusion of macrophages around the foreign body to produce giant cells (Chung et al. 2017).

1.7 Intellectual Property (IP) Associated with Biomedical Materials

Inventors and scientists are continuously putting their efforts towards researches in companies and institutions to advance society through innovations in instruments, methods, software, medical devices and biomaterials. Protection of IP is particularly noteworthy in the biomedical industry. Biomaterials used on or in the human body need wide analyses to confirm biocompatibility, and to assess side effects including clinical aspects (Hornick and Rajan 2015). These evaluations increase the costs of R&D for novel advanced products. Innovators think that some yields will be positive, accept endorsement for sales, produce sufficient income to recover research and advance costs for both fruitful and failed products, and make a revenue (Hornick and Rajan 2015). In recent decades, inventors, their attorneys, the courts, and even congress have fought with the patentability of software, as the original patent laws and even recent amendments do not clearly address it (Hornick and Rajan 2015). Likewise, in spite of the prospective to advance science, nanotechnology, 3D bioprinting technology, and tissue engineering raise more queries about what features of these new inventions and advances can be secured by IP, which cannot be protected, and which should not be protected for ethical and public policy motives (Hornick and Rajan 2015).

Implanted biomaterials and medical devices, surgical treatments and methods, engineered tissues and medicinal drugs have been secured by patents, design patents, trademarks, copyrights, and trade secrets (Hornick and Rajan 2015). Implanted devices remain within the machine category, for those patent laws, and design patents are applicable. Although surgical treatments and methods are not protected in some countries but in US, it is under process category of patent laws (Hornick and Rajan 2015). Medicinal drugs have been protected by patents for compositions of substrates, where the patents are approved for the synthetic chemical structures of the drugs (Hornick and Rajan 2015). IP laws are also applicable for all aspects of 3D bioprinting and nanotechnology (e.g., hardware involved for printing, software for the design of tissue structures, and materials with specific compositions used in this system). The most

noticeable forms of IP for 3D bioprinting and nanotechnology are patent and trade secret protection (Hornick and Rajan 2015). Even though copyrights also protect the software of 3D bioprinting and nanotechnology machine (Hornick and Rajan 2015), the issues of engineered tissues and organs still remain to be solved due to humanized used over time.

1.8 Concluding Remarks and Future Perspectives

Development of biomimetic materials is exponentially increasing, especially for their applications in tissue engineering and regenerative medicine, biosensors, drug/protein delivery, stem cell research, 3D bioprinting and so on. These biomaterials have been fabricated by taking inspiration from existing designs and procedures of nature, along with the understanding of the chemistry and mechanisms of cell biology, nature of diseases, mode of actions and mechanism of biomolecules. It is true that till now, numerous biomaterials have been fabricated, have faced several difficulties *in vitro* and/or *in vivo*. Many materials achieved to their best levels but some of them have failed to achieve their best levels. Research is continuously going on in this field to find better options and for progress of the society. However, the inclusive successful development of biomimetic medical materials solely depends on their practical implementation on or in human body. This process is associated with the development of technology, software, device and so on. The modern progress within materials research promotes further investigation into how to best emulate the structures of natural materials in biomimetic materials. The emerging field of biomimetics deals with new technologies created from biologically stimulated engineering at nano- to macro- levels and 3D-bioprinting. Indeed, these technologies revolutionize materials science and engineering, and provide opportunities to develop tissue engineering scaffolds, devices, and tissue models for biomedical applications by embedding several biomimetic features at the molecular, genetic, and nanometer scales.

In conclusion, the developed biomimetic medical materials should be biocompatible and flexible. They should contain cellular and molecular induction and adhesion sites, sufficient mechanical strength, and possess characteristics of biodegradability and tissue remodeling. To be a model biomedical applicable material, effective *in vivo* results are the primary requirements. A combined package of biomaterial, technology, software, and device could offer a systematic approach for medical application. Besides, IP protection is important in the medical industry. Everything that is used on or in the human body needs wide-ranging analysis to confirm biocompatibility, and to evaluate side effects by Food and Drug Administration of each country.

It is expected that in near future, researchers will able to develop more effective and sophisticated biomimetic medical materials for efficient biomedical applications through further improvement of the understandings of biological functions and human anatomy, and using best leverage advanced technologies especially through wide applications of biomimetics such as nanotechnology and 3D-printing.

Acknowledgement This work was supported by the National Research Foundation of Korea (NRF) Grant (2015R1A2A1A10054592).

References

Aime S, Frullano L, Geninatti Crich S (2002) Compartmentalization of a gadolinium complex in the apoferritin cavity: a route to obtain high relaxivity contrast agents for magnetic resonance imaging. Angew Chem Int Ed 41(6):1017–1019

An X, Butler TW, Washington M, Nayak SK, Kar S (2011) Optical and sensing properties of 1-pyrenecarboxylic acid-functionalized graphene films laminated on polydimethylsiloxane membranes. ACS Nano 5(2):1003–1011

Bacakova L, Novotná K, Parizek M (2014) Polysaccharides as cell carriers for tissue engineering: the use of cellulose in vascular wall reconstruction. Physiol Res 63:S29

Balandin AA, Ghosh S, Bao W, Calizo I, Teweldebrhan D, Miao F, Lau CN (2008) Superior thermal conductivity of single-layer graphene. Nano Lett 8(3):902–907

Bar-Cohen Y (2006) Biomimetics: biologically inspired technologies. CRC/Taylor & Francis, Boca Raton isbn:9780849331633

Bello OS, Adegoke KA, Oyewole RO (2013) Biomimetic materials in our world: a review. IOSR J Appl Chem (IOSR-JAC) 5:22–35

Benyus J (1997) Biomimicry: innovation inspired by nature. William Morrow & Company Inc, New York, isbn:978–0688–16099-9

Betre H, Ong SR, Guilak F, Chilkoti A, Fermor B, Setton LA (2006) Chondrocytic differentiation of human adipose-derived adult stem cells in elastin-like polypeptide. Biomaterials 27(1):91–99

Bhattacharya P, Du D, Lin Y (2014) Bioinspired nanoscale materials for biomedical and energy applications. J R Soc Interface 11(95):20131067

Bode SA, Minten IJ, Nolte RJ, Cornelissen JJ (2011) Reactions inside nanoscale protein cages. Nanoscale 3(6):2376–2389

Boland T, Tao X, Damon BJ, Manley B, Kesari P, Jalota S, Bhaduri S (2007) Drop-on-demand printing of cells and materials for designer tissue constructs. Mater Sci Eng C 27(3):372–376

Branco MC, Schneider JP (2009) Self-assembling materials for therapeutic delivery. Acta Biomater 5 (3):817–831

Caplan AI (2007) Adult mesenchymal stem cells for tissue engineering versus regenerative medicine. J Cell Physiol 213(2):341–347

Chacko RT, Ventura J, Zhuang J, Thayumanavan S (2012) Polymer nanogels: a versatile nanoscopic drug delivery platform. Adv Drug Deliv Rev 64(9):836–851

Chen A, Bao Y, Ge X, Shin Y, Du D, Lin Y (2012) Magnetic particle-based immunoassay of phosphorylated p53 using protein cage template lead phosphate and carbon nanospheres for signal amplification. RSC Adv 2(29):11029–11034

Chen C, Bang S, Cho Y, Lee S, Lee I, Zhang S, Noh I (2016) Research trends in biomimetic medical materials for tissue engineering: 3D bioprinting, surface modification, nano/micro-technology and clinical aspects in tissue engineering of cartilage and bone. Biomater Res 20(1):10

Chen F, Ni Y, Liu B, Zhou T, Yu C, Su Y, Zhu X, Yu X, Zhou Y (2017) Self-crosslinking and injectable hyaluronic acid/RGD-functionalized pectin hydrogel for cartilage tissue engineering. Carbohydr Polym 166:31–44

Chilkoti A, Christensen T, MacKay JA (2006) Stimulus responsive elastin biopolymers: applications in medicine and biotechnology. Curr Opin Chem Biol 10 (6):652–657

Christensen K, Xu C, Chai W, Zhang Z, Fu J, Huang Y (2015) Freeform inkjet printing of cellular structures with bifurcations. Biotechnol Bioeng 112 (5):1047–1055

Chung L, Maestas DR Jr, Housseau F, Elisseeff JH (2017) Key players in the immune response to biomaterial scaffolds for regenerative medicine. Adv Drug Deliv Rev 114:184–192

Cui H, Nowicki M, Fisher JP, Zhang LG (2017) 3D bioprinting for organ regeneration. Adv Healthc Mater 6(1):1601118

Eggermont M, (2008) Biomimetics as problem-solving, creativity and innovation tool. CDEN/C 2E2. Winnipeg, University of Manitoba, Canada, 114:59–67

Entekhabi E, Nazarpak MH, Moztarzadeh F, Sadeghi A (2016) Design and manufacture of neural tissue engineering scaffolds using hyaluronic acid and polycaprolactone nanofibers with controlled porosity. Mater Sci Eng C 69:380–387

Erik D, Stephen M (2002) Bio-inspired materials chemistry. Adv Mater 14:1–14

Fan K, Cao C, Pan Y, Lu D, Yang D, Feng J, Song L, Liang M, Yan X (2012) Magnetoferritin nanoparticles for targeting and visualizing tumour tissues. Nat Nanotechnol 7(7):459

Fan M, Ma Y, Zhang Z, Mao J, Tan H, Hu X (2015) Biodegradable hyaluronic acid hydrogels to control release of dexamethasone through aqueous Diels–Alder chemistry for adipose tissue engineering. Mater Sci Eng C 56:311–317

Gao W (2015) The chemistry of graphene oxide. In: Graphene oxide. Springer, Cham, pp 61–95

Gardner AB, Lee SK, Woods EC, Acharya AP (2013) Biomaterials-based modulation of the immune system. Bio Med Res Int Article ID 732182, 2013:1–7

Geim AK, Novoselov KS (2007) The rise of graphene. Nat Mater 6(3):183

Gelain F, Horii A, Zhang S (2007) Designer self-assembling peptide scaffolds for 3-D tissue cell cultures and regenerative medicine. Macromol Biosci 7(5):544–551

Georgakilas V, Otyepka M, Bourlinos AB, Chandra V, Kim N, Kemp KC, Hobza P, Zboril R, Kim KS (2012) Functionalization of graphene: covalent and non-covalent approaches, derivatives and applications. Chem Rev 112(11):6156–6214

Groen N, Guvendiren M, Rabitz H, Welsh WJ, Kohn J, de Boer J (2016) Stepping into the omics era: opportunities and challenges for biomaterials science and engineering. Acta Biomater 34:133–142

Gu BK, Choi DJ, Park SJ, Kim MS, Kang CM, Kim CH (2016) 3-dimensional bioprinting for tissue engineering applications. Biomater Res 20(1):12. https://doi.org/10.1186/s40824-016-0058-2

Gudapati H, Dey M, Ozbolat I (2016) A comprehensive review on droplet-based bioprinting: past, present and future. Biomaterials 102:20–42

Guvendiren M, Molde J, Soares RM, Kohn J (2016) Designing biomaterials for 3D printing. ACS Biomater Sci Eng 2(10):1679–1693

Harrison PM, Arosio P (1996) The ferritins: molecular properties, iron storage function and cellular regulation. Biochim Biophys Acta 1275(3):161–203

Hatayama T, Nakada A, Nakamura H, Mariko W, Tsujimoto G, Nakamura T (2017) Regeneration of gingival tissue using in situ tissue engineering with collagen scaffold. Oral Surg, Oral Med, Oral Pathol, Oral Radiol 124(4):348–354

Helms B, Meijer EW (2006) Dendrimers at work. SCIENCE-NEW YORK THEN WASHINGTON 313 (5789):929

Hengstenberg A, Bloch A, Dietzel D, Schuhmann W (2001) Spatially resolved detection of neurotransmitter secretion from individual cells by means of scanning electrochemical microscopy. Angew Chem Int Ed 40:905–908

Highley CB, Rodell CB, Burdick JA (2015) Direct 3D printing of shear-thinning hydrogels into self-healing hydrogels. Adv Mater 27(34):5075–5079

Hoffman AS (2012) Hydrogels for biomedical applications. Adv Drug Deliv Rev 64:18–23

Hölzl K, Lin S, Tytgat L, Van Vlierberghe S, Gu L, Ovsianikov A (2016) Bioink properties before, during and after 3D bioprinting. Biofabrication 8(3):032002

Hong S, Sycks D, Chan HF, Lin S, Lopez GP, Guilak F, Leong KW, Zhao X (2015) 3D printing of highly stretchable and tough hydrogels into complex, cellularized structures. Adv Mater 27(27):4035–4040

Hornick JF, Rajan K (2015) Chapter 16: intellectual property in 3d printing and nanotechnology, 3D bioprinting and nanotechnology in tissue engineering. John F. Hornick. Published by Elsevier Inc.

Hou Y, Cai K, Li J, Chen X, Lai M, Hu Y, Luo Z, Ding X, Xu D (2013) Effects of titanium nanoparticles on adhesion, migration, proliferation, and differentiation of mesenchymal stem cells. Int J Nanomedicine 8:3619

Hsieh PC, MacGillivray C, Gannon J, Cruz FU, Lee RT (2006) Local controlled intramyocardial delivery of platelet-derived growth factor improves postinfarction ventricular function without pulmonary toxicity. Circulation 114(7):637–644

Hu SH, Chen YW, Hung WT, Chen IW, Chen SY (2012) Quantum-dot-tagged reduced graphene oxide nanocomposites for bright fluorescence bioimaging and Photothermal therapy monitored in situ. Adv Mater 24(13):1748–1754

Hu C, Liu Y, Yang Y, Cui J, Huang Z, Wang Y, Yang L, Wang H, Xiao Y, Rong J (2013) One-step preparation of nitrogen-doped graphene quantum dots from oxidized debris of graphene oxide. J Mater Chem B 1 (1):39–42

Huang X, Qi X, Boey F, Zhang H (2012) Graphene-based composites. Chem Soc Rev 41(2):666–686

Jakab K, Norotte C, Marga F, Murphy K, Vunjak-Novakovic G, Forgacs G (2010) Tissue engineering by self-assembly and bio-printing of living cells. Biofabrication 2(2):022001

Jang J, Kim TG, Kim BS, Kim SW, Kwon SM, Cho DW (2016) Tailoring mechanical properties of decellularized extracellular matrix bioink by vitamin B2-induced photo-crosslinking. Acta Biomater 33:88–95

Jang J, Park HJ, Kim SW, Kim H, Park JY, Na SJ, Kim HJ, Park MN, Choi SH, Park SH, Kim SW (2017) 3D printed complex tissue construct using stem cell-laden decellularized extracellular matrix bioinks for cardiac repair. Biomaterials 112:264–274

Jeong B, Akter R, Han OH, Rhee CK, Rahman MA (2013) Increased electrocatalyzed performance through dendrimer-encapsulated gold nanoparticles and carbon nanotube-assisted multiple bienzymatic labels: highly sensitive electrochemical immunosensor for protein detection. Anal Chem 85(3):1784–1791

Ji S, Guvendiren M (2017) Recent advances in bioink design for 3D bioprinting of tissues and organs. Front Bioeng Biotechnol 5:23

Julian FVV, Olga AB, Nikolaj RB, Adrian B, Anja KP (2006) Biomimetics: its practice and theory. J R Soc Interface 3:471–482

Jung CS, Kim BK, Lee J, Min BH, Park SH (2017) Development of printable natural cartilage matrix bioink for 3D printing of irregular tissue shape. Tissue Eng Regen Med 15:1–8. https://doi.org/10.1007/s13770-017-0104-8

Kang X, Wang J, Wu H, Aksay IA, Liu J, Lin Y (2009) Glucose oxidase–graphene–chitosan modified electrode for direct electrochemistry and glucose sensing. Biosens Bioelectron 25(4):901–905

Kersey FR, Merkel TJ, Perry JL, Napier ME, DeSimone JM (2012) Effect of aspect ratio and deformability on nanoparticle extravasation through nanopores. Langmuir 28(23):8773–8781

Kim JE, Kim SH, Jung Y (2016) Current status of three-dimensional printing inks for soft tissue regeneration. Tissue Eng Regen Med 13(6):636–646

Kolos E, Ruys AJ (2013) Biomimetic scaffold materials used in tissue engineering. J Biomim Biomater Tissue Eng 18:e101. https://doi.org/10.4172/1662-100X.1000e101

Kutlusoy T, Oktay B, Apohan NK, Süleymanoğlu M, Kuruca SE (2017) Chitosan-co-hyaluronic acid porous cryogels and their application in tissue engineering. Int J Biol Macromol 103:366–378

Lee WC, Loh KP, Lim CT (2018) When stem cells meet graphene: opportunities and challenges in regenerative medicine. Biomaterials 155:236–250

Li M, Yang X, Ren J, Qu K, Qu X (2012) Using graphene oxide high near-infrared absorbance for Photothermal treatment of Alzheimer's disease. Adv Mater 24 (13):1722–1728

Li N, Zhang Q, Gao S, Song Q, Huang R, Wang L, Liu L, Dai J, Tang M, Cheng G (2013) Three-dimensional graphene foam as a biocompatible and conductive scaffold for neural stem cells. Sci Rep 3:1604

Li C, Faulkner-Jones A, Dun AR, Jin J, Chen P, Xing Y, Yang Z, Li Z, Shu W, Liu D, Duncan RR (2015) Rapid formation of a supramolecular polypeptide–DNA hydrogel for in situ three-dimensional multilayer bioprinting. Angew Chem Int Ed 54(13):3957–3961

Liao S, Chan CK, Ramakrishna S (2008) Stem cells and biomimetic materials strategies for tissue engineering. Mater Sci Eng C 28(8):1189–1202

Lim KS, Schon BS, Mekhileri NV, Brown GC, Chia CM, Prabakar S, Hooper GJ, Woodfield TB (2016) New visible-light photoinitiating system for improved print fidelity in gelatin-based bioinks. ACS Biomater Sci Eng 2(10):1752–1762

Lin X, Xie J, Niu G, Zhang F, Gao H, Yang M, Quan Q, Aronova MA, Zhang G, Lee S, Leapman R (2011) Chimeric ferritin nanocages for multiple function loading and multimodal imaging. Nano Lett 11(2):814–819

Liu G, Lin Y (2007) Electrochemical quantification of single-nucleotide polymorphisms using nanoparticle probes. J Am Chem Soc 129(34):10394–10401

Liu JC, Heilshorn SC, Tirrell DA (2004) Comparative cell response to artificial extracellular matrix proteins containing the RGD and CS5 cell-binding domains. Biomacromolecules 5(2):497–504

Liu G, Wang J, Lea SA, Lin Y (2006a) Bioassay labels based on apoferritin nanovehicles. Chembiochem 7 (9):1315–1319

Liu G, Wu H, Wang J, Lin Y (2006b) Apoferritin-templated synthesis of metal phosphate nanoparticle labels for electrochemical immunoassay. Small 2 (10):1139–1143

Liu Z, Robinson JT, Sun X, Dai H (2008) PEGylated nanographene oxide for delivery of water-insoluble cancer drugs. J Am Chem Soc 130(33):10876–10877

Liu Y, Dong X, Chen P (2012) Biological and chemical sensors based on graphene materials. Chem Soc Rev 41(6):2283–2307

Loessner D, Meinert C, Kaemmerer E, Martine LC, Yue K, Levett PA, Klein TJ, Melchels FP, Khademhosseini A, Hutmacher DW (2016) Functionalization, preparation and use of cell-laden gelatin methacryloyl–based hydrogels as modular tissue culture platforms. Nat Protoc 11(4):727

Maeda M, Tani S, Sano A, Fujioka K (1999) Microstructure and release characteristics of the minipellet, a collagen-based drug delivery system for controlled release of protein drugs. J Control Release 62 (3):313–324

MaHam A, Tang Z, Wu H, Wang J, Lin Y (2009) Protein-based nanomedicine platforms for drug delivery. Small 5(15):1706–1721

Mazur A, Litt I, Shorr E (1950) Chemical properties of ferritin and their relation to its vasodepressor activity. J Biol Chem 187:473–484

Müller M, Becher J, Schnabelrauch M, Zenobi-Wong M (2015) Nanostructured Pluronic hydrogels as bioinks for 3D bioprinting. Biofabrication 7(3):035006

Murphy SV, Atala A (2014) 3D bioprinting of tissues and organs. Nat Biotechnol 32(8):773

Nagarajan R (2008) Nanoparticles: building blocks for nanotechnology, nanoparticles: synthesis, stabilization, passivation, and functionalization, chapter 1: ACS Symposium Series, 996:2–14. ISBN:9780841269699eISBN:9780841221390

Nakamura T, Konno K (1954) Studies on ferritin. J Biochem 41(4):499–502

Napier ME, JM DS (2007) Nanoparticle drug delivery platform. J Macromol Sci Part C: Polym Rev 47 (3):321–327

Nassar W, El-Ansary M, Sabry D, Mostafa MA, Fayad T, Kotb E, Temraz M, Saad AN, Essa W, Adel H (2017) Erratum to: umbilical cord mesenchymal stem cells derived extracellular vesicles can safely ameliorate the progression of chronic kidney diseases. Biomater Res 21(1):3

Nayak TR, Andersen H, Makam VS, Khaw C, Bae S, Xu X, Ee PL, Ahn JH, Hong BH, Pastorin G, Ozyilmaz B (2011) Graphene for controlled and accelerated osteogenic differentiation of human mesenchymal stem cells. ACS Nano 5(6):4670–4678

Nguyen DG, Funk J, Robbins JB, Crogan-Grundy C, Presnell SC, Singer T, Roth AB (2016) Bioprinted 3D primary liver tissues allow assessment of organ-level response to clinical drug induced toxicity *in vitro*. PLoS One 11(7):e0158674

Oh JK, Drumright R, Siegwart DJ, Matyjaszewski K (2008) The development of microgels/nanogels for drug delivery applications. Pro Polym Sci 33(4):448–477

Ouyang L, Highley CB, Rodell CB, Sun W, Burdick JA (2016) 3D printing of shear-thinning hyaluronic acid hydrogels with secondary cross-linking. ACS Biomater Sci Eng 2(10):1743–1751

Ozbolat IT, Moncal KK, Gudapati H (2017) Evaluation of bioprinter technologies. Addit Manuf 13:179–200

Pan D, Zhang J, Li Z, Wu M (2010) Hydrothermal route for cutting graphene sheets into blue-luminescent graphene quantum dots. Adv Mater 22(6):734–738

Pan T, Song W, Cao X, Wang Y (2016) 3D bioplotting of gelatin/alginate scaffolds for tissue engineering: influence of crosslinking degree and pore architecture on physicochemical properties. J Mater Sci Technol 32 (9):889–900

Park S, Ruoff RS (2009) Chemical methods for the production of graphenes. Nat Nanotechnol 4(4):217

Park JH, Jang J, Lee JS, Cho DW (2016) Current advances in three-dimensional tissue/organ printing. Tissue Eng Regen Med 13(6):612–621

Pati F, Jang J, Ha DH, Kim SW, Rhie JW, Shim JH, Kim DH, Cho DW (2014) Printing three-dimensional tissue analogues with decellularized extracellular matrix bioink. Nat Commun 5:3935

Patterson J, Martino MM, Hubbell JA (2010) Biomimetic materials in tissue engineering. Mater Today 13 (1–2):14–22

Peng J, Gao W, Gupta BK, Liu Z, Romero-Aburto R, Ge L, Song L, Alemany LB, Zhan X, Gao G, Vithayathil SA (2012) Graphene quantum dots derived from carbon fibers. Nano Lett 12(2):844–849

Pittenger MF, Mackay AM, Beck SC, Jaiswal RK, Douglas R, Mosca JD, Moorman MA, Simonetti DW, Craig S, Marshak DR (1999) Multilineage potential of adult human mesenchymal stem cells. Science 284(5411):143–147

Ramón-Azcón J, Ahadian S, Estili M, Liang X, Ostrovidov S, Kaji H, Shiku H, Ramalingam M, Nakajima K, Sakka Y, Khademhosseini A (2013) Dielectrophoretically aligned carbon nanotubes to control electrical and mechanical properties of hydrogels to fabricate contractile muscle myofibers. Adv Mater 25(29):4028–4034

Raphael B, Khalil T, Workman VL, Smith A, Brown CP, Streuli C, Saiani A, Domingos M (2017) 3D cell bioprinting of self-assembling peptide-based hydrogels. Mater Lett 190:103–106

Rashid ST, Alexander GJ (2013) Induced pluripotent stem cells: from Nobel prizes to clinical applications. J Hepatol 58(3):625–629

Ribeiro M, de Moraes MA, Beppu MM, Garcia MP, Fernandes MH, Monteiro FJ, Ferraz MP (2015) Development of silk fibroin/nanohydroxyapatite composite hydrogels for bone tissue engineering. Eur Polym J 67:66–77

Rolland JP, Maynor BW, Euliss LE, Exner AE, Denison GM, DeSimone JM (2005) Direct fabrication and harvesting of monodisperse, shape-specific nanobiomaterials. J Am Chem Soc 127 (28):10096–10100

Schneider A, Garlick JA, Egles C (2008) Self-assembling peptide nanofiber scaffolds accelerate wound healing. PLoS One 3(1):e1410

Scuderi P, Lam K, Ryan K, Petersen E, Sterling K, Finley P, Ray CG, Slymen D, Salmon S (1986 Dec 13) Raised serum levels of tumour necrosis factor in parasitic infections. Lancet 328(8520):1364–1365

Segers VF, Tokunou T, Higgins LJ, MacGillivray C, Gannon J, Lee RT (2007) Local delivery of protease-resistant stromal cell derived factor-1 for stem cell recruitment after myocardial infarction. Circulation 116(15):1683–1692

Shafiee A, Atala A (2016) Printing technologies for medical applications. Trends Mol Med 22(3):254–265

Shan C, Yang H, Song J, Han D, Ivaska A, Niu L (2009) Direct electrochemistry of glucose oxidase and biosensing for glucose based on graphene. Anal Chem 81(6):2378–2382

Shao Y, Zhang S, Engelhard MH, Li G, Shao G, Wang Y, Liu J, Aksay IA, Lin Y (2010) Nitrogen-doped graphene and its electrochemical applications. J Mater Chem 20(35):7491–7496

Sharma AK, Gothwal A, Kesharwani P, Alsaab H, Iyer AK, Gupta U (2017) Dendrimer nanoarchitectures for cancer diagnosis and anticancer drug delivery. Drug Discov Today 22(2):314–326

Sheehy EJ, Cunniffe GM, O'Brien FJ (2018) Collagen-based biomaterials for tissue regeneration and repair. In: Peptides and proteins as biomaterials for tissue regeneration and repair. Woodhead Publishing, Duxford, pp 127–150

Shin SR, Bae H, Cha JM, Mun JY, Chen YC, Tekin H, Shin H, Farshchi S, Dokmeci MR, Tang S, Khademhosseini A (2011) Carbon nanotube reinforced hybrid microgels as scaffold materials for cell encapsulation. ACS Nano 6(1):362–372

Shin YC, Kim J, Kim SE, Song SJ, Hong SW, Oh JW, Lee J, Park JC, Hyon SH, Han DW (2017) RGD peptide and graphene oxide co-functionalized PLGA nanofiber scaffolds for vascular tissue engineering. Regen biomater 4(3):159–166

Silva GA, Czeisler C, Niece KL, Beniash E, Harrington DA, Kessler JA, Stupp SI (2004) Selective differentiation of neural progenitor cells by high-epitope density nanofibers. Science 303(5662):1352–1355

Soni KS, Desale SS, Bronich TK (2016) Nanogels: an overview of properties, biomedical applications and obstacles to clinical translation. J Control Release 240:109–126

Suci PA, Kang S, Young M, Douglas T (2009) A streptavidin-protein cage janus particle for polarized targeting and modular functionalization. J Am Chem Soc 131:9164–9165

Sun X, Liu Z, Welsher K, Robinson JT, Goodwin A, Zaric S, Dai H (2008) Nano-graphene oxide for cellular imaging and drug delivery. Nano Res 1(3):203–212

Takahashi K, Yamanaka S (2006) Induction of pluripotent stem cells from mouse embryonic and adult fibroblast cultures by defined factors. Cell 126(4):663–676

Tan YJ, Tan X, Yeong WY, Tor SB (2016) Hybrid microscaffold-based 3D bioprinting of multi-cellular constructs with high compressive strength: a new biofabrication strategy. Sci Rep 6:39140

Tang Z, Wu H, Zhang Y, Li Z, Lin Y (2011) Enzyme-mimic activity of ferric nano-core residing in ferritin and its biosensing applications. Anal Chem 83 (22):8611–8616

Tetsuka H, Asahi R, Nagoya A, Okamoto K, Tajima I, Ohta R, Okamoto A (2012) Optically tunable amino-functionalized graphene quantum dots. Adv Mater 24 (39):5333–5338

Tomalia DA, Naylor AM, Goddard WA (1990) Starburst dendrimers: molecular-level control of size, shape, surface chemistry, topology, and flexibility from atoms to macroscopic matter. Angew Chem Int Ed 29 (2):138–175

Toole BP (2004) Hyaluronan: from extracellular glue to pericellular cue. Nat Rev Cancer 4(7):528

Turyanska L, Bradshaw TD, Sharpe J, Li M, Mann S, Thomas NR, Patane A (2009) The biocompatibility of Apoferritin-encapsulated PbS quantum dots. Small 5(15):1738–1741

Uchida M, Klem MT, Allen M, Suci P, Flenniken M, Gillitzer E, Varpness Z, Liepold LO, Young M, Douglas T (2007) Biological containers: protein cages as multifunctional Nanoplatforms. Adv Mater 19:1025–1042

Vunjak-Novakovic G, Scadden DT (2011) Biomimetic platforms for human stem cell research. Cell Stem Cell 8(3):252–261

Walimbe T, Panitch A, Sivasankar PM (2017) A review of hyaluronic acid and hyaluronic acid-based hydrogels

for vocal fold tissue engineering. J Voice 31 (4):416–423
Wang Y, Li Y, Tang L, Lu J, Li J (2009) Application of graphene-modified electrode for selective detection of dopamine. Electrochem Commun 11(4):889–892
Wang Y, Li Z, Hu D, Lin CT, Li J, Lin Y (2010a) Aptamer/graphene oxide nanocomplex for in situ molecular probing in living cells. J Am Chem Soc 132(27):9274–9276
Wang Y, Shao Y, Matson DW, Li J, Lin Y (2010b) Nitrogen-doped graphene and its application in electrochemical biosensing. ACS Nano 4(4):1790–1798
Wang C, Liu N, Allen R, Tok JB, Wu Y, Zhang F, Chen Y, Bao Z (2013a) A rapid and efficient self-healing Thermo-reversible elastomer crosslinked with graphene oxide. Adv Mater 25(40):5785–5790
Wang X, Cai X, Hu J, Shao N, Wang F, Zhang Q, Xiao J, Cheng Y (2013b) Glutathione-triggered "off–on" release of anticancer drugs from dendrimer-encapsulated gold nanoparticles. J Am Chem Soc 135 (26):9805–9810
Wang X, Zhang Y, Li T, Tian W, Zhang Q, Cheng Y (2013c) Generation 9 polyamidoamine dendrimer encapsulated platinum nanoparticle mimics catalase size, shape, and catalytic activity. Langmuir 29 (17):5262–5270
Wang Y, Li Z, Weber TJ, Hu D, Lin CT, Li J, Lin Y (2013d) In situ live cell sensing of multiple nucleotides exploiting DNA/RNA aptamers and graphene oxide nanosheets. Anal Chem 85(14):6775–6782
Weiss NO, Zhou H, Liao L, Liu Y, Jiang S, Huang Y, Duan X (2012) Graphene: an emerging electronic material. Adv Mater 224(43):5782–5825
Wu P, Qian Y, Du P, Zhang H, Cai C (2012) Facile synthesis of nitrogen-doped graphene for measuring the releasing process of hydrogen peroxide from living cells. J Mater Chem 22(13):6402–6412
Wüst S, Müller R, Hofmann S (2015) 3D bioprinting of complex channels—effects of material, orientation, geometry, and cell embedding. J Biomed Mater Res A 103(8):2558–2570
Xie X, Zhou Y, Bi H, Yin K, Wan S, Sun L (2013) Large-range control of the microstructures and properties of three-dimensional porous graphene. Sci Rep 3:2117
Yang K, Hu L, Ma X, Ye S, Cheng L, Shi X, Li C, Li Y, Liu Z (2012) Multimodal imaging guided photothermal therapy using functionalized graphene nanosheets anchored with magnetic nanoparticles. Adv Mater 24(14):1868–1872
Yang K, Feng L, Shi X, Liu Z (2013a) Nano-graphene in biomedicine: theranostic applications. Chem Soc Rev 42(2):530–547
Yang Y, Asiri AM, Tang Z, Du D, Lin Y (2013b) Graphene based materials for biomedical applications. Mater Today 16(10):365–373
Zhang S, Holmes TC, DiPersio CM, Hynes RO, Su X, Rich A (1995) Self-complementary oligopeptide matrices support mammalian cell attachment. Biomaterials 16(18):1385–1393
Zhang L, Xia J, Zhao Q, Liu L, Zhang Z (2010) Functional graphene oxide as a nanocarrier for controlled loading and targeted delivery of mixed anticancer drugs. Small 6(4):537–544
Zhang L, Lu Z, Zhao Q, Huang J, Shen H, Zhang Z (2011a) Enhanced chemotherapy efficacy by sequential delivery of siRNA and anticancer drugs using PEI-grafted graphene oxide. Small 7(4):460–464
Zhang W, Guo Z, Huang D, Liu Z, Guo X, Zhong H (2011b) Synergistic effect of chemo-photothermal therapy using PEGylated graphene oxide. Biomaterials 32(33):8555–8561
Zhang Y, Tang Z, Wang J, Wu H, Lin CT, Lin Y (2011c) Apoferritin nanoparticle: a novel and biocompatible carrier for enzyme immobilization with enhanced activity and stability. J Mater Chem 21 (43):17468–17475
Zhang M, Bai L, Shang W, Xie W, Ma H, Fu Y, Fang D, Sun H, Fan L, Han M, Liu C (2012) Facile synthesis of water-soluble, highly fluorescent graphene quantum dots as a robust biological label for stem cells. J Mater Chem 22(15):7461–7467
Zhang H, Zhai Y, Wang J, Zhai G (2016) New progress and prospects: the application of nanogel in drug delivery. Mater Sci Eng C 60:560–568
Zhen Z, Tang W, Chen H, Lin X, Todd T, Wang G, Cowger T, Chen X, Xie J (2013) RGD-modified apoferritin nanoparticles for efficient drug delivery to tumors. ACS Nano 7(6):4830–4837
Zhou M, Zhai Y, Dong S (2009) Electrochemical sensing and biosensing platform based on chemically reduced graphene oxide. Anal Chem 81(14):5603–5613
Zhu J, Tang C, Kottke-Marchant K, Marchant RE (2009) Design and synthesis of biomimetic hydrogel scaffolds with controlled organization of cyclic RGD peptides. Bioconjug Chem 20(2):333–339
Zhu Y, Murali S, Cai W, Li X, Suk JW, Potts JR, Ruoff RS (2010) Graphene and graphene oxide: synthesis, properties, and applications. Adv Mater 22 (35):3906–3924
Zhu S, Zhang J, Qiao C, Tang S, Li Y, Yuan W, Li B, Tian L, Liu F, Hu R, Gao H (2011) Strongly green-photoluminescent graphene quantum dots for bioimaging applications. Chem comm 47 (24):6858–6860

Part II

Nanomaterials as an Emerging Biomimetic Materials

Protein Cage Nanoparticles as Delivery Nanoplatforms

2

Bongseo Choi, Hansol Kim, Hyukjun Choi, and Sebyung Kang

2.1 Introduction

Along with the innovative development of nanotechnology, a wide range of nanoscale delivery vehicles, including liposomes, micelles, inorganic and polymeric nanoparticles, and protein cage nanoparticles, has been developed to effectively deliver therapeutic and/or diagnostic reagents to the target sites (Allen and Cullis 2013; Brigger et al. 2002; Lee et al. 2016; Rösler et al. 2001; Wang et al. 2012). The nanoscale and modifiable surface of delivery nanoplatforms generally result in efficient passive delivery of cargo molecules mainly relying on enhanced permeability and retention (EPR) effects of nanoparticles in tumor tissues (Brigger et al. 2002). EPR effects of delivery nanoplatforms frequently allow a long circulation time in the bloodstream and deep penetration of delivered cargoes, such as therapeutic and/or diagnostic reagents. For the localized treatment of diseases, minimizing side-effects, and target-specific diagnosis of symptoms in early stage, the active targeted delivery of diagnostic or/and therapeutic reagents to desired sites using nanoparticles has been widely attempted.

Among various delivery nanoplatforms, protein cage nanoparticles are considered to be excellent candidates for multifunctional delivery nanoplatforms due to their well-defined architectures and high biocompatibility (Lee et al. 2016; Maham et al. 2009). A variety of protein cage nanoparticles, such as ferritin, lumazine synthase, encapsulin, and virus-like particles, have been extensively studied and their atomic resolution crystal structures have been solved allowing us to easily manipulate them genetically and chemically (Fig. 2.1). Protein cage nanoparticles have three distinct interfaces: interior and exterior surfaces as well as the interfaces between subunits. These versatile interfaces allow them to be utilized as delivery nanoplatforms for diverse applications (Douglas and Young 2006; Uchida et al. 2010). The defined interior spaces and/or surfaces of protein cage nanoparticles are used as rooms for synthesizing size-constraint biomimetic nanomaterials or for encapsulating diagnostic and/or therapeutic reagents (Bode et al. 2011; Flenniken et al. 2009; Kang and Douglas 2010; Lee et al. 2016). The exterior surfaces of protein cage nanoparticles provide the sites for presenting various types of molecules including affinity tags, antibodies, fluorophores, carbohydrates, nucleic acids, and targeting peptides (Kang et al. 2012, 2014; Kim et al. 2016; Min et al. 2014a, b; Moon et al. 2013, 2014a, b). Chimeric protein cage nanoparticles having multifunctions can also be generated by modulating assembly of

B. Choi · H. Kim · H. Choi · S. Kang (✉)
Department of Biological Sciences, School of Life Sciences, Ulsan National Institute of Science and Technology (UNIST), Ulsan, South Korea
e-mail: sabsab7@unist.ac.kr

I. Noh (ed.), *Biomimetic Medical Materials*, Advances in Experimental Medicine and Biology 1064,
https://doi.org/10.1007/978-981-13-0445-3_2

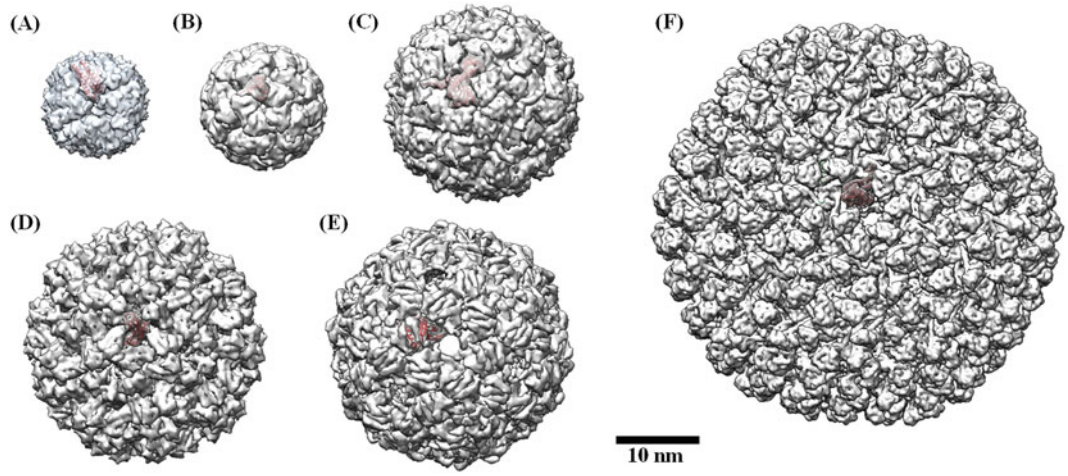

Fig. 2.1 Surface diagram representations of various types of protein cage nanoparticles. (**a**) Ferritin (PDB:2JD6) (**b**) Lumazine synthase (PDB:1HQK) (**c**) Encapsuline (PDB:3DKT) (**d**) CCMV (PDB:1CWP) (**e**) bacteriophage Qβ (PDB: 1qbe) (**f**) bacteriophage P22 procapsid (PDB:3IYI). One of subunits is represented as ribbon diagram in red. All the images are generated by using UCSF chimera

pre-functionalized subunits either in cells or *in vitro* (Kang et al. 2008a, b, 2009; Suci et al. 2010). The highly symmetric and uniform, but multivalent nature of protein cage nanoparticle makes them attractive as multifunctional delivery nanoplatforms. In this chapter, we will briefly discuss about recent development of protein cage nanoparticles as delivery nanoplatforms and their broad usages in biomedical fields.

2.2 Therapeutic and/or Diagnostic Agent Delivery Nanoplatforms

Nature provides a wide range of protein cage nanoparticles which have their own unique biochemical and biophysical properties, such as size, composition, stability and biological activity. The various types of protein cage nanoparticles having different origins and compositions have been used depending on their applications.

2.2.1 Small-Sized Protein Cage Nanoparticles: Ferritin, Lumazine Synthase, and Encapsulin

Ferritins are iron storage proteins found in almost all living organisms from bacteria to animals (Theil et al. 2013). Ferritins are composed of 24 subunits and self-assemble into highly symmetric 12 nm closed shells having 8 nm inner diameter cavity. Recently, RGD-modified ferritin was used to encapsulate doxorubicin (Dox) up to 73.49wt% by pre-complexing with Cu(II) and, similarly, cisplatin which are Pt-based drugs up to 50 molecules via metal-ferritin interaction and selectively delivered them to the target sites (Zhen et al. 2013). Non-covalent loading and unloading of hydrophobic drug-like molecules to ferritin was also demonstrated by chemically conjugating β-cyclodextrins (β-CDs) on the surface of ferritin which spontaneously capture hydrophobic drug molecules and reversibly release them (Kwon et al. 2012). For the targeted

delivery of ferritin, monosaccharides, mannoses or galactoses, were chemically attached to the surface of ferritin (Kang et al. 2014). Mannose- or galactose-displaying ferritins recognized and tightly bound to DC-SIGN or ASGP-R lectins on the surface of the mammalian cells, DCEK or HepG2 cells. Antibodies are ideal ligands for targeted delivery of various therapeutics and/or diagnostics because they have extremely high binding affinity and specificity for their target molecules and a variety of antibodies against virtually any desired targets can be readily obtained on demand. Thirteen residue Fc-binding peptides (FcBP) were genetically inserted onto the surface of ferritin to couple antibodies and ferritin without altering the targeting capability of displayed antibodies (Kang et al. 2012). FcBP-presenting ferritin formed stable non-covalent complexes with both IgGs derived from human and rabbit. Using a human anti-HER2 antibody and a rabbit anti-folate receptor antibody along with fluorescently labeled FcBP-ferritin, the specific binding of these complexes to breast cancer cells and folate receptor over-expressing cells were respectively demonstrated by fluorescent cell imaging (Kang et al. 2012).

Similar antibody-mediated targeted delivery nanoplatforms were also established with lumazine synthase. The lumazine synthase, isolated from hyperthermophile *Aquifex aeolicus* (AaLS), consists of 60 identical subunits assembled into icosahedral capsid architecture with an exterior diameter of 15 nm and an 8 nm interior cavity (Zhang et al. 2001). While AaLS is an enzyme that catalyzes the penultimate step in riboflavin biosynthesis inside the cell (Zhang et al. 2003), its hollow spherical architecture has been used as a template for the encapsulation of cargo proteins (Azuma et al. 2017; Beck et al. 2015; Frey et al. 2016; Seebeck et al. 2006; Wörsdörfer et al. 2011, 2012). Instead of Fc-binding peptides, antibody Fc-binding domain (ABD) from protein A was genetically fused to the C-termini of AaLS subunit and ABD-displaying AaLS (ABD-AaLS) were successfully produced without altering cage architecture and stability (Kim et al. 2016). It was demonstrated that ABD-AaLS effectively capture various types of antibodies derived from diverse species, such as human, rabbit, and mouse, on demand and the resulting complexes have the capability of selective recognition and binding to their target cells guided by antibodies displayed on the surface of ABD-AaLS (Kim et al. 2016). AaLS exhibits an unusual heat stability and genetic and chemical versatility. The AaLS templates acquired two different types of cell-specific targeting peptides, RGD4C and SP94 peptides, in two different positions individually and corresponding cargo molecules, either detecting molecules, NHS-fluorescein and fluorescein-5-maleimide, or therapeutic molecules, aldoxorubicin and bortezomib (BTZ), were chemically attached in combination without disrupting the overall cage architecture. RGD4C- and SP94-AaLS individually exhibited specific binding capability toward their target cells, KB and HepG2 cells respectively, and the enhanced cytotoxicity of delivered Dox and BTZ. (Min et al. 2014a, b)

Encapsulin, another heat stable protein cage nanoparticle isolated from thermophile *Thermotoga maritima*, is assembled from 60 copies of identical 31 kDa monomers having a thin and icosahedral symmetric cage structure with interior and exterior diameters of 20 and 24 nm, respectively (Giessen 2016; Sutter et al. 2008). Encapsulin has a large enough central cavity and tendency to encapsulate a large amount of therapeutic and/or diagnostic reagents. SP94-peptides were presented on the exterior surface of engineered encapsulin through either chemical conjugation or genetic insertion and SP94-encapsulin exhibited specific binding capability to hepatocellular carcinoma

cells, HepG2, and an ability to carry imaging probes or prodrug molecules (Moon et al. 2014a, b). In a similar approach, FcBP was introduced onto the surface loop region of encapsulin and FcBP-displaying encapsulin was demonstrated to selectively recognize and specifically bind to squamous cell carcinoma 7 (SCC-7) cells, which overexpress a cell surface glycoprotein CD44 involved in cell-cell interactions, cell adhesion and migration, over Hela, HepG2, MDA-MB-231 and KB cells (Moon et al. 2014a, b).

2.2.2 Large-Sized Protein Cage Nanoparticles: Virus-Like Particles (VLPs)

Virus-like particle (VLP) is one of the most widely used protein cage nanoparticles for biomedical applications (Ma et al. 2012). VLPs are generally derived from viral capsids, especially bacterial and plant viruses. Similar to the other protein cage nanoparticles, VLPs have a uniform size distribution and a symmetric and well-defined multivalent structure. The cowpea mosaic virus (CPMV) and the cowpea chlorotic mottle virus (CCMV) are plant viruses and self-assemble into an icosahedral symmetric cage structure having an overall outer diameter of 28 nm (Brumfield et al. 2004; Ochoa et al. 2006; Sutter et al. 2008). CPMV exhibits a natural affinity to bind to and penetrate mammalian cells and fluorescent dye-labeled CPMVs were used for intravital imaging of vascular development (Leong et al. 2010; Lewis et al. 2006). Covalent conjugation of anticancer drugs, Dox, to the CPMV was achieved and Dox-CPMV conjugates exhibited superior cytotoxic effect in Hela cells to that of free Dox (Aljabali et al. 2013). The light-absorbing molecules, zinc phthalocyanines (ZnPC), were loaded into CCMV VLPs using pH- and ionic-strength mediated structural changes and the ZnPC-loaded CCMV VLPs were used for photodynamic therapy. RAW 264.7 macrophages efficiently took up ZnPC-loaded CCMV VLPs and were effectively killed upon red light irradiation (Brasch et al. 2011).

In addition to plant viruses, bacterial viruses, bacteriophage MS2, Qβ, and P22, have been used widely in biomedical applications (Lee et al. 2016; Ma et al. 2012; Shukla and Steinmetz 2015). Bacteriophage MS2 (Peabody 2003) and Qβ (Brown et al. 2009) contain RNA molecules as their genomes and they are composed of 180 subunits to form closed icosahedral shells with an outer diameter of 28 nm similar to that of CPMV and CCMV. MS2 has been used for the delivery of nucleic acids, such as siRNA, miRNA, and antisense ssDNA, anticancer drugs including Dox and 5-fluorouracil, and ricin toxin (Ashley et al. 2011; Galaway and Stockley 2013; Pan et al. 2012a, b; Wu et al. 2005). For the photodynamic therapy, the interior surface of MS2 VLPs was chemically conjugated with 180 photodynamic agents, porphyrins, and the exterior was decorated with approximately 20 copies of a Jurkat-specific aptamer using an oxidative coupling reaction targeting an unnatural amino acid. The doubly modified MS2 VLPs selectively targeted the Jurkat cells and killed more than 76% of them upon 20 min illumination (Stephanopoulos et al. 2010). Similar approach using Qβ VLPs as alternative photodynamic agent carriers was reported (Rhee et al. 2012). Alkyne-derivatized Qβ VLPs were prepared by acylation of the wild-type Qβ VLPs with *N*-hydroxysuccinimide ester and subsequently the zinc tetraaryl porphyrins and glycan, Siaα2-6Galβ1-4GlcNAc, were attached by the copper-catalyzed azide-alkyne cycloaddition (CuAAC) reaction as photodynamic agents and a specific ligand for the B-cell CD22 receptor, respectively. It was shown that the doubly modified Qβ VLPs selectively bind to CD22 receptor bearing Chinese hamster ovary (CHO) cells and efficiently generate singlet oxygen upon full-spectrum xenon lamp irradiation showing dose-dependent phototoxicity (Rhee et al. 2012). Fullerenes (C60) were also used as an alternate photosensitizing moiety and their successful cellular uptake into HeLa cells was reported (Steinmetz et al. 2009).

P22 VLPs have approximately twice the outer diameter (~60 nm) of other VLPs that are commonly used (~28 nm) (Kang et al. 2008a, b). With the aid of approximately 300 copies of internal scaffolding proteins, four hundred and twenty copies of identical 46 kDa capsid subunits initially assemble into a 58-nm icosahedral procapsid structure which transforms into 64-nm mature capsid upon DNA packaging (Prevelige et al. 1988). Recently, P22 VLPs have been popularly used for encapsulation of a wide variety of proteins, including fluorescent proteins, influenza nucleoproteins, alcohol dehydrogenase D, and hydrogenase complexes by truncating scaffolding proteins and genetically fusing a cargo protein of interest to the N-terminus (Jordan et al. 2016; O'Neil et al. 2012; Patterson et al. 2012, 2013, 2014; Qazi et al. 2016; Schwarz and Douglas 2015; Sharma et al. 2017). P22 VLPs have genome-free hollow architectures, with sufficient space for accommodating small chemotherapeutic agents and/or diagnostic probes within their cavity. While catechol ligands were attached to the interior surface of the P22 WB VLPs through thiol-maleimide Michael-type addition with *N*-(3,4-dihydroxyphenethyl)-3-maleimidopropanamide, hepatocellular carcinoma (HCC) cell targeting SP94 peptides were chemically conjugated to the exterior surface of them (Min et al. 2014a, b). Anticancer drug, BTZ, formed a stable complex with catechol ligand within P22 VLPs at neutral and alkaline pH through the boric acid-diol complexation and became dissociated under cancerous acidic conditions to kill them. The doubly modified P22 VLPs encapsulated up to 280 molecules of BTZ per particle at pH 9.0 and release them completely within 12 h with a half-life of approximately 5 h at pH 5.5. They efficiently bound to and killed HepG2 hepatocellular carcinoma cells in a dose-dependent manner (Min et al. 2014a, b).

The blood brain barrier (BBB) is often an insurmountable obstacle for a large number of candidate drugs, including peptides, antibiotics, and chemotherapeutic agents. P22 VLPs were tailored to deliver analgesic ziconotide across a BBB model by genetically incorporating ziconotide into scaffolding protein in the interior cavity and chemically attaching cell penetrating HIV-Tat peptide on the exterior of the capsid (Anand et al. 2015). P22 VLPs containing ziconotide were successfully transported in several BBB models of rat and human brain microvascular endothelial cells (BMVEC) using a recyclable noncytotoxic endocytic pathway (Anand et al. 2015).

2.3 Vaccine Delivery Nanoplatforms

To date, vaccination is considered as the most effective way for control and prevention of infectious diseases. Most vaccines currently available are based on live attenuated or killed pathogens against their own original disease-causing pathogens (Berzofsky et al. 2001). However, they often cause severe side-effects at some frequency in population and there are limitations for developing vaccines for non-pathogen derived diseases, such as cancer, in these approaches. Although subunit vaccines that are derived from specific components of disease-causing pathogens or tissues have been developed to circumvent these drawbacks, they generally exhibited limited immunogenicity and longevity (Bachmann and Jennings 2010). In contrast, protein cage nanoparticles self-assemble and form highly symmetric morphology mimicking disease-causing viruses without infectious genetic materials. They are efficiently taken up by professional antigen presenting cells probably due to their nanometer-range size and surface patterns and lead to the efficient induction of strong humoral and cellular immune responses (Bachmann and Jennings 2010; Chackerian 2007; Grgacic and Anderson 2006; Kushnir et al. 2012; Plummer and Manchester 2011; Schwarz and Douglas 2015). Protein cage nanoparticles have been genetically, chemically, and/or post-translationally modified to be used as delivery nanoplatforms for exogenous antigenic molecules.

2.3.1 Chemical Conjugation of Antigenic Molecules to Protein Cage Nanoparticles

Qβ VLPs were investigated as potential delivery nanoplatforms for chemically conjugating self-antigens that induce neutralizing autoantibody responses (Jennings and Bachmann 2009; Maurer et al. 2005; Tissot et al. 2008). Fourteen different self-molecules were individually attached on the surface of Qβ VLPs and four out of them were selected and clinically tested (Jennings and Bachmann 2009). Clinical studies with AngQβ, which target angiotensin II, reported that three immunizations with 300 μg of AngQβ reduced blood pressure in patients with mild to moderate hypertension during the daytime and especially in the early morning (Tissot et al. 2008). Similarly, approximately 585 nicotine molecules were chemically attached to a Qβ VLP to form NicQβ and NicQβ induced strong antibody responses in preclinical studies (Maurer et al. 2005). Vaccinated mice with NicQβ significantly reduced nicotine levels in the brain compared with control group upon intravenous nicotine challenge. In a phase I study, 32 healthy non-smokers were immunized with NicQβ and all volunteers who received NicQβ showed nicotine-specific IgM antibodies at day 7 and nicotine-specific IgG antibodies at day 14 (Maurer et al. 2005).

Similarly, a model antigen, ovalbumin (OVA), was chemically conjugated to the exterior of a small heat shock protein (sHsp), which consists of 24 identical protein subunits forming a near spherical shell of 12 nm exterior and 6.5 nm interior diameter, and a single intranasal vaccination of mice with OVA-sHsp resulted in accelerated and intensified OVA-specific IgG1 responses within 5 days (Richert et al. 2012). It was also shown that pretreatment of mice with P22 VLPs further accelerated the onset of the antibody response to OVA-sHsp, demonstrating the utility of conjugating antigens to VLPs for pre-, or possibly post-exposure prophylaxis of lung, all without the need for adjuvant (Richert et al. 2012).

The effective generation of robust cytotoxic $CD8^+$ T cell immune responses is considered a primary goal in cancer immunotherapy because functional cytotoxic $CD8^+$ T cells not only kill their target cells directly but also secrete the cytokine IFN-γ. E2 protein cage nanoparticles were used as nanoplatforms for simultaneous delivery of $CD8^+$ T cell-specific OT-1 peptide (SIINFEKL) and adjuvant, CpG molecules, to dendritic cells (DCs). E2 is a non-viral protein cage nanoparticle composed of 60 identical subunits forming a hollow dodecahedral shell with 25 nm outer diameter. OT-1 peptides and CpGs were chemically conjugated to E2 and they were effectively delivered to DCs being displayed on MHC I threefold greater than the control. Co-delivery of OT-1 peptides and CpGs by E2 to DCs showed increased and prolonged cytotoxic $CD8^+$ T cell activation (Molino et al. 2013).

2.3.2 Genetic Insertion of Antigenic Molecules to Protein Cage Nanoparticles

In addition to chemical conjugation of antigenic molecules, genetic modifications have been widely used for VLP-based vaccine development. Bacteriophage MS2 VLP was used for displaying viral epitope and binding motif on its surface. Peptides from the V3 loop of HIV gp120 and the ECL2 loop of the HIV coreceptor, CCR5, were genetically inserted into the surface of MS2 VLPs and these genetically modified MS2 VLPs showed the potent immunogenicity (Peabody et al. 2008). The RNA bacteriophage AP205 was also investigated as a nanoplatform for heterologous display of many antigens. The AP205 VLP is composed of 180 copies of the capsid protein and both its N-terminus and C-terminus are tolerant to the fusion of long and complex epitopes. A fusion of a gonadotropin releasing hormone (GnRH) epitope to AP205 VLPs successfully induced antibodies and vaccination of mice with AP205 VLPs genetically fused with an extracellular domain of the Influenza A M2 protein resulted in 100% protection from lethal infection with influenza

virus (Tissot et al. 2010). The insect virus flock house virus (FHV) has been also widely used for antigen display and delivery in animals (Chen et al. 2006; Manayani et al. 2007; Scodeller et al. 1995). FHV also forms icosahedral capsid consisting of 180 copies of the capsid protein and has several surface exposed loops which are popular sites for inserting antigenic epitopes. Chimeric FHV VLPs that carry both Hepatitis C virus (HCV) and hepatitis B virus (HBV) epitopes simultaneously was constructed and they elicited anti-HCV and anti-HBV responses in guinea pig (Chen et al. 2006). The principal neutralizing domain, IGPGRAF sequence, from the V3 loop of HIV-1 was genetically inserted into the surface of FHV VLPs and these hybrid VLPs induced strong and broad specific immune response in guinea pigs against different V3 loop sequences (Scodeller et al. 1995). In addition to peptide epitopes, large antigens were displayed on the surface of FHV VLPs through genetic insertions. The 181 amino acid ANTXR2 VWA domain was inserted into a loop of capsid protein and displayed on the surface of modified FHV VLPs (Manayani et al. 2007). Vaccination with engineered FHV VLPs induced a potent immune response against lethal toxin and protected rats against lethal toxin challenge after a single administration without adjuvant (Manayani et al. 2007).

VLP is not the only one type of protein cage nanoparticles used for antigen display and delivery. The ectodomain of A/New Caledonia/20/1999 (1999 NC) haemagglutinin (HA) was genetically fused to the N-terminus of ferritin subunit to form HA-ferritin. HA-ferritin self-assembled and spontaneously generated eight trimeric viral spikes on its surface (Kanekiyo et al. 2013). Immunization with HA-ferritin elicited haemagglutination inhibition antibody titers more than tenfold higher than those from the licensed inactivated vaccine (Kanekiyo et al. 2013). Antibodies elicited by HA-ferritin neutralized H1N1 viruses from 1934 to 2007 protected ferrets from an unmatched 2007 H1N1 virus challenge (Kanekiyo et al. 2013). Further structure-based development of an H1 HA stem-only immunogen was carried out. H1 HA stabilized stem (H1-SS) without the immunodominant head domain was generated and genetically fused to ferritin to form H1-SS-ferritin. Vaccination with H1-SS-ferritin in mice and ferrets elicited broadly cross-reactive antibodies that completely protected mice and partially protected ferrets against lethal heterosubtypic H5N1 influenza virus challenge (Kanekiyo et al. 2013). AaLS and encapsulin were also used as delivery nanoplatforms to polyvalently display germline-targeting HIV-1 gp120 outer domain immunogens (eOD-GT6) and the receptor-binding portion of Epstein-Barr virus (EBV) gp350, respectively. eOD-GT6-AaLS successfully activated germline and mature VRC01-class B cells that produce broadly neutralizing antibodies (bNAbs) against HIV-1 (Jardine et al. 2013) and EBV gp350-encapsulin induced neutralizing antibody responses in mice and non-human primates that significantly exceeded the level obtained with soluble EBV gp350 protein (Kanekiyo et al. 2015).

Exterior surface is not the only place where protein cage nanoparticles can carry antigenic epitopes. A variety of antigenic peptides and proteins can be encapsulated into spacious interior cavity of protein cage nanoparticles and/or inserted into the protein sequences. The conserved nucleoprotein (NP) from influenza was genetically fused to SP and NP-encapsulated P22 VLPs were successfully generated (Patterson et al. 2013). Vaccination of mice with NP-encapsulated P22 VLPs resulted in multi-strain protection against 100 times lethal doses of influenza in an NP specific cytotoxic $CD8^+$ T cell-dependent manner (Patterson et al. 2013). Ferritin and AaLS were evaluated as efficient vaccine platforms for systematic studies of epitope-specific immune responses (Han et al. 2014; Ra et al. 2014). Antigenic peptides, OT-1 (SIINFEKL) or OT-2 (ISQAVHAAHAEINEAGR) which are derived from ovalbumin, were genetically introduced to various sites of ferritin and AaLS, effectively delivered to DCs, and processed within endosomes. Vaccination of naïve mice with antigenic peptide bearing

ferritin and AaLS induced an efficient differentiation of OT-1 specific $CD8^+$ T cells into functional effector cytotoxic T cells and an effective differentiation of proliferated OT-2 specific $CD4^+$ T cells into functional $CD4^+$ Th1 and Th2 cells which produces IFN-γ/IL-2 and IL-10/IL-13 cytokines, respectively (Han et al. 2014; Ra et al. 2014). As an extension of these studies for cancer vaccine development, antigenic OT-1 peptide was genetically incorporated into three different positions of the encapsulin subunit and their efficacies of inducing DC-mediated antigen-specific T cell cytotoxicity followed by B16-OVA tumor rejection were evaluated (Choi et al. 2016). Vaccination of mice with OT-1-Encap effectively activated OT-1 peptide specific cytotoxic $CD8^+$ T cells before or even after B16-OVA melanoma tumor generation and led to subsequent infiltration of OT-1-specific cytotoxic $CD8^+$ T cells into the tumor sites upon tumor challenges, providing tumor suppression (Choi et al. 2016).

2.3.3 Post-translational Addition of Antigenic Molecules to Protein Cage Nanoparticles

Genetic fusion of antigenic proteins to the viral capsid proteins may be the most commonly used approach to display antigenic proteins on VLPs. However, genetic fusion of two different proteins, antigenic proteins and viral capsid proteins, often leads to misfolding of antigenic proteins and/or impairing VLP assembly. To circumvent these issues, antigenic proteins and VLPs were individually expressed with extra glue domains and then covalently combined together post-translationally using recently developed SpyTag/SpyCatcher (ST/SC) protein ligation system (Moon et al. 2016; Zakeri et al. 2012). In the ST/SC protein ligation system, the 15 kDa SC protein recognizes the 13-amino acid ST (AHIVMVDAYKPTK) and they spontaneously form an irreversible isopeptide covalent bond. ST and SC can be genetically fused to antigenic proteins and VLPs, respectively or reciprocally, and they maintain their individual functions as well as stability of the fused proteins (Moon et al. 2016; Zakeri et al. 2012).

AP205 VLPs were genetically fused to SC (SC-AP205 VLPs) and subsequently ligased with ST-fused malaria antigens, including cysteine-rich Inter-Domain Region (CIDR) and *P. falciparum* sexual-stage antigen (Pfs25) (Brune et al. 2016). Covalent couplings between SC-AP205 VLPs and ST-fused malaria antigens were quantitatively achieved (Brune et al. 2016). Vaccination with SC-AP205 VLPs decorated with malarial antigens efficiently induced antibody responses after only a single immunization (Brune et al. 2016). ST-AP205 VLPs were also generated and used for ligating full-length 3d7 circumsporozoite protein (CSP) fused with SC or Pfs48/45 protein fused with SC (Janitzek et al. 2016). The CSP is an attractive target for malaria vaccine and the immunogenicity of CSP-AP205 VLPs was evaluated in mice (Janitzek et al. 2016). 112 CSP molecules were presented on the surface of an AP205 VLP (180 subunits) on average and mice vaccinated with CSP-AP205 VLPs generated 2.6 fold higher antibody titers over a course of 7 months than those of the control group (Janitzek et al. 2016). CSP-AP205 VLPs also induced production of IgG2a antibodies which are linked with a more efficient clearing of intracellular parasite infection (Janitzek et al. 2016). Genetic fusion of ST or SC to the N-terminus and/or C-terminus of AP205 VLPs produced stable, nonaggregated VLPs expressing one SC, one ST or two ST per capsid protein (Thrane et al. 2016). Eleven different vaccine antigens fused to SC or ST were attempted to be ligased to ST- or SC-AP205 VLPs and antigen-AP205 VLP conjugates were obtained with coupling efficiencies of ranging from 22% to 88% (Thrane et al. 2016). AP205 VLPs displaying Pfs25 or VAR2CSA drastically increased antibody titer, affinity, longevity and functional efficacy compared to corresponding monomeric protein vaccines. AP205 VLPs displaying cancer or allergy-associated self-

antigens, including PD-L1, CTLA-4 and IL-5, also effectively broke B cell self-tolerance eliciting potent and durable antibody responses upon vaccination (Thrane et al. 2016). As extension of these studies, the amount and efficacy of antibodies induced by three different nanoplatforms were evaluated side-by-side (Leneghan et al. 2017). *Plasmodium falciparum* malaria transmission blocking antigen Pfs25 was selected as a transmission blocking malaria vaccine (TBV) candidate and it was genetically fused to IMX313, which is a multimerization domain derived from the chicken complement inhibitor C4b-binding protein, chemically crosslinked onto the surface of Qβ VLPs, or conjugated through ST/SC ligation to SC-AP205 VLPs. While chemically-crosslinked Pfs25-Qβ VLPs elicited the highest quantity of anti-Pfs25 antibodies, Pfs25-AP205 VLPs elicited the highest quality anti-Pfs25 antibodies for transmission blocking upon mosquito feeding (Leneghan et al. 2017). It is anticipated that Pfs25 displayed on AP205 VLPs maintains its native conformation better than that of Qβ VLPs producing more functionally relevant monoclonal antibodies (Leneghan et al. 2017).

2.4 MRI Contrasting Agent (CA) Delivery Nanoplatform

Magnetic resonance imaging (MRI) is one of most powerful *in vivo* imaging techniques that provide highly resolved anatomical and functional information without using harmful ionizing radiation. However, it is difficult to distinguish selected tissues of interest, such as diseased area, from background tissues because they generally produce similar signal intensities. To overcome this issue, contrast agents (CAs) are frequently used to increase the sensitivity of MR to tissues of interest (Caravan 2006). Both positive (T_1-weighted, brightening) and negative (T_2-weighted, darkening) contrast agents are being actively explored for *in vivo* applications. Paramagnetic gadolinium ion (Gd(III)) complexed with poly(aminocarboxylate) compound chelating agents, such as tetraazacyclododecane tetraacetic acid (DOTA) and diethylenetriamine pentaacetic acid (DTPA), is the most frequently used positive contrast agent for contrast enhancement by reducing spin-lattice relaxation times (Caravan 2006; Lauffer 1987) and ferromagnetic iron oxide nanoparticles is the most popularly used negative contrast agents for contrast enhancement by promoting T_2 shortening (Shukla and Steinmetz 2015). A variety of protein cage nanoparticles have been used as templating nanoplatforms for both positive and negative contrast agents.

2.4.1 Positive (T_1) Contrast Agents: Gd(III)-Chelating Agent/Protein Cage Nanoparticle Conjugates

Paramagnetic gadolinium ion (Gd(III)) enhances the image contrast with increased signal intensity from T_1-weighted image acquisition due to the greatly reduced spin-lattice relaxation times produced by the interaction between the proton and unpaired electron spins of Gd(III) (Caravan 2006; Lauffer 1987). However, the free form of Gd(III) is toxic and, therefore, should be complexed with chelating agents or sequestered by composites (Caravan 2006). Furthermore, covalent conjugation of Gd(III)-chelating agent complexes to macromolecules generally improves both the blood circulation time and relaxivity value for high resolution/contrast MR image acquisition (Anderson et al. 2006; Datta et al. 2008; Ferreira et al. 2012; Liepold et al. 2009). Our discussion will focus on covalent protein cage nanoparticle conjugates with Gd(III)-chelating agent complexes.

CCMV VLPs were used as a templating macromolecules to attach Gd(III)-DOTA and each particle contained 60 Gd(III)-DOTAs on average. The resulting Gd(III)-DOTA-CCMV conjugates exhibited ionic and particle T_1 relaxivities of 46 and 2806 $mM^{-1}s^{-1}$, respectively, at 60 MHz (Liepold et al. 2007). To increase the number of Gd(III) ions per particle and conjugate size, various VLPs and chemical methods were applied (Anderson et al. 2006; Datta et al. 2008; Garimella et al. 2011; Hooker

et al. 2007; Min et al. 2013; Pokorski et al. 2011; Prasuhn et al. 2007; Qazi et al. 2013). 360 and more than 500 Gd(III)-DTPAs were attached onto the P22 and MS2 VLPs and they generated enhanced T_1 relaxivities up to 20503 and 7200 $mM^{-1}s^{-1}$ per particle at 60 MHz, respectively (Anderson et al. 2006; Min et al. 2013). The potential use of Gd(III)-DTPA-P22 conjugates as *in vivo* MRI contrast agents was also demonstrated by imaging the blood vessels of a mouse including the carotid, mammary arteries, the jugular vein and, the superficial vessels of the head (Min et al. 2013). Another Gd(III)-chelating agent complex, Gd(III) hydroxypyridonate (Gd(III)-HOPO), was also polyvalently attached to MS2 VLPs obtaining 180 Gd(III) ions per nanoparticle and the resulting Gd(III)-HOPO-MS2 exhibited maximum ionic and particle T_1 relaxivities of 41 and 7416 $mM^{-1}s^{-1}$, respectively, at 60 MHz (Datta et al. 2008; Garimella et al. 2011; Hooker et al. 2007).

Polymerization chemistry along with VLPs allowed conjugation of remarkable amounts of Gd(III) ions to VLPs. The polymerization of oligo(ethylene glycol)-methacrylate (OEGMA) and its azido-functionalized analogue (OEGMA-N3) was directly grafted from the outer surface of Qβ VLPs by atom transfer radical polymerization (ATRP) and the resulting surface-grafted Qβ VLPs held 610 Gd(III) ions exhibiting maximum ionic and particle T_1 relaxivities of 11.6 and 7092 $mM^{-1}s^{-1}$, respectively, at 60 MHz (Pokorski et al. 2011). Approximately 1900 Gd(III) ions were loaded into P22 VLP cavity by using the branched polymerization of p-SCN-Bn-DTPA-Gd(III) and 2-azido-1-azidomethyl-ethylamine (DAA) via stepwise click reactions inside of P22 VLPs and they exhibited maximum ionic and particle T_1 relaxivities of 21.7 and 41300 $mM^{-1}s^{-1}$, respectively, at 28 MHz (Qazi et al. 2013). Similar polymerization approach was applied to non-VLP protein cage nanoparticle, sHsp. Gd(III)-DTPA containing branched polymers were grown inside of sHsp via stepwise click reactions and the resulting Gd(III)-DTPA-sHsp exhibited maximum ionic and particle T_1 relaxivities of 25 and 4200 $mM^{-1}s^{-1}$, respectively, at 31 MHz (Liepold et al. 2009).

In both preclinical and clinical settings, a demand for MRI contrast agents with improved relaxivity at higher magnetic fields (>300 MHz or 7 T) is being hugely increased. The T_1 enhancement ability tends to decrease significantly (more than tenfold) as the magnetic field is increased and often causes a major problem in *in vivo* MRI at high field. AaLS was polyvalently decorated with Gd(III)-DOTA to evaluate its potential as an *in vivo* MR CA at the high magnetic field strength of 7 T. Each AaLS was conjugated with 60 Gd(III)-DOTAs on its surface and the T_1 relaxivities of Gd(III)-DOTA-AaLS were 30.2 and 16.5 $mM^{-1}s^{-1}$ at 60 and 300 MHz, respectively, making it attractive as a T_1 contrast agent at high field (7 T) (Song et al. 2015). 3D MR angiography of mice demonstrated the feasibility of vasculature imaging within 2 h of intravenous injection of Gd(III)-DOTA-AaLS and a significant reduction of T_1 values in the tumor region at 7 h post-injection in the SCC-7 flank tumor model implied potential use of Gd(III)-DOTA-AaLS as an tumor-targeting MR CA at high magnetic field (Song et al. 2015).

2.4.2 Negative (T_2) Contrast Agents: Iron-Oxide Nanoparticle/ Protein Cage Nanoparticle Core-Shells

Ferritin is probably the best protein cage nanoparticle for preparation of ferrimagnetic iron oxide nanoparticles because it inherently sequestrates irons *in vivo* and converts and stores them as forms of iron oxide (Fe_2O_3) (Uchida et al. 2006). Recombinant human H chain ferritin (rHFn) was used as size-constrained nanoplatforms for ferromagnetic iron oxide nanoparticle synthesis and it generated a series of iron oxide nanoparticles with diameters ranging from 3.6 to 5.9 nm with increasing iron loading amounts from 1000 to 5000 iron ions per rHFn (Uchida et al. 2008). The iron oxide-mineralized rHFn exhibited comparable MR signals to known iron oxide-based MRI CAs, such as ferumoxtran-10, and they were readily taken up by macrophages *in vitro* and provided strong

T_2-weighted MR contrast (Uchida et al. 2008). The iron oxide-mineralized rHFn were also used to image vascular macrophages *in vivo* in murine carotid arteries through MRI (Terashima et al. 2011). The iron oxide-mineralized rHFn accumulated in vascular macrophages in mice atherosclerotic lesions without any additional macrophage targeting moieties allowing *in vivo* MR imaging of atherosclerosis (Terashima et al. 2011). Recently, the iron oxide-mineralized rHFn were demonstrated to be targeted to numerous types of cancer cell lines that express high transferrin receptor 1 (TfR1) levels (Fan et al. 2012). As a following study, the iron oxide-mineralized rHFn with the core size of 5.3 nm were prepared and exhibited extremely high relaxivity (T_2) of up to 224 $mM^{-1}s^{-1}$ (Cao et al. 2014). TfR1-positive MDA-MB-231 or U87 tumor-bearing mice were treated with the iron oxide-mineralized rHFn and tumor sites either in thigh or brain were successfully visualized with MRI (Cao et al. 2014). This study indicated that the iron oxide-mineralized rHFn can cross the endothelium, epithelium, and BBB layers (Cao et al. 2014). *In vivo* MRI of vascular inflammation and angiogenesis in experimental carotid disease and abdominal aortic aneurysm (AAA) were also performed with RGD peptide displaying rHFn which mineralized iron oxide nanoparticles within its cavity (RGD-HFn-Fe_3O_4) (Kitagawa et al. 2017). RGD-HFn-Fe_3O_4 was taken up more than HFn-Fe_3O_4 in both the ligated left carotid arteries and AAAs probably due to active targeting of cells and thus exhibited significantly enhanced MRI signals (Kitagawa et al. 2017).

VLPs have been also popularly used as templating nanoplaforms for negative MRI CAs. BMV VLPs derived from plant virus, brome mosaic virus, were disassembled and reassembled with pre-formed ferromagnetic iron oxide nanoparticles to generate core-shell hybrid composites comprising an iron oxide core and a BMV capsid protein shell (Huang et al. 2011). The resulting hybrid composites showed T_2 relaxivity of 376 $mM^{-1}s^{-1}$, which is 4- to 6-fold higher than commercially available contrast agents, and penetrated into tissue and transferred long-distance through the vasculature in *Nicotiana benthamiana* leaves (Huang et al. 2011). Similar core-shell formation approach using Rotavirus or Simian virus 40 (SV40) VLPs derived from mammalian viruses along with the ferromagnetic iron oxide nanoparticles was carried out and it was demonstrated that the resulting core-shell hybrid composites (Chen et al. 2012; Enomoto et al. 2013) were efficiently internalized by their target cells significantly improving cellular MRI sensitivity compared with commercially available surface passivated iron oxide nanoparticles (Chen et al. 2012).

2.5 Conclusion

Macromolecular composites, including synthetic polymers, dendrimers, liposomes, carbohydrates, and inorganic nanoparticles, have been extensively studied for development of versatile *in vivo* delivery nanoplatforms. Although protein cage nanoparticles are in the very early stages of development as *in vivo* delivery nanoplatforms for diagnostics and/or therapeutics, they are a promising class of macromolecular composites for development of *in vivo* delivery nanoplatforms because they have a high biocompatibility and well-defined monodisperse structure which are hardly achieved by other types of macromolecular composites. Protein cage nanoparticles also have the genetic and chemical plasticity that can be used to acquire diverse functions, such as cargo encapsulation, targeting ligand presentation, and functional molecule conjugation, by design depending on their purposes. Numerous studies discussed in this chapter present that various encapsulation strategies of cargo molecules in combination with diverse presentation strategies of targeting ligand molecules are applicable to many protein cage nanoparticles and protein cage nanoparticles are promising *in vivo* delivery nanoplatforms for diagnosis, prevention, and therapy of diseases. Although there are some clinical trials using protein cage nanoparticle-based delivery nanoplatforms undergone and planned, further through studies related to their fate within target cells, *in vivo* immune alteration caused by them, and their bio-distribution and

pharmacodynamics upon *in vivo* administration should be carried out before clinical applications can be considered.

References

Aljabali AAA, Shukla S, Lomonossoff GP, Steinmetz NF, Evans DJ (2013) CPMV-DOX delivers. Mol Pharm 10 (1):3–10. https://doi.org/10.1021/mp3002057

Allen TM, Cullis PR (2013) Liposomal drug delivery systems: from concept to clinical applications. Adv Drug Deliv Rev 65(1):36–48. https://doi.org/10.1016/j.addr.2012.09.037

Anand P, O'Neil A, Lin E, Douglas T, Holford M (2015) Tailored delivery of analgesic ziconotide across a blood brain barrier model using viral nanocontainers. Sci Rep 5:12497. https://doi.org/10.1038/srep12497

Anderson EA, Isaacman S, Peabody DS, Wang EY, Canary JW, Kirshenbaum K (2006) Viral nanoparticles Donning a paramagnetic coat: conjugation of MRI contrast agents to the MS2 capsid. Nano Lett 6 (6):1160–1164. https://doi.org/10.1021/nl060378g

Ashley CE, Carnes EC, Phillips GK, Durfee PN, Buley MD, Lino CA, Padilla DP, Phillips B, Carter MB, Willman CL, Brinker CJ, Caldeira JC, Chackerian B, Wharton W, Peabody DS (2011) Cell-specific delivery of diverse cargos by bacteriophage MS2 virus-like particles. ACS Nano 5(7):5729–5745. https://doi.org/10.1021/nn201397z

Azuma Y, Zschoche R, Hilvert D (2017) The C-terminal peptide of Aquifex aeolicus riboflavin synthase directs encapsulation of native and foreign guests by a cage-forming lumazine synthase. J Biol Chem 292 (25):10321–10327. https://doi.org/10.1074/jbc.C117.790311

Bachmann MF, Jennings GT (2010) Vaccine delivery: a matter of size, geometry, kinetics and molecular patterns. Nat Rev Immunol 10(11):787–796. https://doi.org/10.1038/nri2868

Beck T, Tetter S, Künzle M, Hilvert D (2015) Construction of Matryoshka-type structures from supercharged protein nanocages. Angew Chem Int Ed 54 (3):937–940. https://doi.org/10.1002/anie.201408677

Berzofsky JA, Ahlers JD, Belyakov IM (2001) Strategies for designing and optimizing new generation vaccines. Nat Rev Immunol 1(3):209–219. https://doi.org/10.1038/35105075

Bode SA, Minten IJ, Nolte RJM, Cornelissen JJLM (2011) Reactions inside nanoscale protein cages. Nanoscale 3 (6):2376–2389. https://doi.org/10.1039/C0NR01013H

Brasch M, de la Escosura A, Ma Y, Uetrecht C, Heck AJR, Torres T, Cornelissen JJLM (2011) Encapsulation of Phthalocyanine supramolecular stacks into virus-like particles. J Am Chem Soc 133(18):6878–6881. https://doi.org/10.1021/ja110752u

Brigger I, Dubernet C, Couvreur P (2002) Nanoparticles in cancer therapy and diagnosis. Adv Drug Deliv Rev 54 (5):631–651. https://doi.org/10.1016/S0169-409X(02)00044-3

Brown SD, Fiedler JD, Finn MG (2009) Assembly of hybrid bacteriophage Qβ virus-like particles. Biochemistry 48(47):11155–11157. https://doi.org/10.1021/bi901306p

Brumfield S, Willits D, Tang L, Johnson JE, Douglas T, Young M (2004) Heterologous expression of the modified coat protein of Cowpea chlorotic mottle bromovirus results in the assembly of protein cages with altered architectures and function. J Gen Virol 85(4):1049–1053. https://doi.org/10.1099/vir.0.19688-0

Brune KD, Leneghan DB, Brian IJ, Ishizuka AS, Bachmann MF, Draper SJ, Biswas S, Howarth M (2016) Plug-and-display: decoration of virus-like particles via isopeptide bonds for modular immunization. Sci Rep 6:19234. https://doi.org/10.1038/srep19234

Cao C, Wang X, Cai Y, Sun L, Tian L, Wu H, He X, Lei H, Liu W, Chen G, Zhu R, Pan Y (2014) Targeted in vivo imaging of microscopic tumors with Ferritin-based nanoprobes across biological barriers. Adv Mater 26(16):2566–2571. https://doi.org/10.1002/adma.201304544

Caravan P (2006) Strategies for increasing the sensitivity of gadolinium based MRI contrast agents. Chem Soc Rev 35(6):512–523. https://doi.org/10.1039/B510982P

Chackerian B (2007) Virus-like particles: flexible platforms for vaccine development. Expert Review of Vaccines 6(3):381–390. https://doi.org/10.1586/14760584.6.3.381

Chen Y, Xiong X, Liu X, Li J, Wen Y, Chen Y, Dai Q, Cao Z, Yu W (2006) Immunoreactivity of HCV/HBV epitopes displayed in an epitope-presenting system. Mol Immunol 43(5):436–442. https://doi.org/10.1016/j.molimm.2005.03.002

Chen W, Cao Y, Liu M, Zhao Q, Huang J, Zhang H, Deng Z, Dai J, Williams DF, Zhang Z (2012) Rotavirus capsid surface protein VP4-coated Fe3O4 nanoparticles as a theranostic platform for cellular imaging and drug delivery. Biomaterials 33 (31):7895–7902. https://doi.org/10.1016/j.biomaterials.2012.07.016

Choi B, Moon H, Hong SJ, Shin C, Do Y, Ryu S, Kang S (2016) Effective delivery of antigen–encapsulin nanoparticle fusions to dendritic cells leads to antigen-specific cytotoxic T cell activation and tumor rejection. ACS Nano 10(8):7339–7350. https://doi.org/10.1021/acsnano.5b08084

Datta A, Hooker JM, Botta M, Francis MB, Aime S, Raymond KN (2008) High relaxivity gadolinium hydroxypyridonate-viral capsid conjugates: nanosized

MRI contrast agents. J Am Chem Soc 130 (8):2546–2552. https://doi.org/10.1021/Ja0765363
Douglas T, Young M (2006) Viruses: making friends with Old Foes. Science 312(5775):873. https://doi.org/10.1126/science.1123223
Enomoto T, Kawano M, Fukuda H, Sawada W, Inoue T, Haw KC, Kita Y, Sakamoto S, Yamaguchi Y, Imai T, Hatakeyama M, Saito S, Sandhu A, Matsui M, Aoki I, Handa H (2013) Viral protein-coating of magnetic nanoparticles using simian virus 40 VP1. J Biotechnol 167(1):8–15. https://doi.org/10.1016/j.jbiotec.2013.06.005
Fan K, Cao C, Pan Y, Lu D, Yang D, Feng J, Song L, Liang M, Yan X (2012) Magnetoferritin nanoparticles for targeting and visualizing tumour tissues. Nat Nano 7(7):459–464. https://doi.org/10.1038/nnano.2012.90
Ferreira MF, Mousavi B, Ferreira PM, Martins CIO, Helm L, Martins JA, Geraldes CFGC (2012) Gold nanoparticles functionalised with stable, fast water exchanging Gd3+ chelates as high relaxivity contrast agents for MRI. Dalton Trans 41(18):5472–5475. https://doi.org/10.1039/c2dt30388d
Flenniken ML, Uchida M, Liepold LO, Kang S, Young MJ, Douglas T (2009) A library of protein cage architectures as nanomaterials. Curr Top Microbiol Immunol 327:71–93
Frey R, Hayashi T, Hilvert D (2016) Enzyme-mediated polymerization inside engineered protein cages. Chem Commun 52(68):10423–10426. https://doi.org/10.1039/C6CC05301G
Galaway FA, Stockley PG (2013) MS2 viruslike particles: a robust, semisynthetic targeted drug delivery platform. Mol Pharm 10(1):59–68. https://doi.org/10.1021/mp3003368
Garimella PD, Datta A, Romanini DW, Raymond KN, Francis MB (2011) Multivalent, high-relaxivity MRI contrast agents using rigid Cysteine-reactive Gadolinium complexes. J Am Chem Soc 133 (37):14704–14709. https://doi.org/10.1021/ja204516p
Giessen TW (2016) Encapsulins: microbial nanocompartments with applications in biomedicine, nanobiotechnology and materials science. Curr Opin Chem Biol 34:1–10. https://doi.org/10.1016/j.cbpa.2016.05.013
Grgacic EVL, Anderson DA (2006) Virus-like particles: passport to immune recognition. Methods 40 (1):60–65. https://doi.org/10.1016/j.ymeth.2006.07.018
Han J-A, Kang YJ, Shin C, Ra J-S, Shin H-H, Hong SY, Do Y, Kang S (2014) Ferritin protein cage nanoparticles as versatile antigen delivery nanoplatforms for dendritic cell (DC)-based vaccine development. Nanomedicine 10(3):561–569. https://doi.org/10.1016/j.nano.2013.11.003
Hooker JM, Datta A, Botta M, Raymond KN, Francis MB (2007) Magnetic resonance contrast agents from viral capsid shells: a comparison of exterior and Interior Cargo strategies. Nano Lett 7(8):2207–2210. https://doi.org/10.1021/nl070512c
Huang X, Stein BD, Cheng H, Malyutin A, Tsvetkova IB, Baxter DV, Remmes NB, Verchot J, Kao C, Bronstein LM, Dragnea B (2011) Magnetic virus-like nanoparticles in N. benthamiana Plants: a new paradigm for environmental and agronomic biotechnological research. ACS Nano 5(5):4037–4045. https://doi.org/10.1021/nn200629g
Janitzek CM, Matondo S, Thrane S, Nielsen MA, Kavishe R, Mwakalinga SB, Theander TG, Salanti A, Sander AF (2016) Bacterial superglue generates a full-length circumsporozoite protein virus-like particle vaccine capable of inducing high and durable antibody responses. Malar J 15:545. https://doi.org/10.1186/s12936-016-1574-1
Jardine J, Julien J-P, Menis S, Ota T, Kalyuzhniy O, McGuire A, Sok D, Huang P-S, MacPherson S, Jones M, Nieusma T, Mathison J, Baker D, Ward AB, Burton DR, Stamatatos L, Nemazee D, Wilson IA, Schief WR (2013) Rational HIV immunogen design to target specific germline B cell receptors. Science (New York, NY) 340(6133):711–716. https://doi.org/10.1126/science.1234150
Jennings GT, Bachmann MF (2009) Immunodrugs: therapeutic VLP-based vaccines for chronic diseases. Annu Rev Pharmacol Toxicol 49(1):303–326. https://doi.org/10.1146/annurev-pharmtox-061008-103129
Jordan PC, Patterson DP, Saboda KN, Edwards EJ, Miettinen HM, Basu G, Thielges MC, Douglas T (2016) Self-assembling biomolecular catalysts for hydrogen production. Nat Chem 8(2):179–185. https://doi.org/10.1038/nchem.2416
Kanekiyo M, Wei C-J, Yassine HM, McTamney PM, Boyington JC, Whittle JRR, Rao SS, Kong W-P, Wang L, Nabel GJ (2013) Self-assembling influenza nanoparticle vaccines elicit broadly neutralizing H1N1 antibodies. Nature 499(7456):102–106. https://doi.org/10.1038/nature12202
Kanekiyo M, Bu W, Joyce MG, Meng G, Whittle JRR, Baxa U, Yamamoto T, Narpala S, Todd J-P, Rao SS, McDermott AB, Koup RA, Rossmann MG, Mascola JR, Graham BS, Cohen JI, Nabel GJ (2015) Rational design of an Epstein-Barr Virus vaccine targeting the receptor-binding site. Cell 162(5):1090–1100. https://doi.org/10.1016/j.cell.2015.07.043
Kang S, Douglas T (2010) Some enzymes just need a space of their own. Science 327(5961):42–43. https://doi.org/10.1126/science.1184318
Kang S, Lander GC, Johnson JE, Prevelige PE (2008a) Development of bacteriophage P22 as a platform for molecular display: genetic and chemical modifications of the procapsid exterior surface. Chembiochem 9 (4):514–518. https://doi.org/10.1002/cbic.200700555
Kang S, Oltrogge LM, Broomell CC, Liepold LO, Prevelige PE, Young M, Douglas T (2008b) Controlled assembly of bifunctional chimeric protein cages and composition analysis using noncovalent Mass spectrometry. J Am Chem Soc 130 (49):16527–16529. https://doi.org/10.1021/ja807655t

Kang S, Suci PA, Broomell CC, Iwahori K, Kobayashi M, Yamashita I, Young M, Douglas T (2009) janus-like protein cages. Spatially controlled dual-functional surface modifications of protein cages. Nano Lett 9 (6):2360–2366. https://doi.org/10.1021/nl9009028

Kang HJ, Kang YJ, Lee Y-M, Shin H-H, Chung SJ, Kang S (2012) Developing an antibody-binding protein cage as a molecular recognition drug modular nanoplatform. Biomaterials 33:5423–5430. https://doi.org/10.1016/j.biomaterials.2012.03.055

Kang YJ, Yang HJ, Jeon S, Kang Y-S, Do Y, Hong SY, Kang S (2014) Polyvalent display of monosaccharides on Ferritin protein cage nanoparticles for the recognition and binding of cell-surface lectins. Macromol Biosci 14(5):619–625. https://doi.org/10.1002/mabi.201300528

Kim H, Kang YJ, Min J, Choi H, Kang S (2016) Development of an antibody-binding modular nanoplatform for antibody-guided targeted cell imaging and delivery. RSC Adv 6(23):19208–19213. https://doi.org/10.1039/C6RA00233A

Kitagawa T, Kosuge H, Uchida M, Iida Y, Dalman RL, Douglas T, McConnell MV (2017) RGD targeting of human ferritin iron oxide nanoparticles enhances in vivo MRI of vascular inflammation and angiogenesis in experimental carotid disease and abdominal aortic aneurysm. J Magn Reson Imaging 45 (4):1144–1153. https://doi.org/10.1002/jmri.25459

Kushnir N, Streatfield SJ, Yusibov V (2012) Virus-like particles as a highly efficient vaccine platform: diversity of targets and production systems and advances in clinical development. Vaccine 31(1):58–83. https://doi.org/10.1016/j.vaccine.2012.10.083

Kwon C, Kang YJ, Jeon S, Jung S, Hong SY, Kang S (2012) Development of protein-cage-based delivery Nanoplatforms by Polyvalently displaying β-Cyclodextrins on the surface of Ferritins through Copper(I)-catalyzed Azide/Alkyne cycloaddition. Macromol Biosci 12(11):1452–1458. https://doi.org/10.1002/mabi.201200178

Lauffer RB (1987) Paramagnetic metal complexes as water proton relaxation agents for NMR imaging: theory and design. Chem Rev 87(5):901–927. https://doi.org/10.1021/cr00081a003

Lee EJ, Lee NK, Kim I-S (2016) Bioengineered protein-based nanocage for drug delivery. Adv Drug Deliv Rev 106:157–171. https://doi.org/10.1016/j.addr.2016.03.002

Leneghan DB, Miura K, Taylor IJ, Li Y, Jin J, Brune KD, Bachmann MF, Howarth M, Long CA, Biswas S (2017) Nanoassembly routes stimulate conflicting antibody quantity and quality for transmission-blocking malaria vaccines. Sci Rep 7:3811. https://doi.org/10.1038/s41598-017-03798-3

Leong HS, Steinmetz NF, Ablack A, Destito G, Zijlstra A, Stuhlmann H, Manchester M, Lewis JD (2010) Intravital imaging of embryonic and tumor neovasculature using viral nanoparticles. Nat Protoc 5(8):1406–1417. https://doi.org/10.1038/nprot.2010.103

Lewis JD, Destito G, Zijlstra A, Gonzalez MJ, Quigley JP, Manchester M, Stuhlmann H (2006) Viral nanoparticles as tools for intravital vascular imaging. Nat Med 12(3):354–360. https://doi.org/10.1038/nm1368

Liepold L, Anderson S, Willits D, Oltrogge L, Frank JA, Douglas T, Young M (2007) Viral capsids as MRI contrast agents. Magn Reson Med 58(5):871–879. https://doi.org/10.1002/mrm.21307

Liepold LO, Abedin MJ, Buckhouse ED, Frank JA, Young MJ, Douglas T (2009) supramolecular protein cage composite MR contrast agents with extremely efficient relaxivity properties. Nano Lett 9(12):4520–4526. https://doi.org/10.1021/Nl902884p

Ma Y, Nolte RJM, Cornelissen JJLM (2012) Virus-based nanocarriers for drug delivery. Adv Drug Deliv Rev 64 (9):811–825. https://doi.org/10.1016/j.addr.2012.01.005

Maham A, Tang Z, Wu H, Wang J, Lin Y (2009) Protein-based nanomedicine platforms for drug delivery. Small 5(15):1706–1721. https://doi.org/10.1002/smll.200801602

Manayani DJ, Thomas D, Dryden KA, Reddy V, Siladi ME, Marlett JM, Rainey GJA, Pique ME, Scobie HM, Yeager M, Young JAT, Manchester M, Schneemann A (2007) A viral nanoparticle with dual function as an Anthrax Antitoxin and vaccine. PLoS Pathog 3(10): e142. https://doi.org/10.1371/journal.ppat.0030142

Maurer P, Jennings GT, Willers J, Rohner F, Lindman Y, Roubicek K, Renner WA, Müller P, Bachmann MF (2005) A therapeutic vaccine for nicotine dependence: preclinical efficacy, and phase I safety and immunogenicity. Eur J Immunol 35(7):2031–2040. https://doi.org/10.1002/eji.200526285

Min J, Jung H, Shin H-H, Cho G, Cho H, Kang S (2013) Implementation of P22 viral capsids as intravascular magnetic resonance T1 contrast Conjugates via site-selective attachment of Gd(III)-chelating agents. Biomacromolecules 14(7):2332–2339. https://doi.org/10.1021/bm400461j

Min J, Kim S, Lee J, Kang S (2014a) Lumazine synthase protein cage nanoparticles as modular delivery platforms for targeted drug delivery. RSC Adv 4 (89):48596–48600. https://doi.org/10.1039/C4RA10187A

Min J, Moon H, Yang HJ, Shin H-H, Hong SY, Kang S (2014b) Development of P22 viral capsid nanocomposites as anti-cancer drug, Bortezomib (BTZ), delivery nanoplatforms. Macromol Biosci 14 (4):557–564. https://doi.org/10.1002/mabi.201300401

Molino NM, Anderson AKL, Nelson EL, Wang S-W (2013) biomimetic protein nanoparticles facilitate enhanced dendritic cell activation and cross-presentation. ACS Nano 7(11):9743–9752. https://doi.org/10.1021/nn403085w

Moon H, Kim WG, Lim S, Kang YJ, Shin H-H, Ko H, Hong SY, Kang S (2013) Fabrication of uniform layer-by-layer assemblies with complementary protein cage nanobuilding blocks via simple His-tag/metal

recognition. J Mater Chem B 1(35):4504–4510. https://doi.org/10.1039/C3TB20554A

Moon H, Lee J, Kim H, Heo S, Min J, Kang S (2014a) Genetically engineering encapsulin protein cage nanoparticle as a SCC-7 Cell targeting optical nanoprobe. Biomaterials research 18:21. https://doi.org/10.1186/2055-7124-18-21

Moon H, Lee J, Min J, Kang S (2014b) Developing genetically engineered encapsulin protein cage nanoparticles as a targeted delivery nanoplatform. Biomacromolecules 15:3794–3801. https://doi.org/10.1021/bm501066m

Moon H, Bae Y, Kim H, Kang S (2016) Plug-and-playable fluorescent cell imaging modular toolkits using the bacterial superglue, SpyTag/SpyCatcher. Chem Commun 52(97):14051–14054. https://doi.org/10.1039/C6CC07363H

O'Neil A, Prevelige PE, Basu G, Douglas T (2012) coconfinement of fluorescent proteins: spatially enforced communication of GFP and mCherry encapsulated within the P22 capsid. Biomacromolecules 13(12):3902–3907. https://doi.org/10.1021/bm301347x

Ochoa WF, Chatterji A, Lin T, Johnson JE (2006) Generation and structural analysis of reactive empty particles derived from an icosahedral virus. Chem Biol 13 (7):771–778. https://doi.org/10.1016/j.chembiol.2006.05.014

Pan Y, Jia T, Zhang Y, Zhang K, Zhang R, Li J, Wang L (2012a) MS2 VLP-based delivery of microRNA-146a inhibits autoantibody production in lupus-prone mice. Int J Nanomedicine 7:5957–5967. https://doi.org/10.2147/IJN.S37990

Pan Y, Zhang Y, Jia T, Zhang K, Li J, Wang L (2012b) Development of a microRNA delivery system based on bacteriophage MS2 virus-like particles. FEBS J 279 (7):1198–1208. https://doi.org/10.1111/j.1742-4658.2012.08512.x

Patterson DP, Prevelige PE, Douglas T (2012) Nanoreactors by programmed enzyme encapsulation inside the capsid of the bacteriophage P22. ACS Nano 6(6):5000–5009. https://doi.org/10.1021/nn300545z

Patterson DP, Rynda-Apple A, Harmsen AL, Harmsen AG, Douglas T (2013) Biomimetic antigenic nanoparticles elicit controlled protective immune response to influenza. ACS Nano 7(4):3036–3044. https://doi.org/10.1021/nn4006544

Patterson DP, Schwarz B, Waters RS, Gedeon T, Douglas T (2014) Encapsulation of an enzyme cascade within the bacteriophage P22 virus-like particle. ACS Chem Biol 9(2):359–365. https://doi.org/10.1021/cb4006529

Peabody DS (2003) A viral platform for chemical modification and multivalent display. Journal of Nanobiotechnology 1 (1):5. https://doi.org/10.1186/1477-3155-1-5

Peabody DS, Manifold-Wheeler B, Medford A, Jordan SK, Caldeira JC, Chackerian B (2008) Immunogenic display of diverse peptides on virus-like particles of RNA phage MS2. J Mol Biol 380(1):252–263. https://doi.org/10.1016/j.jmb.2008.04.049

Plummer EM, Manchester M (2011) Viral nanoparticles and virus-like particles: platforms for contemporary vaccine design. Wiley Interdiscip Rev Nanomed Nanobiotechnol 3(2):174–196. https://doi.org/10.1002/wnan.119

Pokorski JK, Breitenkamp K, Finn MG (2011) Functional virus-based polymer-protein nanoparticles by atom transfer radical polymerization. J Am Chem Soc 133 (24):9242–9245. https://doi.org/10.1021/ja203286n

Prasuhn JDE, Yeh RM, Obenaus A, Manchester M, Finn MG (2007) Viral MRI contrast agents: coordination of Gd by native virions and attachment of Gd complexes by azide-alkyne cycloaddition. Chem Commun 12:1269–1271. https://doi.org/10.1039/B615084E

Prevelige PE, Thomas D, King J (1988) Scaffolding protein regulates the polymerization of P22 coat subunits into icosahedral shells in vitro. J Mol Biol 202 (4):743–757. https://doi.org/10.1016/0022-2836(88)90555-4

Qazi S, Liepold LO, Abedin MJ, Johnson B, Prevelige P, Frank JA, Douglas T (2013) P22 viral capsids as nanocomposite high-relaxivity MRI contrast agents. Mol Pharm 10(1):11–17. https://doi.org/10.1021/mp300208g

Qazi S, Miettinen HM, Wilkinson RA, McCoy K, Douglas T, Wiedenheft B (2016) Programmed self-assembly of an active P22-Cas9 nanocarrier system. Mol Pharm 13(3):1191–1196. https://doi.org/10.1021/acs.molpharmaceut.5b00822

Ra J-S, Shin H-H, Kang S, Do Y (2014) Lumazine synthase protein cage nanoparticles as antigen delivery nanoplatforms for dendritic cell-based vaccine development. Clin Exp Vaccine Res 3(2):227–234. https://doi.org/10.7774/cevr.2014.3.2.227

Rhee J-K, Baksh M, Nycholat C, Paulson JC, Kitagishi H, Finn MG (2012) Glycan-targeted virus-like nanoparticles for photodynamic therapy. Biomacromolecules 13(8):2333–2338. https://doi.org/10.1021/bm300578p

Richert LE, Servid AE, Harmsen AL, Rynda-Apple A, Han S, Wiley JA, Douglas T, Harmsen AG (2012) A virus-like particle vaccine platform elicits heightened and hastened local lung mucosal antibody production after a single dose. Vaccine 30(24):3653–3665. https://doi.org/10.1016/j.vaccine.2012.03.035

Rösler A, Vandermeulen GWM, Klok H-A (2001) Advanced drug delivery devices via self-assembly of amphiphilic block copolymers. Adv Drug Deliv Rev 53(1):95–108. https://doi.org/10.1016/S0169-409X(01)00222-8

Schwarz B, Douglas T (2015) Development of virus-like particles for diagnostic and prophylactic biomedical applications. Wiley Interdiscip Rev Nanomed Nanobiotechnol 7(5):722–735. https://doi.org/10.1002/wnan.1336

Scodeller EA, Tisminetzky SG, Porro F, Schiappacassi M, De Rossi A, Chiecco-Bianchi L, Baralle FE (1995) A new epitope presenting system displays a HIV-1 V3 loop sequence and induces neutralizing antibodies. Vaccine 13(13):1233–1239. https://doi.org/10.1016/0264-410X(95)00058-9

Seebeck FP, Woycechowsky KJ, Zhuang W, Rabe JP, Hilvert D (2006) A simple tagging system for protein encapsulation. J Am Chem Soc 128(14):4516–4517. https://doi.org/10.1021/ja058363s

Sharma J, Uchida M, Miettinen HM, Douglas T (2017) Modular interior loading and exterior decoration of a virus-like particle. Nano 9(29):10420–10430. https://doi.org/10.1039/C7NR03018E

Shukla S, Steinmetz NF (2015) Virus-based nanomaterials as PET and MR contrast agents: from technology development to translational medicine. Wiley Interdiscip Rev Nanomed Nanobiotechnol 7 (5):708–721. https://doi.org/10.1002/wnan.1335

Song Y, Kang YJ, Jung H, Kim H, Kang S, Cho H (2015) Lumazine synthase protein nanoparticle-Gd(III)-DOTA conjugate as a T1 contrast agent for high-field MRI. Sci Rep 5:15656. https://doi.org/10.1038/srep15656

Steinmetz NF, Hong V, Spoerke ED, Lu P, Breitenkamp K, Finn MG, Manchester M (2009) Buckyballs meet viral nanoparticles: candidates for biomedicine. J Am Chem Soc 131(47):17093–17095. https://doi.org/10.1021/ja902293w

Stephanopoulos N, Tong GJ, Hsiao SC, Francis MB (2010) Dual-surface modified virus capsids for targeted delivery of photodynamic agents to cancer cells. ACS Nano 4(10):6014–6020. https://doi.org/10.1021/nn1014769

Suci P, Kang S, Gmur R, Douglas T, Young M (2010) Targeted delivery of a photosensitizer to aggregatibacter actinomycetemcomitans biofilm. Antimicrob Agents Chemother 54(6):2489–2496. https://doi.org/10.1128/aac.00059-10

Sutter M, Boehringer D, Gutmann S, Gunther S, Prangishvili D, Loessner MJ, Stetter KO, Weber-Ban E, Ban N (2008) Structural basis of enzyme encapsulation into a bacterial nanocompartment. Nat Struct Mol Biol 15(9):939–947. https://doi.org/10.1038/nsmb.1473

Terashima M, Uchida M, Kosuge H, Tsao PS, Young MJ, Conolly SM, Douglas T, McConnell MV (2011) Human Ferritin cages for imaging vascular macrophages. Biomaterials 32(5):1430–1437. https://doi.org/10.1016/j.biomaterials.2010.09.029

Theil EC, Behera RK, Tosha T (2013) Ferritins for Chemistry and for life. Coord Chem Rev 257(2):579–586. https://doi.org/10.1016/j.ccr.2012.05.013

Thrane S, Janitzek CM, Matondo S, Resende M, Gustavsson T, de Jongh WA, Clemmensen S, Roeffen W, van de Vegte-Bolmer M, van Gemert GJ, Sauerwein R, Schiller JT, Nielsen MA, Theander TG, Salanti A, Sander AF (2016) Bacterial superglue enables easy development of efficient virus-like particle based vaccines. J Nanobiotechnol 14:30. https://doi.org/10.1186/s12951-016-0181-1

Tissot AC, Maurer P, Nussberger J, Sabat R, Pfister T, Ignatenko S, Volk H-D, Stocker H, Müller P, Jennings GT, Wagner F, Bachmann MF (2008) Effect of immunisation against angiotensin II with CYT006-AngQb on ambulatory blood pressure: a double-blind, randomised, placebo-controlled phase IIa study. Lancet 371(9615):821–827. https://doi.org/10.1016/S0140-6736(08)60381-5

Tissot AC, Renhofa R, Schmitz N, Cielens I, Meijerink E, Ose V, Jennings GT, Saudan P, Pumpens P, Bachmann MF (2010) Versatile virus-like particle carrier for epitope based vaccines. PLoS One 5(3):e9809. https://doi.org/10.1371/journal.pone.0009809

Uchida M, Flenniken ML, Allen M, Willits DA, Crowley BE, Brumfield S, Willis AF, Jackiw L, Jutila M, Young MJ, Douglas T (2006) Targeting of cancer cells with ferrimagnetic ferritin cage nanoparticles. J Am Chem Soc 128(51):16626–16633. https://doi.org/10.1021/ja0655690

Uchida M, Terashima M, Cunningham CH, Suzuki Y, Willits DA, Willis AF, Yang PC, Tsao PS, McConnell MV, Young MJ, Douglas T (2008) A human ferritin iron oxide nano-composite magnetic resonance contrast agent. Magn Reson Med 60(5):1073–1081. https://doi.org/10.1002/mrm.21761

Uchida M, Kang S, Reichhardt C, Harlen K, Douglas T (2010) The ferritin superfamily: supramolecular templates for materials synthesis. Biochim Biophys Acta Gen Subj 1800:834–845. https://doi.org/10.1016/j.bbagen.2009.12.005

Wang AZ, Langer R, Farokhzad OC (2012) Nanoparticle delivery of cancer drugs. Annu Rev Med 63 (1):185–198. https://doi.org/10.1146/annurev-med-040210-162544

Wörsdörfer B, Woycechowsky KJ, Hilvert D (2011) Directed evolution of a protein container. Science 331 (6017):589–592. https://doi.org/10.1126/science.1199081

Wörsdörfer B, Pianowski Z, Hilvert D (2012) Efficient in vitro encapsulation of protein cargo by an engineered protein container. J Am Chem Soc 134 (2):909–911. https://doi.org/10.1021/ja211011k

Wu M, Sherwin T, Brown WL, Stockley PG (2005) Delivery of antisense oligonucleotides to leukemia cells by RNA bacteriophage capsids. Nanomedicine 1 (1):67–76. https://doi.org/10.1016/j.nano.2004.11.011

Zakeri B, Fierer JO, Celik E, Chittock EC, Schwarz-Linek-U, Moy VT, Howarth M (2012) Peptide tag forming a rapid covalent bond to a protein, through engineering a bacterial adhesin. Proc Natl Acad Sci U S A 109(12): E690–E697. https://doi.org/10.1073/pnas.1115485109

Zhang X, Meining W, Fischer M, Bacher A, Ladenstein R (2001) X-ray structure analysis and crystallographic refinement of lumazine synthase from the hyperthermophile Aquifex aeolicus at 1.6 Å resolution: determinants of thermostability revealed from

structural comparisons. J Mol Biol 306(5):1099–1114. https://doi.org/10.1006/jmbi.2000.4435

Zhang X, Meining W, Cushman M, Haase I, Fischer M, Bacher A, Ladenstein R (2003) A structure-based model of the reaction catalyzed by Lumazine synthase from Aquifex aeolicus. J Mol Biol 328(1):167–182. https://doi.org/10.1016/S0022-2836(03)00186-4

Zhen Z, Tang W, Chen H, Lin X, Todd T, Wang G, Cowger T, Chen X, Xie J (2013) RGD-modified Apoferritin nanoparticles for efficient drug delivery to tumors. ACS Nano 7(6):4830–4837. https://doi.org/10.1021/nn305791q

Cell Membrane Coated Nanoparticles: An Emerging Biomimetic Nanoplatform for Targeted Bioimaging and Therapy

3

Veena Vijayan, Saji Uthaman, and In-Kyu Park

3.1 Cell Membrane Coated Nanoparticles

Recent advances in nanotechnology have opened doors to the problems which were once regarded impossible. Nanotechnology has offered many new ways to tackle the problems in the clinical world through the novel features offered by nanoparticles in the field of drug delivery, vaccination, detoxification, gene delivery, antimicrobial purposes and so on (Gao et al. 2015; Hu et al. 2013; Kroll et al. 2016). One major use of nanoparticles is its ability to functionalize surfaces with moieties which include targeting ligands, polymers, enzymes and also biomolecules. Targeted drug delivery had side effect which tends the use of large doses throughout the body to achieve the necessary results. Even now for various diseases, targeted drug delivery seems to be a mere topic of discussion, as in conventional methods it is quite difficult for the drugs to reach specific regions through concentration-dependent diffusion.

V. Vijayan · I.-K. Park (✉)
Department of Biomedical Sciences, BK21 PLUS Centre for Creative Biomedical Scientists, Chonnam National University, Chonnam National University Medical School, Gwangju 61469, South Korea
e-mail: pik96@jnu.ac.kr

S. Uthaman
Department of Polymer Science and Engineering, Chungnam National University, Daejeon 34134, South Korea

Nanoparticle based drug delivery offers numerous advantages (Tan et al. 2015; Chen et al. 2016). The amount of success achieved through this technique has brought in a widespread of research focus in enhancing and engineering nanoparticles with specific physicochemical properties which include smaller size, surface charge, surface hydrophilicity and geometry and also in superior accumulation. Nanoparticles (NPs) are exogenous materials which are recognized by the immune system and by renal and hepatic clearance. The inherent issue can be solved by making the nanosystems more biocompatible. A recent advancement in biomimetic nanoengineering with the cell membrane-coated nanoparticle comprises of a core-shell structure with the core material coated by a material derived from the source cell. Biomimetic NPs attain special functions which include ligand recognition and targeting, long blood circulation, immune escaping and offer a wide variety of applications in photothermal therapy, drug delivery, detoxification and vaccination (Chen et al. 2016; Ding et al. 2015; Hu et al. 2011, 2013; Rao et al. 2017a, b, c, etc.). One of the first kind in this development consisted of a cell membrane-coated nanoparticle with the inclusion of red blood cells (RBCs) as the source cell, wherein the RBC membrane being derived through hypotonic treatment and being coated onto negatively charged polymeric nanoparticles through extrusion (Hu et al. 2011). Further modifications have

I. Noh (ed.), *Biomimetic Medical Materials*, Advances in Experimental Medicine and Biology 1064,
https://doi.org/10.1007/978-981-13-0445-3_3

allowed for "active targeting" of nanoparticles with ligands that are bound to the surface receptors on target cells or tissues. It was indicative that active targeting has not only enhanced retention but also the cellular uptake of nanoparticles by these target cells. Currently, the much focused type of ligands comprises of small molecules, peptides, antibodies and aptamers which have been widely used in direct targeted delivery of drugs through these nanocarriers (Parodi et al. 2013a, b).

Another appealing feature of nanoparticles is that they can modify their geometrical conformation and also their surface characteristics in favor to the drug release at targeted sites of surrounding tissues. Targeted delivery of nanoparticles has paved new ways in effectively delivering the drugs to the target sites (Zhang et al. 2017a; Gao et al. 2016; Hu et al. 2011, 2013; Parodi et al. 2013a, b).

Cell membrane-coated nanoparticles have indeed proven to be a promising area in future research. Importantly the nanoparticles can moreover be functionalized by coating particles with membrane derived from source cells of different types. The resulting membrane-coated nanoparticles have high biocompatibility, prolonged circulation and tumor-targeting ability based on the nature of the membrane used. Different types of cell membranes have distinct functions in targeted drug delivery, photothermal therapy and combinational therapy. (Ren et al. 2017; Fu et al. 2015; He et al. 2016a; Chen et al. 2016; Li et al. 2017a, b) In the context of these, preclinical trials on targeted drug delivery has turned the spotlight in creating fine-tuned nanomaterials and nanostructures deployed for drug delivery. Of lately, biomimetic delivery systems have been the of interest due to its nature-inspired materials that could harness these natural occurring biological features and channel it into forming a superior targeted drug delivery system. One such implementation is in the use of coating the nanoparticles with these natural cell membranes for biofunctionalization. These naturally occurring membranes do provide a bilayer medium intended for a transmembrane protein anchorage and also preclude the loss of reliability and their functionalities which occurs during the formation of drug followed by the delivery. (Kroll et al. 2016; Luk and Zhang 2015; Zhang et al. 2017a, b).

3.2 Preparation of Cell Membrane Coated NPs

3.2.1 Isolation of Plasma Membrane from Different Cell Sources

Cell membranes, a biological membrane separating the interior of cells from outside the cells are composed of lipid bilayer with embedded proteins with specific biological functions. To derive the plasma membrane from the cell, initially, the intracellular components should be emptied by a sequence of hypotonic lysis or repeated freeze-thaw procedure, mechanical disruption of the membrane. Soluble proteins are removed through differential centrifugation and finally nanovesicles were formed by extrusion. Briefly, the cells are lysed firstly using a subcellular fractionation buffer, centrifuged at different degrees starting from low speed to high speed up to 40,000 rpm (100,000 × g) and sonicated in between in ice. The final pellet obtained is the membrane pellet which is re-suspended in standard lysis buffer. (Subcellular fractionation protocol, Abcam 2016; Sun et al. 2016; Suski et al. 2014) Finally the cell membrane pellets were extruded through a porous polycarbonate membrane to form plasma membrane vesicle.

3.2.2 Incorporation of Core Particles into Membrane Vesicles

After the progressive removal of the intracellular components, the plasma membrane vesicle thus obtained should be coated onto a core particle. This can be achieved either through physical extrusion, sonication or by means of electroporation. In the case of extrusion, the two components are coextruded through a 200 nm polycarbonate membrane which results in the mechanical adsorption and fusion of membrane vesicles on the surface of the nanoparticle (Ren et al. 2017; Chen et al. 2016; Luk et al. 2016). Simple

co-incubation of membrane vesicles and core nanoparticles under sonication results in the formation of membrane-coated nanoparticles but the demerit of this is that the coating formed might not be uniform and the size might be uneven (He et al. 2016a, b). Electroporation induces multiple pores in the cell membrane as the cells are exposed to the strong external electric field. The nanoparticles can diffuse into the cells through these pores. Microfluidic electroporation is also used to obtain the membrane coated nanoparticles, which uses different microfluidic chips to improve the transfection performance and decrease the voltage which is used for electroporation. Microfluidic chips have various merits which include high throughput, quantitative format, robustness, parallel dependence and versatility (Rao et al. 2017b) (Fig. 3.1).

3.3 Core Particles for Membrane Coating

3.3.1 Organic Nanoparticles

Organic NPs are the NPs which are composed of organic compounds like lipids and polymers. These types of NPs are synthesized through emulsification process and by precipitation methods. (Allouche 2013). The most commonly used organic nanoparticles which are used as core nanoparticles are poly (lactic-co-glycolic acid) (PLGA) NPs, which is Food and Drug Administration (FDA) approved and biodegradable, biocompatible and non-toxic. They are used either alone or encapsulated with any NIR dye or anticancer agents. Indocyanine green (ICG) is the only U.S. FDA approved NIR dye. It is known to have remarkable optical features which are extensively used for fluorescence imaging and photothermal. Since it has certain drawbacks such as nonselectivity for cancer cells, rapid clearance with a short halftime and low singlet oxygen quantum, it needs to be delivered with some nano delivery systems.

PLGA core forms the perfect delivery system due to its combination with a high drug loading capacity and also its biocompatible membrane coating (Dehaini et al. 2017). This core along with RBC membrane coating can be extensively used in delivering the anti-cancer drug DOX to solid tumors (Luk et al. 2016), also in reducing hypoxia in tumors with the encapsulation of perfluorocarbon (PFC) to deliver oxygen. (Gao et al. 2017b) and encapsulation with hemoglobin (Hb) and doxorubicin (DOX) – chemotherapy and targeted oxygen supply to reduce hypoxia -cancer cell membrane- (Tian et al. 2017). PLGA loaded with paclitaxel cytotoxic T lymphocyte (CTL) membrane along with a low dose irradiation is used in tumor localization stimulus for drug delivery (Zhang et al. 2017a). Gelatin nanogels are used to encapsulate DOX, with mesenchymal stem cells for tumor-targeted drug delivery (Gao et al. 2016). Liposomes are also used as a core to encapsulate cytotoxic anticancer drug emtansine and further macrophage membrane coating owes for specific metastasis targeting (Cao et al. 2016).

Human Serum Albumin (HSA) nanoparticles increase the stability of ICG and extend the systemic circulation time for the accumulation in tumor. To solve the problem of low singlet oxygen quantum, perfluorocarbon (PFC) is used to increase the oxygen supply in the tumor microenvironment. This Indocyanine green (ICG) and PFC RBC enhances PDT and PTT. (Ren et al. 2016).

3.3.2 Inorganic Nanoparticles

There are a variety of inorganic NPs used as core NPs and further camouflaged with different membrane vesicles. Inorganic NPs can be easily and cheaply synthesized. They exhibit magnetic, electrical and optical properties which could be customized by controlling the shape, size, surface interactions of the NPs (Tan et al. 2009). Silica nanorattle – encapsulated with DOX and mesenchymal stem cell membrane coating on this is used for tumor-tropic therapy with increased and prolonged intratumoral drug distribution and enhanced tumor cell apoptosis (Li et al. 2011). Janus microcapsules have surface areas and can be used to perform multiplexed biomolecular

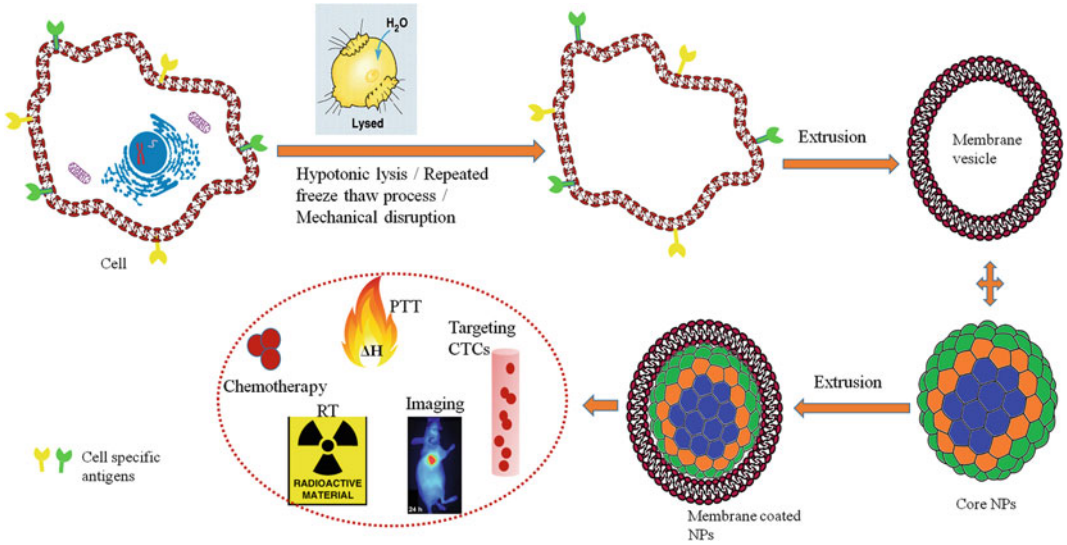

Fig. 3.1 General Scheme of membrane coated nanoparticle: membrane derivation, the formation of vesicle and fusion of core NPs and vesicle. *PTT* photothermal therapy, *CTC* circulating tumor cells, *RT* radiotherapy

detection, where one side of the Janus capsules are modified for target recognition and the other side functionalized with noble metals which have a combination of specific recognition to a cancer cell and photothermal performance. Leukocyte cell membrane coated Janus microcapsules have gold nanoparticles on one side and the membrane coating on another side. (He et al. 2016a, b)

Magnetic o-carboxymethyl-chitosan (CMC) nanoparticle is used as core to co-encapsulate hydrophobic – hydrophilic chemotherapeutic drugs paclitaxel (PTX) and DOX. When RBC membrane (anchored with Arg- Gly- Asp) coating is provided onto this nanoparticles, CMC core exhibited great tumor growth inhibition (Fu et al. 2015). Magnetic iron oxide nanoparticles enter the RBC vesicles through microfluidic electroporation, provide prolonged circulation, and minimized accelerated blood clearance finds application in MR imaging (Rao et al. 2015). Upconversion NPs can convert light from NIR range to the visible range which in turn opens the way for fluorescence imaging applications with unique optical properties like narrow emission peaks, low toxicity, and good photostability. RBC membrane coating over this particle pave the way for efficient tumor imaging (Rao et al. 2017b).

3.4 Types, Functions, and Mechanism of Membrane Coatings

3.4.1 Blood Cells Component Coated NPs

3.4.1.1 Platelet Membrane Coated NPs

Platelet or thrombocyte is an important component of blood which is essential for the maintenance of homeostasis. Functionalizing the nanoparticles with platelet membrane enables the nanoparticles to circulate throughout the bloodstream without any immune system attack. It also facilitates biomimetic targeting by interacting with platelet surface markers and different targets. The platelet membrane coating binds to the damaged blood vessels and certain pathogens, allowing the core biocompatible nanoparticle to deliver the payload. The platelets with unique surface moieties function immune evasion, sub endothelial adhesion, and pathogen interactions make it appropriate to be used as a nanocarrier. This platelet membrane mimics the

platelets in terms of the complete set of surface moieties, antigens, and proteins present on the native platelets. Platelet membrane-coated nanoparticles find itself fitted in variety of applications like drug delivery (Li et al. 2016), treatment of immune thrombocytopenia (Wei et al. 2016), cancer treatment (Hu et al. 2015a).

P- Selectin is a protein which is overexpressed on the platelet membrane which has high specificity towards CD 44 receptors which are upregulated on the surface of cancer cells. Thus platelet membrane-coated nanoparticles extend their applications being used in anticancer therapy where platelet membrane coating helps in active targeting to the tumor site and sequentially deliver the anticancer core nanoparticle. This platelet membrane coating helps the anticancer drug from sudden burst release.

3.4.1.2 RBC Membrane-Coated Nanoparticles

Red blood cells (RBCs) which are also termed as erythrocytes belong to the most common type of blood cells which are mostly involved in the oxygen supply in the body. RBCs have a long circulation life in the body (lifetime of 100–120 days) before getting cleared by the immune system. Nanoparticles are coated with different types of cell membranes to achieve prolonged circulation, which in turn promises better targeting of tissues through both passive and active mechanisms. For prolonged circulation, surface coatings should be chosen in such a way that it should prevent the nanoparticles from early uptake by the reticuloendothelial system. RBC has unique physicochemical characteristics such as self-markers on their surface which suppresses immune attack and makes it the viable candidate to be used in long-circulating carriers. Because of this RBC coating, the core nanoparticles are likely to have improved drug tolerability, therapeutic efficacy (Ren et al. 2017; Fu et al. 2015; Gao et al. 2017b). This conventional chemical conjugation approach seems to be rather impractical because of the major difficulty in functionalizing nanoparticles with the complex surface chemistry of the biological cell. In such case, the cell membrane-coated nanoparticles solve the above problem by translocating the protein makeup on the RBC surface and reduce accelerated blood clearance. RBC membrane capped nanoparticles can be used for personalized diagnosis and therapy (Luk et al. 2014). RBC membrane coatings can be incorporated into numerous nanoparticles through techniques previously discussed in the earlier sections.

RBC membrane-coated nanoparticle is the first cell membrane coated nanoparticle where RBC becomes the source cell and the RBC membrane derived by hypotonic treatment is coated onto anionic polymeric nanoparticles for long-circulating cargo delivery (Hu et al. 2011). RBC coated nanoparticles finds it applications widespread in drug delivery, tumor targeting and imaging (Luk et al. 2016; Fu et al. 2015; Rao et al. 2017a, b; Jiang et al. 2017a, b), therapeutics for broad-spectrum toxin neutralization (Hu et al. 2013). RBC- platelet hybrid membrane-coated nanoparticles encompasse on hybrid functionalities of RBCs and platelet, that is RBC membrane enhances the longer circulation of NPs and introduction of platelet membrane adds a targeting ligand which helps to improve localization to target (Dehaini et al. 2017). RBC coating over Human serum albumin (HSA) NPs with Indocyanine green (ICG) and perfluorocarbon (PFC) enables the particle to be used for enhanced phototherapy (Ren et al. 2017). RBC membrane coating over monoclonal antibody NPs for effective drug delivery and tumor treatment (Gao et al. 2017a)

3.4.2 Immune Cell Membrane Coated NPs

3.4.2.1 Macrophage Membrane Coated Nanoparticles

Macrophages are typical white blood cells that identify, engulf and digest cellular debris and foreign substances, which do not have specific biomarkers of healthy body cells. Macrophages are present in the tumor microenvironment by direct association with tumor progression and metastasis (Qian and Pollard 2010). When the nanoparticles are camouflaged with macrophage membranes, the cell-cell adhesion becomes possible for cancer targeting. The macrophage

membrane-derived vesicles contain the associated membrane proteins from natural macrophages thus making it ideal for cancer targeting and imaging (Rao et al. 2017c). Macrophages can actively bind to a cancer cell through interactions with α4 integrins of macrophages and that of vascular adhesion molecule-1 (VCAM-1) of the cancer cells. The macrophage membrane is derived by draining their intracellular contents through the combined procedures of hypotonic cytolysis, membrane disruption and series of centrifugation. These derived membranes are then coated on nanoparticles through mechanical extrusion. The macrophage membrane-coated nanoparticles also find its place in photothermal cancer therapy when the core nanoparticle is a photothermal agent and its optical absorption lies in the NIR region showing good biocompatibility, reduced opsonization, prolonged circulating time and enhanced tumor accumulation (Xuan et al. 2016). Macrophage membrane coating over a pH-sensitive liposome for the delivery of anticancer drug emtansine facilitates specifically targeting to metastatic sites and thereby enhancing the therapeutic efficacy (Cao et al. 2016) (Fig. 3.2).

3.4.2.2 Neutrophil Cell Membrane-Coated Nanoparticles

Neutrophils are granulocytes which are most abundant types of white blood cells which form an essential part of the innate immune system. Neutrophils are not like other WBCs; they are not confined to a specific area of circulation and can move freely through the walls of veins and body tissues to instantly attack antigens. The role of neutrophils is vital in cancer as it plays an active role in the progression of cancer. Neutrophils are recruited in tumors through the secretion of chemoattractants from tumors. The antitumor response is compromised with the increased number of circulating neutrophils which negatively influence the cytotoxic activity of NK cells and lymphocytes (Treffers et al. 2016). Neutrophil membrane-coated nanoparticles can be synthesized by coating nanoparticles with neutrophil membranes. This neutrophil membrane coated nanoparticle can be used to target circulating tumor cells (CTCs) in circulation. And loading the nanoparticle with a second-generation proteasome inhibitor can find a therapeutic application by preventing de novo metastasis and inhibition of already formed metastasis (Kang et al. 2017) (Fig. 3.3).

3.4.2.3 Cytotoxic T Cell Membrane-Coated Nanoparticles

Cytotoxic T cell generally known as Tc/CTL is a T lymphocyte (a type of WBC) that kills cancer cells and other infected cells. Cytotoxic T lymphocytes can promote carefully chosen target cells death (apoptosis) with the use of a combination of granule and receptor-mediated mechanisms. CTLs have exquisite specificity for an antigen that can recognize the T cell receptors on the target cells and present antigen derived peptide fragments which appear to be on the cell surface to be inserted into the groove of class I major histocompatibility molecules (MHC). CTL becomes attractive as mediators of antitumor immunity with a variety of properties. Their property to recirculate throughout the body in seeking out antigen can be widely utilized in the treatment of systemic disease. MHC class I complex can activate cytolysis just through the recognition of a single peptide. CTLs do also employ noneffector mechanisms along with the production of interferon gamma, which is a cytokine comprising of several antitumor properties (Maher and Davies 2004). Because of the above-mentioned properties of CTL, cytotoxic T cell membrane camouflaged nanoparticles can be used as cancer targeting nanoparticles. This CTL membrane-coated nanoparticle along with local low dose irradiation was exclusively used for target gastric cancer. In this system, poly(lactic-co-glycolic acid) nanoparticles co-loaded with paclitaxel were coated with CTL membrane and through an application of low dose irradiation at the tumor site showed significantly inhibited tumor growth. Low dose irradiation resulted in the upregulation of adhesion molecules in tumor vessels which in turn aides to the localization of the CTL membrane-coated nanoparticles (Zhang et al. 2017a).

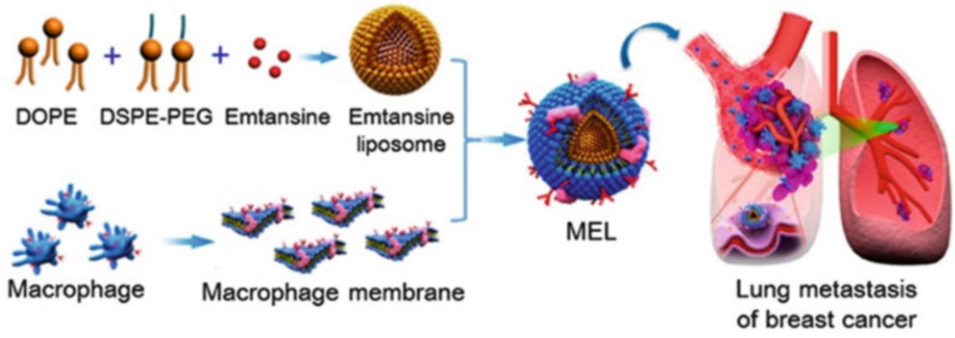

Fig. 3.2 Scheme of Macrophage-Membrane-Coated Liposome loaded with emtansine for suppressing lung metastasis of breast cancer. (Cao et al. 2016. Copyright ©2016 American Chemical Society)

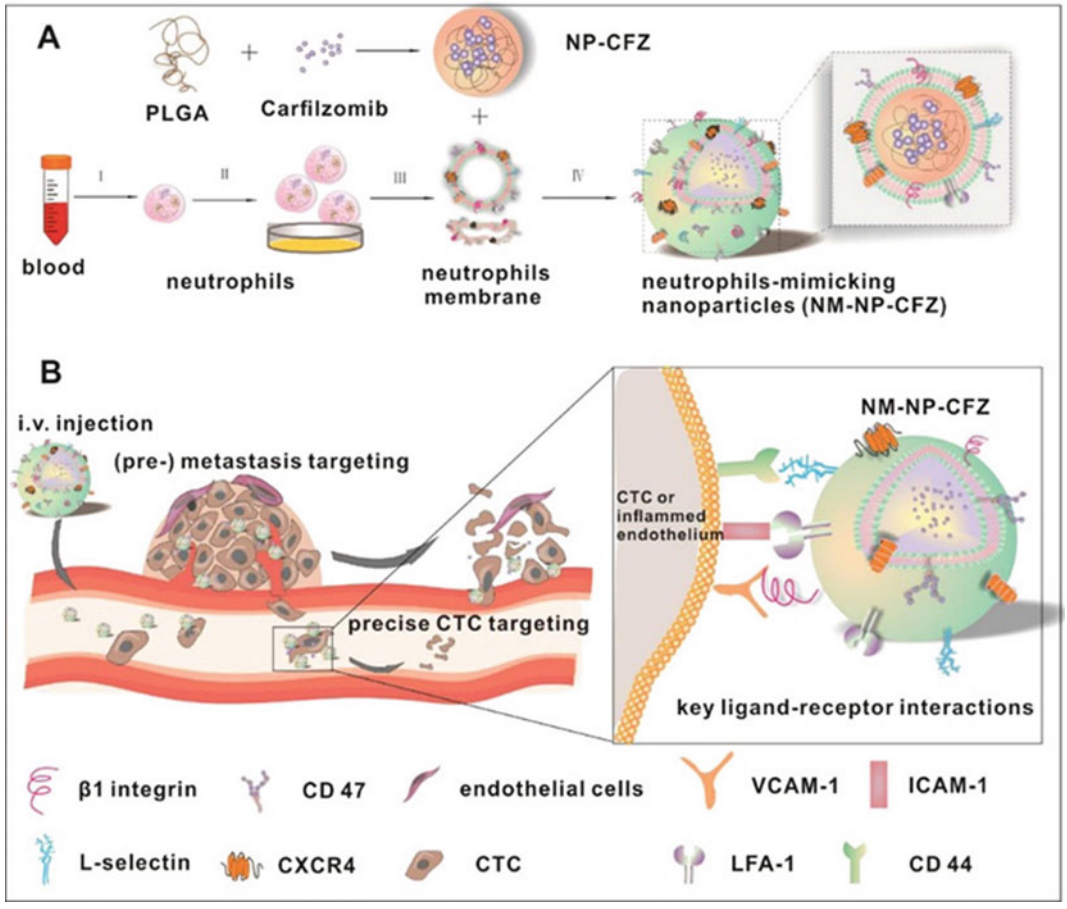

Fig. 3.3 Scheme of neutrophil membrane-coated nanoparticles loaded with carfilzomib for targeting circulating tumor cells (CTCs). (Kang et al. 2017, Copyrights received ©2017 American Chemical Society)

3.4.2.4 Leukocytes Cell Membrane-Coated Nanoparticles

Leukocytes are a type of white blood cells which form a part of the immune system and are involved in protecting the body against infectious diseases and foreign invaders, hence their membrane has the property to evade the immune system and localize at target tissues thus exhibiting their targeting ability through cellular membrane interactions. Leukocyte membrane-coated nanoparticles avoid opsonization, delay uptake by mononuclear phagocyte system. These leukocyte membranes facilitate the transport of chemotherapeutics across the endothelium by preferential binding to inflamed endothelium, thus eluding the lysosomal pathway (Parodi et al. 2013a, b). Nanoporous silicon particles were also used as the core to deliver cargoes and protect this therapeutic cargo for enhanced efficacy (Parodi et al. 2013a, b). Other than nanoparticles, microspheres are also coated with leukocyte membrane. The dual functionalized Janus capsule has photothermal effects which in turn can be used as a photoactive cancer cell detector to kill the cancer cells. This photothermal effect is seen when one compartment of the capsule has a gold shell which has strong NIR absorbance under laser irradiation. Cancer cell walls get ruptured due to violent evaporation of water under NIR irradiation finally leading to cell death (He et al. 2016a, b).

3.4.3 Cancer Cell Membrane-Coated Nanoparticles

Cancer cells adhere to one another through homotypic binding allowing the growth of the tumor. The membrane of cancer cells when coated over nanoparticles helps in homotypic targeting and self- recognition internalization by the source cells. This membrane coating over different nanoparticles makes it an appropriate candidate for the application of anticancer vaccination and drug delivery (Fang et al. 2014), also in dual modal imaging guided by photothermal therapy (Chen et al. 2016), targeted oxygen interference therapy to overcome hypoxia-induced chemoresistance (Tian et al. 2017), MRI (Zhu et al. 2016).

Cancer cell membrane derivation was accomplished by emptying the intracellular contents through a series of hypotonic lysing, mechanical membrane disruption and differential centrifugation. Cancer cell membrane vesicles were then formed by physical extrusion through a 400 nm porous polycarbonate membrane. For coating, this membrane vesicle over the nanoparticle, both the core nanoparticle and membrane vesicle were coextruded through a 200 nm porous polycarbonate membrane. Cancer cell membrane coated NPs allow membrane-bound tumor-associated antigens along with immunological adjuvants to efficiently deliver to antigen presenting cells by stimulating anticancer immune responses. Homotypic cell membrane increases the particle-to-cell adhesion and has the prospective capability to target distant body sites that are inclined to cancer metastasis. Targeting the source cell via homotypic binding mechanism paves way for anticancer drug delivery and the colocalization of multiple antigens together with immunological adjuvants in a stabilized form which facilitates uptake of membrane-bound tumor antigens for efficient presentation and downstream immune activation in the case of cancer immunotherapy (Fang et al. 2014). When the core nanoparticle is NIR dye like ICG, it helps in image-guided photothermal therapy when laser irradiated. Complete tumor irradiation was obtained with such cancer cell membrane coated ICG nanoparticles as it possessed homologous targeted binding to achieve high tumor accumulation. (Chen et al. 2016) (Fig. 3.4). If the core nanoparticle is magnetic nanoparticles, it paves way for the MRI application. It shows the excellent self-targeting homing ability to homologous tumor even in competition with other heterologous tumors and further anticancer drug encapsulation provides potency for tumor treatment. (Zhu et al. 2016). Conformal cancer cell membrane coating over poly (lactic-co-glycolic acid) PLGA core which is encapsulated with hemoglobin and anticancer drug Doxorubicin attained a high selective

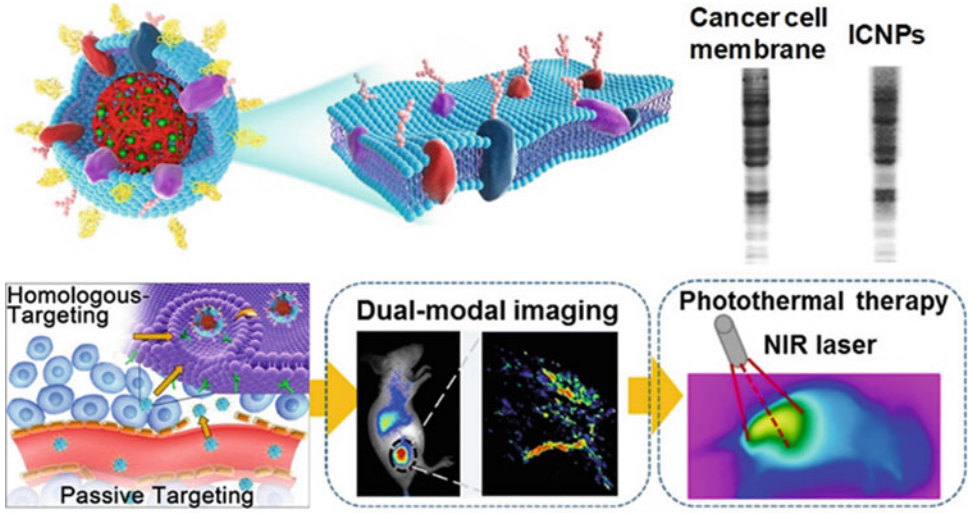

Fig. 3.4 Synthesis of Cancer cell membrane coated NPs for image-guided Photothermal therapy. (Chen et al. 2016. Copyrights received © 2016, American Chemical Society)

targeted delivery of doxorubicin and oxygen to homologous tumors breaking the hypoxia-induced chemoresistance (Tian et al. 2017).

3.4.4 Stem Cell Coated Nanoparticles

Most systemically administered nanoparticles which circulate itself in the blood get rapidly sequestered by the reticuloendothelial system (RES) even by the assistance of tumor-associated EPR effect and conjugation with these targeted moieties. The nanoparticles which get accumulated on tumor are in terms very less to initiate therapeutic effect. Stem cells are known to possess self-renewable capacity with high replicative potential in multilineage differentiation capacity. Generally, embryonic stem cells are widely used for therapeutic purposes due to its higher totipotency and indefinite lifespan. Tumors send out chemo-attractants such as the vascular endothelial growth factor (VEGF) to recruit mesenchymal stem cells in the formation of supporting stroma for the tumor and pericytes intended for angiogenesis. The stem cell membrane coated nanoparticle has an inherent tumoritropic property which could be an interesting alternative.

Stem cell membrane coated nanoparticle is not only attractive in tumor based targeting but also finds application in many molecular recognition moieties due to their easy isolation. Mesenchymal stem cell membrane coated gelatin nanogels derived from bone marrow are developed for highly efficient tumor based targeted drug delivery. These nanogels also consist of a unilamellar membrane coating which is functionalized with a tumor-targeted antigen which is also associated with stem cells. They showcase excellent mesenchymal stem cell mimicking cancer targeting capability in in-vitro and in enhanced tumor accumulation in in vivo. Because of this membrane coating, the tumoritropic property is well preserved and clearance through RES is decreased (Gao et al. 2016).

3.5 Characterizations of Cell Membrane-Coated Nanoparticles

The membrane coated NP's need to be characterized for their physiochemical and biological functions. The membrane coatings on the nanoparticles can be confirmed by the changes in size, surface charge, protein

composition etc. Transmission Electron Microscopy (TEM) reveals the superficial coverage of the membrane coating confirms the presence of cell membrane coating over the nanoparticles. The shape of the final membrane-coated nanoparticles and core-shell structure is also revealed by TEM. Scanning electron microscopy (SEM) explains the morphology of the membrane coated nanoparticle. Generally, the membrane coating is very thin approximately around 10 nm. Dynamic light scattering (DLS) gives insight into the information regarding the hydrodynamic size of the membrane coated nanoparticles. Zeta potential measurements done here suggests successful coating as well as the surface charge on the core particles after membrane coating,

The successful functionalization of nanoparticles with these cell membrane antigens was confirmed by analysis of the protein content of the membrane coated nanoparticles. This was analyzed using Gel electrophoresis/polyacrylamide gel electrophoresis (PAGE)/SDS PAGE followed by protein staining which shows the protein profile when compared to the raw cell lysate. Western blotting analysis confirms on various intracellular protein markers, the presence of surface antigens and adhesion proteins on the membrane coated nanoparticles. In this analysis carried on for protein markers in the nucleus, mitochondria and cytosol should be down-regulated on the final nanoparticles. The membrane coated nanoparticles can be fluorescent labeled and visualized using confocal laser scanning microscope to check the nanoparticle internalization.

3.6 Applications of Cell Membrane-Coated Nanoparticles

The main advantage of cell membrane-coated nanoparticles is their easy functionalization. Different type of membrane coatings and core materials paves the way for different biological applications, which includes drug delivery, phototherapy, radiotherapy, in anticancer vaccination, etc.

3.6.1 Photo Therapy

Phototherapy is used for cancer treatment due to its selective and localized therapeutic effects through laser irradiation. In photothermal therapy the near-infrared (NIR) lasers photoabsorbers are employed for thermal ablation of cancer cells through NIR laser irradiation. Whereas Photodynamic therapy uses a photosensitizer which is excited with specific band light thus generating singlet oxygen which creates local hyperthermia to kill cancer cells. Different types of membrane-coated nanoparticles have been used to enhance phototherapy. RBC membrane coating onto ICG-HSA NPs through extrusion prolonged circulation time and increased singlet oxygen generation for photodynamic therapy. In this, the core HSA NPs was synthesized by encapsulating ICG and perfluorotributylamine (PFTBA) and coated with RBC membrane vesicle through extrusion (Ren et al. 2017). In another study, magnetic NPs were forced to enter RBC vesicles through electroporation method and the resulted NPs helped in MR image-guided photothermal therapy (Rao et al. 2017a; Ren et al. 2016). Cancer cell membrane coating on PLGA NPs with ICG through extrusion demonstrated specific homologous targeting towards cancer with excellent fluorescence and photoacoustic imaging-guided photothermal therapy. Briefly, the core NPs was ICG-loaded PLGA polymeric core and the cancer cell membrane vesicles were fused on the surface by extrusion. This biomimetic NPs showed excellent monodispersity, photothermal property, fluorescence/photoacoustic dual-modal imaging properties and moreover homologous tumor targeting ability (Chen et al. 2016). In another cancer cell membrane coated study, phosphorescence image-guided photodynamic therapy was carried out. In this Platinum (II) porphyrinic nanoscale metal-organic framework (NMOF) with Zirconium (Zr_6 cluster) in which the porphyrin- NMOF with high photosensitizer loading has O_2 sensing and phosphorescence guided PDT (Li et al. 2017a, b) Gold nanoshells when coated with macrophage membrane (through repeated extrusion) become a photothermal conversion

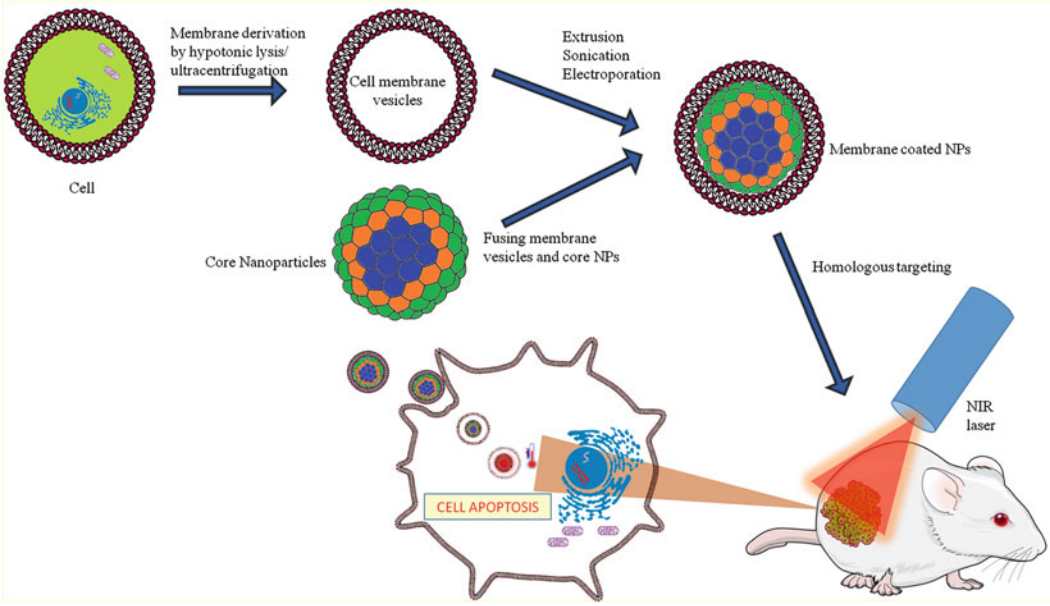

Fig. 3.5 Schematic diagram showing general mechanism of membrane coated NPs in Photothermal therapy

agent for effective photothermal therapy in cancer (Xuan et al. 2016). Janus capsules when modified with gold nanoparticles in one part and leukocyte membrane on the other part was also shown to have specific targeting towards cancer cells and increased PTT (He et al. 2016a).

3.6.2 Drug Delivery

Various types of membrane coating were used for targeted drug delivery (Fig. 3.5). RBC-NPs were used to deliver DOX for the treating solid tumors (Luk and Zhang 2015). RBC membrane coatings over hydrophilic–hydrophobic anticancer drugs DOX and PTX were used for combined chemotherapy. They co-encapsulated both hydrophobic and hydrophilic chemotherapeutic drugs into magnetic O-carboxymethyl chitosan particle which hides in the bloodstream and activates magnetically and gets accumulated in tumor cells and releases drugs into the cytoplasm, the erythrocyte membrane vesicle was coated onto the NPs through a series of extrusion (Fu et al. 2015). When RBC membrane modified by pre-inserting streptavidin and incorporating a biotinylated form of ^{D}CDX peptide, possessed the capability to cross the blood-brain barrier and thus can be used to deliver DOX against brain glioma (Chai et al. 2017). RBC membrane coatings over upconversion nanoparticles (UCNPs) were used as PDT agents and enable targeted drug delivery and phototherapy (Ding et al. 2015). Monoclonal antibodies are coated with RBC membrane and different types of antibodies are intracellularly delivered (Gao et al. 2017a). pH-sensitive liposomes coated with macrophage membrane successfully delivered anticancer drug emtansine against lung metastasis of breast cancer (Cao et al. 2016). Platelet coated NPs with docetaxel and vancomycin are used for disease-targeted therapy (Hu et al. 2015b). Table 3.1 summarizes the application of various membrane-coated nanoparticles.

3.7 Conclusion and Future Perspective

Nanoparticles coated with different types of cell membranes could be employed for a variety of biological applications including drug delivery,

Table 3.1 Applications of different types of membrane coated NPs

Type of NPs	Membrane derivation	Core particle	Application	References
RBC/erythrocyte coated NPs	Hypotonic treatment followed by extrusion	1. HSA NPs with ICG and PFTBA	Enhanced phototherapy	Ren et al. (2017)
	Sonication approach	2. Magnetic NPs	Toxin nanosponge	Ren et al. (2016)
	Hypotonic treatment and sonication	3. PLGA NPs	Drug delivery to treat solid tumors	Hu et al. (2013)
	Microfluidic electroporation	4. PLGA NPs coloaded with DOX	Combinational chemotherapy	Luk et al. (2016)
		5. Magnetic O-carboxymethyl-chitosan nanoparticles coloaded with PTX and DOX	enhanced Radiotherapy	Fu et al. (2015)
		6. PLGA core with PFC	Enhanced tumor imaging	Gao et al. (2017b)
		7. DSPE-PEG functionalized UCNPs		Rao et al. (2017b)
				Hu et al. (2011)
Leucocyte coated NPs	Coincubation	1. Janus particles	Photothermal cancer treatment	He et al. (2016a, b)
		2. Nanoporous Silicon NPs	Drug delivery	Parodi et al. (2013a, b)
Neutrophil coated NPs	Percoll gradient separation followed by emulsion/solvent evaporation	1. PLGA NPs loaded with carfilzomib	Targeting CTCs in circulation and premetastatic niche	Kang et al. (2017)
Platelet coated NPs	Repeated freeze-thaw process followed by sonication	1. PLGA NPs with Docetaxel and Vancomycin	Disease-targeted delivery	Hu et al. (2015b)
		2. Si NPs, TRAIL conjugation		Li et al. (2016)
		3. TRAIL-DOX NPs		Wei et al. (2016)
				Hu et al. (2015a)
Cancer cell membrane coated NPs	Extrusion	1. PLGA core with DOX and Hb	Oxygen interfered chemotherapy	Tian et al. (2017)
		2. PLGA core with ICG	Photothermal therapy, Photoacoustic imaging	Chen et al. (2016)
		3. PLGA with adjuvants	Phosphorescence image-guided photodynamic therapy	Fang et al. (2014)
		4. Fe3O4 and DOX	Anticancer vaccination and drug delivery	Li et al. (2017a, b)
		5. Pt(II) porphyrin nanoscale metal-organic framework with Zirconium cluster	MRI	

(continued)

Table 3.1 (continued)

Type of NPs	Membrane derivation	Core particle	Application	References
Macrophage membrane coated NPs	Hypotonic lysis and extrusion	1. UCNPs	Effective cancer imaging	Rao et al. (2017c)
		2. Au nanoshells coated mesoporous silica NPs	Enhanced cancer photothermal therapy	Xuan et al. (2016)
		3. Liposomes with emtansine	Specific metastasis targeting	Cao et al. (2016)
Cytotoxic T lymphocyte membrane coated NPs	Hypotonic lysis and extrusion	1. PLGA with PTX	Enhanced tumor accumulation and drug delivery	Zhang et al. (2017a)
Stem cell coated NPs		Gelatin nanogels	efficient tumor targeting and drug delivery	Gao et al. (2016)

phototherapy, photodynamic therapy, imaging applications, anticancer vaccines and so on. The membrane coating enhances the particle interaction, in turn, helping for prolonged circulation in blood, escape blood clearance. Nanoparticles coated with a particular cell membrane will provide a homologous targeting and enhanced tumor accumulation.

The membrane coated nanoparticles indeed mimic the source cells. The membrane coated NPs improve the therapeutic efficacy of drugs and other therapeutic cargos through specific delivery and enhanced accumulation in the tumor. Further modification of the isolated cell membranes like double membrane coating and incorporation of novel therapeutics endows a new strategy in biomimetic platforms.

References

Allouche J (2013) Synthesis of organic and bioorganic nanoparticles: an overview of the preparation methods. In: Nanomaterials: a danger or a promise? Springer, London, pp 27–74. https://doi.org/10.1007/978-1-4471-4213-3

Cao H, Dan Z, He X, Zhang Z, Yu H, Yin Q, Li Y (2016) Liposomes coated with isolated macrophage membrane can target lung metastasis of breast cancer. ACS Nano 27;10(8):7738–7748. https://doi.org/10.1021/acsnano.6b03148

Chai Z, Hu X, Wei X, Zhan C, Lu L, Jiang K, Su B, Ruan H, Ran D, Fang RH, Zhang L (2017) A facile approach to functionalizing cell membrane-coated nanoparticles with neurotoxin-derived peptide for brain-targeted drug delivery. J Control Release 264:102. https://doi.org/10.1016/j.jconrel.2017.08.027

Chen Z, Zhao P, Luo Z, Zheng M, Tian H, Gong P, Gao G, Pan H, Liu L, Ma A, Cui H (2016) Cancer cell membrane–biomimetic nanoparticles for homologous-targeting dual-modal imaging and Photothermal therapy. ACS Nano 10 (11):10049–10057. https://doi.org/10.1021/acsnano.6b04695

Dehaini D, Wei X, Fang RH, Masson S, Angsantikul P, Luk BT, Zhang Y, Ying M, Jiang Y, Kroll AV, Gao W (2017) Erythrocyte–platelet hybrid membrane coating for enhanced nanoparticle functionalization. Adv Mater 29(16):1606209. https://doi.org/10.1002/adma.201606209

Ding H, Lv Y, Ni D, Wang J, Tian Z, Wei W, Ma G (2015) Erythrocyte membrane-coated NIR-triggered biomimetic nanovectors with programmed delivery for photodynamic therapy of cancer. Nanoscale 7 (21):9806–9815. https://doi.org/10.1039/C5NR02470F

Fang RH, Hu CM, Luk BT, Gao W, Copp JA, Tai Y, O'Connor DE, Zhang L (2014) Cancer cell membrane-coated nanoparticles for anticancer vaccination and drug delivery. Nano Lett 14(4):2181–2188. https://doi.org/10.1021/nl500618u

Fu Q, Lv P, Chen Z, Ni D, Zhang L, Yue H, Yue Z, Wei W, Ma G (2015) Programmed co-delivery of paclitaxel and doxorubicin boosted by camouflaging with erythrocyte membrane. Nanoscale 7 (9):4020–4030. https://doi.org/10.1039/C4NR07027E

Gao W, Zhang L (2015) Coating nanoparticles with cell membranes for targeted drug delivery. J Drug Target 23(7–8):619–626. https://doi.org/10.3109/1061186X.2015.1052074

Gao C, Lin Z, Jurado-Sánchez B, Lin X, Wu Z, He Q (2016) Stem cell membrane coated nanogels for highly efficient in vivo tumor targeted drug delivery. Small 12 (30):4056–4062. https://doi.org/10.1002/smll.201600624

Gao L, Han L, Ding X, Xu J, Wang J, Zhu J, Lu W, Sun J, Yu L, Yan Z, Wang Y (2017a) An effective intracellular delivery system of monoclonal antibody for treatment of tumors: erythrocyte membrane-coated self-associated antibody nanoparticles. Nanotechnology 28(33):335101. https://doi.org/10.1088/1361-6528/aa7c43

Gao M, Liang C, Song X, Chen Q, Jin Q, Wang C, Liu Z (2017b) Erythrocyte membrane enveloped perfluorocarbon as nanoscale artificial red blood cells to relieve tumor hypoxia and enhance cancer radiotherapy. Adv Mater 29(35). https://doi.org/10.1002/adma.201701429

He W, Frueh J, Wu Z, He Q (2016a) Leucocyte membrane-coated janus microcapsules for enhanced photothermal cancer treatment. Langmuir 32 (15):3637–3644. https://doi.org/10.1021/acs.langmuir.5b04762

He W, Frueh J, Wu Z, He Q (2016b) How leucocyte cell membrane modified janus microcapsules are phagocytosed by cancer cells. ACS Appl Mater Interfaces 8(7):4407–4415. https://doi.org/10.1021/acsami.5b10885

Hu CM, Zhang L, Aryal S, Cheung C, Fang RH, Zhang L (2011) Erythrocyte membrane-camouflaged polymeric nanoparticles as a biomimetic delivery platform. Proc Natl Acad Sci 108(27):10980–10985. https://doi.org/10.1073/pnas.1106634108

Hu CM, Fang RH, Copp J, Luk BT, Zhang L (2013) A biomimetic nanosponge that absorbs pore-forming toxins. Nat Nanotechnol 8(5):336–340. https://doi.org/10.1038/nnano.2013.54

Hu Q, Sun W, Qian C, Wang C, Bomba HN, Gu Z (2015a) Anticancer platelet mimicking nanovehicles. Adv Mater 27(44):7043–7050. https://doi.org/10.1002/adma.201503323

Hu CM, Fang RH, Wang KC, Luk BT, Thamphiwatana S, Dehaini D, Nguyen P, Angsantikul P, Wen CH, Kroll AV, Carpenter C (2015b) Nanoparticle biointerfacing by platelet membrane cloaking. Nature 526 (7571):118–121. https://doi.org/10.1038/nature15373

Jiang X, Wang K, Zhou Z, Zhang Y, Sha H, Xu Q, Wu J, Wang J, Wu J, Hu Y, Liu B (2017a) Erythrocyte membrane nanoparticles improve the intestinal absorption of paclitaxel. Biochem Biophys Res Commun 488 (2):322–328. https://doi.org/10.1016/j.bbrc.2017.05.042

Jiang Q, Luo Z, Men Y, Yang P, Peng H, Guo R, Tian Y, Pang Z, Yang W (2017b) Red blood cell membrane-camouflaged melanin nanoparticles for enhanced photothermal therapy. Biomaterials 143:29–45. https://doi.org/10.1016/j.biomaterials.2017.07.027

Kang T, Zhu Q, Wei D, Feng J, Yao J, Jiang T, Song Q, Wei X, Chen H, Gao X, Chen J (2017) Nanoparticles coated with neutrophil membranes can effectively treat cancer metastasis. ACS Nano 11(2):1397–1411. https://doi.org/10.1021/acsnano.6b06477

Kroll AV, Fang RH, Zhang L (2016) Biointerfacing and applications of cell membrane-coated nanoparticles. Bioconjug Chem 28(1):23–32. https://doi.org/10.1021/acs.bioconjchem.6b00569

Li L, Guan Y, Liu H, Hao N, Liu T, Meng X, Fu C, Li Y, Qu Q, Zhang Y, Ji S (2011) Silica nanorattle–doxorubicin-anchored mesenchymal stem cells for tumor-tropic therapy. ACS Nano 5(9):7462–7470. https://doi.org/10.1021/nn202399w

Li J, Ai Y, Wang L, Bu P, Sharkey CC, Wu Q, Wun B, Roy S, Shen X, King MR (2016) Targeted drug delivery to circulating tumor cells via platelet membrane-functionalized particles. Biomaterials 76:52–65. https://doi.org/10.1016/j.biomaterials.2015.10.046

Li SY, Cheng H, Qiu WX, Zhang L, Wan SS, Zeng JY, Zhang XZ (2017a) Cancer cell membrane-coated biomimetic platform for tumor targeted photodynamic therapy and hypoxia-amplified bioreductive therapy. Biomaterials 142:149–161. https://doi.org/10.1016/j.biomaterials.2017.07.026

Li SY, Xie BR, Cheng H, Li CX, Zhang MK, Qiu WX, Liu WL, Wang XS, Zhang XZ (2017b) A biomimetic theranostic O2-meter for cancer targeted photodynamic therapy and phosphorescence imaging. Biomaterials 151:1. https://doi.org/10.1016/j.biomaterials.2017.10.021

Luk BT, Zhang L (2015) Cell membrane-camouflaged nanoparticles for drug delivery. J Control Release 220:600–607. https://doi.org/10.1016/j.jconrel.2015.07.019

Luk BT, Hu CM, Fang RH, Dehaini D, Carpenter C, Gao W, Zhang L (2014) Interfacial interactions between natural RBC membranes and synthetic polymeric nanoparticles. Nanoscale 6(5):2730–2737. https://doi.org/10.1039/C3NR06371B

Luk BT, Fang RH, Hu CM, Copp JA, Thamphiwatana S, Dehaini D, Gao W, Zhang K, Li S, Zhang L (2016) Safe and immunocompatible nanocarriers cloaked in RBC membranes for drug delivery to treat solid tumors. Theranostics 6(7):1004 https://doi.org/10.7150%2Fthno.14471

Maher J, Davies ET (2004) Targeting cytotoxic T lymphocytes for cancer immunotherapy. Br J Cancer 91(5):817–821. https://doi.org/10.1038/sj.bjc.6602022

Parodi A, Quattrocchi N, van de Ven AL, Chiappini C, Evangelopoulos M, Martinez JO, Brown BS, Khaled SZ, Yazdi IK, Enzo MV, Isenhart L (2013a) Biomimetic functionalization with leukocyte membranes imparts cell like functions to synthetic particles. Nat Nanotechnol 8(1):61 https://doi.org/10.1038%2Fnnano.2012.212

Parodi A, Quattrocchi N, Van De Ven AL, Chiappini C, Evangelopoulos M, Martinez JO, Brown BS, Khaled SZ, Yazdi IK, Enzo MV, Isenhart L (2013b) Synthetic nanoparticles functionalized with biomimetic leukocyte membranes possess cell-like functions. Nat Nanotechnol 8(1):61–68. https://doi.org/10.1038/nnano.2012.212

Qian BZ, Pollard JW (2010) Macrophage diversity enhances tumor progression and metastasis. Cell 141 (1):39–51. https://doi.org/10.1016/j.cell.2010.03.014

Rao L, Bu LL, Xu JH, Cai B, Yu GT, Yu X, He Z, Huang Q, Li A, Guo SS, Zhang WF (2015) Red blood cell membrane as a biomimetic nanocoating for prolonged circulation time and reduced accelerated blood clearance. Small 11(46):6225–6236. https://doi.org/10.1002/smll.201502388

Rao L, Cai B, Bu LL, Liao QQ, Guo SS, Zhao XZ, Dong WF, Liu W (2017a) Microfluidic electroporation-facilitated synthesis of erythrocyte membrane-coated magnetic nanoparticles for enhanced imaging-guided cancer therapy. ACS Nano 11:3496–3505. https://doi.org/10.1021/acsnano.7b00133

Rao L, Meng QF, Bu LL, Cai B, Huang Q, Sun ZJ, Zhang WF, Li A, Guo SS, Liu W, Wang TH (2017b) Erythrocyte membrane coated Upconversion nanoparticles with minimal protein adsorption for enhanced tumor imaging. ACS Appl Mater Interfaces 9(3):2159–2168. https://doi.org/10.1021/acsami.6b14450

Rao L, He Z, Meng QF, Zhou Z, Bu LL, Guo SS, Liu W, Zhao XZ (2017c) Effective cancer targeting and imaging using macrophage membrane camouflaged upconversion nanoparticles. J Biomed Mater Res A 105(2):521–530. https://doi.org/10.1002/jbm.a.35927

Ren X, Zheng R, Fang X, Wang X, Zhang X, Yang W, Sha X (2016) Red blood cell membrane camouflaged magnetic nanoclusters for imaging-guided photothermal therapy. Biomaterials 92:13–24. https://doi.org/10.1016/j.biomaterials.2016.03.026

Ren H, Liu J, Li Y, Wang H, Ge S, Yuan A, Hu Y, Wu J (2017) Oxygen self-enriched nanoparticles functionalized with erythrocyte membranes for long circulation and enhanced phototherapy. Acta Biomater 59:269–282. https://doi.org/10.1016/j.actbio.2017.06.035

Subcellular fractionation protocol, Abcam 2016

Sun H, Su J, Meng Q, Yin Q, Chen L, Gu W, Zhang P, Zhang Z, Yu H, Wang S, Li Y (2016) Cancer cell biomimetic nanoparticles for targeted therapy of homotypic tumors. Adv Mater 28(43):9581–9588. https://doi.org/10.1002/adma.201602173

Suski JM, Lebiedzinska M, Wojtala A, Duszynski J, Giorgi C, Pinton P, Wieckowski MR (2014) Isolation of plasma membrane associated membranes from rat liver. Nat Protoc 9(2):312–322. https://doi.org/10.1038/nprot.2014.016

Tan MC, Chow GM, Ren L, Zhang Q (2009) Inorganic nanoparticles for biomedical applications. InNanoSci Biomed:272–289 Springer, Berlin/Heidelberg. https://doi.org/10.1007/978-3-540-49661-8_11

Tan S, Wu T, Zhang D, Zhang Z (2015) Cell or Cell Membrane-Based Drug Delivery Systems. Theranostics 5(8):863–881

Tian H, Luo Z, Liu L, Zheng M, Chen Z, Ma A, Liang R, Han Z, Lu C, Cai L (2017) Cancer cell membrane biomimetic oxygen Nanocarrier for breaking hypoxia induced Chemoresistance. Adv Funct Mater 27(38). https://doi.org/10.1002/adfm.201703197

Treffers LW, Hiemstra IH, Kuijpers TW, Berg TK, Matlung HL (2016) Neutrophils in cancer. Immunol Rev 273(1):312–328. https://doi.org/10.1111/imr.12444

Wei X, Gao J, Fang RH, Luk BT, Kroll AV, Dehaini D, Zhou J, Kim HW, Gao W, Lu W, Zhang L (2016) Nanoparticles camouflaged in platelet membrane coating as an antibody decoy for the treatment of immune thrombocytopenia. Biomaterials 111:116–123. https://doi.org/10.1016/j.biomaterials.2016.10.003

Xuan M, Shao J, Dai L, Li J, He Q (2016) Macrophage cell membrane camouflaged au nanoshells for in vivo prolonged circulation life and enhanced cancer photothermal therapy. ACS Appl Mater Interfaces 8(15):9610–9618. https://doi.org/10.1021/acsami.6b00853

Zhang L, Li R, Chen H, Wei J, Qian H, Su S, Shao J, Wang L, Qian X, Liu B (2017a) Human cytotoxic T-lymphocyte membrane-camouflaged nanoparticles combined with low-dose irradiation: a new approach to enhance drug targeting in gastric cancer. Int J Nanomedicine 12:2129 https://doi.org/10.2147%2FIJN.S126016

Zhang Y, Zhang J, Chen W, Angsantikul P, Spiekermann KA, Fang RH, Gao W, Zhang L (2017b) Erythrocyte membrane coated nanogel for combinatorial antivirulence and responsive antimicrobial delivery against Staphylococcus aureus infection. J Control Release 263:185. https://doi.org/10.1016/j.jconrel.2017.01.016

Zhu JY, Zheng DW, Zhang MK, Yu WY, Qiu WX, Hu JJ, Feng J, Zhang XZ (2016) Preferential cancer cell self-recognition and tumor self-targeting by coating nanoparticles with homotypic cancer cell membranes. Nano Lett 16(9):5895–5901. https://doi.org/10.1021/acs.nanolett.6b02786

Graphene-Based Nanomaterials and Their Applications in Biosensors

4

Young Jun Kim and Bongjin Jeong

4.1 Graphene

4.1.1 Key Properties of Graphene

Graphene has been drawing tremendous attraction since the crystal graphene had been first observed by Novoselov in 2004 based on scotch-tape method (Novoselov et al. 2004). The name of the one-atom thick 2-D material, graphene is composed of two concepts, graphite and -ene. The thickness of graphene is the separation distance of the graphite, which is 0.335 nm recording the thinnest among all the nanomaterials developed until now. Graphene is 100–300 times stronger than steel with its Young's modulus of 0.5–1.0 TPa and intrinsic strength of 130 GPa (Lee et al. 2008). The electron mobility at room temperature is 2.5×10^5 cm^2 V^{-1} s^{-1} (Mayorov et al. 2011) with tis maximum current density reaching a few million times larger than copper (Liu et al. 2007). The single atom thick crystal material has high thermal conductivity of 3000 WmK^{-1} (Balandin et al. 2008) and high optical transmittance of 97.7% (Nair et al. 2008). Rightly these superb properties contributed Nobel Prize for Physics in 2010 and have been widely used for applications including sensors, electronics, energies and biology.

Two approaches are usually applied for the synthesis of graphene, bottom-up and top-down methods. In bottom-up method graphite is oxidized under very harsh condition to produce well-dispersed graphene oxide in aqueous medium, which in turn reduced to graphene. However, the reduction process does not produce completely -reduced graphene form. The chemical process generates graphene with some defects causing to be called reduced graphene oxide instead of graphene. In the top-down method chemical vapors are crystalized on a proper substrate form single-layer graphene. However, this is not suitable for mass production process. Many different types of exfoliation methods have been developed due to advantages of producing large amount of graphene in a relatively simple process.

4.1.2 Mechanical Exfoliation

The first discovery of graphene was processed based on mechanical exfoliation method using graphite, in which graphene is stacked together linked by van der Waals force. Although the van der Waals force itself is weak the force between graphenes in graphite is very strong since the van der Waals force works all over the surface of graphene. In order to produce graphene through

Y. J. Kim (✉) · B. Jeong
BioMedicalIT Department, Electronics and Telecommunications Research Institute (ETRI), Daejeon, South Korea
e-mail: junkim@etri.re.kr; jbj0919@etri.re.kr

I. Noh (ed.), *Biomimetic Medical Materials*, Advances in Experimental Medicine and Biology 1064,
https://doi.org/10.1007/978-981-13-0445-3_4

exfoliation the van der Waals force is the first thing to overcome. Also another point to consider in exfoliation is lubricating effect in the lateral direction.

Sonication turned out to be a useful tool in exfoliation process due to advantage of producing large amount of graphene. When sonicated graphite powder is dispersed in solvents such as N, N-dimethylformamide (DMF) or N-methylpyrrolidone (NMP). However due to limit in dispersibility of graphene in those solvents, the concentration of graphene produced from sonication exfoliation is usually too low (~ 0.01 mg/mL) to be of any practical use. When the difference in surface energy between graphene and solvent is minimum, exfoliation tends to occur more easily. From the mechanistic point of view exfoliation is facilitated by liquid cavitation which in turn generates micro-bubbles. When the bubbles explode around the graphite the impulse helps to generate exfoliation process (Ciesielski and Samori 2014). However, sonication process has been reported to generate oxygen containing defects such as aldehyde, carboxylic acid, and ethers (Skaltsas et al. 2013).

Ball milling is another way for exfoliating graphite into graphene. In contrast to the sonication method where normal force is the major contributor, in the ball milling process shear force is the dominant factor. Another factor of force in the ball milling process is the balls which act on graphite through collisions. The ball milling can be processed either by wet or dry condition. In the wet process typically graphite is dispersed using solvents that are in good match with the surface energy of the graphite. Although mostly DMF and NMP are used as the matching solvents, combined use of 1-pyrenen carboxylic acid and methanol turned out to result in more efficient exfoliation than DMF alone (Aparna et al. 2013).

In spite of the scalability in production, the above-mentioned mechanical methods for exfoliation have to be developed to produce enhanced yield in monolayer graphene. Fragmentation effects also have to be reduced. In the case of sonication many interacting factors such as power, frequency, and time have to be optimized. Also detects of the graphene has to be minimized and uniformness of the product has to be enhanced.

4.1.3 Synthesis of Graphene

Although many different processes for exfoliation have been developed for large-scale production, the peeling-off method cannot avoid defects especially when it comes to producing large-scale graphene. Synthetic methods have been reported to be advantageous in this respect (Dreyer et al. 2010; Choi et al. 2010). Chemical vapor deposition (CVD) has been mostly widely used due to processibility of generating single-layer graphene over relatively large area (Li et al. 2009). For example, centimeter-scale graphene was able to be produced on a copper substrate using CVD method. Chemical synthetic method for graphene has also been widely used since the chemical wet process is suitable for large production. In the chemical process graphite is oxidized to produce graphene oxide (GO), which in turn is chemically reduced to reduced form of graphene oxide (rGO) (Li et al. 2008). Since the quality of rGO in the chemical synthetic method depends largely on the efficiency of reduction process, many different methods and reducing agents have been developed to obtain high quality rGO.

4.1.4 Characterization of Graphene

As described in the exfoliation and synthetic method for graphene, the product is usually a mixture of a single- and multi-layer of graphene. Many of the characterization methods for graphene is focused on the differentiating those species. Since, in the chemical synthetic method, GO is reduced to rGO, differentiation between these species and degree of reduction are critical aspects to be understood.

UV-visible spectroscopy can be used to identify GO and rGO. GO is characteristic of two absorption maxima (λ_{MAX}) at 234 nm and 299 nm. The shorter λ_{MAX} is attributed to π-π^* transition in the aromatic C=C bonds while the

longer λ_{MAX} is caused by n- π^* transition in C=O bonds. In the case of rGO, λ_{MAX} appears at 269 nm which corresponds to π-π^* transition in the aromatic C=C bonds. The red shift of π-π^* transition in the aromatic C=C bonds for rGO indicates more delocalization of p-orbitals when GO is reduced to rGO (Paredes et al. 2008)

Raman spectroscopy is an efficient tool to identify pristine graphite, GO and rGO. Pristine graphite shows a very sharp G peak at 1581 cm^{-1}, which is caused by the in-plane vibration in the sp^2 carbons. When graphite is oxidized, the G peak shits to 1589 cm^{-1} in somewhat broadened mode and disordered structural pattern of GO, which has been caused by oxidation, produces a D band at 1352 cm^{-1} (Wang et al. 2009a, b, c). When GO is reduced to rGO, the G peak blue-shifts to 1582 cm^{-1} which is close to the G peak from the pristine graphite. Therefor the relative peak intensity between D and G can be used to understand the degree of defect in graphene.

XPS can be effectively used to understand the extent of reduction of GO. Since oxidized form of carbons in GO occurs as C-O (ethers and hydroxyls) and C=O (carbonyl) in addition to C-C (unoxidized carbons), C atoms in GO reveals at three different energies, 284.6 eV for C-C, 286.7 eV for C-O and 288.4 eV for C=O.

Atomic force microscopy (AFM) is a useful tool to identify single-layer graphene, of which thickness is reported to be 0.32 ~ 1.2 nm. More accurate way to characterize single-layer graphene than AFM is transmission electron microscopy (TEM), in which observation of transparency and edge of the graphene directly reveals whether the graphene is single-layered, double-layered or triple-layered, as well statistical analysis of the thickness (Hernandez et al. 2008).

4.1.5 Functionalization of Graphene

Even though graphene has great potential for applications in electronics, sensors, and various composites, in order to be of any practical utility, some barriers have to be overcome such as zero band gap, low dispersibility and inertness to chemical modifications. Many different methods for functionalizing graphene have been developed to enhance the real applicability of graphene. Functionalization on graphene can be processed either through covalent bonding or through non-covalent bonding. In this review functionalization of graphene will be focused mainly on method via covalent bonding. From the organic chemistry point of view, the chemical reactions can generally be processed by condensation reaction, addition reaction and substitution reaction, which can also be subdivided into nucleophilic and electrophilic substitution reactions.

In the condensation-type modification of graphene, thionyl chloride ($SOCl_2$) chemistry is widely used to enable further functionalization on graphene. GO, which contains diverse oxygen-containing functional groups such as hydroxyl, epoxy and carboxylic groups is a good starting point to initiate functionalization process. The carboxylic acid on GO was reacted with $SOCl_2$ to generate –COCl group which is labile to various types of nucleophiles. Indeed, alkylamine (RNH_2) was reacted with –COCl to produce amide bond (-CONHR). Now the functional group R is linked with GO through amide bond, enabling the product with easy dispersibility in various types of solvents including THF, carbon tetrachloride (CCl_4) and dichloroethane (Niyogi et al. 2006). Isocynate compound (RNCO) has been used to prepare amide bone (-CONHR) via reaction with carboxylic acid. Also the functionalization enables compatibility of GO with various polymers to produce graphene-polymer composite (Stankovich et al. 2006).

Different from condensation reaction which is mostly carried out via GO, addition reaction on graphene turned out to be a useful tool to enable direction chemical modification on graphene. Diazonium salt is an effective compound to carry out functionalization on graphene via free radicals which can be generated by heating the diazonium compound. Based on this chemistry, nitrophenyl diazonium compound (BF^-_4 N^+_2-C_4H_4-NO_2) was reacted on graphene to produce nirophenyl group. The addition reaction turned out to affect conductivity of graphene by transforming sp^2 carbons to sp^3 carbons. Based on this, conductivity of graphene was able to

adjusted in a controlled manner, which in turn generated band gap on graphene making possible of applications as semiconducting materials (Sinitskii et al. 2010; Niyogi et al. 2010).

Substitution reactions can occur at epoxy groups on GO using diverse types of nucleophilic functionalities. Primary amine groups are good candidate for the purpose. Amines with varying length of alkyl groups ($C_nH_{2n}NH_2$) were used to ad alkyl groups on GO (Bourlinos et al. 2003). When the alkyl chain was relatively short (n = 2, 4, 8, 12) the reaction was able to proceed at room temperature. However, when the alkyl chain was long (n = 18) the reaction had to be refluxed to complete the reaction.

4.2 Graphene Quantum Dots (GQDs)

Graphene quantum dot (GQD) is a graphene fragmented within around 20 nm. Although semiconductor quantum dots (SQDs) have been attracting much attention, more diverse and wider applications of GQDs are limited due to problems related with cost, toxicity, biocompatibility and chemical modification. In contrast, GQDs are understood be superior to SQDs with those problems. In this section synthetic methods and optical properties of GQDs are described.

4.2.1 Synthesis of GQDs

GQDs are generally prepared in two approaches, top-down and bottom-up. In the top-down method GQDs are prepared by exfoliating graphite followed by fragmentation step. The top-down method involves harsh reaction conditions and produces GQDs with irregular morphology and wide size distribution. Graphite is usually a starting material and is converted into GO using a modified version of the Hummers procedure (Hummers and Offeman 1958), in which sulfuric acid, sodium nitrate and potassium permanganate are involved. In the case of bottom-up method very uniform GQDs are produced. However, bottom-up preparation of GQDs involves complex synthetic steps.

Many different top-down methods have been developed and the major difference among them is how GO is converted into GQDs. Hydrothermal cutting is one of the widely used top-down method, in which relatively strong basic compound such NaOH is used as scissors for the carbon precursors. Pan et al. prepared GQD with diameter of 5–13 nm in aqueous media by thermally reducing GO to graphene and chemical oxidation of the graphene followed by hydrothermal reduction to GQD (Pan et al. 2010). From a mechanistic point of view, oxidation process generates epoxy groups in linear fashion along carbon lattice, which upon further oxidation are converted to carbonyl groups. Under hydrothermal condition the linear mode of oxidation acts as defect site for to be cut to produce GQDs.

Solvothermal method was used to produce GQDs. GO in DMF was sonicated and heated at 200 °C to produce GQDs with average diameter of 5.3 nm and thickness of 1.2 nm indicating most of the GQDs are in single layered or bi-layered state. The resulting GQOs displayed strong fluorescence with photoluminescence quantum yield of 11.4% (Zhu et al. 2011).

Microwave has been utilized for synthesizing GQDs (Li et al. 2012; Zhu et al. 2010; Chen et al. 2010, 2012). Use of microwave has advantage over the hydrothermal and oxidation procedure by providing high energy rapidly and uniformly throughout the reaction medium which results in short reaction time and enhanced uniformity of GQDs. One-pot microwave approach in the absence of stabilizer was reported to produce greenish yellow luminescent GQDs from GO (Li et al. 2012). Epoxy groups were oxidized to form a line of mixture of functional groups composed of minor amount of epoxy and majority of carbonyl groups. The greenish yellow-luminescent GQDs were mostly single and bi-layered graphene with average diameter of 4.5 nm with photoluminescence (PL) quantum yield of 11.7%. By treating the GQDs with

NaBH4 blue-luminescent GQDs were obtained almost without change in dimension with PL quantum yield of 22.9%.

Electrochemical methods also have been used to prepare GQDs (Li et al. 2011; Zhang et al. 2012) based on anode oxidation and anion intercalation which in turn help exfoliate carbon anode. When graphite is used as a working electrode in the preparation of carbon dots, the high redox potential ranging from ±1.5 V to ±3 V can oxidize carbon-carbon single bond enabling oxidative cleavage (Lu et al. 2009). Also potential cycling allows the involving electrolytes to be intercalated into carbon anode. Zhang reported high yield process by exfoliating graphite based on electrochemical method. Dependency of the functionalization mode on temperature was reported. When the hydrazine reduction was processed at ambient temperature, reduction was exerted mostly on basal epoxy and hydroxyl groups. However, when the temperature was increased the reduction produced amidation on the edge carboxylic groups leading to hydrazide formation between two adjacent carboxylic groups.

In a bottom-up method, a polycyclic aromatic molecule, hexa-peri-hexabenzocoronene, was pyrolzed, oxidized and functionalized followed by reduction to produce GQDs (Liu et al. 2011). Yan et al. produced GQDs by oxidizing dendritic polyphenylene precursors. In order to provide solubility of the resulting GQDs phenyl rings were substituted with 3 long alkyl groups (Yan et al. 2010).

4.2.2 Luminescence Properties of GQDs

According to the calculation based on density function theory, the energy gap of GQDs of $\pi - \pi^*$ transition decrease as the size of GQDs increase (Eda et al. 2010). Depending on the way a graphene sheet is cut along the crystallographic direction, the edges can form zigzag or armchair mode. It is reported that types of edges affect the optoelectronic and magnetic properties of GQDs. Such size-dependent properties arise from quantum confinement effect (Chan and Nie 1998; Michalet et al. 2005; Smith and Nie 2010). In general, the smaller GQDs display luminescence at shorter wave length (Freeman and Willner 2012).

Also PL of GQDs tend to be affected by pH (Pan et al. 2010; Zhu et al. 2012). While hydrothermally prepared GQDs under basic condition display strong PL, GQDs prepared under acidic conditions show negligible PL. Under acidic conditions protonation of the zigzag edges disrupts the emissive triplet carbene state. In contrast under basic condition detachment of protons from the zigzag edges revive PL. Also PL patterns are affected by solvents and concentration of GQDs (Fan et al. 2012).

4.3 Applications of Graphene for Biosensors

4.3.1 Introduction

Many different types of sensing systems have been developed in order to maximize detection performance as well as to minimize handling procedures and the size of the sensors. Since electrical and fluorescent properties are the most prominent characteristics of graphene derivatives, sensing systems based on electrochemical and fluorescent properties of graphene have been much studied.

Use of graphene as an electrode in electrochemical applications has advantage in catalytic efficiency which is superior to that of carbon nanotube (CNT) with wide range of electrochemical potential of 2.5 V in 0.1 M PBS at pH 7.0 (Alwarappan et al. 2009). Graphene has lower - charge-transfer resistance than graphite and glass carbon electrodes (GCEs) (Zhou et al. 2009). Electrical properties of were investigated for different redox systems, $Ru(NH_3)_6^{3+/2+}$, $Fe(CN)_6^{3-/4-}$, $Fe^{3+/2+}$ and dopamine (Tang et al. 2009). Two different electrodes were compared, bare

glassy carbon (GC) and glassy carbon modified with rGO sheet film (rGSF). Much faster apparent electron-transfer rate constant (k° app) was observed on rGSF than on GC for both $Ru(NH_3)_6^{3+/2+}$, $Fe(CN)_6^{3-/4-}$.

4.3.2 Graphene-Based Immunosensors

Immunoassay takes advantage of the interaction between antibody and antigen. Enzyme-linked immunoassay (ELISA) is a standard clinical diagnostic method, in which a capture antibody is in complexation with an antigen and a detection antibody in a sandwich-type fashion. One of the key factors for high sensitivity in electrochemical detection is how efficient the electron transfer is on the electrode surface. Highly conductive property of graphene is well suited for this purpose and much application has been developed to enhance the electrical conductivity on electrode surface by using graphene as surface modification medium. Many different types of protein-based cancer biomarkers have been detected using electrochemical immunoassay. Alpha-fetoprotein (AFP), a biomarker for hepatocellular cancer, was assayed on graphene-modified electrode in the hope of enhancing sensing performance by facilitating electron transfer rate of the electrode using graphene (Du et al. 2010).

Ultrasensitive immunoassay was processed by generating polyaniline (PAN) via catalysis with Horse-radish peroxidase (HRP)-conjugated AuNP (HRP-AuNP) (Fig. 4.1) (Lai et al. 2014). In the presence of poly(diallyldimethylammonium chloride) (PDDA) GO was reduced by hydrazine to produce composite of rGO/PDDA. AuNPs were mixed with the composite of rGO/PDDA to prepare rGO/AuNP. The rGO/AuNP was dispersed in water to be dropped on the screen-printed carbon electrode (SPCE), onto which anti-human IgG(anti-HIgG) was added. Due to high surface area of the rGO/AuNP nanocomposite provides large amount of anti-HIgG may be position, which would lead to highly sensitive assay system. In order to process immunoassay, HIgG was added followed by HRP-conjugated AuNP to form sandwich-typed complexation. Aniline monomer and H_2O_2 were added to form PAN. The aniline monomers are polymerized through catalysis by HRP oxidation of aniline by HRP-AuNP. Thus produced PAN is electrochemically determined for immunoassay. The nanocomposite system was reported to be able to detect 9.7 pg/mL of IgG with dynamic range covering 4 orders of magnitude. Such a high sensitivity is reported to have been contributed by the amplification effect of HRP-AuNP and the acceleration of electron transfer by rGO/AuNP.

Ultrasensitive electrochemical immunoassay system (limit of detection 100 fg/mL, 700aM) was reported using rGO (Fig. 4.2) (Monsur et al. 2012). Indium tin oxide (ITO) electrode was functionalized with amine group using amine-functionalized benzenediazonium. The amine functionalized ITO surface was coated with GO, in which the primary amine on the ITO surface was reacted with carboxylic acid positioned at the edge of GO. Then the GO on the ITO surface was electrochemically reduced to prepare rGO on ITO surface. Using π-π interaction of the aromatic rings positioned between ITO surface and polymer, the N-acryloxysuccinimide-functionalized poly(BMA-r-PEGMA-r-NAS) was coated on the rGO surface. IgG was tethered on the polymer coating through reaction of the primary amines in IgG with N-succinimide in the polymer. Then ELISA was processed via sandwich-type complexation with antigen and HRP-labeled secondary anti-IgG.

GQDs were used for immunoassay taking advantage of the unique luminescent and resonance energy transfer (RET) properties of GQDs to recognize 10 ng/mL of human IgG (Fig. 4.3) (Zhao et al. 2013). When mouse anti-human immunoglobulin G (mIgG) functionalized GQDs came in contact with graphene, the luminescent GQDs became quenched through π-π*

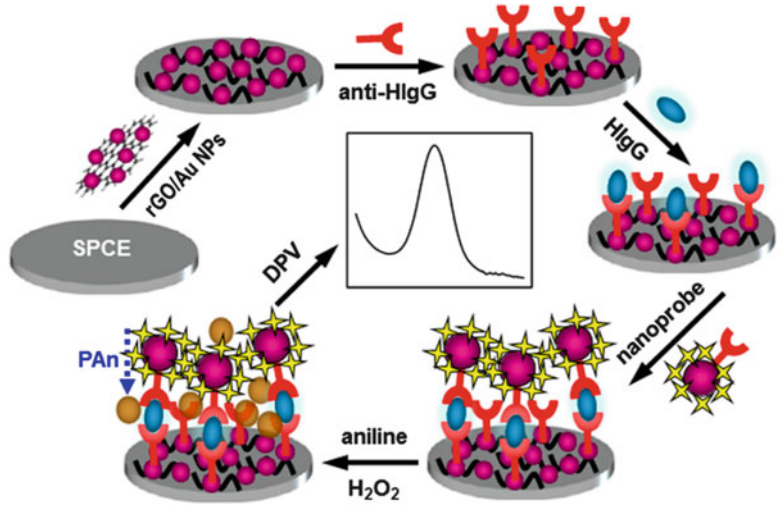

Fig. 4.1 Schematic view of the preparation for ultrasensitive detection of IgG based on rGO/AuNP system. (Lai et al. 2014. Copyright © Lai et al.)

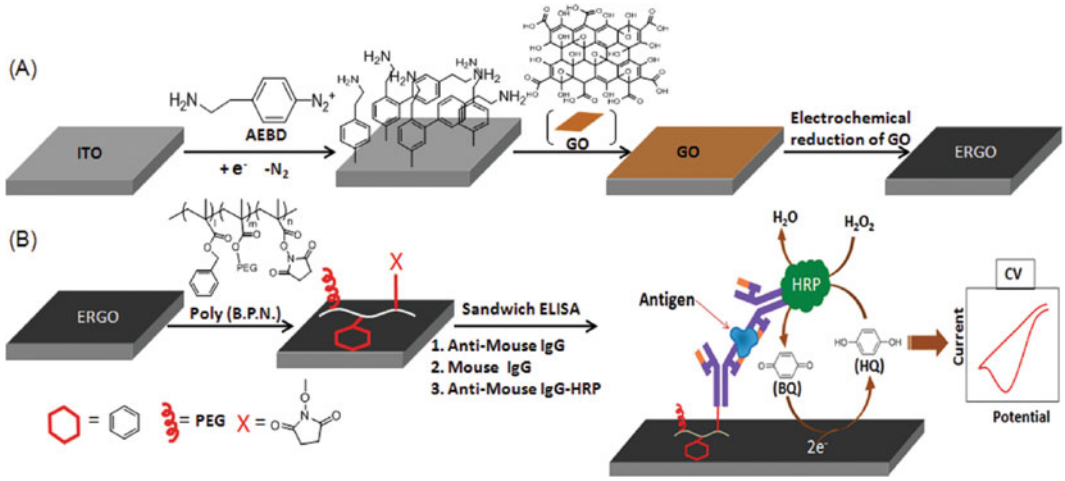

Fig. 4.2 Schematic view of the preparation and working principle for the ultrasensitive electrochemical immunoassay. (Monsur et al. 2012 Copyright © Monsur et al.)

stacking interaction. To this quenched system human IgG was added to restore some degree of luminescence caused by interruption of the π-π* stacking interaction due to the intervening IgG.

4.3.3 Graphene-Based Detection of Oligonucleotides

DNA also can be recognized on graphene-based electrode via electrochemical analysis. Graphene-based electrode can catalytically oxidize the four DNA bases, A, G, C, and T, enabling direct detection of a single-nucleotide polymorphism (SNPP in a short oligonucleotide (Zhou et al. 2009). Immobilization of single-stand DNA can be processed either through adsorption or covalent bonding. Simple adsorption of single-strand DNA were processed on GO or rGO. Reduction of GO was processed electrochemically (Giovanni et al. 2012), thermally (Yang et al. 2013) or polyaniline-electrochemically (Wang et al. 2011). Covalent immobilization of DNA was processed by reacting amine-functionalized

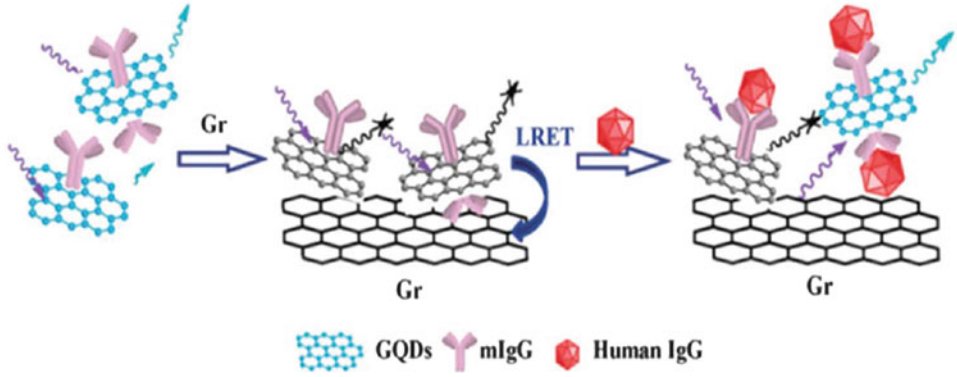

Fig. 4.3 GQD as an immunoassay system via luminescence resonance energy transfer (LRET). (Zhao et al. 2013. Copyright © Zhao et al.)

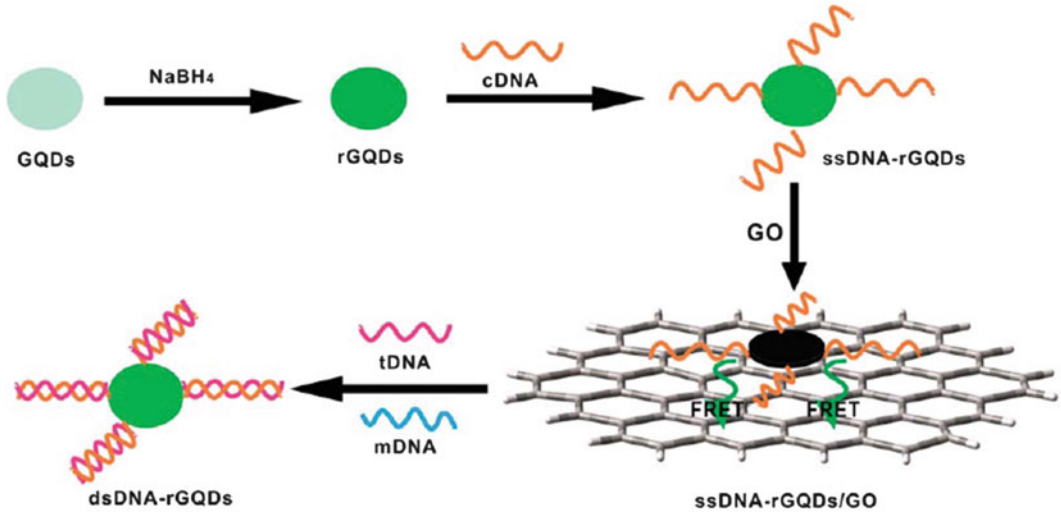

Fig. 4.4 GQDs-based DNA detection system based on fluorescence resonance energy transfer (FRET). (Qian et al. 2014. Copyright © Qian Z S et al.)

DNA on the oxygen containing rGO via carbodiimide (Bonanni et al. 2012).

Quain et al. reported fluorescence resonance energy transfer (FRET)-based DNA assay with limit of detection (LOD) of 75 pM and dynamic range of 6.7 ~ 46 nM (Fig. 4.4.) (Qian et al. 2014). GQDs were treated with $NaBH_4$ to produce reduced GQDs (rGQDs), which can fluorescence prominently. Single-strand DNA (ssDNA) probes were tethered on rGQDs (ssDNA-rGQDs) through condensation reaction. The ssDNA-rGQDs came in contact with GO through π-π interaction leading to fluorescence quenching. When target DNA was added to form double-strand DNA (dsDNA), the dsDNA interrupts the π-π interaction to detach ssDNA-rGQDs from GO leading to restoring of fluorescence.

Zhang et al. presented a molecular beacon (MB)-based miroRNA detection system utilizing GQDs (Fig. 4.5) (Zhang et al. 2015). Molecular beacons are oligonucleotides designed with stem and loop structures (Broude 2002; Wang et al. 2009a; Stobiecka and Chałupa 2015; Tang et al. 2009). The oligonucleotides are equipped with a fluorophore at one end and a quencher at the other. MicroRNAs were able to be

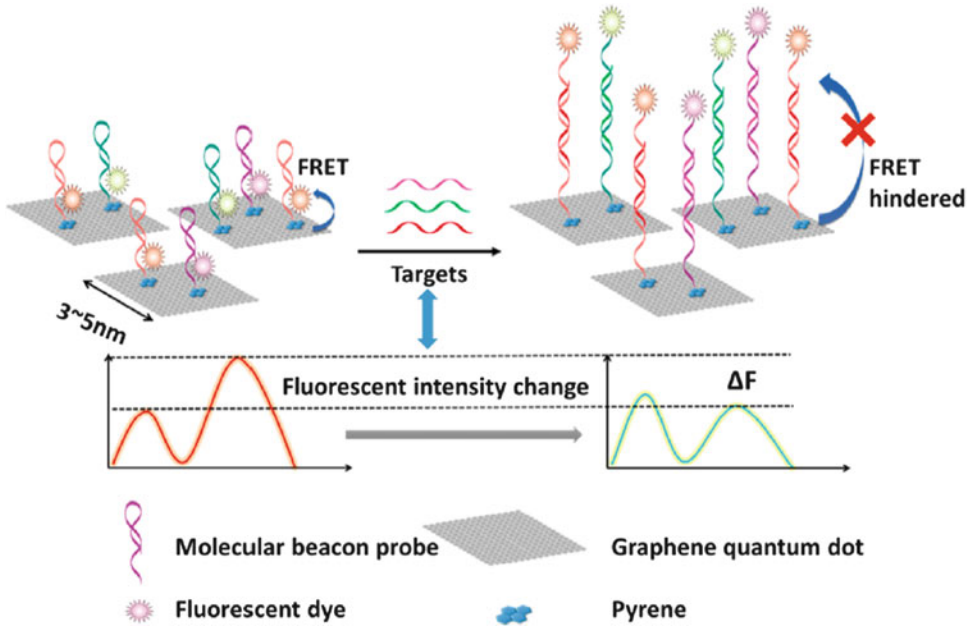

Fig. 4.5 Schematic view illustrating the detection mechanism of the py-MB detection system. (Zhang et al. 2015. Copyright © Zhang H et al.)

analyzed with LOD of 100 pM and dynamic range of 0.1 ~ 200 nM. Pyrene-functionalized MB (py-MB) probes were prepared with 5′ modification on pyrene and 3′ modification of the fluorescence dyes, Cy3 and Cy5, while leaving the loop part of the sequence complementary to the target miRNA. The π-π interaction between pyrene part of the py-MBs and GQDs tethers the py-MBs on GQDs. When no target miRNAs came in contact with the probe py-MBs, FRET occurs between GQDs and the fluorescence dyes. However, when target miRNAs are added, double strands are formed preventing FRET from occurring.

References

Alwarappan S, Erdem A, Liu C, Li C-Z (2009) Probing the electrochemical properties of graphene Nanosheets for biosensing applications. J Phys Chem C 113 (20):8853–8857. https://doi.org/10.1021/jp9010313

Aparna R, Sivakumar N, Balakrishnan A, Nair AS, Nair SV, Subramanian KRV (2013) An effective route to produce few-layer graphene using combinatorial ball milling and strong aqueous exfoliants. J Renew Sustain Energy 5(3):033123–033123. https://doi.org/10.1063/1.4809794

Balandin AA, Ghosh S, Bao W, Calizo I, Teweldebrhan D, Miao F, Lau CN (2008) Superior thermal conductivity of single-layer graphene. Nano Lett 8(3):902–907. https://doi.org/10.1021/nl0731872

Bonanni A, Ambrosi A, Pumera M (2012) On oxygen-containing groups in chemically modified Graphenes. Chem Eur J 18(15):4541–4548. https://doi.org/10.1002/chem.201104003

Bourlinos AB, Gournis D, Petridis D, Szabó T, Szeri A, Dékány I (2003) Graphite oxide: chemical reduction to graphite and surface modification with primary aliphatic amines and amino acids. Langmuir 19 (15):6050–6055. https://doi.org/10.1021/la026525h

Broude NE (2002) Stem-loop oligonucleotides: a robust tool for molecular biology and biotechnology. Trends Biotechnol 20(6):249–256. https://doi.org/10.1016/S0167-7799(02)01942-X

Chan WCW, Nie S (1998) Quantum dot bioconjugates for ultrasensitive nonisotopic detection. Science 281 (5385):2016–2018. https://doi.org/10.1126/science.281.5385.2016

Chen W, Yan L, Bangal PR (2010) Preparation of graphene by the rapid and mild thermal reduction of graphene oxide induced by microwaves. Carbon 48 (4):1146–1152. https://doi.org/10.1016/j.carbon.2009.11.037

Chen S, Liu J-W, Chen M-L, Chen X-W, Wang J-H (2012) Unusual emission transformation of graphene quantum dots induced by self-assembled aggregation. Chem Commun 48(61):7637–7639. https://doi.org/10.1039/C2CC32984K

Choi W, Lahiri I, Seelaboyina R, Kang YS (2010) Synthesis of graphene and its applications: a review. Crit Rev Solid State Mater Sci 35(1):52–71. https://doi.org/10.1080/10408430903505036

Ciesielski A, Samori P (2014) Graphene via sonication assisted liquid-phase exfoliation. Chem Soc Rev 43 (1):381–398. https://doi.org/10.1039/C3CS60217F

Dreyer DR, Park S, Bielawski CW, Ruoff RS (2010) The chemistry of graphene oxide. Chem Soc Rev 39 (1):228–240. https://doi.org/10.1039/B917103G

Du D, Zou Z, Shin Y, Wang J, Wu H, Engelhard MH, Liu J, Aksay IA, Lin Y (2010) Sensitive Immunosensor for Cancer biomarker based on dual signal amplification strategy of graphene sheets and multienzyme functionalized carbon Nanospheres. Anal Chem 82(7):2989–2995. https://doi.org/10.1021/ac100036p

Eda G, Lin Y-Y, Mattevi C, Yamaguchi H, Chen H-A, Chen IS, Chen C-W, Chhowalla M (2010) Blue photoluminescence from chemically derived graphene oxide. Adv Mater 22(4):505–509. https://doi.org/10.1002/adma.200901996

Fan L, Hu Y, Wang X, Zhang L, Li F, Han D, Li Z, Zhang Q, Wang Z, Niu L (2012) Fluorescence resonance energy transfer quenching at the surface of graphene quantum dots for ultrasensitive detection of TNT. Talanta 101(Suppl C):192–197. https://doi.org/10.1016/j.talanta.2012.08.048

Freeman R, Willner I (2012) Optical molecular sensing with semiconductor quantum dots (QDs). Chem Soc Rev 41(10):4067–4085. https://doi.org/10.1039/C2CS15357B

Giovanni M, Bonanni A, Pumera M (2012) Detection of DNA hybridization on chemically modified graphene platforms. Analyst 137(3):580–583. https://doi.org/10.1039/C1AN15910K

Hernandez Y, Nicolosi V, Lotya M, Blighe FM, Sun Z, De S, McGovern IT, Holland B, Byrne M, Gun'Ko YK, Boland JJ, Niraj P, Duesberg G, Krishnamurthy S, Goodhue R, Hutchison J, Scardaci V, Ferrari AC, Coleman JN (2008) High-yield production of graphene by liquid-phase exfoliation of graphite. Nat Nanotechnol 3:563–568. https://doi.org/10.1038/nnano.2008.215

Hummers WS, Offeman RE (1958) Preparation of graphitic oxide. J Am Chem Soc 80(6):1339–1339. https://doi.org/10.1021/ja01539a017

Lai G, Zhang H, Tamanna T, Yu A (2014) Ultrasensitive immunoassay based on electrochemical measurement of enzymatically produced polyaniline. Anal Chem 86 (3):1789–1793. https://doi.org/10.1021/ac4037119

Lee C, Wei X, Kysar JW, Hone J (2008) Measurement of the elastic properties and intrinsic strength of monolayer graphene. Science 321(5887):385–388. https://doi.org/10.1126/science.1157996

Li D, Müller MB, Gilje S, Kaner RB, Wallace GG (2008) Processable aqueous dispersions of graphene nanosheets. Nat Nanotechnol 3:101–105. https://doi.org/10.1038/nnano.2007.451

Li X, Cai W, An J, Kim S, Nah J, Yang D, Piner R, Velamakanni A, Jung I, Tutuc E, Banerjee SK, Colombo L, Ruoff RS (2009) Large-area synthesis of high-quality and uniform graphene films on copper foils. Science 324(5932):1312–1314. https://doi.org/10.1126/science.1171245

Li Y, Hu Y, Zhao Y, Shi G, Deng L, Hou Y, Qu L (2011) An electrochemical avenue to green-luminescent graphene quantum dots as potential Electron-acceptors for photovoltaics. Adv Mater 23(6):776–780. https://doi.org/10.1002/adma.201003819

Li L-L, Ji J, Fei R, Wang C-Z, Lu Q, Zhang J-R, Jiang L-P, Zhu J-J (2012) A facile microwave avenue to Electrochemiluminescent two-color graphene quantum dots. Adv Funct Mater 22(14):2971–2979. https://doi.org/10.1002/adfm.201200166

Liu F, Ming P, Li J (2007) Ab initio. Phys Rev B 76 (6):064120–064120

Liu R, Wu D, Feng X, Müllen K (2011) Bottom-up fabrication of Photoluminescent graphene quantum dots with uniform morphology. J Am Chem Soc 133 (39):15221–15223. https://doi.org/10.1021/ja204953k

Lu J, J-x Y, Wang J, Lim A, Wang S, Loh KP (2009) One-pot synthesis of fluorescent carbon nanoribbons, nanoparticles, and graphene by the exfoliation of graphite in ionic liquids. ACS Nano 3(8):2367–2375. https://doi.org/10.1021/nn900546b

Mayorov AS, Gorbachev RV, Morozov SV, Britnell L, Jalil R, Ponomarenko LA, Blake P, Novoselov KS, Watanabe K, Taniguchi T, Geim AK (2011) Micrometer-scale ballistic transport in encapsulated graphene at room temperature. Nano Lett 11 (6):2396–2399. https://doi.org/10.1021/nl200758b

Michalet X, Pinaud FF, Bentolila LA, Tsay JM, Doose S, Li JJ, Sundaresan G, Wu AM, Gambhir SS, Weiss S (2005) Quantum dots for live cells, in vivo imaging, and diagnostics. Science 307(5709):538–544. https://doi.org/10.1126/science.1104274

Monsur A, Haque J, Park H, Sung D, Jon S, Choi S-Y, Kim K (2012) An electrochemically reduced graphene oxide-based electrochemical Immunosensing platform for ultrasensitive antigen detection. Anal Chem 84:1871−1878. https://doi.org/10.1021/ac202562v

Nair RR, Blake P, Grigorenko AN, Novoselov KS, Booth TJ, Stauber T, Peres NMR, Geim AK (2008) Fine structure constant defines visual transparency of graphene. Science 320(5881):1308–1308. https://doi.org/10.1126/science.1156965

Niyogi S, Bekyarova E, Itkis ME, McWilliams JL, Hamon MA, Haddon RC (2006) Solution properties of graphite and graphene. J Am Chem Soc 128(24):7720–7721. https://doi.org/10.1021/ja060680r

Niyogi S, Bekyarova E, Itkis ME, Zhang H, Shepperd K, Hicks J, Sprinkle M, Berger C, Lau CN, deHeer WA, Conrad EH, Haddon RC (2010) Spectroscopy of covalently functionalized graphene. Nano Lett 10 (10):4061–4066. https://doi.org/10.1021/nl1021128

Novoselov KS, Geim AK, Morozov SV, Jiang D, Zhang Y, Dubonos SV, Grigorieva IV, Firsov AA

(2004) Electric field effect in atomically thin carbon films. Science 306(5696):666–669. https://doi.org/10.1126/science.1102896

Pan D, Zhang J, Li Z, Wu M (2010) Hydrothermal route for cutting graphene sheets into blue-luminescent graphene quantum dots. Adv Mater 22(6):734–738. https://doi.org/10.1002/adma.200902825

Paredes JI, Villar-Rodil S, Martínez-Alonso A, Tascón JMD (2008) Graphene oxide dispersions in organic solvents. Langmuir 24(19):10560–10564. https://doi.org/10.1021/la801744a

Qian ZS, Shan XY, Chai LJ, Ma JJ, Chen JR, Feng H (2014) A universal fluorescence sensing strategy based on biocompatible graphene quantum dots and graphene oxide for the detection of DNA. Nanoscale 6(11):5671–5674. https://doi.org/10.1039/C3NR06583A

Sinitskii A, Dimiev A, Corley DA, Fursina AA, Kosynkin DV, Tour JM (2010) Kinetics of Diazonium functionalization of chemically converted graphene nanoribbons. ACS Nano 4(4):1949–1954. https://doi.org/10.1021/nn901899j

Skaltsas T, Ke X, Bittencourt C, Tagmatarchis N (2013) Ultrasonication induces oxygenated species and defects onto exfoliated graphene. J Phys Chem C 117 (44):23272–23278. https://doi.org/10.1021/jp4057048

Smith AM, Nie S (2010) Semiconductor nanocrystals: structure, properties, and band gap engineering. Acc Chem Res 43(2):190–200. https://doi.org/10.1021/ar9001069

Stankovich S, Dikin DA, Dommett GHB, Kohlhaas KM, Zimney EJ, Stach EA, Piner RD, Nguyen ST, Ruoff RS (2006) Graphene-based composite materials. Nature 442:282–286. https://doi.org/10.1038/nature04969

Stobiecka M, Chałupa A (2015) Biosensors based on molecular beacons. Chem Pap 69(1):62–76. https://doi.org/10.1515/chempap-2015-0026

Tang L, Wang Y, Li Y, Feng H, Lu J, Li J (2009) Preparation, structure, and electrochemical properties of reduced graphene sheet films. Adv Funct Mater 19 (17):2782–2789. https://doi.org/10.1002/adfm.200900377

Wang J, Chen J, Chang P, LeBlanc A, Li D, Abbruzzesse JL, Frazier ML, Killary AM, Sen S (2009a) MicroRNAs in plasma of pancreatic ductal adenocarcinoma patients as novel blood-based biomarkers of disease. Cancer Prev Res 2(9):807–813. https://doi.org/10.1158/1940-6207.capr-09-0094

Wang H, Robinson JT, Li X, Dai H (2009b) Solvothermal reduction of chemically exfoliated graphene sheets. J Am Chem Soc 131(29):9910–9911. https://doi.org/10.1021/ja904251p

Wang K, Tang Z, Yang CJ, Kim Y, Fang X, Li W, Wu Y, Medley CD, Cao Z, Li J, Colon P, Lin H, Tan W (2009c) Molecular engineering of DNA: molecular beacons. Angew Chem Int Ed 48(5):856–870. https://doi.org/10.1002/anie.200800370

Wang Z, Zhang J, Chen P, Zhou X, Yang Y, Wu S, Niu L, Han Y, Wang L, Chen P, Boey F, Zhang Q, Liedberg B, Zhang H (2011) Label-free, electrochemical detection of methicillin-resistant staphylococcus aureus DNA with reduced graphene oxide-modified electrodes. Biosens Bioelectron 26(9):3881–3886. https://doi.org/10.1016/j.bios.2011.03.002

Yan X, Cui X, Li L-s (2010) Synthesis of large, stable colloidal graphene quantum dots with tunable size. J Am Chem Soc 132(17):5944–5945. https://doi.org/10.1021/ja1009376

Yang T, Li Q, Li X, Wang X, Du M, Jiao K (2013) Freely switchable impedimetric detection of target gene sequence based on synergistic effect of ERGNO/PANInanocomposites. Biosens Bioelectron 42(Suppl C):415–418. https://doi.org/10.1016/j.bios.2012.11.007

Zhang M, Bai L, Shang W, Xie W, Ma H, Fu Y, Fang D, Sun H, Fan L, Han M, Liu C, Yang S (2012) Facile synthesis of water-soluble, highly fluorescent graphene quantum dots as a robust biological label for stem cells. J Mater Chem 22(15):7461–7467. https://doi.org/10.1039/C2JM16835A

Zhang H, Wang Y, Zhao D, Zeng D, Xia J, Aldalbahi A, Wang C, San L, Fan C, Zuo X, Mi X (2015) Universal fluorescence biosensor platform based on graphene quantum dots and pyrene-functionalized molecular beacons for detection of MicroRNAs. ACS Appl Mater Interfaces 7(30):16152–16156. https://doi.org/10.1021/acsami.5b04773

Zhao H, Chang Y, Liu M, Gao S, Yu H, Quan X (2013) A universal immunosensing strategy based on regulation of the interaction between graphene and graphene quantum dots. Chem Commun 49(3):234–236. https://doi.org/10.1039/C2CC35503E

Zhou M, Zhai Y, Dong S (2009) Electrochemical sensing and biosensing platform based on chemically reduced graphene oxide. Anal Chem 81(14):5603–5613. https://doi.org/10.1021/ac900136z

Zhu Y, Murali S, Stoller MD, Velamakanni A, Piner RD, Ruoff RS (2010) Microwave assisted exfoliation and reduction of graphite oxide for ultracapacitors. Carbon 48(7):2118–2122. https://doi.org/10.1016/j.carbon.2010.02.001

Zhu S, Zhang J, Qiao C, Tang S, Li Y, Yuan W, Li B, Tian L, Liu F, Hu R, Gao H, Wei H, Zhang H, Sun H, Yang B (2011) Strongly green-photoluminescent graphene quantum dots for bioimaging applications. Chem Commun 47(24):6858–6860. https://doi.org/10.1039/C1CC11122A

Zhu S, Zhang J, Liu X, Li B, Wang X, Tang S, Meng Q, Li Y, Shi C, Hu R, Yang B (2012) Graphene quantum dots with controllable surface oxidation, tunable fluorescence and up-conversion emission. RSC Adv 2 (7):2717–2720. https://doi.org/10.1039/C2RA20182H

Graphene-Functionalized Biomimetic Scaffolds for Tissue Regeneration

5

Yong Cheol Shin, Su-Jin Song, Suck Won Hong, Jin-Woo Oh, Yu-Shik Hwang, Yu Suk Choi, and Dong-Wook Han

5.1 Introduction

Tissues of animals, including human beings, are in principle classified into four types based on their origin and function: connective, muscular, nervous, and epithelial tissues. The tissues are fundamental and essential components of the body, and sometimes they can be injured as they are frequently used depending on each function. A mild damage can be healed naturally, but a severe injury is quite difficult to naturally heal, leads to serious health implications. In recent years, a tissue engineering approach has emerged as a new approach to healing these severely damaged tissues. In tissue engineering approaches, biomimetic scaffolds, which can not only structurally support, but can also functionally promote cell behaviors, are designed and developed for promoting tissue regeneration (Langer and Vacanti 1993; Dvir et al. 2011). Up to now, many scaffolds having various structures and compositions have been developed and employed for biomedical applications, and a variety of bioactive materials has been further functionalized into the scaffolds in order to improve their biofunctionality (Vasita and Katti 2006; Zhao et al. 2013; O'Brien 2011; Dvir et al. 2011; Guo et al. 2015; Wolf et al. 2015; Shin et al. 2016b). In addition to various biomolecules possessing diverse biological and pharmacological activities, such as proteins, peptides, lipids, carbohydrates, and nucleic acids, more recent efforts have focused on the potentials of nanomaterials. The term "*nanomaterials*" are commonly defined as materials with smaller than 100 nm in size at least one dimension, including thickness, width, length, or diameter (MacDiarmid 2001; Hood 2004; Shin et al. 2017d). The nanomaterials exhibit unique properties that are not observed in the bulk materials composed of the same components (Valiev 2002; Dobrovolskaia and McNeil 2007; Liu and Webster 2007; Ray 2010; Zhou et al. 2011; Lin et al. 2012; Cherukula et al. 2016). Therefore, there is a rapidly growing interest in the potentials of nanomaterials.

Y. C. Shin
Research Center for Energy Convergence Technology, Pusan National University, Busan, South Korea

S.-J. Song · S. W. Hong · D.-W. Han (✉)
Department of Cogno-Mechatronics Engineering, College of Nanoscience & Nanotechnology, Pusan National University, Busan, South Korea
e-mail: swhong@pusan.ac.kr; nanohan@pusan.ac.kr

J.-W. Oh
Department of Nanoenergy Engineering, College of Nanoscience & Nanotechnology, Pusan National University, Busan, South Korea
e-mail: ojw@pusan.ac.kr

Y.-S. Hwang
Department of Maxillofacial Biomedical Engineering, School of Dentistry, Kyung Hee University, Seoul, South Korea
e-mail: yshwang@khu.ac.kr

Y. S. Choi
School of Human Sciences, University of Western Australia, Crawley, WA, Australia
e-mail: yusuk.choi@uwa.edu.au

I. Noh (ed.), *Biomimetic Medical Materials*, Advances in Experimental Medicine and Biology 1064,
https://doi.org/10.1007/978-981-13-0445-3_5

Graphene and its derivatives are one of the promising nanomaterials, and there have been tremendous efforts to explore their potentials and possible applications in various fields, such as biology, chemistry, physics, and nanoscience. Graphene is a two-dimensional (2D) atomic layer of graphite, where carbon atoms are assembled in a honeycombed lattice structure. The graphene nanomaterials can be categorized into three primary groups, including graphene, graphene oxide (GO) and reduced graphene oxide (rGO). These graphene family nanomaterials have been reported to have unique characteristics, such as remarkable electrical, mechanical, biological, and chemical properties (Gómez-Navarro et al. 2008; Tang et al. 2009; Wang et al. 2011; Sanchez et al. 2011; Papageorgiou et al. 2017). In particular, GO and rGO have oxygen-containing functional groups on their surface, results in facilitated interactions with cells or biomolecules (Nayak et al. 2011; Lee et al. 2011; Yue et al. 2012). In addition, the oxygen-containing functional groups allow graphene family nanomaterials to be easily incorporated with scaffold materials, which in turn, they can afford the opportunity to fabricate desirable tissue engineering scaffolds having the distinctive advantages of graphene family nanomaterials. Moreover, it has been reported that the graphene family nanomaterials can be used as stimulating factors for not only promoting cellular behaviors, but also for enhancing the differentiation of various cells towards particular lineages, including neurogenic, osteogenic, chondrogenic, myogenic, and adipogenic lineages (Ruiz et al. 2011; Kalbacova et al. 2010; Lee et al. 2011, 2015a, c; Park et al. 2011; Li et al. 2013; Nayak et al. 2011; Ku and Park 2013; Shin et al. 2015a; Patel et al. 2016b; Seong et al. 2010) (Fig. 5.1). Therefore, substantial efforts have been devoted to designing and developing graphene family nanomaterial-functionalized biomimetic scaffolds for tissue engineering and tissue regeneration.

Herein, we are attempting to provide an overview of recent findings in the fields of tissue regeneration concerning the graphene family nanomaterial-functionalized biomimetic scaffolds, and to highlight the promising perspectives for the possible applications of graphene family nanomaterials.

5.2 Skin Tissue Regeneration

Skin is a complex organ mainly consisting of epithelial and connective tissues, and it is composed of three distinct layers of epidermis, dermis and subcutaneous fat layers. The skin covers whole body, and it plays a primary role in protecting our body from external pathogens and damages. Because skin is the primary defense mechanism against surrounding environment, it is vulnerable to injury. In case of severe skin damages, it takes a long time to heal and requires additional surgical treatment. Therefore, a lot of efforts have been made to effectively heal the serious skin damage, and many commercially available products have been developed. Nonetheless, there are still some limitations in healing widespread or deep wounds (i.e., full-thickness wounds), and intensive efforts have been under way to accelerate the healing process through a tissue engineering approach (Lu et al. 2012; Collins and Birkinshaw 2013; Chaudhari et al. 2016; Zhou et al. 2016b; Shin et al. 2016b; Yin et al. 2016; Ho et al. 2017).

To provide suitable microenvironments for wound healing, most scaffolds are generally fabricated in the form of a 3D porous network structure or hydrogel for mimicking the natural extracellular matrix (Li et al. 2002; Drury and Mooney 2003; Li and Xia 2004; Murugan and Ramakrishna 2006; Teo and Ramakrishna 2006; Liu et al. 2012; Norouzi et al. 2015). It has been commonly believed for a long time that the collagen, the main component of extracellular matrix, is the most suitable materials for scaffolds, but during recent years, many studies have focused on the biomimetic composite scaffolds fabricated using various biodegradable polymers and bioactive materials. Graphene family nanomaterials have also attracted a great attention as a novel candidate for scaffold materials, which can promote skin tissue regeneration (Fan et al. 2010; Lu et al. 2012; Shin et al. 2013; Lee et al. 2014; Nishida et al. 2014; Cha et al. 2014; Sayyar

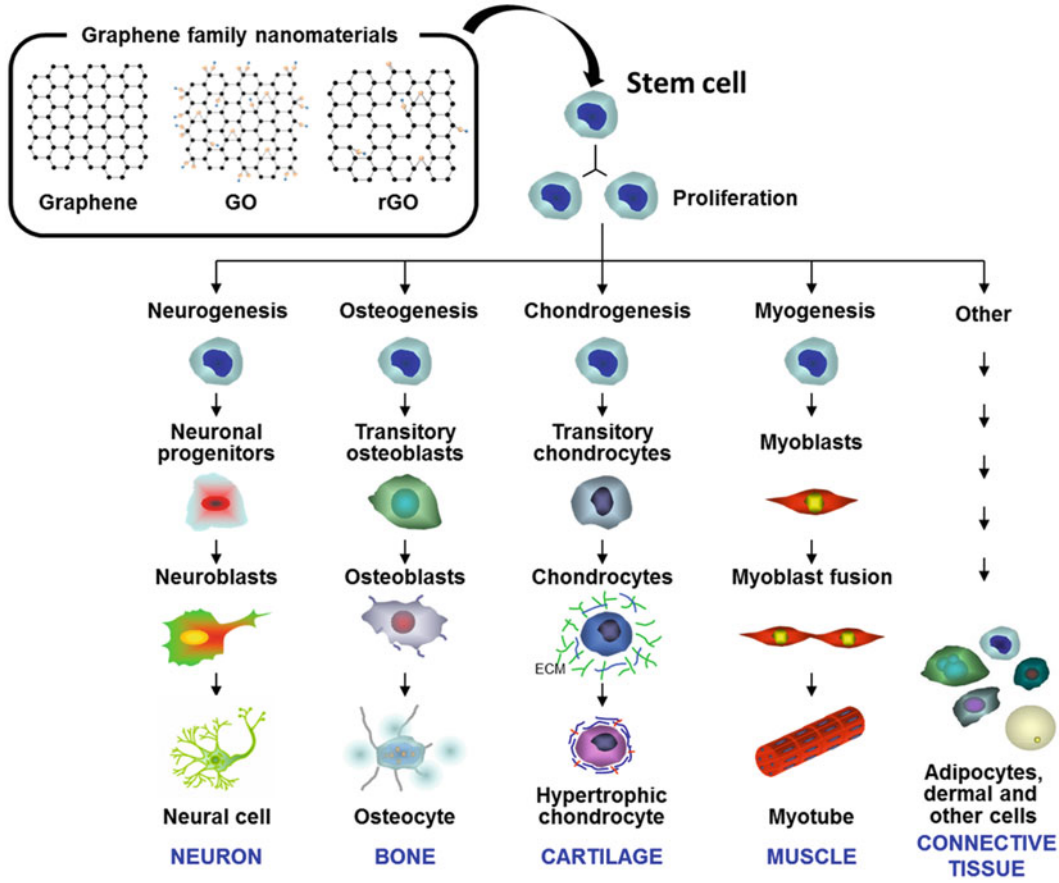

Fig. 5.1 Stimulating effects of graphene family nanomaterials on the differentiation of various cells. (Reproduced from Seong et al. 2010, Copyright (2010) IOP Publishing Ltd.)

et al. 2015; Murray et al. 2015; Zhang et al. 2016a; Unnithan et al. 2016).

Graphene and its derivatives can be easily incorporated into polymer scaffolds. Lu et al. and Lee et al. proved that graphene- or GO-incorporated composite scaffolds were successfully fabricated by electrospinning, and the composite scaffolds were beneficial to cell growth and wound healing (Lu et al. 2012; Lee et al. 2014). Lu et al. revealed that the polyvinyl alcohol (PVA) and chitosan scaffolds containing graphene have higher healing effects on the skin wounds of mice and rabbits than PVA-chitosan scaffolds without graphene (Fig. 5.2). In addition, they proposed a possible wound healing mechanism of graphene. The graphene is composed of carbon atoms arranged in a hexagonal lattice structure, leads to a different electron transfer process towards cells (Lu et al. 2012). Although an electron can be easily transferred from graphene into cells because of the cell membrane potential, the electron movement is dependent on the cell types. In case of eukaryotic cells, the electrons escaping from graphene are difficult to enter the nucleus because of the nuclear membrane, and thus they cannot affect DNA or other genetic materials of eukaryotic cells. Whereas since there is no nuclear membrane in prokaryotic cells, electrons are able to easily enter their nucleus, which can damage DNA or other genetic materials of prokaryotes. In general, the microbes, which inhibit the wound healing process, are prokaryotic cells, which in turn, the damages and impeded proliferations of

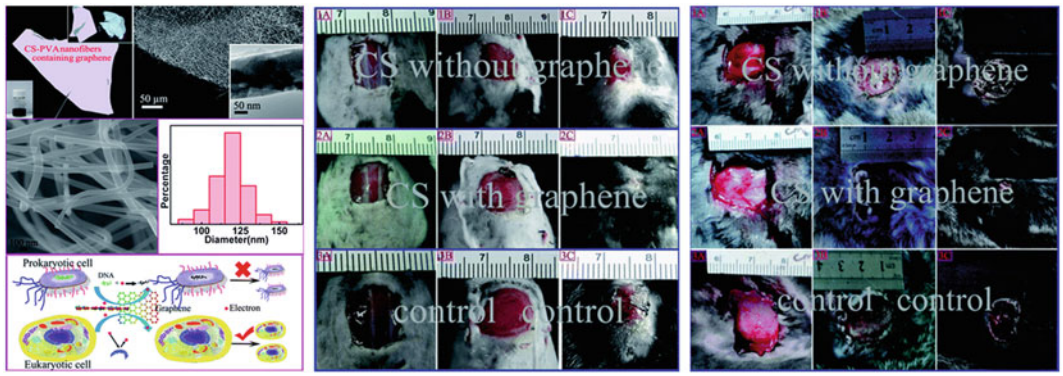

Fig. 5.2 Wound healing effects of PVA-chitosan scaffolds containing graphene in mice and rabbits models and possible wound healing mechanism of graphene. (Reproduced from Lu et al. 2012, Copyright (2012) Royal Society of Chemistry) *Abbreviations: *CS* chitosan, *PVA* polyvinyl alcohol

prokaryotic cells by graphene are beneficial to the wound healing. On the other hand, the GO can also promote wound healing by enhancing the growth of fibroblasts (Lee et al. 2014). The GO-functionalized scaffolds have a more hydrophilic surface and a higher surface energy than hydrophobic polymer scaffolds due to the hydrophilic groups of GO, such as hydroxyl, carboxyl, carbonyl, and epoxy groups. These increases in surface hydrophilicity can promote the cell adhesion and proliferation of dermal fibroblasts, which can benefit skin wound healing.

In order for composite materials to be used as scaffolds for tissue regeneration, they should have suitable and tunable mechanical properties. The excellent mechanical properties are one of the major advantages of graphene family nanomaterials, which enable them to be employed as scaffold materials, and the functionalization of graphene materials has been found to reinforce polymer hydrogel composites (Fan et al. 2010; Shin et al. 2013; Cha et al. 2014). Various types of hydrogels have been extensively utilized as scaffold materials for tissue regeneration, because they can provide a 3D microenvironment, which is structurally similar to the natural extracellular matrix. However, the increasing the cross-linking density to obtain high mechanical properties of hydrogels can sometimes reduce the permeability and biodegradability of hydrogels due to the dense pore structure of hydrogels, and it is also not favorable for cell behaviors and exchange processes of nutrients, biochemical stimuli and cell metabolites (Engler et al. 2006; Nichol et al. 2010; Shin et al. 2013). One way to overcome this problem is to control the mechanical properties of hydrogels by functionalizing graphene family nanomaterials into hydrogels. It has been reported that the mechanical properties of gelatin methacrylate (GelMA) hydrogels can be significantly improved by incorporating with GO (Shin et al. 2013). This can be attributed to the strong non-covalent cross-linking interactions between GO and GelMA hydrogel (Wan et al. 2011; Sharma et al. 2017). On the other hand, the incorporated GO did not affect the intrinsic characteristics of GelMA hydrogels, including biodegradability, porosity and internal morphology. In addition, the GO-incorporated hydrogels containing 2.0 mg/mL of GO exhibited the outstanding biocompatibility to NIH-3T3 fibroblasts. Meanwhile, these reinforcing effects of GO on polymer hydrogels can be further enhanced by surface modification of GO. Cha et al. showed that the GO modified with methacrylate groups is more effective to improve mechanical properties of hydrogels by covalent interactions of chemically modified GO (methacrylated GO) and polymer hydrogels (Cha et al. 2014). The methacrylate groups on GO could prevent aggregation of GO within polymer solution. The stable dispersions of GO within hydrogels could reduce the structural defects of hydrogels, thereby

enhancing their structural integrity and resistance to fractures without adverse effects on their rigidity. Moreover, they demonstrated that the encapsulated fibroblasts within hydrogels favorably proliferated due to the minimization of changes in rigidity, which can influence cell behaviors. These results indicated that the graphene family nanomaterials can be utilized as reinforcing agents to control the mechanical properties of composite scaffolds, and the graphene-functionalized scaffolds have been demonstrated to possess a good biocompatibility *in vitro*.

The *in vivo* biocompatibility and bioactivity of graphene-functionalized scaffolds have been also investigated (Nishida et al. 2014). Nishida et al. prepared GO-coated collagen scaffolds, and evaluated their *in vivo* healing effects in skin incisional models in rats. It was revealed that the GO-coated collagen scaffolds (0.01 wt% of GO) did not induce severe inflammatory responses, and the ingrowth of fibroblastic cells and blood vessels was significantly promoted as compared with collagen scaffold without GO coating. In addition, the GO-coated scaffolds easily resorbed as newly ingrown tissues were reconstructed. On the other hand, the promoting effects of GO-coated collagen scaffolds on tissue regeneration were greatly affected by the concentration of GO. It has been found that the biological effects of graphene family nanomaterials are highly dependent on their concentrations (Zhang et al. 2010b; Akhavan et al. 2012; Lee et al. 2012b; Park et al. 2015a; Kim et al. 2015a). Moreover, these effects of graphene family nanomaterials in dose-dependent manner can also affect the properties of scaffolds, such as degradation rate, thermal stability, conductivity, and interactions with cells. According to the recent findings, the physicochemical, mechanical, thermal, electrical, and biological properties of scaffolds are closely related to the incorporating content of graphene family nanomaterials (Murray et al. 2015; Sayyar et al. 2015; Unnithan et al. 2016; Zhang et al. 2016a). Therefore, even if graphene-functionalized scaffolds exhibit outstanding biocompatibility and biofunctionality, it is very important to determine the graphene material or its content, and to design scaffolds with suitable properties for a target application to specific tissue regenerations.

5.3 Neuronal Tissue Regeneration

Graphene family nanomaterials have exceptional electrical conductivity, which makes them attractive for potential applications in neuronal tissue regeneration. The graphene family nanomaterials have been shown to exhibit superior conductivity compared with the graphite materials, whereas their resistivities are quite lower than those of graphite materials (Zhang et al. 2010a; Qiu et al. 2016). Therefore, numerous studies have focused on applying graphene-functionalized scaffolds directing neural tissue regeneration (Park et al. 2011; Li et al. 2013; Tang et al. 2013; Akhavan and Ghaderi 2013; Akhavan et al. 2014; Serrano et al. 2014; Jakus et al. 2015; Baniasadi et al. 2015; Song et al. 2015; Akhavan et al. 2016; Zhang et al. 2016b; Martín et al. 2017; Golafshan et al. 2017). The cytotoxicity effects of graphene and its derivatives on neuronal cells were also directly dependent on their concentrations (Zhang et al. 2010b). The cytotoxicity of graphene family nanomaterials may attributed to the oxidative stress as similar to the other carbon nanomaterials (Lam et al. 2004; Hussain et al. 2006; Zhang et al. 2010b; Lee et al. 2012b). In addition to concentrations, there are, of course, many other factors that influence the cytotoxicity effects of graphene family nanomaterials, such as size, aggregation, surface chemistry, and exposure time. Nevertheless, the graphene family nanomaterials showed less cytotoxicity than other carbon nanomaterials, including fullerene, carbon nanotube and carbon black, indicating that the graphene-functionalized scaffolds can be favorably exploited in neuronal tissue regeneration (Zhang et al. 2010b; Zhou et al. 2016a; Baweja and Dhawan 2018).

The easiest way to use graphene family nanomaterials as a scaffold is to fabricate graphene-coated substrates (Park et al. 2011; Lee et al. 2012a). Park et al. prepared graphene-coated films by transferring graphene onto glass

substrates, and examined the growth and differentiation of human neural stem cells (hNSCs) (Park et al. 2011). It was shown that the hNSCs quite stably adhered to graphene-coated region, followed by differentiation into neurons and neuroglia cells. Whereas hNSCs on glass region were aggregated and were less differentiated into neurons than the graphene-coated region. In general, the neural differentiation of hNSCs is promoted when they are surrounded by a substantial number of neuroglia cells (Song et al. 2002). Therefore, a substantial number of cells on graphene-coated region can effectively promote the differentiation of hNSCs into neurons. In addition, the genes related to the calcium signaling pathway were also up-regulated on graphene-coated substrates, and the neural activity of hNSCs was confirmed by the increase in intracellular calcium ion concentrations. The similar results were reported for rat adrenal pheochromocytoma cells (PC-12 cells) where the neurite outgrowth of PC-12 cells was remarkably enhanced on graphene-coated substrates as compared with that on bare glass substrates (Lee et al. 2012a). Meanwhile, rGO can be also used as scaffold materials for accelerating the differentiation of hNSCs. Akhavan et al. documented that the rGO-coated substrates can effectively accelerate the differentiation of hNSCs into neurons rather than neuroglia cells (Akhavan et al. 2014). Interestingly, they synthesized rGO using Asian red ginseng as a reducing agent to secure high biocompatibility. The commonly used reducing agent for the synthesis of rGO is a hydrazine, but it is highly toxic to cells. However, they could obtain the higher biocompatibility of rGO by using ginseng as a green reductant than that using hydrazine. In addition, it was proved that the rGO synthesized using ginseng was found to have a more stable dispersibility, improved graphitic structure, increased hydrophilicity, and biocompatibility due to the presence of ginsenoside molecules on its surface. Furthermore, these improved physicochemical properties and biocompatibility played a key role in accelerating the differentiation of hNSCs into neurons. These results indicate that graphene-functionalized substrates are beneficial to neuronal cell growth and differentiation.

Graphene family nanomaterial-functionalized composite scaffolds have been also found to have promising potentials to facilitate neuronal tissue regeneration (Song et al. 2015; Baniasadi et al. 2015; Zhang et al. 2016b; Golafshan et al. 2017). The incorporation of graphene family nanomaterial can allow control over the physicochemical, thermal, mechanical and electrical properties of polymer-based scaffolds. These characteristics of scaffolds are very important for neuronal tissues because they communicate with each other using electrical signals. The functionalization of graphene family nanomaterials into polymer scaffolds imparts excellent mechanical properties and formation of conductive networks to them. In addition, the graphene incorporation can improve the tensile strength, elongation, toughness of polymer scaffolds without significant alteration of their rigidity (Golafshan et al. 2017). The rigidity is critical factors that can significantly affect cell behaviors of soft tissues, including nerve tissues. Therefore, the functionalization of graphene family nanomaterials is highly useful in neural tissue regeneration and engineering. Moreover, the improved mechanical and electrical properties of scaffolds can effectively promote the neuronal cell behaviors, including initial adhesion, spreading and proliferation (Song et al. 2015; Golafshan et al. 2017). Although it is very important to optimize the appropriate amount of graphene, there is no doubt that the functionalization of graphene family nanomaterials is a very valuable approach for developing tissue engineering scaffolds for neural tissue regeneration. On the other hand, specific configuration of graphene-functionalized scaffolds can further enhance the neuronal cell behaviors. Zhang et al. reported that the aligned poly(L-lactide) (PLLA) nanofibrous scaffolds coated with GO greatly promoted the behaviors of schwann cells and PC-12 cells (Zhang et al. 2016b). The GO coating can improve the mechanical and biomedical properties of scaffolds, and the alignment structure can guide the neurite outgrowth, suggesting

that the aligned nanofibrous scaffolds coated with GO have great potentials to be employed as a nerve guidance conduit for nerve regeneration.

The improvement of electrical signaling in neural networks is another very crucial aspect for regeneration of nerve tissues. It is a universally acknowledged fact that the exceptional electrical conductivity of graphene family nanomaterials is quite helpful in enhancing electrical signaling of neural networks and nerve tissues (Park et al. 2011; Tang et al. 2013; Akhavan and Ghaderi 2013; Li et al. 2013; Akhavan et al. 2014; Serrano et al. 2014; Jakus et al. 2015; Martín et al. 2017). The details of neural network formation on graphene-functionalized scaffolds and their interactions with neural networks have been described by Tang et al. and Akhavan et al. (Tang et al. 2013; Akhavan and Ghaderi 2013) (Fig. 5.3). They demonstrated the capabilities of graphene to improve neural network formation, electrical signaling and neural performance by monitoring the intracellular Ca^{2+} fluctuation in neural networks on graphene substrates. It was shown that the graphene films have a good biocompatibility to NSCs, and the density of mature neurons on graphene films is much higher than that on tissue culture plastics. In addition, the mature neurons on graphene films could be organized into functionally active neural networks, and the increased neural network activities were confirmed by the enhanced frequency and amplitude of spontaneous postsynaptic currents as well as the increased intracellular spontaneous and synchronous Ca^{2+} spikes. Because the neural network activities are significantly affected by the interactions between neurons and substrate materials, the intrinsic electrical properties of substrate materials can strongly influence the neural and synaptic activities (Schmidt et al. 1997; Parak et al. 2001; Cellot et al. 2011). Hence, electrical coupling of neuronal cells and graphene substrates is able to enhance the neural network activities because of exceptional electrical conductivity and large surface area of graphene.

It has been extensively acknowledged that in many cases, cell behaviors in the 3D environments are quite different from those in the 2D environments. Therefore, in more recent years, many attempts have been made to develop a graphene-functionalized 3D scaffold to provide a more similar environment to the natural extracellular matrix (Li et al. 2013; Serrano et al. 2014; Akhavan et al. 2016; Martín et al. 2017). In particular, nerve tissues are composed of complex 3D neural networks, which cannot be reproduced in a 2D culture system. Li et al. suggested that the porous graphene foam scaffolds can be a

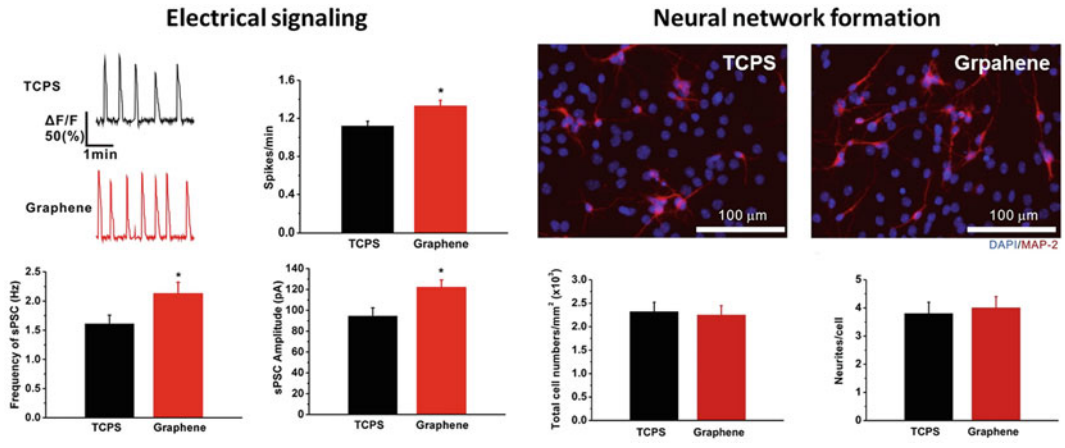

Fig. 5.3 The improvement of neural network formation and electrical signaling in neural networks on graphene-functionalized scaffolds. (Reproduced from Tang et al. 2013, Copyright (2013) Elsevier Ltd.) *Abbreviations: *sPSC* spontaneous postsynaptic current, *TCPS* tissue culture plastics

promising candidate to address these limitations (Li et al. 2013) (Fig. 5.4). In their study, the 3D graphene foams were prepared using a chemical vapor deposition method with Ni foam templates, followed by coating with laminin, and the cellular behaviors of NSCs, including adhesion, proliferation and differentiation, were examined. In addition, the potentials of 3D graphene foams as a conductive platform, which can mediate electrical stimulation for NSCs were explored. It was indicated that the 3D graphene foams have suitable physicochemical and electrical properties to provide favorable 3D microenvironments for cell growth. The 3D network structure with interconnected pores allows the NSCs to successfully adhere and proliferate in a 3D fashion. Additionally, the unique nanoscale rippled and wrinkled features on the surface of 3D graphene foams could offer a mechanical interlocking with cells, leads to enhanced cell adhesion and proliferation (Li et al. 2010). Moreover, these specific topographical cues of 3D graphene foams, including curvature, anisotropic microstructure and roughness, could provide contact guidance to cells, which results in the promoted differentiation of NSCs towards neuronal lineage. On the other hand, an external electrical stimulation was also successfully delivered to NSCs through 3D graphene foams, and a good electrical coupling of 3D graphene foams with differentiated NSCs was clearly observed due to the superior electrical properties and large surface area of 3D graphene foam scaffolds. According to another study, the *in vivo* performance of graphene-based 3D scaffolds was verified (Jakus et al. 2015). The 3D-printed graphene scaffolds composed of graphene flakes and poly(lactic-co-glycolic acid) (PLGA) possessed a good mechanical integrity, electrical conductivity and biocompatibility. The expression of neurogenic relevant genes was also up-regulated in human mesenchymal stem cells on 3D-printed graphene scaffolds. They further investigated the *in vivo* performance of the 3D-printed graphene scaffolds in a female BALB/c mouse model. The results showed that a severe immune response or fibrous encapsulation was not observed, and the scaffolds were actively degraded by macrophages. Moreover, the ability of scaffolds to be intraoperatively manipulated, surgically implemented and handled has also been demonstrated. These results imply that the graphene-functionalized 3D scaffolds can be also promising candidates for neural tissue regeneration.

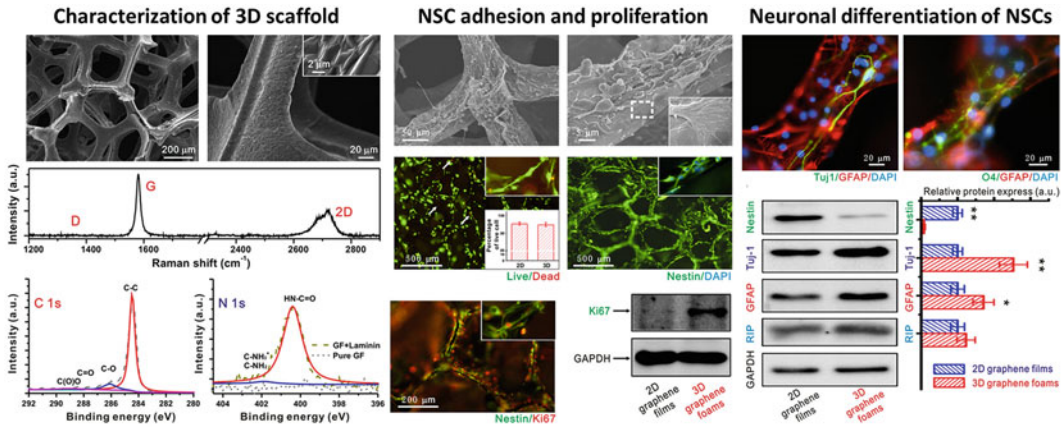

Fig. 5.4 Graphene-functionalized 3D scaffold for neuronal tissue regeneration. (Reproduced from Li et al. 2013, Copyright (2013) Nature Publishing Group) *Abbreviations: *GAPDH* glyceraldehyde-3-phosphate dehydrogenase, *GFAP* glial fibrillary acidic protein, *NSC* neural stem cell, *O4* oligodendrocyte marker, *sPSC* spontaneous postsynaptic current, *TCPS* tissue culture plastics

5.4 Other Tissue Regeneration

In addition to the applications of graphene-functionalized scaffolds to skin and neuronal regeneration, their potentials have been examined for various types of tissues. Among them, herein, we are attempting to briefly summarize the major literature concerning the representative applications to the regeneration of muscle, cardiac and bone tissues.

Numerous studies regarding the graphene-functionalized scaffolds for muscle tissue regeneration have been conducted as the stimulating effects of graphene family nanomaterials on myogenic differentiation were demonstrated (Ku and Park 2013; Ahadian et al. 2014; Shin et al. 2015a, c, 2017b; Bajaj et al. 2014; Ciriza et al. 2015; Lee et al. 2016b; Jo et al. 2016; Krueger et al. 2016; Chaudhuri et al. 2014, 2015, 2016; Patel et al. 2016a). Most studies focus on promoting myogenic differentiation and muscle tissue regeneration by coating graphene family nanomaterials onto substrates or incorporating them into polymer-based scaffolds. It has been revealed that the stimulating effects of GO or rGO can be attributed to the fact that the oxygen-containing functional groups on GO or rGO surface are able to increase in the adsorption of serum proteins from the culture media *via* electrostatic interactions, which results in the strong activation of insulin-like growth factor-1 (IGF-1) signaling pathway (Lee et al. 2011; Ku and Park 2013; Shin et al. 2015a, 2017c; Chaudhuri et al. 2016). In addition, the myogenic differentiation can be further enhanced by introducing external electrical stimulation since muscle cells are activated by electrical stimulation (Ahadian et al. 2014; Bajaj et al. 2014; Krueger et al. 2016; Jo et al. 2016). Electrical conductivity can be imparted to non-conductive polymer-based scaffolds by incorporating graphene family nanomaterials, and the other properties of scaffolds can be also manipulated. The efficient myogenic differentiation could be achieved using graphene family nanomaterial-based scaffolds, but when the scaffolds were used together with electrical stimulation, the myogenic differentiation was further accelerated and promoted (Ahadian et al. 2014). Moreover, the expression levels of gene related to the myotube formation and contraction ability were substantially up-regulated under the application of electrical stimulation (Fig. 5.5). These findings suggested that the use of graphene-functionalized scaffolds in a combination with electrical stimulation can be a novel strategy for muscle tissue regenerations. Meanwhile, because

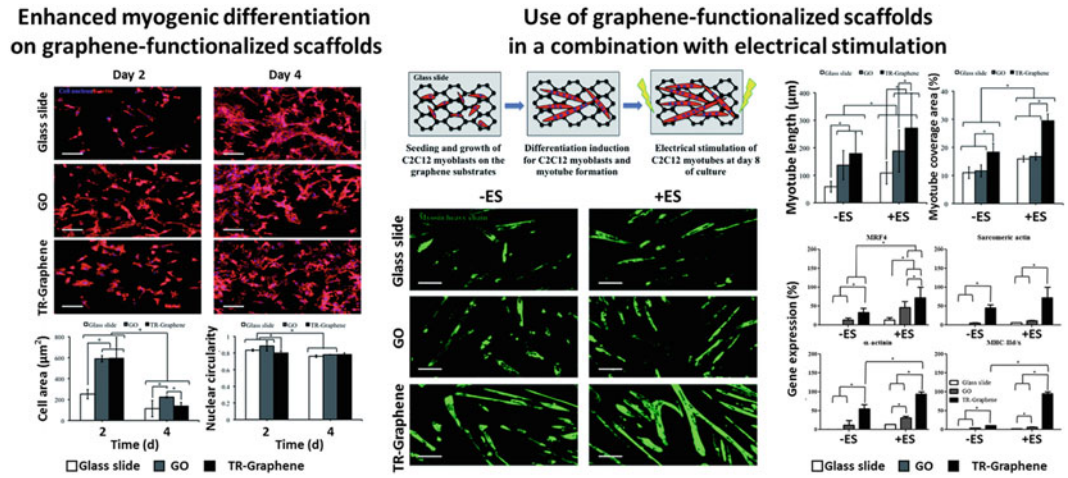

Fig. 5.5 Enhanced myogenic differentiation using graphene-functionalized scaffold in a combination with electrical stimulation. (Reproduced from Ahadian et al. 2014, Copyright (2014) Royal Society of Chemistry) *Abbreviations: *ES* electrical stimulation, *GO* graphene oxide, *TR-Graphene* thermally reduced graphene

myocardial tissues lack the ability to regenerate themselves when they are damaged, studies on myocardial tissue regeneration using graphene-functionalized scaffolds have been steadily carried out (Park et al. 2014, 2015b; Shin et al. 2016a). The rGO-incorporated GelMA hydrogels showed significantly lower electrical impedance values than pristine GelMA hydrogels, and good cytocompatibility to cardiomyocytes (Shin et al. 2016a). Considering that the homogeneous cell distribution is desired for a myocardial repair and regeneration, significantly improved initial homogeneous adhesion and spreading of cardiomyocytes on rGO-incorporated GelMA hydrogels could facilitate the myocardial tissue regeneration. The expression of cardiac markers, including sarcomeric α-actinin and connexin 43, and the spontaneous beating rates of cardiomyocytes were also increased on rGO-incorporated GelMA hydrogels, indicating that the rGO-functionalized GelMA hydrogels can be used as a promising scaffold for cardiac tissue regeneration. The underlying mechanism for the ability of graphene-functionalized scaffolds to enhance cardiomyogenic differentiation was proposed by Park et al. (2014). They described that the graphene-functionalized substrates increased the gene expressions of cardiomyogenic differentiation-related extracellular matrix proteins, such as type I collagen (Col I), type III collagen (Col III), type IV collagen (Col IV), fibronectin, and laminin. In addition, the focal adhesion kinase (FAK) expression was also up-regulated on graphene-functionalized substrates, followed by the up-regulation of phosphatidylinositol 3-kinase (PI3K)/Akt signal transduction pathways, and subsequently the cardiomyogenic differentiation was promoted.

The graphene-functionalized scaffolds for applications to bone tissue regeneration have also been extensively explored (Nayak et al. 2011; Depan et al. 2011; Kumar and Chatterjee 2015; Liao et al. 2015; Shuai et al. 2015; Elkhenany et al. 2015; Wang et al. 2015; Park et al. 2016; Nie et al. 2017; Marrella et al. 2017; Peng et al. 2017). Bone tissues, a type of dense connective tissue, are generally considered to belong to a hard tissue. Therefore, scaffolds for bone tissue regeneration should also have good mechanical properties. In addition to polymer materials, a calcium phosphate material, such as hydroxyapatite, tricalcium phosphate and biphasic calcium phosphate, has been widely used as scaffolds for bone tissue engineering. However, their inherent poor mechanical properties, such as brittleness, low wear resistance and low fracture toughness, are often quoted as disadvantages (Liu et al. 2014; Shin et al. 2015b, 2017d; Lee et al. 2015b). In order to overcome these disadvantages, graphene family nanomaterials have emerged as novel reinforcing nanofillers. The functionalization of graphene family nanomaterials can reinforce the mechanical properties of composite scaffolds (Depan et al. 2011; Liao et al. 2015; Shuai et al. 2015; Peng et al. 2017; Marrella et al. 2017). The reinforcing effects of graphene family nanomaterials on the mechanical properties of composite scaffolds can be explained by the fact that the interfacial interactions between graphene family nanomaterials and composite scaffolds through π-π stacking interaction, hydrogen bonding or electrostatic interaction can achieve the reinforced mechanical properties of scaffolds (Yoon et al. 2012; Ionita et al. 2013; Shin et al. 2017a; Peng et al. 2017; Marrella et al. 2017). The functionalized graphene family nanomaterials can behave as an interface phase between composite scaffolds, and can directly transfer physico-mechanical stress from scaffolds to graphene family nanomaterials, results in the improved mechanical properties (Peng et al. 2017) (Fig. 5.6). Moreover, it has been proved that the graphene and its derivatives can accelerate the osteogenic differentiation without hindering cell growth, which makes graphene-functionalized scaffolds a promising candidate for bone tissue regeneration (Lee et al. 2011, 2015a, 2016a; Nayak et al. 2011; Akhavan et al. 2013; Kim et al. 2015b, 2017). Hence, many studies have been recently reported to improve the bone regeneration by functionalizing graphene family nanomaterials into commercially available bone grafts in various industrial fields as well as research area (Lee et al. 2015a, b; Shin et al. 2015b; Park et al. 2016; Kim et al. 2017;

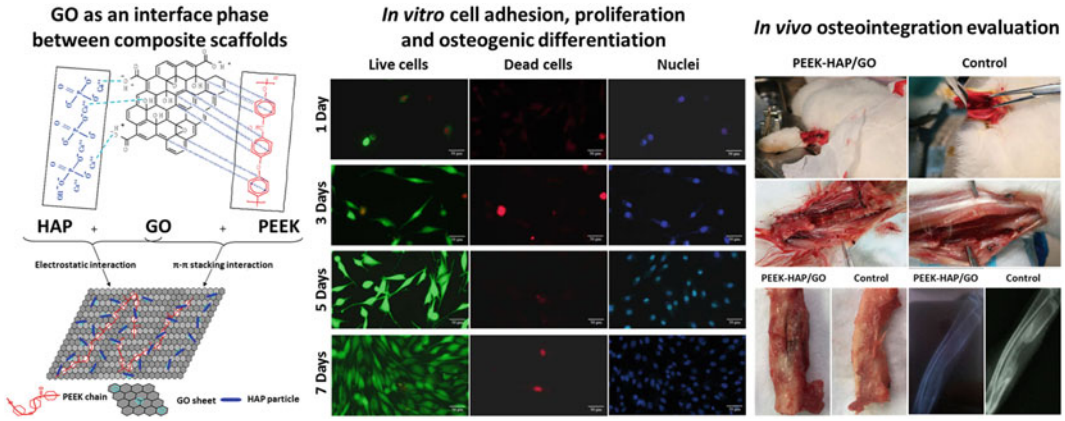

Fig. 5.6 Reinforcing effects of GO on mechanical properties of scaffolds, and *in vitro* and *in vivo* performance evaluation of graphene-functionalized scaffolds. (Reproduced from Peng et al. 2017, Copyright (2017) Peng et al.) *Abbreviations: *GO* graphene oxide, *HAP* hydroxyapatite, *PEEK* polyetheretherketone

Peng et al. 2017). In particular, the potentials of graphene family nanomaterials have become more prominent as the *in vivo* performance of the graphene-functionalized scaffolds, composed of commercially available polyetheretherketone (PEEK) and hydroxyapatite powders and GO, in new bone formation capability has been demonstrated in a rabbit bone defect model (Peng et al. 2017) (Fig. 5.6). Therefore, the functionalization of graphene family nanomaterials is a highly versatile strategy for bone tissue regeneration.

On the other hand, in addition to the cases described here, there are a variety of applications of graphene-functionalized biomimetic scaffolds for tissue regeneration (Shin et al. 2017d; Lee et al. 2011; Chen et al. 2012a, b; Shah et al. 2014; Díez-Pascual and Díez-Vicente 2016; Lalwani et al. 2017). For example, Díez-Pascual et al. prepared the poly(propylene fumarate) (PPF)-based nanocomposites incorporating poly(ethylene glycol) (PEG)-modified GO, and investigated their antibacterial activity against human pathogenic bacteria and cytotoxicity against human dermal fibroblasts (Díez-Pascual and Díez-Vicente 2016). It was shown that the PPF/PEG-GO nanocomposites exhibit an excellent antibacterial activity, whereas they do not show cytotoxicity against human dermal fibroblasts. These antibacterial activity might be due to the fact that the direct contact between the bacteria and the sharp edges of GO can induce membrane damages in bacteria, and oxidative stress induced by GO can damage the cellular components of bacteria (Akhavan and Ghaderi 2010; Akhavan et al. 2011; Chang et al. 2011; Lu et al. 2012). These results suggested that the GO-functionalized composites with excellent antibacterial activity can be used as effective scaffolds for tissue regeneration by preventing pathogen infection while facilitating cellular behaviors. Taken together, given the outstanding physicochemical, thermomechanical, electrical, and biological properties of graphene family nanomaterials, graphene-functionalized biomimetic scaffolds are particularly promising candidates for the regeneration of various tissues.

5.5 Conclusions and Perspectives

Herein, we summarized and discussed the possible applications of graphene-functionalized biomimetic scaffolds for tissue regeneration. According to the recent literature, it is clear that the graphene-functionalized biomimetic scaffolds are highly beneficial to tissue regeneration regardless of the types of graphene nanomaterials. In particular, the fact that the scaffolds possessing desired properties can be readily fabricated by

functionalizing graphene family nanomaterials is good enough to attract our great attention for the promising potentials of graphene-functionalized scaffolds. However, the potential toxic effects and the detailed mechanism underlying the biological effects of graphene family nanomaterials have still not been fully elucidated. In addition, the biological properties of graphene-functionalized scaffolds are quite strongly dependent on many parameters, including the size, concentration, surface chemistry, shape, and preparation method of graphene nanomaterials. This indicates that the further systematic and comprehensive studies must be carried out before their practical applications, and we should deliberately design and employ the graphene-functionalized scaffolds. Nevertheless, the splendid advantages of graphene family nanomaterials described in here rationally suggest that the graphene-functionalized scaffolds are particularly promising strategy for tissue regeneration and tissue engineering, even if many puzzles remain challenges to employing graphene-functionalized scaffolds for biomedical applications.

References

Ahadian S, Ramón-Azcón J, Chang H, Liang X, Kaji H, Shiku H, Nakajima K, Ramalingam M, Wu H, Matsue T (2014) Electrically regulated differentiation of skeletal muscle cells on ultrathin graphene-based films. RSC Adv 4(19):9534–9541

Akhavan O, Ghaderi E (2010) Toxicity of graphene and graphene oxide nanowalls against bacteria. ACS Nano 4(10):5731–5736

Akhavan O, Ghaderi E (2013) Differentiation of human neural stem cells into neural networks on graphene nanogrids. J Mater Chem B 1(45):6291–6301

Akhavan O, Ghaderi E, Esfandiar A (2011) Wrapping bacteria by graphene nanosheets for isolation from environment, reactivation by sonication, and inactivation by near-infrared irradiation. J Phys Chem B 115 (19):6279–6288

Akhavan O, Ghaderi E, Akhavan A (2012) Size-dependent genotoxicity of graphene nanoplatelets in human stem cells. Biomaterials 33(32):8017–8025

Akhavan O, Ghaderi E, Shahsavar M (2013) Graphene nanogrids for selective and fast osteogenic differentiation of human mesenchymal stem cells. Carbon 59:200–211

Akhavan O, Ghaderi E, Abouei E, Hatamie S, Ghasemi E (2014) Accelerated differentiation of neural stem cells into neurons on ginseng-reduced graphene oxide sheets. Carbon 66:395–406

Akhavan O, Ghaderi E, Shirazian SA, Rahighi R (2016) Rolled graphene oxide foams as three-dimensional scaffolds for growth of neural fibers using electrical stimulation of stem cells. Carbon 97:71–77

Bajaj P, Rivera JA, Marchwiany D, Solovyeva V, Bashir R (2014) Graphene-based patterning and differentiation of C2C12 myoblasts. Adv Healthc Mater 3 (7):995–1000

Baniasadi H, Sa AR, Mashayekhan S (2015) Fabrication and characterization of conductive chitosan/gelatin-based scaffolds for nerve tissue engineering. Int J Biol Macromol 74:360–366

Baweja L, Dhawan A (2018) Chapter 12 Computational approaches for predicting nanotoxicity at the molecular level. In: Dhawan A, Anderson D, Shanker R (eds) Nanotoxicology: experimental and computational perspectives, vol 35. Royal Society of Chemistry, CambrIdge, pp 304–327. https://doi.org/10.1039/9781782623922-00304

Cellot G, Toma FM, Varley ZK, Laishram J, Villari A, Quintana M, Cipollone S, Prato M, Ballerini L (2011) Carbon nanotube scaffolds tune synaptic strength in cultured neural circuits: novel frontiers in nanomaterial–tissue interactions. J Neurosci 31 (36):12945–12953

Cha C, Shin SR, Gao X, Annabi N, Dokmeci MR, Tang XS, Khademhosseini A (2014) Controlling mechanical properties of cell-laden hydrogels by covalent incorporation of graphene oxide. Small 10(3):514–523

Chang Y, Yang S-T, Liu J-H, Dong E, Wang Y, Cao A, Liu Y, Wang H (2011) In vitro toxicity evaluation of graphene oxide on A549 cells. Toxicol Lett 200 (3):201–210

Chaudhari AA, Vig K, Baganizi DR, Sahu R, Dixit S, Dennis V, Singh SR, Pillai SR (2016) Future prospects for scaffolding methods and biomaterials in skin tissue engineering: a review. Int J Mol Sci 17(12):1974

Chaudhuri B, Bhadra D, Mondal B, Pramanik K (2014) Biocompatibility of electrospun graphene oxide–poly (ε-caprolactone) fibrous scaffolds with human cord blood mesenchymal stem cells derived skeletal myoblast. Mater Lett 126:109–112

Chaudhuri B, Bhadra D, Moroni L, Pramanik K (2015) Myoblast differentiation of human mesenchymal stem cells on graphene oxide and electrospun graphene oxide–polymer composite fibrous meshes: importance of graphene oxide conductivity and dielectric constant on their biocompatibility. Biofabrication 7(1):015009

Chaudhuri B, Mondal B, Kumar S, Sarkar SC (2016) Myoblast differentiation and protein expression in electrospun graphene oxide (GO)-poly (-ε-caprolactone, PCL) composite meshes. Mater Lett 182:194–197

Chen G-Y, Pang D-P, Hwang S-M, Tuan H-Y, Hu Y-C (2012a) A graphene-based platform for induced pluripotent stem cells culture and differentiation. Biomaterials 33(2):418–427

Chen Y, Qi Y, Tai Z, Yan X, Zhu F, Xue Q (2012b) Preparation, mechanical properties and biocompatibility of graphene oxide/ultrahigh molecular weight polyethylene composites. Eur Polym J 48(6):1026–1033

Cherukula K, Manickavasagam Lekshmi K, Uthaman S, Cho K, Cho C-S, Park I-K (2016) Multifunctional inorganic nanoparticles: Recent progress in thermal therapy and imaging. Nanomaterials 6(4):76

Ciriza J, del Burgo LS, Virumbrales-Muñoz M, Ochoa I, Fernandez LJ, Orive G, Hernandez RM, Pedraz JL (2015) Graphene oxide increases the viability of C2C12 myoblasts microencapsulated in alginate. Int J Pharm 493(1):260–270

Collins MN, Birkinshaw C (2013) Hyaluronic acid based scaffolds for tissue engineering – a review. Carbohydr Polym 92(2):1262–1279

Depan D, Girase B, Shah JS, Misra RDK (2011) Structure–process–property relationship of the polar graphene oxide-mediated cellular response and stimulated growth of osteoblasts on hybrid chitosan network structure nanocomposite scaffolds. Acta Biomater 7(9):3432–3445

Díez-Pascual AM, Díez-Vicente AL (2016) Poly (propylene fumarate)/polyethylene glycol-modified graphene oxide nanocomposites for tissue engineering. ACS Appl Mater Interfaces 8(28):17902–17914

Dobrovolskaia MA, McNeil SE (2007) Immunological properties of engineered nanomaterials. Nat Nanotechnol 2(8):469–478

Drury JL, Mooney DJ (2003) Hydrogels for tissue engineering: scaffold design variables and applications. Biomaterials 24(24):4337–4351

Dvir T, Timko BP, Kohane DS, Langer R (2011) Nanotechnological strategies for engineering complex tissues. Nat Nanotechnol 6(1):13–22

Elkhenany H, Amelse L, Lafont A, Bourdo S, Caldwell M, Neilsen N, Dervishi E, Derek O, Biris AS, Anderson D (2015) Graphene supports *in vitro* proliferation and osteogenic differentiation of goat adult mesenchymal stem cells: potential for bone tissue engineering. J Appl Toxicol 35(4):367–374

Engler AJ, Sen S, Sweeney HL, Discher DE (2006) Matrix elasticity directs stem cell lineage specification. Cell 126(4):677–689

Fan H, Wang L, Zhao K, Li N, Shi Z, Ge Z, Jin Z (2010) Fabrication, mechanical properties, and biocompatibility of graphene-reinforced chitosan composites. Biomacromolecules 11(9):2345–2351

Golafshan N, Kharaziha M, Fathi M (2017) Tough and conductive hybrid graphene-PVA: alginate fibrous scaffolds for engineering neural construct. Carbon 111:752–763

Gómez-Navarro C, Burghard M, Kern K (2008) Elastic properties of chemically derived single graphene sheets. Nano Lett 8(7):2045–2049

Guo B, Lei B, Li P, Ma PX (2015) Functionalized scaffolds to enhance tissue regeneration. Regen Biomater 2(1):47–57

Ho J, Walsh C, Yue D, Dardik A, Cheema U (2017) Current advancements and strategies in tissue engineering for wound healing: a comprehensive review. Adv Wound Care 6(6):191–209

Hood E (2004) Nanotechnology: looking as we leap. Environ Health Perspect 112(13):A740

Hussain SM, Javorina AK, Schrand AM, Duhart HM, Ali SF, Schlager JJ (2006) The interaction of manganese nanoparticles with PC-12 cells induces dopamine depletion. Toxicol Sci 92(2):456–463

Ionita M, Pandele MA, Iovu H (2013) Sodium alginate/graphene oxide composite films with enhanced thermal and mechanical properties. Carbohydr Polym 94 (1):339–344

Jakus AE, Secor EB, Rutz AL, Jordan SW, Hersam MC, Shah RN (2015) Three-dimensional printing of high-content graphene scaffolds for electronic and biomedical applications. ACS Nano 9(4):4636–4648

Jo H, Sim M, Kim S, Yang S, Yoo Y, Park J-H, Yoon TH, Kim M-G, Lee JY (2016) Electrically conductive graphene/polyacrylamide hydrogels produced by mild chemical reduction for enhanced myoblast growth and differentiation. Acta Biomater 48:100–109

Kalbacova M, Broz A, Kong J, Kalbac M (2010) Graphene substrates promote adherence of human osteoblasts and mesenchymal stromal cells. Carbon 48(15):4323–4329

Kim MJ, Lee JH, Shin YC, Jin L, Hong SW, Han D-W, Kim Y-J, Kim B (2015a) Stimulated myogenic differentiation of C2C12 murine myoblasts by using graphene oxide. J Korean Phys Soc 67(11):1910–1914

Kim T-H, Shah S, Yang L, Yin PT, Hossain MK, Conley B, Choi J-W, Lee K-B (2015b) Controlling differentiation of adipose-derived stem cells using combinatorial graphene hybrid-pattern arrays. ACS Nano 9(4):3780–3790

Kim J-W, Shin YC, Lee J-J, Bae E-B, Jeon Y-C, Jeong C-M, Yun M-J, Lee S-H, Han D-W, Huh J-B (2017) The effect of reduced graphene oxide-coated biphasic calcium phosphate bone graft material on osteogenesis. Int J Mol Sci 18(8):1725

Krueger E, Chang AN, Brown D, Eixenberger J, Brown R, Rastegar S, Yocham KM, Cantley KD, Estrada D (2016) Graphene foam as a three-dimensional platform for myotube growth. ACS Biomater Sci Eng 2 (8):1234–1241

Ku SH, Park CB (2013) Myoblast differentiation on graphene oxide. Biomaterials 34(8):2017–2023

Kumar S, Chatterjee K (2015) Strontium eluting graphene hybrid nanoparticles augment osteogenesis in a 3D tissue scaffold. Nanoscale 7(5):2023–2033

Lalwani G, D'Agati M, Gopalan A, Rao M, Schneller J, Sitharaman B (2017) Three-dimensional macroporous graphene scaffolds for tissue engineering. J Biomed Mater Res A 105(1):73–83

Lam C-W, James JT, McCluskey R, Hunter RL (2004) Pulmonary toxicity of single-wall carbon nanotubes in mice 7 and 90 days after intratracheal instillation. Toxicol Sci 77(1):126–134

Langer R, Vacanti JP (1993) Tissue engineering. Science 260(5110):920–926

Lee WC, Lim CHY, Shi H, Tang LA, Wang Y, Lim CT, Loh KP (2011) Origin of enhanced stem cell growth and differentiation on graphene and graphene oxide. ACS Nano 5(9):7334–7341

Lee JH, Shin YC, Jin OS, Han D-W, Kang SH, Hong SW, Kim JM (2012a) Enhanced neurite outgrowth of PC-12 cells on graphene-monolayer-coated substrates as biomimetic cues. J Korean Phys Soc 61(10):1696–1699

Lee JH, Shin YC, Jin OS, Lee EJ, Han D-W, Kang SH, Hong SW, Ahn JY, Kim SH (2012b) Cytotoxicity evaluations of pristine graphene and carbon nanotubes in fibroblastic cells. J Korean Phys Soc 61(6):873–877

Lee EJ, Lee JH, Shin YC, Hwang D-G, Kim JS, Jin OS, Jin L, Hong SW, Han D-W (2014) Graphene oxide-decorated PLGA/collagen hybrid fiber sheets for application to tissue engineering scaffolds. Biomater Res 18 (1):18-24.

Lee JH, Shin YC, Jin OS, Kang SH, Hwang Y-S, Park J-C, Hong SW, Han D-W (2015a) Reduced graphene oxide-coated hydroxyapatite composites stimulate spontaneous osteogenic differentiation of human mesenchymal stem cells. Nanoscale 7(27):11642–11651

Lee JH, Shin YC, Lee S-M, Jin OS, Kang SH, Hong SW, Jeong C-M, Huh JB, Han D-W (2015b) Enhanced osteogenesis by reduced graphene oxide/hydroxyapatite nanocomposites. Sci Rep 5:18833

Lee WC, Lim CH, Su C, Loh KP, Lim CT (2015c) Cell-assembled graphene biocomposite for enhanced chondrogenic differentiation. Small 11(8):963–969

Lee JH, Lee S-M, Shin YC, Park JH, Hong SW, Kim B, Lee JJ, Lim D, Lim Y-J, Huh JB (2016a) Spontaneous osteodifferentiation of bone marrow-derived mesenchymal stem cells by hydroxyapatite covered with graphene nanosheets. J Biomater Tissue Eng 6 (10):818–825

Lee JH, Lee Y, Shin YC, Kim MJ, Park JH, Hong SW, Kim B, Oh J-W, Park KD, Han D-W (2016b) *In situ* forming gelatin/graphene oxide hydrogels for facilitated C2C12 myoblast differentiation. Appl Spectrosc Rev 51(7-9):527–539

Li D, Xia Y (2004) Electrospinning of nanofibers: reinventing the wheel? Adv Mater 16(14):1151–1170

Li WJ, Laurencin CT, Caterson EJ, Tuan RS, Ko FK (2002) Electrospun nanofibrous structure: a novel scaffold for tissue engineering. J Biomed Mater Res 60 (4):613–621

Li X, MacEwan MR, Xie J, Siewe D, Yuan X, Xia Y (2010) Fabrication of density gradients of biodegradable polymer microparticles and their use in guiding neurite outgrowth. Adv Funct Mater 20 (10):1632–1637

Li N, Zhang Q, Gao S, Song Q, Huang R, Wang L, Liu L, Dai J, Tang M, Cheng G (2013) Three-dimensional graphene foam as a biocompatible and conductive scaffold for neural stem cells. Sci Rep 3:1604

Liao J, Qu Y, Chu B, Zhang X, Qian Z (2015) Biodegradable CSMA/PECA/graphene porous hybrid scaffold for cartilage tissue engineering. Sci Rep 5:9879

Lin N, Huang J, Dufresne A (2012) Preparation, properties and applications of polysaccharide nanocrystals in advanced functional nanomaterials: a review. Nanoscale 4(11):3274–3294

Liu H, Webster TJ (2007) Nanomedicine for implants: a review of studies and necessary experimental tools. Biomaterials 28(2):354–369

Liu W, Thomopoulos S, Xia Y (2012) Electrospun nanofibers for regenerative medicine. Adv Healthc Mater 1(1):10–25

Liu Y, Dang Z, Wang Y, Huang J, Li H (2014) Hydroxyapatite/graphene-nanosheet composite coatings deposited by vacuum cold spraying for biomedical applications: Inherited nanostructures and enhanced properties. Carbon 67:250–259

Lu B, Li T, Zhao H, Li X, Gao C, Zhang S, Xie E (2012) Graphene-based composite materials beneficial to wound healing. Nanoscale 4(9):2978–2982

MacDiarmid AG (2001) "Synthetic metals": a novel role for organic polymers (Nobel lecture). Angew Chem Int Ed 40(14):2581–2590

Marrella A, Lagazzo A, Barberis F, Catelani T, Quarto R, Scaglione S (2017) Enhanced mechanical performances and bioactivity of cell laden-graphene oxide/alginate hydrogels open new scenario for articular tissue engineering applications. Carbon 115:608–616

Martín C, Merino S, González-Domínguez JM, Rauti R, Ballerini L, Prato M, Vázquez E (2017) Graphene improves the biocompatibility of polyacrylamide hydrogels: 3D polymeric scaffolds for neuronal growth. Sci Rep 7:10942

Murray E, Thompson BC, Sayyar S, Wallace GG (2015) Enzymatic degradation of graphene/polycaprolactone materials for tissue engineering. Polym Degrad Stab 111:71–77

Murugan R, Ramakrishna S (2006) Nano-featured scaffolds for tissue engineering: a review of spinning methodologies. Tissue Eng 12(3):435–447

Nayak TR, Andersen H, Makam VS, Khaw C, Bae S, Xu X, Ee P-LR, Ahn J-H, Hong BH, Pastorin G (2011) Graphene for controlled and accelerated osteogenic differentiation of human mesenchymal stem cells. ACS Nano 5(6):4670–4678

Nichol JW, Koshy ST, Bae H, Hwang CM, Yamanlar S, Khademhosseini A (2010) Cell-laden microengineered gelatin methacrylate hydrogels. Biomaterials 31 (21):5536–5544

Nie W, Peng C, Zhou X, Chen L, Wang W, Zhang Y, Ma PX, He C (2017) Three-dimensional porous scaffold by self-assembly of reduced graphene oxide and nano-

hydroxyapatite composites for bone tissue engineering. Carbon 116:325–337
Nishida E, Miyaji H, Takita H, Kanayama I, Tsuji M, Akasaka T, Sugaya T, Sakagami R, Kawanami M (2014) Graphene oxide coating facilitates the bioactivity of scaffold material for tissue engineering. Jpn J Appl Phys 53(6S):06JD04
Norouzi M, Boroujeni SM, Omidvarkordshouli N, Soleimani M (2015) Advances in skin regeneration: application of electrospun scaffolds. Adv Healthc Mater 4(8):1114–1133
O'Brien FJ (2011) Biomaterials & scaffolds for tissue engineering. Mater Today 14(3):88–95
Papageorgiou DG, Kinloch IA, Young RJ (2017) Mechanical properties of graphene and graphene-based nanocomposites. Prog Mater Sci 90:75–127
Parak WJ, George M, Kudera M, Gaub HE, Behrends JC (2001) Effects of semiconductor substrate and glia-free culture on the development of voltage-dependent currents in rat striatal neurones. Eur Biophys J 29 (8):607–620
Park SY, Park J, Sim SH, Sung MG, Kim KS, Hong BH, Hong S (2011) Enhanced differentiation of human neural stem cells into neurons on graphene. Adv Mater 23(36):H263–H267
Park J, Park S, Ryu S, Bhang SH, Kim J, Yoon JK, Park YH, Cho SP, Lee S, Hong BH (2014) Graphene–regulated cardiomyogenic differentiation process of mesenchymal stem cells by enhancing the expression of extracellular matrix proteins and cell signaling molecules. Adv Healthc Mater 3(2):176–181
Park E-J, Lee G-H, Han BS, Lee B-S, Lee S, Cho M-H, Kim J-H, Kim D-W (2015a) Toxic response of graphene nanoplatelets in vivo and in vitro. Arch Toxicol 89(9):1557–1568
Park J, Kim B, Han J, Oh J, Park S, Ryu S, Jung S, Shin J-Y, Lee BS, Hong BH (2015b) Graphene oxide flakes as a cellular adhesive: prevention of reactive oxygen species mediated death of implanted cells for cardiac repair. ACS Nano 9(5):4987–4999
Park KO, Lee JH, Park JH, Shin YC, Huh JB, Bae J-H, Kang SH, Hong SW, Kim B, Yang DJ (2016) Graphene oxide-coated guided bone regeneration membranes with enhanced osteogenesis: spectroscopic analysis and animal study. Appl Spectrosc Rev 51 (7-9):540–551
Patel A, Mukundan S, Wang W, Karumuri A, Sant V, Mukhopadhyay SM, Sant S (2016a) Carbon-based hierarchical scaffolds for myoblast differentiation: Synergy between nano-functionalization and alignment. Acta Biomater 32:77–88
Patel M, Moon HJ, Ko DY, Jeong B (2016b) Composite system of graphene oxide and polypeptide thermogel as an injectable 3D scaffold for adipogenic differentiation of tonsil-derived mesenchymal stem cells. ACS Appl Mater Interfaces 8(8):5160–5169
Peng S, Feng P, Wu P, Huang W, Yang Y, Guo W, Gao C, Shuai C (2017) Graphene oxide as an interface phase between polyetheretherketone and hydroxyapatite for tissue engineering scaffolds. Sci Rep 7:46604
Qiu C, Bennet KE, Khan T, Ciubuc JD, Manciu FS (2016) Raman and conductivity analysis of graphene for biomedical applications. Materials 9(11):897
Ray PC (2010) Size and shape dependent second order nonlinear optical properties of nanomaterials and their application in biological and chemical sensing. Chem Rev 110(9):5332–5365
Ruiz ON, Fernando KS, Wang B, Brown NA, Luo PG, McNamara ND, Vangsness M, Sun Y-P, Bunker CE (2011) Graphene oxide: a nonspecific enhancer of cellular growth. ACS Nano 5(10):8100–8107
Sanchez VC, Jachak A, Hurt RH, Kane AB (2011) Biological interactions of graphene-family nanomaterials: an interdisciplinary review. Chem Res Toxicol 25(1):15–34
Sayyar S, Murray E, Thompson BC, Chung J, Officer DL, Gambhir S, Spinks GM, Wallace GG (2015) Processable conducting graphene/chitosan hydrogels for tissue engineering. J Mater Chem B 3(3):481–490
Schmidt CE, Shastri VR, Vacanti JP, Langer R (1997) Stimulation of neurite outgrowth using an electrically conducting polymer. Proc Natl Acad Sci U S A 94 (17):8948–8953
Seong JM, Kim B-C, Park J-H, Kwon IK, Mantalaris A, Hwang Y-S (2010) Stem cells in bone tissue engineering. Biomed Mater 5(6):062001
Serrano MC, Patiño J, García-Rama C, Ferrer ML, Fierro JLG, Tamayo A, Collazos-Castro JE, del Monte F, Gutierrez MC (2014) 3D free-standing porous scaffolds made of graphene oxide as substrates for neural cell growth. J Mater Chem B 2(34):5698–5706
Shah S, Yin PT, Uehara TM, Chueng STD, Yang L, Lee KB (2014) Guiding stem cell differentiation into oligodendrocytes using graphene-nanofiber hybrid scaffolds. Adv Mater 26(22):3673–3680
Sharma G, Thakur B, Naushad M, Kumar A, Stadler FJ, Alfadul SM, Mola GT (2017) Applications of nanocomposite hydrogels for biomedical engineering and environmental protection. Environ Chem Lett. https://doi.org/10.1007/s10311-017-0671-x
Shin SR, Aghaei-Ghareh-Bolagh B, Dang TT, Topkaya SN, Gao X, Yang SY, Jung SM, Oh JH, Dokmeci MR, Tang XS (2013) Cell-laden microengineered and mechanically tunable hybrid hydrogels of gelatin and graphene oxide. Adv Mater 25(44):6385–6391
Shin YC, Lee JH, Jin L, Kim MJ, Kim YJ, Hyun JK, Jung TG, Hong SW, Han DW (2015a) Stimulated myoblast differentiation on graphene oxide-impregnated PLGA-collagen hybrid fibre matrices. J Nanobiotechnol 13:21
Shin YC, Lee JH, Jin OS, Kang SH, Hong SW, Kim B, Park J-C, Han D-W (2015b) Synergistic effects of reduced graphene oxide and hydroxyapatite on osteogenic differentiation of MC3T3-E1 preosteoblasts. Carbon 95:1051–1060

Shin YC, Lee JH, Kim MJ, Hong SW, Kim B, Hyun JK, Choi YS, Park J-C, Han D-W (2015c) Stimulating effect of graphene oxide on myogenesis of C2C12 myoblasts on RGD peptide-decorated PLGA nanofiber matrices. J Biol Eng 9(1):22

Shin SR, Zihlmann C, Akbari M, Assawes P, Cheung L, Zhang K, Manoharan V, Zhang YS, Yüksekkaya M, Kt W (2016a) Reduced graphene oxide-GelMA hybrid hydrogels as scaffolds for cardiac tissue engineering. Small 12(27):3677–3689

Shin YC, Shin DM, Lee EJ, Lee JH, Kim JE, Song SH, Hwang DY, Lee JJ, Kim B, Lim D, Hyon S-H, Lim Y-J, Han D-W (2016b) Hyaluronic acid/PLGA core/shell fiber matrices loaded with EGCG beneficial to diabetic wound healing. Adv Healthc Mater 5 (23):3035–3045

Shin YC, Jin L, Lee JH, Jun S, Hong SW, Kim C-S, Kim Y-J, Hyun JK, Han D-W (2017a) Graphene oxide-incorporated PLGA-collagen fibrous matrices as biomimetic scaffolds for vascular smooth muscle cells. Sci Adv Mater 9(2):232–237

Shin YC, Kang SH, Lee JH, Kim B, Hong SW, Han D-W (2017b) Three-dimensional graphene oxide-coated polyurethane foams beneficial to myogenesis. J Biomater Sci Polym Ed. https://doi.org/10.1080/09205063.09202017.01348738

Shin YC, Kim J, Kim SE, Song S-J, Hong SW, Oh J-W, Lee J, Park J-C, Hyon S-H, Han D-W (2017c) RGD peptide and graphene oxide co-functionalized PLGA nanofiber scaffolds for vascular tissue engineering. Regen Biomater 4(3):159–166

Shin YC, Song S-J, Hong SW, Jeong SJ, Chrzanowski W, Lee J-C, Han D-W (2017d) Multifaceted biomedical applications of functional graphene nanomaterials to coated substrates, patterned arrays and hybrid scaffolds. Nanomaterials 7(11):369

Shuai C, Feng P, Gao C, Shuai X, Xiao T, Peng S (2015) Graphene oxide reinforced poly (vinyl alcohol): nanocomposite scaffolds for tissue engineering applications. RSC Adv 5(32):25416–25423

Song H, Stevens CF, Gage FH (2002) Astroglia induce neurogenesis from adult neural stem cells. Nature 417 (6884):39–44

Song J, Gao H, Zhu G, Cao X, Shi X, Wang Y (2015) The preparation and characterization of polycaprolactone/graphene oxide biocomposite nanofiber scaffolds and their application for directing cell behaviors. Carbon 95:1039–1050

Tang L, Wang Y, Li Y, Feng H, Lu J, Li J (2009) Preparation, structure, and electrochemical properties of reduced graphene sheet films. Adv Funct Mater 19 (17):2782–2789

Tang M, Song Q, Li N, Jiang Z, Huang R, Cheng G (2013) Enhancement of electrical signaling in neural networks on graphene films. Biomaterials 34(27):6402–6411

Teo WE, Ramakrishna S (2006) A review on electrospinning design and nanofibre assemblies. Nanotechnology 17(14):R89

Unnithan AR, Park CH, Kim CS (2016) Nanoengineered bioactive 3D composite scaffold: a unique combination of graphene oxide and nanotopography for tissue engineering applications. Compos Part B 90:503–511

Valiev R (2002) Materials science: nanomaterial advantage. Nature 419(6910):887–889

Vasita R, Katti DS (2006) Nanofibers and their applications in tissue engineering. Int J Nanomedicine 1(1):15

Wan C, Frydrych M, Chen B (2011) Strong and bioactive gelatin-graphene oxide nanocomposites. Soft Matter 7 (13):6159–6166

Wang Y, Li Z, Wang J, Li J, Lin Y (2011) Graphene and graphene oxide: biofunctionalization and applications in biotechnology. Trends Biotechnol 29(5):205–212

Wang L, Lu C, Li Y, Wu F, Zhao B, Dong X (2015) Green fabrication of porous silk fibroin/graphene oxide hybrid scaffolds for bone tissue engineering. RSC Adv 5(96):78660–78668

Wolf MT, Dearth CL, Sonnenberg SB, Loboa EG, Badylak SF (2015) Naturally derived and synthetic scaffolds for skeletal muscle reconstruction. Adv Drug Deliv Rev 84:208–221

Yin H, Ding G, Shi X, Guo W, Ni Z, Fu H, Fu Z (2016) A bioengineered drug-eluting scaffold accelerated cutaneous wound healing in diabetic mice. Colloids Surf B-Biointerfaces 145:226–231

Yoon OJ, Sohn IY, Kim DJ, Lee N-E (2012) Enhancement of thermomechanical properties of poly (D, L-lactic-*co*-glycolic acid) and graphene oxide composite films for scaffolds. Macromol Res 20(8):789–794

Yue H, Wei W, Yue Z, Wang B, Luo N, Gao Y, Ma D, Ma G, Su Z (2012) The role of the lateral dimension of graphene oxide in the regulation of cellular responses. Biomaterials 33(16):4013–4021

Zhang H-B, Zheng W-G, Yan Q, Yang Y, Wang J-W, Lu Z-H, Ji G-Y, Yu Z-Z (2010a) Electrically conductive polyethylene terephthalate/graphene nanocomposites prepared by melt compounding. Polymer 51 (5):1191–1196

Zhang Y, Ali SF, Dervishi E, Xu Y, Li Z, Casciano D, Biris AS (2010b) Cytotoxicity effects of graphene and single-wall carbon nanotubes in neural phaeochromocytoma-derived PC12 cells. ACS Nano 4(6):3181–3186

Zhang C, Wang L, Zhai T, Wang X, Dan Y, Turng L-S (2016a) The surface grafting of graphene oxide with poly (ethylene glycol) as a reinforcement for poly (lactic acid) nanocomposite scaffolds for potential tissue engineering applications. J Mech Behav Biomed Mater 53:403–413

Zhang K, Zheng H, Liang S, Gao C (2016b) Aligned PLLA nanofibrous scaffolds coated with graphene oxide for promoting neural cell growth. Acta Biomater 37:131–142

Zhao C, Tan A, Pastorin G, Ho HK (2013) Nanomaterial scaffolds for stem cell proliferation and differentiation in tissue engineering. Biotechnol Adv 31(5):654–668

Zhou Z-Y, Tian N, Li J-T, Broadwell I, Sun S-G (2011) Nanomaterials of high surface energy with exceptional properties in catalysis and energy storage. Chem Soc Rev 40(7):4167–4185

Zhou K, Motamed S, Thouas GA, Bernard CC, Li D, Parkington HC, Coleman HA, Finkelstein DI, Forsythe JS (2016a) Graphene functionalized scaffolds reduce the inflammatory response and supports endogenous neuroblast migration when implanted in the adult brain. PLoS One 11(3):e0151589

Zhou T, Wang N, Xue Y, Ding T, Liu X, Mo X, Sun J (2016b) Electrospun tilapia collagen nanofibers accelerating wound healing via inducing keratinocytes proliferation and differentiation. Colloids Surf B-Biointerfaces 143:415–422

Part III

Biomimetic Materials in Tissue Engineering

Influence of Biomimetic Materials on Cell Migration

6

Min Sung Kim, Mi Hee Lee, Byeong-Ju Kwon, Min-Ah Koo, Gyeung Mi Seon, Dohyun Kim, Seung Hee Hong, and Jong-Chul Park

6.1 Biomimetic Materials in Tissue Engineering

Tissue engineering is a multi-disciplinary field that purposes tot the advance of biological replacements that recover, maintain, or promote the tissue function (Langer and Vacanti 1993; Ma 2004, 2005; Rice et al. 2005). To regulate the tissue formation in three dimensions (3D) situation, highly porous structure of scaffold is important in a typical tissue engineering strategy. In addition the scaffolds supply the synthetic extracellular matrix (ECMs) or microenvironments for attachment, proliferation, differentiation, regeneration or tissue genesis by the defining of 3D geometry for tissue engineering (Ma 2004, 2005; Liu and Ma 2004). As a result in tissue engineering, chemical and physical structures, or biologically functional moiety are significant to the biomaterials.

The diverse materials have been studied as scaffolds for tissue regeneration to satisfy the tremendous needs in tissue engineering. Because of the lack of degradation in biological situation (Liu and Ma 2004), some metals were not suitable for scaffold applications although they were used for medical implants due to their excellent mechanical properties (Catledge et al. 2004). The ceramic or inorganic materials; calcium phosphates or hydroxyapatite (HAP), has been studied for mineralized tissue engineering because of their excellent osteo-conductivity, however they were also limited due to their lowly porous structures or brittleness. On the contrary, polymers can be great candidate for scaffolds because they have good design flexibility so that the structure or composition can be modified to the particular demands. For these reasons, polymers have been widely studied in diverse tissue engineering applications, including bone, cartilage tissue engineering (Rice et al. 2005; Liu and Ma 2004; Meinel et al. 2005; Huang et al. 2007).

The emulating the advantageous features of the natural ECM may be valuable for the scaffold to serve as the impermanent ECM for regeneration of cells. However, it is unnecessary for the scaffold to completely copy the natural ECM, because the process of neo tissue genesis in tissue engineering is not correctly the same as the developmental or wound healing program. The tissue

M. S. Kim · M.-A. Koo · G. M. Seon · S. H. Hong
J.-C. Park (✉)
Cellbiocontrol Laboratory, Department of Medical Engineering, Yonsei University College of Medicine, Seoul, South Korea

Brain Korea 21 Plus Project for Medical Science, Yonsei University College of Medicine, Seoul, South Korea;
drmin9@yuhs.ac; sseon1227@yuhs.ac; seungheestar@yuhs.ac; parkjc@yuhs.ac

M. H. Lee · B.-J. Kwon · D. Kim
Cellbiocontrol Laboratory, Department of Medical Engineering, Yonsei University College of Medicine, Seoul, South Korea
e-mail: leemh1541@yuhs.ac; bjkwon@yuhs.ac; doh2yun@yuhs.ac

I. Noh (ed.), *Biomimetic Medical Materials*, Advances in Experimental Medicine and Biology 1064,
https://doi.org/10.1007/978-981-13-0445-3_6

engineering could accelerate the regeneration process compared to the natural development program, so the natural ECM is not suitable for scaffold in tissue engineering applications. Highly interconnected macro-or micro-pore structures helps cells to make quick and uniform population, this is essential for the tissue engineering and regenerative process however mature tissue matrix sometimes does not possess those structures. Therefore the optimal tissue engineering applications for accelerating of tissue regeneration require the appropriate designed scaffold features; pore size, porosity, inter pore connectivity. Lastly, the feasible pathogen transmission and immune rejection should be always concerned when using the natural ECM.

The biomaterials play a critical role in the most tissue engineering approaches (Hubbell 1995). The biomaterials can perform as a substrate to help the cells attach or migrate. It also helps cells to be implanted with a mixture of various cell types as a cell delivery vehicle, or be utilized as a drug carrier to initiate the specific cellular function in the localized area (Marler et al. 1998; Murphy and Mooney 1999). The advance of biomaterials for tissue engineering applications has focused on the devising of biomimetic materials that can interact with surrounding tissues by biomolecular identification (Hubbell 1999; Healy 1999; Sakiyama-Elbert and Hubbell 2001). The extracellular matrix (ECM) proteins are not particularly adsorbed on the surface of biomaterials after they are exposed to the biological conditions, then the cells interact with the surface of biomaterials through the adsorption of ECM proteins.

Biomolecular identification of materials by cells can be performed by two major devising approaches. One strategy is to incorporate the cell-binding peptides into biomaterials via physical or chemical adjustment. The cell-binding peptides contain both a long chain of ECM proteins and short peptide sequences derived from unscathed ECM proteins that can cause certain interactions with cell receptors. The biomimetic materials possibly imitate various roles of ECM in tissues. For example, the surface of biomaterials which is cell non-adhesive inherently can change to the cell adhesive surface by the immobilization of signaling peptides (Shin et al. 2002). The specific protease enzymes can also make the material degradable using the union of peptide sequences into materials (West and Hubbell 1999) or the union of peptide can cause the cellular responses (Suzuki et al. 2000). The other strategy is to endue biomaterials with bioactivity by union of soluble bioactive molecules; growth factors and plasmid DNA into biomaterial carriers. The materials released these bioactive molecules and start or modulate the new tissue formation (Whitaker et al. 2001; Richardson et al. 2001; Babensee et al. 2000).

6.2 Cell Migration

Cell migration plays important role in physiological phenomenon and cancer metastasis, immune response or embryonic development. The interaction between cell and the extracellular matrix (ECM) highly regulate the cell specific process characteristics. Cell polarization and protrusion at the leading edge also can influence on the cell migration and these phenomena are dependent on attachment of cells to the ECM or actin polymerization. The cell translocation or retraction of the rear which caused by the transmission of traction forced was followed by these events (Vicente-Manzanares et al. 2005; Lock et al. 2008).

Focal adhesions (FAs) are complexes of various proteins, and these mediate the signal transduction or adhesion to the ECM (Yamada and Geiger 1997). The actin cytoskeleton is connected to the ECM by FAs physically through the transmembrane heterodimer cell receptors; integrins, and also through the focal adhesion kinase (FAK) and vinculin which comprise the signaling pathways and mechano-transductive pathways (Huttenlocher and Horwitz 2011). The repeating cycles of FA assembly and disassembly during cell migration is caused by the rapid change in the protein composition over time in response to the external signals (Huttenlocher and Horwitz 2011; Zaidel-Bar et al. 2003). The characteristics of FA; size or morphology might determine the cell migrations (Kim and Wirtz

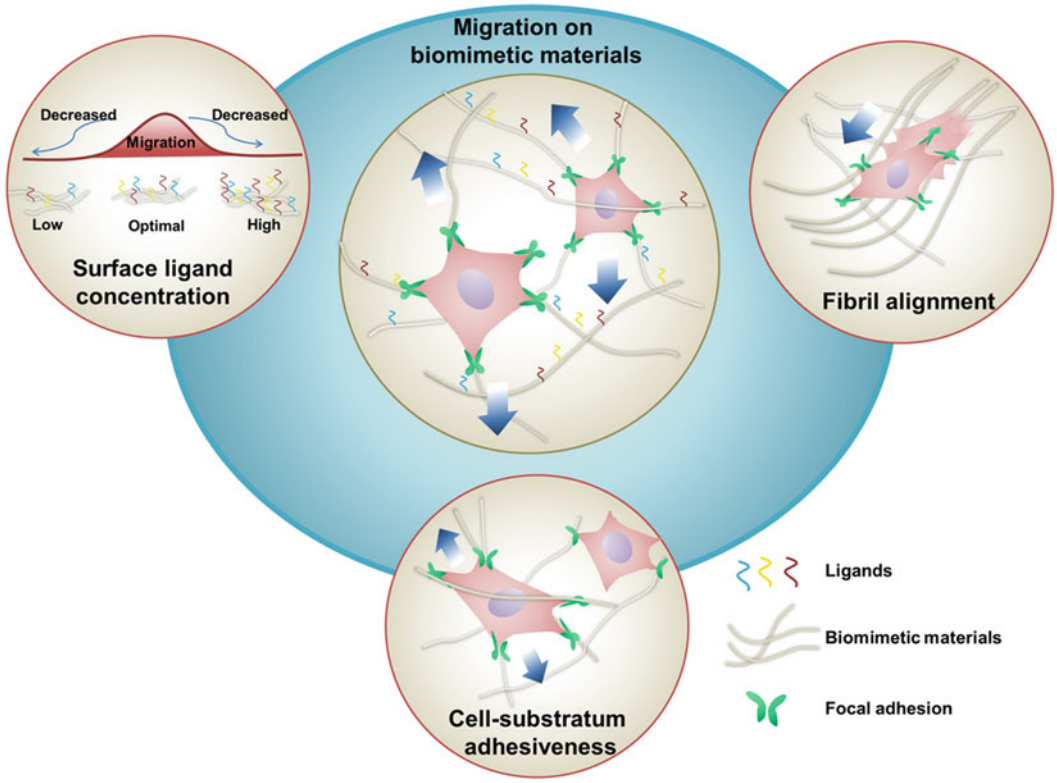

Fig. 6.1 Schematic diagram of cell migration on biomimetic materials

2013). The diverse size of FAs using the nano-patterned surface correlated with the particular cell migratory events (Slater et al. 2015). In addition, studies about the relationship between the cell migration and physical/chemical properties of the substrate have been performed. The ligand density by substrate, the expression levels of integrins and the ligand-inegrin affinity affected to the cell migration too (Palecek et al. 1997; Bergman and Zygourakis 1999). Also the adhesiveness level of cell substratum is related with the maximum speed of the cells (Palecek et al. 1997; Bergman and Zygourakis 1999; Kim et al. 2013).

The tremendous studies about the cell migration have been performed, however the molecular mechanism coordinating the cell motility is still not fully understood. It is well known that the external stimulation can regulate the cell response, such as mechano-transduction signals or stiffness, dimensionality of the ECM (Friedl and Wolf 2010; Petrie et al. 2009). Therefore, it is well accepted that the modulation of physical or chemical material parameters make the biomaterials alter the cell motility. Figure 6.1 showed the schematic diagram of cell migration on the biomimetic materials. In this review, cell migration on biomimetic materials has been introduced at mimicking the natural properties of the *in vitro* or *in-vivo* matrix.

6.2.1 Cell Migration with Collagen

The most plentiful protein in mammals, collagen type I has a triplehelical structure and this is made of three polypeptide chains which contain the gly-X-Y holding th 4-hydroxypoline and proline (Kadler et al. 2007). Collagens could be purified from human tissues (placenta) or animal tissues (skin, tendon). The increase of PH or temperature of precursor solution can reconstitute the ECM

protein into the fibrous matrix (Patterson et al. 2010). Collagen type I is widely used by treated with proteases for removing the small nonhelical telopeptides which presents at the end of the triple helical domain and is used for the cross species immunogenic character of the most proteins. However, the disease transmission and concerns of immunogenicity still remain for clinical application of this material (Lynn et al. 2004). Some recombinant human collagen type I and III are commercially sold, and methods for recombinant collagen expression have been studied for avoiding those risks (Ruggiero and Koch 2008).

The even macroscopic or permanent microscopic alignment of fibrous collagen matrix could be obtained by the dipole moment of fibrous collagen. The alignment of fibrous collagen under the strong magnetic field has been studied for inducing the directed cell migration; for example the neuritis grow along the direction of fibrous alignment (Ceballos et al. 1999).

6.2.2 Cell Migration with Fibrin

The fibrin is a special protein network which is formed in spontaneous tissue repair for clinically using from cryo-precipitated human blood plasma or autologous sources. The circulating glycoprotein homodimer of heterotrimer; which is called polymerization of fibrinogen combine the fibrin matrix spontaneously in the existence of thrombin protease. Fibrino-peptide on the fibrinogen is cleaved by the thrombin which prohibit the chemical or physical self –assembly or the molecule polymerization. The chemically cross linked network by the XIIIa which is blood transglutaminase factor and the fibrous structure of its compound (Patterson et al. 2010) depend on the formation of the cross-linked character (Lorand and Graham 2003; Standeven et al. 2007; Weisel 2004). Normally the fibrin is not the ECM because it is not generated by the cells around the local environment, however ECM is very important material that it is a critical member of regenerative matrices and plays role of a provisional matrix by remodeling and replacing with ECM molecules.

The proteolytic degradation may effect on the mechanism of cell migration in fibrous collagen matrix, however the migration of cells in fibrin is almost related with the cell associated proteolytic activity. The differences of cellular response in the fibril collagen may result from the small scaffold size of the fibrous matrices and the strong fibrous interactions, and the nature of network formation and covalent stabilization.

6.2.3 Cell Migration with Glycosaminoglycans

The long unbranched polysaccharides augmented the structure of ECM proteins in the biochemical or biomechanical functions. The components of ECM proteoglycans are not attaché to the core of protein covalently, and are entagled in the extracellular space except for the hyaluronic acid case. The glycosaminoglycans directly effect on the tissue regeneration through the interactions of cell-surface receptors, however the strong anionic polymers supply the compressive strength to the ECM by absorbing the water (Toole 2004).

Hyaluronic acid hydrogels have been studied for diverse uses; such as the dermal wound healing by keratinocyte transferring or cartilage repair by chondrocyte transplantation (Price et al. 2007; Tognana et al. 2007). Some cell surface receptors including CD44, RHAMM, and ICAM-1, interact with the hyaluronic acid and the incorporation of other functional biomolecules increase the biological activity of hyaluronic acid (Turley et al. 2002). The degradation of hyaluronic acid gel is due to the dyaluronidase (Kim et al. 2008), meanwhile the cell migration is driven by the diverse MMPs activities so using the MMP-sensitive cross-linkers could improve the migration of cells into the hydrogels. Also the wound healing or proliferation of fibroblasts can be improved by the functionalizing of hyaluronic acid gels with protein fragments or peptides from the fibronectin (Park et al. 2003; Ghosh et al. 2006). The migration of cells in-vivo is coupled to the degradation of ECM molecules via cell secreted or cell associated proteases expression, because the

matrix degradation is enzymatically rather than hydrolytically. Therefore the most of hydrogels for the biological applications including fibrin or hyaluronic acid hydrogels are degradable.

The degradation of synthetic hydrogels is mediated by cell and can be controlled by the incorporation of protease substrate sequences (Kim et al. 2008; Chau et al. 2008; Lévesque and Shoichet 2007; Lutolf et al. 2003). For rendering of covalent cross linking (Kim et al. 2008; Lévesque and Shoichet 2007; Lutolf et al. 2003) or self-assembling (Chau et al. 2008) to the degradation of hydrogels enzymatically. Furthermore, hydrogels which contains the incorporation of the enzyme units can control the degradation too. The organization or deposition of collagen type II by encapsulation of chondrocytes in vitro effected on the duration or timing of lipase exposure, and the presence of lipase can be caused the degradation of caprolactone units contained photo cross linked PEG gels (Rice and Anseth 2007). The erosion of the hydrogels for space of cell spreading or ECM production, can direct the cell migration or cell to cell connection, produce the channels and three-dimensional structures for example the interconnected channels made by two-photon methodology. The combination of photolabile tethered biologically active functionalities can effects on the locally modified chemical environments and also can enhance the chondrogenic differentiation of encapsulated human MSCs upon removal of RGD (Kloxin et al. 2009).

6.2.4 Migration in Tenascin-C Mimetic Peptide Amphiphile Nanofiber Gel

The glycoprotein tenascin-C is very important in spinal cord regeneration (Yu et al. 2011; Zhang et al. 1997). The expression of the axon ingrowth is shown highly in spinal cord injury and regions (Zhang et al. 1997). The spinal cord injury inhibit the tenascin-C expression, and the inhibition of tenascin-C reduce the supraspinal synapse formation and axon regrowth with the neurons of spinal motor and recovery of damaged locomotor (Yu et al. 2011). Tenascin-C also can guide the neural progenitors in development of brain (Thomas et al. 1996). The expression of protein that contribute to the stem cell niche by altering the response to the growth factors is increased in the subventicular zone (SVZ), and this protein also promote the FGF2 sensitivity and decrease the BMP4 sensitivity, which enchance the acquisition of EGF receptor (Garcion et al. 2004). The expression of tenascin-C is also increased in the rostral migration stream in the extracellular space (Thomas et al. 1996), which is a pathway that the migration of neuroblasts from SVZ to the olfactory bulb, where they changed into the new internerouns.

The integrin-dependent pathways which helped cell adhesion can activate the tenascin-C. Many studies have discovered that the enascin-C with a linear peptides can promote the length of neurite (Meiners et al. 2001) via interaction with $\alpha_7\beta_1$-integrin (Mercado et al. 2004). The electrospun polyamide fibers were connected with the peptides covalently, and these were coated onto the coverslips (Ahmed et al. 2006). Some primary neurons; spinal motor, dorsal root ganglion and cerebellar granule neurons induce the increase of average lengths of neurite when they cultured in vitro in the tenascin-C peptide coated with the polyamide fibers (Ahmed et al. 2006). The materials with this peptide have effected on the non-neuronal systems too. Recently, one study showed that this peptide coated with self-assembled nanofibers could enhance the osteogenic differentiation of rat mesencymal stem cells (Sever et al. 2014).

The signaling of neurons to increase their length of neurite and the ratio of cells which positively on β-III-tubulin relative to backbone PA gels could be effected by the incorporation of the tenascin-C and PA gels. The length of neurite or the ratio of to β-III-tubulin-positive cells was not increased significantly by adding the scrTN-C PA gels. However, when the β_1-integrin blocking antibody treated to the gels, length of neurite and the ratio of positive cells to β-III-tubulin with neurites were dropped in TN-C PA gels, but not in scrTN-C PA gels because the

scrTN-C PA gels were not seriously different from the TN-C PA gels. According to these results, the length and number of cells with neurite is raised by the TN-C PA, and also β_1-integrin interaction affected too. However the mechanism on the peptide sequence is not fully understood because the TN-C PA is not seriously different from the scrTN-C PA.

The promotion of cell migration by the development of PA was the main purpose, and Eric et al. showed that the native channel for the migration like the rostral migration stream was existed by using the material with physical directional signals such as aligned fibers (Eric et al. 2016). The migration of native or transplanted cells could be directed by the neural stem cells or neural progenitor cells to the regions of neuronal loss. The expression of tenacin-C in the RMS is also detected when the neuroblasts moved on the surface of astrocytes (Thomas et al. 1996). The β1 integrin is very important in migration of neural cell (Jacques et al. 1998; Leone et al. 2005), therefore the incorporation of a tenascin-C derived from β1 integrin and nanofibers could enhance the migration of NPC derived cells. Compared to the backbone PA alone, the incorporation of PA mixtures which including the backbone PA and TN-C PA promote the migration of cells, meanwhile the backbone PA alone and incorporation of PA and scrTN-C did not influence on the cell migration.

6.2.5 Human Microvascular Endothelial Cell Migration on Biomimetic Surfactant Polymers

The migration of cell has been studied a lot in vitro because it is very important in physiological and pathological procedures (Kouvroukoglou et al. 2000; Hubbell et al. 1991; Garcia et al. 1998; Asthagiri et al. 1999; Byzova et al. 2000; Chon et al. 1997; Lauffenburger and Horwitz 1996; Nehls et al. 1998). Cell migration plays a role in various situations such as regeneration of damaged vascular wall, angiogenesis or colonization of cells in biomaterials. The EC migration is significantly important for succeeding of EC seeding on the surface to the implantation. At low density of cell seeding, the speedy migration and colonization is important, and some materials can induce these advantageous features. The migration of cells also important in the regions of cell loss because of the fluid shear stress, even confluent monolayer of ECs covered the implantation area.

The receptor cytoskeleton interactions, cytoskeletal formation or reorganization, and the detachment of tail ends, cell adhesion onto the surface are mediated with the migration of cells. The integrins or ligand interactions with factors could decide the direction or speed of cell migration (Kouvroukoglou et al. 2000; Domanico et al. 1997; Friedl et al. 1998; Maheshwari et al. 2000; Palecek et al. 1997; Simon et al. 1997). The integrin/ligand binding affinities, integrin expression levels, and ligand levels are the member of these factors (Maheshwari et al. 2000; Palecek et al. 1997; Simon et al. 1997). The average speed of cell migration has been shown that the cell to surface adhesive strength is dependent on the variety of cell types theoretically and experimentally (Maheshwari et al. 2000; Palecek et al. 1997; Wu et al. 1994). The $\alpha_4\beta_1$ and the $\alpha_5\beta_1$, the particular integrins could influence on the migration of cells to the fibronectin, as well as the $\alpha_v\beta_3$ and $\alpha_v\beta_5$ which is vitronectin receptors involved in the migration of diverse types of cells, such as endothelial cells in angiogenesis (Maheshwari et al. 2000; Simon et al. 1997; Eliceiri et al. 1998).

The RGDS, YIGSRG (the adhesive sequence of laminin), the example of adhesive peptide sequences which are covalently immobilized, have influenced on the changes of cell persistence (the time between significant directional changes) and cell speed (Kouvroukoglou et al. 2000; Olbrich et al. 1996; Mann and West 2002). The migration of fibroblasts was decreased by adding the RGDs on the surfaces compared to the non-adhesive peptides (RDGS or RGES) (Olbrich et al. 1996), and RGDS and YIGSRG surfaces increased the random migration or persistence time of endothelial cells that non-adhesive peptides (Kouvroukoglou et al. 2000). However, the increase of surface peptide

density which composed of three different adhesive peptides inhibited the migration of smooth muscle cells seriously (Mann and West 2002). Therefore, the density of surface ligand and receptor affinity can influence on the adhesion strength to the surface, shear stability, signaling and EC migration (Garcia et al. 1998; Asthagiri et al. 1999; Palecek et al. 1997; Chan et al. 1999; Ruoslahti and Obrink 1996; Xiao and Truskey 1996).

One study showed that the series of biomimetic polymers which could be used to change the surface of existing biomaterials were designed for enhancing the appropriate adhesion and function of ECs on the biomaterial surfaces (Sagnella et al. 2004). The limiting the undesirable platelet activation and adhesions was caused by the maltose sugars which acts as a steric guard against the adsorption of non-particular proteins likely to the glycocalyx functions (Holland et al. 1998; Qiu et al. 1998). The surfactant polymer on the hydrophobic surface is self-assembled by the side chains of alkyl, so that the EC adhesion increased by the appropriate orientation of The RGD peptides.

The controlling the density of surface peptides could change the rate of EC migration or activity on these surfaces (Sagnella et al. 2004). The 100% of RGD polymers could induce the strong adhesion of ECs and wide spreading than other surfaces because it has the highest density of surface peptide. On 100% of RGD surfaces, HMVEC spread more even the cells were seeded at confluent density, because the increased integrin binding sites per area induced the cells to attach in more places and effectively spread out further. However the shorter distance migrating time and the lower cell density were observed in the smaller surface area covered by the migrating HMVEC population on the 100% RGD surface.

In increased ligand concentration, the decrease of cell migration is related with the increase of cell spreading for EC and other cell types (Palecek et al. 1997; Mann and West 2002; Burgess et al. 2000; Gobin and West 2002; DiMilla et al. 1993). The increase of the concentration of RGDS, VAPG, or KQAGDV inhibited the smooth muscle cell migration (Mann and West 2002). Previous study showed that the changing of surface ligands could control the adhesive strength via cell migration. Another study identified that 8 RGD per collagen monomer induce the highest coefficient of random migration of mouse melanoma cell via 3D collagen scaffold, however the density of peptide decreased above or below this number (Burgess et al. 2000). At concentration of 3.5 μmol/ml of RGDS, the migration of fibroblast and smooth muscle cells in ECM-like PEG hydrogels was highest, however the migration was decreased at above or below of this concentration (Gobin and West 2002). Similarly, full concentration of ECM proteins increased cell migration too (Palecek et al. 1997; DiMilla et al. 1993), so these results suggested that the highest migration is caused by appropriate ligand concentration which is optimal density.

The 100% of RGD surface showed slower migration that 75% RGD surface, and lower RGD promoted the migration of HMVEC even more. At the initial edge of 50% surface, HMVEC migrated further and showed higher density of cells with increase of radial distance than other surfaces. However, more decreased density of peptides induced drop of migration behavior. Unlike the described studies related in surfaces (Burgess et al. 2000; Gobin and West 2002; DiMilla et al. 1993), cell adhesion or growth were not influenced by biomimetic polymer system when the attached peptide did not exist. The adsorption of non-particular protein was inhibited by the glycocalyx-like properties of the oligosaccharide- rich surface (Holland et al. 1998; Ruegsegger and Marchant 2001). The EC adhesion and long term growth were not assisted by the 25% of RGD surface (Murugesan et al. 2002). Therefore, the density of peptide or, cell receptor density, ligand-receptor affinity could affect migration of cells (Palecek et al. 1997; Simon et al. 1997).

6.2.6 Biomimetic-Engineered Poly (Ethylene Glycol) Hydrogel for Smooth Muscle Cell Migration

Smooth muscle cell (SMC) migration plays a key role in a variety of physiological and pathological situations, ranging from vascular development to intimal hyperplasia after vascular injury (Willis et al. 2004; Gerthoffer 2007; Louis and Zahradka 2010). During vascular development, migration of pericytes and smooth muscle precursor cells occurs after the formation of an endothelial cell tube, assisting in the development of vessel wall construction and biomechanical functionality of the blood vessels (Gerthoffer 2007; Louis and Zahradka 2010). In response to vascular injury, SMCs up-regulate the secretion of matrix metallo-proteinases (MMPs) and increase their rate of cell migration, which is required for wound healing and vascular repair (Louis and Zahradka 2010). The development of materials that facilitate SMC migration has been a critical strategy in vascular tissue engineering because of the essential role of cell migration in vascular remodeling (Mann et al. 2001a, b; Almany Seliktar 2005; Liu Chan-Park 2010). However, excessive SMC migration, followed by SMC proliferation, if uncontrolled, will induce pathogenic vascular remodeling, which is a key step in the development of intimal hyperplasia (Willis et al. 2004; Louis and Zahradka 2010). Therefore, understanding the mechanisms involved in SMC migration and the development of strategies to regulate this process have become emerging areas of research.

Published studies of SMC migration on two-dimensional (2D) surfaces have suggested that cell migration is largely governed by the balance between attachment and detachment, presenting a biphasic dependence on cell-substratum adhesiveness (DiMilla et al. 1993). However, conditions for cell migration in vivo are more complex. Besides providing a variety of biochemical cues to guide cell function, the extracellular matrix (ECM) also imposes biophysical resistance to cell movement (Friedl and Brocker 2000; Friedl et al. 1998; Even-Ram and Yamada 2005).

Naturally derived materials, such as collagen gel and fibrin gel (Li et al. 2003; Shi et al. 2010; Ucuzian et al. 2010), have been utilized to investigate cell migration in three dimensions, because they possess many critical biological functions such as cell adhesion and biodegradability (Rosso et al. 2005; Chen and Hunt 2007). However, biological materials used in vitro have some deficiencies, including relatively poor mechanical properties, batch-to-batch variability, and limited design flexibility, which restrict their potential to become an ideal model (Rosso et al. 2005; Chen and Hunt 2007; Pampaloni et al. 2007).

The role of SMC migration as an essential process in physiological and pathological vessel wall remodeling makes the study of mechanisms involved in cell migration a major focus of research (Willis et al. 2004; Gerthoffer 2007; Louis and Zahradka 2010). In contrast to cell migration on 2D surfaces, 3D cell migration is more complex, because migration is mediated not only by biochemical factors (e.g., adhesive ligand concentration), but also by biophysical factors (e.g., network cross-linking density) (Friedl and Brocker 2000; Friedl et al. 1998; Even-Ram and Yamada 2005).

Cell-matrix adhesion is a governing parameter of cell migration on 2D surfaces (DiMilla et al. 1993), consequently, it is reasonable to anticipate that cell-matrix adhesion also will play a key role in 3D cell migration. To explore the effect of a single parameter (e.g., adhesive ligand concentration) on cell migration in a 3D model, the interdependence of variables (e.g., adhesive ligand concentration vs. hydrogel network property) should be considered. To investigate the effect of adhesive ligand concentration on the hydrogel network, studies of mass swelling ratio as a function of RGD-PEGMA concentration were performed. The results indicated that the hydrogel network was not affected by the inclusion of RGD-PEGMA, while adhesive ligand concentration was in the range of 0–2.5 mM. Therefore, this concentration range (0–2.5 mM) was chosen to study the effect of adhesive ligand concentration on SMC migration. Similar to previous studies of cell migration on 2D surfaces (DiMilla et al. 1993; Wu et al. 2012) and within 3D matrices

(Lutolf and Hubbell 2003; Gobin and West 2002; Raeber et al. 2007), a biphasic relationship between migration distances and cell-matrix adhesiveness was found (Lin et al. 2014). Since cell migration is a product of the net force between counteracting detachment and adhesion forces, it is hypothesized that at a low ligand concentration, weak cell-matrix adhesiveness results in a decrease in traction forces for forward movement, which subsequently slows cell migration. In contrast, in the presence of a high ligand concentration in the 3D network, strong cell-matrix adhesiveness inhibits cell detachment, which results in decreased migration (Lutolf and Hubbell 2003; Gobin and West 2002).

The effect of the hydrogel network on cell migration in 3D gels was evaluated by varying the concentration of GIA-PEGDA in the hydrogels. Mass swelling ratio studies showed that a variation in GIA-PEGDA concentrations results in a significant change in mass swelling ratios of the hydrogels (Lin et al. 2014), which is an important parameter that is closely related to the biophysical properties of the hydrogel network (e.g., mesh size, cross-linking density) (Beamish et al. 2009; Lutolf and Hubbell 2003; Munoz-Pinto et al. 2009; Beamish et al. 2010). At a constant concentration of RGD-PEGMA (0.441 mM, the concentration that shows maximum migration in 5% GIA-PEGDA gels) in the swollen hydrogel, increasing GIA-PEGDA concentrations significantly decreases migration distances (Lin et al. 2014). This observation is consistent with previous studies, in which the network properties of PEG hydrogels were tuned by PEG molecular weight. Therefore, along with cell-matrix adhesiveness and proteolysis, network cross-linking density plays a critical role in 3D cell migration.

6.2.7 3D Printing of Biomimetic Microstructures for Cancer Cell Migration

The cancer cells move to another site from the origin region via the circulatory or lymphatic system, this is a complex event of chain and called metastasis (Lauffenburger and Horwitz 1996; Steeg 2006). The patients who have the metastasizing stage of cancer will not survive less than a year (Decaestecker et al. 2007). Some tumors; glioblastomas, are dramatically increased by the migration, therefore the understanding about the migration of cancer cells could help to study the metastasis. The study about various factors to affect migration of cells is very important to advance the method for treating or targeting the cancer disease. Additionally the designing of accurate 3D model of cancer tissue is aided by the current drug test in 2D culture.

One study used the chick embryo's thin chorioallantoic membrane (CAM) mixed with fluorescently labeled cancer cells for observing the migration of cancer cells in vivo to develop more accurate model (Leong et al. 2012). Another study showed that the process of breast cancer metastasis was mimicked by using the transgenic mice (Jenkinson et al. 2004), however the effectiveness of the mice model needed more time to mature the metastasizing cancers and was very expensive (Zhou et al. 2011). For studying about metastasis, in vitro 2-D models have been designed (Jenkinson et al. 2004; Yamada and Cukierman 2007; Watson et al. 1995), for example; the micro-carrier bead assays or monolayer wound model (Decaestecker et al. 2007; Ghajar et al. 2007; Mathew et al. 1997; Chaffer et al. 2006). Additionally, the migration assay of single cell is very useful in migration analysis of separating cells from the cell growth (Decaestecker et al. 2007; Albrecht-Buehler 1977). Recently, in vitro 3-D models of migration system have been studied for more researching of cell migration (Rolli et al. 2010; Mak et al. 2011; Pathak and Kumar 2012), for example the linear polydimethylsiloxane (PDMS) channels was used to analyze the effectiveness of channel width and shape on the migration speed (Heuzé et al. 2011). Another study showed that the physical spatial gradients induce the response of cell migration (Mak et al. 2011), so that the feedback of mechanism about the metastasis of cancer cells into raised aggressiveness was identified. The increased width of channels also decreased the migration speed of cancer cells (Irimia and Toner 2009; Mathew et al. 1997).

One study showed that biomimetic 3D microstructure was created for study about migration of cancer cells by the technique of micro-fabrication (Lin et al. 2014). The scanning polymerization and projection polymerization were used for 3D bioprinting, and this maskless fabrication technique could make the delicate micro-pores and structures. Micromirror Device-based Projection Printing (DMD-PP) is a new technology to make three-dimensional structures in micro-scale biocompatible hydrogels (Lu and Chen 2008; Grogan et al. 2013; Suri et al. 2011; Soman et al. 2012a, b; Gauvin et al. 2012; Fozdar et al. 2011; Han et al. 2010; Zhang et al. 2012). Grogan et al. (2013) used the array of micro-mirrors to make scaffold of 3D structure by projecting the designed images onto the solution of photopolymerizable prepolymer (Grogan et al. 2013). The biomaterials are more pliable and have stiffness for micro-scale structures (Brown et al. 2005) than the PDMS platforms (Mak et al. 2011; Balaban et al. 2001; Vedula et al. 2012).

In addition, the versatility of the DMD-PP process allows rapid alterations of scaffold mechanical properties by altering the composition of the prepolymer solution. The DMD-PP method allows one to create 3D, biomimetic scaffolds in biomaterials with varying pattern design.

One study showed that the channel width did not influence on the migration speed of T1/2 cells, and these results similar with the in vivo study of cancer cell metastasis which identified that the morphology or physical interactions were changed via intravasation (Pathak and Kumar 2012; Gupta and Massagué 2006; Takeda et al. 2002). The procedure of cancer metastasis can describe the enhancing of migration speed by the thin channels (Pathak and Kumar 2012) and also explain the angiogenesis in advancement of tumors (Steeg 2006; Zetter 1998). The geometric signals could influence on the area of Hela cells or migration speed; dropping or promoting of cell area and migration speed. These results suggested that the size of vessel if important to the aggressiveness or metastasis of cancer cells (Gallego-Perez et al. 2012). So the different result in 10 T1/2 and Hela cells in geometric signals could suggest the appropriate plan to study about the metastasis of cancer.

6.3 What Is Coming Next in Cell Migration with Biomimetic Materials Research?

Until now, research on cell migration with biomimetic materials has been carried out using diverse ways; the molecular and structural levels of 2-D and 3-D situation. While all of these ways can make effective results, the methods for the homogeneous distribution and biocompatibility of scaffolds by cell migration needed to be focused with biomimetic materials. The studies about developing the plan for applying the effective methods should be progressed for cell migration with biomimetic materials.

Acknowledgement This research was supported by the Bio & Medical Technology Development Program of theNRF funded by the Korean government, MSIP (2017M3A9B3063638).

References

Ahmed I, Liu HY, Mamiya PC, Ponery AS, Babu AN, Weik T, Schindler M, Meiners S (2006) Three-dimensional nanofibrillar surfaces covalently modified with tenascin-C-derived peptides enhance neuronal growth in vitro. J Biomed Mater Res A 76:851–860

Albrecht-Buehler G (1977) The phagokinetic tracks of 3T3 cells. Cell 11(2):395–404

Almany L, Seliktar D (2005) Biosynthetic hydrogel scaffolds made from fibrinogen and polyethylene glycol for 3D cell cultures. Biomaterials 26:2467–2477

Asthagiri AR, Nelson CM, Horwitz AF, Lauffenburger DA (1999) Quantitative relationship among integrin-ligand binding, adhesion, and signaling via focal adhesion kinase and extracellular signal-regulated kinase 2. J Biol Chem 274:27119–27127

Babensee JE, McIntire LV, Mikos AG (2000) Growth factor delivery for tissue engineering. Pharm Res 17:497–504

Balaban NQ, Schwarz US, Riveline D, Goichberg P, Tzur G, Sabanay I, Mahalu D, Safran S, Bershadsky A, Addadi L, Geiger B (2001) Force and focal adhesion assembly: a close relationship studied using elastic micropatterned substrates. Nat Cell Biol 3 (5):466–472

Beamish JA, Fu AY, Choi A, Haq-Siddiqi NA, Kottke-Marchant K, Marchant RE (2009) The influence of RGDbearing hydrogels on the re-expression of contractile vascular smooth muscle cell phenotype. Biomaterials 30:4127–4135

Beamish JA, Zhu J, Kottke-Marchant K, Marchant RE (2010) The effects of monoacrylated poly (ethylene glycol) on the properties of poly (ethylene glycol) diacrylate hydrogels used for tissue engineering. J Biomed Mater Res A 92:441–450

Bergman AJ, Zygourakis K (1999) Migration of lymphocytes on fibronectin-coated surfaces: temporal evolution of migratory parameters. Biomaterials 20:2235–2244

Brown XQ, Ookawa K, Wong JY (2005) Evaluation of polydimethylsiloxane scaffolds with physiologically-relevant elastic moduli:interplay of substrate mechanics and surface chemistry effects on vascular smooth muscle cell response. Biomaterials 26(16):3123–3129

Burgess BT, Myles JL, Dickinson RB (2000) Quantitative analysis of adhesion-mediated cell migration in three-dimensional gels of RGD-grafted collagen. Ann Biomed Eng 28:110–118

Byzova TV, Kim W, Midura RJ, Plow EF (2000) Activation of integrin alpha(V)beta(3) regulates cell adhesion and migration to bone sialoprotein. Exp Cell Res 254:299–308

Catledge SA, Vohra YK, Bellis SL, Sawyer AA (2004) Mesenchymal stem cell adhesion and spreading on nanostructured biomaterials. J Nanosci Nanotechnol 4:986–989

Ceballos D, Navarro X, Dubey N, Wendelschafer-Crabb-G, Kennedy WR, Tranquillo RT (1999) Magnetically aligned collagen gel filling a collagen nerve guide improves peripheral nerve regeneration. Exp Neurol 158:290–300

Chaffer CL, Brennan JP, Slavin JL, Blick T, Thompson EW, Williams ED (2006) Mesenchymal-to-epithelial transition facilitates bladder cancer metastasis: role of fibroblast growth factor receptor-2. Cancer Res 66 (23):11271–11278

Chan BP, Bhat VD, Yegnasubramanian S, Reichert WM, Truskey GA (1999) An equilibrium model of endothelial cell adhesion via integrin-dependent and integrin-independent ligands. Biomaterials 20:2395–2403

Chau Y, Luo Y, Cheung ACY, Nagai Y, Zhang S, Kobler JB, Zeitels SM, Langer R (2008) Incorporation of a matrix metalloproteinase-sensitive substrate into self-assembling peptides – a model for biofunctional scaffolds. Biomaterials 29:1713–1719

Chen R, Hunt JA (2007) Biomimetic materials processing for tissue-engineering processes. J Mater Chem 17:3974–3979

Chon JH, Wang HS, Chaik EL (1997) Role of fibronectin and sulfated proteoglycans in endothelial cell migration on a cultured smooth muscle layer. J Surg Res 72:53–59

Decaestecker C, Debeir O, Van Ham P, Kiss R (2007) Can anti-migratory drugs be screened in vitro? A review of 2D and 3D assays for the quantitative analysis of cell migration. Med Res Rev 27(2):149–176

DiMilla PA, Stone JA, Quinn JA, Albelda SM, Lauffenburger DA (1993) Maximal migration of human smooth muscle cells on fibronectin and type IV collagen occurs at an intermediate attachment strength. J Cell Biol 122:729–737

Domanico SZ, Pelletier AJ, Havran WL, Quaranta V (1997) Integrin alpha 6A beta 1 induces CD81-dependent cell motility without engaging the extracellular matrix migration substrate. Mol Biol Cell 8:2253–2265

Eliceiri BP, Klemke R, Stromblad S, Cheresh DA (1998) Integrin alphavbeta3 requirement for sustained mitogen-activated protein kinase activityduring angiogenesis. J Cell Biol 140:1255–1263

Eric J, Álvarezb Z, Goldberger JE, Boekhovenb J, Kesslerd JA, Kuhne HG, Stupp SI (2016) A tenascin-C mimetic peptide amphiphile nanofiber gel promotes neurite outgrowth and cell migration of neurosphere-derived cells. Acta Biomater 37:50–58

Even-Ram S, Yamada KM (2005) Cell migration in 3D matrix. Curr Opin Cell Biol 17(5):524–532

Fozdar DY, Soman P, Lee JW, Han LH, Chen S (2011) Three-dimensional polymer constructs exhibiting a tunable negative Poisson's ratio. Adv Funct Mater 21 (14):2712–2720

Friedl P, Brocker EB (2000) The biology of cell locomotion within three-dimensional extracellular matrix. Cell Mol Life Sci 57:41–64

Friedl P, Wolf K (2010) Plasticity of cell migration: a multiscale tuning model. J Cell Biol 188:11–19

Friedl P, Zanker KS, Brocker EB (1998) Cell migration strategies in 3-D extracellular matrix: differences in morphology, cell matrix interactions, and integrin function. Microsc Res Tech 43:369–378

Gallego-Perez D, Higuita-Castro N, Denning L, DeJesus J, Dahl K, Sarkar A, Hansford DJ (2012) Microfabricated mimics of in vivo structural cues for the study of guided tumor cell migration. Lab Chip 12 (21):4424–4432

Garcia AJ, Huber F, Boettiger D (1998) Force required to break alpha5beta1 integrin-fibronectin bonds in intact adherent cells is sensitive to integrin activation state. J Biol Chem 273:10988–10993

Garcion E, Halilagic A, Faissner A, ffrench-Constant C (2004) Generation of an environmental niche for neural stem cell development by the extracellular matrix molecule tenascin C. Development 131:3423–3432

Gauvin R, Chen YC, Lee JW, Soman P, Zorlutuna P, Nichol JW, Bae H, Chen S, Khademhosseini A (2012) Microfabrication of complex porous tissue engineering scaffolds using 3D projection stereolithography. Biomaterials 33(15):3824–3834

Gerthoffer WT (2007) Mechanisms of vascular smooth muscle cell migration. Circ Res 100:607–621

Ghajar CM, Suresh V, Peyton SR, Raub CB, Meyskens FL Jr, George SC, Putnam AJ (2007) A novel three-

dimensional model to quantify metastatic melanoma invasion. Mol Cancer Ther 6(2):552–556
Ghosh K, Ren XD, Shu XZ, Prestwich GD, Clark RAF (2006) Fibronectin functional domains coupled to hyaluronan stimulate adult human dermal fibroblast responses critical for wound healing. Tissue Eng 12:601–613
Gobin AS, West JL (2002) Cell migration through defined, synthetic ECM analogs. FASEB J 16:751–753
Grogan SP, Chung PH, Soman P, Chen P, Lotz MK, Chen S, D'Lima DD (2013) Digital micromirror device projection printing system for meniscus tissue engineering. Acta Biomater 9(7):7218–7226
Gupta GP, Massagué J (2006) Cancer metastasis: building a framework. Cell 127(4):679–695
Han LH, Suri S, Schmidt CE, Chen S (2010) Fabrication of three-dimensional scaffolds for heterogeneous tissue engineering. Biomed Microdevices 12(4):721–725
Healy KE (1999) Molecular engineering of materials for bioreactivity. Curr Opin Solid State Mater Sci 4:381–387
Heuzé ML, Collin O, Terriac E, Lennon-Duménil AM, Piel M (2011) Cell migration in confinement: a micro-channel-based assay. Methods Mol Biol 769:415–434
Holland NB, Yongxing Q, Ruegsegger M, Marchant RE (1998) Biomimetic engineering of non-adhesive glycocalyx-like surfaces using oligosaccharide surfactant polymers. Nature 392:799–801
Huang L, Hu J, Lang L, Wang X, Zhang P, Jing X, Wang X, Chen X, Lelkes PI, Macdiarmid AG, Wei Y (2007) Synthesis and characterization of electroactive and biodegradable ABA block copolymer of polylactide and aniline pentamer. Biomaterials 28:1741–1751
Hubbell JA (1995) Biomaterials in tissue engineering. Biotechnology 13:565–576
Hubbell JA (1999) Bioactive biomaterials. Curr Opin Biotechnol 10:123–129
Hubbell JA, Massia SP, Desai NP, Drumheller PD (1991) Endothelial cell-selective materials for tissue engineering in the vascular graft via a new receptor. Biotech 9 (6):568–572
Huttenlocher A, Horwitz AR (2011) Integrins in cell migration. Cold Spring Harb Perspect Biol 3:a005074
Irimia D, Toner M (2009) Spontaneous migration of cancer cells under conditions of mechanical confinement. Integr Biol (Camb) 1(8–9):506–512
Jacques TS, Relvas JB, Nishimura S, Pytela R, Edwards GM, Streuli CH, ffrench-Constant C (1998) Neural precursor cell chain migration and division are regulated through different beta1 integrins. Development 125:3167–3177
Jenkinson SR, Barraclough R, West CR, Rudland PS (2004) S100A4 regulates cell motility and invasion in an in vitro model for breast cancer metastasis. Br J Cancer 90:253–262
Kadler KE, Baldock C, Bella J, Boot-Handford RP (2007) Collagens at a glance. J Cell Sci 120:1955–1958
Kim DH, Wirtz D (2013) Focal adhesion size uniquely predicts cell migration. FASEB J 27:1351–1361
Kim J, Park Y, Tae G, Lee KB, Hwang SJ, Kim IS, Noh I, Sun K (2008) Synthesis and characterization of matrix metalloprotease sensitive-low molecular weight hyaluronic acid based hydrogels. J Mater Sci Mater Med 19:3311–3318
Kim MC, Neal DM, Kamm RD, Asada HH (2013) Dynamic modeling of cell migration and spreading behaviors on fibronectin coated planar substrates and micropatterned geometries. PLoS Comput Biol 9: e1002926
Kloxin AM, Kasko AM, Salinas CN, Anseth KS (2009) Photodegradable hydrogels for dynamic tuning of physical and chemical properties. Science 324:59–63
Kouvroukoglou S, Dee KC, Bizios R, McIntire LV, Zygourakis K (2000) Endothelial cell migration on surfaces modified with immobilized adhesive peptides. Biomaterials 21:1725–1733
Langer R, Vacanti JP (1993) Tissue engineering. Science 260:920–926
Lauffenburger DA, Horwitz AF (1996) Cell migration: a physically integrated molecular process. Cell 84:359–369
Leone DP, Relvas JB, Campos LS, Hemmi S, Brakebusch C, Fassler R, Ffrench-Constant C, Suter U (2005) Regulation of neural progenitor proliferation and survival by beta1 integrins. J Cell Sci 118:2589–2599
Leong HS, Chambers AF, Lewis JD (2012) Assessing cancer cell migration and metastatic growth in vivo in the chick embryo using fluorescence intravital imaging. Methods Mol Biol 872:1–14
Lévesque SG, Shoichet MS (2007) Synthesis of enzyme-degradable, peptide-cross-linked dextran hydrogels. Bioconjug Chem 18:874–886
Li S, Moon JJ, Miao H, Jin G, Chen BP, Yuan S, Hu Y, Usami S, Chien S (2003) Signal transduction in matrix contraction and the migration of vascular smooth muscle cells in three-dimensional matrix. J Vasc Res 40:378–388
Lin L, Zhu J, Kottke-Marchant K, Marchant RE (2014) Biomimetic-engineered poly (ethylene glycol) hydrogel for smooth muscle cell migration. Tissue Eng Part A 20:864–873
Liu Y, Chan-Park MB (2010) A biomimetic hydrogel based on methacrylated dextran-graft-lysine and gelatin for 3D smooth muscle cell culture. Biomaterials 31:1158–1170
Liu X, Ma PX (2004) Polymeric scaffolds for bone tissue engineering. Ann Biomed Eng 32:477–486
Lock JG, Wehrle-Haller B, Strömblad S (2008) Cell–matrix adhesion complexes: master control machinery of cell migration. Semin Cancer Biol 18:65–76
Lorand L, Graham RM (2003) Transglutaminases: crosslinking enzymes with pleiotropic functions. Nat Rev Mol Cell Biol 4:140–156
Louis SF, Zahradka P (2010) Vascular smooth muscle cell motility: from migration to invasion. Exp Clin Cardiol 15:e75–e85

Lu Y, Chen S (2008) Direct write of microlens array using digital projection photopolymerization. Appl Phys Lett 92:041109

Lutolf MP, Hubbell JA (2003) Synthesis and physicochemical characterization of end-linked poly (ethylene glycol)-co-peptide hydrogels formed by Michael-type addition. Biomacromolecules 4:713–722

Lutolf MP, Lauer-Fields JL, Schmoekel HG, Metters AT, Weber FE, Fields GB, Hubbell JA (2003) Synthetic matrix metalloproteinase-sensitive hydrogels for the conduction of tissue regeneration: engineering cell-invasion characteristics. Proc Natl Acad Sci U S A 100:5413–5418

Lynn AK, Yannas IV, Bonfield W (2004) Antigenicity and immunogenicity of collagen. J Biomed Mater Res B71:343–354

Ma PA (2004) Scaffolds for tissue fabrication. Mater Today 7:30–40

Ma PX (2005) Tissue engineering. Encyclo Polym Sci Technol 12:261–291

Maheshwari G, Brown G, Lauffenburger DA, Wells A, Griffith LG (2000) Cell adhesion and motilitydepend on nanoscale RGD clustering. J Cell Sci 113:1677–1686

Mak M, Reinhart-King CA, Erickson D (2011) Microfabricated physical spatial gradients for investigating cell migration and invasion dynamics. PLoS One 6(6):e20825

Mann BK, West JL (2002) Cell adhesion peptides alter smooth muscle cell adhesion, proliferation, migration, and matrix protein synthesis on modified surfaces and in polymer scaffolds. J Biomed Mater Res 60:86–93

Mann BK, Gobin AS, Tsai AT, Schmedlen RH, West JL (2001a) Smooth muscle cell growth in photopolymerized hydrogels with cell adhesive and proteolytically degradable domains: synthetic ECM analogs for tissue engineering. Biomaterials 22:3045–3051

Mann BK, Schmedlen RH, West JL (2001b) Tethered-TGF-b increases extracellular matrix production of vascular smooth muscle cells. Biomaterials 22:439–444

Marler JJ, Upton J, Langer R, Vacanti JP (1998) Transplantation of cells in matrices for tissue engineering. Adv Drug Deliv Rev 33:165–182

Mathew AC, Rajah TT, Hurt GM, Abbas Abidi SM, Dmytryk JJ, Pento JT (1997) Influence of antiestrogens on the migration of breast cancer cells using an in vitro wound model. Clin Exp Metastasis 15(4):393–399

Meinel L, Fajardo R, Hofmann S, Langer R, Chen J, Snyder B, Vunjak-Novakovic G, Kaplan D (2005) Silk implants for the healing of critical size bone defects. Bone 37:688–698

Meiners S, Nur-e-Kamal MS, Mercado ML (2001) Identification of a neurite outgrowth-promoting motif within the alternatively spliced region of human tenascin-C. J Neurosci 21:7215–7225

Mercado MLT, Nur-e-Kamal A, Liu H-Y, Gross SR, Movahed R, Meiners S (2004) Neurite outgrowth by the alternatively spliced region of human tenascin-C is mediated by neuronal alpha7beta1 integrin. J Neurosci 24:238–247

Munoz-Pinto DJ, Bulick AS, Hahn MS (2009) Uncoupled investigation of scaffold modulus and mesh size on smooth muscle cell behavior. J Biomed Mater Res A 90:303–316

Murphy WL, Mooney DJ (1999) Controlled delivery of inductive proteins, plasmid DNA and cells from tissue engineering matrices. J Periodontal Res 34:413–419

Murugesan GM, Ruegsegger MA, Kligman F, Marchant RE, Kottke-Marchant K (2002) Integrin-dependent interaction of human vascular endothelial cells on biomimetic peptide surfactant polymers. Cell Commun Adhes 9:1–15

Nehls V, Herrmann R, Huhnken M (1998) Guided migration as a novel mechanism of capillarynetwork remodeling is regulated by basic fibroblast growth factor. Histochem Cell Biol 109:319–329

Olbrich KC, Andersen TT, Blumenstock FA, Bizios R (1996) Surfaces modified with covalentlyimmobilized adhesive peptides affect fibroblast population motility. Biomaterials 17:759–764

Palecek SP, Loftus JC, Ginsberg MH, Lauffenburger DA, Horwitz AF (1997) Integrin-ligand binding properties govern cell migration speed through cell-substratum adhesiveness. Nature 385:537–540

Pampaloni F, Reynaud EG, Stelzer EH (2007) The third dimensional bridges the gap between cell culture and live tissues. Nat Rev Mol Cell Biol 8:839–845

Park YD, Tirelli N, Hubbel JA (2003) Photopolymerized hyaluronic acid-based hydrogels and interpenetrating networks. Biomaterials 24:893–900

Pathak A, Kumar S (2012) Independent regulation of tumor cell migration by matrix stiffness and confinement. Proc Natl Acad Sci U S A 109(26):10334–10339

Patterson J, Martino M, Hubbell J (2010) Biomimetic materials in tissue engineering. Mater Today 13:14–22

Petrie RJ, Doyle AD, Yamada KM (2009) Random versus directionally persistent cell migration. Nat Rev Mol Cell Biol 10:538–549

Price RD, Berry MG, Navsaria HA (2007) Hyaluronic acid: the scientific and clinical evidence. J Plast Reconstr Aesthet Surg 60:1110–1119

Qiu YZ, Zhang T, Ruegsegger M, Marchant RE (1998) Novel nonionic oligosaccharide surfactant polymers derived from poly(vinylamine) with pendant dextran and hexanoyl groups. Macromolecules 31:165–171

Raeber GP, Lutolf MP, Hubbell JA (2007) Mechanisms of 3-D migration and matrix remodeling of fibroblasts within artificial ECMs. Acta Biomater 3:615–629

Rice MA, Anseth KS (2007) Controlling cartilaginous matrix evolution in hydrogels with degradation triggered by exogenous addition of an enzyme. Tissue Eng 13:683–691

Rice MA, Dodson BT, Arthur JA, Anseth KS (2005) Cell-based therapies and tissue engineering. Otolaryngol Clin N Am 38:199–214

Richardson TP, Murphy WL, Mooney DJ (2001) Polymeric delivery of proteins and plasmid DNA for tissue engineering and gene therapy. Crit Rev Eukaryot Gene Expr 11:47–58

Rolli CG, Seufferlein T, Kemkemer R, Spatz JP (2010) Impact of tumor cell cytoskeleton organization on invasiveness and migration: a microchannel-based approach. PLoS One 5(1):e8726

Rosso F, Marino C, Giordano A, Barbarisi M, Parmeggiani D, Barbarisi A (2005) Smart materials as scaffolds for tissue engineering. J Cell Physiol 203:465–470

Ruegsegger MA, Marchant RE (2001) Reduced protein adsorption and platelet adhesion bycontrolle d variation of oligomaltose surfactant polymer coatings. J Biomed Mater Res 56:159–167

Ruggiero F, Koch M (2008) Making recombinant extracellular matrix proteins. Methods 45:75–85

Ruoslahti E, Obrink B (1996) Common principles in cell adhesion. Exp Cell Res 227(1):1–11

Sagnella SM, Kligman F, Anderson EH, King JE, Murugesan G, Marchant RE, Kottke-Marchant K (2004) Human microvascular endothelial cell growth and migration on biomimetic surfactant polymers. Biomaterials 25(7–8):1249–1259

Sakiyama-Elbert SE, Hubbell JA (2001) Functional biomaterials: design of novel biomaterials. Annu Rev Mater Res 31:183–201

Sever M, Mammadov B, Guler MO, Tekinay AB (2014) Tenascin-C mimetic peptide nanofibers direct stem cell differentiation to osteogenic lineage. Biomacromolecules 15:4480–4487

Shi Z, Ji X, Berardi DE, Qazi H, Tarbell JM (2010) Interstitial flow induces MMP-1 expression and vascular SMC migration in collagen I gels via an ERK1/2-dependent and c- Jun-mediated mechanism. Am J Physiol Heart Circ Physiol 298:H127

Shin H, Jo S, Mikos AG (2002) Modulation of marrow stromal osteoblast adhesion on biomimetic oligo(poly (ethylene glycol) fumarate) hydrogels modified with Arg-Gly-Asp peptides and a poly(ethylene glycol) spacer. J Biomed Mater Res 61:169–179

Simon KO, Nutt EM, Abraham DG, Rodan GA, Duong LT (1997) The alphavbeta3 integrin regulates alpha5beta1-mediated cell migration toward fibronectin. J Biol Chem 272:29380–29389

Slater JH, Boyce PJ, Jancaitis MP, Gaubert HE, Chang AL, Markey MK, Frey W (2015) Modulation of endothelial cell migration via manipulation of adhesion site growth using nanopatterned surfaces. ACS Appl Mater Interfaces 7:4390–4400

Soman P, Lee JW, Phadke A, Varghese S, Chen S (2012a) Spatial tuning of negative and positive Poisson's ratio in a multi-layer scaffold. Acta Biomater 8 (7):2587–2594

Soman P, Tobe BTD, Lee JW, Winquist AM, Singec I, Vecchio KS, Snyder EY, Chen S (2012b) Three-dimensional scaffolding to investigate neuronal derivatives of human embryonic stem cells. Biomed Microdevices 14(5):829–838

Standeven KF, Carter AM, Grant PJ, Weisel JW, Chernisy I, Masova L, Lord ST, Ariens RAS (2007) Functional analysis of fibrin γ-chain cross-linking by activated factor XIII: determination of a cross-linking pattern that maximizes clot stiffness. Blood 110:902–907

Steeg PS (2006) Tumor metastasis: mechanistic insights and clinical challenges. Nat Med 12:895–904

Suri S, Han LH, Zhang W, Singh A, Chen S, Schmidt CE (2011) Solid freeform fabrication of designer scaffolds of hyaluronic acid for nerve tissue engineering. Biomed Microdevices 13(6):983–993

Suzuki Y, Tanihara M, Suzuki K, Saitou A, Sufan W, Nishimura Y (2000) Alginate hydrogel linked with synthetic oligopeptide derived from BMP-2 allows ectopic osteoinduction in vivo. J Biomed Mater Res 50:405–409

Takeda A, Stoeltzing O, Ahmad SA, Reinmuth N, Liu W, Parikh A, Fan F, Akagi M, Ellis LM (2002) Role of angiogenesis in the development and growth of liver metastasis. Ann Surg Oncol 9(7):610–616

Thomas LB, Gates MA, Steindler DA (1996) Young neurons from the adult subependymal zone proliferate and migrate along an astrocyte, extracellular matrix-rich pathway. Glia 17:1–14

Tognana E, Borrione A, DeLuca C, Pavesio A (2007) Hyalograft® C: hyaluronan-based scaffolds in tissue-engineered cartilage. Cells Tissues Organs 186:97–103

Toole BP (2004) Hyaluronan: from extracellular glue to pericellular cue. Nat Rev Cancer 4:528–539

Turley EA, Noble PW, Bourguignon LYW (2002) Signaling properties of hyaluronan receptors. J Biol Chem 277:4589–4592

Ucuzian AA, Brewster LP, East AT, Pang Y, Gassman AA, Greisler HP (2010) Characterization of the chemotactic and mitogenic response of SMCs to PDGF-BB and FGF-2 in fibrin hydrogels. J Biomed Mater Res A 94:988–996

Vedula SR, Leong MC, Lai TL, Hersen P, Kabla AJ, Lim CT, Ladoux B (2012) Emerging modes of collective cell migration induced by geometrical constraints. Proc Natl Acad Sci U S A 109(32):12974–12979

Vicente-Manzanares M, Webb DJ, Horwitz AR (2005) Cell migration at a glance. J Cell Sci 118:4917–4919

Weisel JW (2004) The mechanical properties of fibrin for basic scientists. Biophys Chem 112:267–276

Watson SA, Morris TM, Robinson G, Crimmin MJ, Brown PD, Hardcastle JD (1995) Inhibition of organ invasion by the matrix metalloproteinase inhibitor batimastat (BB-94) in two human colon carcinoma metastasis models. Cancer Res 55(16):3629–3633

West JL, Hubbell JA (1999) Polymeric biomaterials with degradation sites for protease involved in cell migration. Macromolecules 32:241–244

Whitaker MJ, Quirk RA, Howdle SM, Shakesheff KM (2001) Growth factor release from tissue engineering scaffolds. J Pharm Pharmacol 53:1427–1437

Willis AI, Pierre-Paul D, Sumpio BE, Gahtan V (2004) Vascular smooth muscle cell migration: current research and clinical implications. Vasc Endovasc Surg 38:11

Wu P, Hoying JB, Williams SK, Kozikowski BA, Lauffenburger DA (1994) Integrin-binding peptide in solution inhibits or enhances endothelial cell migration, predictablyfrom cell adhesion. Ann Biomed Eng 22:144–152

Wu J, Mao Z, Gao C (2012) Controlling the migration behaviors of vascular smooth muscle cells by methoxy poly(ethylene glycol) brushes of different molecular weight and density. Biomaterials 33:810–820

Xiao Y, Truskey GA (1996) Effect of receptor-ligand affinityon the strength of endothelial cell adhesion. Biophys J 71:2869–2884

Yamada KM, Geiger B (1997) Molecular interactions in cell adhesion complexes. Curr Opin Cell Biol 9:76–85

Yamada KM, Cukierman E (2007) Modeling tissue morphogenesis and cancer in 3D. Cell 130:601–610

Yu YM, Cristofanilli M, Valiveti A, Ma L, Yoo M, Morellini F, Schachner M (2011) The extracellular matrix glycoprotein tenascin-C promotes locomotor recovery after spinal cord injury in adult zebrafish. Neuroscience 183:238–250

Zaidel-Bar R, Ballestrem C, Kam Z, Geiger B (2003) Early molecular events in the assembly of matrix adhesions at the leading edge of migrating cells. J Cell Sci 116:4605–4613

Zetter BR (1998) Angiogenesis and tumor metastasis. Annu Rev Med 49:407–424

Zhang Y, Winterbottom JK, Schachner M, Lieberman AR, Anderson PN (1997) Tenascin-C expression and axonal sprouting following injury to the spinal dorsal columns in the adult rat. J Neurosci Res 49:433–450

Zhang AP, Qu X, Soman P, Hribar KC, Lee JW, Chen S, He S (2012) Rapid fabrication of complex 3D extracellular microenvironments by dynamic optical projection stereolithography. Adv Mater 24(31):4266–4270

Zhou ZN, Boimel PJ, Segall JE (2011) Tumor-stroma: In vivo assays and intravital imaging to study cell migration and metastasis. Drug Discov Today Dis Model 8 (2-3):95–112

Biomimetic Scaffolds for Bone Tissue Engineering

7

Joon Yeong Park, Seung Hun Park, Mal Geum Kim, Sang-Hyug Park, Tae Hyeon Yoo, and Moon Suk Kim

Table of Content

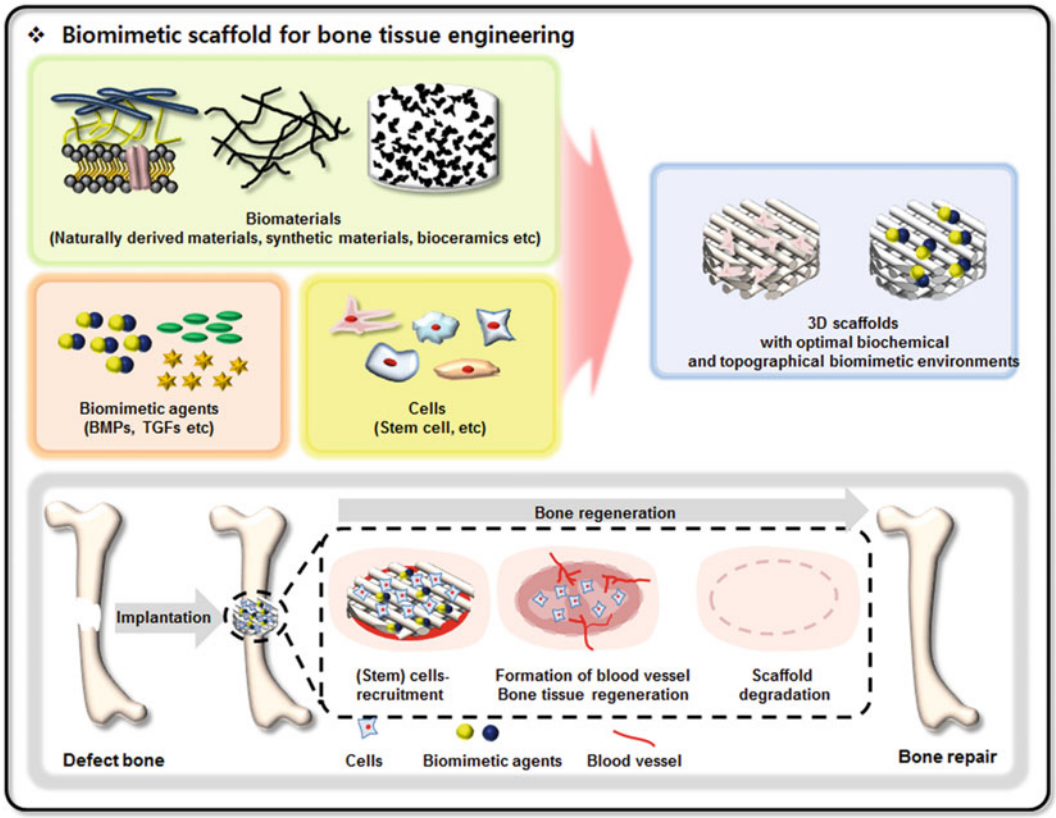

TOC was drawn by Joon Yeong Park using software of Adobe Photoshop7.0

I. Noh (ed.), *Biomimetic Medical Materials*, Advances in Experimental Medicine and Biology 1064,
https://doi.org/10.1007/978-981-13-0445-3_7

7.1 Introduction

Tissue regeneration in living organisms is mediated by biologic regulatory factors that promote tissue renewal, restoration, and growth (Ceafalan and Popescu 2016). Scaffolds are important tools used in tissue engineering for the regeneration of lost or damaged tissues.

From the biological point of view, scaffolds should support the in vivo development of an extracellular matrix in sites of lost or damaged tissues (Kim et al. 2011). In addition, scaffolds should allow influx of nutrient substances from the surrounding tissue or biologic medium and the exit of waste formed in the tissue. Thus, scaffolds should create unique opportunities to regenerate tissues.

Biomimetic scaffolds can be formed using materials that have been designed to elicit specified cellular responses mediated by regulatory factors inside of the engineered environments (Chen et al. 2016). Biomimetic scaffolds are formed into three-dimensional (3D) architectures suitable for cell seeding and cultivation. With biomimetic scaffolds, (stem) cells can be cultivated or differentiated at the right time, in the right place, and into the right phenotype. Biomimetic scaffolds, particularly, are guided by the need to restore cell signaling and match the mechanical behavior of the tissue being engineered (Huang et al. 2016). Additionally, the biological agents inside of biomimetic scaffolds should serve as templates for cell growth and provide significant control over the cellular environment to manipulate cellular processes (Monteiro and Yelick 2017).

Biomimetic scaffolds can be used to closely mimic the generation of authentic tissue, which represents the environment of cells in a living organism, while enabling tight control over the cell environment and cellular processes (Skylar-Scott et al. 2016). Biomimetic scaffolds can be manufactured for precise control of patterning and mobilization of biological agents such as ligands, hormones, and cytokines (Moeinzadeh and Jabbari 2015).

Bone, a tissue containing a dense mineralized matrix, can withstand significant compressive loads (Tracy et al. 2016). Although bone has the innate ability to repair and regenerate, various clinical bone graft procedures are employed in orthopedic and craniofacial medicine (Kashte et al. 2017; Park and Park 2016; Gentile et al. 2017; Lee et al. 2017a). Autologous bones are common, but allografts, xenografts, and alloplast grafts have also been widely utilized.

From the mechanical point of view, biomimetic scaffolds for bone regeneration must bear external loading and provide the shape to the tissue that is to be regenerated (Tatman et al. 2015; Domingues et al. 2016; Behzadi et al. 2017; Lee et al. 2017b). Thus, biomimetic scaffolds for bone regeneration require mechanical stability to support the needed geometry, along with large interconnected pores for cell infiltration. Thus, the mechanical properties of biomimetic scaffolds must be similar to the properties of the replaced bone tissue to prevent stress shielding.

Biomimetic scaffolds for bone regeneration also should have important properties such as stiffness, mechanical resistance, and permeability. Additionally, the scaffold should undergo controlled degradation (Senthebane et al. 2017; Makhni et al. 2016). The degradation rate must be as close as possible to the tissue growth rate to maintain stability and structure at implanted site during the bone tissue regeneration process.

As described, the mechanical properties and degradation of the scaffold depend mainly on the biomaterial properties and the 3D structure, geometry, and porosity of the scaffold. In many cases, biomimetic scaffolds are designed to mimic the biochemistry and/or structure of native bone tissue.

Joon Yeong Park and Seung Hun Park are equal first authors.

J. Y. Park · S. H. Park · M. G. Kim · T. H. Yoo
M. S. Kim (✉)
Department of Molecular Science and Technology, Ajou University, Suwon, South Korea
e-mail: pjy16@ajou.ac.kr; hpt88@ajou.ac.kr; kmg@ajou.ac.kr; taehyeonyoo@ajou.ac.kr; moonskim@ajou.ac.kr

S.-H. Park
Department of Biomedical Engineering, Pukyong National University, Busan, South Korea
e-mail: shpark1@pknu.ac.kr

Here, we discuss the design of biomimetic scaffolds, kinds of biomaterials and methods used to fabricate biomimetic scaffolds, growth factors used with biomimetic scaffold for bone regeneration, mobilization of biological agents into biomimetic scaffolds, and studies on (pre)clinical bone regeneration from biomimetic scaffolds. Then, future prospects for biomimetic scaffolds are discussed.

7.2 Design Considerations for Biomimetic Scaffolds

Biomimetic scaffolds are first evaluated in in vitro environments with various compositions of culture media, mechanical stimuli, temperatures, cells, and cell activity that affect the growth of new bone tissue.

Then, the feasibility of using a biomimetic scaffold is determined by considering the bone regeneration processes occurring in vivo based on gender, age, size and kind of bone defect, mechanical and biochemical stimuli, vascularization, and inflammatory and immunological processes expected during bone regeneration using a scaffold (Mastrogiacomo et al. 2005; Guo et al. 2006).

Thus, the methods to fabricate biomimetic scaffolds must be considered, with several basic factors such as porosity, surface/volume ratio, structure, surface shape, and chemistry of the polymer, and composition, structure, and molecular weight of the biomaterial should be considered (Mondschein et al. 2017; Singh et al. 2014; Chua et al. 2016; Sheikh et al. 2017).

Biomimetic scaffolds must promote cellular growth inside of their structures and must react in a controlled manner in vitro and in the specific implantation site *in vivo*. The processes of bone regeneration are complex, so there are many requirements for the design of biomimetic scaffolds. Some of the most important design considerations are indicated below.

7.2.1 Biomimetics

Biomimetic scaffolds should be prepared by patterning, binding of cytokines and/or ligands, and the sustained release of these molecules (Yin et al. 2017; Park et al. 2017). Biomimetic scaffolds should be produced based on an understanding of cells and tissue morphologies and structures in humans. Biomimetic scaffolds should meet certain design requirements to restore the functions of the regenerated bone tissue and show optimal biochemical and topographical features to allow the infiltration of local or implanted mesenchymal stem cells (MSCs) and other osteoprogenitor cells.

7.2.2 Biocompatibility

Biomimetic scaffolds should be compatible with normal cellular activity, including molecular signaling without eliciting or evoking local or systemic adverse responses in the host. Cytotoxicity, genotoxicity, immunogenicity, mutagenicity, and thrombogenicity in the host should be eliminated, minimized, or controlled before the implantation of a biomimetic scaffold.

7.2.3 Biodegradability

Biomimetic scaffolds should degrade at a rate appropriate for their *in vitro* or *in vivo* environments, preferably at a controlled rate, to create space for the formation of new bone tissue. The degraded materials from biomimetic scaffolds should be biocompatible and must be able to be metabolized and eliminated from the body.

7.2.4 Mechanical Properties

Biomimetic scaffolds should show suitable mechanical strength to meet with mechanical requirements for target bone tissues and should retain their structures to serve a mechanical function after implantation. Mechanical properties such as the elastic modulus, tensile strength, fracture toughness, fatiguability, and elongation percentage should be as close as possible to those of the target bone tissues.

7.3 Techniques to Fabricate Biomimetic Scaffolds

Various manufacturing methods have been used to instill specific properties into biomimetic scaffolds. Generally, conventional methods of solvent casting/particulate leaching, phase inversion/particulate leaching, gas foaming, electrospinning, and injection can be used to prepare biomimetic scaffolds (Barabaschi et al. 2015; Holzwarth and Ma 2011; Bhaskar and Lim 2017). These methods provide biomimetic scaffolds with internal structure, including a pore size between 100 and 1000 microns and porosity up to 90%, but result in a randomly arranged structure and limited permeability. Recently, printed scaffolds with oriented structures have been developed, but their porosity is still difficult to control.

7.4 Biomaterials for Biomimetic Scaffolds

To develop biomimetic scaffolds for use in clinical bone tissue engineering, the biomaterials should be biocompatible, possess appropriate mechanical properties, and have characteristics similar to bone. This section reviews naturally derived biomaterials, synthetic biomaterials, and ceramics and their composites that are currently in use and that have been adapted for the manufacture of biomimetic scaffolds to support biological signaling for bone tissue growth and regeneration.

7.4.1 Naturally Derived Biomaterials

Naturally derived biomaterials are biomaterials produced by living organisms. Naturally derived biomaterials have a number of advantages, including the elicitation of only mild inflammatory responses *in vivo*, excellent biocompatibility, and relative availability and ease of acquisition from natural sources (Aamodt and Grainger 2016; Fan and Guan 2016; Li et al. 2016). Another feature of such biomaterials is that they are eventually degraded into CO_2 and water by microorganisms.

Naturally derived biomaterials exhibit batch-to-batch variations in composition that are strongly dependent on the isolation procedure used and differences in immunogenic and mechanical properties. There are several (pre) clinically applicable naturally derived biomaterials with optimized physical and mechanical properties for ideal performance.

Naturally derived biomaterials such as collagen, chitosan, hyaluronic acid, alginate, and fibrin are inherently biocompatible, showing minimal adverse immunogenicity, and are widely used in the fabrication of biomimetic scaffolds described in following paragraph.

Collagen is the major protein component of the extracellular matrix that is relatively abundant and shows outstanding biocompatibility (Ghazanfari et al. 2016). Even though there are serious concerns about the safety of animal tissue-derived collagen, collagen is the material used most commonly for biomedical applications. Collagen-based biomimetic scaffolds can be fabricated through various methods that determine, for example, 3D shape and the inclusion of hydrogels and nanofibers. However, collagen typically lacks the desired mechanical strength. Thus, the mechanical strength of collagen can be increased by chemical treatment or cross-linking. Collagens, therefore, are some of the most promising biomaterials for the preparation of biomimetic scaffolds.

Chitosan is also an abundant biomaterial derived from the shell-crusts of crustacean animals (Correia et al. 2015). It is obtained by the full or partial deacetylation of chitin by alkaline hydrolysis. Chitosan is a biodegradable, biocompatible, non-antigenic, non-toxic, and biofunctional material. Thus, chitosan has been used to form various scaffolds. Specifically, the cationic amino groups on chitosan chains can interact electrostatically with anionic groups or can be modified or functionalized by chemical or physical methods to increase the mechanical strength of these scaffolds.

Hyaluronic acid (HA) is a naturally derived biomaterial found in most connective tissues of the body, including the skin, cartilage, and vitreous humor (Drury and Mooney 2003). HA can be obtained on a large scale without the risk of transmitting animal-derived pathogens. Because HA serves many physiological functions, including regulation of water in tissues and matrices, HA can be widely used to form scaffolds with structural and space-filling properties. HA is an anionic, non-sulfated glycosaminoglycan polyanion. HA properties are significantly improved by cross-linking. Overall, HA is highly biocompatible with tissues and thus is frequently used as a biomaterial to create biomimetic scaffolds for bone regeneration.

Alginate has also been used to make biocompatible, biodegradable, and hydrophilic biomimetic scaffolds (Lee et al. 2017c). Alginate is an anionic polymer with carboxyl groups, and thus it undergoes simple and reversible gelation through interaction with divalent cations such as Ca^{2+}, Sr^{2+}, and Ba^{2+}. Because of this gelation ability, alginates have been widely used as scaffolds of microbeads and/or hydrogels. Additionally, alginate can mix with other naturally derived biomaterials to increase the integrity and mechanical strength of scaffolds.

Fibrin is composed of two essential components: fibrinogen and purified thrombin (Nanditha et al. 2017). When fibrinogen is mixed with thrombin, these materials polymerize to form long fibrin strands that aggregate in structured fibrin clots. Because fibrin is completely biodegradable and highly angiogenic, fibrin is a promising material for the fabrication of bone biomimetic scaffolds to be used for bone tissue regeneration and wound healing.

Other naturally derived biomaterials that will not be discussed here include proteins, albumin, gelatin, heparin, silk, chondroitin 6-sulfate, and acellular dermis.

7.4.2 Synthetic Biomaterials

In contrast to naturally derived biomaterials, synthetic biomaterials can be obtained that (a) show consistent composition and no batch-to-batch variation; (b) allow large-scale production; (c) can be used to create precise designable geometric forms; (d) can be customized with a wide range of mechanical properties; (e) show predictable mechanical properties; (f) and induce minimal immune responses.

Although the synthetic biomaterial itself or its degradation production can induce inflammatory responses, various synthetic biomaterials such as polylactic acid (PLA), polyglycolic acid (PGA), and their copolymers poly(DL-lactic acid-co-glycolic acid) (PLGA), poly(ε-caprolactone) (PCL), and others are the materials most widely used to fabricate biomimetic scaffolds for bone tissue regeneration.

PLA, PGA, and PLGA with different ratios of glycolic acid and lactic acid are the synthetic polyesters most widely used for the fabrication of scaffolds. Scaffolds fabricated from PLA, PGA, and PLGA are degraded under normal physiological conditions. The degradation rate depends on several conditions such as the degree of crystallinity and amorphousness, molecular weight, copolymer ratios, and environment at the implantation site.

Although the degradation byproducts can induce tissue inflammation associated with the generation of acidic species, PLA, PGA, and PLGA are commercially available and FDA-approved biomaterials that show promise for the fabrication of biomimetic scaffolds for bone tissue regeneration (Jing et al. 2016; Kim et al. 2015; Lin et al. 2017; Armitage and Oyen 2015).

PCL is another biodegradable biomaterial that is considered soft- and hard-tissue compatible and shows biocompatibility similar to that of PLA, PGA, and PLGA. The degradation rate of PCL is slower than that of PGA, PLA, or PLGA. Thus, PCL is ideally suited for long-term implantation applications. PCL is available in a commercial grade and is an FDA-approved biomaterial. Blending or copolymerization of PCL with PGA and PLA can adjust the degradation rate relative to that of PCL alone. Copolymers of PCL with PGA and PLA can be used to satisfy specific demands for bone tissue growth at the appropriate time scale.

Most synthetic biomaterials, therefore, possess appropriate mechanical and biochemical properties and are suitable for fabrication of bone biomimetic scaffolds with adjustable morphological structures.

7.4.3 Ceramics

Even though most naturally derived biomaterials are highly biocompatible, and PLA, PGA, PLGA, and PCL can easily be formed into scaffolds with controlled mechanical properties and biodegradability, biomaterials alone are limited in their applicability to bone regeneration because of their low osteoinductive capacity.

In contrast, bioceramics exhibit good osteoconductivity, high compressive strength, and good bone integration (Dorozhkin 2010; Smith et al. 2015). Bioceramics consist of inorganic oxides and salts. Thus, biomaterial composites that include bioceramics can be used to fabricate osteoinductive and osteoconductive biomimetic scaffolds. Biomimetic scaffolds fabricated from bioceramic composites can biodegrade and exhibit good mechanical strength and the ability to conform.

Calcium phosphates, the mineral components of bone, are composed of calcium ions (Ca^{2+}), orthophosphates (PO_4^{3-}), metaphosphates, or pyrophosphates ($P_2O_7^{4-}$). The most common calcium phosphate, a central component of bone, is hydroxyapatite (HAp), which has a crystalline structure of $Ca_{10}(PO^4)_6(OH)_2$. HAp shows high bioactivity, biocompatibility, and osteoconductivity (Frezzo and Montclare 2016; Koupaei and Karkhaneh 2016).

HAp can be obtained from natural sources or can be synthetized from calcium carbonate and monoammonium phosphate. HAp exhibits osteoconductive characteristics that facilitate bone regeneration.

Other calcium phosphates include calcium sulfate (CS), calcium carbonate, dicalcium phosphate, octacalcium phosphate, β-tricalcium phosphate (TCP), biphasic calcium phosphate, and β-calcium pyrophosphate. Commercially available calcium phosphates are made into many physical forms such as particles, blocks, and cements. In addition, calcium phosphates can be used in biomaterial composites for bone tissue engineering. These composites can be used to fabricate osteoconductive biomimetic scaffolds.

7.5 Growth Factors for Bone Regeneration Using Biomimetic Scaffolds

Biomimetic scaffolds can be manufactured through patterning and mobilization of growth factors such as ligands, hormones, and cytokines. The use of growth factors with biomimetic scaffolds can trigger biochemical signaling for cellular processes such as growth, proliferation, or differentiation. Several growth factors recruit MSCs, differentiate MSCs into chondrocytes and osteoblasts, and promote the proliferation of osteoblasts and chondrocytes for bone regeneration. The growth factors most commonly used in biomimetic scaffolds for bone tissue engineering are summarized below.

Bone morphogenetic proteins (BMPs) can recruit MSCs, differentiate MSCs into chondrocytes and osteoblasts, and promote osteoblast-mediated matrix mineralization (Bessa et al. 2008). BMPs are the prototypical bone regenerative growth factors. When BMPs are incorporation into scaffolds, they promote the growth of new bone tissue inside of these scaffolds. Thus, BMP is most common used growth factors on biomimetic scaffold.

Transforming growth factors-β (TGFs-β) also cause MSCs to differentiate into chondrocytes and may stimulate the proliferation of MSCs, osteoblasts, and chondrocytes (Dinh et al. 2015). Basic fibroblast growth factors (bFGF) also induce MSCs and promote chondrocytes and osteoblast proliferation (Chim et al. 2013). Platelet-derived growth factors (PDGF) similarly increase the proliferation of chondrocytes and osteoblasts, although bone resorption has been shown to be PDGF concentration-dependent (Sánchez et al. 2017). PDGF exhibits chemotactic and mitogenic action on osteoblasts.

Bone regeneration depends on rapid vascularization into the bone scaffold. Thus, the scaffold can be functionalized by the use of growth factors such as vascular endothelial growth factor (VEGF) or bFGF that have angiogenic properties (Wang et al. 2017). VEGF or bFGF both enhance vessel growth into scaffolds.

7.6 Loading of Growth Factors into Biomimetic Scaffolds

To prepare bone scaffolds as biomimetic environments, growth factors can be immobilized on the scaffold. Non-covalent bonding (physical adsorption) and covalent bonding (chemical adsorption) approaches are both well established and allow the introduction of growth factors into a scaffold (Wang et al. 2017).

Physical adsorption occurs through weak interactions such as hydrogen bonding, van der Waals forces, and hydrophobic bonding. Although the introduction of growth factors into a scaffold is quite simple, the strength of the interactions for physical adsorption is dependent on the chemistry of scaffold biomaterial surfaces. Thus, physical adsorption alone may not sufficiently stabilize the growth factors inside a scaffold. Furthermore, growth factor content and conformation cannot be precisely controlled.

In contrast, chemical adsorption can be used to stably introduce growth factors into a scaffold by chemical cross-linking. The growth factors are anchored directly onto the functional groups of the scaffold surface. However, this method may result in side reactions such as scaffold breakdown or structural change in growth factors.

Both adsorption methods can be used to prepare biomimetic scaffolds. Various strategies such as modifying the local concentration of growth factors in the scaffold must be considered. Growth factors in the scaffold must be stable and active throughout the bone regeneration period. Currently, FDA-approved BMP-loaded scaffolds such as INFUSE® and Op-1® are available for orthopedic applications (Pinel and Pluhar 2012).

7.7 Biomimetic Scaffolds for (Pre) clinical Bone Regeneration

Clinical use of biomimetic scaffolds is currently in an embryonic stage, because most research on biomimetic scaffolds is conducted in animal models. Several preclinical studies have examined biomimetic scaffolds from alginate, chitosan, and synthetic polymers (Table 7.1) (Moeinzadeh and Jabbari 2015; Guo et al. 2006; Chua et al. 2016; Sheikh et al. 2017; Park et al. 2017; Bhaskar and Lim 2017; Koupaei and Karkhaneh 2016; Bessa et al. 2008; Wang et al. 2017; Pinel and Pluhar 2012; Re'em et al. 2012; Chen et al. 2011; Kon et al. 2010; Gervaso et al. 2012; Sartori et al. 2017; Zhang et al. 2013; Gotterbarm et al. 2006; Huh et al. 2017; Islam et al. 2015; Ahn et al. 2009; He et al. 2016; Correia et al. 2012; Fuchs et al. 2009; Mitsak et al. 2011; Jang et al. 2016; Chen et al. 2014; Wang et al. 2016; Wu et al. 2012; Lee et al. 2016; Shao et al. 2006; Erisken et al. 2008; Xu et al. 2015; Huang et al. 2013; Nie et al. 2009; Han et al. 2008; Da et al. 2013; Cui et al. 2011; Gupta et al. 2016; Kwon et al. 2015, 2017; Kemppainen and Hollister 2010; Yao et al. 2017; Foroughi et al. 2012; Wongwitwichot et al. 2010). Preclinical studies describing the use of biomimetic scaffolds and stem cells for bone regeneration are presented in the table. Biomimetic scaffold have been used in basic and preclinical research for the treatment of damaged or diseased bone tissues using various adult stem cells. Even though a number of biomimetic scaffolds are available, research must continue to better understand how bone tissues develop in biomimetic scaffolds and which biomimetic scaffold types should be applied in specific clinical situations.

7.8 Future Challenges and Conclusion

Recently, research has been focused on biomimetic scaffolds that mimic the structure and biochemistry of native environments in a living

Table 7.1 Biomimetic scaffolds for (pre)clinical bone regeneration

Biomaterials	Biomaterials for biomimetic scaffolds	Biomimetic agents	Cells	Models	References
Naturally biomaterials	Alginate	TGF-β1, BMP-4	h-MSCs	Rabbit subchondral defects	Moeinzadeh and Jabbari (2015), Bhaskar and Lim (2017), Bessa et al. (2008), Wang et al. (2017), Pinel and Pluhar (2012) and Re'em et al. (2012)
	Chitosan-gelatin/chitosan-gelatin-HAp	TGF-β1, BMP-2 plasmid	r-BMSCs	Rabbit osteochondral defects	Moeinzadeh and Jabbari (2015), Bhaskar and Lim (2017), Wang et al. (2017) and Chen et al. (2011)
	COL1/COL1-HAp	HAp	–	Sheep osteochondral defects	Kon et al. (2010)
	Collagen/HAp	HAp	–	–	Chua et al. (2016), Sheikh et al. (2017) and Gervaso et al. (2012)
	Collagen/Mg-HAp	Mg-HAp	h-MSCs	Mouse skin incisions	Sartori et al. (2017)
	Collagen/PLA	–	r-BMSCs	Rabbit osteochondral defects	Holzwarth and Ma (2011) and Zhang et al. (2013)
	Collagen/TCP	β-TCP	–	Minipig osteochondral defects	Gotterbarm et al. (2006)
	Gelatin/TCP/SF	α-TCP	MG-63	–	Huh et al. (2017)
	Gelatin/chitosan/TCP/CS	β-TCP/CS	–	–	Islam et al. (2015)
	Hyaluronate-Atelocollagen/TCP-HAp	β-TCP-HAp	–	Rabbit osteochondral defects	Ahn et al. (2009)
	Silk fibroin/cellulose nanowhiskers-chitosan	–	MG-63	–	He et al. (2016)
	Silk fibroin	–	h-ADSCs	–	Correia et al. (2012)
	Silk fibroin	–	h-OECs	–	Fuchs et al. (2009)
Synthetic biomaterials	PCL	–	h-fibroblasts	Mouse backs area	Mitsak et al. (2011)
	PCL	BMP2	h-PLSCs	Nude mouse dorsal area	Park et al. (2017), Bessa et al. (2008), Wang et al. (2017) and Pinel and Pluhar (2012)
	PCL	–	h-DPSCs	Nude mouse dorsal area	Jang et al. (2016)
	PCL/COL1	–	Chondrocytes	Nude mouse dorsal area	Chen et al. (2014)

	PCL/graphene	–	h-ADSCs	–	Wang et al. (2016)
	PCL/MP	MP particular	–	–	Wu et al. (2012)
	PCL/PLGA	HAp	r-BMSCs	–	Sheikh et al. (2017) and Lee et al. (2016)
	PCL/TCP	β-TCP	Rabbit BMSCs	Rabbit osteochondral defects	Koupaei and Karkhaneh (2016) and Shao et al. (2006)
	PCL/TCP	β-TCP nanoparticle	–	–	Erisken et al. (2008)
	PCL/PEG	–	h-iPS	–	Xu et al. (2015)
	PHEMA/HA/TCP, HPMA/HA/TCP	HAp/β-TCP	-	–	Huang et al. (2013)
	PLGA/HAp	BMP-2 plasmid	–	Mouse bone defects	Bhaskar and Lim (2017), Wang et al. (2017) and Nie et al. (2009)
	PLGA/BMSCs	TGF-β3	Rabbit BMSCs	–	Guo et al. (2006), Bhaskar and Lim (2017), Wang et al. (2017) and Han et al. (2008)
	PLGA/β-TCP	β-TCP	Rabbit BMSCs	Rabbit osteochondral defects	Da et al. (2013)
	PLGA/β-TCP	β-TCP	Minipig chondrocytes	Minipig osteochondral defects	Cui et al. (2011)
	PLGA/TCP-HAp	TCP/HAp	r-BMSCs	–	Gupta et al. (2016)
	PLGC/hDPSCs	–	h-DPSCs	Rat cranial defects	Kwon et al. (2015)
	PLLA	β-TCP	MG-63	Rat cranial defects	Kwon et al. (2017)
	Poly(glycerol sebacate)	–	Pig chondrocytes	–	Kemppainen and Hollister (2010)
	PVA/TCP	β-TCP	Chondrocytes, SMSCs	–	Yao et al. (2017)
Ceramic biomaterials	HAp	P3HB	–	–	Foroughi et al. (2012)
	TCP, TCP/HAp	β-TCP, HAp	–	Mouse dorsal area	Wongwitwichot et al. (2010)

ADSC adipose-derived stem cell, *BMSC* bone marrow-derived mesenchymal stem cell, *COL1* collagen type I, *DPSC* dental pulp stem cell, *HPMA* 2-hydroxypropyl methacrylate, *iPS* induced pluripotent stem cells, *MP* magnesium phosphate, *OEC* outgrowth endothelial cell, *PEG* poly(ethylene glycol), *PHEMA* poly(2-hydroxyethyl methacrylate), *PLSC* periodontal ligament stem cell, PVA poly(vinyl alcohol), *P3HB* poly-3-hyroxybutyrate, *SMSC* synovium mesenchymal stem cell

organism. Biomimetic scaffolds must be able to accommodate the incorporation of growth factors needed to promote the desired cellular differentiation and maturation and to support the growth and differentiation of (stem) cells for bone regeneration. An overview of biomaterials for the fabrication of biomimetic scaffolds for bone regeneration has been presented here. A number of materials have been successfully applied in animal models, and there will no doubt be significant crossover for human applications of biomimetic scaffolds for better, safer, and more integrated bone regeneration. The challenges are that biomimetic scaffolds must possess the appropriate mechanical and 3D structural properties to mimic in vivo environments and must address immune reactions and bone regeneration in clinical situations. Our knowledge of clinically relevant technologies for biomimetic scaffolds is now growing exponentially and will require collaborative research among biomaterial, biological, and clinical scientists.

Acknowledgments This work was supported by a grant from a Basic Science Research Program (2016R1A2B3007448) and Priority Research Centers Program (2010-0028294) through the National Research Foundation of Korea (NRF) funded by the Ministry of Education.

Conflicts of Interest The authors declare no conflict of interest.

References

Aamodt JM, Grainger DW (2016) Extracellular matrix-based biomaterial scaffolds and the host response. Biomaterials 86:68–82

Ahn JH, Lee TH, Oh JS, Kim SY, Kim HJ, Park IK, Choi BS, Im GI (2009) Novel hyaluronate-atelocollagen/beta-TCP-hydroxyapatite biphasic scaffold for the repair of osteochondral defects in rabbits. Tissue Eng Part A 15:2595–2604

Armitage OE, Oyen ML (2015) Hard-soft tissue interface engineering. Adv Exp Med Biol 881:187–204

Barabaschi GD, Manoharan V, Li Q, Bertassoni LE (2015) Engineering pre-vascularized scaffolds for bone regeneration. Adv Exp Med Biol 881:79–94

Behzadi S, Luther GA, Harris MB, Farokhzad OC, Mahmoudi M (2017) Nanomedicine for safe healing of bone trauma: opportunities and challenges. Biomaterials 146:168–182

Bessa PC, Casal M, Reis RL (2008) Bone morphogenetic proteins in tissue engineering: the road from laboratory to clinic, part II (BMP delivery). J Tissue Eng Regen Med 2:81–96

Bhaskar S, Lim S (2017) Engineering protein nanocages as carriers for biomedical applications. NPG Asia Mater 9:e371

Ceafalan LC, Popescu BO (2016) Juxtacerebral tissue regeneration potential: telocytes contribution. Adv Exp Med Biol 913:397–402

Chen J, Chen H, Li P, Diao H, Zhu S, Dong L, Wang R, Guo T, Zhao J, Zhang J (2011) Simultaneous regeneration of articular cartilage and subchondral bone in vivo using MSCs induced by a spatially controlled gene delivery system in bilayered integrated scaffolds. Biomaterials 32:4793–4805

Chen CH, Shyu VB, Chen JP, Lee MY (2014) Selective laser sintered poly-epilson-carprolactone scaffold hybridized with collagen hydrogel for cartilage tissue engineering. Biofabrication 6:015004

Chen C, Bang S, Cho Y, Lee S, Lee I, Zhang S, Noh I (2016) Research trends in biomimetic medical materials for tissue engineering: 3D bioprinting, surface modification, nano/micro-technology and clinical aspects in tissue engineering of cartilage and bone. Biomater Res 20:10

Chim SM, Tickner J, Chow ST, Kuek V, Guo B, Zhang G, Rosen V, Erber W, Xu J (2013) Angiogenic factors in bone local environment. Cytokine Growth Factor Rev 24:297–310

Chua ILS, Kim HW, Lee JH (2016) Signaling of extracellular matrices for tissue regeneration and therapeutics. Tissue Eng Regen Med 13:1–12

Correia C, Bhumiratana S, Yan LP, Oliveira AL, Gimble JM, Rockwood D, Kaplan DL, Sousa RA, Reis RL, Vunjak-Novakovic G (2012) Development of silk-based scaffolds for tissue engineering of bone from human adipose-derived stem cells. Acta Biomater 8:2483–2492

Correia CR, Reis RL, Mano JF (2015) Multiphasic, multistructured and hierarchical strategies for cartilage regeneration. Adv Exp Med Biol 881:143–160

Cui W, Wang Q, Chen G, Zhou S, Chang Q, Zuo Q, Ren K, Fan W (2011) Repair of articular cartilage defects with tissue-engineered osteochondral composites in pigs. J Biosci Bioeng 111:493–500

Da H, Jia SJ, Meng GL, Cheng JH, Zhou W, Xiong Z, Mu YJ, Liu J (2013) The impact of compact layer in biphasic scaffold on osteochondral tissue engineering. PLoS ONE 8:e54838

Dinh T, Braunagel S, Rosenblum BI (2015) Growth factors in wound healing. the present and the future? Clin Podiatr Med Surg 32:109–119

Domingues RM, Chiera S, Gershovich P, Motta A, Reis RL, Gomes ME (2016) Enhancing the biomechanical performance of anisotropic nanofibrous scaffolds in tendon tissue engineering: reinforcement with cellulose nanocrystals. Adv Healthc Mater 5:1364–1375

Dorozhkin SV (2010) Bioceramics of calcium orthophosphates. Biomaterials 31:1465–1485

Drury JL, Mooney DJ (2003) Hydrogels for tissue engineering: scaffold design variables and applications. Biomaterials 24:4337–4351

Erisken C, Kalyon DM, Wang H (2008) Functionally graded electrospun polycaprolactone and b-tricalcium phosphate nanocomposites for tissue engineering applications. Biomaterials 29:4065–4073

Fan Z, Guan J (2016) Antifibrotic therapies to control cardiac fibrosis. Biomater Res 20:13

Foroughi MR, Karbasi S, Ebrahimi-Kahrizsangi R (2012) Physical and mechanical properties of a poly-3-hydroxybutyratecoated nanocrystalline hydroxyapatite scaffold for bone tissue engineering. J Porous Mater 19:667–675

Frezzo JA, Montclare JK (2016) Natural composite systems for bioinspired materials. Adv Exp Med Biol 940:143–166

Fuchs S, Jiang X, Schmidt H, Dohle E, Ghanaati S, Orth C, Hofmann A, Motta A, Migliaresi C, Kirkpatrick CJ (2009) Dynamic processes involved in the pre-vascularization of silk fibroin constructs for bone regeneration using outgrowth endothelial cells. Biomaterials 30:1329–1338

Gentile P, Ferreira AM, Callaghan JT, Miller CA, Atkinson J, Freeman C, Hatton PV (2017) Multilayer nanoscale encapsulation of biofunctional peptides to enhance bone tissue regeneration in vivo. Adv Healthc Mater. https://doi.org/10.1002/adhm.20160118

Gervaso F, Scalera F, Padmanabhan SK, Licciulli A, Deponti D, Giancamillo AD, Domeneghini C, Peretti GM, Sannino A (2012) Development and mechanical characterization of a collagen/hydroxyapatite bilayered scaffold for osteochondral defect replacement. Key Eng Mater 493:890–895

Ghazanfari S, Khademhosseini A, Smit TH (2016) Mechanisms of lamellar collagen formation in connective tissues. Biomaterials 97:74–84

Gotterbarm T, Richter W, Jung M, Berardi Vilei S, Mainil-Varlet P, Yamashita T, Breusch SJ (2006) An in vivo study of a growth-factor enhanced, cell free, two-layered collagen-tricalcium phosphate in deep osteochondral defects. Biomaterials 27:3387–3395

Guo X, Zheng Q, Yang S, Shao Z, Yuan Q, Pan Z, Tang S, Liu K, Quan D (2006) Repair of full-thickness articular cartilage defects by cultured mesenchymal stem cells transfected with the transforming growth factor beta1 gene. Biomed Mater 1:206–215

Gupta V, Lyne DV, Barragan M, Berkland CJ, Detamore MS (2016) Microsphere-based scaffolds encapsulating tricalcium phosphate and hydroxyapatite for bone regeneration. J Mater Sci Mater Med 27:121

Han SH, Kim YH, Park MS, Kim IA, Shin JW, Yang WI, Jee KS, Park KD, Ryu GH, Lee JW (2008) Histological and biomechanical properties of regenerated articular cartilage using chondrogenic bone marrow stromal cells with a PLGA scaffold in vivo. J Biomed Mater Res A 87:850–861

He JX, Tan WL, Han QM, Cui SZ, Shao W, Sang F (2016) Fabrication of silk fibroin/cellulose whiskers–chitosan composite porous scaffolds by layer-by-layer assembly for application in bone tissue engineering. J Mater Sci 51:4399–4410

Holzwarth JM, Ma PX (2011) Biomimetic nanofibrous scaffolds for bone tissue engineering. Biomaterials 32:9622–9629

Huang J, Ten E, Liu G, Finzen M, Yu W, Lee JS, Saiz E, Tomsia AP (2013) Biocomposites of pHEMA with HA/beta-TCP (60/40) for bone tissue engineering: Swelling, hydrolytic degradation, and in vitro behavior. Polymer 54:1197–1207

Huang BJ, Hu JC, Athanasiou KA (2016) Cell-based tissue engineering strategies used in the clinical repair of articular cartilage. Biomaterials 98:1–22

Huh J, Lee J, Kim W, Yeo M, Kim G (2017) Preparation and characterization of gelatin/α-TCP/SF biocomposite scaffold for bone tissue regeneration. Int J Biol Macromol. https://doi.org/10.1016/j.ijbiomac.2017.09.030

Islam MM, Khan MA, Rahman MM (2015) Preparation of gelatin based porous biocomposite for bone tissue engineering and evaluation of gamma irradiation effect on its properties. Mater Sci Eng C Mater Biol Appl 49:648–655

Jang JY, Park SH, Park JH, Lee BK, Yun JH, Lee B, Kim JH, Min BH, Kim MS (2016) In vivo osteogenic differentiation of human dental pulp stem cells embedded in an injectable in vivo-forming hydrogel. Macromol Biosci 16:1158–1169

Jing Y, Quan C, Liu B, Jiang Q, Zhang C (2016) A mini review on the functional biomaterials based on poly (lactic acid) stereocomplex. Polym Rev 56:262–286

Kashte S, Jaiswal AK, Kadam S (2017) Artificial bone via bone tissue engineering: current scenario and challenges. Tissue Eng Regen Med 14:1–14

Kemppainen JM, Hollister SJ (2010) Tailoring the mechanical properties of 3D-designed poly(glycerol sebacate) scaffolds for cartilage applications. J Biomed Mater Res A 94:9–18

Kim MS, Kim JH, Min BH, Chun HJ, Han DK, Lee HB (2011) Polymeric scaffolds for regenerative medicine. Polym Rev 51:1–30

Kim DY, Kwon DY, Kwon JS, Kim JH, Min BH, Kim MS (2015) Injectable in situ-forming hydrogels for regenerative medicines. Polym Rev 55:407–452

Kon E, Filardo G, Delcogliano M, Fini M, Salamanna F, Giavaresi G, Martin I, Marcacci M (2010) Platelet autologous growth factors decrease the osteochondral regeneration capability of a collagen-hydroxyapatite scaffold in a sheep model. BMC Musculoskelet Disord 11:220

Koupaei N, Karkhaneh A (2016) Porous crosslinked polycaprolactone hydroxyapatite networks for bone tissue engineering. Tissue Eng Regen Med 13:251–260

Kwon DY, Kwon JS, Park SH, Park JH, Jang SH, Yin XY, Yun JH, Kim JH, Min BH, Lee JH, Kim WD, Kim MS (2015) A computer-designed scaffold for bone

regeneration within cranial defect using human dental pulp stem cells. Sci Rep 5:12721
Kwon DY, Park JH, Jang SH, Park JY, Jang JW, Min BH, Kim WD, Lee HB, Lee J, Kim MS (2017) Bone regeneration by means of a three-dimensional printed scaffold in a rat cranial defect. J Tissue Eng Regen Med. https://doi.org/10.1002/term.2532
Lee P, Manoukian OS, Zhou G, Wang Y, Chang W, Yu X, Kumbar SG (2016) Osteochondral scaffold combined with aligned nanofibrous scaffolds for cartilage regeneration. RSC Adv 6:72246
Lee BH, Shirahama H, Kim MH, Lee JH, Cho NJ, Tan LP (2017a) Colloidal templating of highly ordered gelatin methacryloyl-based hydrogel platforms for three-dimensional tissue analogues. NPG Asia Mater 9:e412
Lee H, Liao JD, Sivashanmugan K, Liu BH, Su YH, Yao CK, Juang YD (2017b) Hydrothermal fabrication of highly porous titanium bio-scaffold with a load-bearable property. Materials 10:e726
Lee WK, Lim YY, Leow AT, Namasivayam P, Ong Abdullah J, Ho CL (2017c) Biosynthesis of agar in red seaweeds: a review. Carbohydr Polym 164:23–30
Li Z, Yang J, Loh XJ (2016) Polyhydroxyalkanoates: opening doors for a sustainable future. NPG Asia Mater 8:e265
Lin YJ, Huang CC, Wan WL, Chiang CH, Chang Y, Sung HW (2017) Recent advances in CO2 bubble-generating carrier systems for localized controlled release. Biomaterials 133:154–164
Makhni MC, Caldwell JM, Saifi C, Fischer CR, Lehman RA, Lenke LG, Lee FY (2016) Tissue engineering advances in spine surgery. Regen Med 11:211–222
Mastrogiacomo M, Muraglia A, Komlev V, Peyrin F, Rustichelli F, Crovace A, Cancedda R (2005) Tissue engineering of bone: search for a better scaffold. Orthod Craniofac Res 8:277–284
Mitsak AG, Kemppainen JM, Harris MT, Hollister SJ (2011) Effect of polycaprolactone scaffold permeability on bone regeneration in vivo. Tissue Eng Part A 17:1831–1839
Moeinzadeh S, Jabbari E (2015) Morphogenic peptides in regeneration of load bearing tissues. Adv Exp Med Biol 881:95–110
Mondschein RJ, Kanitkar A, Williams CB, Verbridge SS, Long TE (2017) Polymer structure-property requirements for stereolithographic 3D printing of soft tissue engineering scaffolds. Biomaterials 140:170–188
Monteiro N, Yelick PC (2017) Advances and perspectives in tooth tissue engineering. J Tissue Eng Regen Med 11:2443–2461
Nanditha S, Chandrasekaran B, Muthusamy S, Muthu K (2017) Apprising the diverse facets of platelet rich fibrin in surgery through a systematic review. Int J Surg 46:186–194
Nie H, Ho ML, Wang CK, Wang CH, Fu YC (2009) BMP-2 plasmid loaded PLGA/HAp composite scaffolds for treatment of bone defects in nude mice. Biomaterials 30:892–901
Park JS, Park KH (2016) Light enhanced bone regeneration in an athymic nude mouse implanted with mesenchymal stem cells embedded in PLGA microspheres. Biomater Res 20:4
Park SH, Kwon JS, Lee BS, Park JH, Lee BK, Yun JH, Lee BY, Kim JH, Min BH, Yoo TH, Kim MS (2017) BMP2-immobilized injectable hydrogel for osteogenic differentiation of human periodontal ligament stem cells. Sci Rep 7:6603
Pinel CB, Pluhar GE (2012) Clinical application of recombinant human bone morphogenetic protein in cats and dogs: a review of 13 cases. Can Vet J 53:767–774
Re'em T, Witte F, Willbold E, Ruvinov E, Cohen S (2012) Simultaneous regeneration of articular cartilage and subchondral bone induced by spatially presented TGF-beta and BMP-4 in a bilayer affinity binding system. Acta Biomater 8:3283–3293
Sánchez M, Anitua E, Delgado D, Sanchez P, Prado R, Orive G, Padilla S (2017) Platelet-rich plasma, a source of autologous growth factors and biomimetic scaffold for peripheral nerve regeneration. Expert Opin Biol Ther 17:197–212
Sartori M, Pagani S, Ferrari A, Costa V, Carina V, Figallo E, Maltarello MC, Martini L, Fini M, Giavaresi G (2017) A new bi-layered scaffold for osteochondral tissue regeneration: in vitro and in vivo preclinical investigations. Mater Sci Eng C Mater Biol Appl 70:101–111
Senthebane DA, Rowe A, Thomford NE, Shipanga H, Munro D, Mazeedi MAMA, Almazyadi HAM, Kallmeyer K, Dandara C, Pepper MS, Parker MI, Dzobo K (2017) The role of tumor microenvironment in chemoresistance: to survive, keep your enemies closer. Int J Mol Sci 18:e1586
Shao X, Goh JC, Hutmacher DW, Lee EH, Zigang G (2006) Repair of large articular osteochondral defects using hybrid scaffolds and bone marrow-derived mesenchymal stem cells in a rabbit model. Tissue Eng 12:1539–1551
Sheikh Z, Hamdan N, Ikeda Y, Grynpas M, Ganss B, Glogauer M (2017) Natural graft tissues and synthetic biomaterials for periodontal and alveolar bone reconstructive applications: a review. Biomater Res 21:9
Singh D, Singh D, Zo S, Han SS (2014) Nano-biomimetics for nano/micro tissue regeneration. J Biomed Nanotechnol 10:3141–3161
Skylar-Scott MA, Liu MC, Wu Y, Dixit A, Yanik MF (2016) Guided homing of cells in multi-photon microfabricated bioscaffolds. Adv Healthc Mater 5:1233–1243
Smith BT, Shum J, Wong M, Mikos AG, Young S (2015) Bone tissue engineering challenges in oral and maxillofacial surgery. Adv Exp Med Biol 881:57–78
Tatman PD, Gerull W, Sweeney-Easter S, Davis JI, Gee AO, Kim DH (2015) Multiscale biofabrication of articular cartilage: bioinspired and biomimetic approaches. Tissue Eng Part B Rev 21:543–559
Tracy CJ, Sanders DN, Bryan JN, Jensen CA, Castaner LJ, Kirk MD, Katz ML (2016) Intravitreal implantation of

genetically modified autologous bone marrow-derived stem cells for treating retinal disorders. Adv Exp Med Biol 854:571–577

Wang W, Caetano G, Ambler WS, Blaker JJ, Frade MA, Mandal P, Diver C, Bártolo P (2016) Enhancing the hydrophilicity and cell attachment of 3D printed PCL/graphene scaffolds for bone tissue engineering. Materials 9:992

Wang Z, Wang Z, Lu WW, Zhen W, Yang D, Peng S (2017) Novel biomaterial strategies for controlled growth factor delivery for biomedical applications. NPG Asia Mater 9:e435

Wongwitwichot P, Kaewsrichan J, Chua KH, Ruszymah BH (2010) Comparison of TCP and TCP/HA hybrid scaffolds for osteoconductive activity. Open Biomed Eng J 4:279–285

Wu F, Liu C, O'Neil B, Wei J, Ngothai Y (2012) Fabrication and properties of porous scaffold of magnesium phosphate/polycaprolactone biocomposite for bone tissue engineering. Appl Surf Sci 258:7589–7595

Xu R, Taskin MB, Rubert M, Seliktar D, Besenbacher F, Chen M (2015) hiPS-MSCs differentiation towards fibroblasts on a 3D ECM mimicking scaffold. Sci Rep 5:8480

Yao H, Kang J, Li W, Liu J, Xie R, Wang Y, Liu S, Wang DA, Ren L (2017) Novel beta-TCP/PVA bilayered hydrogels with considerable physical and bio-functional properties for osteochondral repair. Biomed Mater. https://doi.org/10.1088/1748-605X/aa8541

Yin L, Yuvienco C, Montclare JK (2017) Protein based therapeutic delivery agents: contemporary developments and challenges. Biomaterials 134:91–116

Zhang S, Chen L, Jiang Y, Cai Y, Xu G, Tong T, Zhang W, Wang L, Ji J, Shi P, Ouyang HW (2013) Bi-layer collagen/microporous electrospun nanofiber scaffold improves the osteochondral regeneration. Acta Biomater 9:7236–7247

Recent Progress in Vascular Tissue-Engineered Blood Vessels

8

Jun Chen, Grant C. Alexander, Pratheek S. Bobba, and Ho-Wook Jun

8.1 Introduction

Cardiovascular disease (CVD) is regarded as the leading cause of mortality and morbidity in America and worldwide (Zhang et al. 2017). According to the 2017 statistic report from the American Heart Association, it was estimated that the deaths caused by CVD in the world were 31.5% of the all global deaths (Benjamin et al. 2017). In addition, about 92.1 million U.S. adults are suffering from some type of CVD, and of great concern nearly half of the population (43.9%) of U.S. adults are expected to get some kind of CVD by 2030 (Benjamin et al. 2017).

The golden standard procedure to treat CVD is to bypass the blocked vessels with an autologous vein harvested from the patient through coronary bypass graft surgery (Seifu et al. 2013). However, a great number of patients still fail to obtain immediate treatment because suitable native vessels are often unavailable due to inherent disease, amputation, or previous harvest. In addition, it was reported that the autologous veins often fail to function after 10–12 years post-implantation (Liu et al. 2011). Thus, other types of grafts such as synthetic grafts or materials were developed to offer a better treatment option. Synthetic materials (Dacron and expanded polytetrafluorethlyne (ePTFE)) are also used to treat the disease. However, limitations such as thrombosis, poor mechanical properties, low patency rate, and long fabrication time significantly impact that use of these synthetic grafts and materials in clinical use (Liu et al. 2011).

Recently, tissue engineering has become a promising alternative approach to fabricate vascular substitutes to address the shortcomings of current options. The ideal tissue engineered blood vessels (TEBVs) should have similar properties as native blood vessels; for instance: (1) mimic the three layered vessel structures including intima (endothelial cell (EC) layer), media (smooth muscle cell (SMC) layer), and adventitia (fibroblast cell (FB) layer) in a tubular construct, (2) nonthrombogenic and nonimmunogenic, (3) good mechanical stability to withstand physiological blood pressure, and (4) able to vasoconstrict and vasodilate under physiological conditions (Fernandez et al. 2014). For future clinical application, a relatively low cost and short production time should also be considered. To date, significant progress has been made in generating TEBVs *in vitro* and *in vivo*. In this book chapter, we summarize the cell sources and methods to make TEBVs, the recent progress in TEBV production, and the recent progress in clinical studies.

J. Chen · G. C. Alexander · P. S. Bobba · H.-W. Jun (✉)
Department of Biomedical Engineering, University of Alabama at Birmingham, Birmingham, AL, USA
e-mail: cj1016@uab.edu; alexang2@uab.edu; pbobba@uab.edu; hwjun@uab.edu

I. Noh (ed.), *Biomimetic Medical Materials*, Advances in Experimental Medicine and Biology 1064,
https://doi.org/10.1007/978-981-13-0445-3_8

8.2 Fabrication of TEBV Through Tissue Engineering

Tissue engineering involves three independent and crucial factors which contribute to the formation of new vessels: (1) cells, (2) degradable scaffolds in which the cells will be seeded to produce the extracellular matrix and the subsequent in neotissue formation, and (3) humoral and mechanical signals among cells. In this section, we will focus on the first two factors to generate TEBVs (Naito et al. 2011).

8.2.1 Cell Source for TEBV

As mentioned earlier, the native blood vessels consist of ECs, SMCs, and FBs as internal, middle and outside layers, respectively. Specifically, the EC layer is a single layer of cells that are arranged parallel to the blood flow, while the middle layer consists of concentric layers of SMCs. The fibroblast layer is made of myofibroblasts that are able to produce collagen fibers. So far, TEBVs have been reported to be engineered by using one, two, or all three of these types of cells. The ideal cell source to make the TEBVs is an autologous cell source, which can then divide and differentiate into mature cells. Up to now, several types of cell sources have been used to fabricate TEBVs (Ercolani et al. 2015).

One of the cell sources are autologous SMCs, ECs and FBs taken from a patient's saphenous vein or mammary artery, as these vessels tend to be more flexible and less prone to thrombosis (Buijtenhuijs et al. 2004). This cell source is advantageous as it significantly reduces the chance of rejection of the cells by the immune system. One study reported the use of autologously sourced fibroblasts to engineer blood vessels that showed similar mechanical (burst pressure) and antithrombogenic properties to natural blood vessels. These properties were achieved by layering cell sheets formed from cultured fibroblasts and seeding the interior of the engineered blood vessels with autologous endothelial cells. This method also avoided the need for synthetic materials or smooth muscle cells in the production of the blood vessels (L'Heureux et al. 2006). Although these cells are preferred for coronary procedures as they are similar to the autologous vein, they are not always available for use because patients with cardiovascular disease may not have sufficient amount of unaffected tissue to be used for the procedure. Other issues include the incompatibility between the size and shape of the source cells with the area in which they would be utilized.

Because of the aforementioned drawbacks of sourcing autologous cells directly from the vein, stem cells have become an alternative cell source to generate TEBVs. One of the advantages of using stem cells in tissue engineering is that they can both regenerate themselves and differentiate into other types of cells. Embryonic stem cells are stem cells taken from human embryos at the blastocyst stage prior to implantation in the uterus and which have the capability to differentiate into any type of cell in the body (Rippon and Bishop 2004). Because of their wide differentiation capability, these cells have been used to produce both endothelial and smooth muscle cells for tissue blood vessel engineering. For example, one study reported the use of embryonic stem cells differentiated into endothelial cells to improve perfusion in the ischemic hindlimb of a mouse (Huang et al. 2010). Another study reported the success of using embryonic stem cell to derive endothelial cells to form stable blood vessels *in vivo*. However, one challenge associated with using embryonic stem cells to engineer blood vessels is the production of plentiful differentiated cells (Wang et al. 2007). Also, because these cells are usually acquired from a donor, the risk of immune rejection in the affected subject is also present (Thomson et al. 1998).

Another form of stem cells used in blood vessel engineering is adult stem cells. Similar to embryonic stem cells, these cells have the ability to provide an endless supply of themselves through regeneration and also allow for some differentiation. However, the degree of differentiation that is possible from adult stem cells is not as great as that of embryonic stem cells. Adult stem cells are commonly sourced from the

marrow of long bones and have already undergone some degree of differentiation (Bishop et al. 2002). Adult stem cells obtained from bone marrow can mature into endothelial cells and blood cells. Mesenchymal stem cells, a type of adult stem cell, can differentiate into bone, adipose, and even muscle and endothelial cells (Krawiec and Vorp 2012). One study noted the successful attachment of smooth muscle cells derived from adult adipose stem cells to a vascular graft scaffold (Harris et al. 2011). One drawback of adult stem cells not seen in embryonic stem cells is their limited ability to differentiate into specific cell types. For example, some adult stem cells may only differentiate into smooth muscle cells while others only differentiate into endothelial cells. Another limitation of adult stem cells is the difficulty to find sufficient numbers of appropriate and unaffected cells in patients with cardiovascular disease (Wang et al. 2014). Despite these two drawbacks, adult stem cells hold one major advantage over embryonic stem cells: the ability to be sourced autologously. As these stem cells can be sourced from the patient's own body, they hold the benefit of self-regeneration and differentiation without the risk of immunological rejection (Bishop et al. 2002). Induced pluripotent stem cells (hiPSc) have also been used in blood vessel engineering, and seem to solve the issues that come with both adult and embryonic stem cells. While embryonic stem cells have the ability to differentiate into any type of cell (pluripotency), they are difficult to obtain and have the risk of immunologic rejection (Thomson et al. 1998). Adult stem cells can be obtained autologously and limit immunologic rejection, but do not have the range of variability seen in embryonic stem cells (Wang et al. 2014). Induced pluripotent stem cells are obtained from adult cells that are reverted to an embryonic stem cell state. These induced stem cells can be differentiated into a variety of mature cell types, such as smooth muscle cells and endothelial cells. This allows induced pluripotent cells to be sourced autologously. Furthermore, the adult cells they are induced from are also numerous in the body. One study noted the use of aortic fibroblasts to develop induced pluripotent stem cells that were then differentiated into smooth muscle cells to be used in vascular tissue engineering (Wang et al. 2014). Another study noted the use of induced pluripotent stem cells to generate mesenchymal stem cells that improved vascular tissue regeneration upon implantation (Lian et al. 2010).

Yet another cell type utilized in vascular tissue engineering is endothelial progenitor cells (EPCs). Progenitor cells are similar to adult stem cells in that they are more specific than embryonic stem cells: they are directed to differentiate and mature into a specific target cell type. Endothelial progenitor cells specifically differentiate and mature into endothelial cells that form the inner lining of blood vessels (Szmitko 2003). These cells are commonly sourced from primitive bone marrow shortly after birth and normally circulate in the blood and aggregate at sites of injury to replenish injured endothelium (Urbich and Dimmeler. 2004). Because of their role in restoring the endothelium, they have been used in the treatment of ischemia in vascular tissue and cancer (Au et al. 2008). One study reported that grafts seeded with EPCs explanted in sheep remained patent for over 4 months, and also contributed to the relaxation of vessels through the release of nitric oxide (Kaushal et al. 2001). Another study noted that widespread vascular networks formed in mice that had been implanted with both mesenchymal and endothelial progenitor cells. Furthermore, these structures remained patent for over 4 weeks (Melero-Martin et al. 2008). Although EPCs hold the advantage of reduced immunologic rejection by being sourced autologously, they also hold some drawbacks. The functionality and sustainability of vessels made from EPCs is not well defined. For example, one study noted that adult peripheral EPCs form unstable vessels that do not last more than 3 weeks, while EPCs from the umbilical cord form functional vessels that remain patent for more than 4 months (Au et al. 2008). Further study on EPCs and their functionality is required before they can be used efficiently in vascular tissue engineering.

8.2.2 Methods for In Vitro Fabrication of TEBV

Currently, TEBVs can be generally fabricated through the following methods: (1) assembly of cells within scaffolds, (2) self-assembly with cell sheets, (3) 3D-printing.

8.2.2.1 Assembly of Cells Within Scaffolds

This method includes first seeding the cells in a scaffold, then rolling the cells within the scaffolds into a three dimensional vessel structure using a tubular template, and finally culturing the vessels in static culture or in a bioreactor until the TEBVs are mature. Another approach is to seed the cells into the lumen of a synthetic tubular scaffold, and then culture the cell-seeded scaffold in static or in a bioreactor until the TEBVs are mature (Niklason et al. 1999). Sometimes, cell seeded scaffolds will be implanted in the host to produce the TEBV *in vivo,* instead of producing the TEBV *in vitro.*

The scaffolds used in this method can be decellularized or synthetic scaffolds (Zeng et al. 2010). Decellularized scaffolds are always obtained by removing cellular antigenic components from allogeneic tissues cultured *in vitro*, such as tubular tissues or cell sheets that keep a structured and undamaged extracellular matrix (ECM). Removal of the cells from the tissues can be achieved by physical stirring, enzymatic digestion, and use of a chemical surfactant (Xing et al. 2014). For instance, a TEBV of small diameter was fabricated by seeding ECs or EPCs on a decellularized scaffold derived from porcine SMCs through a biomimetic perfusion system. The seeded EPCs preserved their cobblestone cell morphology and also expressed endothelial cells markers such as CD31, CD144, and von Willibrand factor. Importantly, after the TEBV was implanted into the carotid artery, it remained patent for 30 days and showed little neointimal hyperplasia (Quint et al. 2011).

The advantages of using decellularized scaffolds are: (1) they are non-immunogenic, and (2) decellularized scaffolds can be stored as off-the-shelf products because of their acelluar properties. The disadvantages of decellularized scaffold are that the scaffold degrades very quickly and it is also difficult to modify the scaffold (Fernandez et al. 2014).

Another type of scaffold used is synthetic scaffolds, which are divided into synthetic nondegradable scaffolds and biodegradable scaffolds. Some common nondegradable synthetic scaffolds are expanded polytetrafluoroethylene (ePTFE), Dacron, and polyurethane, which have been used to produce large blood vessel substitutes (McQuade et al. 2009).

One commonly used one is Poly (ε-caprolactone) (PCL). PCL can be degraded slowly by hydrolysis through its ester bond, and is thus usually employed for long-term use. Some other examples are polyglycolic acid (PGA) (Niklason et al. 1999), pol(yglycolic acid)-poly(L-lactic acid) (PGA-PLLA) (Wu et al. 2004), poly (glycerol sebacate) (PGS) (Motlagh et al. 2006), polyhydroxyalkanoates (PHA) (Ma et al. 2010; Cheng et al. 2008), collagen (Shepherd et al. 2008) and silk (Liu et al. 2011). Synthetic and natural degradable scaffolds can be made into tubular scaffolds which mimic the ECM via electrospinning. The electrospinning method involves several steps: (1) the polymer solution is loaded into a syringe and pumped with a syringe pump, (2) the solution is applied with a high DC voltage, which results in a formation of cone shape liquid droplet known as the Taylor cone, (3) a liquid jet of polymer solution is generated from the Taylor cone by the high voltage and then travels to the collector, which has an electrode of the opposite polarity of the polymer, (4) the solid polymer is deposited on the collector as the polymer solvent evaporated during the traveling phase (Hasan et al. 2014). A tubular scaffold can be fabricated by use of a rotating mandrel. After the tubular scaffold is obtained, cells can be seeded onto the scaffold to produce the TEBV. Since the cells are seeded onto the scaffolds, the TEBV is mechanically stable to withstand physiological conditions (Fernandez et al. 2014). In addition, cells seeded onto the scaffold can response to the fluid shear stress, for instance, EC will produce nitric oxide upon stimuli to induce antithrombogenicity. However, the limitations of this method are (1) cells need to be autologous;

(2) high cost; (3) need to prepare the TEBV very far ahead before surgery (Fernandez et al. 2014).

8.2.2.2 Assembly of TEBV Using Cell Sheets

Another way to generate TEBVs is *in vitro* assembly of cell sheets into tubular structures (L'Heureux et al. 1998, 2006). This method is scaffold-free and involves a method known as cell sheet technology.

The cell sheets can be produced in several ways. The most known method is to culture the cells with medium containing ascorbic acid, as the ascorbic acid will induce the ECM formation. It takes 30 days to obtain the cell sheets with ECM (L'Heureux et al. 1998).

A modified cell sheet method was developed to obtain cell sheets without damage. This method is based on several steps: (1) cells are seeded onto a temperature-responsive culture dish, which is coated with a temperature responsive polymer, Poly(Nisopropylacrylamide) (PIPAAM). (2) The cells are cultured at 37 °C until cell sheet formation. (3) The cell sheets are harvested by placing the culture dish at 25 °C (Yamada et al. 1990). The principle for this technology is that when the culture dish is at 37 °C, the PIPAAM coated surface is hydrophobic, so the cells can attach and proliferate on the surface; when the temperature goes below 32 °C, PIPAAM becomes hydrophilic and the cells cannot adhere to the surface anymore, and thus the intact cell sheet will detach for collection (Okano et al. 1995; Kushida et al. 1999; Matsuura et al. 2014). After the cell sheets are harvested, the cell sheets are rolled into a vascular structure and then cultured until the different layers fuse and a mature vessel forms. The advantage of the cell sheet method is that no scaffold is needed. The number of sheets and the cell layer orientations can also be easily controlled through this approach.

Another way to make the cell layered sheet is known as layer-by-layer technology. Layer-by-layer technology is a common approach used to fabricate multilayer polymeric films using different types of polymer interactions. However, layer-by-layer technology was also applied to build up multilayer cell sheets. For instance, cells coated with a single layer made of gelatin and fibronectin (FN) showed ability to accumulate into ordered cell layer sheets because the FN-gelatin coated surface is like the ECM, which allows the second layer of cells to attach on the first layer of cells, leading to the formation of cell sheet layers. Construction of 3D tissues with blood-capillary networks using human dermal fibroblast cells (hFC) and human umbilical vein endothelial cells (HUVEC) was demonstrated in this study (Nishiguchi et al. 2011). The advantage of using this technology is that the layer number and type and location of the cell can be controlled by altering the seeded cell number and order (Matsusaki et al. 2007). Thus, this method provides a rapid way to fabricate cell layered 3D tissues and shows potential to fabricate cell sheets to assemble TEBVs.

8.2.2.3 Fabrication of TEBV Using 3D-Printing

Recently, three-dimensional (3D) printing has been used to fabricate 3D functional living tissues. 3D printing involves several steps: (1) imaging the damaged tissue and its environment using X-ray, CT, or MRI, (2) the three central design approaches of biomimicry, self-assembly, and mini-tissues are used, (3) materials are chosen (synthetic polymers, natural polymers, and ECM) for the bioprinting process, (4) cell types are chosen for bioprinting, and (5) the chosen cells and materials integrate with bioprinting methods such as inkjet, microextrusion, or laser-assisted printers. 3D printing can be used to produce either a single vascular structure or a vascular network. We will highlight some recent studies in the next section (Murphy and Atala 2014; Kang et al. 2016).

8.3 Recent Progress in Vascular TEBV

Though successful fabrication of TEBVs has been reported in many studies, several drawbacks of those developed TEBVs, such as long production time, poor mechanical stability, thrombogenicity, and immunogenicity still

remain as obstacles that limit clinical use. In addition, methods to generate TEBVs with good cell alignment and contractile SMC, obtain a confluent endothelium on the SMC layer in the lumen, and find alternative cell sources for more native TEBV mimics have been gaining widespread attention in the field. In this section, we will focus on recent representative studies regarding fabrication of TEBVs using the cells, methods, and scaffolds we discussed earlier to solve those drawbacks.

In the recent related studies, several groups worked on developing technology to produce mechanically stable TEBVs with a shorter maturation time. For instance, functional and mechanically robust tissue engineered blood vessels known as nTEVM were developed using human fibroblast-derived ECM seeded with SMCs via combining cell sheet technology and decellularization (Fig. 8.1). Specifically, the decellularized matrix scaffolds were obtained by culturing dermal fibroblasts (DF) or saphenous vein fibroblasts (SVF) for 3 weeks in the medium with ascorbic acid, and then decellularizing the fibroblast sheets. Then, human umbilical artery SMCs were seeded on the decellularized matrix scaffolds and cultured for 1 week. Finally, the SMC cell sheets were wrapped around a 4.5 mm cylindrical mandrel and cultured for 3 weeks to obtain a tubular construct. This approach significantly decreased the TEBV production time by 1–2 weeks compared to the method that directly cultured SMC sheets to make the tissue engineered blood vessels (sTEVM) (Fig. 8.4). In addition, based on the immunostaining, the nTEVM were positive for SMC markers such as α-SM-actin and calponin (Fig. 8.2). Thus, the nTEVM demonstrated vascular contraction. The burst pressure of the nTEVM was also significantly higher (~2000 mm Hg) than that of native blood vessels (Bourget et al. 2012).

Another continuous related study was reported recently. In this study, an off-the-shelf tissue-engineered fibroblast-derived vascular scaffold (FDVS) was fabricated using a similar method to what we described earlier; then, the fibroblast sheets were rolled into a tubular structure using a mandrel, followed by decellularization and endothelialization. The EC seeded tubular endothelialized construct was perfused in a bioreactor for 1 week to obtain a TEBV. It took around 8 weeks to culture and produce the decellularized scaffold, and an additional 4 weeks for culture and endothelialization. The burst pressure of the vascular construct seeded with endothelial cells cultured in the bioreactor was 1498 ± 187 mmHg, indicating good mechanical integrity of the TEBV. Also, the decellularized scaffold could be stored for up to 1 month. The advantages of this study are that it allowed preparation of the scaffold in advance and storage until needed for production the TEBV for the patients, which significantly shifted a large part of the online production time (TEBV production) to the off-line phase time, and thus a reduction of the total online time to make the EC seeded TEBV from 11 weeks to 4 weeks (Tondreau et al., 2015).

In addition to the off-the-shelf scaffold for TEBV production described above using dermal fibroblast cells, other "off-the-shelf "grafts with burst pressure around 4000 mm Hg were developed by injecting fibroblast-seeded fibrin gel into a tubular mold and then culturing them for 2 weeks in static culture followed by 3 weeks in a bioreactor (Syedain et al. 2014). After the grafts were decellularized, the grafts were highly stable and could be stored at 4 °C. The grafts were implanted into the femoral artery of sheep for up to 24 weeks. Throughout the *in vivo* study, all grafts were patent without any mineralization after 24 weeks. No significant differences were observed in graft thickness, stiffness, and collagen concentration compared to native vessels, and complete endothelialization occurred at 24 weeks. Later, the off-the-shelf tissue engineered acellular vascular grafts were implanted in three growing lambs aged between 8 weeks and 50 weeks; the *in vivo* performance of the TEBVs was evaluated up to 44 weeks. The results demonstrated that the grafts were capable of growth after implantation; furthermore, the lambs' weight increased by 366% after implantation (Syedain et al. 2016).

Different cell sources to produce TEBVs have attracted much attention recently. For instance,

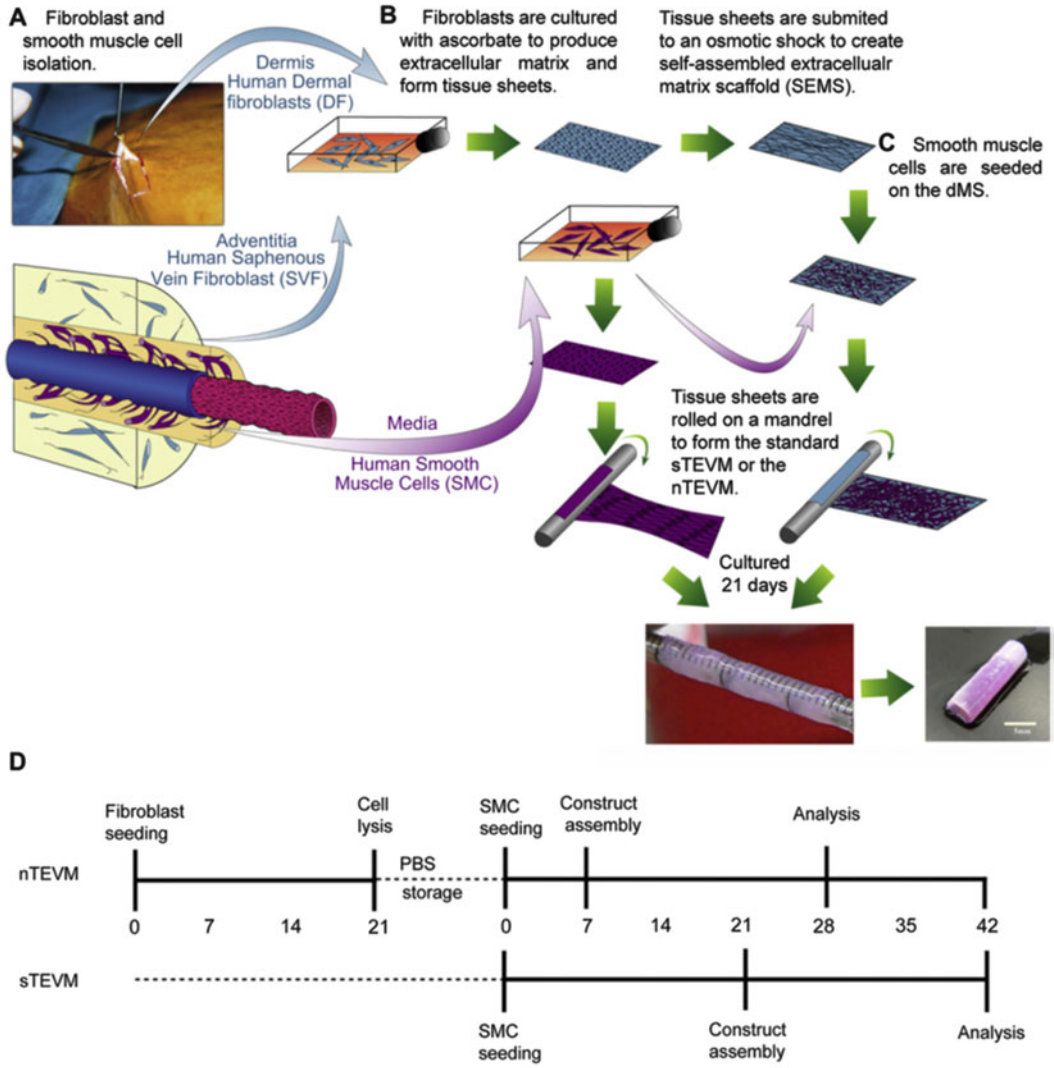

Fig. 8.1 Schematic view of the processes and timeline required for the production of the vascular constructs. (**a**) Human fibroblasts are isolated either from skin or saphenous vein biopsies and smooth muscle cells are isolated from the media of an umbilical artery. (**b**) The tissue sheets are peeled off from the flask and decellularized to produce a dMS or rolled to produce a sTEVM. (**c**) Production of the nTEVM; the dMS are seeded with smooth muscle cells and the sheets are rolled around a tubular mandrel. (**d**) Timeline of the experiment comparing the time required for nTEVM versus sTEVM fabrication, showing that the use of a dMS reduces the production of a vascular construct by 1–2 weeks. (Reused with permission Bourget et al. 2012)

due to the similarity of DF to the human adipose-derived stromal cells (ASC) and the potential to increase TEBV patency, the possibility of using ASC as a novel source to produce TEBVs was investigated. Due to the limitations of obtaining sufficient contractile mature SMCs, ASCs were also studied as a cell source for functional SMCs (Rodriguez et al. 2006). The results demonstrated that ACS can produce mechanically stable TEBVs with sufficient endothelialization within 10 weeks (Fig. 8.3). Importantly, ACS-derived TEBVs can withstand physiological

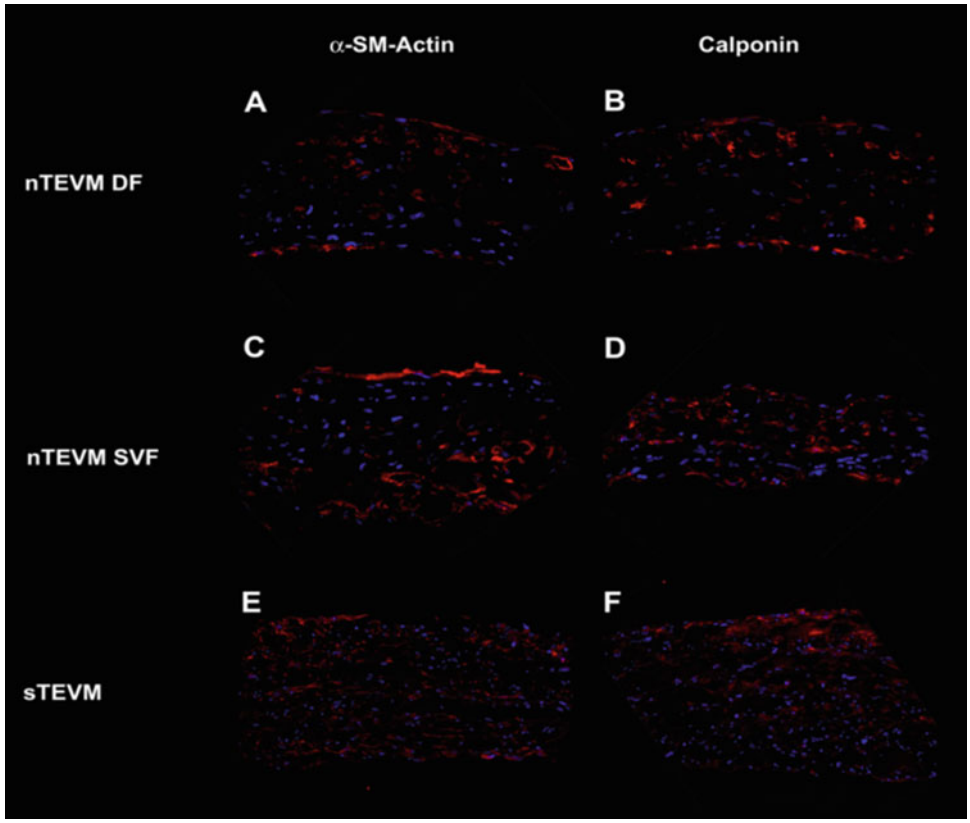

Fig. 8.2 Vascular constructs were stained for SMC markers (**a, c, e**) a-SM-actin (red), and (**b, d, f**) calponin (red). nTEVM constructs produced from (**a, b**) dermal fibroblast, or (**c, d**) saphenous vein fibroblasts seeded with SMCs stained positive for both of these markers. (**e, f**) similar results were obtained for the sTEVM. Scale bar = 100 mm. (Reused with permission Bourget et al. 2012)

blood pressure and had better compliance than fibroblast-derived TEBVs (DF-TEBV) but similar burst pressures, elastic moduli, failure strains, and suture strengths as DF-TEBVs (Tondreau et al. 2015).

Additionally, hiPSCs have been shown to differentiate into contractile SMCs on nanofiber scaffolds through transforming growth factor β1 (TGF-β1) treatment. The hiPSCs-derived SMCs showed high expression of SMC markers, such as α-SMA, CNN1, and SM22a (Wang et al. 2014). Furthermore, vascular smooth muscle cells (VSMCs) obtained from hiPSC differentiation were able to assemble into TEBVs using PLGA grafts. The VSMC TEBVs were generated by culturing the VSMC-seeded PLGA grafts in a bioreactor for 9 weeks. Importantly, the VSMC-based TEBVs remained complete and patent after the grafts were implanted into rat aorta for 2 weeks and could integrate into the native vessels of the host. This study demonstrated that hiPSC-TEBV might offer a chance to treat patients with dysfunctional vascular cells (Gui et al. 2016).

Moreover, hiPSCs can also differentiate into endothelial cells. For example, functional and durable blood vessels were successfully fabricated *in vivo* using endothelial cells and mesenchymal precursor cells derived from hiPSCs. Importantly, the endothelial cells derived from hiPSCs could form stable functional blood vessels and lasted for 280 days in an *in vivo*

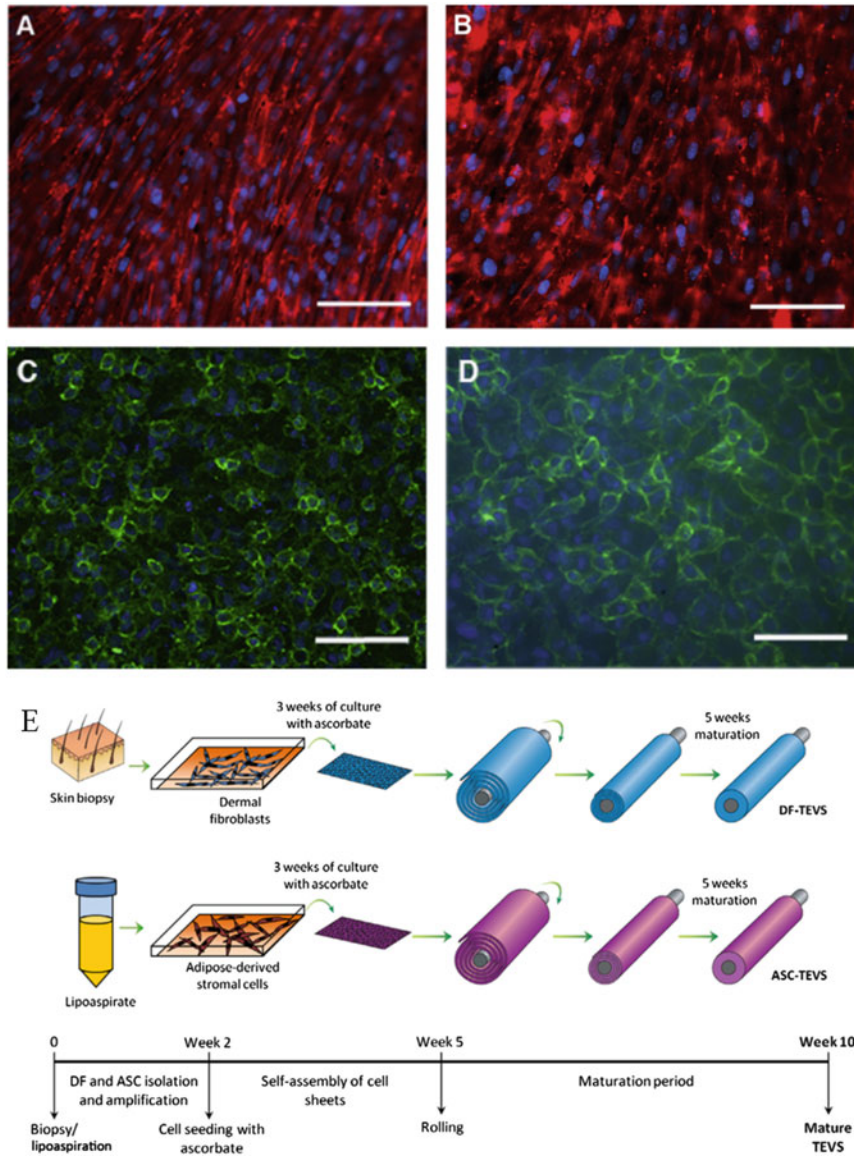

Fig. 8.3 Top view confocal imaging of the endothelium on DF (**a**) and ASC (**b**) sheets as well as on the luminal surface of DF–TEVS (**c**) and ASC–TEVS (**d**). EC on top of DF and ASC cell sheets (**a** and **b**) were submitted to mechanical stimulation on a GyroTwisterTM 3-D shaker plate at 35 rpm for 6 days. These dynamic culture conditions induced the spindled shape of EC and their alignment parallel to the flow. Inversely, no mechanical stimulation was applied to EC inside the DF– and ASC–TEVS and they displayed a polygonal cobblestone-like shape. Labeling for PECAM is shown in red in panel **a–b** and in green in panels **c–d**. All nuclei were counterstained with Hoechst (in blue). Representative micrographs are presented (n = 3). Scale bars: 100 lm. (**e**). Schematic view of the tissue-engineered vascular substitutes (TEVS) production method. Mature TEVS were produced in 10 weeks. Typically, the first step consists in the isolation and amplification of dermal fibroblasts (DF) from a skin biopsy or adipose-derived stromal cells (ASC) from a lipoaspiration procedure. For this study, this step was performed beforehand and banked cells were used. Cell sheets of DF and ASC were produced by culturing cells for 3 weeks with ascorbate. Individual cell sheets were then rolled around 4.7-mm mandrels to form the TEVS. DF- and ASC-TEVS were maintained in culture with ascorbate for a maturation period of 5 weeks before histological and mechanical characterization. (Reproduced with permission Vallières et al. 2015)

mouse model. These results indicate the potential of autologous hiPSC-derived vascular precursors to treat vascular disease (Samuel et al. 2013).

Besides hiPSCs, a bone marrow hMSC-based TEBV was developed by wrapping aligning hEPC-seeded hMSC sheets in a layer-by-layer fashion around a mandrel. It was reported to take around only 5 weeks to obtain a mature hMSC-based TEBV with hEPCs and a burst pressure around 342 mmHg, which is higher than that of human physiological vascular vein pressure (below 200 mmHg). This TEBV can mimic the native porcine femoral vein, as the TEBV diameter decreases upon additional of phenylephrine; also, the NO release amount upon drug treatment was similar to that of native porcine femoral vein (Jung et al. 2015).

In addition to improving the TEBV properties and fabrication process by use of a decellularized scaffold and alternative cell resources, a method combining pNIPAm-assisted cell sheet technology and electrospun PCL aligned nanofiber micropatterned scaffold was reported. The most important advantages of using this method were that: (1) the SMCs could differentiate into contractile human aortic smooth muscle cells (AoSMCs) for use in the TEBV, and (2) PCL can enhance the cell strength sheet in order to make the sheet easy to harvest, as PCL serves plays a similar role as internal elastic lamina in blood vessels (IEL) (Rayatpisheh et al. 2014).

Another study reported that TEBVs made using electrospun sulfated silk fibroin nanofibers demonstrated improved anticoagulant activities due to the sulfuric group incorporated into the silk fibroin nanofibers; also, the porcine vascular ECs and SMCs could attach and proliferate on the silk scaffold and expressed genes for specific cellular phenotype, such as SM-MHC2, α-SM actin, and collagen type I for SMCs, and CD146, vWF, and VE-C gene makers for ECs (Liu et al. 2011). Moreover, an alternative method to increase the scaffold anti-thrombogenicity included coating the scaffold with heparin, as heparin is a highly sulfated polysaccharide. It was reported that heparin coated decellularized vessels seeded with EPCs demonstrated improved anti-thrombogenicity and also inhibited neointimal hyperplasia after the grafts were implanted into dogs for 3 months. The EPCs might also contribute to the decrease in thrombogenicity (Zhou et al. 2012 2011). Interestingly, by combining the highly tubular interconnected porous SF scaffolds coated with heparin, the neovascularization *in vivo* was significantly improved (Zhu et al. 2014).

For synthetic nondegradable scaffolds in recent years, several studies focused on *in vivo* evaluation of the use of polyurethane as a scaffold for vascular prostheses. Polyurethane scaffolds were found to be non-cytotoxic and have good mechanical stability. The HUVEC-seeded polyurethane scaffolds were implanted into the abdominal area of rats for 7 weeks, 14 weeks, 3 months, and 6 months. A 95% patency rate of the polyurethane vascular scaffolds and host cell growth were observed (Grasl et al. 2010; Bergmeister et al. 2012). In addition, the *in vivo* performance, ability to form the vascular wall, and pro-inflammatory properties of TEBVs made using bacterially-synthesized cellulose (BC) as a scaffold were evaluated in a sheep model. However, the TEBVs only showed a burst strength around 800 mm Hg. Vascular wall-like structure formation comprised of vascular SMC and endothelial cells was observed in the scaffold, and the patency rate was around 50% (Scherner et al. 2014).

Besides the progress in TEBV production, some recent studies focused on generating tissue engineered blood vessel models of specific disease. For instance, a Hutchison-Gilford Progeria Syndrome (HGPS) model was developed using TEBVs made with Human iPSC-derived SMCs. Briefly, fibroblasts were first obtained from a HGPS patient; then, the fibroblast were converted into hiPSCs and then differentiated into HGPS-iSMCs. The TEBVs made with HGPS-iSMCs demonstrated HGPS phenotype, such as higher amounts of calcification and thicker walls, but decreased cellularity compared to the TEBVs made from normal healthy cells and MSC-derived TEBVs (Fig. 8.4) (Atchison et al. 2017). Another study reported building up a TEBV atherosclerosis model that consisted of LDL or TNF-α-treated EC and SMC, and LDL

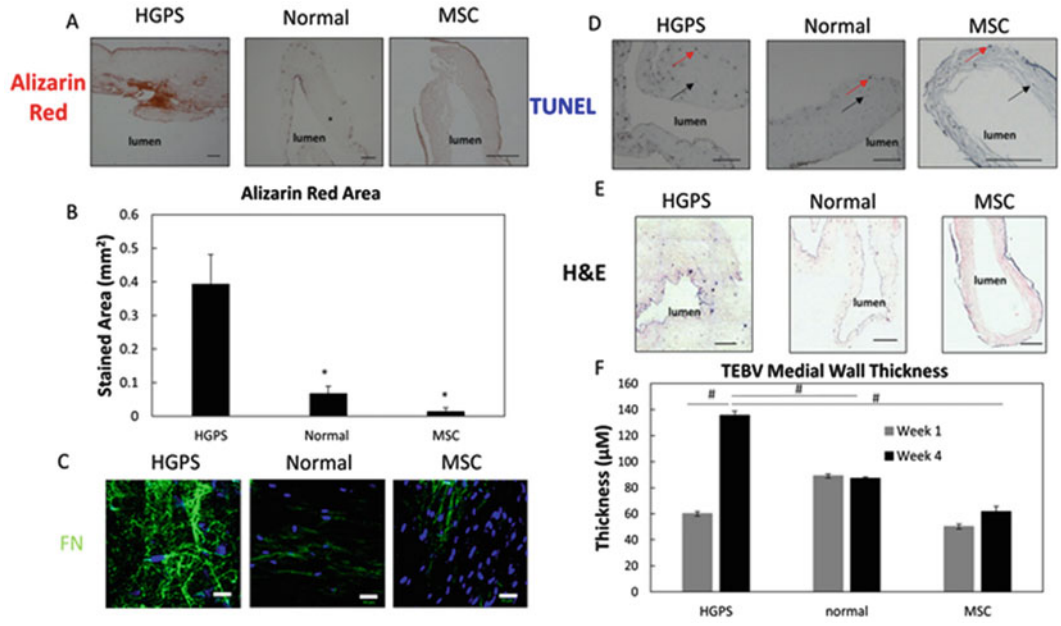

Fig. 8.4 Progeria disease characterization of TEBVs fabricated from MSC or iPSC-derived SMC TEBVs from healthy and Progeria patients. (**a**) Histochemical analysis of HGPS iSMC, normal iSMC, and MSC TEBVs at week 4 with Alizarin Red staining (Scale bar, 200 μm). (**b**) Quantification of A, total area positive for Alizarin Red. (**c**) Representative images of immunofluorescence staining with fibronectin antibodies at week 4 of perfusion on TEBVs fabricated from HGPS iSMCs, normal iSMCs, and MSCs and seeded with hCB-ECs in the lumen (Scale bar, 50 μm). (**d**) Histochemical analysis of MSC, normal iSMC and HGPS iSMC TEBVs at week 4 with TUNEL staining. Red arrows indicate TUNEL positive cells and black arrows indicate TUNEL negative cells (Scale bar, 200 μm). (**e**) Histochemical analysis of HGPS iSMC, normal iSMC, and MSC TEBVs at week 4 with H&E (Scale bar, 200 μm). (**f**) The average thickness of MSC, normal iSMC and HGPS iSMC TEBVs at week 1 and week 4 based on H&E images in E. n = 3 TEBVs for each TEBV cell type. *P < 0.05, **P < 0.01, #P < 0.000. (Reused with permission Atchison et al. 2017)

treated monocytes. The TEBV was fabricated by seeding the cells within a tubular PGA-P4HB composite scaffold and culturing the TEBV in a bioreactor. The total TEBV fabrication time was around 5 weeks. After the endothelium activation, monocytes were circulated into the system and the attachment of monocytes to the activated endothelium and monocyte migration through the endothelium cell layer were observed (Fig. 8.5) (Robert et al. 2013).

As mentioned earlier, 3D-printing also has been used to make vascular structures. One study reported the development of 3D vascular networking by directly 3D bioprinting cell-resonpsive bio-ink that contains gelatin methacryloyl (GelMA), sodium alginate, and 4-arm poly(ethylene glycol)-tetra-acrylate (PEGTA). A stable structure was obtained by first crosslinking alginate with Ca^{2+} and then photocrosslinking the GelMA and PEGTA using UV light (Fig. 8.6). The cells could be encapsulated in the stable structures by mixing the cells with the polymer solution before any crosslinking procedures. The developed blend bio-ink also allowed the endothelial and stem cells to spread and proliferate after encapsulation, which resulted in the formation of perfusable vessels with organized structures (Fig. 8.7). The advantages of this reported method were that the size and diameter of the vascular tube made by this method are changeable, and a vascular network can be fabricated through this method. Also,

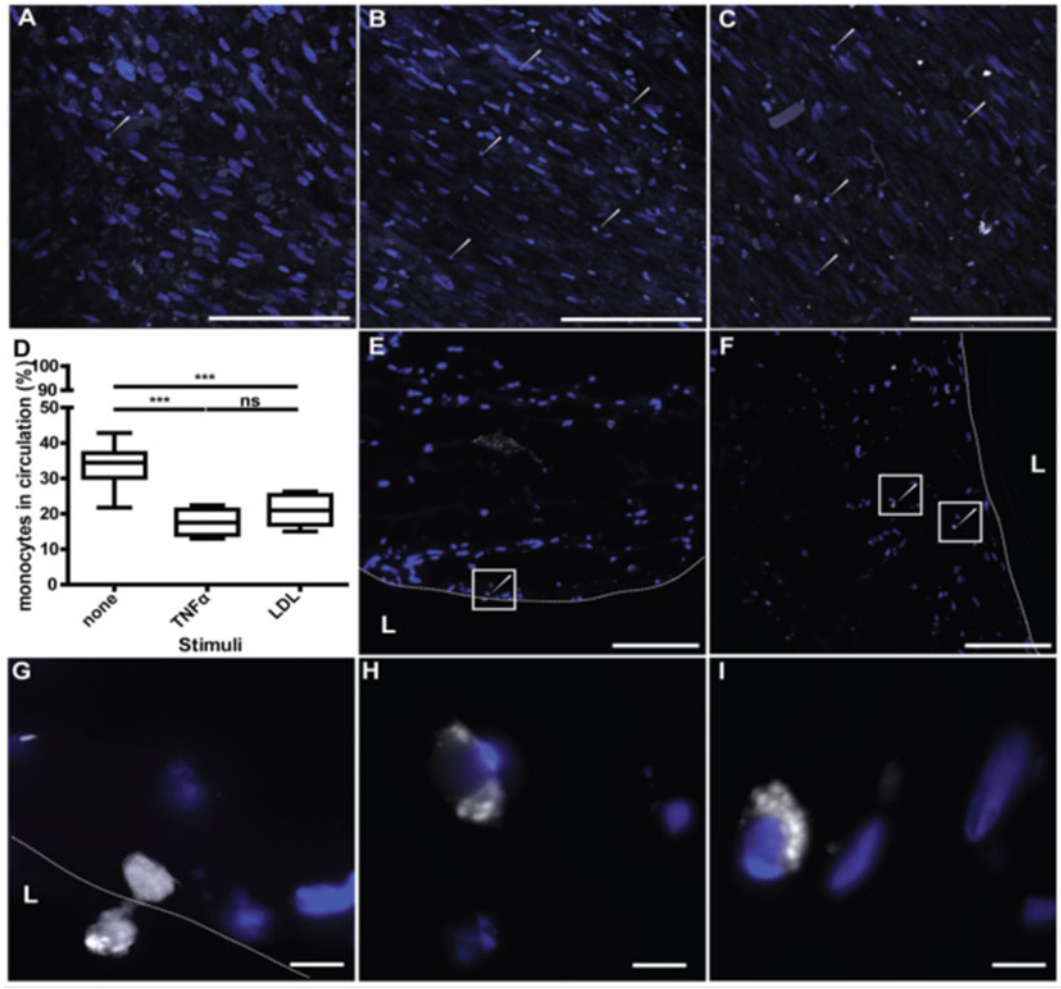

Fig. 8.5 (**a, d**) After pre-treatment in the absence or the presence of 3 h TNFa (10 ng/ml) (**b, d**) or 24 hours LDL (20 mg/ml) (**c–i**) 16106 fluorescently labelled monocytes (white) per ml were injected into the circulation loop and circulated for 24 h. Tissues were analyzed by confocal microscopy and after cryosectionning. In addition, monocytes remaining in the circulation were counted. More monocytes (white arrows) adhered after pre-treatment with TNFa (**b**) or LDL (**c**) compared to the not stimulated (**a**). Less monocyte remained into the circulation after TNFa or LDL pre-treatment compared to the absence of stimuli (**d**). Monocytes adhesion and migration in the tissue was further analyzed by microscopy of cryosections after LDL pre-treatment. Microscopic observations demonstrated adhesion and migration of monocytes through the endothelium (dash line) (**e, g**) and accumulation of monocytes into the tissue (**f, h–i**). Bars represent 200 mm (**a–c**, **e–f**) and 20 mm (**g–i**). (Reused with permission Robert et al. 2013)

this method was simple, as it only involved a multilayered coaxial nozzle device and cell-laden blend bio-ink (Jia et al. 2016). Another example was demonstrated by Chen et al. They developed a new platform for rapid construction of vascularized tissues through 3D microscale continuous optical bioprinting using HUVECs and 10 T1/2 cells, gelatin methacrylate, hyaluronic acid and photoinitiator lithium phenyl-2,4,6 trimethylbenzoylphosphinate (Fig. 8.8). The prevascularized tissues printed by this method showed good cell viability and

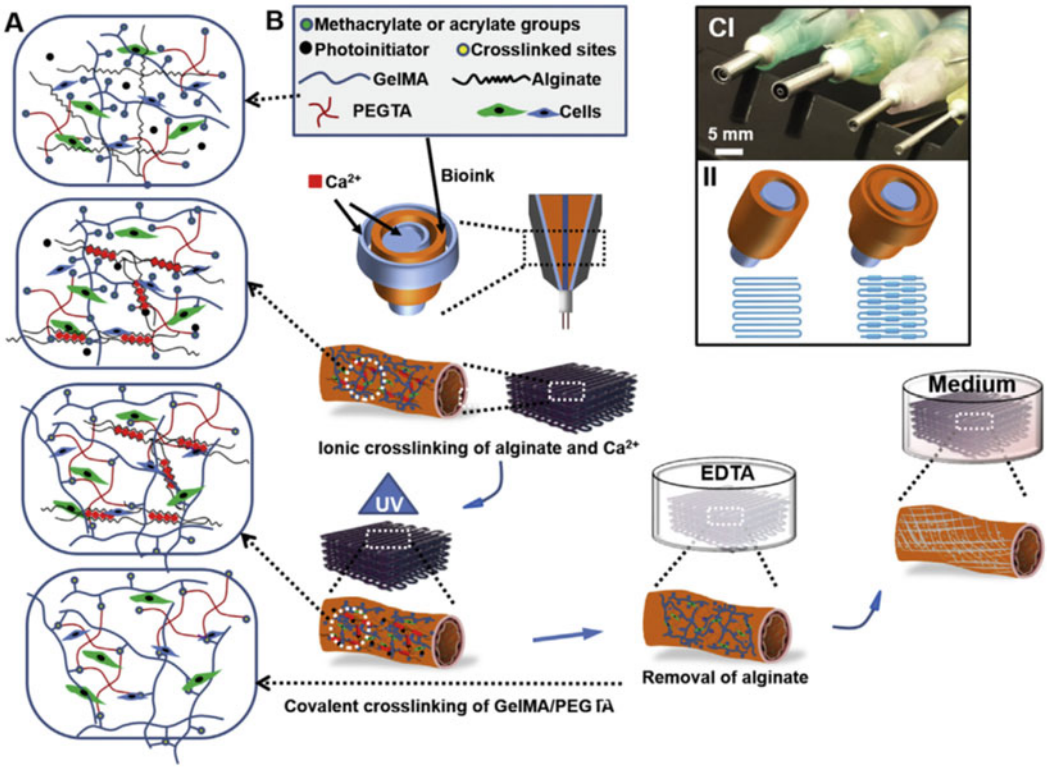

Fig. 8.6 (**a**) Schematic diagram showing two independent crosslinking processes of the bioink, where alginate, GelMA, and PEGTA are ionically and covalently crosslinked, respectively, upon exposure to CaCl2 solution and UV light. (**b**) Schematics showing the procedure of bioprinting perfusable hollow tubes with the cell-encapsulating blend bioink and subsequent vascular formation. (**c**) The designed multilayered coaxial nozzles and schematic diagram showing fabrication of perfusable hollow tubes with constant diameters and changeable sizes. (Reused with permission Jia et al. 2016)

HUVEC network formation *in vivo* after a 2 week implantation period (Zhu et al. 2017).

8.4 Recent Progress in Clinical Studies of TEBV

While the creation of a TEBV in the laboratory setting is a major milestone in the progress towards blood vessel replacement, the ultimate goal is a fully functional, biocompatible, bioresponsive TEBV that is readily available and can be quickly utilized in the clinical environment. Researchers, in conjunction with medical doctors, have been working towards this goal for years now with varying levels of success (Fig. 8.9) (Drews et al. 2017). Here, we will focus on the most progress and advances within the recent years.

8.4.1 Clinical Study Results

Many patients could benefit from a viable TEBV, such as those who must undergo arterial bypass surgery, who need grafts for dialysis access, and who have congenital cardiovascular defects, just to name a few (Patterson et al. 2012). This has been widely recognized for several decades, first in the 1980s with the first successful creation of living blood vessels *in vitro* by Weinberg and Bell, then with the first successful clinical

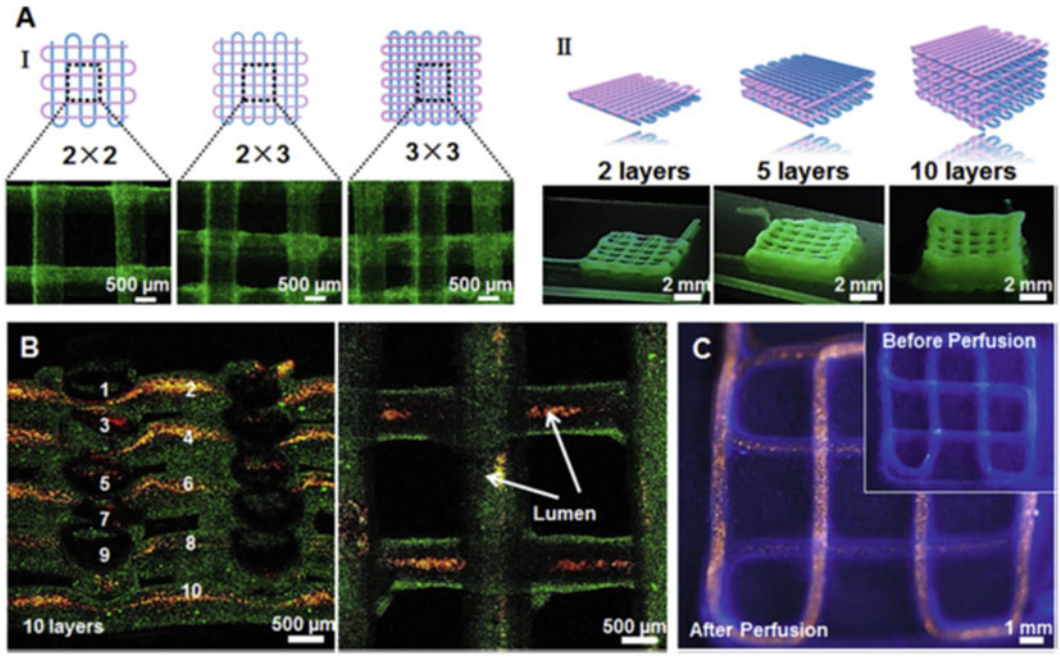

Fig. 8.7 (**a**) Schematics and corresponding fluorescence micrographs of the bioprinted tubular constructs with different aspect ratios of internal grids (I) and numbers of layers (II). (**b**) Confocal micrographs showing a uniform 3D structure composed of 10 layers of bioprinted tubes (containing green fluorescent beads), which were perfused with red fluorescentmicrobeads inside the lumens. (**c**) Fluorescence photographs before (inset) and after injection with red fluorescent microbeads into the lumen of the single, continuous bioprinted tube. (For interpretation of the references to colour in this figure legend, the reader is referred to the web version of this article.) (Reused with permission Jia et al. 2016)

application of a TEBV in 1999, with continuing progress up to the present day (Weinberg and Bell 1986). These were monumental steps toward the dream of fully autologous TEBV in clinical practice.

For example, Shinoka et al. conducted the first clinical trial in children with congenital heart disease in Japan in which 25 TEBV grafts were implanted between 2001 and 2004, with follow up that ranged from 4.3 to most recently 10.3 years. At the 5.8 year follow up, all grafts were patent, and there was no graft-related mortality, no evidence of formation of aneurysms in the grafts, no graft infection or rupture, and no ectopic calcification observed in the grafts (Hibino et al. 2010). Admittedly, after a mean follow-up time of 10.3 years there was some graft stenosis noted in 28% of the patients, but they either stabilized or were resolved after angioplasty and stenting procedures. Nevertheless, on the whole, grafts remained patent and functional, even years after the implantation procedure (Fig. 8.10) (Hibino et al. 2010; Drews et al. 2017). Furthermore, even at the 10.3 year follow up, there was no evidence of aneurysm formation, graft rupture, or calcification (Drews et al. 2017). In 2011, Shinoka et el began the first Food and Drug Administration-approved clinical trial in the United States investigating the use of TEBV in children with congenital heart defects; while the study is ongoing and results are to date unpublished, the trends have been similar to the Japanese study cohort. These exciting results demonstrate the feasibility and clinical potential of TEBV.

A second example is by the L'Heureux group, who implanted autologous TEBV fabricated utilizing sheet-based tissue engineering for

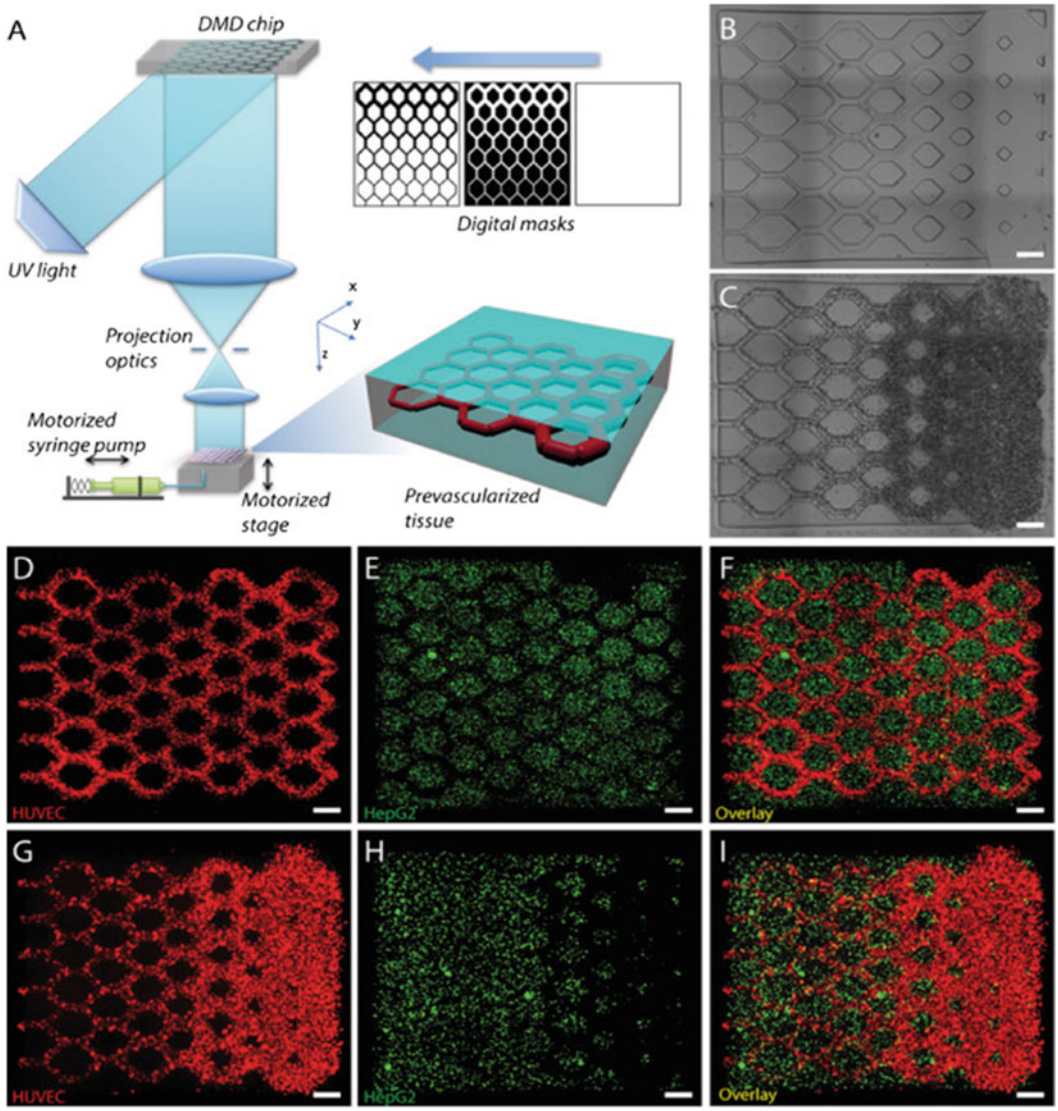

Fig. 8.8 3D bioprinting of the prevascularized tissue constructs. (**a**) Schematic of the bioprinting platform. (**b**) Bioprinted acellular construct featuring intended channels with gradient widths. (**c**) Bioprinted cellular construct with HUVECs and 10T1/2 (50:1) encapsulated in the intended channels. (**d–f**) Fluorescent images demonstrating the bioprinting of heterogeneous cell-laden tissue constructs with uniform channel width. HUVECs (red) are encapsulated in the intended channels and HepG2 (green) are encapsulated in the surrounding area. (**g–i**) Fluorescent images demonstrating the bioprinting of heterogeneous cell-laden tissue constructs with gradient channel widths. Scale bars, 250 μm. (Reused with permission Zhu et al. 2017)

hemodialysis access (L'Heureux et al. 2007a, b; McAllister et al. 2009). Cells were extracted from ten patients, grown into sheets of fibroblasts, wrapped around stainless steel mandrels, and allowed to mature and fuse together over a 10 week period; afterwards, they were endothelialized and preconditioned to *in vivo* flows and pressures (McAllister et al. 2009; L'Heureux et al. 2007a, b). The whole process took between 6 and 9 months, with an average

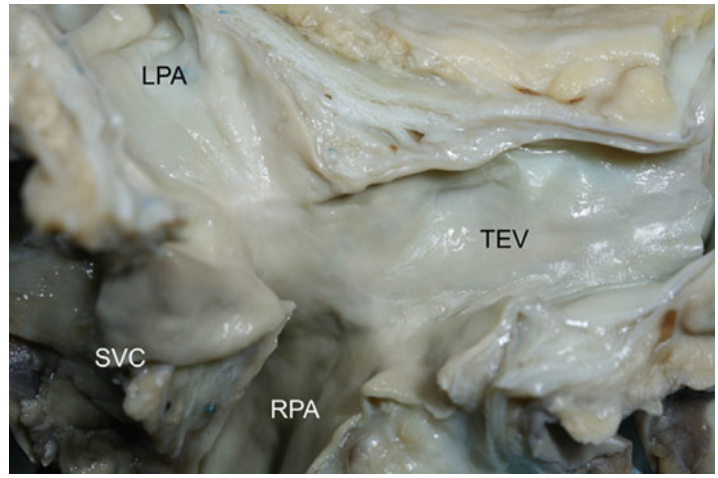

Fig. 8.9 Gross image of a TEBV 13 years after implantation. The appearance is similar to native vein. LPA, left pulmonary artery; RPA, right pulmonary artery; SVC, superior vena cava; TEV, tissue-engineered vessel. (Reused with permission Drews et al. 2017)

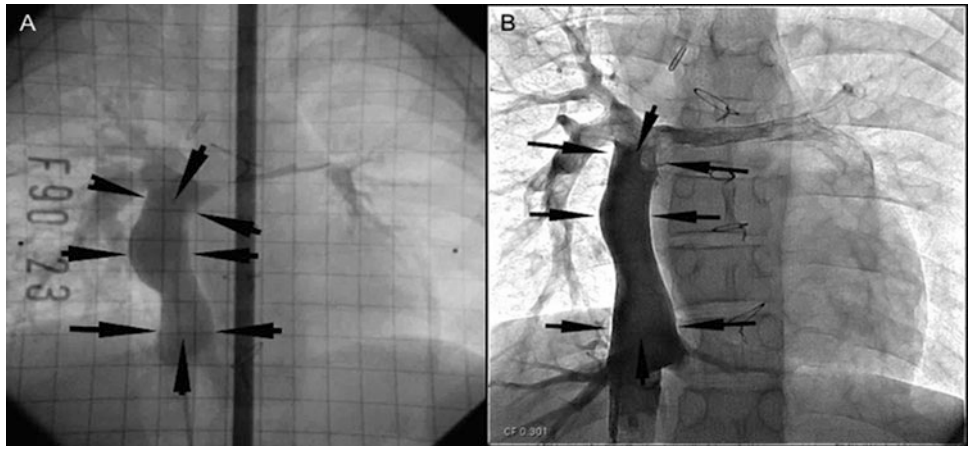

Fig. 8.10 Postoperative growth of a TEBV. A TEBV was implanted in a 5-year-old patient undergoing a Fontan procedure. Angiography 2 years (**a**) and 11 years (**b**) after implantation demonstrate growth, with length of the graft increased from 43.4 to 60.4 cm. (Reused with permission Drews et al. 2017)

period of 7.5 months. Cumulatively speaking, 78% of the grafts maintained primary patency 1 month after implantation, and 60% maintained patency at 3 and 6 months (McAllister et al. 2009). Thus, the L'Heureux group demonstrated successful TEBV implantation in an extremely difficult patient population (end-stage renal disease with at least one previous hemodialysis access graft failure), high arteriovenous hemodynamic flow loads and pressures, and repeated graft puncture for hemodialysis (L'Heureux et al. 2007a, b; McAllister et al. 2009).

The L'Heureux group also attempted the first human use of a nonliving, allogeneic, completely biological TEBV for hemodialysis access, which they reported in 2014 (Wystrychowski et al.

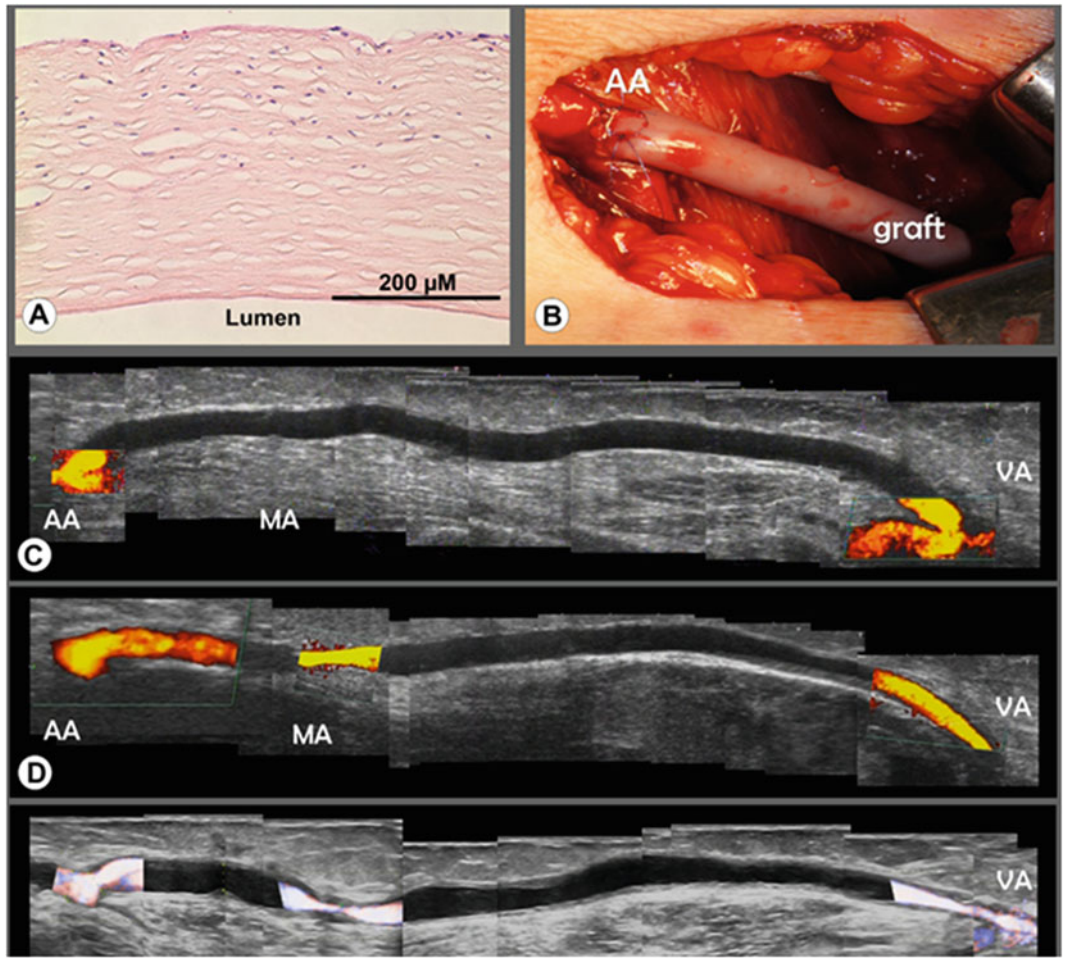

Fig. 8.11 Graft of patient 1. (**a**) Preimplantation hematoxylin and eosin staining of the de-vitalized graft showed the same organization as a living graft, but with dense nuclear remnants in the outer layers. (**b**) Macroscopic view shows the implanted. (Reused with permission Wystrychowski et al. 2014)

2014). These particular grafts were composed of extracellular matrix and fibroblasts which were dehydrated and devitalized prior to long term (6–-9 months) storage. Three patients then received the allogeneic grafts as brachial-axillary arteriovenous shunts for hemodialysis access (Fig. 8.11). The grafts showed no signs of degradation, graft-related infection, or aneurysm formation; they also demonstrated hemodialysis functionality; however, problems with graft stenosis and thrombosis remained (Wystrychowski et al. 2014). Nevertheless, this study demonstrated the potential of nonliving, allogeneic, off the shelf grafts for human use: grafts maintained requisite mechanical strength and did not cause immune response, major milestones in TEBV development. Thus, this study represents a critical advance in the field, as it would be ideal for grafts to be available off

the shelf without concern of degradation or loss of function during the storage time.

8.4.2 Challenges

Despite decades of research, autologous vein and artery grafts remain the clinical gold standard today. Significant challenges remain before TEBV can be adopted for widespread clinical use. These challenges include: (1) similar burst pressure strength (>1700 mm Hg), (2) stable vessel diameter over long time periods, (3) biocompatibility, including non-thrombogenicity, non-inflammatory, maintenance of vessel patency, and structural stability of the TEBV, (4) demonstrated feasibility and consistency in the manufacturing process on a large scale, and (5) the prohibitively long time is takes to create an autologous TEBV (L'Heureux et al. 2007a, b). Furthermore, tissue engineering-based approaches must demonstrate improvements in efficacy and quality of life above synthetic material and native vein approaches that are common clinical practice today. Aside from the purely clinical aspect, challenges also exist in the regulatory, reimbursement, and cost-effectiveness areas for TEBV.

One of the greatest ongoing challenges to the clinical application of TEBV is postoperative vessel stenosis. Shinoka et al. reported asymptomatic graft narrowing (stenosis) in 24% (six) of patients who received a TEBV at 5.8 year follow up; four of these six patients underwent successful balloon angioplasty treatment (REF: late term results). The number of patients with TEBV stenosis increased to 28% (seven) by 10.3 years of follow up (Drews et al. 2017). While this treatment cohort was relatively small, these still represent unacceptable rates of postoperative vessel stenosis; thus, research is ongoing to find ways to limit and prevent stenosis after TEBV implantation.

L'Heureux also encountered challenges with both the autologous and allogeneic TEBV studies. This included instances of aneurysm formation within the graft, thrombosis, graft dilation, stenosis, and strong acute immune response (McAllister et al. 2009; Wystrychowski et al. 2014). Unacceptably long production times (7.5 months) also hamper widespread adoption of autologous graft use (McAllister et al. 2009). While L'Heureux et al. bypassed common challenges of TEBV (infection, poor mechanical strength, use of synthetic or exogenous materials, chemical modification leading to inflammation, etc.), many challenges remain.

8.5 Summary and Future Perspective

Although the concept, fabrication, and implementation of TEBVs have progressed quickly since the original idea more than 30 years ago, a great deal of research and work still remains. TEBVs clearly offer distinct advantages over synthetic grafts, which suffer from limitations such as thrombosis, poor patency, and inadequate mechanical properties; however, more progress is needed before TEBVs can replace autologous grafts, the current gold standard.

Recent advances in cell technology, such as the development of iPSCs, offer a variety of potential cell sources for use in TEBVs. Autologous fully differentiated cells, stem cells, induced pluripotent stem cells, and progenitor cells are all potential sources for use in fabricating TEBVs. Moreover, a variety of methods to create the TEBVs currently exist, including (but not limited to) cell assembly, self-assembly with cell sheets, 3D bioprinting, and layer-by-layer technology. Undoubtedly, as scientific progress is made, better and higher-precision methods will be developed and utilized.

Importantly, TEBVs have already been utilized both in animal models as well as within the clinic for human use. Significant reductions in production and maturation time, off-the-shelf TEBV scaffolds, and improvements in cell sources have all contributed to these recent advances, utilizations, and *in vivo* studies with TEBVs. Although major milestones have been accomplished, including successful long-term TEBV implantation in humans for patients with congenital heart disease and hemodialysis access, many challenges remain to be overcome before

TEBVs will be accepted for widespread clinical use. Despite these challenges, TEBVs have a bright future, and there is little doubt that advances in science and technology will lead to improvements in TEBVs and subsequent pervasive use within the clinic.

References

Atchison L, Zhang H, Cao K, Truskey GA (2017) A tissue engineered blood vessel model of Hutchinson-Gilford progeria syndrome using human iPSC-derived smooth muscle cells. Sci Rep 7(1):8168–8180. https://doi.org/10.1038/s41598-017-08632-4

Au P, Daheron LM, Duda DG, Cohen KS, Tyrrell JA, Lanning RM, Fukumura D, Scadden DT, Jain RK (2008) Differential in vivo potential of endothelial progenitor cells from human umbilical cord blood and adult peripheral blood to form functional long-lasting vessels. Blood 111(3):1302–1305. https://doi.org/10.1182/blood-2007-06-094318

Benjamin EJ, Blaha MJ, Chiuve SE, Cushman M, Das SR, Deo R, de Ferranti SD, Floyd J, Fornage M, Gillespie C (2017) Heart disease and stroke statistics—2017 update: a report from the American Heart Association. Circulation 135(10):e146–e603. https://doi.org/10.1161/CIR.0000000000000485

Bergmeister H, Grasl C, Walter I, Plasenzotti R, Stoiber M, Schreiber C, Losert U, Weigel G, Schima H (2012) Electrospun small-diameter polyurethane vascular grafts: ingrowth and differentiation of vascular-specific host cells. Artif Organs 36(1):54–61. https://doi.org/10.1111/j.1525-1594.2011.01297.x

Bishop AE, Buttery LDK, Polak JM (2002) Embryonic stem cells. J Pathol 197(4):424–429

Bourget J-M, Gauvin R, Larouche D, Lavoie A, Labbé R, Auger FA, Germain L (2012) Human fibroblast-derived ECM as a scaffold for vascular tissue engineering. Biomaterials 33(36):9205–9213. https://doi.org/10.1016/j.biomaterials.2012.09.015

Buijtenhuijs P, Buttafoco L, Poot AA, Daamen WF, Van Kuppevelt TH, Dijkstra PJ, De Vos RA, Sterk LMT, Geelkerken BR, Feijen J (2004) Tissue engineering of blood vessels: characterization of smooth-muscle cells for culturing on collagen-and-elastin-based scaffolds. Biotechnol Appl Biochem 39(2):141–149. https://doi.org/10.1042/BA20030105

Cheng S-T, Chen Z-F, Chen G-Q (2008) The expression of cross-linked elastin by rabbit blood vessel smooth muscle cells cultured in polyhydroxyalkanoate scaffolds. Biomaterials 29(31):4187–4194. https://doi.org/10.1016/j.biomaterials.2008.07.022

Drews JD, Miyachi H, Shinoka T (2017) Tissue-engineered vascular grafts for congenital cardiac disease: clinical experience and current status. Trends Cardiovasc Med 27:521. https://doi.org/10.1016/j.tcm.2017.06.013

Ercolani E, Del Gaudio C, Bianco A (2015) Vascular tissue engineering of small-diameter blood vessels: reviewing the electrospinning approach. J Tissue Eng Regen Med 9(8):861–888. https://doi.org/10.1002/term.1697

Fernandez CE, Achneck HE, Reichert WM, Truskey GA (2014) Biological and engineering design considerations for vascular tissue engineered blood vessels (TEBVs). Curr Opin Chem Eng 3:83–90. https://doi.org/10.1016/j.coche.2013.12.001

Grasl C, Bergmeister H, Stoiber M, Schima H, Weigel G (2010) Electrospun polyurethane vascular grafts: in vitro mechanical behavior and endothelial adhesion molecule expression. J Biomed Mater Res A 93(2):716–723. https://doi.org/10.1002/jbm.a.32584

Gui L, Dash BC, Luo J, Qin L, Zhao L, Yamamoto K, Hashimoto T, Wu H, Dardik A, Tellides G (2016) Implantable tissue-engineered blood vessels from human induced pluripotent stem cells. Biomaterials 102:120–129. https://doi.org/10.1016/j.biomaterials.2016.06.010

Harris LJ, Abdollahi H, Zhang P, McIlhenny S, Tulenko TN, DiMuzio PJ (2011) Differentiation of adult stem cells into smooth muscle for vascular tissue engineering. J Surg Res 168(2):306–314. https://doi.org/10.1016/j.jss.2009.08.001

Hasan A, Memic A, Annabi N, Hossain M, Paul A, Dokmeci MR, Dehghani F, Khademhosseini A (2014) Electrospun scaffolds for tissue engineering of vascular grafts. Acta Biomater 10(1):11–25. https://doi.org/10.1016/j.actbio.2013.08.022

Hibino N, McGillicuddy E, Matsumura G, Ichihara Y, Naito Y, Breuer C, Shinoka T (2010) Late-term results of tissue-engineered vascular grafts in humans. J Thorac Cardiovasc Surg 139(2):431–436. e432. https://doi.org/10.1016/j.jtcvs.2009.09.057

Huang NF, Niiyama H, Peter C, De A, Natkunam Y, Fleissner F, Li Z, Rollins MD, Wu JC, Gambhir SS (2010) Embryonic stem cell–derived endothelial cells engraft into the ischemic hindlimb and restore perfusion. Arterioscler Thromb Vasc Biol 30(5):984–991. https://doi.org/10.1161/ATVBAHA

Jia W, Gungor-Ozkerim PS, Zhang YS, Yue K, Zhu K, Liu W, Pi Q, Byambaa B, Dokmeci MR, Shin SR (2016) Direct 3D bioprinting of perfusable vascular constructs using a blend bioink. Biomaterials 106:58–68. https://doi.org/10.1016/j.biomaterials

Jung Y, Ji H, Chen Z, Chan HF, Atchison L, Klitzman B, Truskey G, Leong KW (2015) Scaffold-free, human mesenchymal stem cell-based tissue engineered blood

vessels. Sci Rep 5:15116. https://doi.org/10.1038/srep15116
Kang H-W, Lee SJ, Ko IK, Kengla C, Yoo JJ, Atala A (2016) A 3D bioprinting system to produce human-scale tissue constructs with structural integrity. Nat Biotechnol 34(3):312–319. https://doi.org/10.1038/nbt.3413
Kaushal S, Amiel GE, Guleserian KJ, Shapira OM, Perry T, Sutherland FW, Rabkin E, Moran AM, Schoen FJ, Atala A (2001) Functional small-diameter neovessels created using endothelial progenitor cells expanded ex vivo. Nat Med 7(9):1035–1040. https://doi.org/10.1038/nm0901-1035
Krawiec JT, Vorp DA (2012) Adult stem cell-based tissue engineered blood vessels: a review. Biomaterials 33 (12):3388–3400. https://doi.org/10.1016/j.biomaterials
Kushida A, Yamato M, Konno C, Kikuchi A, Sakurai Y, Okano T (1999) Decrease in culture temperature releases monolayer endothelial cell sheets together with deposited fibronectin matrix from temperature-responsive culture surfaces. J Biomed Mater Res A 45(4):355–362. https://doi.org/10.1002/(SICI)1097-4636(19990615)45:4<355::AID-JBM10>3.0.CO;2-7
L'Heureux N, Pâquet S, Labbé R, Germain L, Auger FA (1998) A completely biological tissue-engineered human blood vessel. FASEB J 12(1):47–56
L'Heureux N, Dusserre N, Konig G, Victor B, Keire P, Wight TN, Chronos NA, Kyles AE, Gregory CR, Hoyt G (2006) Human tissue engineered blood vessel for adult arterial revascularization. Nat Med 12(3):361. https://doi.org/10.1038/nm1364
L'Heureux N, Dusserre N, Marini A, Garrido S, De La Fuente L, McAllister T (2007a) Technology insight: the evolution of tissue-engineered vascular grafts--from research to clinical practice. Nat Clin Pract Cardiovasc Med 4(7):389. https://doi.org/10.1038/ncpcardio0930
L'Heureux N, McAllister TN, de la Fuente LM (2007b) Tissue-engineered blood vessel for adult arterial revascularization. N Engl J Med 357(14):1451–1453. https://doi.org/10.1056/NEJMc071536
Lian Q, Zhang Y, Zhang J, Zhang HK, Wu X, Zhang Y, Lam FF-Y, Kang S, Xia JC, Lai W-H (2010) Functional mesenchymal stem cells derived from human induced pluripotent stem cells attenuate limb ischemia in mice. Circulation 121(9):1113–1123. https://doi.org/10.1161/CIRCULATIONAHA.109.898312
Liu H, Li X, Zhou G, Fan H, Fan Y (2011) Electrospun sulfated silk fibroin nanofibrous scaffolds for vascular tissue engineering. Biomaterials 32(15):3784–3793. https://doi.org/10.1016/j.biomaterials.2011.02.002
Ma H, Hu J, Ma PX (2010) Polymer scaffolds for small-diameter vascular tissue engineering. Adv Funct Mater 20 (17):2833–2841. https://doi.org/10.1002/adfm.201000922
Matsusaki M, Kadowaki K, Nakahara Y, Akashi M (2007) Fabrication of cellular multilayers with nanometer-sized extracellular matrix films. Angew Chem 119 (25):4773–4776. https://doi.org/10.1002/anie.200701089
Matsuura K, Utoh R, Nagase K, Okano T (2014) Cell sheet approach for tissue engineering and regenerative medicine. J Control Release 190:228–239. https://doi.org/10.1016/j.jconrel.2014.05.024
McAllister TN, Maruszewski M, Garrido SA, Wystrychowski W, Dusserre N, Marini A, Zagalski K, Fiorillo A, Avila H, Manglano X (2009) Effectiveness of haemodialysis access with an autologous tissue-engineered vascular graft: a multicentre cohort study. Lancet 373(9673):1440–1446. https://doi.org/10.1016/S0140-6736(09)60248-8
McQuade K, Gable D, Hohman S, Pearl G, Theune B (2009) Randomized comparison of ePTFE/nitinol self-expanding stent graft vs prosthetic femoralpopliteal bypass in the treatment of superficial femoral artery occlusive disease. J Vasc Surg 49 (1):109–116 e9
Melero-Martin JM, De Obaldia ME, Kang S-Y, Khan ZA, Yuan L, Oettgen P, Bischoff J (2008) Engineering robust and functional vascular networks in vivo with human adult and cord blood–derived progenitor cells. Circ Res 103(2):194–202. https://doi.org/10.1161/CIRCRESAHA.108.178590
Motlagh D, Yang J, Lui KY, Webb AR, Ameer GA (2006) Hemocompatibility evaluation of poly (glycerol-sebacate) in vitro for vascular tissue engineering. Biomaterials 27(24):4315–4324
Murphy SV, Atala A (2014) 3D bioprinting of tissues and organs. Nat Biotechnol 32(8):773–785
Naito Y, Shinoka T, Duncan D, Hibino N, Solomon D, Cleary M, Rathore A, Fein C, Church S, Breuer C (2011) Vascular tissue engineering: towards the next generation vascular grafts. Adv Drug Deliv Rev 63 (4):312–323. https://doi.org/10.1016/j.addr.2011.03.001
Niklason L, Gao J, Abbott W, Hirschi K, Houser S, Marini R, Langer R (1999) Functional arteries grown in vitro. Science 284(5413):489–493. https://doi.org/10.1126/science.284.5413.489
Nishiguchi A, Yoshida H, Matsusaki M, Akashi M (2011) Rapid construction of three-dimensional multilayered tissues with endothelial tube networks by the cell-accumulation technique. Adv Mater 23(31):3506–3510. https://doi.org/10.1002/adma.201101787
Okano T, Yamada N, Okuhara M, Sakai H, Sakurai Y (1995) Mechanism of cell detachment from temperature-modulated, hydrophilic-hydrophobic polymer surfaces. Biomaterials 16(4):297–303. https://doi.org/10.1016/0142-9612(95)93257-E
Patterson JT, Gilliland T, Maxfield MW, Church S, Naito Y, Shinoka T, Breuer CK (2012) Tissue-engineered vascular grafts for use in the treatment of congenital heart disease: from the bench to the clinic and back again. Regen Med 7(3):409–419. https://doi.org/10.2217/rme.12.12
Quint C, Kondo Y, Manson RJ, Lawson JH, Dardik A, Niklason LE (2011) Decellularized tissue-engineered blood vessel as an arterial conduit. Proc Natl Acad Sci

108(22):9214–9219. https://doi.org/10.1073/pnas.1019506108

Rayatpisheh S, Heath DE, Shakouri A, Rujitanaroj P-O, Chew SY, Chan-Park MB (2014) Combining cell sheet technology and electrospun scaffolding for engineered tubular, aligned, and contractile blood vessels. Biomaterials 35(9):2713–2719

Rippon H, Bishop A (2004) Embryonic stem cells. Cell Prolif 37(1):23–34. https://doi.org/10.1111/j.1365-2184.2004.00298.x

Robert J, Weber B, Frese L, Emmert MY, Schmidt D, von Eckardstein A, Rohrer L, Hoerstrup SP (2013) A three-dimensional engineered artery model for in vitro atherosclerosis research. PLoS One 8(11):e79821. https://doi.org/10.1371/journal.pone.0079821

Rodríguez LV, Alfonso Z, Zhang R, Leung J, Wu B, Ignarro LJ (2006) Clonogenic multipotent stem cells in human adipose tissue differentiate into functional smooth muscle cells. Proc Natl Acad Sci 103(32):12167–12172. https://doi.org/10.1073/pnas.0604850103

Samuel R, Daheron L, Liao S, Vardam T, Kamoun WS, Batista A, Buecker C, Schäfer R, Han X, Au P (2013) Generation of functionally competent and durable engineered blood vessels from human induced pluripotent stem cells. Proc Natl Acad Sci 110(31):12774–12779. https://doi.org/10.1073/pnas.1310675110

Scherner M, Reutter S, Klemm D, Sterner-Kock A, Guschlbauer M, Richter T, Langebartels G, Madershahian N, Wahlers T, Wippermann J (2014) In vivo application of tissue-engineered blood vessels of bacterial cellulose as small arterial substitutes: proof of concept? J Surg Res 189(2):340–347. https://doi.org/10.1016/j.jss.2014.02.011

Seifu DG, Purnama A, Mequanint K, Mantovani D (2013) Small-diameter vascular tissue engineering. Nat Rev Cardiol 10(7):410–421. https://doi.org/10.1038/nrcardio.2013.77

Shepherd BR, Jay SM, Saltzman WM, Tellides G, Pober JS (2008) Human aortic smooth muscle cells promote arteriole formation by coengrafted endothelial cells. Tissue Eng A 15(1):165–173. https://doi.org/10.1089/ten.tea.2008.0010

Syedain ZH, Meier LA, Lahti MT, Johnson SL, Tranquillo RT (2014) Implantation of completely biological engineered grafts following decellularization into the sheep femoral artery. Tissue Eng A 20 (11–12):1726–1734. https://doi.org/10.1089/ten.TEA.2013.0550

Syedain Z, Reimer J, Lahti M, Berry J, Johnson S, Tranquillo RT (2016) Tissue engineering of acellular vascular grafts capable of somatic growth in young lambs. Nat Commun 7:12951

Szmitko PE (2003) Endothelial progenitor cells: new hope for a broken heart. Circulation 107(24):3093–3100

Thomson JA, Itskovitz-Eldor J, Shapiro SS, Waknitz MA, Swiergiel JJ, Marshall VS, Jones JM (1998) Embryonic stem cell lines derived from human blastocysts. Science 282(5391):1145–1147. https://doi.org/10.1126/science.282.5391.1145

Tondreau MY, Laterreur V, Gauvin R, Vallières K, Bourget J-M, Lacroix D, Tremblay C, Germain L, Ruel J, Auger FA (2015) Mechanical properties of endothelialized fibroblast-derived vascular scaffolds stimulated in a bioreactor. Acta Biomater 18:176–185. https://doi.org/10.1016/j.actbio.2015.02.026

Urbich C, Dimmeler S (2004) Endothelial progenitor cells. Circ Res 95(4):343–353. https://doi.org/10.1161/01.RES.0000137877.89448.78

Vallières K, Laterreur V, Tondreau MY, Ruel J, Germain L, Fradette J, Auger FA (2015) Human adipose-derived stromal cells for the production of completely autologous self-assembled tissue-engineered vascular substitutes. Acta Biomater 24:209–219

Wang ZZ, Au P, Chen T, Shao Y, Daheron LM, Bai H, Arzigian M, Fukumura D, Jain RK, Scadden DT (2007) Endothelial cells derived from human embryonic stem cells form durable blood vessels in vivo. Nat Biotechnol 25(3):317. https://doi.org/10.1038/nbt1287

Wang Y, Hu J, Jiao J, Liu Z, Zhou Z, Zhao C, Chang L-J, Chen YE, Ma PX, Yang B (2014) Engineering vascular tissue with functional smooth muscle cells derived from human iPS cells and nanofibrous scaffolds. Biomaterials 35(32):8960–8969. https://doi.org/10.1016/j.biomaterials.2014.07.011

Weinberg CB, Bell E (1986) A blood vessel model constructed from collagen and cultured vascular cells. Science 231:397–401. https://doi.org/10.1126/science.2934816

Wu X, Rabkin-Aikawa E, Guleserian KJ, Perry TE, Masuda Y, Sutherland FW, Schoen FJ, Mayer JE, Bischoff J (2004) Tissue-engineered microvessels on three-dimensional biodegradable scaffolds using human endothelial progenitor cells. Am J Phys Heart Circ Phys 287(2):H480–H487. https://doi.org/10.1152/ajpheart.01232.2003

Wystrychowski W, McAllister TN, Zagalski K, Dusserre N, Cierpka L, L'Heureux N (2014) First human use of an allogeneic tissue-engineered vascular graft for hemodialysis access. J Vasc Surg 60 (5):1353–1357

Xing Q, Yates K, Tahtinen M, Shearier E, Qian Z, Zhao F (2014) Decellularization of fibroblast cell sheets for natural extracellular matrix scaffold preparation. Tissue Eng Part C Methods 21(1):77–87. https://doi.org/10.1089/ten.TEC.2013.0666

Yamada N, Okano T, Sakai H, Karikusa F, Sawasaki Y, Sakurai Y (1990) Thermo-responsive polymeric surfaces; control of attachment and detachment of cultured cells. Macromol Rapid Commun 11(11):571–576. https://doi.org/10.1002/marc.1990.030111109

Zeng W, Yuan W, Li L, Mi J, Xu S, Wen C, Zhou Z, Sun J, Ying D, Yang M (2010) The promotion of endothelial

progenitor cells recruitment by nerve growth factors in tissue-engineered blood vessels. Biomaterials 31 (7):1636–1645. https://doi.org/10.1016/j.biomaterials.2009.11.037

Zhang J, Huang H, Ju R, Chen K, Li S, Wang W, Yan Y (2017) In vivo biocompatibility and hemocompatibility of a polytetrafluoroethylene small diameter vascular graft modified with sulfonated silk fibroin. Am J Surg 213(1):87–93. https://doi.org/10.1016/j.amjsurg.2016.04.005

Zhou M, Liu Z, Liu C, Jiang X, Wei Z, Qiao W, Ran F, Wang W, Qiao T, Liu C (2012) Tissue engineering of small-diameter vascular grafts by endothelial progenitor cells seeding heparin-coated decellularized scaffolds. J Biomed Mater Res B Appl Biomater 100(1):111–120. https://doi.org/10.1002/jbm.b.31928

Zhu M, Wang K, Mei J, Li C, Zhang J, Zheng W, An D, Xiao N, Zhao Q, Kong D (2014) Fabrication of highly interconnected porous silk fibroin scaffolds for potential use as vascular grafts. Acta Biomater 10(5):2014. https://doi.org/10.1016/j.actbio.2014.01.022

Zhu W, Xin Q, Zhu J, Ma X, Patel S, Liu J, Wang P, Lai CSE, Gou M, Xu Y, Zhang K, Chen S (2017) Direct 3D bioprinting of prevascularized tissue constructs with complex microarchitecture. Biomaterials 124:106–115

Part IV

Biomimetic Medical Materials and Stem Cells

9 Microenvironmental Regulation of Stem Cell Behavior Through Biochemical and Biophysical Stimulation

Bogyu Choi, Deogil Kim, Inbo Han, and Soo-Hong Lee

9.1 Stem Cells

Stem cells are classified into totipotent, pluripotent, multipotent, and unipotent stem cells based on their differentiation potential (Revel 2009). Stem cells can self-renew and differentiate into other cell types, suggesting their use in various applications such as cell therapy, tissue engineering, and regenerative medicine. Therefore, it is important to develop methods to expand stem cells and induce their differentiation by using biochemical and/or biophysical stimulation to realize this potential.

9.1.1 Pluripotent Stem Cells

Pluripotent stem cells (PSCs) can proliferate perpetually and can differentiate into cells that form the three germ layers, namely, the endoderm, mesoderm, and ectoderm. PSCs are a valuable tool for stem cell therapy, in vitro drug screening, and disease modeling. PSCs include embryonic stem cells (ESCs), ESCs produced by somatic cell nuclear transfer (SCNT-ESCs), and induced PSCs (iPSCs). ESCs are derived from embryos at the developmental stage, SCNT-ESCs are produced by transferring nuclei of somatic cells into enucleated eggs, and iPSCs are artificially generated by reprogramming adult cells. In 2006, Takahashi and Yamanaka achieved a seminal breakthrough in stem cell production (Takahashi and Yamanaka 2006). They found that mouse embryonic fibroblasts (MEFs) can be reprogrammed into iPSCs by exogenous transcription of four factors, Oct4, Sox2, c-Myc, and Klf4. iPSCs are very similar to ESCs but are associated with less ethical concerns and show enhanced patient specificity. For iPSCs, increasing the reprogramming efficiency without the risk from genetic manipulation should be overcome.

9.1.2 Multipotent Stem Cells

Multipotent stem cells such as mesenchymal stem cells (MSCs) derived from the bone marrow, adipose tissue, umbilical cord blood, nerve tissue, dental pulp, hair follicle, or brain can also self-renew and differentiate into different cell types after biochemical and/or biophysical stimulation. MSCs derived from mesodermal tissues differentiate into mesodermal cells such as osteoblasts, chondrocytes, or adipocytes. However, some studies indicate that MSCs can also trans-

B. Choi · D. Kim
Department of Biomedical Science, CHA University, Seongnam-si, South Korea

I. Han
Department of Neurosurgery, CHA University, CHA Bundang Medical Center, Seongnam-si, South Korea
e-mail: hanib@cha.ac.kr

S.-H. Lee (✉)
Department of Medical Biotechnology, Dongguk University, Goyang-si, Gyeonggi-do, South Korea
e-mail: soohong@dongguk.edu

I. Noh (ed.), *Biomimetic Medical Materials*, Advances in Experimental Medicine and Biology 1064,
https://doi.org/10.1007/978-981-13-0445-3_9

differentiate into ectodermal or endodermal lineage cells in vitro when cultured in an induction medium containing some soluble factors (Brzoska et al. 2005; Damien and Allan 2015; Gao et al. 2014; Li et al. 2013). Some MSCs express growth factors and chemokines that induce cell proliferation and angiogenesis (Chen et al. 2008; Doorn et al. 2011; Haynesworth et al. 1996) and exert anti-inflammatory and immunomodulatory effects (Aggarwal and Pittenger 2005; Iyer and Rojas 2008). MSCs have been used for treating various disorders such as spinal cord injury, bone fracture, autoimmune disorder, rheumatoid arthritis, and hematopoietic defects.

9.2 Biochemical Stimulation

Biochemical components such as growth factors, cytokines, enzymes, peptides, chemical reagents, and small molecules are commonly added to cell culture medium to regulate stem cell differentiation. Moreover, biochemical components can be immobilized or precoated on cell culture substrates or scaffolds to induce the differentiation of stem cells into different cell lineages. Biochemical factors bind to receptors present on stem cells or enter stem cells to activate different cellular signaling pathways, thus modulating their behavior. Here, we will explore some existing methods for inducing stem cell differentiation with biochemical factors, as listed in Table 9.1.

9.2.1 Biochemical Differentiation of Multipotent Stem Cells

Osteogenic differentiation can be induced using soluble factors such as ascorbic acid, β-glycerophosphate, bone morphogenetic proteins (BMPs), dexamethasone, NEL-like molecule-1 (NELL-1), phenamil, or tauroursodeoxycholic acid (TUDCA). BMP-2 stimulates the expression of major osteogenic genes such as those encoding osteopontin, osteocalcin, and Runt-related transcription factor 2 (Sun et al. 2015). Although BMPs are suggested to be the most potent osteoinductive proteins, they also induce pro-adipogenesis (Hata et al. 2003; Jin et al. 2006). NELL-1 induces highly specific osteogenic differentiation of MSCs both in vitro and in vivo (Zhang et al. 2010). TUDCA, an endogenous hydrophilic bile acid, suppresses adipogenesis and promotes angiogenesis and osteogenesis by reducing ER stress, preventing unfolded protein response dysfunction, and stabilizing mitochondria (Cha et al. 2014; Cho et al. 2015; Kim et al. 2017; Vang et al. 2014; Yoon et al. 2016). Wnt protein, specifically Wnt3a and Wnt4, is another factor that induces osteogenic differentiation by activating YAP/TAZ accumulation in MSCs (Byun et al. 2014; Park et al. 2015).

Transforming growth factor-β1 (TGF-β1), TGF-β3, kartogenin (KGN), and matrilin-3 are used to enhance chondrogenic differentiation. TGF-β1-tethered photocrosslinkable hydrogel system enhances sulfated glycosaminoglycan accumulation in vitro and cartilage regeneration in vivo (Choi et al. 2015). TGF-β3 is more effective for inducing the chondrogenesis of MSCs than TGF-β1 and TGF-β2 (Barry et al. 2001; Estes et al. 2006). KGN, a new low-molecular-mass heterocyclic molecule, induced selective differentiation of MSCs into chondrocytes and promoted cartilage repair after its intra-articular injection into an animal model of osteoarthritis (Johnson et al. 2012). KGN-conjugated chitosan nanoparticles and microparticles also show potential as efficient intra-articular drug delivery systems for treating osteoarthritis (Kang et al. 2014). Matrilin-3, a non-collagenous extracellular matrix (ECM) protein, enhances the chondrogenic differentiation of adipose tissue-derived MSCs both in vitro and in vivo (Muttigi et al. 2017).

Poly-L-lysine (PLL) is coated on cell culture dishes to enhance cell adhesion through interaction between positive charges on PLL and negative charges on cell membrane (De Kruijff and Cullis 1980; Pachmann and Leibold 1976). Immobilization of PLL on cell culture plates increases the expansion and erythroid differentiation of human hematopoietic stem cells (HSCs) (Fig. 9.1) (Park et al. 2014). Moreover, PLL induces neural differentiation of MSCs (Cai et al. 2012).

Table 9.1 Biochemical factors that regulate cell behavior

Cell	Cell behavior	Biochemical factor	Reference
Human MSC	Chondrogenesis	TGF-β3	Barry et al. (2001)
		BMP-6	Estes et al. (2006)
		KGN	Johnson et al. (2012) and Kang et al. (2014)
		Matrilin-3	Muttigi et al. (2017)
	Osteogenesis	NELL-1	Zhang et al. (2010)
		TUDCA	Cha et al. (2014) and Kim et al. (2017)
Human/murine MSC	Osteogenesis	Wnt3a, Wnt4	Byun et al. (2014) and Park et al. (2015)
Human HSC	Erythropoiesis	PLL	Park et al. (2014)
	Neovascularization	TUDCA	Cho et al. (2015) and Yoon et al. (2016)
Murine MSC	Adipogenesis	BMP-2	Hata et al. (2003) and Jin et al. (2006)
	Chondrogenesis	TGF-β1	Choi et al. (2015)
	Osteogenesis	BMP-2	Sun et al. (2015)
Mouse neural progenitor cell	Neurogenesis	PLL	Cai et al. (2012)
Human PSC	Cardiomyogenesis	CHIR99021, DMH1	Aguilar et al. (2015) and Fonoudi et al. (2015)
	Neurogenesis	CHCHD2,	Zhu et al. (2016)
		Noggin, SB431542	Chambers et al. (2016)
		LDN, CHIR99021	Chambers et al. (2009)
	Astrogenesis	Retionic acid, FGF8, FGF2, EGF	Krencik et al. (2011)
	Pancreatic differentiation	Activin, Wnt, FGF-10, CYC, retinoic acid, DAPT, Ex4, IGF-1, HGF	D'Amour et al. (2006)
		Act A, CHIR, KGF, retinoic acid, SANT1, LDN, PdbU, SANT1, Heparin, Betacellullin, ALK5i, CMRL	Pagliuca et al. (2014)
		GDF8, FGF7, retinoic acid, GSK3βi, VitC, SANT, TPB, LDN, ALK5i II, T3, GSi XX, N-Cys, AXLi	Rezania et al. (2014)
MEF	Reprogramming into iPSC	Oct4, Sox2, c-Myc, Klf4 (OSMK)	Takahashi and Yamanaka (2006)
		OSMK + E-cadherin	Chen et al. (2010) and Redmer et al. (2011)
		ALK5 inhibitors in replace of Sox2	Huangfu et al. (2008a, b), Ichida et al. (2009), Lee et al. (2012), Lin et al. (2009), Mikkelsen et al. (2008), Staerk et al. (2011)

9.2.2 Biochemical Differentiation of Pluripotent Stem Cells

Biochemical differentiation of PSCs in vitro is traditionally achieved by inducing uncontrolled spontaneous differentiation or directed differentiation of these cells into specific cell lineages (Ding et al. 2017). Spontaneous differentiation produces a mixed population of cell lineages from all three germ layers, and the differentiation is uncontrollable. Directed differentiation of PSCs by using soluble factors can be successfully used to generate various cell types such as cardiomyocytes, neural cells, pancreatic beta

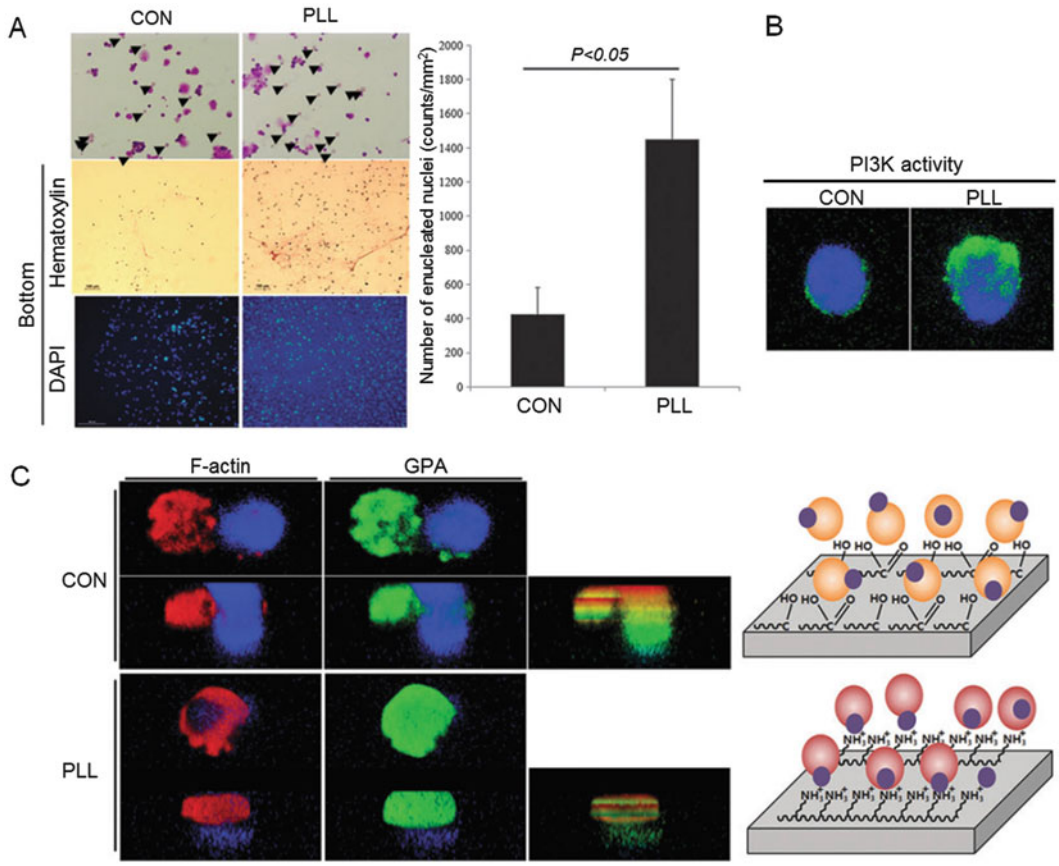

Fig. 9.1 Interaction between HSCs and PLL-coated substrate stimulates downward enucleation. PLL substrate enhances enucleation of HSC (**a**) through stimulation of PI3K activity (**b**). Furthermore, PLL substrate localizes the extruded nuclei downward (**c**), possibly due to the positive charge of PLL substrate

cells, and hepatocytes. However, the efficiency of and purity of cell types obtained through directed differentiation are low.

Functional cardiomyocytes can be produced by culturing EBs in a differentiation medium containing non-essential amino acids such as L-glutamine, β-mercaptoethanol, and 20% fetal bovine serum (FBS), followed by microdissection of beating areas (Zhang et al. 2009). Addition of small-molecule Wnt signaling inhibitors or activators, BMP inhibitors, or shRNA also induces the differentiation of PSCs into cardiomyocytes (Aguilar et al. 2015; Fonoudi et al. 2015; Zhang et al. 2013).

Various protocols have been developed for the neurogenic differentiation of PSCs. Differentiation of PSCs to neuroectoderms can be mediated with CHCHD2, a mitochondrial protein, that suppresses the TGF-β signaling pathway (Zhu et al. 2016). Highly pure astrocyte-like cells have been generated by adding retinoic acid, sonic hedgehog, epidermal growth factor, basic fibroblast growth factor (bFGF), ciliary neurotrophic factor, and 10% FBS to cell culture medium (Krencik et al. 2011). Neural cells can also be generated from PSCs by adding small-molecules to inhibit dual SMAD signaling and activate Wnt signaling (Chambers et al. 2009, 2016). Numerous clinical trials have assessed the potential of human iPSCs and ESCs to undergo neurogenesis for treating spinal cord injury and retinal diseases. However, generation

of mature neural cells from PSCs remains a challenge.

Pancreatic hormone-expressing endocrine cells can be successfully produced from human ESCs by adding and/or removing growth factors such as activin, Wnt, FGF-10, KAAD-cyclopamine (CYC), all-*trans* retinoic acid, γ-secretase inhibitor DAPT, exendin-4, insulin-like growth factor 1, and hepatocyte growth factor to and/or from cell culture medium over five-stages protocol (D'Amour et al. 2006). ViaCyte Inc. (San Diego, CA) is performing clinical trials to assess the efficacy of hESC-derived pancreatic endodermal cells for treating type I diabetes (Agulnick et al. 2015; Kimbrel and Lanza 2015). Addition of activin A, FGF, retinoic acid, BMP inhibitor (LDN), and some gene inhibitors also induces the pancreatic differentiation of PSCs (Pagliuca et al. 2014; Rezania et al. 2014). However, the complexity of these multistep protocols, cost of production, and scaling up should be overcome before using these strategies in clinical practice.

9.2.3 Biochemical Reprogramming Into iPSCs

Takahashi and Yamanaka showed that MEFs could be reprogrammed into iPSCs by inducing forced expression of four transcription factors, namely, OCT4, SOX2, c-MYC, and KLF4 (Yamanaka 4 factors), that are important for ESC function (Takahashi and Yamanaka 2006). This seminal development gave Yamanaka the 2012 Nobel Prize in Physiology or Medicine. Since this pioneering discovery, many researchers have developed various methods to enhance reprogramming efficiency by using biochemical factors. Overexpressed epithelial-cadherin can replace OCT4 during cellular reprogramming, thus enhancing reprogramming efficiency (Chen et al. 2010; Redmer et al. 2011). Addition of high concentration of FBS (>20%), ascorbic acid (vitamin C), histone deacetylase inhibitors, DNA methyltransferase inhibitor (5-azacytidine), or SB431542 (a TGF-β signaling inhibitor) to cell culture medium also enhances reprogramming efficiency (Esteban et al. 2010; Kwon et al. 2016). ALK5 inhibitor, LY364947 or E-616452, can be used to replace Sox2 to reprogram MEFs into iPSCs (Huangfu et al. 2008a, b; Ichida et al. 2009; Lee et al. 2012; Lin et al. 2009; Mikkelsen et al. 2008; Staerk et al. 2011), and CCAAT/enhancer-binding protein alpha (C/EBPα) can boost up the iPSC reprogramming efficiency by upregulating Klf4 and increase several chromatin-modifying complex proteins that activates pluripotency program (Di Stefano et al. 2016).

9.3 Biophysical Stimulation

Many researchers have extensively investigated the effects of various biophysical factors, including matrix stiffness, nanotopography, three-dimensionality, external stress and strain, electrical stimulation, hydrostatic pressure, electromagnetic field, ultrasound, and photostimulation, on cell behavior, as listed in Table 9.2.

9.3.1 Stiffness

In 2006, Engler showed that substrate stiffness regulated stem cell fates and was correlated with in vivo ECM elasticity (Fig. 9.2) (Engler et al. 2006). Human MSCs preferred neurogenesis, myogenesis, and osteogenesis on a soft gel (0.1−1 kPa) mimicking the mechanical stiffness of brain, on an intermediate gel (8−17 kPa) mimicking the mechanical stiffness of muscle, and on very stiff gel (25−40 kPa) mimicking the mechanical stiffness of bone, respectively. Human adipose tissue-derived MSCs undergo adipogenesis on a soft substrate (2 kPa) in the absence of inductive soluble biochemical factors (Young et al. 2013). Neural stem cells (NSCs) expressed high levels of neurogenic biomarker β-tubulin III on substrates having stiffness similar to the brain tissue (Saha et al. 2008). Increase in substrate stiffness increases the expression of type A lamin, a mechanosensitive cellular molecule (Swift et al. 2013). Skeletal muscle stem cells rapidly lose their regenerative potential when

Table 9.2 Biophysical factors that regulate cell behavior

Cell	Cell Behavior	Biophysical Factor	Reference
Human MSC	Differentiation (soft: neurogenesis, intermediate: myogenesis, stiff: osteogenesis)	Stiffness (soft: 0.1–1 kPa, intermediate: 8–17 kPa, stiff: 25–40 kPa)	Engler et al. (2006)
Human MSC	Adipogenesis	Stiffness (soft: 2 kPa)	Young et al. (2013)
Rat NSC	Neurogenesis	Stiffness (~500 Pa)	Saha et al. (2008)
Mouse cell/human MSC	Soft: adipogenesis Stiff: osteogenesis	Stiffness (soft: 0.3 kPa, stiff: 40 kPa)	Swift et al. (2013)
Mouse muscle stem cell	Self-renewal	Stiffness (soft: 12 kPa)	Gilbert et al. (2010)
Human PSC	Neurogenesis	Stiffness (0.1–0.7 kPa)	Keung et al. (2012)
MEF	Reprogramming into iPSC	Stiffness (soft: 0.1 kPa)	Choi et al. (2016)
Human MSC	Osteogenesis	Nanotopography	Dalby et al. (2007)
Mouse ESC	Differentiation	Nanotopography	Lapinte et al. (2013)
Human MSC	Multipotency	Nanotopography	McMurray et al. (2011)
Human iPSC	Pluripotency	Nanotopography	Reimer et al. (2016)
Human MSC	NPo: adipogenesis, NPi: osteogenesis	Nanotopography	Park et al. (2012)
Human PSC	Osteogenesis	Nanotopography	Kingham et al. (2013)
Human iPSC	Cardiogenesis	Topography (microgrooved surface)	Rao et al. (2013)
Human MSC	Neurogenesis	Topography (nanogratings surface)	Yim et al. (2007)
MEF	Reprogamming into iPSC	Topography (microgrooved surface)	Downing et al. (2013)
Human MSC	Myogenesis	Cyclic strain	Gong and Niklason (2008)
Human MSC	Osteogenesis	Cyclic uniaxial tension	Haudenschild et al. (2009)
Human MSC	Chondrogenesis	Dynamic compression	Haudenschild et al. (2009)
Mouse skin fibroblast	Reprogramming into iPSC	Orbital shaking	Sia et al. (2016)
Human PSC	Vascular smooth muscle cell	Tensile stress	Wanjare et al. (2015)
Human MSC	High tension: osteogenesis Low tension: adipogenesis	Intracellular tension	McMurray et al. (2011)
Human MSC	Endothelial differentiation	Shear stress	Dan et al. (2015)
Human iPSC	Cardiomyogenesis	Electrical field	Hirt et al. (2014)
Human NSC	Cell migration	Electrical field	Feng et al. (2012)
Human NSC	Neurogenesis	Electrical field	Pires et al. (2015) and Thrivikraman et al. (2014)
Mouse fibroblast or human dermal fibroblast	Reprogramming into iPSC	Extremely low-frequency electromagnetic field	Baek et al. (2014)
Human MSC	Osteogenesis	LIPUS	Kang et al. (2013)
Human iPS	Neurogenesis	LIPUS	Lv et al. (2013)
Human epidermal stem cell	Proliferation, cell migration	He-Ne laser (632.8 nm)	Liao et al. (2014)
Mouse MSC	Osteogenesis	Visible blue light (405 nm)	Kushibiki and Awazu (2009)

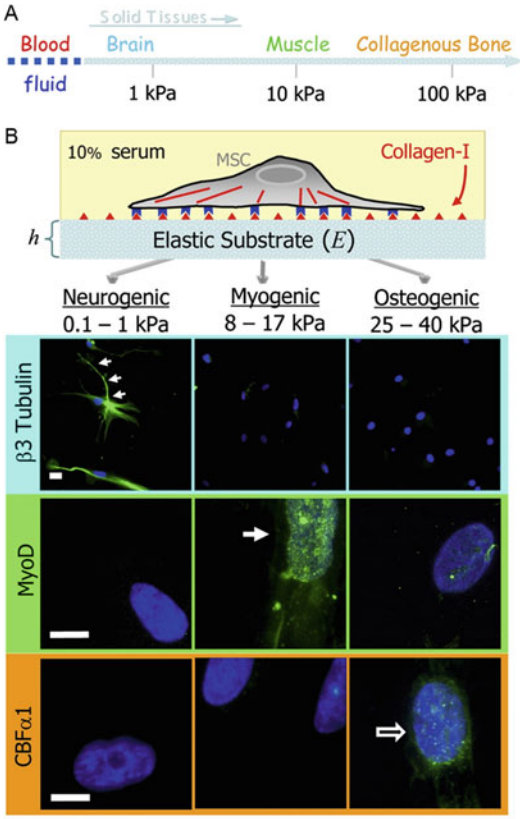

Fig. 9.2 MSC differentiation is regulated by substrate stiffness. Different solid tissues are made up of specific range of elastic modulus (**a**). Through substrate modifications to various matrices that mimic each solid tissue, MSC differentiates to each lineages (**b**)

grown on stiff culture dishes but retain their self-renewal and regenerative capacities when grown on soft hydrogels (Gilbert et al. 2010). Substrates with different stiffness induce the differentiation of different stem cells in a similar manner. Optimal substrate stiffness for the differentiation of stem cells into specific lineages differs based on stem cell source, substrate used, and differentiation protocol used. PSCs also sense and respond with the stiffness of microenvironments. Soft microenvironments (0.1−0.7 kPa) promote early neurogenic differentiation of human PSCs without affecting their proliferation (Keung et al. 2012).

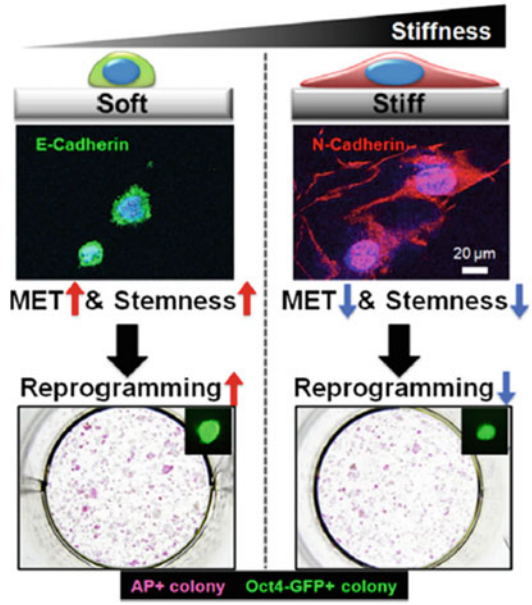

Fig. 9.3 Generation of iPSCs is affected by matrix stiffness. As the substrate softens, MET change and stemness increase, resulting enhanced reprogramming efficiency into iPSCs

Generation of iPSCs is also affected by substrate stiffness. Soft substrates enhance reprogramming efficiency by increasing the expression of MET and pluripotent markers (Fig. 9.3) (Choi et al. 2016).

9.3.2 Topography

Stem cell adhesion, phenotype, and differentiation are highly sensitive to substrate topography (Dalby et al. 2014; Ding et al. 2017; Griffin et al. 2015; Park and Im 2015). The effect of surface topography on stem cell phenotype depends on the shape (pillars, pits, and gratings), dimension (feature size, spacing, and height), arrangement, and composition of a substrate (Dalby et al. 2007; Lapointe et al. 2013; Murphy et al. 2014; Wang et al. 2015). Presence of highly ordered nanoscale pitted patterns in a substrate inhibits the adhesion of cells to the substrate (Dalby et al. 2007).

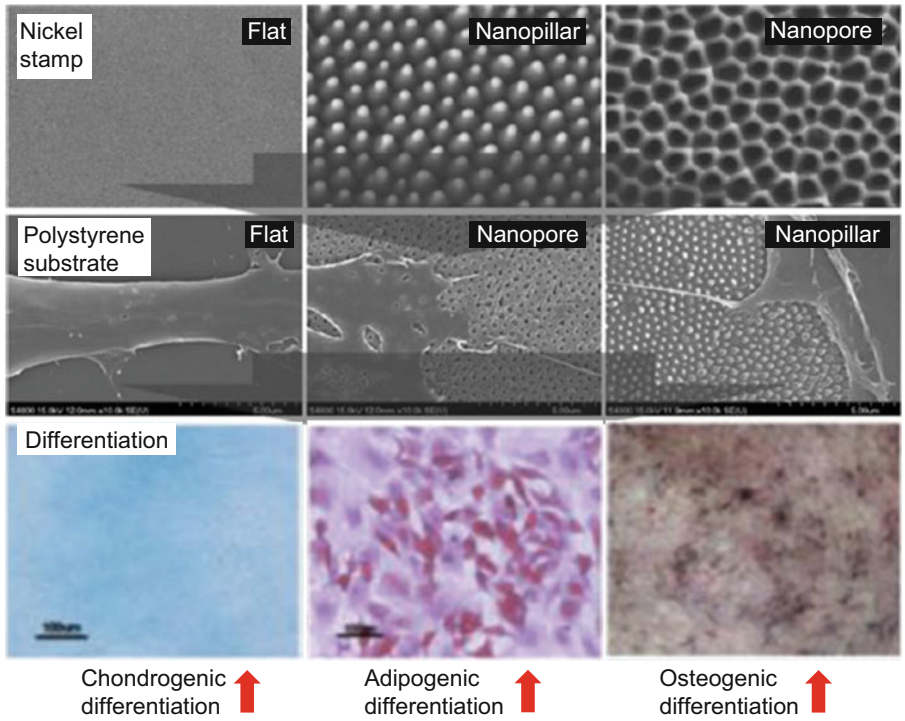

Fig. 9.4 Behavior of ASCs cultured on NPo- and NPi-containing substrates. Fabrication of each nano-featured polystyrene substrates were established using fabricated nickel stamp, and ASC differentiation trends show each flat, NPo, and NPi surface enhances chondrogenic, adipogenic, and osteogenic differentiation, respectively

Expression of human bone marrow-derived MSC (BMSC) and adipose-derived MSC (ASC) markers depends on the size of pits (McMurray et al. 2011). High-density arrangement of smaller topographical features promotes the proliferation and pluripotency of human iPSCs (Reimer et al. 2016).

Substrates with 120-nm diameter pits and an average 300-nm spacing (randomly offset by 50 nm) induce the osteogenesis of human BMSCs (Dalby et al. 2007). Human ASCs cultured on a polystyrene surface containing nanopores (NPo; 200-nm diameter/400-nm depth) undergo enhanced adipogenic differentiation, while those cultured on a polystyrene surface containing nanopillars (NPi; 200-nm diameter/650-nm height) undergo osteogenic differentiation (Fig. 9.4) (Park et al. 2012). Disordered nanotopographies enhance the osteogenesis of human ESCs (Kingham et al. 2013). Fibronectin-coated microgrooves (4-μm width/10-μm depth/10-μm spacing) improve the maturation and function of human iPSC-derived cardiomyocytes (Rao et al. 2013). Human MSCs cultured on 350-nm PDMS nanogratings show significantly upregulated expression of neuronal markers β-tubulin III and microtubule-associated protein 2 compared with human MSCs cultured on microgratings and flat surface (Yim et al. 2007).

Substrate topography also affects the reprogramming of MEFs into iPSCs (Downing et al. 2013). Elongation of MEFs on parallel microgrooved surfaces modulates epigenetic states and improves reprogramming efficiency.

9.3.3 External Stress and Strain

In addition to the intrinsic physical properties of the stem cell microenvironment, such as substrate stiffness, extrinsic mechanical stimuli such as stress or strain are important for regulating the differentiation of stem cells (Keung et al. 2010).

Cyclic strain inhibits the differentiation of hESCs by upregulating the phosphorylation of TGF-β1, activin A, Nodal, and SMAD2/3 and promotes the myogenesis of BMSCs (Gong and Niklason 2008). Cyclic uniaxial tension induces the osteogenesis and dynamic compression induces the chondrogenesis of human BMSCs (Haudenschild et al. 2009). Dynamic culturing with orbital shaking at 100 rpm significantly improves the reprogramming efficiency of iPSCs (Sia et al. 2016). In the presence of uniaxial tensile strain, vascular smooth muscle cells derived from human iPSCs and human ESCs align perpendicular to the strain axis and show increased ECM gene expression (Wanjare et al. 2015). Compressive and tensile forces induced by fluid flow, cell–cell interaction, and cell–matrix interaction regulate MSC behavior in vivo (Hao et al. 2015; Liu and Lee 2014). Human BMSCs with high intracellular tension differentiate into osteoblasts, whereas those with low intracellular tension or low actin–myosin interaction differentiate into adipocytes (McMurray et al. 2011). Shear stress stimulates the differentiation of human MSCs obtained from different tissues into endothelial-like cells (Dan et al. 2015).

9.3.4 Non-contact-Dependent Factors: Electric Field, Ultrasound, and Photostimulation

In addition to cell–matrix interaction-dependent factors such as substrate stiffness and topography, non-contact-dependent factors such as electromagnetic field, low-intensity pulsed ultrasound (LIPUS), and light of varying wavelengths affect stem cell behavior.

Electrical stimulation is of interest for both cardiac and neural differentiation because of its importance in embryonic development. Pulsed biphasic electrical field of 2 V/cm every 4 ms promotes human iPSC-derived cardiomyocytes to develop a phenotype similar to native cardiomyocytes (Hirt et al. 2014). Human ESC-derived NSCs migrate toward positive charged regions in the presence of a small direct-current electrical field (Feng et al. 2012). Application of an electrical field to NSCs or BMSCs grown on an electroconductive matrix enhances their neurogenesis (Pires et al. 2015; Thrivikraman et al. 2014). Extremely low-frequency electromagnetic fields replace SOX2, KLF4, and c-MYC during somatic cell reprogramming of iPSCs (Baek et al. 2014).

Ultrasound frequencies also regulate stem cell behavior. LIPUS enhances the osteogenic differentiation of human ASCs and is used for bone fracture healing and callus distraction (Claes and Willie 2007; Kang et al. 2013). LIPUS stimulation enhances the proliferation and neural differentiation of human iPSC-derived neural crest stem cells (Lv et al. 2013).

Photostimulation also modulates stem cell behavior. Irradiation with helium–neon lasers (632.8 nm), which are used clinically to promote wound healing, induces the proliferation and migration of human epidermal stem cells (Liao et al. 2014). Irradiation with visible blue light (405 nm) enhances the osteogenesis of and bone formation by mouse MSCs (Kushibiki and Awazu 2009).

9.4 Conclusion

Stem cells are a very promising cell source for the cell therapy of various diseases because of their self-renewal and differentiation capacities. For successful application of stem cells and biomaterials in tissue engineering and regenerative medicine, stem cell behavior such as adhesion, proliferation, survival, and differentiation in response to biochemical and biophysical cues

must be precisely regulated. Furthermore, results of biochemical and biophysical stimulation studies involving three-dimensional microenvironments will play an important role in more accurately predicting the in vivo behavior of stem cells.

Acknowledgements This work was supported by a grant from the National Research Foundation (NRF) of Korea funded by the Ministry of Science, ICT & Future Planning (MSIP) (No. NRF-2016R1A2A1A05004987) and the Ministry of Education, Science and Technology (MEST) (No. NRF-2014R1A6A3A04055123).

References

Aggarwal S, Pittenger MF (2005) Human mesenchymal stem cells modulate allogeneic immune cell responses. Blood 105(4):1815–1822. https://doi.org/10.1182/blood-2004-04-1559

Aguilar JS, Begum AN, Alvarez J, Zhang XB, Hong Y, Hao J (2015) Directed cardiomyogenesis of human pluripotent stem cells by modulating Wnt/beta-catenin and BMP signalling with small molecules. Biochem J 469(2):235–241. https://doi.org/10.1042/BJ20150186

Agulnick AD, Ambruzs DM, Moorman MA, Bhoumik A, Cesario RM, Payne JK, Kelly JR, Haakmeester C, Srijemac R, Wilson AZ, Kerr J, Frazier MA, Kroon EJ, D'Amour KA (2015) Insulin-producing endocrine cells differentiated in vitro from human embryonic stem cells function in macroencapsulation devices in vivo. Stem Cells Transl Med 4(10):1214–1222. https://doi.org/10.5966/sctm.2015-0079

Baek S, Quan X, Kim S, Lengner C, Park J-K, Kim J (2014) Electromagnetic fields mediate efficient cell reprogramming into a pluripotent state. ACS Nano 8 (10):10125–10138 %@ 1936-0851

Barry F, Boynton RE, Liu B, Murphy JM (2001) Chondrogenic differentiation of mesenchymal stem cells from bone marrow: differentiation-dependent gene expression of matrix components. Exp Cell Res 268(2):189–200. https://doi.org/10.1006/excr.2001.5278

Brzoska M, Geiger H, Gauer S, Baer P (2005) Epithelial differentiation of human adipose tissue-derived adult stem cells. Biochem Biophys Res Commun 330 (1):142–150. https://doi.org/10.1016/j.bbrc.2005.02.141

Byun MR, Hwang JH, Kim AR, Kim KM, Hwang ES, Yaffe MB, Hong JH (2014) Canonical Wnt signalling activates TAZ through PP1A during osteogenic differentiation. Cell Death Differ 21(6):854–863. https://doi.org/10.1038/cdd.2014.8

Cai L, Lu J, Sheen V, Wang S (2012) Optimal poly (L-lysine) grafting density in hydrogels for promoting neural progenitor cell functions. Biomacromolecules 13(5):1663–1674 %@ 1525-7797

Cha BH, Kim JS, Ahn JC, Kim HC, Kim BS, Han DK, Park SG, Lee SH (2014) The role of tauroursodeoxycholic acid on adipogenesis of human adipose-derived stem cells by modulation of ER stress. Biomaterials 35(9):2851–2858. https://doi.org/10.1016/j.biomaterials.2013.12.067

Chambers SM, Fasano CA, Papapetrou EP, Tomishima M, Sadelain M, Studer L (2009) Highly efficient neural conversion of human ES and iPS cells by dual inhibition of SMAD signaling. Nat Biotechnol 27 (3):275–280. https://doi.org/10.1038/nbt.1529

Chambers SM, Mica Y, Lee G, Studer L, Tomishima MJ (2016) Dual-SMAD inhibition/WNT activation-based methods to induce neural crest and derivatives from human pluripotent stem cells. Methods Mol Biol 1307:329–343. https://doi.org/10.1007/7651_2013_59

Chen L, Tredget EE, Wu PY, Wu Y (2008) Paracrine factors of mesenchymal stem cells recruit macrophages and endothelial lineage cells and enhance wound healing. PLoS One 3(4):e1886. https://doi.org/10.1371/journal.pone.0001886

Chen T, Yuan D, Wei B, Jiang J, Kang J, Ling K, Gu Y, Li J, Xiao L, Pei G (2010) E-cadherin-mediated cell–cell contact is critical for induced pluripotent stem cell generation. Stem Cells 28(8):1315–1325 %@ 1549-4918

Cho JG, Lee JH, Hong SH, Lee HN, Kim CM, Kim SY, Yoon KJ, Oh BJ, Kim JH, Jung SY, Asahara T, Kwon SM, Park SG (2015) Tauroursodeoxycholic acid, a bile acid, promotes blood vessel repair by recruiting vasculogenic progenitor cells. Stem Cells 33 (3):792–805. https://doi.org/10.1002/stem.1901

Choi B, Kim S, Fan J, Kowalski T, Petrigliano F, Evseenko D, Lee M (2015) Covalently conjugated transforming growth factor-beta1 in modular chitosan hydrogels for the effective treatment of articular cartilage defects. Biomater Sci 3(5):742–752. https://doi.org/10.1039/c4bm00431k

Choi B, Park KS, Kim JH, Ko KW, Kim JS, Han DK, Lee SH (2016) Stiffness of hydrogels regulates cellular reprogramming efficiency through mesenchymal-to-epithelial transition and Stemness markers. Macromol Biosci 16(2):199–206

Claes L, Willie B (2007) The enhancement of bone regeneration by ultrasound. Prog Biophys Mol Biol 93 (1):384–398 %@ 0079-6107

D'Amour KA, Bang AG, Eliazer S, Kelly OG, Agulnick AD, Smart NG, Moorman MA, Kroon E, Carpenter MK, Baetge EE (2006) Production of pancreatic hormone-expressing endocrine cells from human embryonic stem cells. Nat Biotechnol 24 (11):1392–1401. https://doi.org/10.1038/nbt1259

Dalby MJ, Gadegaard N, Tare R, Andar A, Riehle MO, Herzyk P, Wilkinson CD, Oreffo RO (2007) The control of human mesenchymal cell differentiation using nanoscale symmetry and disorder. Nat Mater 6 (12):997–1003. https://doi.org/10.1038/nmat2013

Dalby MJ, Gadegaard N, Oreffo RO (2014) Harnessing nanotopography and integrin-matrix interactions to influence stem cell fate. Nat Mater 13(6):558–569. https://doi.org/10.1038/nmat3980

Damien P, Allan DS (2015) Regenerative therapy and immune modulation using umbilical cord blood–derived cells. Biol Blood Marrow Transplant 21 (9):1545–1554 %@ 1083-8791

Dan P, Velot E, Decot V, Menu P (2015) The role of mechanical stimuli in the vascular differentiation of mesenchymal stem cells. J Cell Sci 128 (14):2415–2422. https://doi.org/10.1242/jcs.167783

De Kruijff B, Cullis PR (1980) The influence of poly (l-lysine) on phospholipid polymorphism evidence that electrostatic polypeptide-phospholipid interactions can modulate bilayer/non-bilayer transitions. Biochim Biophys Acta Biomembr 601:235–240 %@ 0005-2736

Di Stefano B, Collombet S, Jakobsen JS, Wierer M, Sardina JL, Lackner A, Stadhouders R, Segura-Morales C, Francesconi M, Limone F, Mann M, Porse B, Thieffry D, Graf T (2016) C/EBPalpha creates elite cells for iPSC reprogramming by upregulating Klf4 and increasing the levels of Lsd1 and Brd4. Nat Cell Biol 18(4):371–381. https://doi.org/10.1038/ncb3326

Ding S, Kingshott P, Thissen H, Pera M, Wang PY (2017) Modulation of human mesenchymal and pluripotent stem cell behavior using biophysical and biochemical cues: a review. Biotechnol Bioeng 114(2):260–280. https://doi.org/10.1002/bit.26075

Doorn J, van de Peppel J, van Leeuwen JP, Groen N, van Blitterswijk CA, de Boer J (2011) Pro-osteogenic trophic effects by PKA activation in human mesenchymal stromal cells. Biomaterials 32(26):6089–6098. https://doi.org/10.1016/j.biomaterials.2011.05.010

Downing TL, Soto J, Morez C, Houssin T, Fritz A, Yuan F, Chu J, Patel S, Schaffer DV, Li S (2013) Biophysical regulation of epigenetic state and cell reprogramming. Nat Mater 12(12):1154 %@ 1476-1122

Engler AJ, Sen S, Sweeney HL, Discher DE (2006) Matrix elasticity directs stem cell lineage specification. Cell 126(4):677–689. https://doi.org/10.1016/j.cell.2006.06.044

Esteban MA, Wang T, Qin B, Yang J, Qin D, Cai J, Li W, Weng Z, Chen J, Ni S, Chen K, Li Y, Liu X, Xu J, Zhang S, Li F, He W, Labuda K, Song Y, Peterbauer A, Wolbank S, Redl H, Zhong M, Cai D, Zeng L, Pei D (2010) Vitamin C enhances the generation of mouse and human induced pluripotent stem cells. Cell Stem Cell 6(1):71–79. https://doi.org/10.1016/j.stem.2009.12.001

Estes BT, Wu AW, Guilak F (2006) Potent induction of chondrocytic differentiation of human adipose-derived adult stem cells by bone morphogenetic protein 6. Arthritis Rheum 54(4):1222–1232. https://doi.org/10.1002/art.21779

Feng JF, Liu J, Zhang XZ, Zhang L, Jiang JY, Nolta J, Zhao M (2012) Guided migration of neural stem cells derived from human embryonic stem cells by an electric field. Stem Cells 30(2):349–355. https://doi.org/10.1002/stem.779

Fonoudi H, Ansari H, Abbasalizadeh S, Larijani MR, Kiani S, Hashemizadeh S, Zarchi AS, Bosman A, Blue GM, Pahlavan S, Perry M, Orr Y, Mayorchak Y, Vandenberg J, Talkhabi M, Winlaw DS, Harvey RP, Aghdami N, Baharvand H (2015) A universal and robust integrated platform for the scalable production of human cardiomyocytes from pluripotent stem cells. Stem Cells Transl Med 4(12):1482–1494. https://doi.org/10.5966/sctm.2014-0275

Gao Y, Bai C, Wang K, Sun B, Guan W, Zheng D (2014) All-trans retinoic acid promotes nerve cell differentiation of yolk sac-derived mesenchymal stem cells. Appl Biochem Biotechnol 174(2):682–692. https://doi.org/10.1007/s12010-014-1100-2

Gilbert PM, Havenstrite KL, Magnusson KE, Sacco A, Leonardi NA, Kraft P, Nguyen NK, Thrun S, Lutolf MP, Blau HM (2010) Substrate elasticity regulates skeletal muscle stem cell self-renewal in culture. Science 329(5995):1078–1081. https://doi.org/10.1126/science.1191035

Gong Z, Niklason LE (2008) Small-diameter human vessel wall engineered from bone marrow-derived mesenchymal stem cells (hMSCs). FASEB J 22 (6):1635–1648. https://doi.org/10.1096/fj.07-087924

Griffin MF, Butler PE, Seifalian AM, Kalaskar DM (2015) Control of stem cell fate by engineering their micro and nanoenvironment. World J Stem Cells 7(1):37

Hao J, Zhang Y, Jing D, Shen Y, Tang G, Huang S, Zhao Z (2015) Mechanobiology of mesenchymal stem cells: perspective into mechanical induction of MSC fate. Acta Biomater 20:1–9. https://doi.org/10.1016/j.actbio.2015.04.008

Hata K, Nishimura R, Ikeda F, Yamashita K, Matsubara T, Nokubi T, Yoneda T (2003) Differential roles of Smad1 and p38 kinase in regulation of peroxisome proliferator-activating receptor gamma during bone morphogenetic protein 2-induced adipogenesis. Mol Biol Cell 14(2):545–555. https://doi.org/10.1091/mbc.E02-06-0356

Haudenschild AK, Hsieh AH, Kapila S, Lotz JC (2009) Pressure and distortion regulate human mesenchymal stem cell gene expression. Ann Biomed Eng 37 (3):492–502. https://doi.org/10.1007/s10439-008-9629-2

Haynesworth SE, Baber MA, Caplan AI (1996) Cytokine expression by human marrow-derived mesenchymal progenitor cells in vitro: effects of dexamethasone and IL-1 alpha. J Cell Physiol 166(3):585–592. https://doi.org/10.1002/(SICI)1097-4652(199603)166:3<585::AID-JCP13>3.0.CO;2-6

Hirt MN, Boeddinghaus J, Mitchell A, Schaaf S, Börnchen C, Müller C, Schulz H, Hubner N, Stenzig J, Stoehr A (2014) Functional improvement

and maturation of rat and human engineered heart tissue by chronic electrical stimulation. J Mol Cell Cardiol 74:151–161 %@ 0022-2828

Huangfu D, Maehr R, Guo W, Eijkelenboom A, Snitow M, Chen AE, Melton DA (2008a) Induction of pluripotent stem cells by defined factors is greatly improved by small-molecule compounds. Nat Biotechnol 26(7):795–797. https://doi.org/10.1038/nbt1418

Huangfu D, Osafune K, Maehr R, Guo W, Eijkelenboom A, Chen S, Muhlestein W, Melton DA (2008b) Induction of pluripotent stem cells from primary human fibroblasts with only Oct4 and Sox2. Nat Biotechnol 26(11):1269–1275. https://doi.org/10.1038/nbt.1502

Ichida JK, Blanchard J, Lam K, Son EY, Chung JE, Egli D, Loh KM, Carter AC, Di Giorgio FP, Koszka K (2009) A small-molecule inhibitor of Tgf-β signaling replaces Sox2 in reprogramming by inducing Nanog. Cell Stem Cell 5(5):491–503 %@ 1934-5909

Iyer SS, Rojas M (2008) Anti-inflammatory effects of mesenchymal stem cells: novel concept for future therapies. Expert Opin Biol Ther 8(5):569–581. https://doi.org/10.1517/14712598.8.5.569

Jin W, Takagi T, Kanesashi SN, Kurahashi T, Nomura T, Harada J, Ishii S (2006) Schnurri-2 controls BMP-dependent adipogenesis via interaction with Smad proteins. Dev Cell 10(4):461–471. https://doi.org/10.1016/j.devcel.2006.02.016

Johnson K, Zhu S, Tremblay MS, Payette JN, Wang J, Bouchez LC, Meeusen S, Althage A, Cho CY, Wu X, Schultz PG (2012) A stem cell-based approach to cartilage repair. Science 336(6082):717–721. https://doi.org/10.1126/science.1215157

Kang KS, Hong JM, Kang JA, Rhie JW, Cho DW (2013) Osteogenic differentiation of human adipose-derived stem cells can be accelerated by controlling the frequency of continuous ultrasound. J Ultrasound Med 32(8):1461–1470. https://doi.org/10.7863/ultra.32.8.1461

Kang ML, Ko JY, Kim JE, Im GI (2014) Intra-articular delivery of kartogenin-conjugated chitosan nano/microparticles for cartilage regeneration. Biomaterials 35(37):9984–9994. https://doi.org/10.1016/j.biomaterials.2014.08.042

Keung AJ, Kumar S, Schaffer DV (2010) Presentation counts: microenvironmental regulation of stem cells by biophysical and material cues. Annu Rev Cell Dev Biol 26:533–556. https://doi.org/10.1146/annurev-cellbio-100109-104042

Keung AJ, Asuri P, Kumar S, Schaffer DV (2012) Soft microenvironments promote the early neurogenic differentiation but not self-renewal of human pluripotent stem cells. Integr Biol 4(9):1049–1058

Kim BJ, Arai Y, Park EM, Park S, Bello AB, Han IB, Lee SH (2017) Osteogenic potential of tauroursodeoxycholic acid (TUDCA) as an alternative to rhBMP-2 in a mouse spinal fusion model. Tissue Eng Part A 24:407–417. https://doi.org/10.1089/ten.TEA.2016.0349

Kimbrel EA, Lanza R (2015) Current status of pluripotent stem cells: moving the first therapies to the clinic. Nat Rev Drug Discov 14(10):681–692. https://doi.org/10.1038/nrd4738

Kingham E, White K, Gadegaard N, Dalby MJ, Oreffo RO (2013) Nanotopographical cues augment mesenchymal differentiation of human embryonic stem cells. Small 9(12):2140–2151. https://doi.org/10.1002/smll.201202340

Krencik R, Weick JP, Liu Y, Zhang ZJ, Zhang SC (2011) Specification of transplantable astroglial subtypes from human pluripotent stem cells. Nat Biotechnol 29(6):528–534. https://doi.org/10.1038/nbt.1877

Kushibiki T, Awazu K (2009) Blue laser irradiation enhances extracellular calcification of primary mesenchymal stem cells. Photomed Laser Surg 27(3):493–498. https://doi.org/10.1089/pho.2008.2343

Kwon D, Kim J-S, Cha B-H, Park K-S, Han I, Park K-S, Bae H, Han M-K, Kim K-S, Lee S-H (2016) The effect of fetal bovine serum (FBS) on efficacy of cellular reprogramming for induced pluripotent stem cell (iPSC) generation. Cell Transplant 25(6):1025–1042 %@ 0963-6897

Lapointe VL, Fernandes AT, Bell NC, Stellacci F, Stevens MM (2013) Nanoscale topography and chemistry affect embryonic stem cell self-renewal and early differentiation. Adv Healthc Mater 2(12):1644–1650. https://doi.org/10.1002/adhm.201200382

Lee J, Xia Y, Son MY, Jin G, Seol B, Kim MJ, Son MJ, Do M, Lee M, Kim D (2012) A novel small molecule facilitates the reprogramming of human somatic cells into a pluripotent state and supports the maintenance of an undifferentiated state of human pluripotent stem cells. Angew Chem Int Ed 51(50):12509–12513 %@ 1521-3773

Li J, Zhu L, Qu X, Li J, Lin R, Liao L, Wang J, Wang S, Xu Q, Zhao RC (2013) Stepwise differentiation of human adipose-derived mesenchymal stem cells toward definitive endoderm and pancreatic progenitor cells by mimicking pancreatic development in vivo. Stem Cells Dev 22(10):1576–1587. https://doi.org/10.1089/scd.2012.0148

Liao X, Xie GH, Liu HW, Cheng B, Li SH, Xie S, Xiao LL, Fu XB (2014) Helium-neon laser irradiation promotes the proliferation and migration of human epidermal stem cells in vitro: proposed mechanism for enhanced wound re-epithelialization. Photomed Laser Surg 32(4):219–225. https://doi.org/10.1089/pho.2013.3667

Lin T, Ambasudhan R, Yuan X, Li W, Hilcove S, Abujarour R, Lin X, Hahm HS, Hao E, Hayek A, Ding S (2009) A chemical platform for improved induction of human iPSCs. Nat Methods 6(11):805–808. https://doi.org/10.1038/nmeth.1393

Liu YS, Lee OK (2014) In search of the pivot point of mechanotransduction: mechanosensing of stem cells.

Cell Transplant 23(1):1–11. https://doi.org/10.3727/096368912X659925

Lv Y, Zhao P, Chen G, Sha Y, Yang L (2013) Effects of low-intensity pulsed ultrasound on cell viability, proliferation and neural differentiation of induced pluripotent stem cells-derived neural crest stem cells. Biotechnol Lett 35(12):2201–2212. https://doi.org/10.1007/s10529-013-1313-4

McMurray RJ, Gadegaard N, Tsimbouri PM, Burgess KV, McNamara LE, Tare R, Murawski K, Kingham E, Oreffo RO, Dalby MJ (2011) Nanoscale surfaces for the long-term maintenance of mesenchymal stem cell phenotype and multipotency. Nat Mater 10 (8):637–644. https://doi.org/10.1038/nmat3058

Mikkelsen TS, Hanna J, Zhang X, Ku M, Wernig M, Schorderet P, Bernstein BE, Jaenisch R, Lander ES, Meissner A (2008) Dissecting direct reprogramming through integrative genomic analysis. Nature 454 (7200):49–55. https://doi.org/10.1038/nature07056

Murphy WL, McDevitt TC, Engler AJ (2014) Materials as stem cell regulators. Nat Mater 13(6):547–557 %@ 1476–1122

Muttigi MS, Kim B, Choi B, Yoshie A, Kumar H, Han I, Park H, Lee SH (2017) Matrilin-3 co-delivery with adipose-derived mesenchymal stem cells promotes articular cartilage regeneration in a rat osteochondral defect model. J Tissue Eng Regen Med 12:667. https://doi.org/10.1002/term.2485

Pachmann K, Leibold W (1976) Insolubilization of protein antigens on polyacrylic plastic beads using poly-L-lysine. J Immunol Methods 12(1–2):81–89 %@ 0022-1759

Pagliuca FW, Millman JR, Gurtler M, Segel M, Van Dervort A, Ryu JH, Peterson QP, Greiner D, Melton DA (2014) Generation of functional human pancreatic beta cells in vitro. Cell 159(2):428–439. https://doi.org/10.1016/j.cell.2014.09.040

Park S, Im GI (2015) Stem cell responses to nanotopography. J Biomed Mater Res A 103 (3):1238–1245. https://doi.org/10.1002/jbm.a.35236

Park KS, Cha KJ, Han IB, Shin DA, Cho DW, Lee SH, Kim DS (2012) Mass-producible nano-featured polystyrene surfaces for regulating the differentiation of human adipose-derived stem cells. Macromol Biosci 12(11):1480–1489. https://doi.org/10.1002/mabi.201200225

Park K-S, Ahn J, Kim JY, Park H, Kim HO, Lee S-H (2014) Poly-l-lysine increases the ex vivo expansion and erythroid differentiation of human hematopoietic stem cells, as well as erythroid enucleation efficacy. Tissue Eng A 20(5–6):1072–1080 %@ 1937-3341

Park HW, Kim YC, Yu B, Moroishi T, Mo J-S, Plouffe SW, Meng Z, Lin KC, Yu F-X, Alexander CM, Wang C-Y, Guan K-L (2015) Alternative Wnt signaling activates YAP/TAZ. Cell 162(4):780–794. https://doi.org/10.1016/j.cell.2015.07.013

Pires F, Ferreira Q, Rodrigues CA, Morgado J, Ferreira FC (2015) Neural stem cell differentiation by electrical stimulation using a cross-linked PEDOT substrate: expanding the use of biocompatible conjugated conductive polymers for neural tissue engineering. Biochim Biophys Acta 1850(6):1158–1168. https://doi.org/10.1016/j.bbagen.2015.01.020

Rao C, Prodromakis T, Kolker L, Chaudhry UA, Trantidou T, Sridhar A, Weekes C, Camelliti P, Harding SE, Darzi A, Yacoub MH, Athanasiou T, Terracciano CM (2013) The effect of microgrooved culture substrates on calcium cycling of cardiac myocytes derived from human induced pluripotent stem cells. Biomaterials 34(10):2399–2411. https://doi.org/10.1016/j.biomaterials.2012.11.055

Redmer T, Diecke S, Grigoryan T, Quiroga-Negreira A, Birchmeier W, Besser D (2011) E-cadherin is crucial for embryonic stem cell pluripotency and can replace OCT4 during somatic cell reprogramming. EMBO Rep 12(7):720–726 %@ 1469-221X

Reimer A, Vasilevich A, Hulshof F, Viswanathan P, van Blitterswijk CA, de Boer J, Watt FM (2016) Scalable topographies to support proliferation and Oct4 expression by human induced pluripotent stem cells. Sci Rep 6:18948. https://doi.org/10.1038/srep18948

Revel A (2009) Multitasking human endometrium: a review of endometrial biopsy as a diagnostic tool, therapeutic applications, and a source of adult stem cells. Obstet Gynecol Surv 64(4):249–257. https://doi.org/10.1097/OGX.0b013e318195136f

Rezania A, Bruin JE, Arora P, Rubin A, Batushansky I, Asadi A, O'Dwyer S, Quiskamp N, Mojibian M, Albrecht T, Yang YH, Johnson JD, Kieffer TJ (2014) Reversal of diabetes with insulin-producing cells derived in vitro from human pluripotent stem cells. Nat Biotechnol 32(11):1121–1133. https://doi.org/10.1038/nbt.3033

Saha K, Keung AJ, Irwin EF, Li Y, Little L, Schaffer DV, Healy KE (2008) Substrate modulus directs neural stem cell behavior. Biophys J 95(9):4426–4438. https://doi.org/10.1529/biophysj.108.132217

Sia J, Sun R, Chu J, Li S (2016) Dynamic culture improves cell reprogramming efficiency. Biomaterials 92:36–45. https://doi.org/10.1016/j.biomaterials.2016.03.033

Staerk J, Lyssiotis CA, Medeiro LA, Bollong M, Foreman RK, Zhu S, Garcia M, Gao Q, Bouchez LC, Lairson LL (2011) Pan-Src family kinase inhibitors replace Sox2 during the direct reprogramming of somatic cells. Angew Chem Int Ed 50(25):5734–5736 %@ 1521-3773

Sun J, Li J, Li C, Yu Y (2015) Role of bone morphogenetic protein-2 in osteogenic differentiation of mesenchymal stem cells. Mol Med Rep 12(3):4230–4237. https://doi.org/10.3892/mmr.2015.3954

Swift J, Ivanovska IL, Buxboim A, Harada T, Dingal PCDP, Pinter J, Pajerowski JD, Spinler KR, Shin

J-W, Tewari M (2013) Nuclear Lamin-a scales with tissue stiffness and enhances matrix-directed differentiation. Science 341(6149):1240104 %@ 0036-8075

Takahashi K, Yamanaka S (2006) Induction of pluripotent stem cells from mouse embryonic and adult fibroblast cultures by defined factors. Cell 126(4):663–676. https://doi.org/10.1016/j.cell.2006.07.024

Thrivikraman G, Madras G, Basu B (2014) Intermittent electrical stimuli for guidance of human mesenchymal stem cell lineage commitment towards neural-like cells on electroconductive substrates. Biomaterials 35 (24):6219–6235. https://doi.org/10.1016/j.biomaterials.2014.04.018

Vang S, Longley K, Steer CJ, Low WC (2014) The unexpected uses of Urso- and Tauroursodeoxycholic acid in the treatment of non-liver diseases. Glob Adv Health Med 3(3):58–69. https://doi.org/10.7453/gahmj.2014.017

Wang P-Y, Clements LR, Thissen H, Tsai W-B, Voelcker NH (2015) Screening rat mesenchymal stem cell attachment and differentiation on surface chemistries using plasma polymer gradients. Acta Biomater 11:58–67 %@ 1742-7061

Wanjare M, Agarwal N, Gerecht S (2015) Biomechanical strain induces elastin and collagen production in human pluripotent stem cell-derived vascular smooth muscle cells. Am J Physiol Cell Physiol 309(4):C271–C281. https://doi.org/10.1152/ajpcell.00366.2014

Yim EK, Pang SW, Leong KW (2007) Synthetic nanostructures inducing differentiation of human mesenchymal stem cells into neuronal lineage. Exp Cell Res 313(9):1820–1829. https://doi.org/10.1016/j.yexcr.2007.02.031

Yoon YM, Lee JH, Yun SP, Han YS, Yun CW, Lee HJ, Noh H, Lee SJ, Han HJ, Lee SH (2016) Tauroursodeoxycholic acid reduces ER stress by regulating of Akt-dependent cellular prion protein. Sci Rep 6:39838. https://doi.org/10.1038/srep39838

Young DA, Choi YS, Engler AJ, Christman KL (2013) Stimulation of adipogenesis of adult adipose-derived stem cells using substrates that mimic the stiffness of adipose tissue. Biomaterials 34(34):8581–8588 %@ 0142-9612

Zhang J, Wilson GF, Soerens AG, Koonce CH, Yu J, Palecek SP, Thomson JA, Kamp TJ (2009) Functional cardiomyocytes derived from human induced pluripotent stem cells. Circ Res 104(4):e30–e41. https://doi.org/10.1161/CIRCRESAHA.108.192237

Zhang X, Zara J, Siu RK, Ting K, Soo C (2010) The role of NELL-1, a growth factor associated with craniosynostosis, in promoting bone regeneration. J Dent Res 89 (9):865–878. https://doi.org/10.1177/0022034510376401

Zhang Y, Liang X, Lian Q, Tse HF (2013) Perspective and challenges of mesenchymal stem cells for cardiovascular regeneration. Expert Rev Cardiovasc Ther 11 (4):505–517. https://doi.org/10.1586/erc.13.5

Zhu L, Gomez-Duran A, Saretzki G, Jin S, Tilgner K, Melguizo-Sanchis D, Anyfantis G, Al-Aama J, Vallier L, Chinnery P, Lako M, Armstrong L (2016) The mitochondrial protein CHCHD2 primes the differentiation potential of human induced pluripotent stem cells to neuroectodermal lineages. J Cell Biol 215(2):187

Decellularized Tissue Matrix for Stem Cell and Tissue Engineering

10

Jung Seung Lee, Yi Sun Choi, and Seung-Woo Cho

10.1 Tissue-Derived Natural Scaffold: Decellularized Matrix

In the scope of tissue engineering and regenerative medicine, investigations of functional biomaterials and development of *in vivo*-like systems are essential to maximize the efficacy of tissue regeneration. Various extracellular matrix (ECM)-derived components and synthetic biomaterials have been utilized to construct tissue-mimicking scaffolds and provide tissue-like microenvironments for improved functionalities of cells (Hubbell 1995; O'brien 2011; Place et al. 2009). However, the complex structural interactions and biomolecular composition of native tissues cannot currently be reconstituted with combinations of available simple fabrication techniques.

To prepare functional scaffolds for successful tissue regeneration, decellularization of organs has been increasingly studied in the last few decades, using different types of xenogenic, allogenic, and autologous tissues (Gilbert et al. 2006). During decellularization through stepwise processes of physical, chemical, and enzymatic methods, most cells within the organ are removed, while the tissue-specific structures and functional biomolecules of the tissue ECM are retained, providing a tissue-specific microenvironment (Fig. 10.1) (Gilbert et al. 2006; Guyette et al. 2014). With the excellent biocompatibility of organ-derived natural materials, various types of cells such as primary cells and stem cells can be reseeded onto the decellularized matrix to fabricate tissue-engineered artificial organs, which show greatly enhanced cellular engraftment and tissue regeneration with improved functionalities compared to conventional scaffolds (Fig. 10.1) (Badylak et al. 2011). The biochemical microenvironment, based on the retained ECMs, glycoproteins, proteoglycans, and tissue-specific functional molecules and mechanical properties similar to those of native tissues, significantly enhanced the regenerative efficacy of the matrix and showed potential in therapeutic replacement of damaged tissues (Badylak et al. 2011; Ott et al. 2008; Reing et al. 2010). Importantly, removal of native cells could minimize immune rejection and immune-related issues, which facilitates the use of these biomaterials in regenerative medicine and further clinical applications (Gilbert et al. 2006).

10.2 Decellularized Matrix as a Functional Bioscaffold for Tissue Engineering

10.2.1 Blood Vessel

Replacement of diseased blood vessels is a common surgical treatment for treating coronary artery and peripheral vascular diseases

J. S. Lee · Y. S. Choi · S.-W. Cho (✉)
Department of Biotechnology, Yonsei University, Seoul, South Korea
e-mail: seungwoocho@yonsei.ac.kr

I. Noh (ed.), *Biomimetic Medical Materials*, Advances in Experimental Medicine and Biology 1064,
https://doi.org/10.1007/978-981-13-0445-3_10

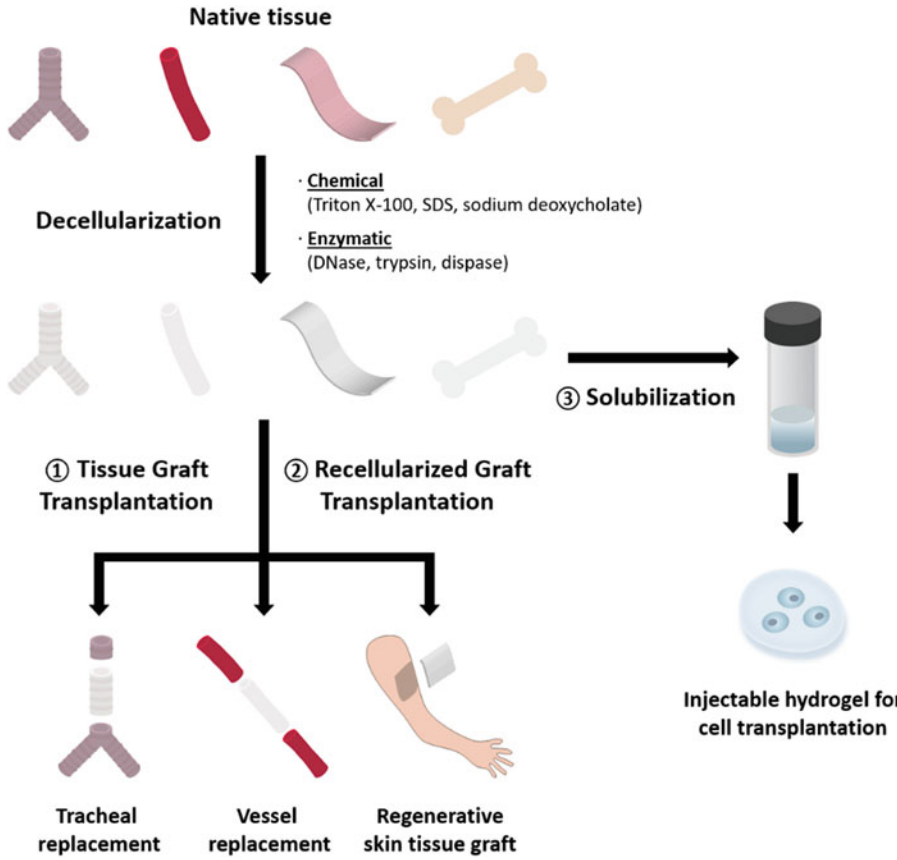

Fig. 10.1 Tissue-engineering strategy using the recellularization of various cell types into decellularized tissue matrices prepared with diverse chemical and enzymatic methodologies. Decellularized matrices from various tissues (e.g. blood vessel, intestine, bladder, skin, trachea, bone, tendon, and skeletal muscle) can be utilized as functional bioscaffolds for tissue regeneration. Solubilized decellularized matrices can be used as injectable hydrogels for cell transplantation

(e.g. atherosclerosis) (Chlupac et al. 2009). Although autologous vessels are a major candidate for bypass graft transplantation, proper vessels might not always be available and harvesting autologous vessels entails substantial surgical costs and complex procedures and causes secondary morbidity (Wilson et al. 1995). Therefore, artificial blood vessels comprised of natural or synthetic polymers have been developed over the last few decades (L'Heureux et al. 2006, 2007). However, these scaffolds usually fail to maintain functional vessels for long-term patency owing to restenosis and thrombosis after transplantation, especially for artificial vessels with diameters below 6 mm (Wilson et al. 1995).

Since the early 1990s, acellular tissue-engineered blood vessels have been highlighted as natural scaffolds for vessel replacement (Wilson et al. 1995; Kaushal et al. 2001; Cho et al. 2005a, 2006). ECM components in decellularized vessels, such as collagen, elastin, and glycosaminoglycan (GAG), can promote repopulation of endothelial cells and smooth muscle cells, resulting in functional vessel construction and host integration without thrombosis (Kaushal et al. 2001). Decellularized vessels can be acquired from various arteries and veins, including carotid arteries (Cho et al. 2005b), iliac arteries (Kaushal et al. 2001), umbilical arteries (Gui et al. 2009), saphenous veins

(Schaner et al. 2004), inferior vena cava (Cho et al. 2005a; Bertanha et al. 2014a; Lee et al. 2014), and jugular veins (Lee et al. 2014). Decellularization of the native vessel includes diverse ionic (e.g. sodium dodecyl sulfate [SDS], deoxycholate) (Gui et al. 2009; Schaner et al. 2004) or non-ionic (e.g. Triton X-100) detergents (Kaushal et al. 2001), and enzymatic (e.g. trypsin, RNase, DNase) treatments (Wilson et al. 1995; Kaushal et al. 2001). Among them, the Triton X-100-based mild chemical procedure has been generally adopted to remove cellular components and retain similar structural integrity, mechanical properties, and ECM components of the native vessel (Samouillan et al. 1999).

For successful fabrication of tissue-engineered blood vessels, rapid endothelialization and host integration with the endothelium and smooth muscle layers are essential for reducing the possibility of restenosis and subsequent graft failure. Diverse cell types have been seeded onto the matrix to potentiate functionality and long-term patency of the artificial decellularized vessels. Stem cells, having the potential to differentiate into endothelial cells, have been considered an ideal candidate to construct the endothelium, which is important for physiological functions involved in inhibiting inflammation, thrombosis, and restenosis after transplantation (Kaushal et al. 2001). For example, endothelial progenitor cells (EPCs) were isolated from peripheral blood and seeded inside the lumen of the decellularized vessel for preconditioning of the graft. The confluent monolayer of EPCs on the decellularized vessel graft greatly extended *in vivo* patency with physiological functionalities (Kaushal et al. 2001; Quint et al. 2011). Smooth muscle cells (SMCs) play major roles in the medial layer of the vessel as supporting cells in the mechanical and physiological functions of native blood vessels (Dora 2001). Thus, several studies coseeded SMCs with ECs and showed significantly enhanced *in vivo* maturation and contractile functionality of the engineered vessel graft (Yazdani et al. 2009; Neff et al. 2011). In addition, bone marrow-derived cells (Cho et al. 2005a) and mesenchymal stem cells (MSCs) (Zhao et al. 2010; Bertanha et al. 2014b) were differentiated into EC-like cells or SMC-like cells and used in reconstruction of endothelium and vessel grafts, resulting in improved long-term patency.

10.2.2 Small Intestine

Decellularized small intestinal submucosa (SIS) is one of the most widely studied decellularized ECM scaffolds. SIS is a thin layer of intestinal tissue that supports the mucosa and joins it to the muscularis propria layer. With the high content of collagens and structural integrity of the decellularized SIS, it has been mostly used as a transplantable natural scaffold for clinical applications (Hodde 2002; Badylak 1993). Indeed, SIS has been used in treating patients requiring blood vessel replacement, bladder reconstruction, dural repair, tendon and ligament substitute, and chronic wound healing (Huynh et al. 1999; Franklin et al. 2002; Badylak et al. 1989, 1999, 2002; Prevel et al. 1995; Cheng and Kropp 2000; Cobb et al. 1999). Other popular clinical usages of SIS scaffolds include reconstruction of urinary bladder (Misseri et al. 2005; Caione et al. 2006), urethra (Jones et al. 2005), diaphragm (Oelschlager et al. 2003), and integument (MacLeod et al. 2004; Zhang et al. 2003). In earlier studies, the whole small intestine tissue section was examined for implantable biomaterial usage. However, having all the layers in the small intestine appeared to be too enzymatically active for clinical uses, especially in wound treatments. Subsequent studies involved examination of the various layers of the small intestine, and it was concluded that the layer consisting solely of the submucosa was the most suitable for implantation usage (Brown-Etris et al. 2002). The submucosal layer appears to be the best option in terms of biofunctionality for transplantation because of its high content of fibroblast growth factor (FGF), transforming growth factor-beta (TGF-β), and collagens (Badylak et al. 1989; Badylak 2004). Not only do the factors induce rapid regeneration of the submucosal layer, but the fibrous collagen network in the layer also gives mechanical strength to the whole intestine.

There are various methods to produce completely decellularized intestine, that include physical, chemical, and enzymatic methods (Luo et al. 2011; Syed et al. 2014; Oliveira et al. 2013), but generally, decellularized SIS does not need complex decellularization steps to remove all cellular and nuclear materials because it already contains relatively few, if any, connective tissue cells. In most cases, mechanical force has been used to delaminate the layers of the small intestine, and the extent of the force used is enough to separate the SIS layer from the small intestine with minimal disruption to the three-dimensional (3D) ECM structures. Despite the relative lack of cellular materials to start with, additional chemical methods including treatments with Triton X-100, peracetic acid, and deoxycholate have been used in many studies to ensure that there are no immune responses upon transplantation (Wu et al. 2011; Totonelli et al. 2012).

For cell therapeutic purposes, stem cells have been used as a cell source for SIS transplantation, since stem cells can differentiate and contribute to the regeneration of the intestinal epithelium. It has been reported that adult stem cells such as human MSCs, including bone-marrow derived cells, can repair the damaged intestinal epithelium (Patil et al. 2013). Other studies for reconstruction of urethral tissue involve the isolation of human MSCs from voided urine that can differentiate into multiple bladder cell lineages (Wu et al. 2011). Urine-derived stem cells and smooth muscle cells could be seeded onto SIS scaffolds to mimic urethral tissues for transplantation.

10.2.3 Bladder

The urinary bladder is a hollow muscular sac where urine is contained until it is evacuated from the body by the parasympathetic nervous system. Spinal cord injury can affect the activity of the urinary bladder and cause bladder dysfunction, eventually leading to urinary tract infections, which significantly affects the quality of life of the patient. The conventional treatment for repairing a damaged urinary bladder involves partial or complete replacement of the bladder with gastrointestinal segments (Kropp et al. 2004). Upon transplantation, several issues can arise, such as metabolic disturbances, increased mucus production, and malignant tissue formation (Soergel et al. 2004). Owing to these problems, more attempts have been made to approach urinary bladder treatment from a tissue engineering perspective. Synthetic materials such as polyvinyl sponge (Kudish 1957) or collagen matrices (Monsour et al. 1987) had been used in experimental and clinical settings, but they usually failed to generate functional bladders due to their lack of biocompatibility and insufficient layer formation of bladder tissues. Since decellularization is an efficient method to produce bioscaffolds for regeneration of diverse organs, an acellular bladder matrix has also been considered for the repair and regeneration of urinary bladder. Bladder augmentation using decellularized matrix has been proposed to improve the function of neurogenic bladder (Obara et al. 2006; Urakami et al. 2007).

The decellularization protocols for the bladder included sodium deoxycholate (Obara et al. 2006; Urakami et al. 2007), Triton X-100 with ammonium hydroxide (Consolo et al. 2016), sodium azide (Sievert et al. 2006), SDS (Youssif et al. 2005), and RNase/DNase treatments (Reddy et al. 2000). Most studies also involved physical lamination and removal of the muscular and serosal layers prior to the chemical and enzymatic procedures to facilitate the later steps (Youssif et al. 2005; Davis et al. 2011). The studies that optimized the protocol to remove almost all the cellular contents while preserving the ECM structural architecture and growth factors combined lamination of the layers and SDS solution treatment (Youssif et al. 2005; Rosario et al. 2008). This method enhanced the reseeding and proliferation of urothelial and bladder stromal cells.

When the decellularized bladder matrix is used without reseeding, it augments the bladder to induce the formation of the urothelial layer (Brown et al. 2002). In other studies that used a seeded matrix of the bladder, urothelial cells are used for the patients needing bladder augmentation (Yoo et al. 1998). For the treatment of patients with bladder cancer, alternative cell

sources such as stem cells are a candidate because the patient's own stem cells can be used to generate more specialized bladder tissue. The stem cells for recellularization of the bladder matrix include bone marrow-derived mesenchymal stem cells (BMMSCs) (Chung et al. 2005), bone marrow-derived endothelial progenitor cells (Chen et al. 2011), adipose-derived stem cells (ADSCs) (Zhu et al. 2010), or amniotic fluid-derived stem cells (De Coppi et al. 2007). It has been shown that the decellularized bladder matrix can provide the cells with an environment suitable to promote cell migration, growth, and differentiation. Therefore, decellularization methods hold a great deal of promise for bladder repair.

10.2.4 Skin

Skin is the largest organ in vertebrates, playing roles as a mechanical barrier against pathogens and excessive water loss, as well as an insulator for temperature moderation. Despite the large advancements in regenerative medicine, treating skin disorders and injuries with fully functional skin tissues has faced substantial limitations. Although autologous dermis transplantation is a popular therapeutic for skin regeneration, development of bioscaffolds that can be applied immediately after severe injuries such as burns is essential to reduce lethality and minimize issues regarding shortages of skin replacement, especially for skin reconstruction of large-scale, full-thickness injuries. Earlier studies developed skin scaffolds from natural polymers and synthetic biodegradable polymers (Eaglstein and Falanga 1997). However, synthetic materials appeared to have poor biocompatibility and low mechanical strength to resist wound contraction (Ono et al. 1999). Moreover, large scale skin defects arising from surgery, acute trauma, chronic wounds, cancer, or vascular disease require skin transplantation, which cannot be accomplished solely with conventional synthetic scaffolds (Ruszczak 2003). Thus, a bioengineered acellular dermal matrix has been the next desirable candidate for skin substitutes.

Recent studies have presented several methods for producing natural matrices derived from decellularized skin tissue (Chen et al. 2004; Hoganson et al. 2010). They demonstrated successful decellularization methods that exhibited low antigenicity, excellent structural integrity, and comparable functional performances to native skin. For eliminating cells from dense skin tissue, SDS (Wainwright 1995; Livesey et al. 1995) and Triton X-100 treatments along with other enzymes such as dispase (Takami et al. 1996) have been employed. The process of skin decellularization usually requires more than just one treatment and takes much longer than the conventional decellularization protocols for other organs due to high collagen density of skin tissue.

Decellularized skin scaffolds are not only useful in skin reconstruction, but also in reconstruction of several other body parts including the esophagus (Bozuk et al. 2006) and urinary tract (Kimuli et al. 2004). To further promote skin regeneration and efficient structural reconstruction of thick skin tissue by decellularized matrices, cell reseeding has also been explored. There have been several studies that utilize ADSCs, a widely investigated stem cell type in regenerative medicine, to enhance wound healing using decellularized skin tissues (Nie et al. 2009; Huang et al. 2012; Altman et al. 2008). The decellularized dermal matrix can act as a functional biomaterial platform to promote ADSC differentiation or as a delivery vehicle to carry stem cells capable of secreting angiogenic factors to the injured sites for accelerated wound healing. Autologous BMMSCs (Zhao et al. 2012) and keratinocyte-like cells differentiated from ADSCs (Chavez-Munoz et al. 2013) have also been used to reconstruct skin tissues using a decellularized skin matrix.

10.2.5 Trachea

Trachea, a cartilaginous airway is one of the most well-studied tissues in regards to engineering concepts based on decellularization techniques. Malignant tracheal injuries often require tissue resection and artificial trachea implantation,

especially when the removed length exceeds 30% of the native trachea (Macchiarini et al. 2008). Therefore, tubular scaffolds made of various biocompatible natural and synthetic polymers have been utilized for the fabrication of tissue-engineered tracheae and successful tracheal replacement (Jungebluth et al. 2011; Grillo 2002). However, anatomical complications and exposure to external pathogens usually induce immune reaction, inflammation, and subsequent restenosis, leading to failures in long-term patency (Grillo 2002).

Therefore, a decellularized trachea has been investigated as an attractive natural scaffold for preparing a functional tissue construct and trachea replacement. Detergent-based (e.g. sodium deoxycholate, SDS, and Triton X-100) and enzymatic (e.g. DNase-I) decellularization methods were adopted to remove cellular components from native tracheal tissues (Macchiarini et al. 2008; Gray et al. 2012; Jungebluth et al. 2014). Generally, decellularization of tracheal tissue is a more time-consuming process compared to that for other organs due to difficulties in eliminating chondrocytes from the cartilaginous layer. However, repeated cycles of the process resulted in depletion of DNA content after decellularization, thus minimizing immune reactions. Decellularized trachea matrix scaffolds successfully preserved trachea-specific 3D structures and ECM components such as collagen, laminin, and GAG, even after the decellularization process (Partington et al. 2013). Moreover, the decellularized trachea showed comparable mechanical properties to a native trachea (Jungebluth et al. 2014; Partington et al. 2013), which is a crucial factor for long-term maintenance and functionality after transplantation, although several studies employed chemical fixation methods for mechanical strength enhancement (Haag et al. 2012).

Decellularized trachea matrix was further engineered with stem cells to improve the efficacy of practical tracheal reconstruction. MSCs differentiated into the chondrogenic lineage (Gray et al. 2012; Go et al. 2010) were seeded or coseeded with epithelial cells on the decellularized matrix to facilitate trachea reconstruction, suggesting the regenerative potential of the engineered matrix. Stem cells are thought to participate directly in tissue regeneration for physiological functions, simultaneously withstanding the mechanical demands required for tracheal functions. A clinical trial using a tissue-engineered trachea was firstly attempted in a patient with end-stage tracheal disease in 2008 by engineering the decellularized matrix with autologous epithelial cells and MSC-derived chondrocytes (Macchiarini et al. 2008). Since then, several clinical applications have also been performed and successful regeneration of the trachea was confirmed in several clinically relevant follow-up studies (Gonfiotti et al. 2014; Jungebluth and Macchiarini 2014). However, the need for additional stent insertions and initial side effects including immune reactions, inflammation, and partial stenosis also occurred in many cases. Therefore, to be accepted as a universal treatment for tracheal reconstruction, decellularized trachea matrix-based approaches need to be further studied in terms of improving host integration without restenosis and satisfying mechanical properties for long-term patency.

10.2.6 Bone

Unlike most tissues in the body, bone is a hard connective tissue made up of different osteogenic lineage cells such as osteoblasts, osteocytes, and osteoclasts and is usually dense with a honeycomb-like network. The hardness comes from the inorganic components of bone including calcium phosphate and calcium carbonate. The mineralization by these inorganic materials gives bone its strength and rigidity (Clarke 2008; Kalfas 2001). One of the most common defects in bone is a bone fracture that occurs when excess force is applied or when osteoporosis lowers bone density. As the bone regeneration process takes a long time and the healing process is accompanied by swelling and pain in daily activities, bone substitutes or supports accelerating bone healing are greatly in demand (Burge et al. 2007).

The requirements for bone grafts include having the mechanical strength, chemical composition, and structural architecture that mimic natural bone. The bone graft must be strong and osteoinductive to generate fully functioning bone tissue. Lack of immunogenicity and biocompatibility are also key requirements for bone grafts, like any other biological grafts. To this end, inorganic materials such as hydroxyapatite (Bucholz et al. 1987, 1989) and calcium phosphate (Jarcho 1981) have been widely used as biomaterials that meet these criteria. Similar to other organs and tissues, decellularization strategy could be applied for generation of functional bone grafts. Since bone tissue has physically different features from other organs in terms of interconnectivity, permeability, and mechanical properties, decellularized bone matrix can provide multifaceted mimicry of the native bone tissue, which is rarely achieved by conventional scaffold systems. Several decellularization protocols using detergent containing Triton X-100 (Woods and Gratzer 2005), trypsin (Gerhardt et al. 2013), SDS (Grayson et al. 2008), or enzymes (Fröhlich et al. 2009) and hydrostatic pressure (Hashimoto et al. 2011) have been tested to decellularize bone tissue. In some studies, demineralization using hydrochloric acid (HCl) was used before decellularization, but this process might cause a reduction in active growth factors (e.g. bone morphogenetic proteins) (Pietrzak et al. 2011).

Owing to the osteogenic potential of decellularized bone matrix, several studies have reported that decellularized bone matrix indeed promotes proliferation and osteogenic differentiation of the seeded stem cells (Hashimoto et al. 2011; Lee et al. 2016; Datta et al. 2005). Decellularized bone scaffolds seeded with BMMSCs have shown successful bone regeneration after transplantation into defective calvarial bone (Lee et al. 2016). Other studies have involved culture of stem cells derived from adipose, dental pulp, and umbilical cord blood on decellularized bone ECM supplemented with growth factors to induce osteogenic differentiation for bone regeneration (Fröhlich et al. 2009; Paduano et al. 2016, 2017; Liu et al. 2010). To further expand the applicability and versatility of decellularized bone graft, recent work solubilized the matrix through enzymatic digestion to generate a hydrogel platform (Paduano et al. 2016; Sawkins et al. 2013). Osteogenic cells from calvaria or dental pulp were cultured on hydrogel made from decellularized bone matrix, significantly enhancing proliferation and odontogenic differentiation. These studies employed gelation of bone ECM, which demonstrated the advantages of using a decellularized bone matrix that could be formulated into various 3D scaffolds and used as a functional biomaterial for enhanced bone regeneration.

10.2.7 Tendon

Tendon is a tough, fibrous connective tissue that connects muscle to bone, usually requiring a high capacity for withstanding a large amount of force or tension during movement and exercise. In tendon tissue, collagen fibers allow tendons to resist tensile stress while proteoglycans give them the ability to resist compression. Tendons need to have sufficient elasticity to store energy for their function and thus control finer movements of the muscle at the same time. Since tendon tends to have a dense and intricate network of collagen and proteoglycans, repairing ruptured tendons is not an easy task (Clayton and Court-Brown 2008). There have been several candidates for tendon grafts including synthetic polymers such as poly (glycolic acid) (PGA), poly(lactic-co-glycolic acid) (PLGA), and polytetrafluoroethylene (PTFE) to provide biological functions as well as mechanical properties (Ouyang et al. 2003; Stoll et al. 2010); however, synthetic materials have shown poor performance in regards to biocompatibility, quality of regeneration, and mechanical durability (Chen et al. 2009).

The decellularization method for tendon repair has been a focus of research because of the naturally aligned, intricate construction of thick collagen and tendon ECMs. With various sources in body, tendon tissues from Achilles (Ko et al. 2016), neck (Ko et al. 2016), tibia (Lee et al. 2013a), flexor

(Youngstrom et al. 2013; Martinello et al. 2014), and diaphragm (Deeken et al. 2011) tendon have been decellularized through protocols involving freeze-thaw cycles (Youngstrom et al. 2013; Deeken et al. 2011) and the use of mechanical forces (Ingram et al. 2007) along with the aid of chemical treatments such as non-ionic detergent (e.g. Triton X-100), ionic detergent (e.g. SDS), and zwitterionic detergent (e.g. tributyl phosphate) (Ko et al. 2016; Deeken et al. 2011; Alberti et al. 2015). Importantly, the dense, aligned fibrous structures, mechanical properties, and stiffness of native tendon tissue could be preserved even after the decellularization, which are all essential for improved and prolonged tendon regeneration and function.

For recellularization of tendon scaffolds, stem cells such as BMMSCs, ADSCs, and tendon-derived stem cells that can differentiate into tenocytes can be used (Martinello et al. 2014; Ning et al. 2015; Yin et al. 2013). It was found that the intrinsic alignment of tendon ECMs preserved in the decellularized tendon scaffold could provide a sufficiently favorable microenvironment for enhancing cell distribution, proliferation, and tenogenic differentiation of stem cells. Other cell candidates also include mesenchymal stromal cells, tenocytes, and fibroblasts (Angelidis et al. 2010; Whitlock et al. 2013; Burk et al. 2013). For improving engraftment efficiency, supporting hydrogels can also be used during cellular repopulation into the decellularized tendon tissue (Martinello et al. 2014). In addition, bioreactors that can provide cyclic mechanical stress after cell seeding onto the decellularized tendons could contribute to better cellular orientation and mechanically stronger tendon regeneration (Angelidis et al. 2010).

10.2.8 Skeletal Muscle

Skeletal muscle is composed of bundles of muscle fibers that together function to generate forces to facilitate voluntary movement (Gans 1982). Even when muscle is damaged, the muscle can repair itself with the biochemical and biophysical cues provided by the ECMs (Hill et al. 2003); however, if the damage exceeds the self-healing capacity, the repair process mediated by ECMs is not efficient, and the lost muscle volume will be replaced with fibrotic scar tissue. Cell transplantation has been attempted to regenerate muscle tissue and restore functions of injured muscle, but cell therapy alone has shown rather marginal regenerative effects on muscle.

With the insufficient therapeutic functional restoration provided by cell transplantation, several synthetic (e.g. poly-ε-caprolactone [PCL]) (Chen et al. 2013) or natural (e.g. fibrin (Layman et al. 2010), gelatin (Layman et al. 2007), and alginate (Ruvinov et al. 2010) biomaterials have been used for treating muscular damage. However, due to immune rejection, low degradability of polymers, bioinertness, and lacking imitation of the natural ECMs, conventional biomaterials were not suitable for the efficient muscle regeneration. The ideal scaffold for addressing muscle damage should replace the native ECMs of musculofascial tissue, which is not an easy task to be accomplished with conventional methods. Therefore, recent studies have focused on using decellularized skeletal muscle tissue to guide skeletal muscle regeneration at the defect site. Decellularized muscle scaffolds are suitable for muscle tissue engineering because they are expected to provide proper biological and biophysical signals to guide differentiation and proliferation of muscle progenitor cells and myoblasts for skeletal muscle regeneration (Stern et al. 2009).

Different approaches for muscle decellularization have been explored using combinations of different treatments. These methods include detergent solutions containing Triton X-100 (Stern et al. 2009; Gillies et al. 2010; Wang et al. 2013; Wolf et al. 2012), SDS (Hurd et al. 2015; Perniconi et al. 2011; DeQuach et al. 2010; Merritt et al. 2010a), or sodium deoxycholate (Wolf et al. 2012), along with other enzymatic treatments involving DNase

(Gillies et al. 2010) and trypsin/ethylenediaminetetraacetic acid (EDTA) (Porzionato et al. 2015). These methods for muscle tissue decellularization successfully removed cellular components from native muscle tissue, while retaining muscle ECMs (e.g. collagens, fibronectin, and laminin), growth factors, and GAG components with the intact muscular architectures providing cell-to-matrix interactions (Stern et al. 2009; Gillies et al. 2010; Wang et al. 2013; Wolf et al. 2012).

Decellularized muscle scaffolds can be engineered by culturing cells on the matrix to improve regeneration efficiency. There are usually two types of platforms on which the cells could be seeded. In earlier studies, most cells were seeded onto the decellularized muscle graft itself (Hurd et al. 2015; Perniconi et al. 2011). The cell candidates for muscle regeneration using decellularized muscle matrix include BMMSCs that can differentiate into muscle cells and induce functional recovery after full-thickness defects (Merritt et al. 2010b). Myoblasts, skeletal muscle stem cells, fibroblasts, and endothelial cells have also been used with decellularized muscle matrix in muscular remodeling (Wolf et al. 2012). However, more recent studies have utilized the biochemical properties of ECM from the decellularized matrix in the form of a hydrogel or surface coating instead of using the whole muscle scaffold; this approach gives the materials more benefits in terms of versatility and applicability (DeQuach et al. 2010, 2012; Ungerleider et al. 2015). Even in their solubilized form, the natural muscle-specific proteins, peptides, and proteoglycans, including heparin sulfate and decorin, could promote differentiation and maturation of the skeletal myoblasts (DeQuach et al. 2010). There have been numerous studies on injectable skeletal muscle matrix-based hydrogels that can induce proliferation of smooth muscle cells and skeletal myoblasts to improve neovascularization in hindlimb ischemia models (DeQuach et al. 2012) and in volumetric muscle loss injury models with the addition of MSCs (Merritt et al. 2010b).

10.3 Whole Organ Decellularization for Functional Organ Replacement

10.3.1 Heart

As one of the major causes of death, heart failure is a fatal disorder, especially for the many patients with end-stage heart disease. Whole heart transplantation has been considered the only treatment option, but donor shortages and immunological issues have substantially limited the application of this approach. Fabrication of functional heart tissue involves complicated issues in terms of mimicking complex structures with mechanical demands, diverse cellular populations, and physiological functions including heart beating.

In 2008, a perfusion-based whole organ decellularization technique was first suggested for the heart (Ott et al. 2008). For efficient decellularization, various detergent solutions containing SDS, Triton X-100, trypsin, and sodium deoxycholate were tested, and SDS has been proven to be an essential compound for successful decellularization of native heart tissue, though there were some differences in composition of the detergents and perfusion time among the species tested (Fig. 10.2) (Ott et al. 2008; Lu et al. 2013; Kitahara et al. 2016; Oberwallner et al. 2014). When detergent is perfused through the coronary artery, most cellular components, lipids and soluble factors were removed after several days of the decellularization process, but structural ECMs, such as collagens, laminin, and fibronectin, were preserved to provide the proper microenvironment for heart tissue (Ott et al. 2008; Maher 2013). Recently, Kitahara *et al.* reported a shorter method for preparing whole decellularized porcine heart tissue that is suitable for clinical applications, which would minimize loss of biofunctional molecules in native cardiac tissue and side effects induced by residual DNA contents (Kitahara et al. 2016). More importantly, the cardiac-specific 3D architecture that supports persistent contractions and relaxations during circulation was maintained without any distortion or collapse. Although substantial advances have

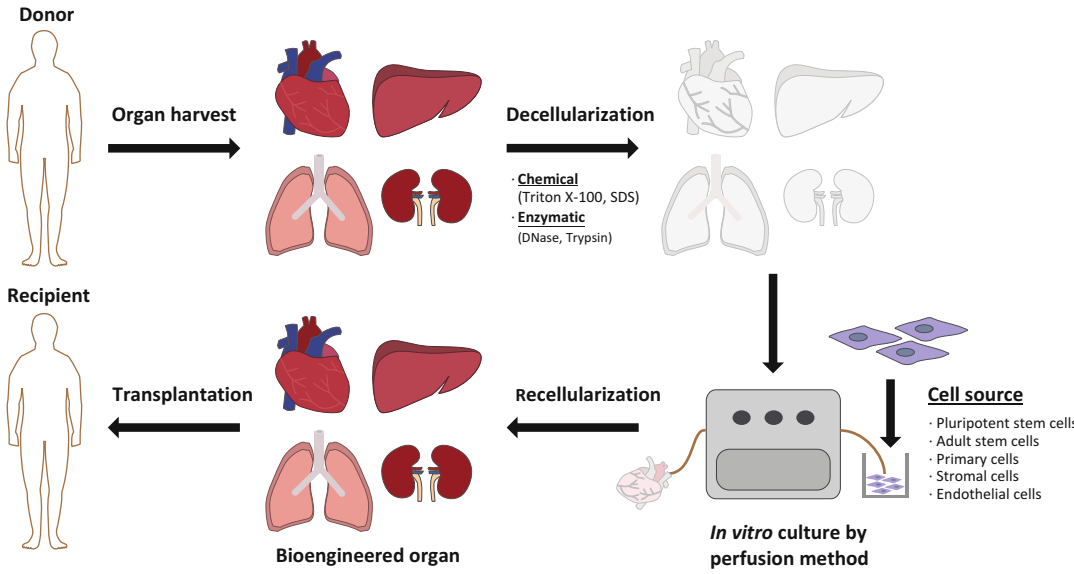

Fig. 10.2 Construction of transplantable bioengineered organs via whole organ decellularization and subsequent recellularization through perfusion-based cell seeding methods. Whole organs (e.g. heart, liver, kidney, and lung) from donors can be decellularized using detergents and recellularized with various cell types to reconstitute native organs with the native circulatory system

been made in whole heart decellularization since the first success in rat heart tissue (Ott et al. 2008), fabricating fully functional whole hearts using decellularized matrix is still a challenging task. To scale-up for human use, the process of removing cells while preserving the biochemical microenvironment and mechanical/structural properties of native cardiac tissue needs to be further optimized. Moreover, functional cell incorporation into the matrix needs to be achieved for physiological functioning of the regenerated heart tissue.

Recellularization using neonatal cardiac cells and endothelial cells resulted in contracting and functional cardiac tissues (Ott et al. 2008). Later, induced pluripotent stem cell (iPSC)-derived cardiovascular progenitor cells were also used in repopulating the decellularized heart (Lu et al. 2013). The progenitor cells were distributed throughout the whole decellularized heart via a perfusion seeding method and efficiently differentiated into cardiomyocytes, smooth muscle cells, and endothelial cells within histologically relevant regions of the decellularized matrix, resulting in spontaneous contractions of the engineered heart tissue (Fig. 10.2). With the potential to differentiate into myogenic lineages, adult stem cells such as BMMSCs and cord blood-derived mesenchymal stem cells (CBMSCs) have also been exploited as promising cell sources for reconstructing a functional heart using a decellularized heart matrix (Kitahara et al. 2016; Oberwallner et al. 2014; Eitan et al. 2009; Wang et al. 2010).

10.3.2 Liver

The liver is one of the largest organs with integral functions in metabolism, detoxification, and biosynthesis of various proteins. The liver can be damaged by various innate or acquired conditions such as genetic abnormality, viral infection, and alcoholic liver cirrhosis, but proper therapies to treat patients with end-stage liver diseases have not been developed as an alternative to orthotopic liver transplantation (Lee and Cho 2012). However, substantial shortages of donor livers and

immune reactions have limited the practical application of liver transplantations to replace damaged livers. Moreover, as the liver is one of the most highly vascularized and largest organs in our body, previous tissue-engineering scaffolds could not generate the complex and interconnected vascular pathways in liver tissue. Perfusion-based decellularization techniques using whole liver tissue have provided insight into solving the hurdles of liver transplantation. In 2010, a whole organ decellularization technique was used in the fabrication of an artificial liver construct in a rat model (Uygun et al. 2010). Perfusion of an SDS-based detergent solution successfully removed cellular components while retaining the hepatic sinusoidal structural ECM components (e.g. collagen type IV and fibronectin) and basement membranous ECM components of the native liver (e.g. laminin-β1). Along with liver tissue-derived ECM components, the retained GAGs and proteoglycans play important roles in improving hepatic functions of the cultured cells, as well as mechanical support of the matrix (Stuart and Panitch 2008). Other decellularizing detergents that have been used include Triton X-100, sodium deoxycholate, and chelating agents such as EDTA and ethylene glycol tetraacetic acid (EGTA). Importantly, decellularized liver tissue contains intact and interconnected vasculature structures in the matrix even after the cell removal process, which is crucial in reconstructing blood circulation for oxygen transfer and nutrient supply for the cells in the whole matrix.

To develop a functional artificial liver construct, various cell types composing native liver tissues were seeded into the decellularized liver matrix. Primary hepatocytes, stem cell-derived hepatocyte-like cells, liver progenitor cells, and hepatic satellite cells were seeded to endow the inherent functionality of the liver such as protein synthesis, urea metabolism, detoxification, and enzymatic activity (Uygun et al. 2010; Soto-Gutierrez et al. 2011; Mazza et al. 2015; Wang et al. 2014). Endothelial cells were also coseeded with hepatocytes to reconstruct physiologically durable vasculature and reduce thrombosis (Baptista et al. 2011). Establishing proper cell seeding methods is another issue for artificial liver construction because of the large volume of tissue matrix and difficulties in evenly distributing the seeded cells throughout whole decellularized matrix (Baptista et al. 2011; Faulk et al. 2015). Multiple cell perfusion via the portal vein has shown efficient cellular engraftment of over 90% of the infused cells compared to other less efficient approaches including direct parenchymal injection or continuous perfusion method (Uygun et al. 2010; Soto-Gutierrez et al. 2011). For constructing a functional bioengineered liver with a decellularized liver matrix, vasculature modifications using antibodies have also been utilized to improve re-endothelialization after cell seeding (Ko et al. 2015). Recently, enzymatically solubilized whole decellularized liver matrix was used in preparing different formats of liver-specific scaffolds for functionally improved hepatocyte culture and transplantation, which has broadened the utility of decellularized liver matrices (Lee et al. 2013b).

10.3.3 Kidney

The kidney filters the blood to make urine for the purpose of removing waste and nitrogen from the body. Despite this important role of the kidney, the number of patients who suffer from chronic renal diseases increases every year with approximately 30 million patients in the United States alone (Stats F 2017). In the case of end-stage renal disease, chronic dialysis or kidney transplantation is indispensable for survival of the patients. Even with the accelerated development of dialysis systems, kidney transplantation is often the ultimate curative treatment for end-stage patients. However, the number of kidney donors is insufficient to meet the demand. It is a devastating fact that after kidney transplantation, the recipients often suffer from acute rejection. Thus, tissue-engineering approaches for functional artificial kidney construction appear to be a necessary alternative to renal transplantation.

In the early conception of tissue engineering a kidney, an extracorporeal device using a

hemofiltration cartridge was developed as an artificial renal tubule (Humes et al. 2002). Cells with endocrine activity were grown along the inner surface of the cartridge. However, it seemed that a more functional bioscaffold is required for the growth and functions of renal cells or precursor cells in order to replace kidney functions in the long term. Therefore, since 2009, decellularization of the whole kidney has started to be considered for artificial kidney reconstruction (Ross et al. 2009). The whole decellularized kidney matrix can retain its naturally occurring renal architectures and ECM structures for the glomerulus and renal tubule including the abundant growth factors and vasculature to promote cell engraftment and renal regeneration (Ross et al. 2009; Song et al. 2013; Caralt et al. 2015).

The first approach to kidney regeneration using decellularization was reported in 2009, in which the whole rat kidney was decellularized so that pluripotent murine embryonic stem cells could be repopulated in the scaffold (Ross et al. 2009). Later, decellularized kidneys from other species have also been investigated for generation of renal ECM scaffolds, including porcine (Song et al. 2013; Batchelder et al. 2015; Sullivan et al. 2012), monkey (Nakayama et al. 2010), and human (Song et al. 2013). To obtain decellularized whole kidney scaffolds, several treatments can be applied, including SDS (Caralt et al. 2015; Batchelder et al. 2015; Nakayama et al. 2010; McKee and Wingert 2016; Wang et al. 2015), Triton X-100 (Caralt et al. 2015; Nakayama et al. 2010; McKee and Wingert 2016; Wang et al. 2015), trypsin (Caralt et al. 2015), and DNase (Sullivan et al. 2012) or combinations of these treatments. In general, SDS and Triton X-100 are the mostly widely adopted methods to remove cellular components from renal tissue.

Functional renal regeneration requires recellularization with various cells into the 3D ECM architectures of the decellularized kidney tissues. Conventionally, cells are seeded through renal arterial perfusion so that they can be distributed throughout the matrix by the native circulatory system (Song et al. 2013; McKee and Wingert 2016). Diverse cell candidates have been tested to repopulate the kidney matrix, and stem cells are regarded as an ideal cell source for kidney regeneration in terms of immune tolerance and differentiation capacity. Stem cells could differentiate into cell types for renal regeneration such as endothelial cells or renal progenitor cells (Caralt et al. 2015; Bonandrini et al. 2014). Embryonic stem cells (ESCs) have been used to repopulate the decellularized kidney matrix since they can differentiate into renal lineage cells. It appeared that renal ECM scaffolds can sufficiently induce renal differentiation of ESCs without the addition of other factors (Ross et al. 2009). It was also reported that the 3D ECM architectures of the decellularized kidney matrix influences not only cell morphology, adhesion, migration, and proliferation, but also the differentiation of the infused ESCs into the meso-endodermal lineage and renal progenitors (Bonandrini et al. 2014). Endothelial cells derived from iPSCs were also utilized for constructing functional renal tissue using decellularized kidney matrix (Song et al. 2013; Caralt et al. 2015; Du et al. 2016). The endothelial cells successfully repopulated the vasculature in the kidney matrix and formed tubules with metabolic activity.

10.3.4 Lung

The lung is one of the major organs of the body involved with the respiratory system for gas exchange. As the lung directly comes into contact with the outside atmosphere containing various toxic materials such as viruses, dust, and air pollutants, it is prone to various diseases, including pneumonia, lung cancer, asthma, and cystic fibrosis (Schoene 1999). In severe cases, partial or whole lung transplantation is the only clinical option for patients, but the organ shortages and immune rejection are issues with lung transplantation like with other organs. Therefore, biological scaffolds for lung reconstruction have been identified as an alternative to lung grafts. However, fabricating lung-specific structures such as alveoli and pulmonary capillaries, which are essential for gas exchange, has been a

challenge in constructing functional lung grafts for clinical applications.

Earlier studies of lung scaffolds dealt with a whole organ perfusion method for decellularization (Ott et al. 2010; Petersen et al. 2012). Decellularization using perfusion was preferred because the whole lung turns into a functional scaffold with intact alveolar and vascular networks and native ECM structures. In the whole lung perfusion method, detergent solutions are flowed into the organ via blood vessels so that the detergents can successfully remove all cellular components along the capillaries. Generally, chemical solutions such as Triton X-100, sodium deoxycholate, SDS, and 3-[(3-cholamidopropyl) dimethylammonio]-1-propanesulfonate (CHAPS) (Ott et al. 2010; Petersen et al. 2010, 2012; O'Neill et al. 2013) have been applied for lung decellularization. In another study, the lung was cut into smaller pieces for more efficient decellularization, while preserving the ECM components, microstructures, and mechanical properties intrinsic to the lung (O'Neill et al. 2013). The decellularized lungs are usually then reseeded with endothelial cells and pulmonary epithelial cells prior to transplantation into the recipient.

The cell sources for lung grafts include ESCs (Longmire et al. 2012), BMMSCs, and ADSCs (Mendez et al. 2014; Bonvillain et al. 2012) that can differentiate into the cell types needed to reconstitute lung tissues, which includes lung progenitor cells and airway epithelial cells. iPSCs, another type of pluripotent stem cells reprogrammed from somatic cells, have also been used to recellularize the decellularized lung scaffolds (Gilpin et al. 2014; Ren et al. 2015). Ren et al. reported that iPSCs reseeded onto a decellularized lung scaffold differentiated into endothelial and perivascular cells, which opened up a new possibility to advance decellularization techniques to vascularized organs with a larger scale (Ren et al. 2015). Other cell sources for recellularization include human umbilical vein endothelial cells, fetal lung cells (Ott et al. 2010), and lung epithelial cells (Petersen et al. 2010). However, the issue of ensuring that specific cell types settle at desired locations during recellularization still remains, which is mainly due to technical difficulties in cell seeding and localization.

References

Alberti KA, Sun J-Y, Illeperuma WR, Suo Z, Xu Q (2015) Laminar tendon composites with enhanced mechanical properties. J Mater Sci 50(6):2616–2625

Altman AM, Matthias N, Yan Y, Song Y-H, Bai X, Chiu ES, Slakey DP, Alt EU (2008) Dermal matrix as a carrier for in vivo delivery of human adipose-derived stem cells. Biomaterials 29(10):1431–1442

Angelidis IK, Thorfinn J, Connolly ID, Lindsey D, Pham HM, Chang J (2010) Tissue engineering of flexor tendons: the effect of a tissue bioreactor on adipoderived stem cell–seeded and fibroblast-seeded tendon constructs. J Hand Surg 35(9):1466–1472

Badylak SF (1993) Small intestinal submucosa (SIS): a biomaterial conducive to smart tissue remodeling. Tissue Eng: Springer, 179–189

Badylak SF (2004) Xenogeneic extracellular matrix as a scaffold for tissue reconstruction. Transpl Immunol 12 (3):367–377

Badylak SF, Lantz GC, Coffey A, Geddes LA (1989) Small intestinal submucosa as a large diameter vascular graft in the dog. J Surg Res 47(1):74–80

Badylak S, Arnoczky S, Plouhar P, Haut R, Mendenhall V, Clarke R, Horvath C (1999) Naturally occurring extracellular matrix as a scaffold for musculoskeletal repair. Clin Orthop Relat Res 367:S333–S343

Badylak S, Kokini K, Tullius B, Simmons-Byrd A, Morff R (2002) Morphologic study of small intestinal submucosa as a body wall repair device. J Surg Res 103 (2):190–202

Badylak SF, Taylor D, Uygun K (2011) Whole-organ tissue engineering: decellularization and recellularization of three-dimensional matrix scaffolds. Annu Rev Biomed Eng 13:27–53

Baptista PM, Siddiqui MM, Lozier G, Rodriguez SR, Atala A, Soker S (2011) The use of whole organ decellularization for the generation of a vascularized liver organoid. Hepatology 53(2):604–617

Batchelder CA, Martinez ML, Tarantal AF (2015) Natural scaffolds for renal differentiation of human embryonic stem cells for kidney tissue engineering. PLoS One 10 (12):e0143849

Bertanha M, Moroz A, Jaldin RG, Silva RA, Rinaldi JC, Golim MA, Felisbino SL, Domingues MA, Sobreira ML, Reis PP (2014a) Morphofunctional characterization of decellularized vena cava as tissue engineering scaffolds. Exp Cell Res 326(1):103–111

Bertanha M, Moroz A, Almeida R, Alves FC, Valério MJA, Moura R, Domingues MAC, Sobreira ML, Deffune E (2014b) Tissue-engineered blood vessel substitute by reconstruction of endothelium using mesenchymal stem cells induced by platelet growth factors. J Vasc Surg 59(6):1677–1685

Bonandrini B, Figliuzzi M, Papadimou E, Morigi M, Perico N, Casiraghi F, Sangalli F, Conti S, Benigni A, Remuzzi A (2014) Recellularization of well-preserved acellular kidney scaffold using embryonic stem cells. Tissue Eng A 20(9-10):1486–1498

Bonvillain RW, Danchuk S, Sullivan DE, Betancourt AM, Semon JA, Eagle ME, Mayeux JP, Gregory AN, Wang G, Townley IK (2012) A nonhuman primate model of lung regeneration: detergent-mediated decellularization and initial in vitro recellularization with mesenchymal stem cells. Tissue Eng A 18 (23-24):2437–2452

Bozuk MI, Fearing NM, Leggett PL (2006) Use of decellularized human skin to repair esophageal anastomotic leak in humans. JSLS 10(1):83

Brown A, Farhat W, Merguerian P, Wilson G, Khoury A, Woodhouse K (2002) 22 week assessment of bladder acellular matrix as a bladder augmentation material in a porcine model. Biomaterials 23(10):2179–2190

Brown-Etris M, Cutshall WD, Hiles MC (2002) A new biomaterial derived from small intestine submucosa and developed into a wound matrix device. Wounds 14(4):150–166

Bucholz RW, Carlton A, Holmes RE (1987) Hydroxyapatite and tricalcium phosphate bone graft substitutes. Orthop Clin N Am 18(2):323–334

Bucholz RW, Carlton A, Holmes R (1989) Interporous hydroxyapatite as a bone graft substitute in tibial plateau fractures. Clin Orthop Relat Res 240:53–62

Burge R, Dawson-Hughes B, Solomon DH, Wong JB, King A, Tosteson A (2007) Incidence and economic burden of osteoporosis-related fractures in the United States, 2005–2025. J Bone Miner Res 22(3):465–475

Burk J, Erbe I, Berner D, Kacza J, Kasper C, Pfeiffer B, Winter K, Brehm W (2013) Freeze-thaw cycles enhance decellularization of large tendons. Tissue Eng Part C Methods 20(4):276–284

Caione P, Capozza N, Zavaglia D, Palombaro G, Boldrini R (2006) In vivo bladder regeneration using small intestinal submucosa: experimental study. Pediatr Surg Int 22(7):593–599

Caralt M, Uzarski JS, Iacob S, Obergfell KP, Berg N, Bijonowski BM, Kiefer KM, Ward HH, Wandinger-Ness A, Miller WM (2015) Optimization and critical evaluation of decellularization strategies to develop renal extracellular matrix scaffolds as biological templates for organ engineering and transplantation. Am J Transplant 15(1):64–75

Chavez-Munoz C, Nguyen KT, Xu W, Hong S-J, Mustoe TA, Galiano RD (2013) Transdifferentiation of adipose-derived stem cells into keratinocyte-like cells: engineering a stratified epidermis. PLoS One 8 (12):e80587

Chen R-N, Ho H-O, Tsai Y-T, Sheu M-T (2004) Process development of an acellular dermal matrix (ADM) for biomedical applications. Biomaterials 25 (13):2679–2686

Chen J, Xu J, Wang A, Zheng M (2009) Scaffolds for tendon and ligament repair: review of the efficacy of commercial products. Expert Rev Med Devices 6 (1):61–73

Chen B-S, Xie H, Zhang S-L, Geng H-Q, Zhou J-M, Pan J, Chen F (2011) Tissue engineering of bladder using vascular endothelial growth factor gene-modified endothelial progenitor cells. Int J Artif Organs 34 (12):1137–1146

Chen M-C, Sun Y-C, Chen Y-H (2013) Electrically conductive nanofibers with highly oriented structures and their potential application in skeletal muscle tissue engineering. Acta Biomater 9(3):5562–5572

Cheng EY, Kropp BP (2000) Urologic tissue engineering with small-intestinal submucosa: potential clinical applications. World J Urol 18(1):26–30

Chlupac J, Filova E, Bacakova L (2009) Blood vessel replacement: 50 years of development and tissue engineering paradigms in vascular surgery. Physiol Res 58: S119

Cho S-W, Park HJ, Ryu JH, Kim SH, Kim YH, Choi CY, Lee M-J, Kim J-S, Jang I-S, Kim D-I (2005a) Vascular patches tissue-engineered with autologous bone marrow-derived cells and decellularized tissue matrices. Biomaterials 26(14):1915–1924

Cho S-W, Lim SH, Kim I-K, Hong YS, Kim S-S, Yoo KJ, Park H-Y, Jang Y, Chang BC, Choi CY (2005b) Small-diameter blood vessels engineered with bone marrow–derived cells. Ann Surg 241(3):506

Cho SW, Lim JE, Chu HS, Hyun HJ, Choi CY, Hwang KC, Yoo KJ, Kim DI, Kim BS (2006) Enhancement of in vivo endothelialization of tissue-engineered vascular grafts by granulocyte colony-stimulating factor. J Biomed Mater Res A 76((2):252–263

Chung SY, Krivorov NP, Rausei V, Thomas L, Frantzen M, Landsittel D, Kang YM, Chon CH, Ng CS, Fuchs GJ (2005) Bladder reconstitution with bone marrow derived stem cells seeded on small intestinal submucosa improves morphological and molecular composition. J Urol 174(1):353–359

Clarke B (2008) Normal bone anatomy and physiology. Clin J Am Soc Nephrol 3(Supplement 3):S131–S139

Clayton RA, Court-Brown CM (2008) The epidemiology of musculoskeletal tendinous and ligamentous injuries. Injury 39(12):1338–1344

Cobb MA, Badylak SF, Janas W, Simmons-Byrd A, Boop FA (1999) Porcine small intestinal submucosa as a dural substitute. Surg Neurol 51(1):99–104

Consolo F, Brizzola S, Tremolada G, Grieco V, Riva F, Acocella F, Fiore G, Soncini M (2016) A dynamic distention protocol for whole-organ bladder decellularization: histological and biomechanical characterization of the acellular matrix. J Tissue Eng Regen Med 10(2):E101–E112

Datta N, Holtorf HL, Sikavitsas VI, Jansen JA, Mikos AG (2005) Effect of bone extracellular matrix synthesized in vitro on the osteoblastic differentiation of marrow stromal cells. Biomaterials 26(9):971–977

Davis NF, Mooney R, Callanan A, Flood HD, McGloughlin TM (2011) Augmentation cystoplasty and extracellular matrix scaffolds: an ex vivo comparative study with autogenous detubularised ileum. PLoS One 6(5):e20323

De Coppi P, Callegari A, Chiavegato A, Gasparotto L, Piccoli M, Taiani J, Pozzobon M, Boldrin L, Okabe M, Cozzi E (2007) Amniotic fluid and bone marrow derived mesenchymal stem cells can be converted to smooth muscle cells in the cryo-injured rat bladder and prevent compensatory hypertrophy of surviving smooth muscle cells. J Urol 177(1):369–376

Deeken C, White A, Bachman S, Ramshaw B, Cleveland D, Loy T, Grant S (2011) Method of preparing a decellularized porcine tendon using tributyl phosphate. J Biomed Mater Res B Appl Biomater 96 ((2):199–206

DeQuach JA, Mezzano V, Miglani A, Lange S, Keller GM, Sheikh F, Christman KL (2010) Simple and high yielding method for preparing tissue specific extracellular matrix coatings for cell culture. PLoS One 5(9):e13039

DeQuach JA, Lin JE, Cam C, Hu D, Salvatore MA, Sheikh F, Christman KL (2012) Injectable skeletal muscle matrix hydrogel promotes neovascularization and muscle cell infiltration in a hindlimb ischemia model. Eur Cells Mater 23:400

Dora KA (2001) Cell-cell communication in the vessel wall. Vasc Med 6(1):43–50

Du C, Narayanan K, Leong MF, Ibrahim MS, Chua YP, Khoo VMH, Wan AC (2016) Functional kidney bioengineering with pluripotent stem-cell-derived renal progenitor cells and decellularized kidney scaffolds. Adv Healthcare Mater 5(16):2080–2091

Eaglstein WH, Falanga V (1997) Tissue engineering and the development of Apligraf®, a human skin equivalent. Clin Ther 19(5):894–905

Eitan Y, Sarig U, Dahan N, Machluf M (2009) Acellular cardiac extracellular matrix as a scaffold for tissue engineering: in vitro cell support, remodeling, and biocompatibility. Tissue Eng Part C Methods 16 (4):671–683

Faulk DM, Wildemann JD, Badylak SF (2015) Decellularization and cell seeding of whole liver biologic scaffolds composed of extracellular matrix. J Clin Exp Hepatol 5(1):69–80

Franklin M, Gonzalez J, Michaelson R, Glass J, Chock D (2002) Preliminary experience with new bioactive prosthetic material for repair of hernias in infected fields. Hernia 6(4):171–174

Fröhlich M, Grayson WL, Marolt D, Gimble JM, Kregar-Velikonja N, Vunjak-Novakovic G (2009) Bone grafts engineered from human adipose-derived stem cells in perfusion bioreactor culture. Tissue Eng A 16 (1):179–189

Gans C (1982) Fiber architecture and muscle function. Exerc Sport Sci Rev 10(1):160–207

Gerhardt LC, Widdows KL, Erol MM, Nandakumar A, Roqan IS, Ansari T, Boccaccini AR (2013) Neocellularization and neovascularization of nanosized bioactive glass-coated decellularized trabecular bone scaffolds. J Biomed Mater Res A 101((3):827–841

Gilbert TW, Sellaro TL, Badylak SF (2006) Decellularization of tissues and organs. Biomaterials 27(19):3675–3683

Gillies AR, Smith LR, Lieber RL, Varghese S (2010) Method for decellularizing skeletal muscle without detergents or proteolytic enzymes. Tissue Eng Part C Methods 17(4):383–389

Gilpin SE, Ren X, Okamoto T, Guyette JP, Mou H, Rajagopal J, Mathisen DJ, Vacanti JP, Ott HC (2014) Enhanced lung epithelial specification of human induced pluripotent stem cells on decellularized lung matrix. Ann Thorac Surg 98(5):1721–1729

Go T, Jungebluth P, Baiguero S, Asnaghi A, Martorell J, Ostertag H, Mantero S, Birchall M, Bader A, Macchiarini P (2010) Both epithelial cells and mesenchymal stem cell–derived chondrocytes contribute to the survival of tissue-engineered airway transplants in pigs. J Thorac Cardiovasc Surg 139(2):437–443

Gonfiotti A, Jaus MO, Barale D, Baiguera S, Comin C, Lavorini F, Fontana G, Sibila O, Rombolà G, Jungebluth P (2014) The first tissue-engineered airway transplantation: 5-year follow-up results. Lancet 383 (9913):238–244

Gray FL, Turner CG, Ahmed A, Calvert CE, Zurakowski D, Fauza DO (2012) Prenatal tracheal reconstruction with a hybrid amniotic mesenchymal stem cells–engineered construct derived from decellularized airway. J Pediatr Surg 47(6):1072–1079

Grayson WL, Bhumiratana S, Cannizzaro C, Chao P-HG, Lennon DP, Caplan AI, Vunjak-Novakovic G (2008) Effects of initial seeding density and fluid perfusion rate on formation of tissue-engineered bone. Tissue Eng A 14(11):1809–1820

Grillo HC (2002) Tracheal replacement: a critical review. Ann Thorac Surg 73(6):1995–2004

Gui L, Muto A, Chan SA, Breuer CK, Niklason LE (2009) Development of decellularized human umbilical arteries as small-diameter vascular grafts. Tissue Eng A 15(9):2665–2676

Guyette JP, Gilpin SE, Charest JM, Tapias LF, Ren X, Ott HC (2014) Perfusion decellularization of whole organs. Nat Protoc 9(6):1451

Haag J, Baiguera S, Jungebluth P, Barale D, Del Gaudio C, Castiglione F, Bianco A, Comin CE, Ribatti D, Macchiarini P (2012) Biomechanical and angiogenic properties of tissue-engineered rat trachea using genipin cross-linked decellularized tissue. Biomaterials 33(3):780–789

Hashimoto Y, Funamoto S, Kimura T, Nam K, Fujisato T, Kishida A (2011) The effect of decellularized bone/bone marrow produced by high-hydrostatic pressurization on the osteogenic differentiation of mesenchymal stem cells. Biomaterials 32(29):7060–7067

Hill M, Wernig A, Goldspink G (2003) Muscle satellite (stem) cell activation during local tissue injury and repair. J Anat 203(1):89–99

Hodde J (2002) Naturally occurring scaffolds for soft tissue repair and regeneration. Tissue Eng 8 (2):295–308

Hoganson DM, O'Doherty EM, Owens GE, Harilal DO, Goldman SM, Bowley CM, Neville CM, Kronengold RT, Vacanti JP (2010) The retention of extracellular matrix proteins and angiogenic and mitogenic cytokines in a decellularized porcine dermis. Biomaterials 31(26):6730–6737

Huang S-P, Hsu C-C, Chang S-C, Wang C-H, Deng S-C, Dai N-T, Chen T-M, Chan JY-H, Chen S-G, Huang S-M (2012) Adipose-derived stem cells seeded on acellular dermal matrix grafts enhance wound healing in a murine model of a full-thickness defect. Ann Plast Surg 69(6):656–662

Hubbell JA (1995) Biomaterials in tissue engineering. Nat Biotechnol 13(6):565–576

Humes HD, Fissell WH, Weitzel WF, Buffington DA, Westover AJ, MacKay SM, Gutierrez JM (2002) Metabolic replacement of kidney function in uremic animals with a bioartificial kidney containing human cells. Am J Kidney Dis 39(5):1078–1087

Hurd SA, Bhatti NM, Walker AM, Kasukonis BM, Wolchok JC (2015) Development of a biological scaffold engineered using the extracellular matrix secreted by skeletal muscle cells. Biomaterials 49:9–17

Huynh T, Abraham G, Murray J, Brockbank K, Hagen P-O, Sullivan S (1999) Remodeling of an acellular collagen graft into a physiologically responsive neovessel. Nat Biotechnol 17(11):1083–1086

Ingram JH, Korossis S, Howling G, Fisher J, Ingham E (2007) The use of ultrasonication to aid recellularization of acellular natural tissue scaffolds for use in anterior cruciate ligament reconstruction. Tissue Eng 13(7):1561–1572

Jarcho M (1981) Calcium phosphate ceramics as hard tissue prosthetics. Clin Orthop Relat Res 157:259–278

Jones JS, Rackley RR, Berglund R, Abdelmalak JB, Deorco G, Vasavada SP (2005) Porcine small intestinal submucosa as a percutaneous mid-urethral sling: 2-year results. BJU Int 96(1):103–106

Jungebluth P, Macchiarini P (2014) Airway transplantation. Thorac Surg Clin 24(1):97–106

Jungebluth P, Alici E, Baiguera S, Blomberg P, Bozóky B, Crowley C, Einarsson O, Gudbjartsson T, Le Guyader S, Henriksson G (2011) Tracheobronchial transplantation with a stem-cell-seeded bioartificial nanocomposite: a proof-of-concept study. Lancet 378 (9808):1997–2004

Jungebluth P, Haag JC, Sjöqvist S, Gustafsson Y, Rodríguez AB, Del Gaudio C, Bianco A, Dehnisch I, Uhlén P, Baiguera S (2014) Tracheal tissue engineering in rats. Nat Protoc 9(9):2164–2179

Kalfas IH (2001) Principles of bone healing. Neurosurg Focus 10(4):1–4

Kaushal S, Amiel GE, Guleserian KJ, Shapira OM, Perry T, Sutherland FW, Rabkin E, Moran AM, Schoen FJ, Atala A (2001) Functional small-diameter neovessels created using endothelial progenitor cells expanded ex vivo. Nat Med 7(9):1035–1040

Kimuli M, Eardley I, Southgate J (2004) In vitro assessment of decellularized porcine dermis as a matrix for urinary tract reconstruction. BJU Int 94(6):859–866

Kitahara H, Yagi H, Tajima K, Okamoto K, Yoshitake A, Aeba R, Kudo M, Kashima I, Kawaguchi S, Hirano A (2016) Heterotopic transplantation of a decellularized and recellularized whole porcine heart. Interact Cardiovasc Thorac Surg 22(5):571–579

Ko IK, Peng L, Peloso A, Smith CJ, Dhal A, Deegan DB, Zimmerman C, Clouse C, Zhao W, Shupe TD (2015) Bioengineered transplantable porcine livers with re-endothelialized vasculature. Biomaterials 40:72–79

Ko E, Alberti K, Lee JS, Yang K, Jin Y, Shin J, Yang HS, Xu Q, Cho S-W (2016) Nanostructured tendon-derived scaffolds for enhanced bone regeneration by human adipose-derived stem cells. ACS Appl Mater Interfaces 8(35):22819–22829

Kropp BP, Cheng EY, Lin H-k, Zhang Y (2004) Reliable and reproducible bladder regeneration using unseeded distal small intestinal submucosa. J Urol 172 ((4):1710–1713

Kudish HG (1957) The use of polyvinyl sponge for experimental cystoplasty. J Urol 78(3):232–235

L'Heureux N, Dusserre N, Konig G, Victor B, Keire P, Wight TN, Chronos NA, Kyles AE, Gregory CR, Hoyt G (2006) Human Tissue Engineered Blood Vessel For Adult Arterial Revascularization. Nat Med 12(3):361

L'Heureux N, McAllister TN, de la Fuente LM (2007) Tissue-engineered blood vessel for adult arterial revascularization. N Engl J Med 357(14):1451–1453

Layman H, Spiga M-G, Brooks T, Pham S, Webster KA, Andreopoulos FM (2007) The effect of the controlled release of basic fibroblast growth factor from ionic gelatin-based hydrogels on angiogenesis in a murine critical limb ischemic model. Biomaterials 28 (16):2646–2654

Layman H, Rahnemai-Azar AA, Pham SM, Tsechpenakis G, Andreopoulos FM (2010) Synergistic angiogenic effect of codelivering fibroblast growth factor 2 and granulocyte-colony stimulating factor from fibrin scaffolds and bone marrow transplantation in critical limb ischemia. Tissue Eng A 17 (1-2):243–254

Lee JS, Cho S-W (2012) Liver tissue engineering: Recent advances in the development of a bio-artificial liver. Biotechnol Bioprocess Eng 17(3):427–438

Lee KI, Lee JS, Kim JG, Kang KT, Jang JW, Shim YB, Moon SH (2013a) Mechanical properties of decellularized tendon cultured by cyclic straining bioreactor. J Biomed Mater Res A 101(11):3152–3158

Lee JS, Shin J, Park H-M, Kim Y-G, Kim B-G, Oh J-W, Cho S-W (2013b) Liver extracellular matrix providing dual functions of two-dimensional substrate coating and three-dimensional injectable hydrogel platform for liver tissue engineering. Biomacromolecules 15 (1):206–218

Lee JS, Lee K, Moon SH, Chung HM, Lee JH, Um SH, Kim DI, Cho SW (2014) Mussel-inspired cell-adhesion peptide modification for enhanced endothelialization of decellularized blood vessels. Macromol Biosci 14(8):1181–1189

Lee DJ, Diachina S, Lee YT, Zhao L, Zou R, Tang N, Han H, Chen X, Ko C-C (2016) Decellularized bone matrix grafts for calvaria regeneration. J Tissue Eng 7:2041731416680306

Liu G, Li Y, Sun J, Zhou H, Zhang W, Cui L, Cao Y (2010) In vitro and in vivo evaluation of osteogenesis of human umbilical cord blood-derived mesenchymal stem cells on partially demineralized bone matrix. Tissue Eng A 16(3):971–982

Livesey SA, Herndon DN, Hollyoak MA, Atkinson YH, Nag A (1995) Transplanted acellular allograft dermal matrix: potential as a template for the reconstruction of viable dermis. Transplantation 60(1):1–9

Longmire TA, Ikonomou L, Hawkins F, Christodoulou C, Cao Y, Jean J, Kwok LW, Mou H, Rajagopal J, Shen SS (2012) Efficient derivation of purified lung and thyroid progenitors from embryonic stem cells. Cell Stem Cell 10(4):398–411

Lu T-Y, Lin B, Kim J, Sullivan M, Tobita K, Salama G, Yang L (2013) Repopulation of decellularized mouse heart with human induced pluripotent stem cell-derived cardiovascular progenitor cells. Nat Commun 4:2307

Luo J-C, Chen W, Chen X-H, Qin T-W, Huang Y-C, Xie H-Q, Li X-Q, Qian Z-Y, Yang Z-M (2011) A multi-step method for preparation of porcine small intestinal submucosa (SIS). Biomaterials 32(3):706–713

Macchiarini P, Jungebluth P, Go T, Asnaghi MA, Rees LE, Cogan TA, Dodson A, Martorell J, Bellini S, Parnigotto PP (2008) Clinical transplantation of a tissue-engineered airway. Lancet 372 (9655):2023–2030

MacLeod T, Sarathchandra P, Williams G, Sanders R, Green C (2004) Evaluation of a porcine origin acellular dermal matrix and small intestinal submucosa as dermal replacements in preventing secondary skin graft contraction. Burns 30(5):431–437

Maher B (2013) How to build a heart. Nature 499 (7456):20

Martinello T, Bronzini I, Volpin A, Vindigni V, Maccatrozzo L, Caporale G, Bassetto F, Patruno M (2014) Successful recellularization of human tendon scaffolds using adipose-derived mesenchymal stem cells and collagen gel. J Tissue Eng Regen Med 8 (8):612–619

Mazza G, Rombouts K, Hall AR, Urbani L, Luong TV, Al-Akkad W, Longato L, Brown D, Maghsoudlou P, Dhillon AP (2015) Decellularized human liver as a natural 3D-scaffold for liver bioengineering and transplantation. Sci Rep 5:13079

McKee RA, Wingert RA (2016) Repopulating decellularized kidney scaffolds: an avenue for ex vivo organ generation. Materials 9(3):190

Mendez JJ, Ghaedi M, Steinbacher D, Niklason LE (2014) Epithelial cell differentiation of human mesenchymal stromal cells in decellularized lung scaffolds. Tissue Eng A 20(11-12):1735–1746

Merritt EK, Hammers DW, Tierney M, Suggs LJ, Walters TJ, Farrar RP (2010a) Functional assessment of skeletal muscle regeneration utilizing homologous extracellular matrix as scaffolding. Tissue Eng A 16 (4):1395–1405

Merritt EK, Cannon MV, Hammers DW, Le LN, Gokhale R, Sarathy A, Song TJ, Tierney MT, Suggs LJ, Walters TJ (2010b) Repair of traumatic skeletal muscle injury with bone-marrow-derived mesenchymal stem cells seeded on extracellular matrix. Tissue Eng A 16(9):2871–2881

Misseri R, Cain MP, Casale AJ, Kaefer M, Meldrum KK, Rink RC (2005) Small intestinal submucosa bladder neck slings for incontinence associated with neuropathic bladder. J Urol 174(4):1680–1682

Monsour M, Mohammed R, Gorham S, French D, Scott R (1987) An assessment of a collagen/vicryl composite membrane to repair defects of the urinary bladder in rabbits. Urol Res 15(4):235–238

Nakayama KH, Batchelder CA, Lee CI, Tarantal AF (2010) Decellularized rhesus monkey kidney as a three-dimensional scaffold for renal tissue engineering. Tissue Eng A 16(7):2207–2216

Neff LP, Tillman BW, Yazdani SK, Machingal MA, Yoo JJ, Soker S, Bernish BW, Geary RL, Christ GJ (2011) Vascular Smooth muscle enhances functionality of tissue-engineered blood vessels in vivo. J Vasc Surg 53(2):426–434

Nie C, Yang D, Morris SF (2009) Local delivery of adipose-derived stem cells via acellular dermal matrix as a scaffold: a new promising strategy to accelerate wound healing. Med Hypotheses 72(6):679–682

Ning L-J, Zhang Y-J, Zhang Y, Qing Q, Jiang Y-L, Yang J-L, Luo J-C, Qin T-W (2015) The utilization of decellularized tendon slices to provide an inductive microenvironment for the proliferation and tenogenic differentiation of stem cells. Biomaterials 52:539–550

O'brien FJ (2011) Biomaterials & scaffolds for tissue engineering. Mater Today 14(3):88–95

O'Neill JD, Anfang R, Anandappa A, Costa J, Javidfar J, Wobma HM, Singh G, Freytes DO, Bacchetta MD, Sonett JR (2013) Decellularization of human and porcine lung tissues for pulmonary tissue engineering. Ann Thorac Surg 96(3):1046–1056

Obara T, Matsuura S, Narita S, Satoh S, Tsuchiya N, Habuchi T (2006) Bladder acellular matrix grafting regenerates urinary bladder in the spinal cord injury rat. Urology 68(4):892–897

Oberwallner B, Brodarac A, Choi YH, Saric T, Anić P, Morawietz L, Stamm C (2014) Preparation of cardiac extracellular matrix scaffolds by decellularization of human myocardium. J Biomed Mater Res A 102 (9):3263–3272

Oelschlager BK, Barreca M, Chang L, Pellegrini CA (2003) The use of small intestine submucosa in the repair of paraesophageal hernias: initial observations of a new technique. Am J Surg 186(1):4–8

Oliveira AC, Garzón I, Ionescu AM, Carriel V, de la Cruz Cardona J, González-Andrades M, del Mar Pérez M, Alaminos M, Campos A (2013) Evaluation of small intestine grafts decellularization methods for corneal tissue engineering. PLoS One 8(6):e66538

Ono I, Tateshita T, Inoue M (1999) Effects of a collagen matrix containing basic fibroblast growth factor on wound contraction. J Biomed Mater Res A 48 (5):621–630

Ott HC, Matthiesen TS, Goh S-K, Black LD, Kren SM, Netoff TI, Taylor DA (2008) Perfusion-decellularized matrix: using nature's platform to engineer a bioartificial heart. Nat Med 14(2):213–221

Ott HC, Clippinger B, Conrad C, Schuetz C, Pomerantseva I, Ikonomou L, Kotton D, Vacanti JP (2010) Regeneration and orthotopic transplantation of a bioartificial lung. Nat Med 16(8):927–933

Ouyang HW, Goh JC, Thambyah A, Teoh SH, Lee EH (2003) Knitted poly-lactide-co-glycolide scaffold loaded with bone marrow stromal cells in repair and regeneration of rabbit Achilles tendon. Tissue Eng 9 (3):431–439

Paduano F, Marrelli M, White LJ, Shakesheff KM, Tatullo M (2016) Odontogenic differentiation of human dental pulp stem cells on hydrogel scaffolds derived from decellularized bone extracellular matrix and collagen type I. PLoS One 11(2):e0148225

Paduano F, Marrelli M, Alom N, Amer M, White LJ, Shakesheff KM, Tatullo M (2017) Decellularized bone extracellular matrix and human dental pulp stem cells as a construct for bone regeneration. J Biomater Sci Polym Ed 28(8):730–748

Partington L, Mordan N, Mason C, Knowles J, Kim H, Lowdell M, Birchall M, Wall I (2013) Biochemical changes caused by decellularization may compromise mechanical integrity of tracheal scaffolds. Acta Biomater 9(2):5251–5261

Patil PB, Chougule PB, Kumar VK, Almström S, Bäckdahl H, Banerjee D, Herlenius G, Olausson M, Sumitran-Holgersson S (2013) Recellularization of acellular human small intestine using bone marrow stem cells. Stem Cells Transl Med 2(4):307–315

Perniconi B, Costa A, Aulino P, Teodori L, Adamo S, Coletti D (2011) The pro-myogenic environment provided by whole organ scale acellular scaffolds from skeletal muscle. Biomaterials 32(31):7870–7882

Petersen TH, Calle EA, Zhao L, Lee EJ, Gui L, Raredon MB, Gavrilov K, Yi T, Zhuang ZW, Breuer C (2010) Tissue-engineered lungs for in vivo implantation. Science 329(5991):538–541

Petersen TH, Calle EA, Colehour MB, Niklason LE (2012) Matrix composition and mechanics of decellularized lung scaffolds. Cells Tissues Organs 195(3):222–231

Pietrzak WS, Ali SN, Chitturi D, Jacob M, Woodell-May JE (2011) BMP depletion occurs during prolonged acid demineralization of bone: characterization and implications for graft preparation. Cell Tissue Bank 12(2):81–88

Place ES, Evans ND, Stevens MM (2009) Complexity in biomaterials for tissue engineering. Nat Mater 8(6):457

Porzionato A, Sfriso MM, Pontini A, Macchi V, Petrelli L, Pavan PG, Natali AN, Bassetto F, Vindigni V, De Caro R (2015) Decellularized human skeletal muscle as biologic scaffold for reconstructive surgery. Int J Mol Sci 16(7):14808–14831

Prevel CD, Eppley BL, Summerlin D-J, Sidner R, Jackson JR, McCarty M, Badylak SF (1995) Small intestinal submucosa: utilization as a wound dressing in full-thickness rodent wounds. Ann Plast Surg 35 (4):381–388

Quint C, Kondo Y, Manson RJ, Lawson JH, Dardik A, Niklason LE (2011) Decellularized tissue-engineered blood vessel as an arterial conduit. Proc Natl Acad Sci 108(22):9214–9219

Reddy PP, Barrieras DJ, Wilson G, Bägli DJ, McLORIE GA, Khoury AE, Merguerian PA (2000) Regeneration of functional bladder substitutes using large segment acellular matrix allografts in a porcine model. J Urol 164(3:936–941

Reing JE, Brown BN, Daly KA, Freund JM, Gilbert TW, Hsiong SX, Huber A, Kullas KE, Tottey S, Wolf MT (2010) The effects of processing methods upon mechanical and biologic properties of porcine dermal extracellular matrix scaffolds. Biomaterials 31 (33):8626–8633

Ren X, Moser PT, Gilpin SE, Okamoto T, Wu T, Tapias LF, Mercier FE, Xiong L, Ghawi R, Scadden DT (2015) Engineering pulmonary vasculature in decellularized rat and human lungs. Nat Biotechnol 33(10):1097–1102

Rosario DJ, Reilly GC, Ali Salah E, Glover M, Bullock AJ, MacNeil S (2008) Decellularization and sterilization of porcine urinary bladder matrix for tissue engineering in the lower urinary tract. Regen Med 3 (2):145–146

Ross EA, Williams MJ, Hamazaki T, Terada N, Clapp WL, Adin C, Ellison GW, Jorgensen M, Batich CD (2009) Embryonic stem cells proliferate and differentiate when seeded into kidney scaffolds. J Am Soc Nephrol 20(11):2338–2347

Ruszczak Z (2003) Effect of collagen matrices on dermal wound healing. Adv Drug Deliv Rev 55 (12):1595–1611

Ruvinov E, Leor J, Cohen S (2010) The effects of controlled HGF delivery from an affinity-binding alginate biomaterial on angiogenesis and blood perfusion in a hindlimb ischemia model. Biomaterials 31 (16):4573–4582

Samouillan V, Dandurand-Lods J, Lamure A, Maurel E, Lacabanne C, Gerosa G, Venturini A, Casarotto D, Gherardini L, Spina M (1999) Thermal analysis characterization of aortic tissues for cardiac valve bioprostheses. J Biomed Mater Res 46(4):531–538

Sawkins M, Bowen W, Dhadda P, Markides H, Sidney L, Taylor A, Rose F, Badylak S, Shakesheff K, White L (2013) Hydrogels derived from demineralized and decellularized bone extracellular matrix. Acta Biomater 9(8):7865–7873

Schaner PJ, Martin ND, Tulenko TN, Shapiro IM, Tarola NA, Leichter RF, Carabasi RA, DiMuzio PJ (2004) Decellularized vein as a potential scaffold for vascular tissue engineering. J Vasc Surg 40(1):146–153

Schoene RB (1999) Lung disease at high altitude. Hypoxia: Springer, pp 47–56

Sievert K-D, Fandel T, Wefer J, Gleason CA, Nunes L, Dahiya R, Tanagho EA (2006) Collagen I: III ratio in canine heterologous bladder acellular matrix grafts. World J Urol 24(1):101–109

Soergel TM, Cain MP, Misseri R, Gardner TA, Koch MO, Rink RC (2004) Transitional cell carcinoma of the bladder following augmentation cystoplasty for the neuropathic bladder. J Urol 172((4):1649–1652

Song JJ, Guyette JP, Gilpin SE, Gonzalez G, Vacanti JP, Ott HC (2013) Regeneration and experimental orthotopic transplantation of a bioengineered kidney. Nat Med 19(5):646–651

Soto-Gutierrez A, Zhang L, Medberry C, Fukumitsu K, Faulk D, Jiang H, Reing J, Gramignoli R, Komori J, Ross M (2011) A whole-organ regenerative medicine approach for liver replacement. Tissue Eng Part C Methods 17(6):677–686

Stats F (2017) National Chronic Kidney Disease Fact Sheet

Stern MM, Myers RL, Hammam N, Stern KA, Eberli D, Kritchevsky SB, Soker S, Van Dyke M (2009) The influence of extracellular matrix derived from skeletal muscle tissue on the proliferation and differentiation of myogenic progenitor cells ex vivo. Biomaterials 30 (12):2393–2399

Stoll C, John T, Endres M, Rosen C, Kaps C, Kohl B, Sittinger M, Ertel W, Schulze-Tanzil G (2010) Extracellular matrix expression of human tenocytes in three-dimensional air–liquid and PLGA cultures compared with tendon tissue: Implications for tendon tissue engineering. J Orthop Res 28(9):1170–1177

Stuart K, Panitch A (2008) Influence of chondroitin sulfate on collagen gel structure and mechanical properties at physiologically relevant levels. Biopolymers 89 (10):841–851

Sullivan DC, Mirmalek-Sani S-H, Deegan DB, Baptista PM, Aboushwareb T, Atala A, Yoo JJ (2012) Decellularization methods of porcine kidneys for whole organ engineering using a high-throughput system. Biomaterials 33(31):7756–7764

Syed O, Walters NJ, Day RM, Kim H-W, Knowles JC (2014) Evaluation of decellularization protocols for production of tubular small intestine submucosa scaffolds for use in oesophageal tissue engineering. Acta Biomater 10(12):5043–5054

Takami Y, Matsuda T, Yoshitake M, Hanumadass M, Walter R (1996) Dispase/detergent treated dermal matrix as a dermal substitute. Burns 22(3):182–190

Totonelli G, Maghsoudlou P, Garriboli M, Riegler J, Orlando G, Burns AJ, Sebire NJ, Smith VV, Fishman JM, Ghionzoli M (2012) A rat decellularized small bowel scaffold that preserves villus-crypt architecture for intestinal regeneration. Biomaterials 33 (12):3401–3410

Ungerleider J, Johnson T, Rao N, Christman K (2015) Fabrication and characterization of injectable hydrogels derived from decellularized skeletal and cardiac muscle. Methods 84:53–59

Urakami S, Shiina H, Enokida H, Kawamoto K, Kikuno N, Fandel T, Vejdani K, Nunes L, Igawa M, Tanagho EA (2007) Functional improvement in spinal cord injury-induced neurogenic bladder by bladder augmentation using bladder acellular matrix graft in the rat. World J Urol 25(2):207–213

Uygun BE, Soto-Gutierrez A, Yagi H, Izamis M-L, Guzzardi MA, Shulman C, Milwid J, Kobayashi N, Tilles A, Berthiaume F (2010) Organ reengineering through development of a transplantable recellularized liver graft using decellularized liver matrix. Nat Med 16(7):814–820

Wainwright D (1995) Use of an acellular allograft dermal matrix (AlloDerm) in the management of full-thickness burns. Burns 21(4):243–248

Wang B, Borazjani A, Tahai M, de Jongh Curry AL, Simionescu DT, Guan J, To, F, Elder SH, Liao J (2010) Fabrication of cardiac patch with decellularized porcine myocardial scaffold and bone marrow mononuclear cells. J Biomed Mater Res A 94(4):1100–1110

Wang L, Johnson JA, Chang DW, Zhang Q (2013) Decellularized musculofascial extracellular matrix for tissue engineering. Biomaterials 34(11):2641–2654

Wang X, Cui J, Zhang BQ, Zhang H, Bi Y, Kang Q, Wang N, Bie P, Yang Z, Wang H (2014) Decellularized liver scaffolds effectively support the proliferation and differentiation of mouse fetal hepatic progenitors. J Biomed Mater Res A 102(4):1017–1025

Wang Y, Bao J, Wu Q, Zhou Y, Li Y, Wu X, Shi Y, Li L, Bu H (2015) Method for perfusion decellularization of porcine whole liver and kidney for use as a scaffold for clinical-scale bioengineering engrafts. Xenotransplantation 22(1):48–61

Whitlock P, Seyler T, Northam C, Smith T, Poehling G, Koman L, Van Dyke M (2013) Effect of cyclic strain on tensile properties of a naturally derived, decellularized tendon scaffold seeded with allogeneic tenocytes and associated messenger RNA expression. J Surg Orthop Adv 22(3):224–232

Wilson GJ, Courtman DW, Klement P, Lee JM, Yeger H (1995) Acellular matrix: a biomaterials approach for coronary artery bypass and heart valve replacement. Ann Thorac Surg 60:S353–S358

Wolf MT, Daly KA, Reing JE, Badylak SF (2012) Biologic scaffold composed of skeletal muscle extracellular matrix. Biomaterials 33(10):2916–2925

Woods T, Gratzer PF (2005) Effectiveness of three extraction techniques in the development of a decellularized bone–anterior cruciate ligament–bone graft. Biomaterials 26(35):7339–7349

Wu S, Liu Y, Bharadwaj S, Atala A, Zhang Y (2011) Human urine-derived stem cells seeded in a modified 3D porous small intestinal submucosa scaffold for urethral tissue engineering. Biomaterials 32 (5):1317–1326

Yazdani SK, Watts B, Machingal M, Jarajapu YP, Van Dyke ME, Christ GJ (2009) Smooth muscle cell seeding of decellularized scaffolds: the importance of bioreactor preconditioning to development of a more native architecture for tissue-engineered blood vessels. Tissue Eng A 15(4):827–840

Yin Z, Chen X, Zhu T, Hu J-j, Song H-x, Shen W-l, Jiang L-y, Heng BC, Ji J-f, Ouyang H-W (2013) The effect of decellularized matrices on human tendon stem/progenitor cell differentiation and tendon repair. Acta Biomater 9(12):9317–9329

Yoo JJ, Meng J, Oberpenning F, Atala A (1998) Bladder augmentation using allogenic bladder submucosa seeded with cells. Urology 51(2):221–225

Youngstrom DW, Barrett JG, Jose RR, Kaplan DL (2013) Functional characterization of detergent-decellularized equine tendon extracellular matrix for tissue engineering applications. PLoS One 8(5):e64151

Youssif M, Shiina H, Urakami S, Gleason C, Nunes L, Igawa M, Enokida H, Tanagho EA, Dahiya R (2005) Effect of vascular endothelial growth factor on regeneration of bladder acellular matrix graft: histologic and functional evaluation. Urology 66(1):201–207

Zhang F, Zhu C, Oswald T, Lei M-P, Lineaweaver WC (2003) Porcine small intestinal submucosa as a carrier for skin flap prefabrication. Ann Plast Surg 51 (5):488–492

Zhao Y, Zhang S, Zhou J, Wang J, Zhen M, Liu Y, Chen J, Qi Z (2010) The development of a tissue-engineered artery using decellularized scaffold and autologous ovine mesenchymal stem cells. Biomaterials 31 (2):296–307

Zhao Y, Zhang Z, Wang J, Yin P, Zhou J, Zhen M, Cui W, Xu G, Yang D, Liu Z (2012) Abdominal hernia repair with a decellularized dermal scaffold seeded with autologous bone marrow-derived mesenchymal stem cells. Artif Organs 36(3):247–255

Zhu W-d, Xu Y-m, Feng C, Fu Q, Song L-j, Cui L (2010) Bladder reconstruction with adipose-derived stem cell-seeded bladder acellular matrix grafts improve morphology composition. World J Urol 28(4):493–498

Biomaterials for Stem Cell Therapy for Cardiac Disease

11

Hyunbum Kim, Seung-Hyun L. Kim, Young-Hwan Choi, Young-Hyun Ahn, and Nathaniel S. Hwang

11.1 Cardiac Disease

11.1.1 Cardiovascular Disease

Worldwide, cardiovascular diseases are the most common cause of death (Joggerst and Hatzopoulos 2009). Globally it resulted up to 17.9 million deaths (32.1%) in 2015 from 12.3 million (25.8%) in 1990 and account for over 75% of CVD deaths in both males and females. Cardiovascular disease includes coronary artery diseases (CAD), for example, angina and myocardial infarction. The additional risk for CAD is that it is the strongest predictor of a future cardiovascular event. People who carried or still carries CAD, have composite risk scores of individuals future risk of cardiovascular disease, combined with several risk factors such as age, sex, smoking, blood pressure, and diabetes.

The goal of treating CAD so far is to maximize the patient's quantity and quality of life. Most importantly, prevention is the key to avoid cardiovascular disease. Ever since the plaque formation has begun, to limit its progression by maintaining a healthy lifestyle with routine exercise is possible. Also by delicately controlling one's blood pressure and cholesterol level is necessary.

11.1.2 Myocardial Infarction

One of the major contributors to the overall mortality risk of severe cardiovascular diseases is acute myocardial infarction (MI), simply known as heart attack. According to the United States Renal Data, approximately 20% of cardiac deaths are caused by MI patients. MI occurs when the flow of oxygen-rich blood to a section of heart muscle suddenly becomes blocked and the cardiomyocytes can't receive oxygen (Pedron et al. 2011). As a result, the portion of heart muscle, especially the left ventricle, fed by the artery begins to collapse. Because of cardiomyocytes lacks the intrinsic regenerative capability to replace the lost cells, myocyte slippage and fibroblast proliferation occur aggressively resulting in replacement of healthy heart tissue to dysfunctional scar tissue (Wang and Guan 2010). The limited oxygen transfer capability of the regenerated scar tissue results in ventricular wall thinning and chamber dilatation, causing congestive heart failure (Li and Guan 2011). Therefore, there is an excessive need for new treatment for the regeneration of dysfunctional heart tissue and reestablish the heart function.

H. Kim · S.-H. L. Kim · Y.-H. Choi · Y.-H. Ahn · N. S. Hwang (✉)
School of Chemical and Biological Engineering, Institute of Chemical Processes, Institute of Engineering Research, Seoul National University, Seoul, South Korea
e-mail: tiggerhy2@hotmail.com; lucy.kim619@snu.ac.kr; yghorse@naver.com; ayh015@snu.ac.kr; nshwang@snu.ac.kr

I. Noh (ed.), *Biomimetic Medical Materials*, Advances in Experimental Medicine and Biology 1064,
https://doi.org/10.1007/978-981-13-0445-3_11

For current clinical treatment of MI, surgical transplantation and synthetic implants, such as artery bypass grafting, has been used to restore the heart function. These strategies serve as mechanical aids such as left ventricular assist devices, which have been shown therapeutic effects at restoring heart function or slowing down the progression of the disease for several years, which improved the quality of life of a patient (Yost et al. 2004; Menasche et al. 2008; Venugopal et al. 2012). However, these approaches are not always effective when it comes to long-term therapy. The limited lifespan, malfunction of transplanted implants and shortage of donors are concerned. Due to the limitations, alternative therapies are needed (Mukherjee et al. 2010; Alcon et al. 2012). For many years, stem-cell and biomaterials-based cardiovascular regeneration therapy has been advocated as a potential treatment strategy for an infracted tissue. It has shown some success in regaining heart muscle function after direct injection of stem cell to the damaged part. Despite its recovery, up to 90% of the injected cells die after injection and cell loss within the myocardium became major issues (Menasche et al. 2003). Showing that injected cells are not significant to be localized, viable and sustain production of beneficial paracrine factors were delivered simultaneously to achieve efficient cellular activity. Moreover, the need of biomaterial engineered stem cell that can efficiently deliver and localized at the damaged cardiac muscle and promote myocardial regeneration has emerged.

Herein, we encompass stem cell and biomaterial-based therapeutic methods for cardiac regeneration. We will discuss current stem cell therapy strategies as well as its drawbacks and next-generation stem cell therapy incorporating with biomaterials for engineering cardiac function with high survival rate, enhanced cellular activity, and differentiation. In addition, we will summarize various examples of cell sources and novel scaffold strategies to regenerate or regain the wounded heart.

11.2 Studies on Cardiovascular Diseases

Cardiovascular diseases have become major causes of death around the globe with increasing obesity and accumulating stress. Especially, myocardial infarction (MI) is the most common and well-known cardiovascular disease. For several decades, major researches have been working towards its treatments. Some of most considerable approaches that have been employed to study MI are as follows.

11.2.1 Stem Cell Injection

Unlike other minimal cardio-related damages, MI generates a considerable amount of tissue loss that cannot be recovered by regeneration of heart from resident cardiac stem cells (McMullen and Pasumarthi 2007). Due to such reason, direct injection of stem cells has become one of the most commonly used strategies for cardiac repair (Assmus et al. 2006; Schachinger et al. 2006).

Various researches have been carried out with mesenchymal stem cells (MSCs) to test their differentiation abilities into lineages like cardiac, osteogenic, and chondrogenic cells (Di Nicola et al. 2002; Liu et al. 2003; Shim et al. 2004). In addition to differentiation capabilities, MSCs have immunosuppressive characteristics such as inhibiting T-cell proliferation and white blood cells (Balana et al. 2006). With these advantages in hands, cardiovascular researches have been performed by deriving cardiac differentiation in MSCs. For instance, application of a DNA-methylating chemical 5-azacytidine (5-Aza) has shown induction of MSC differentiation into cardiomyocytes (Chung et al. 2011).

Furthermore, other strategies have been developed to generate MSCs with cardiomyocyte-like phenotypes (Rangappa et al. 2003).

11.2.2 Biomaterials Incorporating Cellular Transplantation

Even though with the therapeutic potential of stem cells, however, more than 90% of injected stem cells are lost and show poor engraftment and cell fusion (Orlic et al. 2001; Menasche et al. 2003). Even if cells successfully engraft, there is inconsistency in graft sizes and newly grafted tissue cannot provide enough support for normal heart function (Reinecke and Murry 2000; Zhang et al. 2001; Balsam et al. 2004). Due to the low efficiency of cell injections, using cells only for cardiac repair is not favored as much as other methods.

Although cells only or cells on biomaterials are generally used for cardiac recovery, some studies have shown progress in cardiac repair applying only biomaterials. Some of these materials include fibrin glue, fibrin scaffold, and biotinylated peptide nanofibers (Christman et al. 2004a, b). By using only biomaterials into defect models, an immunogenic response decrease and allows integrating chemical factors. Despite these advantages, repairing without incorporating cells cannot generate functional cardiac tissue (Christman et al. 2004a, b; Davis et al. 2006). Other examples of using biomaterials only include external restraints such as passive elastic containment devices. These devices also do not generate immunogenic responses and are easier to manipulate designs. However, devices are restricted for use in preventing ventricular wall expansion or collapse (Chaudhry et al. 2000; Saavedra et al. 2002). Therefore, the most efficient strategy for cellular transplantation in cardiac tissue repair should integrate both cells and biomaterials.

11.3 Arising Stem Cell and Biomaterial Therapy for Cardiovascular Diseases

Until now, researches on MI has been treated using various approaches such as those at the cellular and structural levels, as well as clinical trials. Although these approaches can grant reasonable results, enormous demands for the integration of bioengineered stem cell therapy has been considered. In this section, we will discuss emerging stem cell and biomaterial therapy with cell surface engineering, microbeads and hydrogel patches that can be used to sufficiently restore the function of cardiac tissues.

11.3.1 Cell Surface Engineering

When stem cells are injected, transfused or transplanted to a patient without any prevention of the environmental stress, it might induce donor cell to death (Hofmann et al. 2005), which declares the importance of stem cell engineering to enhance viability, proliferation or differentiation ability to increase the efficacy of stem cell-based therapy. Following its trend, cell surface modification with natural or synthetic biomaterials is rapidly emerging as a cell engineering technique (Fig. 11.1). Cell functions can be modulated by cell surface engineering by modifying various bioactive functional groups on the cell surface such as cellular receptors and their ligands through covalent conjugation, hydrophobic interaction and electrostatic interaction (Teramura and Iwata 2010). One of the key applications includes cell adhesion and migration by exposing exogenous ligands into the cell membrane. Introduction of cell surface glycosylation can also regulate cell microenvironment (Sampathkumar et al. 2006). Coating biopolymer on the cell surface, it can work as a safeguard by camouflaging the donor cells against the donee's

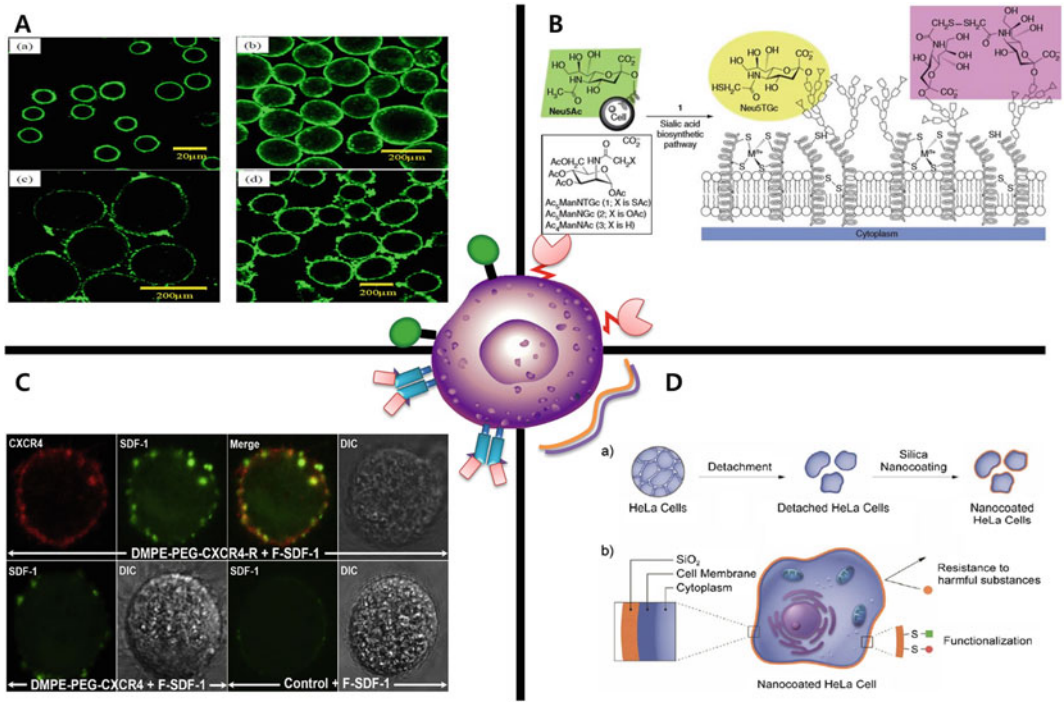

Fig. 11.1 Cell surface bioengineering for cell therapy. (**a**) Bioartificial pancreas coated with polymer chains or thin membranes which masked the cell surface antigens. (Reproduced with permission from Teramura and Iwata 2010, Copyright© 2010, Royal Society of Chemistry). (**b**) Metabolic labeling of surface glycans with functional groups by the biosynthetic sugars. (Reproduced with permission from Sampathkumar et al. 2006, Copyright© 2006, Nature Publishing Group). (**c**) Enhancement of mesenchymal stem cell migration toward cell surface SDF-1 gradient. (Reproduced with permission from Won et al. 2014, Copyright© 2014, Elsevier). (**d**) Cytoprotective silica coating of cell surface through bioinspired silicification. (Reproduced with permission from Lee et al. 2014, Copyright© 2014, John Wiley and Sons)

immune system, as it is especially important in stem cell-based therapies for prolonged *in vivo* persistence and functionality. Moreover, these biomolecules and components can enhance modified donor cell longevity, proliferation, and therapeutic potential.

However, for clinical cell therapy applications, there are criteria for developing clinically available stem cell surface engineering strategies. As cell surface is not a static structure, but rather is a dynamic state, modifying the cell surface is in fact, complicated (Lingwood and Simons 2010). At first, cell surface engineering should minimize alterations in the microenvironment of engineering primary cells. Small changes in pH, temperature and serum starvation can effect on cell viability and differentiation ability (Hofmann et al. 2005). Also, considering the complexity and membrane fluidity of the cell membrane, surface engineering without inhibiting or blocking the surface molecules by modifying cell membrane surface proteins, glycolipids, and polysaccharides, can be a dilemma. Since cell functions, such as cell signaling, proliferation, adhesion, and migration mainly depend on these parameters, several strategies, which are discussed in detail below, have been established to stabilize and retain the function of surface engineered stem cells to work as a suitable tissue regeneration therapy.

As described before, injected cells show poor engraftment and cell fusion to the injured tissue. Thus, cell adhesion and migration to the targeted tissue and interaction between transplanted cells

and injured tissue cells became crucial for cardiac tissue regeneration therapy (Ridker et al. 1998; Assmus et al. 2002). Even though the bioengineered cells successfully injected into injured cardiac tissue, it needs to appropriately differentiate and fuse to the attached area for tissue recovery. At the early stage, studies to show enhancement of the interaction between cell and extracellular matrix (ECM) were addressed. Every tissue has its own unique ECM compositions which are essential for cell binding and tissue functions. By knowing the interaction between tissue and biomaterial, it can give a unique insight into tissue-specific cell guidance (Schlie-Wolter et al. 2013). In MI therapy, type I and type III collagen are known to give significant differences in myocardium development (Sutton and Sharpe 2000). These collagens serve as a framework of aligned myofilaments that distribute force evenly to the ventricular walls to prevent sarcomeric deformation (Erlebacher et al. 1984). Kato et al. demonstrated a strategy of rewiring the cell-surface integrin receptor for adhesion that gave an additional activation of integrin receptors to enhance a biological function of donor cells and cardiac ECM interactions (Kato and Mrksich 2004). Moreover, various natural or synthetic biopolymers are tested for the enhancement of cellular adhesion to tissue. Lee et al. reported a strategy using a bispecific antibody to target human $CD34^+$ cells to infarcted regions which formed bidirectional antibody bridge between the hematopoietic stem cells and injured myocardium. It not only increases fused cells but also, enhanced the function of the left ventricle of infracted heart tissue (Lee et al. 2007). Also, by using biotin-streptoavidin specific interaction, Sarkar et al., successfully engineered adhesion molecule sialyl Lewis X (SLeX) on the surface of mesenchymal stem cells to increase the targeting efficiency of any cell type to specific tissue without altering the cell phenotype and differentiation potential (Sarkar et al. 2008).

Like cell adhesion, stem cell migration to the damaged heart tissue is critical in tissue regeneration. After MI, bone marrow-derived stem cells (BMSCs) are recruited within the myocardium. The differentiation capacity of BMSCs is known to improve the ventricular function of the heart after MI. According to Abbott et al., BMSCs are localized by the local chemotactic factors such as a stromal cell-derived factor-1(SDF-1), which is up-regulated in the cardiac tissue early after MI and is released into the peripheral blood (Abbott et al. 2004). Furthermore, Won et al. investigated SDF-1 and its receptor CXCR4, which plays an important role in recruiting BMSCs and MSCs to fuse into the ischemic myocardium (Won et al. 2014). Since SDF-1 is highly expressed for only 48 h after infarction, by modifying the cell surface with 1,2-dimyristoyl-sn-glycerol-3-phosphoethanolamine (DMPE) and recombinant CXCR4 (rCXCR4) conjugated polyethylene glycol (PEG) within 10mins, they successfully improve the homing efficiency of transplanted MSCs. Hence, stem cell therapy should have to implicate several techniques that can utilize target cells to the damaged cardiac tissue for recovery.

As known, mesenchymal stem cell therapy is highlighted as a new clinical paradigm. However, recent examinations have out turned undesirable results. Preclinical studies revealed the potency of the immune response, which prompts the use of MSC to treat numerous diseases (Ankrum and Karp 2010). Therefore, immune response becomes one of the major problems in stem cell therapy. Even though the donor cells are physiologically alike the host cells, it has a possibility to induce the adaptive immune response. Several attempts have been made by various kinds of natural or synthetic polymers to work as a steric barrier on the transplanted cell surface (Teramura and Iwata 2010). Efficient rendering of cell surface by synthetic modifications can be achieved by covalent attachment of a functional poly (ethylene glycol) (PEG) (Wattendorf and Merkle 2008). PEG is currently considered as a suitable, biocompatible material for inhibition of immune response of the donor cells (Cho et al. 2010). Pegylation makes donor cells antigenically silent, thus protecting them from the immune response (Muruve 2004; Lee et al. 2006; Armstrong et al. 2007). At Wee et al., islets are pegylated by using cyanuric chloride-activated methoxy-polyethylene glycol. When transplanted, it showed almost 90% decrease in antibody binding and decrease in

lymphocyte proliferation, which dedicates successful inhibition of immune response towards transplanted islets (Wee et al. 2008). However, bioinert and non-degradable property was insufficient to prevent the progression of MI (Mathieu et al. 2012). Nevertheless, PEG is continuously studied by its property as a biomatrix for stem cell transplantation, which we will discuss in later part. Furthermore, other synthetic biomaterial can prevent cells from soluble and cellular blood components. Recently, Lee et al. reported cytoprotective coating strategy that can endure enzymatic attack and other toxic compounds. In this respect, this strategy can provide long-term protection of transplanted cells which can survive until the recovery of the damaged cardiac tissue (Lee et al. 2014).

11.3.2 Injectable Hydrogel

Typical stem cell therapy generally utilizes cell itself. On the other hand, several biomaterials can be adopted as delivery carriers for cells or drugs to facilitate cardiac tissue regeneration. Hydrogels have been widely used in regenerative medicine due to their highly adjustable physical and chemical properties (Peppas et al. 2006). Hence, hydrogels are frequently utilized in catheter technology for minimal invasiveness, low cost, and potential for multi-function. Hydrogels can be injected in gel or sol form. Hydrogels that are injected in a sol form, can be injected via three routes: intracoronary, epicardially or transendocardially. The injected solution must transform to gel quickly at the damaged site and also have similar mechanical properties as the ventricular wall for suitable supporting. For example, Liu et al. explored an injectable chitosan hydrogel for cardiac stem cell delivery into myocardium injury and examined the favorable effects of the hydrogel. By investigating the expression of adhesion-related molecules against reactive oxygen species and recruiting key factors for stem cell homing and revascularization, this injectable chitosan hydrogel was beneficial in ischemic myocardium. In addition, Yost et al., developed a collagen type I tubular scaffold that can support cardiomyocyte attachment and elongation (Yost et al. 2004). Collagen which is known as the main components of the myocardial extracellular matrix is important for the phenotypic response of the cardiomyocytes. By applying the tubular design, cardiomyocytes showed comparable *in vivo* phenotype and this potentially is applied in overall construct architecture of transplanted cell fate and behavior.

Moreover, injectable microspheres-based systems have been used in biomedical therapy to deliver growth factors, proteins, and peptides (Babensee et al. 2000; Hoare and Kohane 2008). For instance, Iwakura et al. reported that injectable gelatin microspheres encapsulating basic fibroblast growth factor increased angiogenesis and improved cardiac function in rat MI models (Iwakura et al. 2003). Furthermore, *in situ* cell delivery via microcapsules and microcarriers have been studied to treat many diseases (Hernandez et al. 2010). Because a direct injection of allogenic or xenogenic cells may cause immune rejection, recent researches have been used cell microencapsulation strategies. Due to the membrane barrier surrounding transplanted cells, the access of the host's immune cells can be physically prevented. Also, semipermeable polymeric membrane enables the entry of nutrients for the living of encapsulated cells and the exit of therapeutic cytokines from encapsulated cells.

Recently, Yu et al. reported that the human mesenchymal stem cells encapsulated in RGD modified alginate microspheres effectively improved myocardial repair and regeneration (Fig. 11.2). To improve cell attachment, growth and increase angiogenic growth factor creation, RGD peptides were introduced in the fabrication of alginate microspheres. They identified that the RGD-alginate microspheres encapsulating hMSCs facilitated angiogenesis, and prevented negative LV remodeling, infarct wall thinning and chamber dilation after the outbreak of MI (Yu et al. 2010).

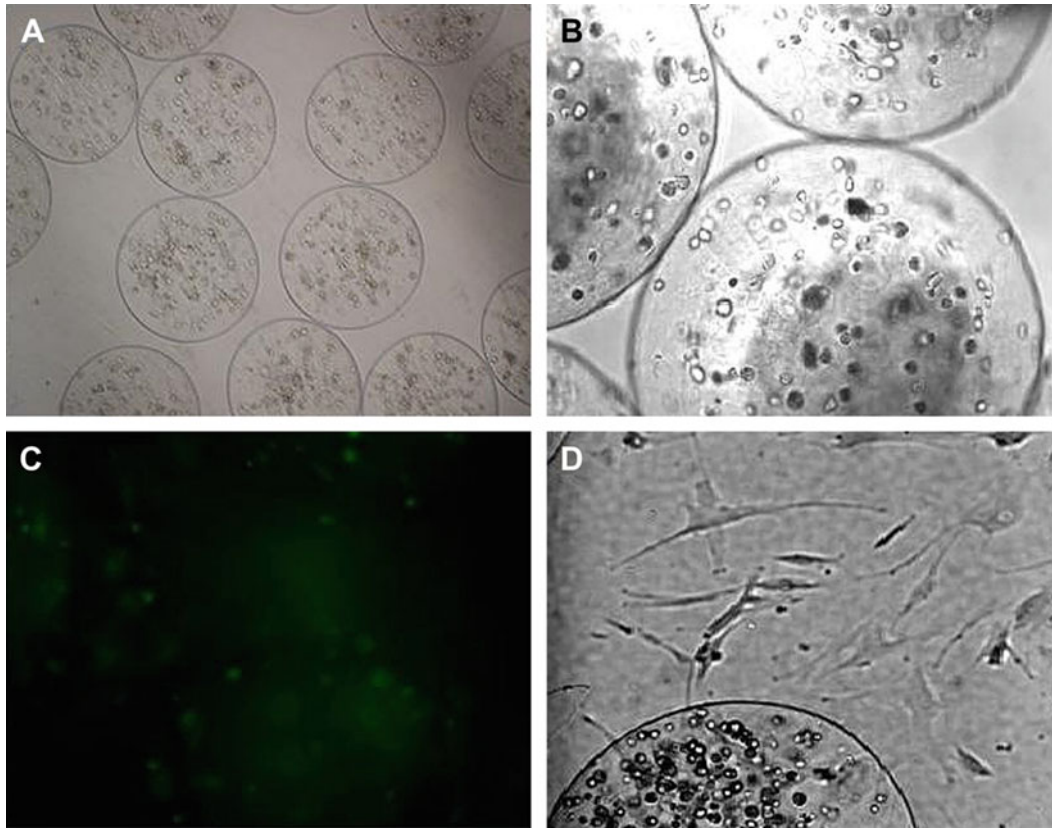

Fig. 11.2 Alginate microbeads encapsulating hMSCs. (**a**, **b**) 2 days after encapsulation, (**c**): Calcein staining (live cells of (**b**)), (**d**) 5 weeks after encapsulation. (Reproduced with permission from Yu et al. 2010, Copyright© 2010, Elsevier)

11.3.3 Stem Cell Delivery Patch

Stem cell delivery using bioactive hydrogel can be therapeutic applications for MI, resulted from a decrease of blood flow into cardiomyocytes. The optional treatments for stem cell delivery include using biomaterials with several approaches (Madden et al. 2010; Wu et al. 2011). In traditional stem cell therapy for MI, the stem cells were injected directly into MI sites, but it revealed that survival and retention of the stem cells lower after surgery (Siepe et al. 2006; Piao et al. 2007). For upregulating these factors, the hydrogel scaffolds have been applied to MI, which has invasive procedure refrained, as delivery vehicles not only for stem cells, also for growth factors and peptides (Christman and Lee 2006). Hydrogel with functionalized properties has resulted in improved cardiac function and effective regeneration when applied to MI (Camci-Unal et al. 2014). There are several ways to utilize the hydrogels, such as injection and patch forms. These have its own benefits and drawbacks. The cardiac patch could be applied to heart without an invasive procedure but existed lacking vascularization. In contrast, injection methods allowed the delicate delivery of materials into the infarcted region but need to be an invasive procedure. We herein demonstrated the hydrogel patch with stem cell engraftment for MI treatments.

To develop the system for stem cell delivery using tissue engineered scaffolds, the suitable materials were selected preferentially and adjusted according to targeted function (e.g., morphological and chemical modification). After which, the stem cells were incubated on scaffolds

or encapsulated within hydrogel during preparing the constructs, followed by transplantation into MI regions. Among the candidates for stem cell therapy for MI, mesenchymal stem cells (MSCs) have been mainly used since it is multipotent to differentiate into cardiomyocytes and releases cytokines and growth factors for promoting endogenous repair pathway (Toma et al. 2002; Kucia et al. 2004). Thus, synergetic effects were anticipated when collaborating between MSCs and hydrogel. The hydrogels for cardiac repair must support heart tissue-like elasticity and be well attached infarcted site with resistance to heart beating (Ye et al. 2011). For this goal, fibrin and/or tissue adhesive materials have been widely applied to MI therapy. For example, Xiong et al. demonstrated that fibrin patch-based delivery of human embryonic stem cell could promote neovascularization and LV contractile functions (Xiong et al. 2011).

Extracellular matrix (ECM) materials, such as hyaluronic acid (HA), collagen, and fibronectin (FN), also represented proper biomaterials. Chi et al. compared MSCs-loaded scaffolds with acellular scaffolds using silk fibroin/hyaluronic acid hydrogel patch. The LV wall thickness and neovascularization in MI zones were enhanced in MSCs-loaded hydrogels (Chi et al. 2012). Moreover, Simpson et al. utilized a rat tail type I collagen and embedded the human MSCs into the collagen matrix, followed by being applied to MI. It revealed that 30% increase in fractional shortening and affected on recruitment and differentiation of native cells (Simpson et al. 2007). Recently, Kang and Kim et al. developed polycaprolactone (PCL) nanofibers as cardiac patch functionalized with immobilizing FN to improve cardiac function (Kang et al. 2014) (Fig. 11.3). With increased elongation and adhesion efficacy of MSCs, the cell-seeded nanofibrous patch enhanced vessel density and MI size and fibrosis decreased compared to acellular patch. These results demonstrated that the ECM-based stem cell-delivery scaffolds can promote the cardiac function after MI with being integrated into host tissue and delivering stem cells stably.

Other methods for stem cell delivery with substrates have been reported. Wei et al. developed hydrogel patch where multilayered MSCs were inserted into a sliced biological scaffold for rat MI model. The cardiac patch could restore left ventricular (LV) cavity and preserve cardiac functions (Wei et al. 2008). Likewise, numerous strategies for MI treatments using tissue-engineered patches have been under investigation for elevating cell viability, integration, and coupling with host tissue. For the advanced healing effects, the scaffolds have to tightly be controlled according to degradation rates, efficient transport of nutrients and wastes (Parsa et al. 2015). Furthermore, long-term approach, not during several weeks but longer period, are needed for evaluating the biomaterial-based stem cell therapy, and suitable cell source should be decided to proceed with clinical applications (Rane and Christman 2011; Ungerleider and Christman 2014).

11.4 Future Outlooks and Directions

Currently, bountiful of companies are corresponding in the development and investment of stem cell-based products, as it became the starting material to treat a wide range of diseases (Kirouac and Zandstra 2008). In hindsight, stem cell therapy has undergone an astonishing improvement from traditional blood transfusions into a promising healthcare industry. The broaden needs of clinical stem cell therapy products for cardiac diseases have also hastened the developments of stem cell engineering with the goal of maximizing the therapeutic achievement in patients. In this chapter, we have highlighted several strategies investigated to rationally design the microarchitecture for stem cells with natural or synthetic biomaterials. Cell products as live therapeutics, it ought to be costly to harvest, purify and expand. In this regard, to successfully hybrid stem cell bioengineering technologies into clinical applications, future research attempts will be needed to optimize additional parameters.

Despite the challenges, the fields of bio-responsive or bio-interactive materials are

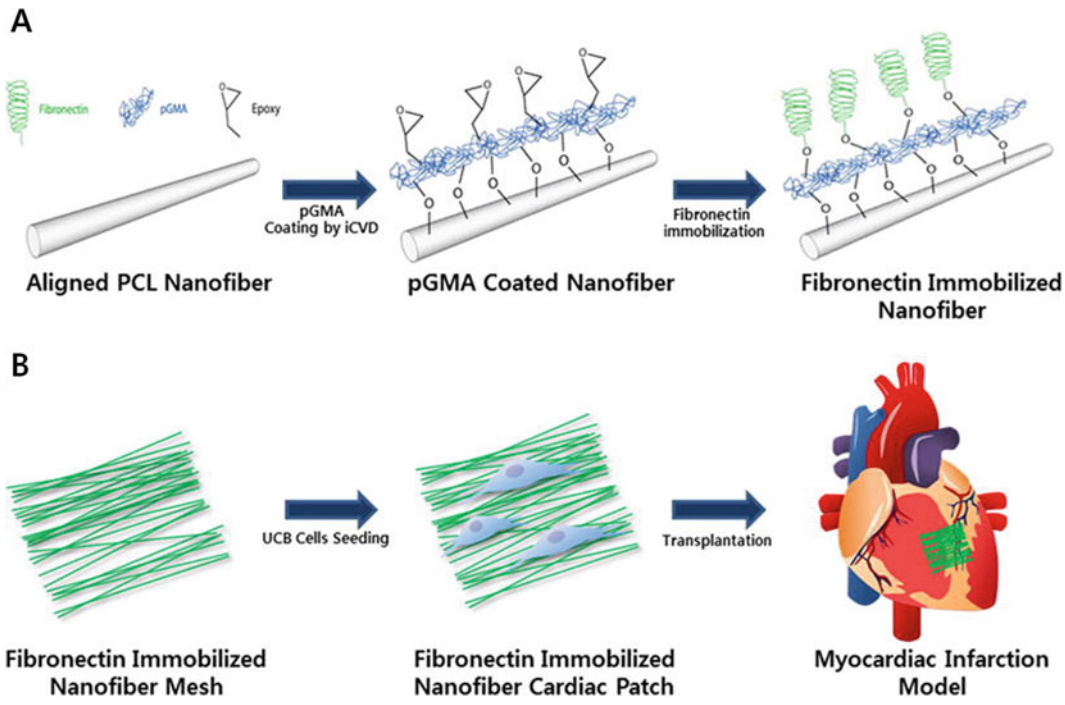

Fig. 11.3 Representative procedure from preparing the substrates (**a**) to transplanting the stem cell seeded biomaterials into myocardial infarction model (**b**). (Reproduced with permission from Kang et al. 2014, Copyright© 2014, Elsevier)

emerging in stem cell engineering for cardiac diseases. Some of the latest attempts of the very useful mechanistic end for a clinical trial are the capability to track the stem cells after they are injected or implanted. For instance, Raman et al., developed paramagnetic particles that can be visualized by MRI or molecular tracers (Hill et al. 2003; Wu et al. 2003). As well, the injectable hydrogel system could regard as a cellular "Trojan horse vehicles" tuned to release drug payloads controllably once they reach the infracted sites. Guo et al., prepared tunable multifunctional nanocarriers and triggered drug release once reaching tumor targets with acidic pH environments. Showed that such on-demand drug release would further show potential in both targetings and treat at once to minimize excessive cytotoxicity of background levels of drugs (Guo et al. 2011). Moreover, multistimulus responsive drug delivery to the targeted area could also trigger a therapeutically effective dose without adverse side effects as microenvironment of disease areas are different. By using polymers that can respond to different stimuli, such as pH, light, temperature, ultrasound, magnetism, or biomolecule, this novel biomaterial can deliver a therapeutic agent and advances in "smart" drug delivery systems (You et al. 2010).

The development of advanced biomaterial analysis tools, such as combinatorial synthesis, has led to developing new and rapid methods to design drug delivery systems of next-generation biomaterials with remarkable functionality and biocompatibility. This field of study holds the promise to further acceleration of the discovery and design processes for stem cell therapies (Petersen and Narasimhan 2008). Novel hydrogel technology to be considered for cardiac cell therapy with tantalizing therapeutic potential is shape memory injectable gels (Thornton et al. 2004). Well-defined injectable macroporous hydrogels by cryotropic gelation of a naturally sourced polymer demonstrated

long-term release of therapeutics in vivo. Transplanted cells at the injection site had enhanced survival, higher local retention, and extended engraftment (Bencherif et al. 2012).

Another direction for the future is merging microfabrication techniques with biomaterial arrangement to manipulate highly vascularized cardiac constructs. The arrangement of advanced constructs, which can be practiced applying electrical and mechanical stimulation at the same time on the engineered cardiac tissues, can be another favorable research parameter. It is expected that stem cell-encapsulated functional hybrid hydrogels will permit us to reconstruct the myocardium after injuries, and improved properties such as electrical conductivity, elasticity, vascularization potential, and oxygen supplementation which can further control cellular behavior, resulting in the regeneration of functional cardiac tissues.

References

Abbott JD, Huang Y, Liu D, Hickey R, Krause DS, Giordano FJ (2004) Stromal cell-derived factor-1alpha plays a critical role in stem cell recruitment to the heart after myocardial infarction but is not sufficient to induce homing in the absence of injury. Circulation 110(21):3300–3305. https://doi.org/10.1161/01.CIR.0000147780.30124.CF

Alcon A, Bozkulak EC, Qyang YB (2012) Regenerating functional heart tissue for myocardial repair. Cell Mol Life Sci 69(16):2635–2656. https://doi.org/10.1007/s00018-012-0942-4

Ankrum J, Karp JM (2010) Mesenchymal stem cell therapy: two steps forward, one step back. Trends Mol Med 16(5):203–209. https://doi.org/10.1016/j.molmed.2010.02.005

Armstrong JK, Hempel G, Koling S, Chan LS, Fisher T, Meiselman HJ, Garratty G (2007) Antibody against poly(ethylene glycol) adversely affects PEG-asparaginase therapy in acute lymphoblastic leukemia patients. Cancer 110(1):103–111. https://doi.org/10.1002/cncr.22739

Assmus B, Schachinger V, Teupe C, Britten M, Lehmann R, Dobert N, Grunwald F, Aicher A, Urbich C, Martin H, Hoelzer D, Dimmeler S, Zeiher AM (2002) Transplantation of progenitor cells and regeneration enhancement in acute myocardial infarction (TOPCARE-AMI). Circulation 106 (24):3009–3017

Assmus B, Honold J, Schachinger V, Britten MB, Fischer-Rasokat U, Lehmann R, Teupe C, Pistorius K, Martin H, Abolmaali ND, Tonn T, Dimmeler S, Zeiher AM (2006) Transcoronary transplantation of progenitor cells after myocardial infarction. N Engl J Med 355 (12):1222–1232. https://doi.org/10.1056/NEJMoa051779

Babensee JE, McIntire LV, Mikos AG (2000) Growth factor delivery for tissue engineering. Pharm Res 17 (5):497–504. https://doi.org/10.1023/A:1007502828372

Balana B, Nicoletti C, Zahanich I, Graf EM, Christ T, Boxberger S, Ravens U (2006) 5-Azacytidine induces changes in electrophysiological properties of human mesenchymal stem cells. Cell Res 16(12):949–960. https://doi.org/10.1038/sj.cr.7310116

Balsam LB, Wagers AJ, Christensen JL, Kofidis T, Weissman IL, Robbins RC (2004) Haematopoietic stem cells adopt mature haematopoietic fates in ischaemic myocardium. Nature 428(6983):668–673. https://doi.org/10.1038/nature02460

Bencherif SA, Sands RW, Bhatta D, Arany P, Verbeke CS, Edwards DA, Mooney DJ (2012) Injectable preformed scaffolds with shape-memory properties. Proc Natl Acad Sci U S A 109(48):19590–19595. https://doi.org/10.1073/pnas.1211516109

Camci-Unal G, Annabi N, Dokmeci MR, Liao R, Khademhosseini A (2014) Hydrogels for cardiac tissue engineering. Npg Asia Mater 6:e99. https://doi.org/10.1038/am.2014.19

Chaudhry PA, Mishima T, Sharov VG, Hawkins J, Alferness C, Paone G, Sabbah HN (2000) Passive epicardial containment prevents ventricular remodeling in heart failure. Ann Thorac Surg 70 (4):1275–1280

Chi NH, Yang MC, Chung TW, Chen JY, Chou NK, Wang SS (2012) Cardiac repair achieved by bone marrow mesenchymal stem cells/silk fibroin/hyaluronic acid patches in a rat of myocardial infarction model. Biomaterials 33(22):5541–5551. https://doi.org/10.1016/j.biomaterials.2012.04.030

Cho YW, Park JH, Park JS, Park K (2010) Pegylation: camouflage of proteins, cells, and nanoparticles against recognition by the body's defense mechanism. In: Pharmaceutical sciences encyclopedia. Wiley, Hoboken

Christman KL, Lee RJ (2006) Biomaterials for the treatment of myocardial infarction. J Am Coll Cardiol 48 (5):907–913. https://doi.org/10.1016/j.jacc.2006.06.005

Christman KL, Fok HH, Sievers RE, Fang Q, Lee RJ (2004a) Fibrin glue alone and skeletal myoblasts in a fibrin scaffold preserve cardiac function after myocardial infarction. Tissue Eng 10(3–4):403–409. https://doi.org/10.1089/107632704323061762

Christman KL, Vardanian AJ, Fang Q, Sievers RE, Fok HH, Lee RJ (2004b) Injectable fibrin scaffold improves cell transplant survival, reduces infarct expansion, and induces neovasculature formation in ischemic myocardium. J Am Coll Cardiol 44(3):654–660. https://doi.org/10.1016/j.jacc.2004.04.040

Chung YS, Huang CY, Ma MC, Chu CC, Chiang HS, Lin LJ, Chou SH (2011) Cardiac injury protection from mouse bone marrow stromal cells with in utero transplantation followed by secondary postnatal boost. Chin J Physiol 54(4):205–218. https://doi.org/10.4077/CJP.2011.AMM078

Davis ME, Hsieh PC, Takahashi T, Song Q, Zhang S, Kamm RD, Grodzinsky AJ, Anversa P, Lee RT (2006) Local myocardial insulin-like growth factor 1 (IGF-1) delivery with biotinylated peptide nanofibers improves cell therapy for myocardial infarction. Proc Natl Acad Sci U S A 103(21):8155–8160. https://doi.org/10.1073/pnas.0602877103

Di Nicola M, Carlo-Stella C, Magni M, Milanesi M, Longoni PD, Matteucci P, Grisanti S, Gianni AM (2002) Human bone marrow stromal cells suppress T-lymphocyte proliferation induced by cellular or nonspecific mitogenic stimuli. Blood 99(10):3838–3843

Erlebacher JA, Weiss JL, Weisfeldt ML, Bulkley BH (1984) Early dilation of the infarcted segment in acute transmural myocardial infarction: role of infarct expansion in acute left ventricular enlargement. J Am Coll Cardiol 4(2):201–208

Guo M, Que C, Wang C, Liu X, Yan H, Liu K (2011) Multifunctional superparamagnetic nanocarriers with folate-mediated and pH-responsive targeting properties for anticancer drug delivery. Biomaterials 32 (1):185–194. https://doi.org/10.1016/j.biomaterials.2010.09.077

Hernandez RM, Orive G, Murua A, Pedraz JL (2010) Microcapsules and microcarriers for in situ cell delivery. Adv Drug Deliv Rev 62(7–8):711–730. https://doi.org/10.1016/j.addr.2010.02.004

Hill JM, Dick AJ, Raman VK, Thompson RB, Yu ZX, Hinds KA, Pessanha BS, Guttman MA, Varney TR, Martin BJ, Dunbar CE, McVeigh ER, Lederman RJ (2003) Serial cardiac magnetic resonance imaging of injected mesenchymal stem cells. Circulation 108 (8):1009–1014. https://doi.org/10.1161/01.CIR.0000084537.66419.7A

Hoare TR, Kohane DS (2008) Hydrogels in drug delivery: progress and challenges. Polymer 49(8):1993–2007. https://doi.org/10.1016/j.polymer.2008.01.027

Hofmann M, Wollert KC, Meyer GP, Menke A, Arseniev L, Hertenstein B, Ganser A, Knapp WH, Drexler H (2005) Monitoring of bone marrow cell homing into the infarcted human myocardium. Circulation 111(17):2198–2202. https://doi.org/10.1161/01.CIR.0000163546.27639.AA

Iwakura A, Fujita M, Kataoka K, Tambara K, Sakakibara Y, Komeda M, Tabata Y (2003) Intramyocardial sustained delivery of basic fibroblast growth factor improves angiogenesis and ventricular function in a rat infarct model. Heart Vessel 18 (2):93–99. https://doi.org/10.1007/s10380-002-0686-5

Joggerst SJ, Hatzopoulos AK (2009) Stem cell therapy for cardiac repair: benefits and barriers. Expert Rev Mol Med 11:e20. https://doi.org/10.1017/S1462399409001124

Kang BJ, Kim H, Lee SK, Kim J, Shen Y, Jung S, Kang KS, Im SG, Lee SY, Choi M, Hwang NS, Cho JY (2014) Umbilical-cord-blood-derived mesenchymal stem cells seeded onto fibronectin-immobilized polycaprolactone nanofiber improve cardiac function. Acta Biomater 10(7):3007–3017. https://doi.org/10.1016/j.actbio.2014.03.013

Kato M, Mrksich M (2004) Rewiring cell adhesion. J Am Chem Soc 126(21):6504–6505. https://doi.org/10.1021/ja039058e

Kirouac DC, Zandstra PW (2008) The systematic production of cells for cell therapies. Cell Stem Cell 3 (4):369–381. https://doi.org/10.1016/j.stem.2008.09.001

Kucia M, Dawn B, Hunt G, Guo YR, Wysoczynski M, Majka M, Ratajczak J, Rezzoug F, Ildstad ST, Bolli R, Ratajczak MZ (2004) Cells expressing early cardiac markers reside in the bone marrow and are mobilized into the peripheral blood after myocardial infarction. Circ Res 95(12):1191–1199. https://doi.org/10.1161/01.RES.0000150856.47324.5b

Lee DY, Park SJ, Nam JH, Byun Y (2006) A new strategy toward improving immunoprotection in cell therapy for diabetes mellitus: long-functioning PEGylated islets in vivo. Tissue Eng 12(3):615–623. https://doi.org/10.1089/ten.2006.12.615

Lee RJ, Fang Q, Davol PA, Gu Y, Sievers RE, Grabert RC, Gall JM, Tsang E, Yee MS, Fok H, Huang NF, Padbury JF, Larrick JW, Lum LG (2007) Antibody targeting of stem cells to infarcted myocardium. Stem Cells 25 (3):712–717. https://doi.org/10.1634/stemcells.2005-0602

Lee J, Choi J, Park JH, Kim MH, Hong D, Cho H, Yang SH, Choi IS (2014) Cytoprotective silica coating of individual mammalian cells through bioinspired silicification. Angew Chem Int Ed Engl 53(31):8056–8059. https://doi.org/10.1002/anie.201402280

Li ZQ, Guan JJ (2011) Hydrogels for cardiac tissue engineering. Polymers 3(2):740–761. https://doi.org/10.3390/polym3020740

Lingwood D, Simons K (2010) Lipid rafts as a membrane-organizing principle. Science 327(5961):46–50. https://doi.org/10.1126/science.1174621

Liu Y, Song J, Liu W, Wan Y, Chen X, Hu C (2003) Growth and differentiation of rat bone marrow stromal cells: does 5-azacytidine trigger their cardiomyogenic differentiation? Cardiovasc Res 58(2):460–468

Madden LR, Mortisen DJ, Sussman EM, Dupras SK, Fugate JA, Cuy JL, Hauch KD, Laflamme MA, Murry CE, Ratner BD (2010) Proangiogenic scaffolds as functional templates for cardiac tissue engineering. Proc Natl Acad Sci U S A 107(34):15211–15216. https://doi.org/10.1073/pnas.1006442107

Mathieu E, Lamirault G, Toquet C, Lhommet P, Rederstorff E, Sourice S, Biteau K, Hulin P, Forest V, Weiss P, Guicheux J, Lemarchand P (2012) Intramyocardial delivery of mesenchymal stem cell-seeded hydrogel preserves cardiac function and attenuates ventricular remodeling after myocardial infarction. PLoS One 7(12):e51991. https://doi.org/10.1371/journal.pone.0051991

McMullen NM, Pasumarthi KB (2007) Donor cell transplantation for myocardial disease: does it complement current pharmacological therapies? Can J Physiol Pharmacol 85(1):1–15. https://doi.org/10.1139/Y06-105

Menasche P, Hagege AA, Vilquin JT, Desnos M, Abergel E, Pouzet B, Bel A, Sarateanu S, Scorsin M, Schwartz K, Bruneval P, Benbunan M, Marolleau JP, Duboc D (2003) Autologous skeletal myoblast transplantation for severe postinfarction left ventricular dysfunction. J Am Coll Cardiol 41(7):1078–1083

Menasche P, Alfieri O, Janssens S, McKenna W, Reichenspurner H, Trinquart L, Vilquin JT, Marolleau JP, Seymour B, Larghero J, Lake S, Chatellier G, Solomon S, Desnos M, Hagege AA (2008) The myoblast autologous grafting in ischemic cardiomyopathy (MAGIC) trial – first randomized placebo-controlled study of myoblast transplantation. Circulation 117 (9):1189–1200. https://doi.org/10.1161/Circulationaha.107.734103

Mukherjee S, Venugopal JR, Ravichandran R, Ramakrishna S, Raghunath M (2010) Multimodal biomaterial strategies for regeneration of infarcted myocardium. J Mater Chem 20(40):8819–8831. https://doi.org/10.1039/c0jm00805b

Muruve DA (2004) Helper-dependent adenovirus vectors elicit intact innate but attenuated adaptive host immune responses in vivo. J Virol 78:5966–5972

Orlic D, Kajstura J, Chimenti S, Jakoniuk I, Anderson SM, Li B, Pickel J, McKay R, Nadal-Ginard B, Bodine DM, Leri A, Anversa P (2001) Bone marrow cells regenerate infarcted myocardium. Nature 410(6829):701–705. https://doi.org/10.1038/35070587

Parsa H, Ronaldson K, Vunjak-Novakovic G (2015) Bioengineering methods for myocardial regeneration. Adv Drug Deliv Rev 96:195–202

Pedron S, van Lierop S, Horstman P, Penterman R, Broer DJ, Peeters E (2011) Stimuli responsive delivery vehicles for cardiac microtissue transplantation. Adv Funct Mater 21(9):1624–1630. https://doi.org/10.1002/adfm.201002708

Peppas NA, Hilt JZ, Khademhosseini A, Langer R (2006) Hydrogels in biology and medicine: from molecular principles to bionanotechnology. Adv Mater 18 (11):1345–1360. https://doi.org/10.1002/adma.200501612

Petersen LK, Narasimhan B (2008) Combinatorial design of biomaterials for drug delivery: opportunities and challenges. Expert Opin Drug Deliv 5(8):837–846. https://doi.org/10.1517/17425247.5.8.837

Piao H, Kwon JS, Piao S, Sohn JH, Lee YS, Bae JW, Hwang KK, Kim DW, Jeon O, Kim BS, Park YB, Cho MC (2007) Effects of cardiac patches engineered with bone marrow-derived mononuclear cells and PGCL scaffolds in a rat myocardial infarction model. Biomaterials 28(4):641–649. https://doi.org/10.1016/j.biomaterials.2006.09.009

Rane AA, Christman KL (2011) Biomaterials for the treatment of myocardial infarction. J Am Coll Cardiol 58 (25):2615–2629. https://doi.org/10.1016/j.jacc.2011.11.001

Rangappa S, Fen C, Lee EH, Bongso A, Sim EK (2003) Transformation of adult mesenchymal stem cells isolated from the fatty tissue into cardiomyocytes. Ann Thorac Surg 75(3):775–779

Reinecke H, Murry CE (2000) Transmural replacement of myocardium after skeletal myoblast grafting into the heart. Too much of a good thing? Cardiovasc Pathol 9 (6):337–344

Ridker PM, Hennekens CH, Roitman-Johnson B, Stampfer MJ, Allen J (1998) Plasma concentration of soluble intercellular adhesion molecule 1 and risks of future myocardial infarction in apparently healthy men. Lancet 351(9096):88–92. https://doi.org/10.1016/S0140-6736(97)09032-6

Saavedra WF, Tunin RS, Paolocci N, Mishima T, Suzuki G, Emala CW, Chaudhry PA, Anagnostopoulos P, Gupta RC, Sabbah HN, Kass DA (2002) Reverse remodeling and enhanced adrenergic reserve from passive external support in experimental dilated heart failure. J Am Coll Cardiol 39 (12):2069–2076

Sampathkumar SG, Jones MB, Yarema KJ (2006) Metabolic expression of thiol-derivatized sialic acids on the cell surface and their quantitative estimation by flow cytometry. Nat Protoc 1(4):1840–1851. https://doi.org/10.1038/nprot.2006.252

Sarkar D, Vemula PK, Teo GS, Spelke D, Karnik R, Wee le Y, Karp JM (2008) Chemical engineering of mesenchymal stem cells to induce a cell rolling response. Bioconjug Chem 19(11):2105–2109. https://doi.org/10.1021/bc800345q

Schachinger V, Erbs S, Elsasser A, Haberbosch W, Hambrecht R, Holschermann H, Yu J, Corti R, Mathey DG, Hamm CW, Suselbeck T, Assmus B, Tonn T, Dimmeler S, Zeiher AM, Investigators R-A (2006) Intracoronary bone marrow-derived progenitor cells in acute myocardial infarction. N Engl J Med 355 (12):1210–1221. https://doi.org/10.1056/NEJMoa060186

Schlie-Wolter S, Ngezahayo A, Chichkov BN (2013) The selective role of ECM components on cell adhesion, morphology, proliferation and communication in vitro. Exp Cell Res 319(10):1553–1561. https://doi.org/10.1016/j.yexcr.2013.03.016

Shim WS, Jiang S, Wong P, Tan J, Chua YL, Tan YS, Sin YK, Lim CH, Chua T, Teh M, Liu TC, Sim E (2004) Ex vivo differentiation of human adult bone marrow stem cells into cardiomyocyte-like cells. Biochem Biophys Res Commun 324(2):481–488. https://doi.org/10.1016/j.bbrc.2004.09.087

Siepe M, Giraud MN, Pavlovic M, Receputo C, Beyersdorf F, Menasche P, Carrel T, Tevaearai HT (2006) Myoblast-seeded biodegradable scaffolds to prevent post-myocardial infarction evolution toward heart failure. J Thorac Cardiovasc Surg 132 (1):124–131. https://doi.org/10.1016/j.jtcvs.2006.01.052

Simpson D, Liu H, Fan THM, Nerem R, Dudley SC (2007) A tissue engineering approach to progenitor cell delivery results in significant cell engraftment and improved myocardial remodeling. Stem Cells 25(9):2350–2357. https://doi.org/10.1634/stemcells.2007-0132

Sutton MG, Sharpe N (2000) Left ventricular remodeling after myocardial infarction: pathophysiology and therapy. Circulation 101(25):2981–2988

Teramura Y, Iwata H (2010) Cell surface modification with polymers for biomedical studies. Soft Matter 6 (6):1081–1091. https://doi.org/10.1039/B913621E

Thornton AJ, Alsberg E, Hill EE, Mooney DJ (2004) Shape retaining injectable hydrogels for minimally invasive bulking. J Urol 172(2):763–768. https://doi.org/10.1097/01.ju.0000130466.84214.f7

Toma C, Pittenger MF, Cahill KS, Byrne BJ, Kessler PD (2002) Human mesenchymal stem cells differentiate to a cardiomyocyte phenotype in the adult murine heart. Circulation 105(1):93–98. https://doi.org/10.1161/hc0102.101442

Ungerleider JL, Christman KL (2014) Concise review: injectable biomaterials for the treatment of myocardial infarction and peripheral artery disease: translational challenges and progress. Stem Cells Transl Med 3 (9):1090–1099. https://doi.org/10.5966/sctm.2014-0049

Venugopal JR, Prabhakaran MP, Mukherjee S, Ravichandran R, Dan K, Ramakrishna S (2012) Biomaterial strategies for alleviation of myocardial infarction. J R Soc Interface 9(66):1–19. https://doi.org/10.1098/rsif.2011.0301

Wang F, Guan J (2010) Cellular cardiomyoplasty and cardiac tissue engineering for myocardial therapy. Adv Drug Deliv Rev 62(7–8):784–797. https://doi.org/10.1016/j.addr.2010.03.001

Wattendorf U, Merkle HP (2008) PEGylation as a tool for the biomedical engineering of surface modified microparticles. J Pharm Sci 97(11):4655–4669. https://doi.org/10.1002/jps.21350

Wee YM, Lim DG, Kim YH, Kim JH, Kim SC, Yu E, Park MO, Choi MY, Park YH, Jang HJ, Cho EY, Cho MH, Han DJ (2008) Cell surface modification by activated polyethylene glycol prevents allosensitization after islet transplantation. Cell Transplant 17(10–11):1257–1269

Wei HJ, Chen CH, Lee WY, Chiu I, Hwang SM, Lin WW, Huang CC, Yeh YC, Chang Y, Sung HW (2008) Bioengineered cardiac patch constructed from multilayered mesenchymal stem cells for myocardial repair. Biomaterials 29(26):3547–3556. https://doi.org/10.1016/j.biomaterials.2008.05.009

Won YW, Patel AN, Bull DA (2014) Cell surface engineering to enhance mesenchymal stem cell migration toward an SDF-1 gradient. Biomaterials 35(21):5627–5635. https://doi.org/10.1016/j.biomaterials.2014.03.070

Wu JC, Chen IY, Sundaresan G, Min JJ, De A, Qiao JH, Fishbein MC, Gambhir SS (2003) Molecular imaging of cardiac cell transplantation in living animals using optical bioluminescence and positron emission tomography. Circulation 108(11):1302–1305. https://doi.org/10.1161/01.CIR.0000091252.20010.6E

Wu J, Zeng FQ, Huang XP, Chung JCY, Konecny F, Weisel RD, Li RK (2011) Infarct stabilization and cardiac repair with a VEGF-conjugated, injectable hydrogel. Biomaterials 32(2):579–586. https://doi.org/10.1016/j.biomaterials.2010.08.098

Xiong QA, Hill KL, Li QL, Suntharalingam P, Mansoor A, Wang XH, Jameel MN, Zhang PY, Swingen C, Kaufman DS, Zhang JY (2011) A fibrin patch-based enhanced delivery of human embryonic stem cell-derived vascular cell transplantation in a porcine model of postinfarction left ventricular remodeling. Stem Cells 29(2):367–375. https://doi.org/10.1002/stem.580

Ye ZY, Zhou Y, Cai HB, Tan WS (2011) Myocardial regeneration: roles of stem cells and hydrogels. Adv Drug Deliv Rev 63(8):688–697. https://doi.org/10.1016/j.addr.2011.02.007

Yost MJ, Baicu CF, Stonerock CE, Goodwin RL, Price RL, Davis JM, Evans H, Watson PD, Gore CM, Sweet J, Creech L, Zile MR, Terracio L (2004) A novel tubular scaffold for cardiovascular tissue engineering. Tissue Eng 10(1–2):273–284. https://doi.org/10.1089/107632704322791916

You JO, Almeda D, Ye GJ, Auguste DT (2010) Bioresponsive matrices in drug delivery. J Biol Eng 4:15. https://doi.org/10.1186/1754-1611-4-15

Yu JS, Du KT, Fang QZ, Gu YP, Mihardja SS, Sievers RE, Wu JC, Lee RJ (2010) The use of human mesenchymal stem cells encapsulated in RGD modified alginate microspheres in the repair of myocardial infarction in the rat. Biomaterials 31(27):7012–7020. https://doi.org/10.1016/j.biomaterials.2010.05.078

Zhang M, Methot D, Poppa V, Fujio Y, Walsh K, Murry CE (2001) Cardiomyocyte grafting for cardiac repair: graft cell death and anti-death strategies. J Mol Cell Cardiol 33(5):907–921. https://doi.org/10.1006/jmcc.2001.1367

Part V

Immunoresponses of Biomimetic Medical Materials

Immunomodulation of Biomaterials by Controlling Macrophage Polarization

12

Hyeong-Cheol Yang, Hee Chul Park, Hongxuan Quan, and Yongjoon Kim

12.1 Introduction

Implantation of biomaterials in the body is accompanied by immune responses against tissue injuries that occur during implantation, presence of foreign bodies, and toxic property of the biomaterials. The immune responses to biomaterials include acute inflammation, chronic inflammation, and foreign body reactions. Before acute inflammation, a provisional matrix is formed on the surface of implanted materials. The provisional matrix comprises a fibrin network, platelets, and inflammatory cells, which recruits neutrophils [polymorphonuclear leukocytes (PMNs)] to trigger acute inflammation. The neutrophils then phagocytose and degrade foreign substances such as microorganisms and biomaterials. The detailed effect of neutrophils on biomaterials is described in another chapter. PMNs predominate for the first 24–48 h after implantation and are then replaced by monocytes/macrophages (Fig. 12.1).

Monocyte-derived macrophages play a central role in innate immune responses against foreign materials and participate in phagocytosis, angiogenesis, fibroblast recruitment, and granulation tissue formation. Because of their multifunctionality, macrophages can reside within the inflammation site for several weeks or months, depending on the severity of the injury and the toxicity of the biomaterials. Their ability to release various types of cytokines and their phenotype plasticity contribute to macrophages playing several roles in the immune response process. They secrete both proinflammatory cytokines, such as tumor necrosis factor (TNF)-α, interleukin (IL)-1β, and IL-6, and antiinflammatory cytokines, such as transforming growth factor (TGF)-α and IL-10. Macrophages also produce vascular endothelial growth factor (VEGF) for neovascularization. They simultaneously release several cytokines, the release profiles or patterns of which are dependent on the phenotype of the activated macrophage. In general, macrophage phenotypes are classified into either M1 (classically activated) or M2 (alternatively activated), and M2 is further subdivided into M2a, M2b, and M2c. The M1 phenotype, known as the proinflammatory type, produces proinflammatory cytokines, as described above, and induces an inflammatory response to protect tissues from foreign substances (Fig. 12.2). In contrast, macrophages with the M2 phenotype produce antiinflammatory cytokines, suppress inflammation, and enhance tissue healing and regeneration. In the normal wound-healing process, M1 macrophages appear first to clean the injured site, followed by M2 macrophages to complete the wound-healing process; furthermore, the phenotype do not show an extreme

H.-C. Yang (✉) · H. C. Park · H. Quan · Y. Kim
Department of Dental Biomaterials Science and Dental Research Institute, School of Dentistry, Seoul National University, Seoul, South Korea
e-mail: yanghc@snu.ac.kr; pipichul@snu.ac.kr; baobei@snu.ac.kr; yjak87@snu.ac.kr

I. Noh (ed.), *Biomimetic Medical Materials*, Advances in Experimental Medicine and Biology 1064,
https://doi.org/10.1007/978-981-13-0445-3_12

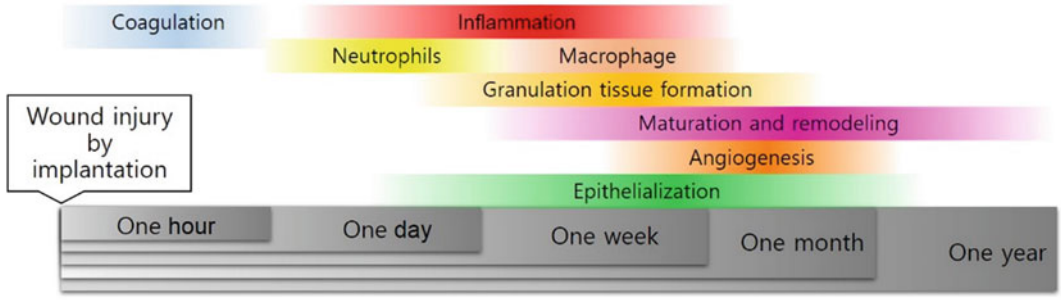

Fig. 12.1 Time line of wound healing process after implantation of biomaterials

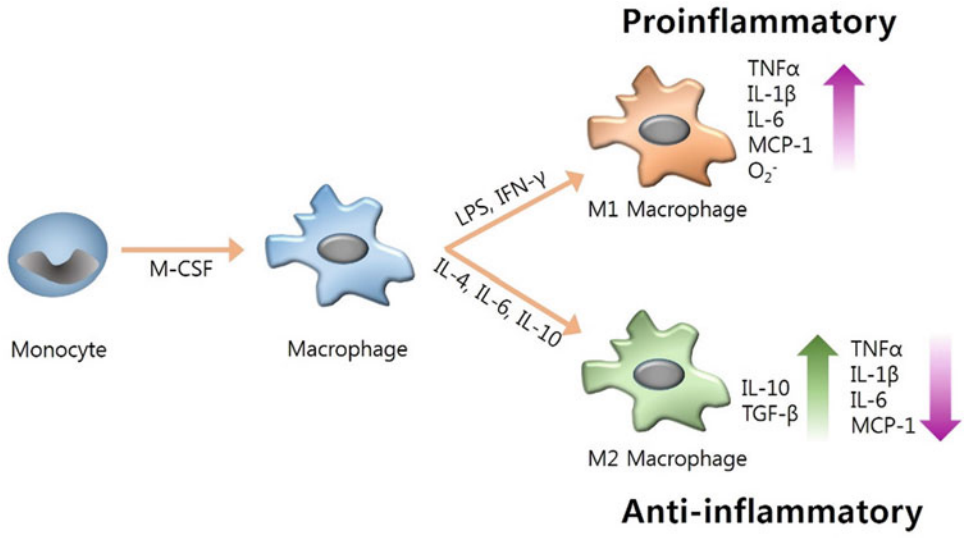

Fig. 12.2 Phenotype of M1 and M2 macrophages

pattern but exhibit a mixed population of the two phenotypes with a preferred ratio. That is, a high M1/M2 ratio develops first, and a low M1/M2 ratio develops later to regenerate the tissues.

When macrophages are unable to phagocytose biomaterials because of their size, they fuse together to form multinuclear foreign body giant cells (FBGCs), a frustrated form of macrophages. FBGCs produce a group of cytokines that are different from the cytokine-release profiles of the M1 and M2 macrophages and produce reactive oxygen species, which can damage implanted biomaterials. They also promote fibrous encapsulation via the release of TGF-β. The fibrous capsule surrounds the medical device, isolates it from the tissue, and disturbs its inherent function. Thus, in general, the appearance of FBGCs is not desired as an immune response to biomaterials.

This chapter mainly focuses on the effects of various biomaterials on macrophages, particularly on their phenotypes. Here the association between the chemical/physical properties of biomaterials and the M1/M2 ratio is described to suggest the importance of the macrophage phenotype in a foreign body reaction (FBR). In addition, we introduce several strategies that modulate macrophage phenotypes to obtain favorable FBRs.

12.2 Role of Macrophages on Biodegradable Materials

Biomaterials are either biodegradable and non-biodegradable. Biodegradable materials can be either synthetically prepared or obtained from natural sources. The biodegradability of materials depends on the intrinsic chemical/physical properties and their modification for optimization, such as decellularization of extracellular matrix (ECM) scaffolds and the crosslinking of polymers. Keane et al. (2012) found that the decellularization of porcine small intestinal ECM induced a change in the macrophage phenotypes to a predominance of M2 over M1. The association between ECM decellularization and macrophage phenotype can also be implied by the results of a recent study that demonstrated that collagen scaffolds supplemented with cellular components such as DNA, mitochondria, or cell membranes promote the occurrence of M1 macrophages (Londono et al. 2017). The biodegradation of ECM scaffolds needs macrophage participation (Valentin et al. 2009), and macrophage-derived proteolytic (MMP) enzymes might also play an important role in ECM degradation. Several studies have demonstrated that M1 and M2 macrophages have different MMP expression profiles. M1-polarized human macrophages showed high protein expressions of MMP-1, -3, and -10, whereas M2-polarized macrophages showed high protein expressions of MMP-12 (Roch et al. 2014). Classical activation (M1) of mouse macrophages induced an increase in MMP-13, -14, and -25 mRNA expressions (Hayes et al. 2014) and a decrease in MMP-19 expression. In contrast, MMP-19 mRNA expression increased in alternatively activated (M2) mouse macrophages. MMP enzymatic activities also vary depending on the macrophage phenotype. The MMP activity of M2 macrophages was higher than that of M1 macrophages (Roch et al. 2014). The differences between M1 and M2 cells with respect to MMP expression levels and enzyme activity imply that macrophage phenotype affects the biodegradability of ECM scaffolds.

In addition to the degree of decellularization, the degree of ECM scaffold crosslinking also affects the M1/M2 ratio. High M1/M2 ratios in carbodiimide-crosslinked scaffolds derived from the porcine small intestine submucosa (SIS) were observed during the 16 weeks after implantation compared with those in non-crosslinked scaffolds (Badylak et al. 2008). M1 macrophages predominated over M2 macrophages at the interface of the host tissues and crosslinked mesh derived from the porcine dermis; non-crosslinked meshes displayed a relatively low M1/M2 ratio (Brown et al. 2012).

12.3 Role of Macrophages on Non-biodegradable Materials

12.3.1 Polarization of Macrophages by Wear Debris Particles

Early studies on the interaction between macrophages and non-biodegradable biomaterials have mainly focused on the role of macrophages in wear debris-induced inflammation around a failed prosthesis. The co-presence of macrophages and prosthetic material-derived small particles in tissues that surround artificial joints suggest the involvement of macrophages and their phagocytic activity in periprosthetic osteolysis (Willert and Semlitsch 1977). *In vitro* and animal studies have provided strong evidences to support the participation of macrophages in wear debris–associated pathogenesis. Human monocytes/macrophages secret proinflammatory TNF-α and IL-6 in the presence of titanium particles (Blaine et al. 1996; Maloney et al. 1996), and TNF-α medicated implant particle-induced osteoclastogenesis in a murine model (Merkel et al. 1999). Macrophages exhibited inflammatory responses against bone cement particles (Ingham et al. 2000; Wimhurst et al. 2001), and ultrahigh molecular weight polyethylene particles also induced macrophage migration and osteolysis (Ren et al. 2011); therefore, it is fairly evident that small particles of non-degradable biomaterials such as metal, ceramics, and polymers can activate

macrophages. The secretion of inflammatory cytokines by particle-activated macrophages implies that M1 macrophages are involved in wear debris-induced inflammation, proved by a clinical study wherein an increase in the M1/M2 ratio was demonstrated in tissues retrieved from a revised joint replacement (Rao et al. 2012). The M1 phenotype also appeared in macrophage cultures that were exposed to microsized TiO_2 particles above certain concentrations (Schoenenberger et al. 2016). In this case, the protein expressions of TNF-α and IL-10, representative proinflammatory cytokines, were upregulated to approximately 10–15 folds compared with those of the unexposed control of M0 THP-1 macrophages; however, using the same macrophage cell line, another previous study demonstrated that titanium alloy particles of a failed hip prosthesis did not induce the release of TNF-α in vitro (Akisue et al. 2002). Only LPS-treated particles promoted TNF-α secretion, which indicated that wear debris alone could not evoke inflammation and osteolysis. Thus, the role of wear debris in macrophage polarization remains controversial, and the precise mechanism underlining wear debris-induced pathogenesis remains unknown. Finally, Pajarinen et al. (2013) showed that M1 macrophages exhibited inflammatory responses more intensely than M0 and M2 macrophages, demonstrating the potential importance of the macrophage phenotype in prosthetic failure. In this context, the suppression of M1 macrophages has been attempted for treating or preventing prosthetic failure.

IL-4, a strong suppressor of the M1 phenotype and an inducer of M2 polarization (Martinez et al. 2009), reduces the production of proinflammatory cytokines in human peripheral blood monocytes that were exposed to poly(methyl methacrylate) (PMMA) particles or particles retrieved from titanium alloy wear (Trindade et al. 1999; Im and Han 2001). The effect of IL-4 was also demonstrated in in vivo studies. Daily injection of IL-4 reduced polyethylene particle-induced osteolysis in a mouse calvarial and air pouch model (Rao et al. 2013; Wang et al. 2013b). The in vitro and in vivo results indicated that IL-4 can suppress wear debris-induced inflammation by modulating the macrophage phenotype from M1 toward M2. IL-10 also mitigated the release of TNF-α and IL-6 from titanium- and PMMA-treated human macrophages (Pollice et al. 1998; Trindade et al. 2001). In addition to proteinaceous molecules such as IL-4 and IL-10, bioactive small molecules, including flavonoids and alkaloids, can promote macrophage polarization. The flavonoid apigenin reversed M1 macrophages to M2 macrophages and decreased proinflammatory cytokine levels in a rodent model (Feng et al. 2016). Pentamethoxyflavanone, another type of flavonoid, facilitated a shift from the M1 macrophage phenotype to the M2 macrophage phenotype (Feng et al. 2014). The results imply that bioactive small molecules can be used for reducing biomaterial-derived inflammation. In fact, curcumin, a plant-derived alkaloid that polarizes macrophages toward the M2 phenotype (Gao et al. 2015), suppressed titanium particle-induced inflammation in the mouse air pouch model (Li et al. 2017). Because of the low production cost, chemical stability, and ease of handling, bioactive small chemicals can be attractive alternatives to cytokine molecules, provided their activities are sufficient for polarizing macrophages and the chemicals are applied timely to the pathogenesis site.

12.3.2 Role of Macrophages on Fibrous Encapsulation

Fibrous encapsulation, a late foreign body response to biomaterials, is a dense layer of avascular fibrotic tissue that surrounds implants. Myofibroblasts play an important role in the formation of fibrous encapsulation. Myofibroblasts are generally derived from tissue fibroblasts, which are principally mediated by TGF-β, particularly isoform 1. TGF-β is released by various cells such as macrophages and FBGCs. Hernandez-Pando et al. (2000) found that FBGCs highly expressed TGF-β, which was accompanied by fibrosis. FBGCs are formed by the fusion of macrophages to the surface of a foreign substance. Because IL-4 treatment can induce both FBGCs and M2 macrophages,

FBGCs are considered to be a lineage of M2 macrophages; however, unlike M2 cells, FBGCs express M1 (TNF-α, iNOS, and IL-1β) and M2 (IL-10 and Arg1) markers (Moore et al. 2015), which indicates that FBGCs cannot be categorized according to the typical classification of macrophages (i.e., classically and alternatively activated).

Biomaterial-derived fibrous encapsulation is generally considered to be an undesirable consequence of an immune response. A fibrotic capsule can hinder the function of implanted devices such as a glucose sensor by isolating them from surrounding tissues and can cause discomfort and pain to the patient. Thus, various strategies have been attempted to reduce surface fibrosis of implanted biomaterials. The most commonly introduced method is coating the implants with biocompatible materials, including both synthetic and naturally occurring materials. The natural materials include collagen, gelatin, chitosan, alginate, and hyaluronan. These materials have been proved to be highly biocompatible without an obvious inflammatory tissue response and are frequently used as scaffolds for tissue engineering. Thus, coating the surface of implants with natural materials may reduce FBRs and fibrous encapsulation; however, using natural materials does not guarantee a favorable immune reaction to the implants. Naturally occurring polymers are often immunogenic, and their molecular structures are not necessarily consistent, which can affect the process and degree of tissue and cellular responses. Badylak et al. (2008) showed the importance of macromolecular structure in determining an immune response (Badylak et al. 2008). In their study, SIS induced the normal tissue-remodeling process with an early accumulation of M2 macrophages in a rat model. But carbodiimide-crosslinked SIS provoked chronic inflammation and prolonged (16 weeks) the appearance of M1 macrophages. Although we do not yet completely understand the molecular mechanism that underlies the crosslinking effect of scaffolding on innate immune responses, it is certain that the hierarchical structure and type of polymer should be carefully considered when selecting coating materials. Synthetic and semisynthetic polymers can also affect the reaction to a foreign body and subsequent fibrous encapsulation by preventing surface biofouling, biomolecule adsorption, and subsequent adhesion of inflammatory cells. The passivated or nonfouling surface may reduce the reactions to a foreign body, including a surface fibrosis. Poly(ethylene glycol) (PEG) is the most well-known nonfouling material. Hydrophilicity and the ability to retain water molecules allow PEG to block protein adhesion and inflammatory reactions. Poly(lactic-co-glycotic acid) (PLGA) and poly(vinyl-alcohol) (PVA) have been mostly used as a drug-eluting coating for implants (Bhardwaj et al. 2010), although their antiinflammatory or antifibrotic effects have not yet been clearly demonstrated.

Antiinflammatory drugs have been investigated for their feasibility in reducing implant-associated fibrosis. Several studies have demonstrated that dexamethasone-loaded PLGA effectively attenuated inflammatory reactions and fibrous encapsulation (Hickey et al. 2002; Patil et al. 2004). The controlled release of dexamethasone is most likely important for suppressive drug to exhibit their effects. Drug-loaded PLGA may reduce fibrosis of implanted devices such as a glucose sensor. In an animal study, dexamethasone in a PLGA/PVA matrix could suppress inflammatory reactions and fibrosis on the surface of a biosensor (in this case, a dummy sensor was used) in normal and diabetic rats (Wang et al. 2013a). This result indicates that antiinflammatory drugs are sufficiently applicable in preparing antifibrotic implants. The development of appropriate drug-eluting systems and the selection of effective drugs are necessary for achieving an effective antifibrotic effect.

It is generally agreed that TGF-β plays a central role in fibrous encapsulation. Thus, the inhibition of TGF-β may reduce fibrous encapsulation at the surface of implants. Neutralizing antibodies against TGF-β have been used to suppress or ameliorate fibrosis in various organs such as the kidneys, lungs, and renal system (Yanagita 2012; Giri et al. 1993; Ling et al. 2013). The effects of the TGF-β-neutralizing antibody in the cure of organ fibrosis suggest its use in preventing

fibrotic encapsulation of implants; however, there have been no reports to demonstrate the antifibrotic effect of the TGF-β antibody at the implant surface, possibly because of the lack of an appropriate method by which the antibody is loaded onto implants. In addition to the antibody treatment, gene therapy is considered to attenuate encapsulation. In a previous study, TGF-β1-siRNA, delivered via liposome-based nanoparticles, inhibited peritoneal fibrosis in a mice model (Yoshizawa et al. 2015). In another study, a mammalian target of rapamycin (mTOR)-siRNA was used to inhibit the fibrous encapsulation of a polymer implant (Takahashi et al. 2010). Unfortunately, mTOR-siRNA did not affect the thickness of the fibrous capsule. The authors attributed the ineffectiveness of mTOR-siRNA to an inappropriate gene delivery system. Rujitanaroj et al. (2013) recently successfully reduced fibrous capsule formation with COL1A1-siRNA. A poly(caprolactone-co-ethyl ethylene phosphate) nanofiber was used to control the sustained release of siRNA; therefore, the development of a gene delivery system and the selection of a target gene are important for successfully suppressing capsule formation. Antifibrotic drugs such as nintedanib and pirfenidone are also expected to resolve the encapsulation problem (Raghu and Selman 2015). Because these chemicals are more stable than antibody proteins and siRNA in a biological environment, a greater in vivo effect is expected in future studies. Table 12.1 summarize various methods for reduction of fibrous encapsulation.

12.4 Control of Macrophage Polarization for Improved Biomaterial Outcomes

Biomaterials that do not induce FBR have not yet been developed despite great endeavors of many researchers. The major obstacles for the removal of FBRs are the lack of knowledge about the ideal performance of macrophages, a key player in innate inflammation, and few efficient methods or tools for mitigating FBRs. The early appearance of macrophages at the implantation site is a necessary and unavoidable event that prevents infection-derived inflammation and cleans out cell debris in damaged tissues, which were generated during surgery. Proinflammatory M1 macrophages are involved in early tissue responses. In healthy tissues, M1 macrophages generally subside within 3 days after implantation; however, the prolonged presence of microorganisms can delay M1 quiescence, aggravate inflammation, and disturb the healing and regeneration of surrounding tissues. Unwanted M1 macrophage involvement can lead us to recognize M1 as a target to suppress or remove to achieve FBR reduction. In this context, the phenotype change from M1 to M2 microphages has been attempted on the surface of implanted biomaterials. Fortunately, previous studies have discovered the plasticity of macrophage phenotypes (i.e., M1 macrophages can be converted to M2 microphages and vice versa). Obesity alters the phenotype of adipose tissue macrophages from M2 to M1 (Morris et al. 2011). Prostaglandin E6- and IL-6-induced M2 macrophages were converted to M1 macrophages by CD4+ Th1 cells (Heusinkveld et al. 2011). Deng et al. (2012) demonstrated that IL-10 regulated the change in muscle microphage phenotype from M1 to M2. Those studies suggested methods for modulating macrophage phenotypes and provided evidences of plasticity. Gower et al. (2014) used the potential of IL-10 in the modulation of FBRs. The lentiviral gene that encodes IL-10 was delivered with a poly(lactide-co-glycolide) scaffold to reduce implantation-induced inflammation. The IL-10 delivery significantly decreased leukocyte infiltration and increased IL-10 expression, which indicated that IL-10 successfully mitigated FBRs. IL-4 also induced M2 macrophages in a three-dimensional hydrogel (Cha et al. 2017). IL-4-eluting coating increased the percentage of M2 macrophages at the surface of the implant and diminished the formation of fibrotic capsules (Hachim et al. 2017). These studies indicated that the suppression of M1 macrophages or the M1/M2 ratio is effective for generating a favorable FBR, i.e., less inflammation and a thinner fibrous capsule. The elimination of macrophages by clodronate, a

Table 12.1 Methods for anti-fibrous encapsulation

Methods	Materials or agents	References
Coating with natural materials	Collagen	Badylak et al. (2008)
Coating with non-fouling materials	PEG, PLGA, PVA	Bhardwaj et al. (2010)
Anti-inflammatory drug loading	Dexamethasone	Hickey et al. (2002)
		Patil et al. (2004)
		Wang et al. (2013a)
siRNA loading	TGF-β1-siRNA	Yoshizawa et al. (2015)
	COL1A1-siRNA	Rujitanaroj et al. (2013)
	mTOR-siRNA	Takahashi et al. (2010)

bisphosphate, also successfully diminished giant-cell accumulation and fibrosis of 3D electrospun scaffolds (Dondossola et al. 2016). In addition, the study clearly demonstrated the role of VEGF and neovascularization in fibrosis via the antagonistic effect of VEGF neutralization on the formation of giant cells and fibrosis. VEGF production in macrophages and giant cells caused neovascularization around biomaterials followed by fibrosis. Newly formed blood vessels most likely aggravate inflammatory tissue responses in combination with preexisting giant cells by secondarily supplying macrophages, thus the inhibition of neovascularization at the surface of implants might reduce FBRs toward biomaterials. If so, we speculated whether the antiangiogenic approach always induces favorable FBRs. Considering the presence of new blood vessels in granulation tissues and the importance of angiogenesis in tissue regeneration, antiangiogenic agents can retard the healing of injured tissues that result from implantation surgery; therefore, timely and locally specific inhibition of angiogenesis might be necessary for suppressing the formation of fibrous capsules. With medical devices such as an implantable glucose sensor, reduced blood vessels at the surface of the implant can result in lowered sensitivity. Contrary to the inhibition of neovascularization, the induction of vascularization by the sequential delivery of IFN-γ and IL-4 was also exploited to enhance angiogenesis and healing of bone scaffolding (Spiller et al. 2015). Because M1 and M2 macrophages can promote the initiation and maturation of blood vessel formation, respectively, Spiller et al. expected the development of functional blood vessels adjacent to the scaffold, followed by fast healing. The sequential delivery of cytokines actually enhanced angiogenesis in the study, but the effect on fibrosis was not mentioned.

Although the effect of M2 macrophages on tissue regeneration or healing is affirmed, considering that M2 macrophages fairly often produce TGF-β and that TGF-β leads to the generation of fibrosis, we must be cautious not to excessively and extendedly induce the M2 macrophage phenotype. For the regulation of FBRs, most studies have focused on the modulation of M1 macrophages; however, the regulation of M2 macrophages for the suppression of TGF-β or direct inhibition of TGF-β can be a target for reducing fibrosis. In our laboratory, moderately PEGylated phosphatidylserine (PS) liposomes showed a promising *in vitro* result for the suppression of fibrous encapsulation (Quan et al. 2017). PEGylated PS liposomes did not enhance the generation of TGF-β in RAW 264.7 cells. Meanwhile, the liposomes effectively inhibited the production of TNF-α in LPS-activated macrophages. This result indicated that PEGylated PS liposomes could suppress the M1 phenotype without enhancing TGF-β, a typical characteristic of the M2 phenotype. The *in vivo* effects of the liposomes are being investigated for use as an antifibrosis material.

Scaffold geometry affected the cytokine profiles of human monocytes/macrophages (Almeida et al. 2014). The chitosan scaffold with its larger pores resulted in higher secretion levels of proinflammatory cytokines, suggesting an association between the morphology and macrophage phenotype. More direct evidence for this association was demonstrated in another study wherein intentionally elongated macrophages on

Table 12.2 Methods for the control of macrophage polarization

Methods	Acting effects on macrophages	References
IL-10 loading	M1 → M2	Deng et al. (2012)
IL-4 loading	M1 → M2	Cha et al. (2017)
		Hachim et al. (2017)
PEGylated phosphatidylserine (PS) liposome	Suppression of M1 without M2 induction	Quan et al. (2017)
Scaffold geometry (chitosan scaffold with larger pores)	M1 induction	Almeida et al. (2014)
Surface pattern (microgroove)	M2 induction	McWhorter et al. (2013)

a micropatterned surface exhibited the M2 phenotype (McWhorter et al. 2013). Because the M2 phenotype was abrogated by an inhibitor of actin polymerization, the actin cytoskeleton was most likely involved in the pathway for the shape-induced polarization of macrophages. The effect of the physical environment on macrophage polarization suggests that the modulation of surface geometry can be used for obtaining obtain a favorable FBR toward implanted biomaterials. Table 12.2 summarize the methods for the control of macrophage polarization at the surface of biomaterials.

12.5 Conclusion

Most biomaterials induce FBRs, and the degree of reaction is considerably dependent on the resultant macrophage phenotype on the material's surface. Various studies have focused on the modulation of macrophage phenotypes to obtain favorable FBRs. A supply of cytokines and bioactive small chemicals and the fabrication of surface geometry have sucessfully modified macrophage phenotypes. Although a gap remains between laboratory results and clinical application, the immunomodulative tools described in this chapter may provide a way for developing more biocompatible medical devices.

References

Akisue T, Bauer TW, Farver CF, Mochida Y (2002) The effect of particle wear debris on nfkappab activation and pro-inflammatory cytokine release in differentiated thp-1 cells. J Biomed Mater Res 59(3):507–515

Almeida CR, Serra T, Oliveira MI, Planell JA, Barbosa MA, Navarro M (2014) Impact of 3-d printed pla- and chitosan-based scaffolds on human monocyte/macrophage responses: unraveling the effect of 3-d structures on inflammation. Acta Biomater 10(2):613–622

Badylak SF, Valentin JE, Ravindra AK, McCabe GP, Stewart-Akers AM (2008) Macrophage phenotype as a determinant of biologic scaffold remodeling. Tissue Eng Part A 14(11):1835–1842

Bhardwaj U, Sura R, Papadimitrakopoulos F, Burgess DJ (2010) Plga/pva hydrogel composites for long-term inflammation control following s.C. Implantation. Int J Pharm 384(1–2):78–86

Blaine TA, Rosier RN, Puzas JE, Looney RJ, Reynolds PR, Reynolds SD, O'Keefe RJ (1996) Increased levels of tumor necrosis factor-alpha and interleukin-6 protein and messenger rna in human peripheral blood monocytes due to titanium particles. J Bone Joint Surg Am 78(8):1181–1192

Brown BN, Londono R, Tottey S, Zhang L, Kukla KA, Wolf MT, Daly KA, Reing JE, Badylak SF (2012) Macrophage phenotype as a predictor of constructive remodeling following the implantation of biologically derived surgical mesh materials. Acta Biomater 8 (3):978–987

Cha BH, Shin SR, Leijten J, Li YC, Singh S, Liu JC, Annabi N, Abdi R, Dokmeci MR, Vrana NE et al (2017) Integrin-mediated interactions control macrophage polarization in 3d hydrogels. Adv Healthc Mater. https://doi.org/10.1002/adhm.201700289

Deng B, Wehling-Henricks M, Villalta SA, Wang Y, Tidball JG (2012) IL-10 triggers changes in macrophage phenotype that promote muscle growth and regeneration. J Immunol 189(7):3669–3680

Dondossola E, Holzapfel BM, Alexander S, Filippini S, Hutmacher DW, Friedl P (2016) Examination of the foreign body response to biomaterials by nonlinear intravital microscopy. Nat Biomed Eng 1:0007

Feng L, Song P, Zhou H, Li A, Ma Y, Zhang X, Liu H, Xu G, Zhou Y, Wu X et al (2014) Pentamethoxyflavanone regulates macrophage polarization and ameliorates sepsis in mice. Biochem Pharmacol 89 (1):109–118

Feng X, Weng D, Zhou F, Owen YD, Qin H, Zhao J, Wen Y, Huang Y, Chen J, Fu H et al (2016) Activation of pparγ by a natural flavonoid modulator, apigenin ameliorates obesity-related inflammation via regulation of macrophage polarization. EBioMedicine 9:61–76

Gao S, Zhou J, Liu N, Wang L, Gao Q, Wu Y, Zhao Q, Liu P, Wang S, Liu Y et al (2015) Curcumin induces m2 macrophage polarization by secretion il-4 and/or il-13. J Mol Cell Cardiol 85:131–139

Giri SN, Hyde DM, Hollinger MA (1993) Effect of antibody to transforming growth factor beta on bleomycin induced accumulation of lung collagen in mice. Thorax 48(10):959–966

Gower RM, Boehler RM, Azarin SM, Ricci CF, Leonard JN, Shea LD (2014) Modulation of leukocyte infiltration and phenotype in microporous tissue engineering scaffolds via vector induced IL-10 expression. Biomaterials 35(6):2024–2031

Hachim D, LoPresti ST, Yates CC, Brown BN (2017) Shifts in macrophage phenotype at the biomaterial interface via il-4 eluting coatings are associated with improved implant integration. Biomaterials 112:95–107

Hayes EM, Tsaousi A, Di Gregoli K, Jenkinson SR, Bond AR, Johnson JL, Bevan L, Thomas AC, Newby AC (2014) Classical and alternative activation and metalloproteinase expression occurs in foam cell macrophages in male and female apoe null mice in the absence of t and b lymphocytes. Front Immunol 5:537

Hernandez-Pando R, Bornstein QL, Aguilar Leon D, Orozco EH, Madrigal VK, Martinez Cordero E (2000) Inflammatory cytokine production by immunological and foreign body multinucleated giant cells. Immunology 100(3):352–358

Heusinkveld M, de Vos van Steenwijk PJ, Goedemans R, Ramwadhdoebe TH, Gorter A, Welters MJ, van Hall T, van der Burg SH (2011) M2 macrophages induced by prostaglandin e2 and il-6 from cervical carcinoma are switched to activated m1 macrophages by cd4+ th1 cells. J Immunol (Baltimore, Md: 1950) 187(3):1157–1165

Hickey T, Kreutzer D, Burgess DJ, Moussy F (2002) In vivo evaluation of a dexamethasone/plga microsphere system designed to suppress the inflammatory tissue response to implantable medical devices. J Biomed Mater Res 61(2):180–187

Im GI, Han JD (2001) Suppressive effects of interleukin-4 and interleukin-10 on the production of proinflammatory cytokines induced by titanium-alloy particles. J Biomed Mater Res 58(5):531–536

Ingham E, Green TR, Stone MH, Kowalski R, Watkins N, Fisher J (2000) Production of tnf-alpha and bone resorbing activity by macrophages in response to different types of bone cement particles. Biomaterials 21 (10):1005–1013

Keane TJ, Londono R, Turner NJ, Badylak SF (2012) Consequences of ineffective decellularization of biologic scaffolds on the host response. Biomaterials 33 (6):1771–1781

Li B, Hu Y, Zhao Y, Cheng M, Qin H, Cheng T, Wang Q, Peng X, Zhang X (2017) Curcumin attenuates titanium particle-induced inflammation by regulating macrophage polarization in vitro and in vivo. Front Immunol 8:55

Ling H, Roux E, Hempel D, Tao J, Smith M, Lonning S, Zuk A, Arbeeny C, Ledbetter S (2013) Transforming growth factor beta neutralization ameliorates pre-existing hepatic fibrosis and reduces cholangiocarcinoma in thioacetamide-treated rats. PLoS One 8 (1):e54499

Londono R, Dziki JL, Haljasmaa E, Turner NJ, Leifer CA, Badylak SF (2017) The effect of cell debris within biologic scaffolds upon the macrophage response. J Biomed Mater Res A 105:2109

Maloney WJ, James RE, Smith RL (1996) Human macrophage response to retrieved titanium alloy particles in vitro. Clin Orthop Relat Res 322:268–278

Martinez FO, Helming L, Gordon S (2009) Alternative activation of macrophages: an immunologic functional perspective. Annu Rev Immunol 27(1):451–483

McWhorter FY, Wang T, Nguyen P, Chung T, Liu WF (2013) Modulation of macrophage phenotype by cell shape. Proc Natl Acad Sci U S A 110 (43):17253–17258

Merkel KD, Erdmann JM, McHugh KP, Abu-Amer Y, Ross FP, Teitelbaum SL (1999) Tumor necrosis factor-alpha mediates orthopedic implant osteolysis. Am J Pathol 154(1):203–210

Moore LB, Sawyer AJ, Charokopos A, Skokos EA, Kyriakides TR (2015) Loss of monocyte chemoattractant protein-1 alters macrophage polarization and reduces nfkappab activation in the foreign body response. Acta Biomater 11:37–47

Morris DL, Singer K, Lumeng CN (2011) Adipose tissue macrophages: phenotypic plasticity and diversity in lean and obese states. Curr Opin Clin Nutr Metab Care 14(4):341–346

Pajarinen J, Kouri VP, Jamsen E, Li TF, Mandelin J, Konttinen YT (2013) The response of macrophages to titanium particles is determined by macrophage polarization. Acta Biomater 9(11):9229–9240

Patil SD, Papadimitrakopoulos F, Burgess DJ (2004) Dexamethasone-loaded poly(lactic-co-glycolic) acid microspheres/poly(vinyl alcohol) hydrogel composite coatings for inflammation control. Diabetes Technol Ther 6(6):887–897

Pollice PF, Hsu J, Hicks DG, Bukata S, Rosier RN, Reynolds PR, Puzas JE, O'Keefe RJ (1998) Interleukin-10 inhibits cytokine synthesis in monocytes stimulated by titanium particles: evidence of an anti-inflammatory regulatory pathway. J Orthop Res: Off Publ Orthop Res Soc 16(6):697–704

Quan H, Park HC, Kim Y, Yang HC (2017) Modulation of the anti-inflammatory effects of phosphatidylserine-containing liposomes by pegylation. J Biomed Mater Res A 105(5):1479–1486

Raghu G, Selman M (2015) Nintedanib and pirfenidone. New antifibrotic treatments indicated for idiopathic pulmonary fibrosis offer hopes and raises questions. Am J Respir Crit Care Med 191(3):252–254

Rao AJ, Gibon E, Ma T, Yao Z, Smith RL, Goodman SB (2012) Revision joint replacement, wear particles, and macrophage polarization. Acta Biomater 8 (7):2815–2823

Rao AJ, Nich C, Dhulipala LS, Gibon E, Valladares R, Zwingenberger S, Smith RL, Goodman SB (2013) Local effect of il-4 delivery on polyethylene particle induced osteolysis in the murine calvarium. J Biomed Mater Res A 101((7):1926–1934

Ren P-G, Irani A, Huang Z, Ma T, Biswal S, Goodman SB (2011) Continuous infusion of uhmwpe particles induces increased bone macrophages and osteolysis. Clin Orthop Relat Res 469(1):113–122

Roch T, Akymenko O, Kruger A, Jung F, Ma N, Lendlein A (2014) Expression pattern analysis and activity determination of matrix metalloproteinase derived from human macrophage subsets. Clin Hemorheol Microcirc 58(1):147–158

Rujitanaroj PO, Jao B, Yang J, Wang F, Anderson JM, Wang J, Chew SY (2013) Controlling fibrous capsule formation through long-term down-regulation of collagen type I (COL1A1) expression by nanofiber-mediated siRNA gene silencing. Acta Biomater 9 (1):4513–4524

Schoenenberger AD, Schipanski A, Malheiro V, Kucki M, Snedeker JG, Wick P, Maniura-Weber K (2016) Macrophage polarization by titanium dioxide (tio2) particles: size matters. ACS Biomater Sci Eng 2 (6):908–919

Spiller KL, Nassiri S, Witherel CE, Anfang RR, Ng J, Nakazawa KR, Yu T, Vunjak-Novakovic G (2015) Sequential delivery of immunomodulatory cytokines to facilitate the m1-to-m2 transition of macrophages and enhance vascularization of bone scaffolds. Biomaterials 37:194–207

Takahashi H, Wang Y, Grainger DW (2010) Device-based local delivery of sirna against mammalian target of rapamycin (mtor) in a murine subcutaneous implant model to inhibit fibrous encapsulation. J Control Release 147(3):400–407

Trindade MC, Nakashima Y, Lind M, Sun DH, Goodman SB, Maloney WJ, Schurman DJ, Smith RL (1999) Interleukin-4 inhibits granulocyte-macrophage colony-stimulating factor, interleukin-6, and tumor necrosis factor-alpha expression by human monocytes in response to polymethylmethacrylate particle challenge in vitro. J Orthop Res Off Publ Orthop Res Soc 17 (6):797–802

Trindade MC, Lind M, Nakashima Y, Sun D, Goodman SB, Schurman DJ, Smith RL (2001) Interleukin-10 inhibits polymethylmethacrylate particle induced interleukin-6 and tumor necrosis factor-alpha release by human monocyte/macrophages in vitro. Biomaterials 22(15):2067–2073

Valentin JE, Stewart-Akers AM, Gilbert TW, Badylak SF (2009) Macrophage participation in the degradation and remodeling of extracellular matrix scaffolds. Tissue Eng Part A 15(7):1687–1694

Wang Y, Papadimitrakopoulos F, Burgess DJ (2013a) Polymeric "smart" coatings to prevent foreign body response to implantable biosensors. J Control Release 169(3):341–347

Wang Y, Wu NN, Mou YQ, Chen L, Deng ZL (2013b) Inhibitory effects of recombinant il-4 and recombinant il-13 on uhmwpe-induced bone destruction in the murine air pouch model. J Surg Res 180(2):e73–e81

Willert HG, Semlitsch M (1977) Reactions of the articular capsule to wear products of artificial joint prostheses. J Biomed Mater Res 11(2):157–164

Wimhurst JA, Brooks RA, Rushton N (2001) Inflammatory responses of human primary macrophages to particulate bone cements in vitro. J Bone Joint Surg 83 (2):278–282

Yanagita M (2012) Inhibitors/antagonists of tgf-beta system in kidney fibrosis. Nephrol Dial Transplant Off Publ Eur Dial Transplant Assoc Eur Ren Assoc 27 (10):3686–3691

Yoshizawa H, Morishita Y, Watanabe M, Ishibashi K, Muto S, Kusano E, Nagata D (2015) Tgf-beta(1)-sirna delivery with nanoparticles inhibits peritoneal fibrosis. Gene Ther 22(4):333–340

Artificial Methods for T Cell Activation: Critical Tools in T Cell Biology and T Cell Immunotherapy

13

Kyung-Ho Roh

13.1 Introduction

T lymphocytes play a conductor role in the immune system by orchestrating complex interactions between innate and adaptive immune cells. Protection from various infections as well as cancers is provided in an antigen-specific manner with immunological memory as a result of the functions of healthy T lymphocytes.

The special capability of T cells – to recognize antigens from various pathogens or endogenous mutations in a very specific, sensitive, and selective manner - is conferred by a clonally restricted receptor molecule, the T cell receptor (TCR). Therefore, any discussion regarding biomaterials that are designed for the engineering of T cell functions cannot be made without a proper discussion of the structure and the function of TCR and its related molecules. The TCR is membrane bound, and specifically interacts with not a soluble antigen by itself but an antigenic peptide combined with a molecule encoded by the major histocompatibility complex (pMHC) which is expressed on a membrane of an antigen presenting cell (APC) or a target cell. Thus, the cellular interface between the T cell and the counterpart cell is very important in determining T cell functions, and has been described as the immunological synapse (IS).

We will first briefly review the biology of TCR and IS. And we will focus our discussion to the biomimetic designs that have been developed to study and/or engineer T cell functions through recapitulating or modifying TCR-pMHC interactions and the spatiotemporal molecular dynamics within the IS.

13.2 T Cell Receptor (TCR)

The TCR is a heterodimer of either *alpha and beta* chains or *gamma and delta* chains, and the T cell that expresses the corresponding pairs is called αβ T cell or γδ T cell, respectively (Davis and Bjorkman 1988). The αβ TCR demonstrates a high degree of antigen specificity and thus becomes a hallmark molecule of the adaptive immune system along with the antibody of the B cell. By contrast, γδ T cells recognize classes of antigens present on ranges of pathogens, whose functions more belong to innate immunity. In this chapter, we will focus our discussion on αβ T cells.

The α and β TCR chains are classified as members of the immunoglobulin superfamily. Each chain contains one variable and one constant domain which are structurally homologous to the variable and constant domains of immunoglobulins. The TCR variable domain contains three complementary determining regions (CDR1-3) that are hypervariable. The

K.-H. Roh (✉)
Department of Chemical and Materials Engineering, University of Alabama in Huntsville, Huntsville, AL, USA
e-mail: kyung-ho.roh@uah.edu

I. Noh (ed.), *Biomimetic Medical Materials*, Advances in Experimental Medicine and Biology 1064,
https://doi.org/10.1007/978-981-13-0445-3_13

interaction between αβ TCRs and antigen is determined by the combined affinities 1) between CDR1 or 2 loops and conserved regions of the MHC molecule and 2) between CDR3 and antigenic pMHC (Garcia et al. 1996).

In order to provide immune protection from a wide range of pathogens with antigen specificity, healthy human individuals might possess 10^7~10^8 different TCR specificities (clonotypes) (Arstila et al. 1999). In fact, the theoretically possible TCR diversity (number of different pairs of α and β TCR chains that can be produced) far exceeds the number of TCR repertoire present at a given point in time (Nikolich-Zugich et al. 2004). This amazing diversity of immune receptors (TCR and immunoglobulins) originates from their unique genetic features. Unlike most other genes that contain single complete genes in a given locus, the genes encoding TCR chains (along with the genes encoding immunoglobulin heavy and κ or λ light chains) are composed of families of gene segments that should be rearranged before they can be transcribed. For humans, TCR α and β chain genes are located on chromosomes 14 and 7, respectively. Each TCR chain is composed of gene segments that encodes the leader peptide, the variable, and the constant regions. The germline DNAs for variable region in chromosome 14 (TCR α chain) consist of many alternative variable (V) and joining (J) segments. In chromosome 7 (TCR β chain), an additional set of segments called diversity (D) gene segments are located between V segments and J segments. In the recombination process, a mechanistic rule guarantees that each TCR chain is precisely formed by joining of only one of each V and J segments (TCR α chain), or V, D, and J segments (TCR β chain). This is achieved by recombination that is restricted to only occur between the two different types of recombination signal sequences (RSSs) flanking each V, D, and J genes. This random combinatorial way of forming TCR α and β chains using alternative gene segments significantly contributes to the diversity of TCR antigen specificities. Another major mechanism to diversify the TCR repertoire is junctional diversity. As part of the recombination process, the junctions between the V and J segments or between V, D, and J segments are additionally diversified with palindromic (P) sequences of cleaved sites (by action of recombination activating gene proteins (RAG1 and RAG2) as well as randomly added new sequences (N-nucleotides) by action of terminal deoxynucleotidyl transferase (TdT). As CDR3 is encoded at the junctions between the V and J segments or between V, D, and J segments, this mechanism to create junctional diversity heavily contributes to the increase of functional diversity in TCR repertoire.

Even if there are exceptions (Padovan et al. 1993; Davodeau et al. 1995; Heath et al. 1995; Cochran et al. 2001), allelic exclusion of genes for the TCR α and β chains occurs in most developing T cells in the thymus (thymocytes). So a given immature T cell would likely express one kind of functional αβ TCR. Among the enormous TCR repertoire that are randomly generated by the above-mentioned mechanisms (order of 10^{15} for the αβ receptor) (Nikolich-Zugich et al. 2004), i.e. the repertoire of thymocytes, only a small fraction of thymocytes survive after the two following selection processes. First, only the thymocytes bearing receptors capable of binding self-MHC molecules can survive (positive selection). Second, thymocytes bearing high-affinity receptors for self-MHC molecules or self-peptide presented by self-MHC are eliminated (negative selection). The surviving thymocytes without apoptosis after both selection processes become mature T cells bearing receptors that are "self-restricted" as well as "self-tolerant". It is worth mentioning that some of the gene rearrangement (particularly TCR α-chain) occur simultaneously involving RAG-1, RAG-2, and TdT activities during the positive selection.

Both TCR α and β chains have a positively-charged transmembrane domain and a short cytoplasmic tail at its C-terminus (Blumberg et al. 1990). The cytoplasmic region of αβ TCR is not long enough to transduce the signal initiated by interaction with antigenic pMHC. The accessory molecules that are critical for TCR signal transduction and even for the successful expression of TCR are designated as the CD3 complex. The CD3 complex is composed of three dimers (γε,

δε, and ζζ or ζη) formed by five invariant polypeptide chains (γ, δ, ε, η, and ζ). A negatively-charged residue within the transmembrane regions of all CD3 chains interacts with positively charged amino acid residues in the transmembrane region of each TCR chain, which helps the association between CD3 and TCR polypeptide chains (Call and Wucherpfennig 2004). The cytoplasmic tails of the CD3 chains contain a common sequence called the immunoreceptor tyrosine-based activation motif (ITAM), which interacts with tyrosine kinases to play a major role in signal transduction. The CD3 ζ and η chains each contain three ITAMs, whereas the γ, δ, and ε chains each contain only a single copy of ITAM.

13.3 T Cell Activation

The molecular details of signaling cascades following T cell activation and the subsequent alteration of numerous gene expressions is beyond the scope of this chapter. Instead, we will review the most critical molecular components and cellular behaviors that should primarily be considered when developing the biomimetic design of biomaterials that engineer T cell functions. The initial interest lies on the molecular components and their functions within the interface between a T cell and an antigen presenting cell (APC).

Due to the unique role of T cells which respond to pathogens in an antigen-specific manner, the interaction between TCR and pMHC determine its fate and function in almost every stage of a T cell's life span from its early development in the thymus to the fully activated and terminally differentiated effector stage in the periphery. As mentioned earlier, within the thymus, interactions between TCR and self-MHC molecules or self-peptide presented by self-MHC molecules and the consequent intracellular signals determine the fate of developing T cells. The T cells that have completed their development stages exit the thymus and circulate the bloodstream and the lymph through secondary lymphoid organs such as lymph nodes and the spleen in surveillance of foreign antigens. These "non-activated" T cells that have not encountered foreign antigens are called "naïve".

In addition to TCR, there are two kinds of co-receptors designated as CD4 and CD8 on the T cell membrane, and an individual T cell is committed to express only one kind of co-receptor before it is fully developed and exit the thymus. Reflecting their respective effector functions and roles, CD4+ and CD8+ T cells are called "helper" T cells and "cytotoxic" T cells, respectively. TCRs on CD4+ T cells only interact with exogenous peptides presented by class II MHC molecules which are only expressed by phagocytic professional ACPs such as dendritic cells (DCs), macrophages, and B cells. Meanwhile, TCRs on CD8+ T cells only interact with self- or virus-originated peptides presented by class I MHC molecules which are expressed by most cells including professional APCs. Despite this critical difference between CD4+ and CD8+ T cells, the naïve population of both types are commonly required to be properly activated before they can function as effector cells.

As described earlier, the interaction between TCR and the foreign peptide presented by either class I or class II MHC molecules expressed on the plasma membrane of professional APCs becomes a primary signal for T cell activation and dictates the initial activation of naïve T cell. However, a mere TCR-pMHC interaction is not sufficient to fully activate a naïve T cell. The additional requirement is called co-stimulation, and there are multiple molecular interactions between a T cell and an APC that provide co-stimulatory signals. The most important one is the engagement of CD28 on the T cell by CD80 (B7-1) or CD86 (B7-2) on the APC. It is shown that the TCR engaged by pMHC without co-stimulation signals induce the T cell to an "anergic" state (Appleman and Boussiotis 2003). Once the T cell becomes anergic, it maintains this inactivated state even when the T cell is exposed to APC with both antigenic pMHC and costimulatory molecules. The third component that completes the activation of the T cell is various cytokines. Some of these soluble cytokines are secreted either by the T cell itself or by neighboring APC or other cells regulated by

feedback loops. The cytokines secreted by the T cell itself can work as both autocrine and paracrine. As an example, interleukin-2 (IL-2) secreted by T cell is important for the clonal expansion of antigen-specific T cell populations and their differentiation into effector cells.

13.4 Spatiotemporal Molecular Reorganization at the Immunological Synapse

As a result of the interaction between the TCR and its cognate pMHC, the T cell and APC or a target cell form a tightly apposed cellular interface, which is called the immunological synapse (IS). Over the past couple of decades, the spatiotemporal dynamics of molecules within the IS has been extensively studied (Grakoui et al. 1999; Bunnell et al. 2002; Huppa and Davis 2003). The name of IS was initially coined after the initial observation of concentric rings (so called bull's-eye pattern) of membrane receptors and adhesion molecules on T cell membrane upon T cell-APC interaction. Subsequent studies discovered that TCR and CD28 molecules are concentrated within the innermost circle (central supramolecular activation cluster, cSMAC), which are surrounded by peripheral SMAC (pSMAC) of integrins (e.g. LFA-1). Lastly, the outermost ring or distal SMAC (dSMAC) is occupied by proteins that have relatively longer ectodomains (e.g. CD43, CD45). Since then, many studies have been attempted to define the true functions of the IS with the bull's-eye pattern. And continuous TCR signaling is required for maintenance the SMAC structure of IS and extended effector functions (Huppa et al. 2003). Later it was discovered that the lasting TCR signaling is maintained by the microclusters that are continuously and newly generated in the peripheral or distal regions of IS (Yokosuka et al. 2005). It is now well accepted that the microcluster of TCR and other signaling molecules (kinases and adaptors) are the activation signaling cluster. These newly generated TCR microclusters in the distal region are translocated into the central region (cSMAC), where the TCR signaling ceases while TCR molecules break apart from other signaling components. Therefore, cSMAC might function toward the regulation of TCR signaling and molecular recycling. Nevertheless, it has been suggested that the selective and polarized secretion of lytic granules are another function of the cSMAC and the bull's-eye pattern of IS between cytotoxic T cells and target cells (Davis and Dustin 2004).

Furthermore, the bull's-eye pattern is not the unique molecular pattern of IS. For example, a helper T cell forms a multifocal IS in its interaction with a dendritic cell that present the cognate antigens (pMHCs) (Brossard et al. 2005; Dustin et al. 2006). The double positive (CD4 + CD8+) thymocytes also form a decentralized multifocal pattern of TCR accumulation surrounded by ICAM-1 molecules when examined on a lipid bilayer (Hailman et al. 2002).

More recently, owing to the progress in super-resolution microscopy techniques, the spatiotemporal dynamics of TCR and other molecules have been studied in a molecular length scale. And it has been shown that these critical signaling components including TCR complex (e.g. CD3 ζ) (Lillemeier et al. 2010), co-receptor (e.g. CD4) (Roh et al. 2015), adaptor (e.g. Lat) (Lillemeier et al. 2010; Sherman et al. 2011; Williamson et al. 2011), and kinases (e.g. p53lck) (Rossy et al. 2013) are all residing within nano-sized clusters even before the activation of T cells, and these nanoclusters coalesce to form bigger clusters (microclusters) upon engagement of TCR molecules with the cognate pMHCs.

Many steps of these intricate spatial reorganizations within IS and their downstream signaling events are intricately related to cytoskeletal dynamics (e.g. actin rearrangements)

(Miletic et al. 2003; Tskvitaria-Fuller et al. 2003) and integrin adhesion (e.g. LFA-1 to ICAM-1) (Burbach et al. 2007).

13.5 Biomimetic and Artificial Methods to Induce T Cell Activation

To artificially activate T cells, biomimetic design is intrinsically involved. First, biochemical reagents that can effectively engage with the TCR should be selected. Depending on the antigen-specificity requirement, the reagents will be varied, for example, an anti-CD3 antibody for the activation of general T cell population vs. a specific pMHC or a collection of different pMHCs for the activation of antigen-specific T cells. Second, the use of accessory ligands (e.g. for co-stimulatory signals or for effective adhesion) should be considered. Third, the format of presentation (e.g. soluble, plate-bound, membrane-bound, etc.) for such ligands to T cells needs to be determined. All of these design components are deterministic factors for molecular affinity between receptor and ligand and their binding kinetics within immunological kinapses (transient contacts with pro-migratory junctions) and immunological synapses (contacts for a prolonged period with stable junctions) (Fooksman et al. 2010).

Although the exact mechanism of how the very initial TCR triggering is induced is unknown, a number of leading models (van der Merwe and Dushek 2011), namely aggregation model, conformational change model, segregation or redistribution model, serial triggering model (Valitutti et al. 1995), and kinetic proofreading model (McKeithan 1995; Rabinowitz et al. 1996), have been suggested to explain its mechanisms. Historically, various artificial methods of inducing T cell activation have been developed to test these models and hypotheses. In addition, many surface-associated methods were developed as biomimetic tools to study the spatiotemporal dynamics of IS under the microscope. Nevertheless, these various methods can induce varying degrees of T cell activation (Table 13.1) and thus might be useful for particular biomedical applications.

13.5.1 Soluble Reagents

Typically the affinity between TCR and its cognate agonist pMHC has been measured by the use of surface plasmon resonance (SPR). In SPR measurement, one is bound to the surface, and the other binding partner is in the solution, which might well reflect the interactions between soluble reagents and the TCRs on T cell membranes. And from SPR measurements, TCRs have relatively low affinities (K_D values in the range of 1–100 μM) against their cognate agonist pMHCs (Stone et al. 2009), which are combined effects of slow association rates and intermediate dissociation rates. These affinity values are similar to those of antibodies against their antigen in their primary responses, *i.e.* before affinity maturation.

Reflecting these low solution affinity values between TCRs and pMHCs, agonistic pMHC monomers in solution are incapable of inducing T cell activation (Cochran et al. 2000). In fact, the soluble form of high-affinity anti-TCR Fab is incapable of activating T cell either (Yoon et al. 1994). In stark comparison, anti-CD3 antibody in solution can induce T cell activation even if it is partial (Bekoff et al. 1986). Activation can be more robust by using anti-CD28 antibody simultaneously or employing some accessory cells. Thus it is clear that the crosslinking of TCR-CD3 complex is critical for T cell activation. This notion has been further confirmed by well-designed soluble reagents (Fig. 13.1). Cochran et al. (2000, 2001) first introduced maleimide functional groups to the amine side chain of lysine residues within oligopeptides with precisely controlled distance between the lysine residues. By introducing free thiol (cysteine side group) at either α or β chain of recombinant pMHC molecule, 2, 3, or 4 pMHC monomers could be attached to a single peptide chain. All dimer, trimer, and tetramer agonist pMHC could fully activate the T cells (Cochran et al. 2000) and the pMHC dimers coupled through shorter intermolecular distances were

Table 13.1 Comparison of TCR activation platforms and responses

Ligand and presentation platform	Ligand: TCR[a]	TCR activation	Comments	Reference
Soluble				
Agonist pMHC monomers	1:1	No activation	No activation despite binding of monomers to TCR	Cochran et al. (2000)
Agonist pMHC dimers	2:2	Full and sustained	Intermolecular distance is critical	Cochran et al. (2000, 2001)
Agonist/ endogenous pMHC heterodimers	2:2	Full and sustained	CD4 involvement is critical	Krogsgaard et al. (2005)
Anti-TCR fab	1:1	No activation	Low affinity (μM K_d), might not be stable	Yoon et al. (1994)
Anti-CD3 antibody	2:2	Partial	Signaling not blocked by actin depolymerization	Bekoff et al. (1986), Wolff et al. (1993)
Crosslinked anti-CD3	2:2+	Full and transient	CD69 upregulation	Bekoff et al. (1986)
Immobilized surface anchored				
Anti-CD3 antibody	2:2+	Full and sustained	Stable bivalent ligand induces clustering, may generate force for mechanotransduction	Bunnell et al. (2002)
Fluid membrane anchored				
Agonist pMHC monomers	1:1+	Full and sustained if >0.2 pMHC/ μm^2	Requires F-actin, myosin IIA and adhesion to ICAM-1	Grakoui et al. (1999), Varma et al. (2006), Ma et al. (2008), Ilani et al. (2009)

Adapted and modified from Reference Fooksman et al. (2010)
[a]Stoichiometry of engagement
+ Higher-order crosslinking may be present

consistently more potent than those coupled through longer intermolecular distances (Cochran et al. 2001). Furthermore, the same crosslinking strategy was employed by Krogsgaard et al. to construct a heterodimer of agonist pMHC coupled with endogenous pMHC molecules (Krogsgaard et al. 2005). And these heterodimers were capable of inducing T cell activation in a CD4 dependent manner (Krogsgaard et al. 2005). Altogether, T cell activation can be effectively induced by designing soluble reagents that can crosslink the TCR-CD3 complexes. Even if it is still unclear whether and how exactly the strength, duration, and signaling outputs on T cell activations using different soluble reagents are different, the implications on various applications will be further discussed in latter sections.

13.5.2 Surface-Bound Ligands

The physiological TCR and pMHC interactions essentially occur between two cell membrane surfaces. Therefore, simply anchoring the soluble ligands onto a surface might bring a change in the nature of interactions. Indeed, monomeric agonistic pMHCs on either fixed plastic surfaces or fluid lipid bilayers in extremely dilute surface density (< 10 per cell) can effectively trigger the activation of cognate T cells (Ma et al. 2008), while the solution counterparts cannot. This surface-anchorage effect could be interpreted in multiple ways, but it is at least clear that it is dependent on T cell adhesion to the surface and intact cytoskeletal function (Ma et al. 2008; Ilani et al. 2009). Additionally, the above-mentioned SPR-based affinity measurements may not represent the whole picture of how these affinity values and parameters are related to the T cell activation. In

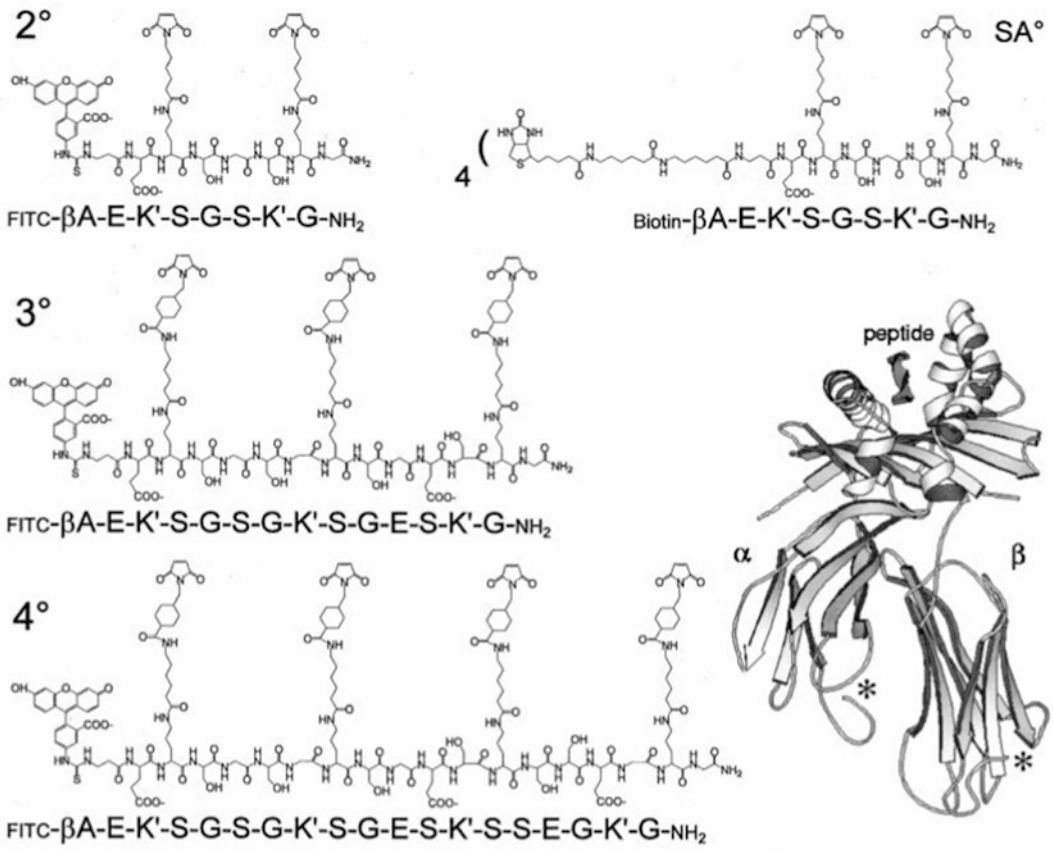

Fig. 13.1 Design and chemical structures of soluble pMHC oligomers: All crosslinkers carry maleimide groups for coupling to cysteine resides introduced into HLA-DR1. Left, fluorescein-labeled, peptide-based crosslinkers for production of MHC dimers (2°), trimers (3°), and tetramers (4°). Upper right, biotin-labeled dimeric crosslinker for production of higher order streptavidin-linked oligomers (SA^o). Lower right, ribbon diagram of the HLA-DR1-peptide complex (Stern et al. 1994), showing the position of cysteine residues (positions marked with asterisks) introduced at the end of either the α or β subunit connecting peptide region. The HLA-DR1 model is shown at approximately 80% of the scale of the chemical diagrams of the cross-linking reagents. Adapted from reference (Cochran et al. 2000). Copyright© 2000, Cell Press

fact, on a plasma membrane, membrane-associated molecules are constricted in 2D diffusion, while the molecules in solution phase are freely movable in 3D. The loss in kinetic degrees of freedom due to the newly formed molecular association between any pair of molecules is considered to be 6 (x, y, and z translation and x, y, and z rotation), 3 (x, y translation and z rotation), or 0 for molecules in soluble (3D), anchored in 2D fluidic membrane, or fixed in immobilizing hard surface, respectively (Fig. 13.2). Therefore, it is expected that the affinity values are intrinsically increased by restricting the soluble activating ligands (pMHCs and other co-stimulatory and integrin binding molecules) onto 2D surfaces (faster on rate and slower off rate). It is indeed commonly observed that more robust T cell activation is induced by surface-bound pMHC or anti-CD3 antibody than by the soluble counterpart.

However, measuring 2D binding properties of TCR and pMHC in practice turned out to be more complicated. Recently, the 2D binding kinetics of TCR-pMHC have been explored using two

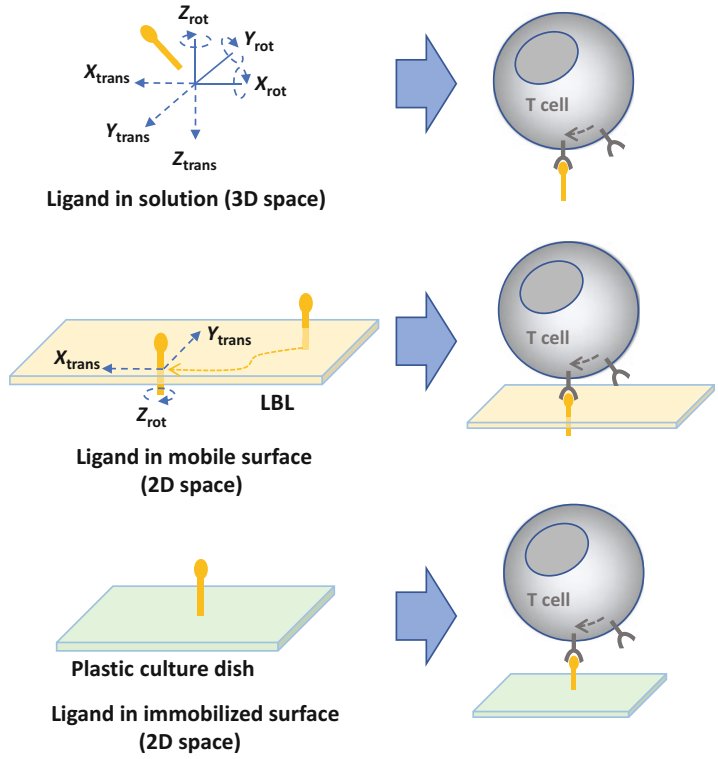

Fig. 13.2 Receptor binding to ligands in a solution (3D), in a lipid bilayer (mobile 2D), and in a solid surface (immobilized 2D). The degrees of freedom before the receptor-ligand binding are 6, 3, and 0, for solution, mobile 2D, and immobilized 2D, respectively. The physiological immune receptor-ligand interactions typically occur at the interface between two opposing cell membranes (immunological synapse)

completely different methods, (i) optical microscopy based on fluorescent resonance energy transfer (FRET) (Huppa et al. 2010) and (ii) mechanical assay based on observation of bonding and deformation (Huang et al. 2010). Intriguingly, in both studies, 2D k_{off} was measured to be significantly faster than the solution (3D) k_{off} values. Again in both studies, the 2D k_{on} values varied in large dynamic ranges (Huang et al. 2010; Huppa et al. 2010) while the 3D counterparts did not (Huang et al. 2010). Furthermore, both the dramatically varying 2D k_{on} rates and fast 2D k_{off} correlated with activation potency, while 3D k_{off} values showed inverse correlation (Huang et al. 2010). All of these interesting data indicated that the TCR-pMHC interaction is subject to mechanical forces, mainly by the actin cytoskeleton, and that the local environment of the direct vicinity of TCR-CD3 complex (e.g. surface density, molecular orientation) dynamically changes upon TCR-pMHC engagement.

Even if measuring 2D binding properties is a very complicated task for the above-mentioned reasons, at least it is clear that localizing TCR triggering signals (pMHC and other ligands) in 2D with biomimetic biomaterial-based design has tremendous implications in T cell activation and functional programing.

13.5.2.1 Immobilized Ligands on Surfaces

As the simplest method of immobilization, ligands (proteins) can be non-specifically adsorbed to 2D surfaces. For in-vitro activation of T cells and resulting T-cell expansions, non-specifically coating the culture dish with anti-CD3 antibodies along with anti-CD28 antibodies has long been used (Lewis et al. 2015). Some examples of antibody clones that are widely employed for this purpose include clone 145-2C11 (anti-mouse CD3ε), OKT3 or HIT3a (anti-human CD3), 37.51 (anti-mouse CD28), and CD28.2 (anti-human CD28).

These antibodies and/or pMHC and recombinant B7 molecules were also immobilized on the surface of synthetic microbeads, which is often called artificial antigen presenting cells (aAPCs) even though the particles are incapable of processing the antigens per se (Curtsinger and Khazaeli 1997; Trickett and Kwan 2003; Walter et al. 2003; Kim et al. 2004; Schilbach et al. 2005; Durai et al. 2009). Both polystyrene beads of 5–6 μm in diameter (so called latex beads) (Curtsinger and Khazaeli 1997; Walter et al. 2003; Schilbach et al. 2005) and commercially available magnetic beads (e.g. Dynabeads®) (Trickett and Kwan 2003; Durai et al. 2009) have been extensively employed as aAPC platforms to expand antigen-nonspecific (with anti-CD3 antibody) or antigen-specific (with pMHC molecule) T cell populations.

Recombinant membrane proteins (e.g. pMHC) or soluble antibodies were successfully incorporated onto the surface of polystyrene beads by non-specific adsorption with or without the aid of co-incubating surfactants (Curtsinger and Khazaeli 1997). For better control over surface density and potentially better molecular orientation, more specific interactions, such as streptavidin to biotin (Walter et al. 2003; Schilbach et al. 2005), anti-Fc antibody or protein A/G to Fc portion of antibody (Trickett and Kwan 2003) or Fc-containing recombinant proteins (Durai et al. 2009), have been employed for the conjugation of T cell activating reagents to the surface of aAPC beads. It is worth mentioning that magnetic Dynabeads® presenting anti-CD3 and anti-CD28 antibodies have been employed as a gold standard for the expansion of CD8+ cytotoxic T cells in recent T cell adoptive therapy trials, due to their easy purification steps using magnets.

In order to observe spatiotemporal dynamics of TCRs and other signaling molecules under microscope, pMHC and B7.1 molecules have also been immobilized on thin glass slides (Lillemeier et al. 2010; Roh et al. 2015). By incubating positively charged poly(L-lysine) (PLL) chains that are conjugated with biotin residues on top of negatively charged glass slides, the surface of the glass slide could be effectively modified with biotin residues. After subsequent incubation with streptavidin, biotinylated pMHC and B7.1 molecules could be immobilized on glass slides. The observation of the T cell membrane molecules interacting with these immobilized activating ligands under the microscope revealed that the TCRs form microclusters, as a result of actin-dependent clustering (concatenation) of smaller nanoclusters, but they could not develop into mature SMACs, potentially due to the spatially fixed activating ligands (Lillemeier et al. 2010).

This observation clearly demonstrates the potential limitations of the surface-immobilized antibodies or natural ligands, which is associated with their incapability of generating dynamic remodeling of physiological IS between T cells and APCs or target cells. This leads us to the discussion of development of artificial platforms with which ligands are presented in a mobile layer.

13.5.2.2 Mobile Ligands Attached to Plasma Membrane-Mimetic Fluidic Surfaces

The molecules within the IS dynamically reorganize during T cell activation as mentioned above. Therefore, the importance of providing lateral mobility of molecular ligands to T cells has long been recognized. The supported lipid bilayer (LBL) has been developed as an effective biomimetic platform to study cell-cell interactions between immune cells (McConnell et al. 1986; Sackmann 1996). The initial observation of the bull's eye pattern of IS was made on top of glass-slide-supported lipid bilayer presenting agonistic pMHC and ICAM-1 (Grakoui et al. 1999). For the preparation of this artificial membrane layer, they first expressed glycosylphosphatidylinositol (GPI)-modified pMHC and ICAM-1 in CHO and BHK cells, respectively, and successfully incorporated them into liposomes containing 1,2-dioleoyl-sn-glycero-3-phosphatidylcholine (DOPC). Finally, these liposomes were incubated on a clean glass slide. Similarly designed mobile LBLs have been employed to study the spatiotemporal dynamics of IS under the microscope (Varma et al. 2006).

Instead of GPI-anchored proteins, others expressed recombinant proteins (pMHC, B7.1, and ICAM-1) with multi-histidine tag (His-tag) for specific association onto glass-slide supported lipid bilayer composed of 1-palmitoyl-2-oleoyl-sn-glycero-3-phosphocholine (POPC) and 1,2-dioleoyl-sn-glycero-3-[(N-(5-amino-1-carboxypentyl)iminodiacetic acid) succinyl] (nickel salt) (DGS-NTA(Ni)) (Huppa et al. 2010; Roh et al. 2015).

In order to mimic the preclustered membrane microdomains on the APC surface, Albani and colleagues introduced neutravidin to the supported LBL. Biotinlyated cholera toxin B (CTB) along with biotinylated antibodies and pMHC complexes were first bound to neutravidin. By utilizing the affinity between CTB and the monosialoganglioside (GM1), the whole protein complex with neutravidin as a scaffolding unit was attached to supported LBL composed of phosphatidylcholine, cholesterol and GM1.

LBL was also formed on glass substrates displaying various patterns of chromium lines (100 nm wide and 5 nm high) fabricated using electron-beam lithography (Mossman et al. 2005). These nanoscale chromium lines became barriers for the lateral movement of pMHC-TCR complex, which created IS with artificial geometric molecular patterns. Within these repatterned molecular structures in IS, the TCR microclusters mechanically trapped in the peripheral regions showed prolonged signaling compared to the central counterparts (Mossman et al. 2005), which reinforced the idea that cSMAC may function as a signal termination site.

The aAPCs with laterally mobile activating ligands have also been constructed in a non-planar geometry, i.e. spherical shape. Liposomes of 60–90 nm in size were constructed with cholesterol and phosphatidylcholine to effectively present agonistic pMHC molecules (60–160 per aAPC) to detect and activate the cognate T cell population (Prakken et al. 2000). Similar to the above-mentioned planar LBL, the affinity between CTB and GM1 has been employed to construct the liposome aAPCs decorated with neutravidin-scaffolded anti-CD3, anti-CD28, and anti-LFA1 monoclonal antibodies (mAbs) (Zappasodi et al. 2008). These lipid aAPCs were similarly effective to the commercially available magnetic bead (anti-CD3, anti-CD28 mAbs) counterpart in activation and expansion of T cells (Zappasodi et al. 2008). The viscous oil droplets (liquid colloids) created by shear-induced rupturing in viscoelastic complex fluids have been surface grafted with anti-CD3 and anti-CD28 mAbs as aAPCs that are more similar to the physiological cells in size (a few microns) (Bourouina et al. 2012). Upon interacting with these aAPCs, T cells were activated to induce intracellular signaling and developed cytoskeleton-dependent dynamics at the interfaces (Bourouina et al. 2012).

In addition to these artificially constructed aAPCs, virus-like particles (VLP) were produced by mammalian cells (HEK293 cells) infected with Moloney murine leukemia virus (Derdak et al. 2006). In order to effectively decorate the VLPs with TCR ligands (either scFv of anti-CD3 antibody or pMHC) as well as the costimulatory ligand (CD80) and the intracellular adhesion molecule (ICAM-1), the recombinant constructs of these molecules were linked to GPI anchor sequences. These molecules were specifically localized into lipid rafts on HEK293 cells, which were heavily transferred to the membranes of budding VLPs. Using this VLP-based aAPC, T cells were successfully stimulated either in antigen-specific or non-specific manner (Derdak et al. 2006). Exosomes (Thery et al. 2002) are another important category of cell-derived vesicles that can act as aAPC. These small (30–150 nm) extracellular vesicles secreted from cellular endosomes of dendritic cells could present pMHC molecules as well as costimulatory and adhesion molecules to CD4+ or CD8+ T cells (Zitvogel et al. 1998). Exosomes derived directly from tumor cells have also been employed to boost the antigen-specific T-cell immune responses in vivo (Wolfers et al. 2001). These anti-tumor activities might be a result of combined effects of direct interaction between exosomes and T cells as well as indirect priming of T cells through exosome targeted DCs (Syn et al. 2017).

13.6 Conclusions

At the basis of the central roles of T cells in the adaptive immune system, there is the specific molecular interaction between TCR and pMHC molecular complex. The antigen recognition in a very selective, sensitive, and specific manner induces the activation of T cells with intricate signaling pathways. As the T cell activation continues, the interface between the T cell and the APC or the target cell develop into mature IS with spatially reorganized molecular structures in various sizes (from molecular nanostructures to cellular microstructures).

A variety of biobimetic artificial methods to induce T cell activation has been pursued. Actually many of these methods were developed as a tool to study the molecular and cellular mechanisms of T cell activations. Here we briefly reviewed these methods in three different categories, i.e. i) soluble, ii) immobilized-surface-bound, and iii) mobile-surface-bound forms.

As adoptive T cell therapy continuously creates tremendous success cases in pre-clinical and clinical studies, the need for effective and clinically-relevant methods of T cell activation and expansion is also ever-growing. Various aAPCs summarized above have tremendous potential, while genetically-modified cell-based aAPCs (Maus et al. 2002) also may have ample room to contribute with their unique attributes (Kim et al. 2004).

Here, we have discussed the physicochemical implications of presenting ligands in different formats (e.g. 3D vs. 2D, immobilized vs. fluidic). These differences may affect the strength, duration, and/or the nature of T cell activations, which in turn may yield different phenotypes and functions of final T cell populations (Li and Kurlander 2010). Therefore, the platform of activation should be carefully selected for each intended purpose, and further studies are warranted to better understand the relationship between the final fate of the T cell and the methods of artificial T cell activation varied by above-mentioned engineering parameters as well as other parameters such as mechanical properties of the substrate (O'Connor et al. 2012).

References

Appleman LJ, Boussiotis VA (2003) T cell anergy and costimulation. Immunol Rev 192:161–180

Arstila TP, Casrouge A, Baron V, Even J, Kanellopoulos J, Kourilsky P (1999) A direct estimate of the human alphabeta T cell receptor diversity. Science 286(5441):958–961

Bekoff M, Kubo R, Grey HM (1986) Activation requirements for normal T cells: accessory cell-dependent and -independent stimulation by anti-receptor antibodies. J Immunol 137(5):1411–1419

Blumberg RS, Alarcon B, Sancho J, McDermott FV, Lopez P, Breitmeyer J, Terhorst C (1990) Assembly and function of the T cell antigen receptor. Requirement of either the lysine or arginine residues in the transmembrane region of the alpha chain. J Biol Chem 265(23):14036–14043

Bourouina N, Husson J, Hivroz C, Henry N (2012) Biomimetic droplets for artificial engagement of living cell surface receptors: the specific case of the T-cell. Langmuir 28(14):6106–6113

Brossard C, Feuillet V, Schmitt A, Randriamampita C, Romao M, Raposo G, Trautmann A (2005) Multifocal structure of the T cell - dendritic cell synapse. Eur J Immunol 35(6):1741–1753

Bunnell SC, Hong DI, Kardon JR, Yamazaki T, McGlade CJ, Barr VA, Samelson LE (2002) T cell receptor ligation induces the formation of dynamically regulated signaling assemblies. J Cell Biol 158 (7):1263–1275

Burbach BJ, Medeiros RB, Mueller KL, Shimizu Y (2007) T-cell receptor signaling to integrins. Immunol Rev 218:65–81

Call ME, Wucherpfennig KW (2004) Molecular mechanisms for the assembly of the T cell receptor-CD3 complex. Mol Immunol 40(18):1295–1305

Cochran JR, Cameron TO, Stern LJ (2000) The relationship of MHC-peptide binding and T cell activation probed using chemically defined MHC class II oligomers. Immunity 12(3):241–250

Cochran JR, Cameron TO, Stone JD, Lubetsky JB, Stern LJ (2001) Receptor proximity, not intermolecular orientation, is critical for triggering T-cell activation. J Biol Chem 276(30):28068–28074

Curtsinger JW, Khazaeli A (1997) A reconsideration of stress experiments and population heterogeneity. Exp Gerontol 32(6):727–729

Davis MM, Bjorkman PJ (1988) T-cell antigen receptor genes and T-cell recognition. Nature 334 (6181):395–402

Davis DM, Dustin ML (2004) What is the importance of the immunological synapse? Trends Immunol 25 (6):323–327

Davodeau F, Peyrat MA, Romagne F, Necker A, Hallet MM, Vie H, Bonneville M (1995) Dual T cell receptor beta chain expression on human T lymphocytes. J Exp Med 181(4):1391–1398

Derdak SV, Kueng HJ, Leb VM, Neunkirchner A, Schmetterer KG, Bielek E, Majdic O, Knapp W, Seed B, Pickl WF (2006) Direct stimulation of T lymphocytes by immunosomes: virus-like particles decorated with T cell receptor/CD3 ligands plus costimulatory molecules. Proc Natl Acad Sci USA 103(35):13144–13149

Durai M, Krueger C, Ye Z, Cheng L, Mackensen A, Oelke M, Schneck JP (2009) In vivo functional efficacy of tumor-specific T cells expanded using HLA-Ig based artificial antigen presenting cells (aAPC). Cancer Immunol Immunother 58(2):209–220

Dustin ML, Tseng SY, Varma R, Campi G (2006) T cell-dendritic cell immunological synapses. Curr Opin Immunol 18(4):512–516

Fooksman DR, Vardhana S, Vasiliver-Shamis G, Liese J, Blair DA, Waite J, Sacristan C, Victora GD, Zanin-Zhorov A, Dustin ML (2010) Functional anatomy of T cell activation and synapse formation. Annu Rev Immunol 28:79–105

Garcia KC, Degano M, Stanfield RL, Brunmark A, Jackson MR, Peterson PA, Teyton L, Wilson IA (1996) An alphabeta T cell receptor structure at 2.5 A and its orientation in the TCR-MHC complex. Science 274(5285):209–219

Grakoui A, Bromley SK, Sumen C, Davis MM, Shaw AS, Allen PM, Dustin ML (1999) The immunological synapse: a molecular machine controlling T cell activation. Science 285(5425):221–227

Hailman E, Burack WR, Shaw AS, Dustin ML, Allen PM (2002) Immature CD4(+)CD8(+) thymocytes form a multifocal immunological synapse with sustained tyrosine phosphorylation. Immunity 16(6):839–848

Heath WR, Carbone FR, Bertolino P, Kelly J, Cose S, Miller JF (1995) Expression of two T cell receptor alpha chains on the surface of normal murine T cells. Eur J Immunol 25(6):1617–1623

Huang J, Zarnitsyna VI, Liu B, Edwards LJ, Jiang N, Evavold BD, Zhu C (2010) The kinetics of two-dimensional TCR and pMHC interactions determine T-cell responsiveness. Nature 464 (7290):932–936

Huppa JB, Davis MM (2003) T-cell-antigen recognition and the immunological synapse. Nat Rev Immunol 3 (12):973–983

Huppa JB, Gleimer M, Sumen C, Davis MM (2003) Continuous T cell receptor signaling required for synapse maintenance and full effector potential. Nat Immunol 4 (8):749–755

Huppa JB, Axmann M, Mortelmaier MA, Lillemeier BF, Newell EW, Brameshuber M, Klein LO, Schutz GJ, Davis MM (2010) TCR-peptide-MHC interactions in situ show accelerated kinetics and increased affinity. Nature 463(7283):963–967

Ilani T, Vasiliver-Shamis G, Vardhana S, Bretscher A, Dustin ML (2009) T cell antigen receptor signaling and immunological synapse stability require myosin IIA. Nat Immunol 10(5):531–539

Kim JV, Latouche JB, Riviere I, Sadelain M (2004) The ABCs of artificial antigen presentation. Nat Biotechnol 22(4):403–410

Krogsgaard M, Li QJ, Sumen C, Huppa JB, Huse M, Davis MM (2005) Agonist/endogenous peptide-MHC heterodimers drive T cell activation and sensitivity. Nature 434(7030):238–243

Lewis MD, de Leenheer E, Fishman S, Siew LK, Gross G, Wong FS (2015) A reproducible method for the expansion of mouse CD8+ T lymphocytes. J Immunol Methods 417:134–138

Li Y, Kurlander RJ (2010) Comparison of anti-CD3 and anti-CD28-coated beads with soluble anti-CD3 for expanding human T cells: differing impact on CD8 T cell phenotype and responsiveness to restimulation. J Transl Med 8:104

Lillemeier BF, Mortelmaier MA, Forstner MB, Huppa JB, Groves JT, Davis MM (2010) TCR and Lat are expressed on separate protein islands on T cell membranes and concatenate during activation. Nat Immunol 11(1):90–96

Ma Z, Sharp KA, Janmey PA, Finkel TH (2008) Surface-anchored monomeric agonist pMHCs alone trigger TCR with high sensitivity. PLoS Biol 6(2):e43

Maus MV, Thomas AK, Leonard DG, Allman D, Addya K, Schlienger K, Riley JL, June CH (2002) Ex vivo expansion of polyclonal and antigen-specific cytotoxic T lymphocytes by artificial APCs expressing ligands for the T-cell receptor, CD28 and 4-1BB. Nat Biotechnol 20(2):143–148

McConnell HM, Watts TH, Weis RM, Brian AA (1986) Supported planar membranes in studies of cell-cell recognition in the immune system. Biochim Biophys Acta 864(1):95–106

McKeithan TW (1995) Kinetic proofreading in T-cell receptor signal transduction. Proc Natl Acad Sci USA 92(11):5042–5046

Miletic AV, Swat M, Fujikawa K, Swat W (2003) Cytoskeletal remodeling in lymphocyte activation. Curr Opin Immunol 15(3):261–268

Mossman KD, Campi G, Groves JT, Dustin ML (2005) Altered TCR signaling from geometrically repatterned immunological synapses. Science 310 (5751):1191–1193

Nikolich-Zugich J, Slifka MK, Messaoudi I (2004) The many important facets of T-cell repertoire diversity. Nat Rev Immunol 4(2):123–132

O'Connor RS, Hao X, Shen K, Bashour K, Akimova T, Hancock WW, Kam LC, Milone MC (2012) Substrate rigidity regulates human T cell activation and proliferation. J Immunol 189(3):1330–1339

Padovan E, Casorati G, Dellabona P, Meyer S, Brockhaus M, Lanzavecchia A (1993) Expression of two T cell receptor alpha chains: dual receptor T cells. Science 262(5132):422–424

Prakken B, Wauben M, Genini D, Samodal R, Barnett J, Mendivil A, Leoni L, Albani S (2000) Artificial antigen-presenting cells as a tool to exploit the immune 'synapse'. Nat Med 6(12):1406–1410

Rabinowitz JD, Beeson C, Lyons DS, Davis MM, McConnell HM (1996) Kinetic discrimination in T-cell activation. Proc Natl Acad Sci USA 93 (4):1401–1405

Roh KH, Lillemeier BF, Wang F, Davis MM (2015) The coreceptor CD4 is expressed in distinct nanoclusters and does not colocalize with T-cell receptor and active protein tyrosine kinase p56lck. Proc Natl Acad Sci USA 112(13):E1604–E1613

Rossy J, Owen DM, Williamson DJ, Yang Z, Gaus K (2013) Conformational states of the kinase Lck regulate clustering in early T cell signaling. Nat Immunol 14(1):82–89

Sackmann E (1996) Supported membranes: scientific and practical applications. Science 271(5245):43–48

Schilbach K, Kerst G, Walter S, Eyrich M, Wernet D, Handgretinger R, Xie W, Rammensee HG, Muller I, Buhring HJ, Niethammer D (2005) Cytotoxic minor histocompatibility antigen HA-1-specific CD8+ effector memory T cells: artificial APCs pave the way for clinical application by potent primary in vitro induction. Blood 106(1):144–149

Sherman E, Barr V, Manley S, Patterson G, Balagopalan L, Akpan I, Regan CK, Merrill RK, Sommers CL, Lippincott-Schwartz J, Samelson LE (2011) Functional nanoscale organization of signaling molecules downstream of the T cell antigen receptor. Immunity 35(5):705–720

Stern LJ, Brown JH, Jardetzky TS, Gorga JC, Urban RG, Strominger JL, Wiley DC (1994) Crystal structure of the human class II MHC protein HLA-DR1 complexed with an influenza virus peptide. Nature 368 (6468):215–221

Stone JD, Chervin AS, Kranz DM (2009) T-cell receptor binding affinities and kinetics: impact on T-cell activity and specificity. Immunology 126(2):165–176

Syn NL, Wang L, Chow EK, Lim CT, Goh BC (2017) Exosomes in Cancer nanomedicine and immunotherapy: prospects and challenges. Trends Biotechnol 35 (7):665–676

Thery C, Zitvogel L, Amigorena S (2002) Exosomes: composition, biogenesis and function. Nat Rev Immunol 2(8):569–579

Trickett A, Kwan YL (2003) T cell stimulation and expansion using anti-CD3/CD28 beads. J Immunol Methods 275(1–2):251–255

Tskvitaria-Fuller I, Rozelle AL, Yin HL, Wulfing C (2003) Regulation of sustained actin dynamics by the TCR and costimulation as a mechanism of receptor localization. J Immunol 171(5):2287–2295

Valitutti S, Muller S, Cella M, Padovan E, Lanzavecchia A (1995) Serial triggering of many T-cell receptors by a few peptide-MHC complexes. Nature 375 (6527):148–151

van der Merwe PA, Dushek O (2011) Mechanisms for T cell receptor triggering. Nat Rev Immunol 11(1):47–55

Varma R, Campi G, Yokosuka T, Saito T, Dustin ML (2006) T cell receptor-proximal signals are sustained in peripheral microclusters and terminated in the central supramolecular activation cluster. Immunity 25 (1):117–127

Walter S, Herrgen L, Schoor O, Jung G, Wernet D, Buhring HJ, Rammensee HG, Stevanovic S (2003) Cutting edge: predetermined avidity of human CD8 T cells expanded on calibrated MHC/anti-CD28-coated microspheres. J Immunol 171(10):4974–4978

Williamson DJ, Owen DM, Rossy J, Magenau A, Wehrmann M, Gooding JJ, Gaus K (2011) Pre-existing clusters of the adaptor Lat do not participate in early T cell signaling events. Nat Immunol 12 (7):655–662

Wolfers J, Lozier A, Raposo G, Regnault A, Thery C, Masurier C, Flament C, Pouzieux S, Faure F, Tursz T, Angevin E, Amigorena S, Zitvogel L (2001) Tumor-derived exosomes are a source of shared tumor rejection antigens for CTL cross-priming. Nat Med 7 (3):297–303

Wolff CH, Hong SC, von Grafenstein H, Janeway CA Jr (1993) TCR-CD4 and TCR-TCR interactions as distinctive mechanisms for the induction of increased intracellular calcium in T-cell signalling. J Immunol 151(3):1337–1345

Yokosuka T, Sakata-Sogawa K, Kobayashi W, Hiroshima M, Hashimoto-Tane A, Tokunaga M, Dustin ML, Saito T (2005) Newly generated T cell receptor microclusters initiate and sustain T cell activation by recruitment of Zap70 and SLP-76. Nat Immunol 6(12):1253–1262

Yoon ST, Dianzani U, Bottomly K, Janeway CA Jr (1994) Both high and low avidity antibodies to the T cell receptor can have agonist or antagonist activity. Immunity 1(7):563–569

Zappasodi R, Di Nicola M, Carlo-Stella C, Mortarini R, Molla A, Vegetti C, Albani S, Anichini A, Gianni AM (2008) The effect of artificial antigen-presenting cells with preclustered anti-CD28/-CD3/-LFA-1 monoclonal antibodies on the induction of ex vivo expansion of functional human antitumor T cells. Haematologica 93(10):1523–1534

Zitvogel L, Regnault A, Lozier A, Wolfers J, Flament C, Tenza D, Ricciardi-Castagnoli P, Raposo G, Amigorena S (1998) Eradication of established murine tumors using a novel cell-free vaccine: dendritic cell-derived exosomes. Nat Med 4(5):594–600

Regulatory T Cell-Mediated Tissue Repair

14

Jihye Hong and Byung-Soo Kim

14.1 Tissue Healing Process

Tissue injury healing can be divided into two parts: the inflammatory phase and the regenerative phase. The beginning of the tissue healing process is indicated by coagulation, as platelets aggregate at the injury sites (Martin and Leibovich 2005). Neutrophils, macrophages, and mast cells then modify the microenvironment to facilitate tissue repair. They clear up the injured site and eliminate the invading microbes and dead cells around the injury site by phagocytosis. After this pro-inflammatory phase, various cytokines contribute to the induction of the regenerative phase or an anti-inflammatory phase. Unlike the pro-inflammatory phase, the cytokines and molecules focus on remodeling the injured tissue sites in the regenerative phase. However, it is not clear whether the pro-inflammatory phase is essential for tissue repair, as prolonged inflammation could cause pain to and other side effects on the injured host (Eming et al. 2007). Numerous studies have been performed to identify the specific leukocyte and immune reaction responsible for the undesired inflammation during tissue repair. Among the immune cells that participate in tissue repair, regulatory T-cells (Treg cells) have been found to be capable of initiating the anti-inflammatory phase.

J. Hong
Interdisciplinary Program for Bioengineering, Seoul National University, Seoul, South Korea
e-mail: minie0120@snu.ac.kr

B.-S. Kim (✉)
Interdisciplinary Program for Bioengineering, Seoul National University, Seoul, South Korea

School of Chemical and Biological Engineering, Seoul National University, Seoul, South Korea

Institute of Chemical Processes, Seoul National University, Seoul, South Korea
e-mail: byunskim@snu.ac.kr

14.2 Role of Regulatory T-Cells

14.2.1 Treg Cells as Immune Suppressors

Treg cells are a type of effector T-cells, and constitute 10% of the $CD4^+$ T-cells. Treg cells were identified in 1995, when the transfer of $CD4^+CD25^-$ T-cells into CD25-depleted mice caused autoimmune diseases such as thyroiditis and gastritis, while $CD4^+CD25^+$ T-cells rescued the mice from these diseases (Sakaguchi et al. 1995). The cells acted as immune suppressors, and had $CD4^+CD25^+Foxp3^+$ properties, with $Foxp3^+$ as their X-chromosome transcription factor. Several studies have identified Foxp3 as an essential transcription factor of Treg cells. Mutations in Foxp3 can compromise the suppressive functions of Treg cells and result in the aggressive development of autoimmune diseases, such as the *scurfy* phenotype in mice and immunodysregulation polyendocrinopathy enteropathy X-linked (IPEX) in

I. Noh (ed.), *Biomimetic Medical Materials*, Advances in Experimental Medicine and Biology 1064,
https://doi.org/10.1007/978-981-13-0445-3_14

humans (Bacchetta et al. 2006; Bennett et al. 2001; Fontenot et al. 2003; Hori et al. 2003). Treg cells produce anti-inflammatory cytokines, including interleukin-10 (IL-10), transforming growth factor-beta (TGF-β), and cytotoxic T-lymphocyte–associated antigen (CTLA)-4 (Liu et al. 2003; Takahashi et al. 2000), thus maintaining immune homeostasis and suppressing the inflammatory pathway by several mechanisms for various circumstances.

TGF-β is the major suppressive cytokine of Treg cells, and contributes to the Treg-mediated T-cell suppressive activity and tissue repair (Li et al. 2006; Schmidt-Weber and Blaser 2004). TGF-β exists on the Treg cell surface and mediates the suppression of $CD4^+CD25^-$ T-cells by cell-cell contact (Nakamura et al. 2001). Although TGF-β-independent suppression is also possible (Piccirillo et al. 2002), TGF-β is involved in the immune regulation of Treg cells, and blocking TGF-β has been found to cause type-1 diabetes in a mouse model (You et al. 2005) and thyroiditis in a rat model (Seddon and Mason 1999). TGF-β also plays a major role in inducing $Foxp3^+$-induced Treg (iTreg) cells in the periphery, with the involvement of interleukin (IL)-2, thus producing periphery-induced Treg (pTreg) cells, which are not found in the thymus (Coombes et al. 2007).

IL-10, one of the $CD4^+CD25^+$ T-cell-secreted cytokines, has been found to be involved in intestine-specific Treg cell activity; Treg cells isolated from IL-10-deficient mice were incapable of rescuing colitis (Asseman et al. 1999). In addition, IL-10 has also been found to contribute to Treg cell activation in colon, lung, and skin, although its roles in other organs are not well known yet (Rubtsov et al. 2008). However, *in vitro* IL-10 deficiency caused no downregulation of Treg cell activity, indicating that IL-10 was part of the Treg cell pathway, and not a necessary cytokine (Thornton and Shevach 1998).

CTLA-4 is the major pathway in the $Foxp3^+$-mediated suppressive function of Treg cells, regulating inflammatory T-cell activation and maintaining immune homeostasis. CTLA-4 deficiency in mice can cause a burst of lymphoproliferative diseases (Tivol et al. 1995; Waterhouse et al. 1995). CTLA-4 deficiency also causes autoimmune diseases, including type-1 diabetes, and inflammatory bowel diseases; even antibody-mediated temporary blockade of CTLA-4 can induce autoimmune symptoms (Lühder et al. 1998; Read et al. 2000; Takahashi et al. 2000). Although the suppression mechanism of CTLA-4 is not well known, its regulation may involve antigen presentation by dendritic cells (DCs) (Wing et al. 2008). Further, a study had revealed that CTLA-4 could induce the secretion of TGF-β and stimulate anti-inflammatory responses by Treg cells (Chen et al. 1998), although CTLA-4 does not require TGF-β for its expression. These cytokines can thus complement each other, maintaining Treg-mediated suppression in a compensatory manner (Tang et al. 2004). Therefore, CTLA-4 participates in most parts of immune control, with $Foxp3^+$ Treg cells as a major regulator of Treg cell suppression.

In addition to these cytokines, Treg cells have additional mechanisms involving granzyme B and IL-35 (Cao et al. 2007; Collison et al. 2007). These immune suppressive characteristics make Treg cells a potential solution for the problems of autoimmunity and transplant rejection. Treg cells are now the focus of attention for their contribution to tissue repair. The mechanism of tissue repair by Treg cells involves the induction of the transition from pro-inflammatory phase to regenerative phase of the immune system. The main pathway in Treg cell-mediated tissue repair is macrophage polarization, as Treg cell secretion of IL-10, IL-4, and IL-13 induces the transition to alternatively activated macrophages (AAM) or anti-inflammatory macrophages (M2) (Tiemessen et al. 2007). This macrophage transition reduces the inflammatory cytokine secretion by macrophages, and macrophage activity is converted into regenerative activity, which is critical for tissue repair (Gordon and Martinez 2010; Mantovani et al. 2013; Stout and Suttles 2004). There are several *in vivo* examples that demonstrate Treg cell-mediated tissue repair, and they are reviewed in Sect. 4.

14.2.2 Diversity of Treg Cells

Regulatory T-cells can be divided into three groups, thymus-derived Treg (tTreg) cells, pTreg cells, and iTreg cells. Their respective roles are not well understood, as tTreg and pTreg cells are highly similar, cooperate *in vivo*, and are hard to separate.

tTreg cells, previously known as natural Treg cells, are matured by the DCs in thymus as in Fig. 14.1 (Martín-Gayo et al. 2010; Watanabe et al. 2005). tTreg cells originally show $Foxp3^+$ $CD4^+CD25^+$ characteristics and are responsive to autoimmunity. They are responsible for most Treg cell activities, suppressing immune responses through various methods.

pTreg cells are not derived from the thymus; they are differentiated from naïve T-cells, usually with TGF-β and IL-2, and can respond to external antigens. Their role in immunity is not clearly known; an exclusion of pTreg cells resulted in autoimmune diseases, showing that pTreg cells cannot prevent autoimmune diseases by themselves (Bonomo et al. 1995). However, recent studies have revealed that pTreg cells play significant roles in the immunity-independency of tTreg cells (Josefowicz et al. 2012; Samstein et al. 2012). pTreg cells can be classified into two groups, type 1 regulatory T-cells (Tr1) and T-helper 3 cells (Th3). Tr1 cells lack the transcription factor Foxp3, but secrete IL-10. Th3 cells also lack Foxp3 and secrete TGF-β, thus contributing to Treg cell suppression.

Lastly, iTreg cells are Treg cells that are induced *in vitro*, and are promising Treg cells for therapeutic applications. iTreg cells include Tr1 cells and Th3 cells induced *in vitro*. As therapeutic Treg cells need to be largely expanded for clinical use, understanding iTreg cells would be an important task for Treg applications.

14.3 Treg Cell Induction and Localization

The induction method for Treg cells is significant, as *in vitro* Treg induction could be a promising method for large-scale production of Treg cells for clinical use. The first induction of Treg cells was by oral administration of antigens, causing the suppression of T-cells for treating experimental autoimmune encephalomyelin (EAE)

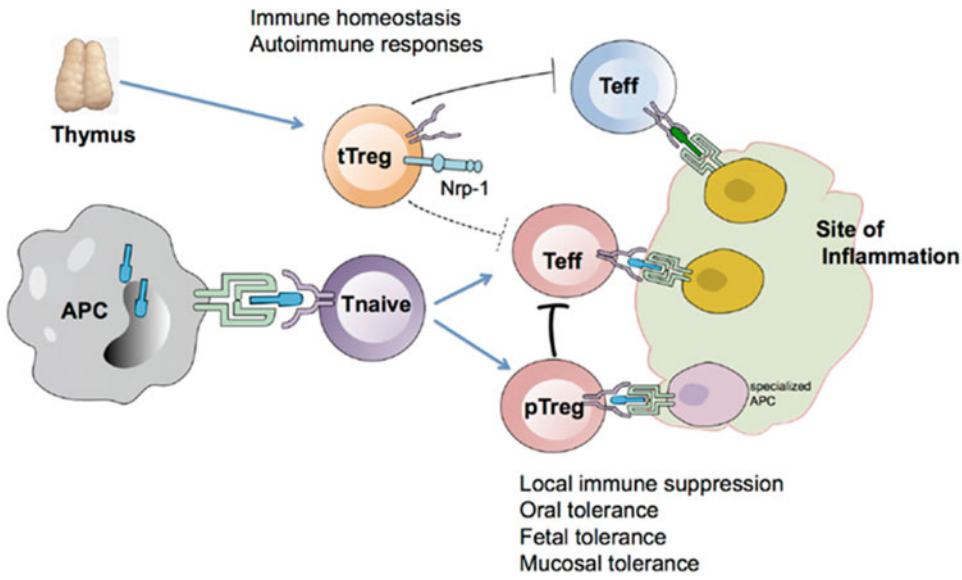

Fig. 14.1 Differentiation and roles in inflammation of Treg and pTreg cells. Thymus-derived tTreg cells and antigen-presenting cell (APC)-derived pTreg cells suppress T-cell immune responses, maintaining immune homeostasis. (Reproduced with permission from Yadav et al. 2013)

(Youhai-Chen et al. 1994). The oral administration of antigens could be fruitful, as one study showed that oral administration in mice increased the proportion of $CD4^+CD25^+$ T-cells and succeeded in increasing CTLA-4 and TGF-β secretion. Surprisingly, orally administered antigen $CD4^+CD25^+$ T-cells were more effective than the control $CD4^+CD25^+$ T-cells, although the induction lasted for only 4 days (Zhang et al. 2001). In addition to oral administration of antigens, several induction methods for Treg cells have been developed *in vivo* and *in vitro*, depending on the types and characteristics of the Treg cells.

14.3.1 IL-10- and TGF-β-Induced Treg Cells

Activation of $CD4^+$ T-cells with IL-10 can induce IL-10-producing Tr1 cells (Groux et al. 1997). Tr1 cell induction has succeeded in both murine and human models, and it suppressed autoimmune colitis.

In 2003, Chen and his colleagues succeeded in inducing TGF-β-secreting Treg cells by providing TGF-β in a murine model (Chen et al. 2003). In an *in vitro* experiment, TGF-β induced Foxp3 expression in $CD4^+CD25^-$ T-cells and stimulated $CD4^+CD25^-$ T-cells to differentiate into $Foxp3^+$ $CD4^+CD25^+$ T-cells in the presence of antigen-presenting cells (APCs). The differentiated Treg cells produced TGF-β, suppressing naive T-cell activity. The induced Treg cells were cell-contact-dependent, as they suppressed naïve T cells through TGF-β. The induced $CD4^+CD25^+$ T-cells were tested *in vivo*, and were found to alleviate house dust mite-induced lung inflammation in mice.

TGF-β also induced Treg cells in the human peripheral blood, distinguishable from IL-10-secreting Tr1 cells; anti-IL-10 could not block the induced suppressive activity in this case (Yamagiwa et al. 2001). pTreg cells in humans are induced by TGF-β, and the transcription of Foxp3 downregulates Smad7, which suppresses TGF-β. Therefore, the absence of Smad7 results in TGF-β expression under positive feedback, upregulating the Foxp3 expression of $CD4^+CD25^-$ T-cells in the periphery (Fantini et al. 2004). The peripherally induced $Foxp3^+CD4^+CD25^+$ T-cells downregulate the immune response in the periphery by antagonizing helper T cells, Th1, Th2, and Th17. IL-6, a pro-inflammatory cytokine, inhibits TGF-β expression, thus interrupting the development of additional Foxp3+ Treg cells and mediating immune homeostasis (Bettelli et al. 2006).

14.3.2 Antigen-Induced Treg Cells

Treg cells can be induced in an antigen-dependent manner through the oral administration of antigen-induced Treg cells. The most promising antigen administration method would be the utilization of DCs for T-cell conversion into Treg cells. In 2001, induction by antigen was achieved by a low dose of antigens, which inhibited T-cell proliferation via TGF-β or IL-2 (Kretschmer et al. 2005). This study revealed that TGF-β enhances antigen-derived Treg cell induction by suppressing T-cell proliferation. In contrast, IL-2 enhanced Treg cell induction, and its absence enhanced Treg cell differentiation.

Th3 cells, a type of iTreg cells, can also be induced by the oral administration of antigens, producing TGF-β, IL-10, and IL-4 (Weiner and Howard 1997; Youhai-Chen et al. 1994). Th3 cells suppressed Th1 and Th2 cells, and their development was enhanced in presence of IL-4 (Weiner 2001).

DCs are a type of APCs necessary for maintaining immune homeostasis (Ohnmacht et al. 2009). Inducing pTreg cells with immature DCs was recently in the spotlight as a potential method for Treg cell differentiation (Groux et al. 2004). In the presence of TGF-β, DCs showed higher activation efficacy than other APCs, especially spleen DCs, which are specialized in Treg cell differentiation (Yamazaki et al. 2007). DCs require a low dose of antigens and can suppress immune responses *in vivo*.

Antigen-induced IL-10-producing T-cells, Tr1 cells, do not express the Foxp3 transcriptional factor, but have the same suppressive effect as $CD4^+CD25^+Foxp3^+$ T-cells (Vieira et al. 2004). Tr1 cells can also be induced by DCs with their IL-27 secretion. One study revealed that tTreg cells could stimulate DCs to produce IL-27 to induce Tr1 cells, and that TGF-β enhanced this induction (Awasthi et al. 2007). Interferon-alpha (IFN-α) or CD2 also enhances Tr1 cell induction *in vitro*, as their co-stimulation increases the efficiency of Tr1 cell induction (Levings et al. 2001; Wakkach et al. 2001). In a human study, stimulation with immature DCs induced IL-10-secreting T-cells with suppressive activity (Jonuleit et al. 2000).

14.3.3 Localization of Treg Cells In Vivo

In 2001, chemokines were proposed as the leading candidates for inducing the localization of Treg cells to inflammation sites (Iellem et al. 2001; Bystry et al. 2001). These studies revealed that $CD4^+CD25^+$ T-cells highly expressed chemokine receptor 4 (CCR4) and chemokine receptor 8 (CCR8), the receptors of chemokine ligand 1 (CCL1), chemokine ligand 17 (CCL17), and chemokine ligand 22 (CCL22). A chemokine-induced localization test showed a correlation between CCR4 and CCR8 and $CD4^+CD25^+$ T-cells, as localized $CD4^+$ cells mostly expressed CD25. Localization tests with different chemokines and blocking revealed that $CD4^+CD25^+$ T-cells responded to CCL1 and CCL22 via CCR4 and CCR8 in synergistic manner. $CD4^+CD25^+$ T-cells also expressed chemokine receptor 5 (CCR5) and were recruited by chemokine ligand 4 (CCL4) *in vitro*. In addition, mature DCs were found to localize Treg cells by expressing ligands such as CCL17 and CCL22, showing that DCs were capable of recruiting Treg cells. Several studies have also demonstrated the importance of chemokines in Treg cell recruitment (Faustino et al. 2013; Lee et al. 2005; Oo et al. 2010).

14.4 Examples of Tissue Therapy Using Treg Cells

14.4.1 Treg Cell-Applied Tissue Repair by Suppressing Pro-inflammatory Immune Reactions

14.4.1.1 Alleviation of Myocardial Infarction by Treg Cells

Myocardial infarction is a high-risk cardiac disease that causes ventricular remodeling, with a high chance of heart failure. The process of healing of cardiac tissues is not well established, because heart muscle regeneration is not well understood and because of the difficulty of preventing ventricular remodeling, which stiffens the wound area and compromises ventricular functioning (Ertl and Frantz 2005).

Treg-deleted mice were found to show low survival rates and high infarct sizes. In contrast, CD28-SA mice, which were induced to have high $Foxp3^+CD4^+$ Treg cell rate in the infarct site, showed low rate of heart failure, few ventricular ruptures, and high survival rate. This may be attributed to the cytokines secreted by the Treg cells, mainly IL-10 and IL-13, which induced a transition from pro-inflammatory M1 macrophages to anti-inflammatory M2 macrophages, and this transition contributes to tissue wound healing and regeneration (Weirather et al. 2014). In a recent experiment, mice were injected with tolerogenic dendritic cells (tDCs), which were primed with cardiac lysate and tumor necrosis factor-alpha (TNF-α). The tDCs were localized properly in the infarcted area; they induced a sufficient number of Treg cells to observe a therapeutic effect. Figure 14.2 showed that the treated mice showed higher survival rates, smaller infarct sizes, and better functioning of the left ventricle than the controls. The successful healing may be attributed to earlier polarization of M1 macrophages to M2 macrophages by Treg cells in the infarcted area, making the immune environment suitable for healing and regeneration. This study implied that tDC implantation could be a promising method for Treg-applied

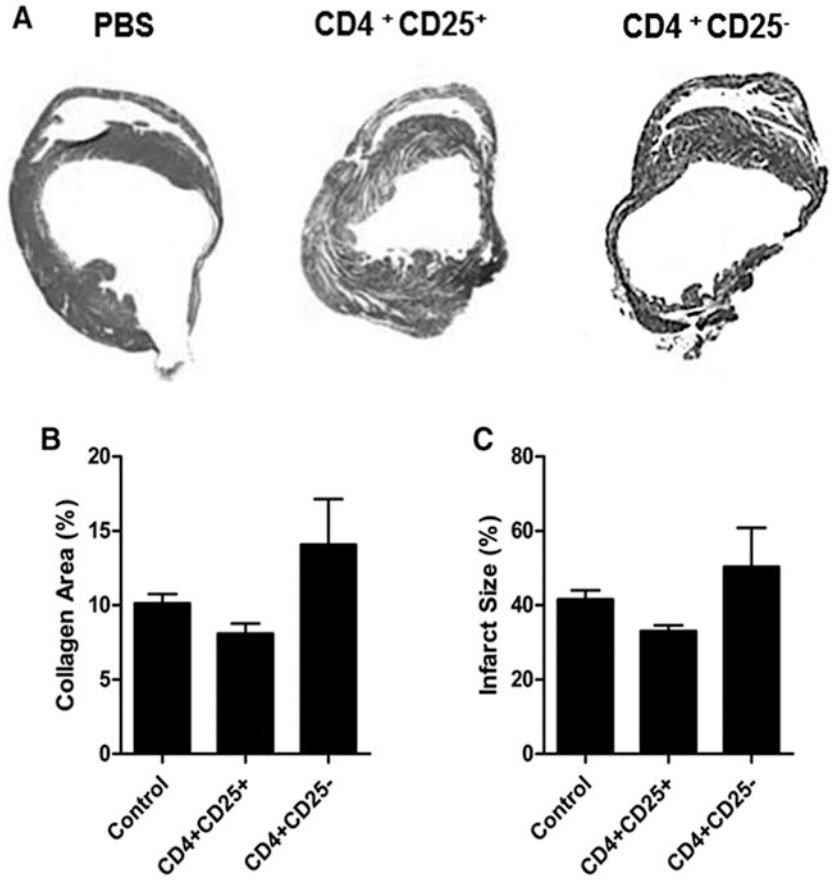

Fig. 14.2 The alleviation of myocardial infarction (MI) by injection of tolerogenic dendritic cell (tDC)-induced Treg cells in a murine MI model. Unlike $CD4^+$ $CD25^-$ T-cells, the injection of $CD4^+CD25^+$ T-cells resulted in reduced infarct size and collagen area in MI heart. (Reproduced with permission from Choo et al. 2017)

clinical therapy, as it does not cause autoimmune problems or require a long time to produce feasible amounts of Treg cells (Choo et al. 2017).

14.4.1.2 Skeletal Muscle Tissue Repair in Mice by Treg Cells

Arnold et al. had suggested the significance of the polarization of macrophages in muscle repair (Arnold et al. 2007). In the early stages of skeletal muscle repair, inflammatory macrophages (M1) contribute to regeneration with phagocytosis activity, eliminating necrotic cells and debris to facilitate muscle regeneration. After the switch to anti-inflammatory phase, macrophages (M2) stimulate myogenic progenitor cells, also known as satellite cells, to differentiate and form new muscle fibers by secreting chemokines. They also enhance monocyte infiltration into the injured site, increasing the macrophage influence in muscle regeneration (Chazaud et al. 2003). Furthermore, Treg cells in muscle tissues secrete amphiregulin, which enhances tissue repair (Burzyn et al. 2013).

Therefore, using Treg cells for muscle repair is an attractive approach, as they can promote macrophage polarization. In a recent study, Treg cell application in muscle repair was demonstrated in a mouse model (Burzyn et al. 2013). Treg cell depletion resulted in the impaired regeneration of injured muscles and reduced satellite cell stimulation in the injured site. In addition, Treg cell-depleted mice were incapable of expressing the

appropriate chemokines for muscle homeostasis and macrophage transition. Therefore, the pro-inflammatory phase of M1 macrophages was prolonged in Treg-deficient mice, preventing proper muscle regeneration.

14.4.1.3 Repair of Ischemia Reperfusion Injury in Kidneys by Treg Cells

Ischemic reperfusion injury (IRI) is the major cause of acute renal injury (AKI), which is responsible for the high mortality in renal transplantation (Kinsey et al. 2008). $CD4^+CD25^+$ $Foxp3^+$ T-cells were found to modulate the inflammation in IRI in mice kidneys (Gandolfo et al. 2009). Gandolfo and his team demonstrated that Treg cells were necessary for tissue repair in IRI and their T-cell suppressive mechanism could alleviate the inflammation in kidneys and improve tissue healing. Decreased Treg cells in the injury site of IRI-induced mice showed higher TNF-α expression and increased infiltration of T-cells in the kidneys. In contrast, the $CD4^+CD25^+Foxp3^+$ T-cell-injected group showed reduced production of inflammatory cytokines, including interferon-gamma (IFN-γ) and TNF-α, and enhanced tissue repair. This result showed the potential of Treg cells as therapeutic agents for IRI.

14.4.1.4 Repair of Lung Injury by Treg Cells

The application of Treg cells in acute lung injury (ALI) has also been tested in mice (D'alessio et al. 2009). Patients with ALI suffer from alveolar inflammation. Transition to the anti-inflammatory phase by transferred Treg cells could be a promising solution for ALI. Lipopolysaccharide (LPS) was injected to mice to induce ALI. *Rag-1*$^{-/-}$ mice that lack normal lymphocytes were compared with wild type mice. *Rag-1*$^{-/-}$ mice were stuck in the pro-inflammatory phase, while the wild type mice showed normal transition, with elevated levels of TGF-β on day 4. The transfer of $CD4^+CD25^+Foxp3^+$ T-cells rescued the *Rag-1*$^{-/-}$ mice. The Treg-transferred mice showed elevated levels of TGF-β and decreased levels of pro-inflammatory cytokines in the alveoli. TGF-β was also found to be the main cytokine of Treg cells, as blocking it diminished the Treg-mediated alveolar improvement. An additional experiment also revealed Treg-induced anti-inflammatory transition in alveolar macrophages. In addition to the anti-inflammatory activity, Treg cells also mediated lung tissue repair in a distinctive manner by secreting amphiregulin (Arpaia et al. 2015). Therefore, the application of Treg cells to lung tissue injury could be a potential solution.

14.4.1.5 Repair of Brain Injury by Treg Cells

Acute brain ischemia or ischemic stroke in mice was treated with Treg cells as an inflammation-mediator (Liesz et al. 2009). Histological analysis of the brain, and mRNA and protein expression levels in cerebral tissues showed that Treg-depleted mice had higher pro-inflammatory cytokines, including TNF-α, IL-1β, and INF-γ, than the controls. These inflammatory cytokines promoted an infarct growth in the brain, and blocking these cytokines resulted in alleviated brain damage. An additional experiment was performed to determine the Treg-secreted cytokines that were responsible for cerebral tissue protection. It was revealed that IL-10-depletion induced the same inflammatory state as was observed in Treg-depleted mice, and an injection of IL-10 rescued the Treg-depleted mice by downregulating pro-inflammatory cytokines and boosting tissue repair.

14.5 Limitations of and Expectations from the Therapeutic Use of Treg Cells

14.5.1 Limitations of Treg Therapy in Humans

No clinical trials of Treg cells have been performed yet. However, numerous studies have shown the possibility of Treg application in humans. Taams et al. achieved human macrophage polarization using $CD4^+CD25^+Foxp3^+$ T-cells (Taams et al. 2005), suggesting that

human Treg cells can be used to induce macrophage transition in the inflammation site.

14.5.1.1 Difficulty of Treg Application in Humans

Among the challenges for therapeutic application of Treg cells, dealing with unexpected side effects is one of the major ones. One of the side effects that can be expected is unknown cytokine interactions in humans. Although murine model experiments have had positive results, the same may not be true in human trials because of the complexity of the immune system. Although administration has augmented the Treg cell population *in vivo*, the side effects should be treated before clinical use.

Furthermore, there is the possibility that *in vivo* results may not always be consistent with the *in vitro* results. *In vivo* experiments can have unexpected side effects or the involvement of unknown and unpredicted mechanisms. Therefore, *in vivo* tests in humans are necessary for the clinical use of Treg cells. Human experiments for treating graft-versus-host disease (GVHD) with Treg cells have shown their potential for alleviating autoimmune diseases (Trzonkowski et al. 2009). Likewise, Treg-applied in-human tests of tissue repair would encourage the therapeutic use of Treg cells.

14.5.1.2 Technical Limitations of Supplying Human Treg Cells for Clinical Use

Clinical application would require large doses of Treg cells. There are two ways to obtain the required amounts of Treg cells: isolation and large scale *ex vivo* expansion of Treg cells or *in vitro* induction of Treg cells.

Distinguishing Treg cells in humans is a major challenge for the isolation of human Treg cells. Several markers have been suggested to distinguish and isolate human Treg cells. Neuropilin-1 (Nrp-1), a Treg marker in a murine model, was found to be non-specific in humans (Milpied et al. 2009). Helios, the well-known marker for Treg cells, distinguished only 70% of human Treg cells. Furthermore, although a previous study suggested Helios as a tTreg marker (Thornton et al. 2010), it cannot distinguish between tTreg and iTreg cells, as its expression is changeable depending on Foxp3 expression circumstances. Therefore, perfect separation of the Treg cells is almost impossible (Gottschalk et al. 2012). In addition to Nrp-1 and Helios, CD39 was suggested as a pTreg marker in humans (Mandapathil et al. 2009). The most widely used marker in Treg cell studies is CD127, an IL-7 receptor (Liu et al. 2006). The downregulation of CD127 was found to inversely correlate with pTreg cells in humans. Several studies have utilized this marker for testing its clinical applicability. In one such study, CD127 was used to isolate Treg cells, which were then injected into patients with high-grade glioma (Ardon et al. 2010). The Treg cells isolated using CD127 showed the same suppressive activity as tTreg cells, suggesting that CD127 might be an appropriate marker for Treg cell isolation.

For the efficient induction of Treg cells *in vitro*, DCs have been used in many studies. DC-based induction is advantageous in many respects. Inducing antigen-specific DCs would be much more convenient than other APCs, and the injection of matured DCs is very simple (Jonuleit et al. 2001).

After proper isolation or induction of Treg cells *in vitro*, there should be appropriate expansion of Treg cells to meet the required Treg dose for clinical treatment. To change the Treg concentration in the human body, large-scale *ex vivo* Treg expansion would be required. The estimated total number of Treg cells in the human body is 1.3×10^{10} (Tang and Lee 2012), while the calculated number of Treg cells in human circulation is 0.2×10^{9}, indicating the limitation for the application of human-obtained Treg cells without expansion. In a human study for treating autoimmune diseases, the targeted-dose of Treg cells was not achieved in the patients, as Treg cell expansion failed to reach the number of Treg cells as planned (Brunstein et al. 2011). Expansion of Treg cells with DCs was found to be more efficient than that with other APCs, successfully augmenting the Treg concentration in patients with myeloma (Banerjee et al. 2006). Further, several studies have recommended

co-stimulation of CD28 to increase the efficiency of Treg cell expansion *in vitro* (Golovina et al. 2008; Lin and Hünig 2003).

14.5.2 Expectations from Treg Cell Therapy in the Future

As mentioned earlier, the establishment of a method for separating Treg cells is important, as Treg cells exist in various types and utilize different suppressive mechanisms. CD127 can be used as a human Treg marker; however, highly purified isolation using CD127 requires verification. To avoid transferring lymphocytes other than Treg cells, a technique to isolate highly purified Treg cells is required. However, if isolation of Treg cells is accomplished, Treg cells can be expanded *ex vivo*, for infusion into patients.

To solve the time-consuming problem of Treg isolation, one study suggested a shortcut for analyzing Treg cells, which would shorten the required time from 4 to 5 days to less than 24 h (Canavan et al. 2012; Ruitenberg et al. 2011). This 7-h protocol would make therapeutic application of Treg cells more plausible, as it can reduce the possibility of reduction of the suppressive activity of *in vitro* iTreg cells.

In conclusion, the clinical application of Treg cells would be breakthrough in tissue repair. Treg cells can be an effective regulator of inflammation in tissue injury, reducing undesirable pain and inflammation in injured sites. Although proper examination and tests would be required before the therapeutic use of Treg cells in the future, their application in tissue repair is a bright prospect.

References

Ardon H, Verbinnen B, Maes W, Beez T, Van Gool S, De Vleeschouwer S (2010) Technical advancement in regulatory T cell isolation and characterization using CD127 expression in patients with malignant glioma treated with autologous dendritic cell vaccination. J Immunol Methods 352(1):169–173. https://doi.org/10.1016/j.jim.2009.10.007

Arnold L, Henry A, Poron F, Baba-Amer Y, Van Rooijen N, Plonquet A, Gherardi RK, Chazaud B (2007) Inflammatory monocytes recruited after skeletal muscle injury switch into antiinflammatory macrophages to support myogenesis. J Exp Med 204 (5):1057–1069. https://doi.org/10.1084/jem.20070075

Arpaia N, Green JA, Moltedo B, Arvey A, Hemmers S, Yuan S, Treuting PM, Rudensky AY (2015) A distinct function of regulatory T cells in tissue protection. Cell 162(5):1078–1089. https://doi.org/10.1016/j.cell.2015.08.021

Asseman C, Mauze S, Leach MW, Coffman RL, Powrie F (1999) An essential role for interleukin 10 in the function of regulatory T cells that inhibit intestinal inflammation. J Exp Med 190(7):995–1004. https://doi.org/10.1084/jem.190.7.995

Awasthi A, Carrier Y, Peron JP, Bettelli E, Kamanaka M, Flavell RA, Kuchroo VK, Oukka M, Weiner HL (2007) A dominant function for interleukin 27 in generating interleukin 10-producing anti-inflammatory T cells. Nat Immunol 8(12):1380. https://doi.org/10.1038/ni1541

Bacchetta R, Passerini L, Gambineri E, Dai M, Allan SE, Perroni L, Dagna-Bricarelli F, Sartirana C, Matthes-Martin S, Lawitschka A (2006) Defective regulatory and effector T cell functions in patients with FOXP3 mutations. J Clin Invest 116(6):1713. https://doi.org/10.1172/JCI25112

Banerjee DK, Dhodapkar MV, Matayeva E, Steinman RM, Dhodapkar KM (2006) Expansion of FOXP3 high regulatory T cells by human dendritic cells (DCs) in vitro and after injection of cytokine-matured DCs in myeloma patients. Blood 108(8):2655–2661. https://doi.org/10.1182/blood-2006-03-011353

Bennett CL, Christie J, Ramsdell F, Brunkow ME, Ferguson PJ, Whitesell L, Kelly TE, Saulsbury FT, Chance PF, Ochs HD (2001) The immune dysregulation, polyendocrinopathy, enteropathy, X-linked syndrome (IPEX) is caused by mutations of FOXP3. Nat Genet 27(1):20. https://doi.org/10.1038/ng.83713

Bettelli E, Carrier Y, Gao W, Korn T, Strom TB, Oukka M, Weiner HL, Kuchroo VK (2006) Reciprocal developmental pathways for the generation of pathogenic effector TH17 and regulatory T cells. Nature 441 (7090):235. https://doi.org/10.1038/nature04753

Bonomo A, Kehn PJ, Shevach EM (1995) Post-thymectomy autoimmunity: abnormal T-cell homeostasis. Immunol Today 16(2):61–67. https://doi.org/10.1016/0167-5699(95)80089-1

Brunstein CG, Miller JS, Cao Q, McKenna DH, Hippen KL, Curtsinger J, DeFor T, Levine BL, June CH, Rubinstein P (2011) Infusion of ex vivo expanded T regulatory cells in adults transplanted with umbilical cord blood: safety profile and detection kinetics. Blood 117(3):1061–1070. https://doi.org/10.1182/blood-2010-07-293795

Burzyn D, Kuswanto W, Kolodin D, Shadrach JL, Cerletti M, Jang Y, Sefik E, Tan TG, Wagers AJ, Benoist C (2013) A special population of regulatory T cells potentiates muscle repair. Cell 155

(6):1282–1295. https://doi.org/10.1016/j.cell.2013.10.054

Bystry RS, Aluvihare V, Welch KA, Kallikourdis M, Betz AG (2001) B cells and professional APCs recruit regulatory T cells via CCL4. Nat Immunol 2(12):1126. https://doi.org/10.1038/ni735

Canavan JB, Afzali B, Scottà C, Fazekasova H, Edozie FC, Macdonald TT, Hernandez-Fuentes MP, Lombardi G, Lord GM (2012) A rapid diagnostic test for human regulatory T-cell function to enable regulatory T-cell therapy. Blood 119(8):e57–e66. https://doi.org/10.1182/blood-2011-09-380048

Cao X, Cai SF, Fehniger TA, Song J, Collins LI, Piwnica-Worms DR, Ley TJ (2007) Granzyme B and perforin are important for regulatory T cell-mediated suppression of tumor clearance. Immunity 27(4):635–646. https://doi.org/10.1016/j.immuni.2007.08.014

Chazaud B, Sonnet C, Lafuste P, Bassez G, Rimaniol A-C, Poron F, Authier F-J, Dreyfus PA, Gherardi RK (2003) Satellite cells attract monocytes and use macrophages as a support to escape apoptosis and enhance muscle growth. J Cell Biol 163(5):1133–1143. https://doi.org/10.1083/jcb.200212046

Chen W, Jin W, Wahl SM (1998) Engagement of cytotoxic T lymphocyte–associated antigen 4 (CTLA-4) induces transforming growth factor β (TGF-β) production by murine CD4+ T cells. J Exp Med 188 (10):1849–1857. https://doi.org/10.1084/jem.188.10.1849

Chen W, Jin W, Hardegen N, K-j L, Li L, Marinos N, McGrady G, Wahl SM (2003) Conversion of peripheral CD4+ CD25− naive T cells to CD4+ CD25+ regulatory T cells by TGF-β induction of transcription factor Foxp3. J Exp Med 198(12):1875–1886. https://doi.org/10.1084/jem.20030152

Choo EH, Lee J-H, Park E-H, Park HE, Jung N-C, Kim T-H, Koh Y-S, Kim E, Seung K-B, Park C (2017) Infarcted myocardium-primed dendritic cells improve remodeling and cardiac function after myocardial infarction by modulating the Treg and macrophage polarization. Circulation. https://doi.org/10.1161/CIRCULATIONAHA.116.023106

Collison LW, Workman CJ, Kuo TT, Boyd K, Wang Y, Vignali KM, Cross R, Sehy D, Blumberg RS, Vignali DA (2007) The inhibitory cytokine IL-35 contributes to regulatory T-cell function. Nature 450(7169):566. https://doi.org/10.1038/nature06306

Coombes JL, Siddiqui KR, Arancibia-Cárcamo CV, Hall J, Sun C-M, Belkaid Y, Powrie F (2007) A functionally specialized population of mucosal CD103+ DCs induces Foxp3+ regulatory T cells via a TGF-β–and retinoic acid–dependent mechanism. J Exp Med 204(8):1757–1764. https://doi.org/10.1084/jem.20070590

D'alessio FR, Tsushima K, Aggarwal NR, West EE, Willett MH, Britos MF, Pipeling MR, Brower RG, Tuder RM, McDyer JF (2009) CD4+ CD25+ Foxp3+ Tregs resolve experimental lung injury in mice and are present in humans with acute lung injury. J Clin Invest 119(10):2898. https://doi.org/10.1172/JCI36498

Eming SA, Krieg T, Davidson JM (2007) Inflammation in wound repair: molecular and cellular mechanisms. J Invest Dermatol 127(3):514–525. https://doi.org/10.1038/sj.jid.5700701

Ertl G, Frantz S (2005) Healing after myocardial infarction. Cardiovasc Res 66(1):22–32. https://doi.org/10.1016/j.cardiores.2005.01.011

Fantini MC, Becker C, Monteleone G, Pallone F, Galle PR, Neurath MF (2004) Cutting edge: TGF-β induces a regulatory phenotype in CD4+ CD25− T cells through Foxp3 induction and down-regulation of Smad7. J Immunol 172(9):5149–5153. https://doi.org/10.4049/jimmunol.172.9.5149

Faustino L, da Fonseca DM, Takenaka MC, Mirotti L, Florsheim EB, Guereschi MG, Silva JS, Basso AS, Russo M (2013) Regulatory T cells migrate to airways via CCR4 and attenuate the severity of airway allergic inflammation. J Immunol 190(6):2614–2621. https://doi.org/10.4049/jimmunol.1202354

Fontenot JD, Gavin MA, Rudensky AY (2003) Foxp3 programs the development and function of CD4+ CD25+ regulatory T cells. Nat Immunol 4 (4):330–336. https://doi.org/10.1038/ni904

Gandolfo MT, Jang HR, Bagnasco SM, Ko G-J, Agreda P, Satpute SR, Crow MT, King LS, Rabb H (2009) Foxp3 + regulatory T cells participate in repair of ischemic acute kidney injury. Kidney Int 76(7):717–729. https://doi.org/10.1038/ki.2009.259

Golovina TN, Mikheeva T, Suhoski MM, Aqui NA, Tai VC, Shan X, Liu R, Balcarcel RR, Fisher N, Levine BL (2008) CD28 costimulation is essential for human T regulatory expansion and function. J Immunol 181 (4):2855–2868. https://doi.org/10.4049/jimmunol.181.4.2855

Gordon S, Martinez FO (2010) Alternative activation of macrophages: mechanism and functions. Immunity 32 (5):593–604. https://doi.org/10.1016/j.immuni.2010.05.007

Gottschalk RA, Corse E, Allison JP (2012) Expression of Helios in peripherally induced Foxp3+ regulatory T cells. J Immunol 188(3):976–980. https://doi.org/10.4049/jimmunol.1102964

Groux H, O'garra A, Bigler M, Rouleau M (1997) A CD4 + T-cell subset inhibits antigen-specific T-cell responses and prevents colitis. Nature 389(6652):737. https://doi.org/10.1038/39614

Groux H, Fournier N, Cottrez F (2004) Role of dendritic cells in the generation of regulatory T cells. Semin Immunol 16(2):99–106. https://doi.org/10.1016/j.smim.2003.12.004

Hori S, Nomura T, Sakaguchi S (2003) Control of regulatory T cell development by the transcription factor Foxp3. Science 299(5609):1057–1061. https://doi.org/10.1126/science.1079490

Iellem A, Mariani M, Lang R, Recalde H, Panina-Bordignon P, Sinigaglia F, D'Ambrosio D (2001) Unique chemotactic response profile and specific

expression of chemokine receptors CCR4 and CCR8 by CD4+ CD25+ regulatory T cells. J Exp Med 194 (6):847–854. https://doi.org/10.1084/jem.194.6.847

Jonuleit H, Schmitt E, Schuler G, Knop J, Enk AH (2000) Induction of interleukin 10–producing, nonproliferating CD4+ T cells with regulatory properties by repetitive stimulation with allogeneic immature human dendritic cells. J Exp Med 192(9):1213–1222. https://doi.org/10.1084/jem.192.9.1213

Jonuleit H, Schmitt E, Steinbrink K, Enk AH (2001) Dendritic cells as a tool to induce anergic and regulatory T cells. Trends Immunol 22(7):394–400. https://doi.org/10.1016/S1471-4906(01)01952-4

Josefowicz SZ, Niec RE, Kim HY, Treuting P, Chinen T, Zheng Y, Umetsu DT, Rudensky AY (2012) Extrathymically generated regulatory T cells control mucosal TH2 inflammation. Nature 482(7385):395. https://doi.org/10.1038/nature10772

Kinsey GR, Li L, Okusa MD (2008) Inflammation in acute kidney injury. Nephron Exp Nephrol 109(4):e102–e107. https://doi.org/10.1159/000142934

Kretschmer K, Apostolou I, Hawiger D, Khazaie K, Nussenzweig MC, von Boehmer H (2005) Inducing and expanding regulatory T cell populations by foreign antigen. Nat Immunol 6(12):1219. https://doi.org/10.1038/ni1265

Lee I, Wang L, Wells AD, Dorf ME, Ozkaynak E, Hancock WW (2005) Recruitment of Foxp3+ T regulatory cells mediating allograft tolerance depends on the CCR4 chemokine receptor. J Exp Med 201 (7):1037–1044. https://doi.org/10.1084/jem.20041709

Levings MK, Sangregorio R, Galbiati F, Squadrone S, de Waal Malefyt R, Roncarolo M-G (2001) IFN-α and IL-10 induce the differentiation of human type 1 T regulatory cells. J Immunol 166(9):5530–5539. https://doi.org/10.4049/jimmunol.166.9.5530

Li MO, Sanjabi S, Flavell RA (2006) Transforming growth factor-β controls development, homeostasis, and tolerance of T cells by regulatory T cell-dependent and-independent mechanisms. Immunity 25 (3):455–471. https://doi.org/10.1016/j.immuni.2006.07.011

Liesz A, Suri-Payer E, Veltkamp C, Doerr H, Sommer C, Rivest S, Giese T, Veltkamp R (2009) Regulatory T cells are key cerebroprotective immunomodulators in acute experimental stroke. Nat Med 15(2):192–199. https://doi.org/10.1038/nm.1927

Lin CH, Hünig T (2003) Efficient expansion of regulatory T cells in vitro and in vivo with a CD28 superagonist. Eur J Immunol 33(3):626–638. https://doi.org/10.1002/eji.200323570

Liu H, Hu B, Xu D, Liew FY (2003) CD4+ CD25+ regulatory T cells cure murine colitis: the role of IL-10, TGF-β, and CTLA4. J Immunol 171 (10):5012–5017. https://doi.org/10.4049/jimmunol.171.10.5012

Liu W, Putnam AL, Xu-Yu Z, Szot GL, Lee MR, Zhu S, Gottlieb PA, Kapranov P, Gingeras TR, Groth BFS (2006) CD127 expression inversely correlates with FoxP3 and suppressive function of human CD4+ T reg cells. J Exp Med 203(7):1701–1711. https://doi.org/10.1084/jem.20060772

Lühder F, Höglund P, Allison JP, Benoist C, Mathis D (1998) Cytotoxic T lymphocyte–associated antigen 4 (CTLA-4) regulates the unfolding of autoimmune diabetes. J Exp Med 187(3):427–432. https://doi.org/10.1084/jem.187.3.427

Mandapathil M, Lang S, Gorelik E, Whiteside TL (2009) Isolation of functional human regulatory T cells (Treg) from the peripheral blood based on the CD39 expression. J Immunol Methods 346(1):55–63. https://doi.org/10.1016/j.jim.2009.05.004

Mantovani A, Biswas SK, Galdiero MR, Sica A, Locati M (2013) Macrophage plasticity and polarization in tissue repair and remodelling. J Pathol 229(2):176–185. https://doi.org/10.1002/path.4133

Martin P, Leibovich SJ (2005) Inflammatory cells during wound repair: the good, the bad and the ugly. Trends Cell Biol 15(11):599–607. https://doi.org/10.1016/j.tcb.2005.09.002

Martín-Gayo E, Sierra-Filardi E, Corbí AL, Toribio ML (2010) Plasmacytoid dendritic cells resident in human thymus drive natural Treg cell development. Blood 115(26):5366–5375. https://doi.org/10.1182/blood-2009-10-248260

Milpied P, Renand A, Bruneau J, Mendes-Da-Cruz DA, Jacquelin S, Asnafi V, Rubio MT, MacIntyre E, Lepelletier Y, Hermine O (2009) Neuropilin-1 is not a marker of human Foxp3+ Treg. Eur J Immunol 39 (6):1466–1471. https://doi.org/10.1002/eji.200839040

Nakamura K, Kitani A, Strober W (2001) Cell contact–dependent immunosuppression by CD4+ CD25+ regulatory T cells is mediated by cell surface–bound transforming growth factor β. J Exp Med 194 (5):629–644. https://doi.org/10.1084/jem.194.5.629

Ohnmacht C, Pullner A, King SB, Drexler I, Meier S, Brocker T, Voehringer D (2009) Constitutive ablation of dendritic cells breaks self-tolerance of CD4 T cells and results in spontaneous fatal autoimmunity. J Exp Med 206(3):549–559. https://doi.org/10.1084/jem.20082394

Oo YH, Weston CJ, Lalor PF, Curbishley SM, Withers DR, Reynolds GM, Shetty S, Harki J, Shaw JC, Eksteen B (2010) Distinct roles for CCR4 and CXCR3 in the recruitment and positioning of regulatory T cells in the inflamed human liver. J Immunol 184(6):2886–2898. https://doi.org/10.4049/jimmunol.0901216

Piccirillo CA, Letterio JJ, Thornton AM, McHugh RS, Mamura M, Mizuhara H, Shevach EM (2002) CD4+ CD25+ regulatory T cells can mediate suppressor function in the absence of transforming growth factor β1 production and responsiveness. J Exp Med 196 (2):237–246. https://doi.org/10.1084/jem.20020590

Read S, Malmström V, Powrie F (2000) Cytotoxic T lymphocyte–associated antigen 4 plays an essential role in the function of CD25+ CD4+ regulatory cells

that control intestinal inflammation. J Exp Med 192 (2):295–302. https://doi.org/10.1084/jem.192.2.295

Rubtsov YP, Rasmussen JP, Chi EY, Fontenot J, Castelli L, Ye X, Treuting P, Siewe L, Roers A, Henderson WR (2008) Regulatory T cell-derived interleukin-10 limits inflammation at environmental interfaces. Immunity 28(4):546–558. https://doi.org/10.1016/j.immuni.2008.02.017

Ruitenberg JJ, Boyce C, Hingorani R, Putnam A, Ghanekar SA (2011) Rapid assessment of in vitro expanded human regulatory T cell function. J Immunol Methods 372(1):95–106. https://doi.org/10.1016/j.jim.2011.07.001

Sakaguchi S, Sakaguchi N, Asano M, Itoh M, Toda M (1995) Immunologic self-tolerance maintained by activated T cells expressing IL-2 receptor alpha-chains (CD25). Breakdown of a single mechanism of self-tolerance causes various autoimmune diseases. J Immunol 155(3):1151–1164

Samstein RM, Josefowicz SZ, Arvey A, Treuting PM, Rudensky AY (2012) Extrathymic generation of regulatory T cells in placental mammals mitigates maternal-fetal conflict. Cell 150(1):29–38. https://doi.org/10.1016/j.cell.2012.05.031

Schmidt-Weber CB, Blaser K (2004) Regulation and role of transforming growth factor-β in immune tolerance induction and inflammation. Curr Opin Immunol 16 (6):709–716. https://doi.org/10.1016/j.coi.2004.09.008

Seddon B, Mason D (1999) Regulatory T cells in the control of autoimmunity: the essential role of transforming growth factor β and interleukin 4 in the prevention of autoimmune thyroiditis in rats by peripheral CD4+ CD45RC− cells and CD4+ CD8− thymocytes. J Exp Med 189(2):279–288. https://doi.org/10.1084/jem.189.2.279

Stout RD, Suttles J (2004) Functional plasticity of macrophages: reversible adaptation to changing microenvironments. J Leukoc Biol 76(3):509–513. https://doi.org/10.1189/jlb.0504272

Taams LS, van Amelsfort JM, Tiemessen MM, Jacobs KM, de Jong EC, Akbar AN, Bijlsma JW, Lafeber FP (2005) Modulation of monocyte/macrophage function by human CD4+ CD25+ regulatory T cells. Hum Immunol 66(3):222–230. https://doi.org/10.1016/j.humimm.2004.12.006

Takahashi T, Tagami T, Yamazaki S, Uede T, Shimizu J, Sakaguchi N, Mak TW, Sakaguchi S (2000) Immunologic self-tolerance maintained by CD25+ CD4+ regulatory T cells constitutively expressing cytotoxic T lymphocyte–associated antigen 4. J Exp Med 192 (2):303–310

Tang Q, Lee K (2012) Regulatory T-cell therapy for transplantation: how many cells do we need? Curr Opin Organ Transplant 17(4):349–354. https://doi.org/10.1097/MOT.0b013e328355a992

Tang Q, Boden EK, Henriksen KJ, Bour-Jordan H, Bi M, Bluestone JA (2004) Distinct roles of CTLA-4 and TGF-β in CD4+ CD25+ regulatory T cell function. Eur J Immunol 34(11):2996–3005. https://doi.org/10.1002/eji.200425143

Thornton AM, Shevach EM (1998) CD4+ CD25+ immunoregulatory T cells suppress polyclonal T cell activation in vitro by inhibiting interleukin 2 production. J Exp Med 188(2):287–296

Thornton AM, Korty PE, Tran DQ, Wohlfert EA, Murray PE, Belkaid Y, Shevach EM (2010) Expression of Helios, an Ikaros transcription factor family member, differentiates thymic-derived from peripherally induced Foxp3+ T regulatory cells. J Immunol 184 (7):3433–3441. https://doi.org/10.4049/jimmunol.0904028

Tiemessen MM, Jagger AL, Evans HG, van Herwijnen MJ, John S, Taams LS (2007) CD4+ CD25+ Foxp3+ regulatory T cells induce alternative activation of human monocytes/macrophages. Proc Natl Acad Sci 104(49):19446–19451. https://doi.org/10.1073/pnas.0706832104

Tivol EA, Borriello F, Schweitzer AN, Lynch WP, Bluestone JA, Sharpe AH (1995) Loss of CTLA-4 leads to massive lymphoproliferation and fatal multiorgan tissue destruction, revealing a critical negative regulatory role of CTLA-4. Immunity 3(5):541–547

Trzonkowski P, Bieniaszewska M, Juścińska J, Dobyszuk A, Krzystyniak A, Marek N, Myśliwska J, Hellmann A (2009) First-in-man clinical results of the treatment of patients with graft versus host disease with human ex vivo expanded CD4+ CD25+ CD127− T regulatory cells. Clin Immunol 133(1):22–26. https://doi.org/10.1016/j.clim.2009.06.001

Vieira PL, Christensen JR, Minaee S, O'Neill EJ, Barrat FJ, Boonstra A, Barthlott T, Stockinger B, Wraith DC, O'Garra A (2004) IL-10-secreting regulatory T cells do not express Foxp3 but have comparable regulatory function to naturally occurring CD4+ CD25+ regulatory T cells. J Immunol 172(10):5986–5993. https://doi.org/10.4049/jimmunol.172.10.5986

Wakkach A, Cottrez F, Groux H (2001) Differentiation of regulatory T cells 1 is induced by CD2 costimulation. J Immunol 167(6):3107–3113. https://doi.org/10.4049/jimmunol.167.6.3107

Watanabe N, Yi-Hong W, Lee HK, Ito T (2005) Hassall's corpuscles instruct dendritic cells to induce CD4+ CD25+ regulatory T cells in human thymus. Nature 436(7054):1181. https://doi.org/10.1038/nature03886

Waterhouse P, Penninger JM, Timms E, Wakeham A, Shahinian A, Lee KP, Thompson CB, Griesser H, Mak TW (1995) Lymphoproliferative disorders with early lethality in mice deficient in Ctla-4. Science 270:985–988

Weiner HL (2001) Induction and mechanism of action of transforming growth factor-β-secreting Th3 regulatory cells. Immunol Rev 182(1):207–214. https://doi.org/10.1034/j.1600-065X.2001.1820117.x

Weiner M, Howard L (1997) Oral tolerance for the treatment of autoimmune diseases. Annu Rev Med 48 (1):341–351. https://doi.org/10.1146/annurev.med.48.1.341

Weirather J, Hofmann U, Beyersdorf N, Ramos GC, Vogel B, Frey A, Ertl G, Kerkau T, Frantz S (2014) Foxp3+ CD4+ T cells improve healing after myocardial infarction by modulating monocyte/macrophage differentiation. Circ Res. https://doi.org/10.1161/CIRCRESAHA.115.303895

Wing K, Onishi Y, Prieto-Martin P, Yamaguchi T, Miyara M, Fehervari Z, Nomura T, Sakaguchi S (2008) CTLA-4 control over Foxp3+ regulatory T cell function. Science 322(5899):271–275. https://doi.org/10.1126/science.1160062

Yadav M, Bluestone JA, Stephan S (2013) Peripherally induced tregs–role in immune homeostasis and autoimmunity. Front Immunol 4(232):1–12. https://doi.org/10.3389/fimmu.2013.00232

Yamagiwa S, Gray JD, Hashimoto S, Horwitz DA (2001) A role for TGF-β in the generation and expansion of CD4+ CD25+ regulatory T cells from human peripheral blood. J Immunol 166(12):7282–7289. https://doi.org/10.4049/jimmunol.166.12.7282

Yamazaki S, Bonito AJ, Spisek R, Dhodapkar M, Inaba K, Steinman RM (2007) Dendritic cells are specialized accessory cells along with TGF-β for the differentiation of Foxp3+ CD4+ regulatory T cells from peripheral Foxp3− precursors. Blood 110(13):4293–4302. https://doi.org/10.1182/blood-2007-05-088831

You S, Belghith M, Cobbold S, Alyanakian M-A, Gouarin C, Barriot S, Garcia C, Waldmann H, Bach J-F, Chatenoud L (2005) Autoimmune diabetes onset results from qualitative rather than quantitative age-dependent changes in pathogenic T-cells. Diabetes 54(5):1415–1422. https://doi.org/10.2337/diabetes.54.5.1415

Youhai-Chen VKK, Inobe J-i, Hafler DA, Weiner HL (1994) Regulatory T cell clones induced by oral tolerance: suppression of autoimmune encephalomyelitis. Science 265:1237. https://doi.org/10.1126/science.7520605

Zhang X, Izikson L, Liu L, Weiner HL (2001) Activation of CD25+ CD4+ regulatory T cells by oral antigen administration. J Immunol 167(8):4245–4253. https://doi.org/10.4049/jimmunol.167.8.4245

Part VI

Functional Biomaterials

ROS-Responsive Biomaterial Design for Medical Applications

15

Jung Bok Lee, Young Min Shin, Won Shik Kim, Seo Yeon Kim, and Hak-Joon Sung

15.1 Introduction

Stimuli-responsive biomaterials represent a major type of state-of- the art approaches to endow biomaterials with smart functions. These biomaterials undergo significant alterations in material structure and property in response to changes of local environmental factors including pH, temperature, enzyme activation, and water absorption. This smart function is useful to release drugs or cells locally at a specific moment when a pathological condition is generated. In particular, production of reactive oxygen species (ROS) serve as a major stimulus because over-production of ROS involves most types of major pathogenesis. The application of ROS-responsive biomaterials requires suitable material designs to program user-defined changes of their structure and property in response to a sudden change in the local ROS level. Thus, both natural and synthetic biomaterials have been used to program this function with exciting successes in this field. In this chapter, the progress in designing and applying ROS-responsive biomaterials within the past 10 years is summarized. The authors aim to provide a comprehensive but concise review of chosen biomaterials being applied to ROS-responsive designs.

J. B. Lee · Y. M. Shin · S. Y. Kim · H.-J. Sung (✉)
Department of Biomedical Science, Yonsei University College of Medicine, Seoul, South Korea
e-mail: JUNGBOKLEE01@yuhs.ac; MSHIN@yuhs.ac; hj72sung@yuhs.ac

W. S. Kim
Department of Otorhinolaryngology, Yonsei University College of Medicine, Seoul, South Korea
e-mail: wskim78@yuhs.ac

15.2 Reactive Oxygen Species (ROS) in Biological System

As the first part of the present chapter, we describe the definition, generation mechanism, and signaling roles of ROS comprehensively based on the past and current reports from the field of redox biology and free radicals. This part provides insight into the main concepts to design ROS-responsive biomaterials for therapeutic delivery and tissue regeneration.

15.2.1 Definition of ROS

Reactive oxygen species (ROS) are a family of reactive molecules and free radicals generated from oxygen. They are produced during normal aerobic metabolism, notably in the mitochondrion from an incomplete reduction of oxygen by electron transfer. The reduction process of two unpaired electrons in a separate orbital electron shell of oxygen generates radicals, including superoxide anion ($O2^-$), hydrogen peroxide (H_2O_2), hydroxyl radical (HO•), hydroxyl ion (HO^-); and nitric oxide (NO^-) (Fig. 15.1). Each ROS type has an intrinsic chemical feature which

I. Noh (ed.), *Biomimetic Medical Materials*, Advances in Experimental Medicine and Biology 1064,
https://doi.org/10.1007/978-981-13-0445-3_15

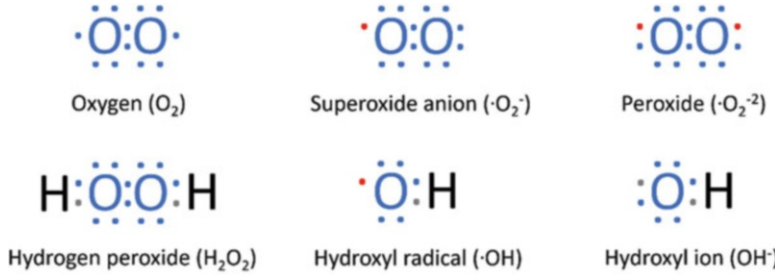

Fig. 15.1 Electron structures of representative reactive oxygen species (ROS)

determines its reactivity with various biological targets (Rhee 2006).

During the past few decades, it has been found that harmful effects of ROS result in critical damages of DNA, proteins and lipids and thus play causative roles in pathogenesis of atherosclerosis, carcinogenesis, neurodegeneration, diabetes, and aging, which is issued as a term of oxidative stress in the biological system (Fakhruddin et al. 2017; Kim et al. 2015a; Nikolay et al. 2015; Simm and Brömme 2005; Ziech et al. 2011). On the other hand, favorable reactions of ROS have been reported recently as ROS participates in communications between intracellular molecules by turning on and off protein expression (Schieber and Chandel 2014). These proteins were found to play supportive roles during tissue regeneration (Dunnill et al. 2017; Serras 2016). These positive behaviors of ROS in signaling is now conferred as "redox biology" or "redox signaling".

15.2.2 ROS Generation

In redox biology, hydrogen peroxide-mediated oxidation of proteins is commonly considered as an initial step for signaling. Cysteine residues in proteins are a major target of hydrogen peroxide and are present as a form of thiolate anion at physiological pH (Finkel 2012). Hydrogen peroxide within a nanomolar range oxidizes thiolate anions to a sulfenic form, and its reversible reaction causes structural alteration of proteins, thereby modulating their functions. However, along with oxidative stress, over-production of intracellular hydrogen peroxide can lead a permanent damage of proteins, resulting in pathogenesis (Sharma et al. 2012).

Generation of hydrogen peroxide is regulated by mitochondria and NADPH oxidases (Fig. 15.2) (Brand 2010). During electron transfer of oxygen, superoxide can be generated and quickly converted into hydrogen peroxide by superoxide dismutase (SOD) in cytosol and mitochondrial matrix (Fridovich 1997). Hence, addition of SOD has been considered as a therapeutic strategy to reduce accumulation of superoxide in an intracellular matrix so that damage or inactivation of functional proteins can be prevented. While only small populations of proteins are affected by superoxide or hydrogen peroxide, most intracellular proteins are influenced by reactive hydroxyl radicals (Chen et al. 2009). Indeed, reactive hydroxyl radicals damage DNA, proteins, and lipids in the cytosol indiscriminately. Reactive hydroxyl radicals are formed from hydrogen peroxide by the Fenton reaction, and their generation is highly regulated to maintain homeostasis with various mechanisms (Winterbourn 1995). Thus, it is important to maintain a level of intracellular hydrogen peroxide to control signaling cascades of cells or to prevent oxidative stress with pathogenesis.

15.2.3 ROS in Regulation of Cell Proliferation

In tissue engineering and regenerative medicine, how to promote tissue regeneration is one of the major objectives. Since enhanced tissue regeneration should be accompanied with favorable cell proliferation, various growth factors have been

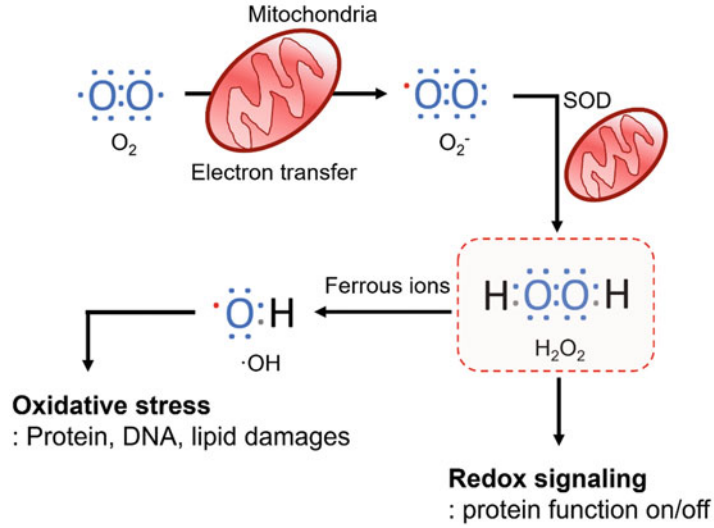

Fig. 15.2 ROS generation in mitochondria: oxidative stress vs. redox signaling

used. For example, platelet-derived growth factor (PDGF) and epidermal growth factor (EGF) binds to their corresponding receptors and thus activate tyrosine kinases, thereby initiating an intracellular signaling pathway related to cell proliferation (Fig. 15.3) (Svegliati et al. 2005; Paulsen et al. 2011). In this process, ROS production can be modulated through action of NADPH oxidases and play a regulatory role in activating or deactivating functional proteins by changing their allosteric protein structures (Hertog et al. 2008). Hydrogen peroxide can be generated by EGF signaling and consequently oxidizes a cysteine residue of protein tyrosine phosphatase 1B to a sulfenic form, thereby inactivating the signaling through dephosphorylation of tyrosine residues in the EGF receptor (EGFR) (Bae et al. 1997).

On the other hand, cancer cells exhibit a high level of ROS production (Cairns et al. 2011). While a high level of ROS production (e.g. reactive hydroxyl radicals) impairs proliferation of normal cells, cancer cells are not susceptible to ROS-induced cell death due to their robust anti-oxidative activities, indicating that the anti-oxidative capacity is dependent on the cell type (Gorrini et al. 2013). As a survival mechanism, cells undergo an adaptation process to adjust their anti-oxidative capacity when their environment is changed in the course of nutrition supply or evaluation process, suggesting that the strategy to operate anti-oxidative activities should be modified considering the developmental and pathological stage, the tissue environment, and the nutrition status of target cell type.

15.2.4 ROS in Regulation of Inflammation

Immune system is defined as a host defense system against invasion of foreign materials such as pathogen, biomaterial and microbes. When this defense system is activated, accumulation of inflammatory cells increases in the infected area to remove the pathogens or other foreign materials. Therefore, the body operates this defense system to prevent various diseases, such as autoimmunity and cardiovascular disease. Since this defense system is also crucial for tissue repair by recruiting and synthesizing essential components, how to regulate the immune response to biomaterial-based implants is a key design factor for successful applications in the field of biomaterials and tissue engineering (Franz et al. 2011). Interestingly, it has been recently reported that ROS can play a mechanistic role as essential second messengers in innate and

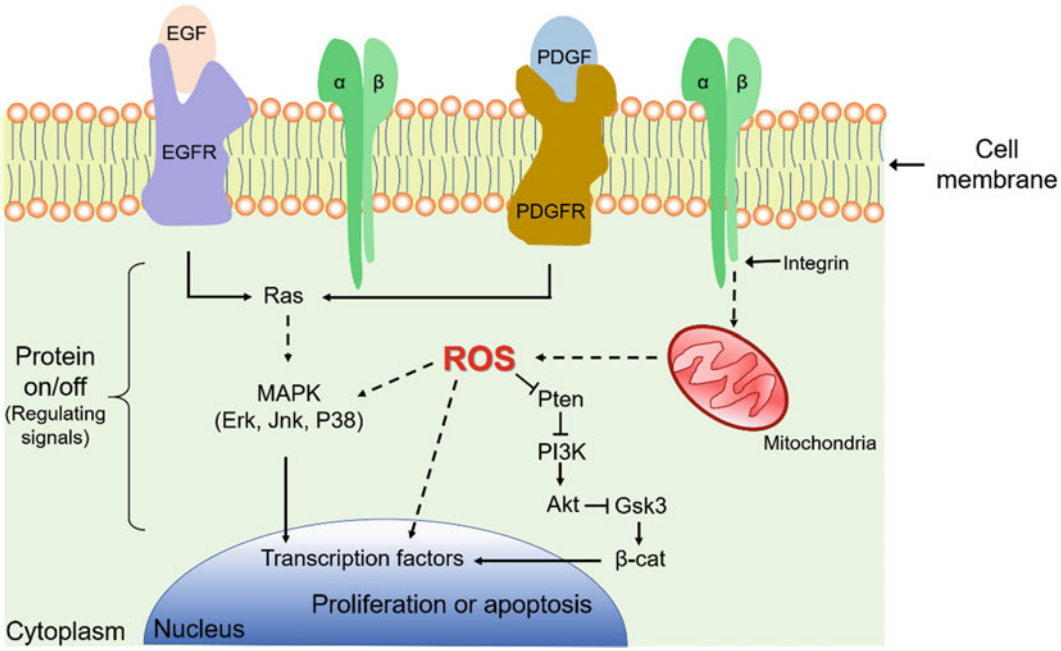

Fig. 15.3 Simple diagram of ROS-mediated signaling for cell proliferation

adaptive immunity (Yang et al. 2013). This mechanistic role of ROS in interaction with immune cells became an urgent subject to study in the context of tissue repair and immune diseases (Mittal et al. 2013).

The innate immunity is non-specific in reponse to tissue infection and injury. For example, binding of lipopolysaccharide onto a toll-like receptor stimulates NADPH oxidase and mitochondrial activity to generate ROS (Chandel et al. 2000; Qin et al. 2005). It was found that the generated ROS boosted the activity of macrophage against bacterial infections. On the other hand, the adaptive immune system also relies on the ROS action in operating their target-specific defense system. For example, antioxidant treatment in order to reduce ROS levels prohibited T cell proliferation and interleukin-2 production, suggesting that proper level of ROS is required for T-cell activation (Chaudhri et al. 1986; Kamiński et al. 2010). Activation and proliferation of B-cells were also regulated by an appropriate ROS level which is driven by cooperative actions of NADPH oxidase and mitochondria (Wheeler and DeFranco 2012; Jang et al. 2015). Together these studies suggest ROS as a key regulatory factor for both for T- and B- cell-mediated immune responses.

For the past 50 years of ROS research, overproduction of ROS has been recognized as a harmful component for cell and tissue repair, resulting in of the status of "oxidative stress". However, a series of leading research groups found a new mechanistic role of ROS as a positive component in cell and tissue repair and opened a new avenue of research entitled "redox biology". Hence, interpreting ROS roles in tissue and cell responses should be target-specific and avoid applying the generalized concept of ROS roles, suggesting that there is an unmet need requiring significant efforts to further investigate ROS mechanisms. Moreover, how to prevent the exposure to excess ROS, how to reduce their over-production, and how to use ROS as an alternative to treat diseases or to repair tissue defects should be considered to develop therapeutics for the next generation.

15.3 ROS-Responsive Materials

In this part, we summarize state-of the-art approaches to design materials to undergo degradation, structural change, functional modulation or physicochemical property switch in response to ROS production ("ROS-responsive materials"). These materials have been used as a form of delivery vehicle, hydrogel, scaffold, or cell culture matrix in the field of drug delivery, tissue engineering and regenerative medicine.

15.3.1 Poly(Propylene Sulfide) (PPS)

PPS is commonly used to design thioether-based polymers, which have been used as a form of drug delivery carrier as its chemical property is switched in solution upon exposure to ROS. When PPS is oxidized, it undergoes structural conversion of hydrophobic sulfide group to be hydrophilic. For example, the sulfide group of PPS becomes hydrophilic polysulfoxide or sulfone in the H_2O_2 rich environment. Sulfone is generated in response to low levels of H_2O_2 concentration with low temperature whereas sulfones are produced in response to strong oxidative acids such as organic peroxyacids (Lee et al. 1998). For drug delivery, PPS is used to design amphiphilic block copolymers for self-assembly of unilamellar nanoparticles which can carry hydrophobic drugs inside and degrade under an oxidative environment, thereby releasing the drugs. For example, PPS-based nanoparticles were found to be stable for several weeks in suspension with DI water at room temperature but underwent degradation by depolymerization in response to H_2O_2 treatment (Napoli et al. 2004a). Due to this ROS-responsive property, PPS-based materials have been applied to biosensing and stimuli-responsive therapeutic delivery in the context of pathogenesis related to inflammation and cancer.

15.3.2 Selenium

Selenium is an essential trace element in the human body and protects cells from oxidative damages as a regulatory component of anti-oxidative enzymes such as glutathione peroxidase and thioredoxin reductase (Mertz 1981; Schroeder et al. 1970; Rotruck et al. 1973). The oxidation mechanism of selenium is similar to that of PPS as it undergoes hydrophobic to hydrophilic transition upon oxidation. Selenium-based polymers showed a higher sensitivity to oxidants due to their lower bond energies of C-Se (244 kJ mol^{-1}) and Se-Se (172 kJ mol^{-1}) bonds when compared to C-S (272 kJ mol^{-1}) and S-S (240 kJ mol^{-1}) bonds in PPS (Xu et al. 2013; Saravanakumar et al. 2017). Since Diselenide has redox sensitive nature, incorporating diselenide linker in a polymer backbone elevates intracellular redox sensitivities (Ziegler 1985; Corti et al. 2005).

15.3.3 Phenylboronic Acid and Phenylboronic Ester

Recently, boronic ester has been used as a ROS responsive component because it degrades upon oxidation (Webb and Levy 1995). Aryl boronic acid and ester bonds are selectively oxidized by H_2O_2 and generate phenol and boronic acid as oxidation products (Song et al. 2014). Because of specific binding affinities of the arylboronic acid and ester functional groups to diols, amino alcohols, cyanide and fluoride, they have been used in the functional polymer design, in particular as a biosensor or glucose-responsive nanoparticles for controlled insulin delivery (Shiino et al. 1994). Conjugating these functional groups to the polymer backbone of nanoparticles enables effective targeting and releasing of drugs, including vaccine molecules or proteins.

15.3.4 Tellurium

Tellurium belongs to the group 16 of the periodic table and resembles the oxidative response of sulfur and selenium. As Tellurium is listed below selenium in the periodic table due to its lower electronegativity, tellurium-containing polymers are anticipated to have a higher sensitivity than that of selenium-based polymers. In the sites of inflammation or tumor progression, the physiological level of ROS is typically as low as 50–100 $\times$ 10^{-6} M. Due to the matched responsiveness, tellurium-based polymers are considered more promising to apply to the sites inflammation and tumor progress compared to the selenium based materials. However, only few studies have explored applying Tellurium to design ROS-responsive drug carriers (Saravanakumar et al. 2017; Xu et al. 2016).

15.3.5 Poly(Thioketal)

Thioketal bonds can be destabilized by superoxide and H_2O_2, followed by oxidation into ketones and organic thiols (or disulfide) (Wilson et al. 2010; Kim et al. 2015b; Nicolaou et al. 2003). Oxidation of thioketal bonds increases the polarity and water solubility of polymers by hydrophobic to hydrophilic conversion as thioketal is oxidized to sulfoxides and sulfones. Due to this property, thioketal-based polymeric carriers deliver therapeutics in ROS rich sites such as cancer (Shim and Xia 2013). Intracellular or tumor acidosis with a weak acidic pH level can serve as a biological trigger to program drug release from thioketal-containing polymers.

15.4 Platforms of ROS-Responsive Biomaterials for Biomedical Applications

Stimuli-responsive materials are designed to undergo modulation of their structure or property like phase transition in response to a change in external environmental factors such as ion, enzyme, pH, light and temperature. Among stimuli-responsive biomaterials, ROS-sensitive platforms have been widely utilized for biomedical applications as a form of scaffold, hydrogel, and drug delivery vehicle (Xu et al. 2016). In this part, we summarize recent approaches to design nanoparticles, scaffolds, and hydrogels based on ROS-responsive materials to enable efficient targeting into pathological sites where ROS are over-produced.

15.4.1 Hydrogels

Hydrogels are composed of hydrophilic or amphiphilic natural/synthetic polymer networks which absorb a large amount of water. Hydrogels have been widely used in biomedical applications including pharmaceutics, tissue engineering, and regenerative medicine (Yu and Ding 2008; Kopeček 2007; Seliktar 2012). Due to their ECM-like three dimensional structure, high water content and biocompatibility, hydrogels have become a common format for the applications (Drury and Mooney 2003; Annabi et al. 2014). Recently, new applications based on ROS responsive hydrogels have drawn remarkable attention as intelligent drug or cell delivery vehicles in the field of tissue engineering and therapeutics delivery.

15.4.1.1 Poly(Propylene Sulfide) (PPS)

Duvall and co-workers utilized an ABC triblock polymer and developed thermo-responsive and ROS-mediated degradable hydrogels (Fig. 15.4) (Gupta et al. 2014). The polymer was poly [(propylenesulfide)-block-(N,N-dimethylacylamide)-block-(N-isopropylacrylamide)] (PPS-b-PDMA-b-PNIPAAM) and formed micelles (micelle solution at $\geq$2.5 wt. %) comprising a hydrophobic PPS core at room temperature (25 °C). Each part of this triblock copolymer was designed to play a different role: (i) the PPS block makes a hydrophobic core which can load hydrophobic drugs into the micelle core, (ii) PNIPAM acts as a trigger of phase transition from insoluble to soluble in water, and (iii) this triblock copolymer makes hydrogels as it

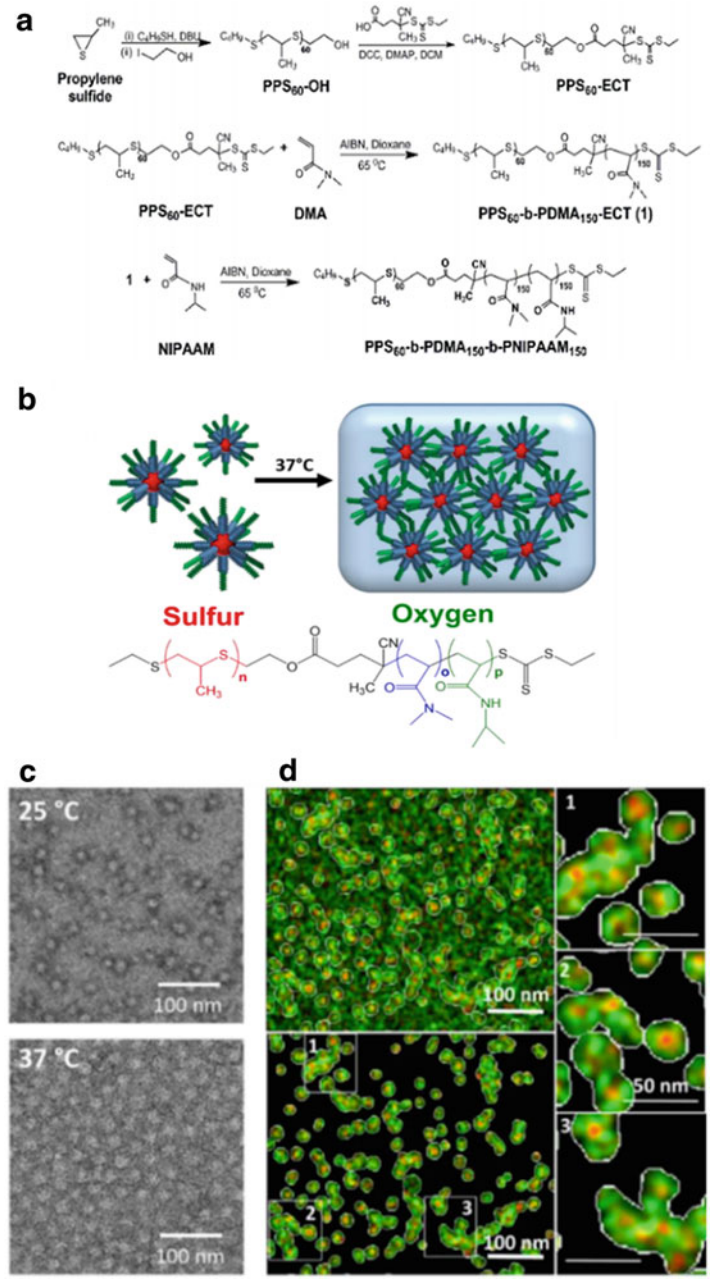

Fig. 15.4
(**a**) Synthesis illustration PPS-b-PDMA-b-PNIPAM triblock-copolymer (**b**) Schematic representation of micelle gelation at 37 °C and polymer architecture coordinating with STEM-EDS element maps. (**c**) TEM images of PPS60-b-PDMA150-b-PNIPAAM150 micelles at 25 and 37 °C. (**d**) STEM-EDS element maps for sulfur (red) and oxygen (green) of PPS60-bPDMA150-b-PNIPAAM150 core-shell compartments at 37 °C with image thresholding and background subtraction. Core-forming PPS produces the red signal for sulfur, while oxygen (appearing green) is present in the PDMA and PNIPAAM corona-forming blocks. (Gupta et al. 2014)

contains the hydrophilic block PDMA. Upon exposure to ROS, PPS block became hydrophilic and disrupted the micelles, leading to gel degradation. This hydrogel has great potential for applying to the conditions of oxidative stress associated pathologies such as atherosclerosis, cancer and arthritis (Winterbourn 2008; Martin et al. 2014).

15.4.1.2 Arylboronic Ester

To induce ROS-responsive behavior, boronoaryl methoxycarbonyl (BAmoc) groups containing di-

and tripeptides were constructed (Ikeda et al. 2014; Zhou et al. 2017; Peltier et al. 2015). These peptides were self-assembled and thereby formed a hydrogel. Under an oxidative environment, the BAmoc unit was destabilized and led to hydrogel degradation. The gel to sol transition of 0.1 wt. % peptide solution took 1~6 h and the duration was dependent on the H_2O_2 concentration. When glucose oxidases were encapsulated, the hydrogel quickly degraded due to H_2O_2 production by the enzymatic reaction. This hydrogel demonstrated a similar gel disruption behavior when blood plasma containing glucoses were treated at the hyperglycemic level. This ROS-responsive hydrogel can be used to detect specific analytes as a diagnostic means of disease when the encapsulated glucose oxidases are replaced with other types of oxidase such as choline oxidase, sarcosine oxidase, or urate oxidase (Xu et al. 2016; Ikeda et al. 2014).

15.4.2 Scaffold

Porous scaffolds are commonly used to regenerate damaged or diseased tissues as they allow for appropriate cell adhesion and proliferation. ROS-responsive scaffolds have been designed to react with ROS in local environments for therapeutic purposes (Xu et al. 2016).

15.4.2.1 Poly(Thioether Ketal)

Poly(thioketal) (PTK) urethane (PTK-UR) scaffolds were designed to degrade in selectively response to cell-generated ROS, leaving the degraded space to tissue in-growth (Martin et al. 2014). Poly(thioketal) has been commonly used to produce ROS-responsive nanoparticles because the thioketal bond is selectively destabilized and degrades by ROS-mediated cleavages of polymer chains. The oxidative degradation mechanism of PTK polymer is shown in Fig. 15.5a. The PTK-UR scaffolds were stable over 25 weeks in PBS whereas they degraded rapidly under ROS environment (Fig. 15.5b). RAW 267.4 macrophages were cultured within the scaffold under treatment of macrophage-activating media condition to determine cell-mediated degradation. As a result, the PTK scaffold degraded in selective response to cell-mediated ROS production. Upon *in vivo* degradation, the PTK-UR scaffold provided proper spaces for cellular infiltration and tissue ingrowth compared to poly(ester urethane) scaffolds undergoing hydrolytic degradation.

15.4.2.2 Oilgoproline Peptide

Biodegradable and porous PEG-b-polycaprolactone copolymeric scaffolds were prepared and crosslinked by proline oligomers (Ac-KP_nK) to program a ROS-responsive property (Yu et al. 2011). In this way, scaffold degradation can be accelerated in response to progressive oxidative stress with chronic inflammation, thereby enabling sustained release of anti-inflammatory drugs to the inflamed site. The degradation behavior of oligoproline peptide conjugated scaffolds was tested under treatment of H_2O_2 and Cu II at 37 °C. To mimic a physiological relevant ROS environment, activated murine macrophages were seeded into scaffolds. As a result, the proline oligomers fully degraded after few weeks, suggesting that this design should be applicable to program site-specific and ROS generation-responsive therapeutic delivery as a form of scaffold or delivery vehicle.

15.4.3 ROS-Triggered Drug Release from Nanoparticles

15.4.3.1 Poly(Propylene Sulfide) (PPS)

Upon oxidation, PPS undergoes a significant switch in its solubility from a hydrophobic status to hydrophilic polysulfoxide or polysulfone, resulting in degradation. Therefore, PPS has been used as a major ROS-responsive component to develop nanoparticles which can deliver and release therapeutics (e.g. drug, antigen, and gene) to a pathogenic site under oxidative stress. For example, Reddy and colleagues prepared PPS-containing poly(ethylene glycol) (PEG) nanoparticles (NPS). Hydrophilic PEG stabilized the NPs structure with a PPS core with an average diameter of 20 nm. These NPs were effectively trapped into a lymph node over 5 days when they

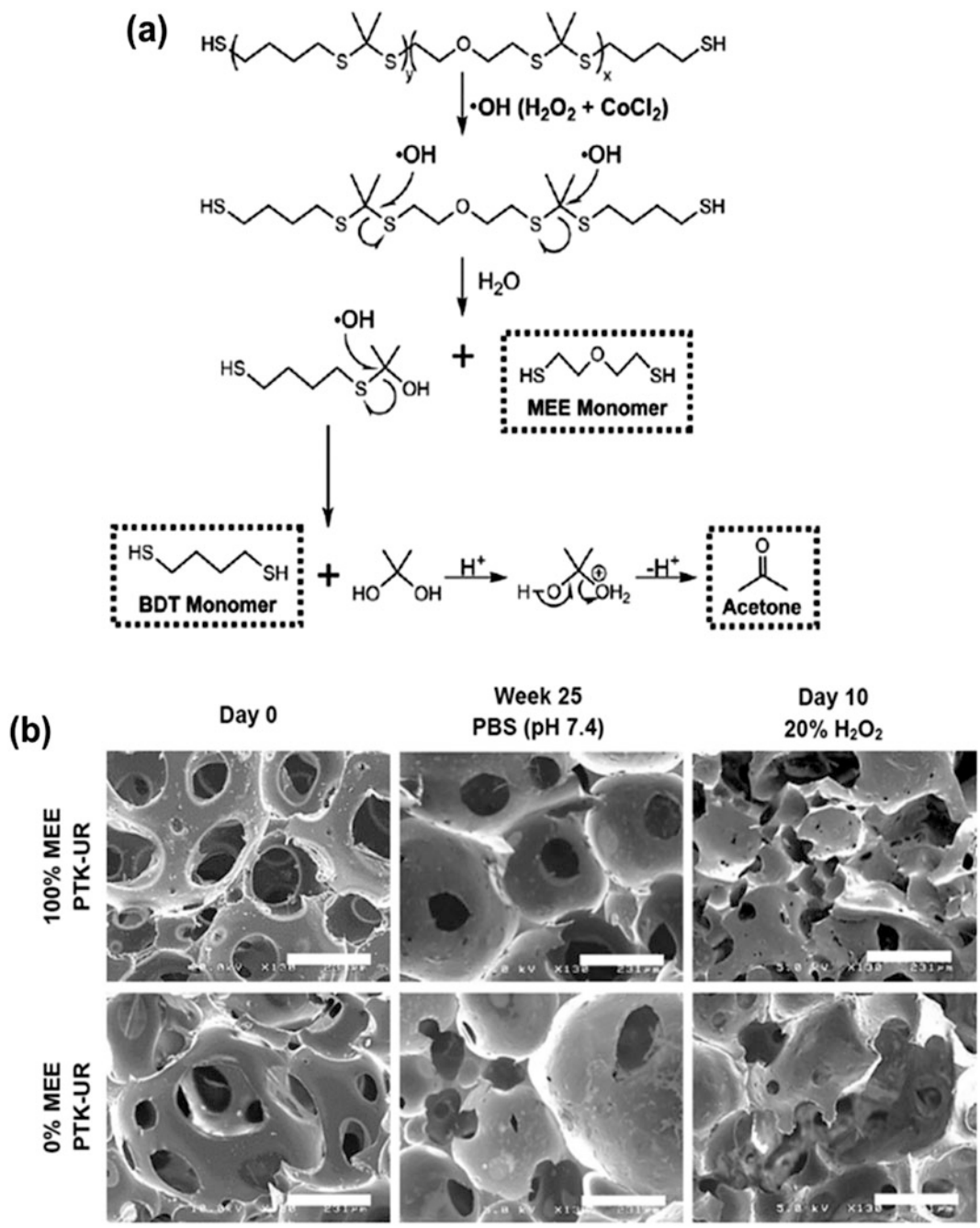

Fig. 15.5 (**a**) Degradation mechanism of PTK polymers and (**b**) SEM images of PTK-UR scaffold *in vitro* degradation incubated in PBS for 25 weeks and 20% H_2O_2 media for 10 days. Scale bars = 231 μm. (Martin et al. 2014).

were injected interstitially into mice due to the stable structure with highly hydrophilic PEG corona and hydrophobic PPS core, indicating a suitable delivery performance in vivo (Reddy et al. 2006). PPS-based micelles showed an effective performance in sustained drug release. PEG_{44}-b-$PPS_{10–40}$ block copolymers were used to form a micelle for delivering cyclosporine A,

and this micelle released the drug for 12 days in a sustained fashion (Velluto et al. 2008). Glucose oxidases were also delivered by encapsulating or chemically conjugated into PPS, thereby enabling glucose-responsive release (Rehor et al. 2005; Napoli et al. 2004b).

15.4.3.2 Selenium

Since Selenium-based polymers are known to be more sensitive to H_2O_2 than sulfide-containing counterparts, these polymers have been used to develop ROS-responsive drug delivery carriers. As the ROS level in cancer cells is higher than that of normal cells, Selenium-based polymers provide a favorable platform for delivering anti-cancer drugs. For example, PEG-b-PUSeSe-b-PEG was synthesized to form micelles through self-assembly in the water with a mean diameter of 76 nm (Fig. 15.6) (Ma et al. 2010). Their capabilities for drug loading and releasing were determined with doxorubicin and Rhodamine B. Their exposure to 0.01% H_2O_2 triggered quick release of Rhodamine B within 4 h, while their exposure gamma-ray radiation triggered release of doxorubicin within 3 h (Ma et al. 2011). Thus, selenium-based polymeric micelles can be applied as a means of therapeutic delivery in the context of radiotherapy treatment for relevant cancer patients.

Recently, small selenium-containing compounds gained an attention due to their therapeutic effects for cancer therapy. For example, when hyperbranched polydiselenides were conjugated with hydrophilic phosphate segments, these materials induced apoptosis of cancer cells. In addition, when they were self-assembled into stable NPs with loading of doxorubicin, these NPs demonstrated effective drug release in oxidative or reductive stimuli-responsive manner (Liu et al. 2012).

15.4.3.3 Phenylboronic Ester

Phenylboronic ester-containing polymers react with H_2O_2 and consequently generate biproducts phenol and boronic acid. Phenylboronic acids have a unique property to react with only H_2O_2 among other ROS types, resulting in oxidation into phenols. Hence, phenylboronic acids have been used to develop H_2O_2-responsive drug delivery carriers or imaging agents (Liu et al. 2012). For instance, arylboronic ester conjugated dextran was used to produce ROS-responsive NPs (Broaders et al. 2011). Degradation of these NPs was accelerated under 1×10^{-3} M H_2O_2, followed by the significantly high presence to CD8+ T-cells whereas ovalbumin encapsulated PLGA (poly(lactic-co-glycolic acid)) NPs did not degrade.

Xu and collaborators used phenylboronic ester-containing polymers to regulate a ROS-responsive protein function. Briefly, when phenylboronic acid was coupled with RNase A (RNase A-4-nitrophenyl 4-(4,4,5,5-tetramethyl-1,3,2-dioxaborolan-2-yl) benzyl carbonate), the enzyme function was temporarily inactive. However, upon entering in tumor cells possessing a high level of intracellular ROS, this material underwent cleavages of phenylboronic ester bond links with RNases. This process resulted in turning on of the enzymatic action to degrade RNAs in target cells and consequent restoration of the anti-cancer activity (Wang et al. 2014).

15.5 Disease-Specific Applications of ROS-Responsive Materials

This part provides a brief review on biomedical applications of ROS-responsive materials towards the clinic side. A growing body of evidence suggests that over-production of ROS locally accompanies major pathogenesis such as cancer (Shim and Xia 2013; Xu et al. 2017; Trachootham et al. 2009), atherosclerosis (Dou et al. 2017), diabetes (Poole et al. 2015), infections (Dwyer et al. 2009), and inflammatory diseases (Chung et al. 2015). The following examples provide insight into development of suitable therapeutic platforms by programing target disease-specific delivery functions

Cancer Selective treatment with maintenance of a high therapeutic activity is a major goal of cancer drug delivery. Because genetic differences between normal and cancer cells results in expression of different phenotypic molecules on cell

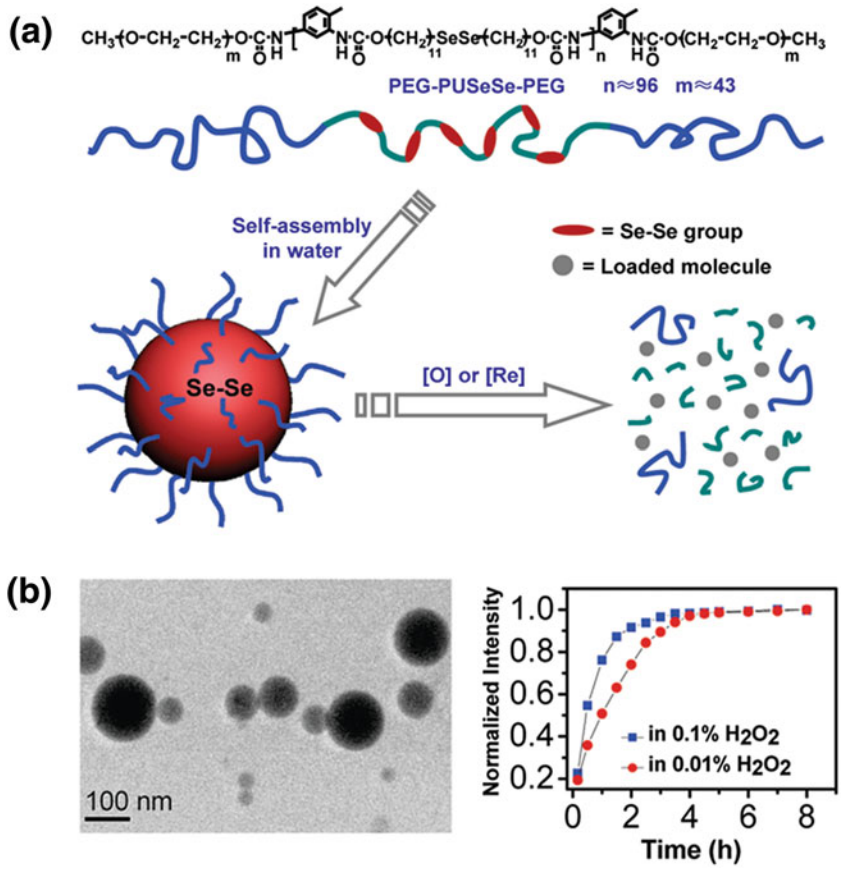

Fig. 15.6 Selenium-based polymer as a ROS-responsive drug delivery carrier. (**a**) Redox responsive disassembly of PEG-PUSeSe-PEG micelles, and (**b**) Cryo-TEM image of PEG-PUSeSe-PEG micelles and the release behavior of Rhodamine B in H_2O_2. (Rehor et al. 2005)

membrane, molecular targeting of cancer drugs such as cetuximab and trastuzumab demonstrated promising therapeutic activities with tolerable side effects (Xu et al. 2017). However, this targeting strategy has major limitations related to the acquired resistance and the genetic instability/heterogeneity of cancer cells. To overcome these limitation, a combinatorial usage of therapeutic vehicles targeting multi-genetic alterations of cancer cells has been approached (Shim and Xia 2013; Trachootham et al. 2009). Since increased aerobic glycolysis, also known as the Warburg effect, increases oxidative stress and represents common characteristics of most cancer cells (Trachootham et al. 2009), targeting these physiological changes in cancer cells has been proposed as an important strategy to develop novel anticancer drugs. A series of evidences suggest that many types of cancer cells have high levels of ROS, which is associated with aberrant growth. Hence, adjusting intracellular ROS levels in cancer cells with redox modulation is proposed as a promising strategy to treat cancer cells with minimal side effects (Shim and Xia 2013).

Atherosclerosis Atherosclerosis is a major cause of mortality all over the world. Various drugs have been extensively investigated and clinically tested for atherosclerosis treatment. However, since most therapeutics tested so far are administered orally, drugs are nonspecifically distributed throughout the body, and side effects to other organs and normal tissues become a

major issue, indicating an unmet need to develop a new strategy. Moreover, oral administration makes it difficult to maintain the effective concentration of therapeutics around atherosclerotic plaques over time, resulting in poor outcomes. Drug delivery using ROS-responsive materials is a promising approach to address the problems in the treatment of the atherosclerosis as ROS involve all steps of atherosclerosis generation including endothelial dysfunction, lipid oxidation, inflammatory cell activation, form cell formation, and smooth muscle cell action (Dou et al. 2017).

Diabetes Diabetes result from a chronic inflammation-imposed environment where ROS contributes to causative mechanisms of endothelial dysfunction and peripheral arterial disease (PAD) (Poole et al. 2015). Diabetic patients have an increased risk of PAD due to hyperglycemia, oxidative stress, and consequential microvascular complications. Therefore, novel agents aiming to decrease oxidative stress can be a promising candidate for anti-PAD treatment of diabetic patients. ROS-responsive release of radical scavenger combined with biocompatible microparticles like PLGA can be suggested as an option for effective delivery with control of sustained release (Poole et al. 2015).

Infection Emergence of antibiotic-resistant bacteria is a serious problem in the clinical setting. The list of bacteria that immune to the actions of antibacterial drugs in the human body has been expanded as it was found that bacteria can become antibiotic-resistant through genetic and epigenetic alterations such as addition of genetic materials from different species, followed by activation of dormant genetic materials among others; or genetic mutation via interactions with antibiotic agents or via antibiotic-induced oxidative stress (Dwyer et al. 2009). Since antibiotic treatment induces ROS production at the target site, delivery vehicles releasing antibiotics upon oxidative stress under infection will serve as a future solution to replace the conventional antibiotic therapy by enabling long-term sustained release of antibiotics and then stopping the release upon attenuation of ROS production.

Inflammation A series of studies have reported that many diseases are triggered by inflammatory mechanisms with concurrent over-production of ROS from activated inflammatory cells. ROS-responsive materials carrying anti-inflammatory drugs can be a promising strategy to control inflammatory diseases. One of the main diseases is an osteoarthritis in which ROS contribute to inflammatory activation in the joint space (Chung et al. 2015). Systemic administration of anti-inflammatory drugs through ROS-sensitive delivery will improve local targeting accuracy and site-specific release of therapeutic agents in an inflammatory joint, thereby reducing systemic side effects.

15.6 Conclusion

As summarized so far, ROS-responsive materials are considered as a promising tool for therapeutic delivery to various pathological sites under oxidative stress. These materials have been applied as a form of implantable scaffold, drug/gene delivery vehicle, and oxidative stress protector. Since ROS is produced locally upon pathogenesis in living organisms, various ROS-responsive materials have been designed to deliver and release therapeutics by material degradation or structure deformation to the local sites of ROS production including various organs, tissues and cells. ROS-responsive materials have been used as a format of coating, implantable, or injectable materials for site-specific delivery of therapeutics and imaging agents in response to over-production of ROS *in vivo*.

As discussed in this chapter, several ROS-responsive micelles or NPs have been developed and utilized to treat diseases in pre-clinical settings. Since type and amount of ROS varies depending upon cell and tissue sources as well as pathogenic conditions, understanding the target-specific mechanism of ROS action is essential for efficient design and fabrication of materials.

Moreover, understanding material-specific ROS-responsive properties is also a key requirement for successful clinical applications. Although this chapter covers only a limited portion of the state-of-the-art approaches in the field, the underlying points are summarized enough to indicate that the research area of ROS-responsive materials has much room to succeed if more precise material designs are customized to meet pathogenesis-specific requirements and applied to gain clinically-relevant effects.

References

Annabi N, Tamayol A, Uquillas JA, Akbari M, Bertassoni LE, Cha C, Camci-Unal G, Dokmeci MR, Peppas NA, Khademhosseini A (2014) 25th anniversary article: rational design and applications of hydrogels in regenerative medicine. Adv Mater (Deerfield Beach, Fla) 26 (1):85–124

Bae YS, Kang SW, Seo MS, Baines IC, Tekle E, Chock PB, Rhee SG (1997) Epidermal growth factor (EGF)-induced generation of hydrogen peroxide: role in EGF receptor-mediated tyrosine phosphorylation. J Biol Chem 272(1):217–221

Brand MD (2010) The sites and topology of mitochondrial superoxide production. Exp Gerontol 45(7):466–472

Broaders KE, Grandhe S, Fréchet JMJ (2011) A biocompatible oxidation-triggered carrier polymer with potential in therapeutics. J Am Chem Soc 133(4):756–758

Cairns RA, Harris IS, Mak TW (2011) Regulation of cancer cell metabolism. Nat Rev Cancer 11:85

Chandel NS, Trzyna WC, McClintock DS, Schumacker PT (2000) Role of oxidants in NF-κB activation and TNF-α gene transcription induced by hypoxia and endotoxin. J Immunol 165(2):1013–1021

Chaudhri G, Clark IA, Hunt NH, Cowden WB, Ceredig R (1986) Effect of antioxidants on primary alloantigen-induced T cell activation and proliferation. J Immunol 137(8):2646–2652

Chen Y, Azad MB, Gibson SB (2009) Superoxide is the major reactive oxygen species regulating autophagy. Cell Death Differ 16:1040

Chung M-F, Chia W-T, Wan W-L, Lin Y-J, Sung H-W (2015) Controlled release of an anti-inflammatory drug using an ultrasensitive ROS-responsive gas-generating carrier for localized inflammation inhibition. J Am Chem Soc 137(39):12462–12465

Corti A, Paolicchi A, Franzini M, Dominici S, Casini AF, Pompella A (2005) The S-thiolating activity of membrane gamma-glutamyltransferase: formation of cysteinyl-glycine mixed disulfides with cellular proteins and in the cell microenvironment. Antioxid Redox Signal 7(7–8):911–918

Dou Y, Chen Y, Zhang X, Xu X, Chen Y, Guo J, Zhang D, Wang R, Li X, Zhang J (2017) Non-proinflammatory and responsive nanoplatforms for targeted treatment of atherosclerosis. Biomaterials 143(Supplement C):93–108

Drury JL, Mooney DJ (2003) Hydrogels for tissue engineering: scaffold design variables and applications. Biomaterials 24(24):4337–4351

Dunnill C, Patton T, Brennan J, Barrett J, Dryden M, Cooke J, Leaper D, Georgopoulos NT (2017) Reactive oxygen species (ROS) and wound healing: the functional role of ROS and emerging ROS-modulating technologies for augmentation of the healing process. Int Wound J 14(1):89–96

Dwyer DJ, Kohanski MA, Collins JJ (2009) Role of reactive oxygen species in antibiotic action and resistance. Curr Opin Microbiol 12(5):482–489

Fakhruddin S, Alanazi W, Jackson KE (2017) Diabetes-induced reactive oxygen species: mechanism of their generation and role in renal injury. J Diabetes Res 2017:30

Finkel T (2012) From sulfenylation to sulfhydration: what a thiolate needs to tolerate. Sci Signal 5(215):pe10–pe10

Franz S, Rammelt S, Scharnweber D, Simon JC (2011) Immune responses to implants – a review of the implications for the design of immunomodulatory biomaterials. Biomaterials 32(28):6692–6709

Fridovich I (1997) Superoxide anion radical (O·2), superoxide dismutases, and related matters. J Biol Chem 272 (30):18515–18517

Gorrini C, Harris IS, Mak TW (2013) Modulation of oxidative stress as an anticancer strategy. Nat Rev Drug Discov 12:931

Gupta MK, Martin JR, Werfel TA, Shen T, Page JM, Duvall CL (2014) Cell protective, ABC triblock polymer-based thermoresponsive hydrogels with ROS-triggered degradation and drug release. J Am Chem Soc 136(42):14896–14902

Hertog Jd, Östman A, Böhmer F-D (2008) Protein tyrosine phosphatases: regulatory mechanisms. FEBS J 275 (5):831–847

Ikeda M, Tanida T, Yoshii T, Kurotani K, Onogi S, Urayama K, Hamachi I (2014) Installing logic-gate responses to a variety of biological substances in supramolecular hydrogel–enzyme hybrids. Nat Chem 6:511

Jang K-J, Mano H, Aoki K, Hayashi T, Muto A, Nambu Y, Takahashi K, Itoh K, Taketani S, Nutt SL, Igarashi K, Shimizu A, Sugai M (2015) Mitochondrial function provides instructive signals for activation-induced B-cell fates. Nat Commun 6:6750

Kamiński MM, Sauer SW, Klemke C-D, Süss D, Okun JG, Krammer PH, Gülow K (2010) Mitochondrial reactive oxygen species control T cell activation by regulating IL-2 and IL-4 expression: mechanism of ciprofloxacin-mediated immunosuppression. J Immunol 184(9):4827–4841

Kim GH, Kim JE, Rhie SJ, Yoon S (2015a) The role of oxidative stress in neurodegenerative diseases. Exp Neurobiol 24(4):325–340

Kim JS, Jo SD, Seah GL, Kim I, Nam YS (2015b) ROS-induced biodegradable polythioketal nanoparticles for intracellular delivery of anti-cancer therapeutics. J Ind Eng Chem 21(Supplement C):1137–1142

Kopeček J (2007) Hydrogel biomaterials: a smart future? Biomaterials 28(34):5185–5192

Lee J-C, Litt MH, Rogers CE (1998) Synthesis and properties of poly(oxyethylene)s containing thioether, sulfoxide, or sulfone groups. J Polym Sci A Polym Chem 36(5):793–801

Liu J, Pang Y, Chen J, Huang P, Huang W, Zhu X, Yan D (2012) Hyperbranched polydiselenide as a self assembling broad spectrum anticancer agent. Biomaterials 33 (31):7765–7774

Ma N, Li Y, Xu H, Wang Z, Zhang X (2010) Dual redox responsive assemblies formed from diselenide block copolymers. J Am Chem Soc 132(2):442–443

Ma N, Xu H, An L, Li J, Sun Z, Zhang X (2011) Radiation-sensitive diselenide block co-polymer micellar aggregates: toward the combination of radiotherapy and chemotherapy. Langmuir 27 (10):5874–5878

Martin JR, Gupta MK, Page JM, Yu F, Davidson JM, Guelcher SA, Duvall CL (2014) A porous tissue engineering scaffold selectively degraded by cell-generated reactive oxygen species. Biomaterials 35 (12):3766–3776

Mertz W (1981) The essential trace elements. Science 213 (4514):1332–1338

Mittal M, Siddiqui MR, Tran K, Reddy SP, Malik AB (2013) Reactive oxygen species in inflammation and tissue injury. Antioxid Redox Signal 20(7):1126–1167

Napoli A, Valentini M, Tirelli N, Muller M, Hubbell JA (2004a) Oxidation-responsive polymeric vesicles. Nat Mater 3(3):183–189

Napoli A, Boerakker MJ, Tirelli N, Nolte RJM, Sommerdijk NAJM, Hubbell JA (2004b) Glucose-oxidase based self-destructing polymeric vesicles. Langmuir 20(9):3487–3491

Nicolaou KC, Mathison CJ, Montagnon T (2003) New reactions of IBX: oxidation of nitrogen- and sulfur-containing substrates to afford useful synthetic intermediates. Angew Chem Int Ed Engl 42 (34):4077–4082

Nikolay VG, Pavel VA, Alexander DN, Irina LZ, Richard OJ (2015) Reactive oxygen species in pathogenesis of atherosclerosis. Curr Pharm Des 21(9):1134–1146

Paulsen CE, Truong TH, Garcia FJ, Homann A, Gupta V, Leonard SE, Carroll KS (2011) Peroxide-dependent sulfenylation of the EGFR catalytic site enhances kinase activity. Nat Chem Biol 8:57

Peltier R, Chen G, Lei H, Zhang M, Gao L, Lee SS, Wang Z, Sun H (2015) The rational design of a peptide-based hydrogel responsive to H2S. Chem Commun 51(97):17273–17276

Poole KM, Nelson CE, Joshi RV, Martin JR, Gupta MK, Haws SC, Kavanaugh TE, Skala MC, Duvall CL (2015) ROS-responsive microspheres for on demand antioxidant therapy in a model of diabetic peripheral arterial disease. Biomaterials 41(Supplement C):166–175

Qin L, Li G, Qian X, Liu Y, Wu X, Liu B, Hong J-S, Block ML (2005) Interactive role of the toll-like receptor 4 and reactive oxygen species in LPS-induced microglia activation. Glia 52(1):78–84

Reddy ST, Rehor A, Schmoekel HG, Hubbell JA, Swartz MA (2006) In vivo targeting of dendritic cells in lymph nodes with poly(propylene sulfide) nanoparticles. J Control Release 112(1):26–34

Rehor A, Botterhuis NE, Hubbell JA, Sommerdijk NAJM, Tirelli N (2005) Glucose sensitivity through oxidation responsiveness. An example of cascade-responsive nano-sensors. J Mater Chem 15(37):4006–4009

Rhee SG (2006) H2O2, a necessary evil for cell signaling. Science 312(5782):1882–1883

Rotruck JT, Pope AL, Ganther HE, Swanson AB, Hafeman DG, Hoekstra WG (1973) Selenium: biochemical role as a component of glutathione peroxidase. Science 179(4073):588–590

Saravanakumar G, Kim J, Kim WJ (2017) Reactive-oxygen-species-responsive drug delivery systems: promises and challenges. Adv Sci (Weinh) 4 (1):1600124

Schieber M, Chandel NS (2014) ROS function in redox signaling and oxidative stress. Curr Biol 24(10):R453–R462

Schroeder HA, Frost DV, Balassa JJ (1970) Essential trace metals in man: selenium. J Chronic Dis 23(4):227–243

Seliktar D (2012) Designing cell-compatible hydrogels for biomedical applications. Science 336 (6085):1124–1128

Serras F (2016) The benefits of oxidative stress for tissue repair and regeneration. Fly 10(3):128–133

Sharma P, Jha AB, Dubey RS, Pessarakli M (2012) Reactive oxygen species, oxidative damage, and antioxidative defense mechanism in plants under stressful conditions. J Bot 2012:26

Shiino D, Murata Y, Kataoka K, Koyama Y, Yokoyama M, Okano T, Sakurai Y (1994) Preparation and characterization of a glucose-responsive insulin-releasing polymer device. Biomaterials 15(2):121–128

Shim MS, Xia Y (2013) A reactive oxygen species (ROS)-responsive polymer for safe, efficient, and targeted gene delivery in cancer cells. Angew Chem Int Ed 52 (27):6926–6929

Simm A, Brömme H-J (2005) Reactive oxygen species (ROS) and aging: do we need them — can we measure them — should we block them? Signal Transduct 5 (3):115–125

Song C-C, Du F-S, Li Z-C (2014) Oxidation-responsive polymers for biomedical applications. J Mater Chem B 2(22):3413–3426

Svegliati S, Cancello R, Sambo P, Luchetti M, Paroncini P, Orlandini G, Discepoli G, Paterno R,

Santillo M, Cuozzo C, Cassano S, Avvedimento EV, Gabrielli A (2005) Platelet-derived growth factor and reactive oxygen species (ROS) regulate Ras protein levels in primary human fibroblasts via ERK1/2: amplification of ROS and Ras in systemic sclerosis fibroblasts. J Biol Chem 280(43):36474–36482

Trachootham D, Alexandre J, Huang P (2009) Targeting cancer cells by ROS-mediated mechanisms: a radical therapeutic approach? Nat Rev Drug Discov 8:579

Velluto D, Demurtas D, Hubbell JA (2008) PEG-b-PPS diblock copolymer aggregates for hydrophobic drug solubilization and release: cyclosporin A as an example. Mol Pharm 5(4):632–642

Wang M, Sun S, Neufeld CI, Perez-Ramirez B, Xu Q (2014) Reactive oxygen species-responsive protein modification and its intracellular delivery for targeted cancer therapy. Angew Chem Int Ed 53 (49):13444–13448

Webb KS, Levy D (1995) A facile oxidation of boronic acids and boronic esters. Tetrahedron Lett 36 (29):5117–5118

Wheeler ML, DeFranco AL (2012) Prolonged production of reactive oxygen species in response to B cell receptor stimulation promotes B cell activation and proliferation. J Immunol 189(9):4405–4416

Wilson DS, Dalmasso G, Wang L, Sitaraman SV, Merlin D, Murthy N (2010) Orally delivered thioketal nanoparticles loaded with TNF-α–siRNA target inflammation and inhibit gene expression in the intestines. Nat Mater 9:923

Winterbourn CC (1995) Toxicity of iron and hydrogen peroxide: the Fenton reaction. Toxicol Lett 82–83 (Supplement C):969–974

Winterbourn CC (2008) Reconciling the chemistry and biology of reactive oxygen species. Nat Chem Biol 4:278

Xu H, Cao W, Zhang X (2013) Selenium-containing polymers: promising biomaterials for controlled release and enzyme mimics. Acc Chem Res 46 (7):1647–1658

Xu Q, He C, Xiao C, Chen X (2016) Reactive oxygen species (ROS) responsive polymers for biomedical applications. Macromol Biosci 16(5):635–646

Xu X, Saw PE, Tao W, Li Y, Ji X, Bhasin S, Liu Y, Ayyash D, Rasmussen J, Huo M, Shi J, Farokhzad OC (2017) ROS-responsive polyprodrug nanoparticles for triggered drug delivery and effective cancer therapy. Adv Mater 29(33). https://doi.org/10.1002/adma.201700141

Yang Y, Bazhin AV, Werner J, Karakhanova S (2013) Reactive oxygen species in the immune system. Int Rev Immunol 32(3):249–270

Yu L, Ding J (2008) Injectable hydrogels as unique biomedical materials. Chem Soc Rev 37(8):1473–1481

Yu SS, Koblin RL, Zachman AL, Perrien DS, Hofmeister LH, Giorgio TD, Sung H-J (2011) Physiologically relevant oxidative degradation of oligo(proline) cross-linked polymeric scaffolds. Biomacromolecules 12 (12):4357–4366

Zhou Y, Li B, Li S, Ardoña HAM, Wilson WL, Tovar JD, Schroeder CM (2017) Concentration-driven assembly and sol–gel transition of π-conjugated oligopeptides. ACS Cent Sci 3(9):986–994

Ziech D, Franco R, Pappa A, Panayiotidis MI (2011) Reactive oxygen species (ROS)—induced genetic and epigenetic alterations in human carcinogenesis. Mutat Res/Fundam Mol Mech Mutagen 711(1):167–173

Ziegler DM (1985) Role of reversible oxidation-reduction of enzyme thiols-disulfides in metabolic regulation. Annu Rev Biochem 54(1):305–329

Fibrin-Based Biomaterial Applications in Tissue Engineering and Regenerative Medicine

16

Chan Ho Park and Kyung Mi Woo

16.1 Background of Fibrin Biomaterials

16.1.1 Background with Biology

Fibrin is a fibrillar biopolymer that is naturally formed during blood clotting. Hemostasis is a primary role of fibrin, but fibrin also functions as a provisional matrix during wound healing. Fibrin possess the properties suitable for its use in regenerative medicine; fibrin is capable of conveying matrix proteins such as fibronectin and growth factors (Makogonenko et al. 2002; Rybarczyk et al. 2003; Mosesson 2005; Laurens et al. 2006a, b; Wolberg 2007; Janmey et al. 2009). Given these features, fibrin has been widely studied in biomedical research for its ability to repair hard and soft tissues (Hubbell 2003; Falanga et al. 2007; Ahmed et al. 2008; Breen et al. 2009a, b; Davis et al. 2011; Oh et al. 2014).

The biological functions of fibrin involve its structure. A number of variables can influence the structure of fibrin, including the local pH, ionic strength, and the concentrations of calcium and thrombin (Mosesson 2005; Wolberg 2007). The thrombin concentration present at the time of gelation has important influences on fibrin clot structure. The low thrombin concentrations produce fibrin clots that are turbid and composed of thick, loosely-woven fibrin strands. Higher concentrations of thrombin produce fibrin clots that are composed of relatively thinner, more tightly-packed fibrin strands (Collet et al. 2000; Wolberg 2007). Thrombin exposes the cryptic fibronectin-binding sites in fibrinogen and that fibronectin mostly bound to polymerized fibrin but rarely bound to fibrinogen (Makogonenko et al. 2002) and modulates the fibronectin-binding capacity of fibrin and that this modulation of thrombin contributes to integrin phosphorylation of the cells (Oh et al. 2012). The structure of the fibrin biomaterials affects their biological functions. Thus, it should be optimized for specific applications in tissue engineering and regenerative medicine.

16.1.2 Biodegradation of Fibrin: Fibrinolysis

The biodegradation process of fibrin material is known as the fibrinolysis or fibrinolytic system, which is mediated by plasmin (Baron and Kneissel 2013; Park et al. 2017). Briefly, fibrin degradation can be catalyzed by cell-surface-associated plasmin, which formed after binding

C. H. Park
Department of Dental Biomaterials, School of Dentistry, Kyungpook National University, Daegu, South Korea
e-mail: chanho@knu.ac.kr

K. M. Woo (✉)
Department of Pharmacology & Dental Therapeutics, Dental Research Institute and BK21 Program, School of Dentistry, Seoul National University, Seoul, South Korea
e-mail: kmwoo@snu.ac.kr

I. Noh (ed.), *Biomimetic Medical Materials*, Advances in Experimental Medicine and Biology 1064,
https://doi.org/10.1007/978-981-13-0445-3_16

soluble plasminogen and plasminogen activators (tissue-type plasminogen activator; t-pA and urokinase-type plasminogen activator; u-pA). In particular, the lysine-binding domains of plasminogen play an important role in the binding of plasminogen to fibrin for the fibrin degradation. In the inhibition of the fibrinolytic system, the plasminogen activator inhibitor-1 (PAI-1) or α2-antiplasmin (α2Ap) neutralize the plasminogen activators and block the interactions between binding domain of plasminogen and fibrin structures. Therefore, the biochemical interactions with plasminogen, fibrin, and plasminogen activators are contributed for controls of fibrin degradation process (Baron and Kneissel 2013; Park et al. 2017).

16.2 Tissue Engineering Applications Using Fibrin Biomaterials

At present, various pre-clinical/clinical approaches have been actively developed for regeneration of damaged tissues and wound healings using fibrin-based biomaterials (Table 16.1). In particular, fibrin can be dimensionally modified (two−/three-dimensional scaffolds) or its phasic characteristics (injectable or implantable matrices) can be fabricated to promote biological interactions in optimal tissue regeneration for wound healing and functioning restorations. According to target tissue defects or physiological environments, several therapeutic techniques have been implemented to improve mechanical, physical, chemical, or biological properties (Lee and Kurisawa 2013; Li et al. 2015).

16.2.1 Skin Tissue Engineering

Skin is the largest organ in the human body and consists of approximately 10% of the whole body weight. It is a crucial barrier between the internal and external with three distinct layers: the epidermis, the dermis, and the hypodermis (or subcutaneous tissue) (Chaudhari et al. 2016; Huang and Fu 2010; MacNeil 2008). The epidermis is the outermost layer to form a highly effective barrier against infectious pathogens from the external environments and maintain appropriate or optimal hydration (Huang and Fu 2010). Although capillary structures are formed under epidermis layer, 95% keratinocyte cells were contained in the epidermis without the vasculature networks. The dermis layer is between the epidermis and the hypodermis with connective tissues which are composed of fibroblasts, macrophages, and adipocytes (Priya et al. 2008). It has the primarily role to generate appropriate stress-strain mechanical responses by matrix components like collagen, elastin, and extrafibrillar matrix (MacNeil 2008). The hypodermis is the lowermost layer and below the dermis of vertebrate skin and has similar cell types to the dermis; fibroblasts, adipose cells, and macrophages. Compared to the dermis, the hypodermis mainly consists of loose connective tissue and subcutaneous fat with large blood vessels and nerves which cannot be found in epidermis and dermis tissues. Therefore, healthy skin tissue has various cell types such as keratinocytes, fibroblasts, or mesenchymal stem cells to regenerate complex tissue constructs and restore their functions (MacNeil 2008).

Fibrin has been utilized to induce skin tissue regeneration as vehicles for bioactive molecules to promote wound healing, delivery carriers for multiple cells like keratinocytes, fibroblast-like cells, and mesenchymal stem cells, or sealants for skin graft fixation to stop the bleeding (Bensaid et al. 2003; Jimenez and Jimenez 2004; Wechselberger et al. 2002).

16.2.2 Cardiac/Vascular Tissue Engineering

The cardiovascular system is the hemodynamic tissue complex with complicated responsiveness. The major components of the system are heart valves, cardiac muscles and the blood vasculatures, which are significantly challenging to regenerate or heal within the limited golden time. The cardiovascular tissues should have

Table 16.1 Tissue engineering applications using fibrin biomaterials

Target tissues	Summary	References
Skin tissue engineering	Rapid wound closure and improvement for elastic tissue regeneration	Huang and Fu (2010), Laurens et al. (2006a, b), Priya et al. (2008)
Cardiac/vascular tissue engineering	Injectable fibrin matrices to decrease infarct size, increase blood flow to ischemic myocardium, and improve cardiac function	Black et al. (2009), Chang and Niklason (2017), Cummings et al. (2004), Flanagan et al. (2007), Grassl et al. (2003), Huang et al. (2007), Ye et al. (2000)
Musculoskeletal tissue engineering	Biomimetic micro-architectures of the natural nanostructured features of bone and cartilage using the fibrin matrices having osteogenic or chondrogenic factors	Ben-Ari et al. (2009), Connelly et al. (2004), Eyrich et al. (2007), Koob et al. (2011), Lee et al. (2012), Neovius and Kratz (2003), Noori et al. (2017), Park et al. (2017), Passaretti et al. (2001), Peretti et al. (2006), Perka et al. (2000), Schek et al. (2004), Westreich et al. (2004)
Nervous tissue engineering	Central and peripheral nervous system regenerations using various concentrated fibrin matrices or chemically-modified fibrin.	Chernousov and Carey (2003), Herbert et al. (1998), Johnson et al. (2010), Sakiyama-Elbert and Hubbell (2000), Sakiyama et al. (1999), Tsai et al. (2006)

flexible responsiveness against various mechanical stimulations such as pressure, blood shear stress, molecular permeability in dynamic fluidics, and immunological responses (Gebara et al. 1997; Pober and Tellides 2012). In particular, severed ischemic cardiac tissue damages or injuries are irreversible or limitedly viable to restore vital functions (Hasan et al. 2015).

Grassl et al. developed and demonstrated the mechanically-modified fibrin-based tubular constructs as vascular grafts (Grassl et al. 2003). By controlling and balancing between fibrinolysis and cell-produced collagen matrix formation, the modified fibrin can be improved in mechanical strength like ultimate tensile strength or tensile modulus (Grassl et al. 2003). Moreover, cardiomyocytes can be encapsulated using the fibrin material and the strategy influenced cell alignments like cardiac muscle bundles for functioning restoration (Black et al. 2009). In particular, 3-D fibrin architectures could guide cardiac cell alignments and maintained synchronous beating in the *in-vitro* environment (Huang et al. 2007)

16.2.3 Musculoskeletal Tissue Engineering

The musculoskeletal complex is the major system to support organs and tissues as well as allow the appropriate movements with structural stabilities. The system has the bone skeleton and fibrous connective tissues. The mineralized tissue or bone in the system plays a critical role to protect the vital organs, provide locomotion of body, and produce blood cells. Moreover, fibrous connective tissues like ligaments, muscles, cartilage, or tendons can contribute the fundamental mobility after integration with bone (ligament, tendon, or cartilage) or muscles (tendon) (Stevens 2008).

In bone constructs, there are two major patterns to generate mechanical responses by remodeling tissues like compact (cortical bone) and trabecular patterns (cancellous bone) (Clarke 2008; Stevens 2008). In particular, the bone remodeling process can be contributed by significant cell activations of osteoblasts for regeneration and osteoclasts for destruction (Stevens 2008) However, if the physiological balance for bone remodeling is lost by diseases or greater defects than osteogenic wound healing, various osteoconductive or osteoinductive materials could be critically considered to promote bone regeneration as well as bone substitutes (Noori et al. 2017; Stevens 2008).

Fibrin matrices fundamentally have numerous proteins and growth factors so, they have widely utilized in bone tissue engineering in various preclinical and clinical scenarios. They can biologically contribute the upregulation of osteoblast expressions and significantly promote bone tissue

regeneration (Ben-Ari et al. 2009; Schek et al. 2004; Stevens 2008). Although fibrin has these great biological or biochemical properties, it is challenging to improve and modify rapid biodegradability and poor mechanical properties for skeletal structure neogenesis. Therefore, fibrin-incorporated bioactive composite materials have been developed using inorganic materials to have similar compositions to bone minerals with mechanical strength and enhance osteogenesis or organic materials to enable 3-D fabrications for favorable architectures with biodegradability and characterize biochemical/biological properties (Stevens 2008).

Of fibrous connective tissues in the musculoskeletal system, the cartilage is major structural component of ears, nose, or joint areas with higher stiffness and less flexibility than other fibrous tissues (Lee et al. 2012; Neovius and Kratz 2003; Passaretti et al. 2001; Peretti et al. 2006). In particular, articular cartilage has no vascular structures or nerves so, nutrition can be diffused to chondrocytes and the articular cartilage can particularly be too slowly remolded to have tissue regeneration or repair (Zhang et al. 2009). It is placed on the surface of joints to provide protection and movements of skeletal structures under compressive forces. Because mechanical responses of articular cartilage structures are significantly considered in frictional, compressive, or shear loading environments, cartilage can be demonstrated as resilient and viscoelastic tissue constructs at the skeletal joints (Zhang et al. 2009).

For the cartilage tissue engineering, fibrin material is widely studied and applied for various preclinical studies with clinical implications like chondrocyte-fibrin constructs or injectable fibrin gel containing cells to promote cartilage formations (Eyrich et al. 2007; Horak et al. 2014; Makris et al. 2015; Vinatier et al. 2009). However, environmental specificity of the cartilage construct under biomechanical stimulations can be a challenge for the cartilage regeneration using 3-D fibrin scaffold so, chondrocyte-associated fibrin sealant or fibrin glue have been popularly utilized.

16.2.4 Nerve Tissue Engineering

Nerve tissue categorizes two major parts like central nervous system (CNS) and peripheral nervous system (PNS) to regulate body functions. It mainly consists of nerve cells (neurons) to transmit impulses and glial cells (neuroglia) to provide nutrients and oxygen to neurons. The CNS has sophisticated dynamic networks with physicochemical communications to exchange sensed information. PNS consists of sensory and motor axons surrounded my myelin sheaths which Schwann cells produced (Johnson et al. 2010, 2013; Schmidt and Leach 2003; Subramanian et al. 2009). In various traumatic injuries or diseased destructions, CNS and PNS have different capacity of regeneration; CNS axons cannot be regenerated but peripheral nerves can be healed by extending new axonal sprouts (Schmidt and Leach 2003).

To guide the directional orientations with new nerve tissue regeneration, various biomaterials have been developed and utilized as the nerve conduits in preclinical and clinical situations (Sakiyama-Elbert and Hubbell 2000; Tsai et al. 2006). In particular, fibrin matrices have been used to fill hollow nerve conduits across the nerve defect regions to promote axonal regeneration and growth (Tsai et al. 2006). Moreover, fibrin scaffolds have been limitedly used for spinal cord regeneration or neural fiber formations at the early stage (Johnson et al. 2010).

16.3 Technical Applications for Tissue Regeneration in Fibrin Biomaterials

For the strategic applications for tissue engineering using fibrin matrices, various fabrication and modification techniques have been developed and applied for preclinical and clinical scenarios (Table 16.2). In particular, target tissues or injured defect dimensions should be significant considerations to manufacture fibrin products for the appropriate medical or surgical treatments. Commonly, fibrin gel has been widely considered

Table 16.2 Technical applications of fibrin for tissue regeneration

Target strategies	Summary	References
Injectable scaffold for tissue regeneration: Delivery system	Cell or biologic (drug) delivery systems for tissue regeneration	Breen et al. (2009a, b), Lee and Mooney (2001), Sacchi et al. (2014), Spicer and Mikos (2010), Tajdaran et al. (2015), Whelan et al. (2014), Yuan Ye et al. (2011)
Modified fibrin matrix for tissue engineering	Chemical modification of fibrin materials to improve mechanical properties and optimize predictable cell/tissue responses	Breen et al. (2009a, b), Hall et al. (2004), Hall and Hubbell (2004), Hall (2007), Lee and Mooney (2001), Park et al. (2017)
3D printing technique	3D bioprinting strategy with the fibrin gel material to manufacture customized architectures for tissue engineering and regenerative medicine	Gu et al. (2016), Lee et al. (2010), Lorber et al. (2014), Pati et al. (2015), Rimann et al. (2015), Xu et al. (2006)
Current clinical application	FDA-approved, clinical applicable products: Plasma-rich fibrin, fibrin sealant, or fibrin glue	Albala and Lawson (2006), Andree et al. (2008), Buchta et al. (2005), Janmey et al. (2009), Molly et al. (2006), Saltz et al. (1991); Santoro et al. (2007); Simonpieri et al. (2012)

as a sealant or a bioadhesive for hemostasis or wound closure (Mehdizadeh and Yang 2013) because the fibrin shows the minimal inflammation, foreign body reaction, or rapid degradation (Schmidt and Leach 2003).

As target cell or favorable biologic delivery systems, the injectable fibrin gel has been investigated as a carrier: such as cardiomyoblast delivery (Camci-Unal et al. 2014), bone marrow cells (Tajdaran et al. 2015), or bioactive factors (Bensaid et al. 2003; Breen et al. 2009a, b; Tajdaran et al. 2015). Injectable fibrin has been popularly investigated for bone tissue engineering applications because it is not seriously considered for any defect shapes or dimensions and simple invasive implant procedure. To improve the effectiveness and efficacy, it is required to mix the fibrin and biological components like bioactive molecules, cells (or stem cells), or other biomaterials (Li et al. 2015). Moreover, fibrin microbeads are recently studied to deliver a single cell into 3-D engineered micro-environments (or scaffolds) or directly into the injured defect sites for cartilage, cardiac muscle, skin or others (Spicer and Mikos 2010; Tajdaran et al. 2015; Whelan et al. 2014; Yuan Ye et al. 2011). It can be advantageous to more predictably control the quantities of cells or biologics with high efficacies. Fibrin-based micro-bead delivery systems can also encapsulate various stem cells to promote bone regeneration (Liu et al. 2017).

Although the fibrin has various advantages for tissue regeneration like great cell-material interactions, rapid biodegradability could be the limitation to induce appropriate tissue formation with sufficient time (Hubbell 2003; Mano et al. 2007). Therefore, the fibrin material has been modified with chemical agents to control degradability or enhance crosslinking for improvements of biological and mechanical properties (Park et al. 2017; Tallawi et al. 2015). In particular, various cell types can affect fibrin degradation rate because different biologics can be produced by biological interactions between cells and fibrin matrices (Brown and Barker 2014). Recently, Park et al. investigated that the cementoblast and osteoblast generated significantly different matrix metalloproteinases (MMPs) in *in-vitro* and modified fibrins for slow biodegradation critically contributed to promote cementogenesis and insert/integrate fibrous connective tissues within the mineralized tissues in *in-vivo* (Park et al. 2017).

For the 3-D scaffolds with geometric or architectural specificities, 3-D additive manufacturing or 3-D printing techniques have been currently highlighted and rapidly developed for biomedical applications (Gu et al. 2016; Lorber et al. 2014; Pati et al. 2015; Rimann et al. 2015; Xu et al. 2006). Of various polymeric materials for 3-D printing systems, the fibrin material is limitedly utilized as the bioink which is the hydrogel

material with biological components like cells or biologics for soft tissue engineering (Gu et al. 2016). Xu et al. demonstrated that the 3-D printing fabrication manufactured the fibrin constructs for neural tissue-guiding scaffolds (Xu et al. 2006) and Lee et al. presented the modified fibrin material with murine neural stem cells was used for build the 3-D architectures for nerve tissue formations (Lee et al. 2010).

16.4 Future Perspectives for Fibrin Biomaterials in Tissue Engineering and Regenerative Medicine

Fibrin has showed the high potential in functioning as an injectable materials, property-controlled materials with cell-material interactions, and 3-D printed scaffolds for tissue engineering and regenerative medicine. However, there are still numerous limitations like the poor mechanical properties for skeletal tissue regeneration, potential disease transmission by unpredictable biological affinities, or deformability of fibrin hydrogels. Many efforts have been contributed to improve the mechanical strength to extend applications with wide spectra and investigate synthetic biopolymeric material composite to characterize as biological or bioactive materials like polyglycolic acid and poly(lactic-co-glycolic acid).

References

Ahmed TA, Dare EV, Hincke M (2008) Fibrin: a versatile scaffold for tissue engineering applications. Tissue Eng Part B Rev 14:199–215

Albala DM, Lawson JH (2006) Recent clinical and investigational applications of fibrin sealant in selected surgical specialties. J Am Coll Surg 202(4):685–697

Andree C, Munder BI, Behrendt P, Hellmann S, Audretsch W, Voigt M et al (2008) Improved safety of autologous breast reconstruction surgery by stabilisation of microsurgical vessel anastomoses using fibrin sealant in 349 free DIEP or fascia-muscle-sparing (fms)-TRAM flaps: a two-centre study. Breast 17(5):492–498

Baron R, Kneissel M (2013) WNT signaling in bone homeostasis and disease: from human mutations to treatments. Nat Med 19(2):179–192

Ben-Ari A, Rivkin R, Frishman M, Gaberman E, Levdansky L, Gorodetsky R (2009) Isolation and implantation of bone marrow-derived mesenchymal stem cells with fibrin micro beads to repair a critical-size bone defect in mice. Tissue Eng A 15 (9):2537–2546

Bensaid W, Triffitt JT, Blanchat C, Oudina K, Sedel L, Petite H (2003) A biodegradable fibrin scaffold for mesenchymal stem cell transplantation. Biomaterials 24(14):2497–2502

Black LD 3rd, Meyers JD, Weinbaum JS, Shvelidze YA, Tranquillo RT (2009) Cell-induced alignment augments twitch force in fibrin gel-based engineered myocardium via gap junction modification. Tissue Eng A 15(10):3099–3108

Breen A, O'Brien T, Pandit A (2009a) Fibrin as a delivery system for therapeutic drugs and biomolecules. Tissue Eng Part B Rev 15:201–214

Breen A, O'Brien T, Pandit A (2009b) Fibrin as a delivery system for therapeutic drugs and biomolecules. Tissue Eng Part B Rev 15(2):201–214

Brown AC, Barker TH (2014) Fibrin-based biomaterials: modulation of macroscopic properties through rational design at the molecular level. Acta Biomater 10 (4):1502–1514

Buchta C, Hedrich HC, Macher M, Hocker P, Redl H (2005) Biochemical characterization of autologous fibrin sealants produced by CryoSeal and Vivostat in comparison to the homologous fibrin sealant product Tissucol/Tisseel. Biomaterials 26(31):6233–6241

Camci-Unal G, Annabi N, Dokmeci MR, Liao R, Khademhosseini A (2014) Hydrogels for cardiac tissue engineering. NPG Asia Mater 6:e99

Chang WG, Niklason LE (2017) A short discourse on vascular tissue engineering. NPJ Regen Med 2

Chaudhari AA, Vig K, Baganizi DR, Sahu R, Dixit S, Dennis V et al (2016) Future prospects for scaffolding methods and biomaterials in skin tissue engineering: a review. Int J Mol Sci 17(12)

Chernousov MA, Carey DJ (2003) alphaVbeta8 integrin is a Schwann cell receptor for fibrin. Exp Cell Res 291 (2):514–524

Clarke B (2008) Normal bone anatomy and physiology. Clin J Am Soc Nephrol 3(Suppl 3):S131–S139

Collet JP, Park D, Lesty C, Soria J, Soria C, Montalescot G et al (2000) Influence of fibrin network conformation and fibrin fiber diameter on fibrinolysis speed: dynamic and structural approaches by confocal microscopy. Arterioscler Thromb Vasc Biol 20:1354–1361

Connelly JT, Vanderploeg EJ, Levenston ME (2004) The influence of cyclic tension amplitude on chondrocyte matrix synthesis: experimental and finite element analyses. Biorheology 41(3–4):377–387

Cummings CL, Gawlitta D, Nerem RM, Stegemann JP (2004) Properties of engineered vascular constructs

made from collagen, fibrin, and collagen-fibrin mixtures. Biomaterials 25(17):3699–3706
Davis HE, Miller SL, Case EM, Leach JK (2011) Supplementation of fibrin gels with sodium chloride enhances physical properties and ensuing osteogenic response. Acta Biomater 7:691–699
Eyrich D, Brandl F, Appel B, Wiese H, Maier G, Wenzel M et al (2007) Long-term stable fibrin gels for cartilage engineering. Biomaterials 28(1):55–65
Falanga V, Iwamoto S, Chartier M, Yufit T, Butmarc J, Kouttab N et al (2007) Autologous bone marrow-derived cultured mesenchymal stem cells delivered in a fibrin spray accelerate healing in murine and human cutaneous wounds. Tissue Eng 13:1299–1312
Flanagan TC, Cornelissen C, Koch S, Tschoeke B, Sachweh JS, Schmitz-Rode T et al (2007) The in vitro development of autologous fibrin-based tissue-engineered heart valves through optimised dynamic conditioning. Biomaterials 28 (23):3388–3397
Gebara MM, Sayre MH, Corden JL (1997) Phosphorylation of the carboxy-terminal repeat domain in RNA polymerase II by cyclin-dependent kinases is sufficient to inhibit transcription. J Cell Biochem 64(3):390–402
Grassl ED, Oegema TR, Tranquillo RT (2003) A fibrin-based arterial media equivalent. J Biomed Mater Res A 66(3):550–561
Gu BK, Choi DJ, Park SJ, Kim MS, Kang CM, Kim CH (2016) 3-dimensional bioprinting for tissue engineering applications. Biomater Res 20(12):12
Hall H (2007) Modified fibrin hydrogel matrices: both, 3D-scaffolds and local and controlled release systems to stimulate angiogenesis. Curr Pharm Des 13 (35):3597–3607
Hall H, Hubbell JA (2004) Matrix-bound sixth Ig-like domain of cell adhesion molecule L1 acts as an angiogenic factor by ligating alphavbeta3-integrin and activating VEGF-R2. Microvasc Res 68(3):169–178
Hall H, Djonov V, Ehrbar M, Hoechli M, Hubbell JA (2004) Heterophilic interactions between cell adhesion molecule L1 and alphavbeta3-integrin induce HUVEC process extension in vitro and angiogenesis in vivo. Angiogenesis 7(3):213–223
Hasan A, Khattab A, Islam MA, Hweij KA, Zeitouny J, Waters R et al (2015) Injectable hydrogels for cardiac tissue repair after myocardial infarction. Adv Sci 2 (11):1500122
Herbert CB, Nagaswami C, Bittner GD, Hubbell JA, Weisel JW (1998) Effects of fibrin micromorphology on neurite growth from dorsal root ganglia cultured in three-dimensional fibrin gels. J Biomed Mater Res 40 (4):551–559
Horak M, Handl M, Podskubka A, Kana R, Adler J, Povysil C (2014) Comparison of the cellular composition of two different chondrocyte-seeded biomaterials and the results of their transplantation in humans. Folia Biol 60(1):1–9
Huang S, Fu X (2010) Naturally derived materials-based cell and drug delivery systems in skin regeneration. J Control Release 142(2):149–159
Huang YC, Khait L, Birla RK (2007) Contractile three-dimensional bioengineered heart muscle for myocardial regeneration. J Biomed Mater Res A 80 ((3):719–731
Hubbell JA (2003) Materials as morphogenetic guides in tissue engineering. Curr Opin Biotechnol 14 (5):551–558
Janmey PA, Winer JP, Weisel JW (2009) Fibrin gels and their clinical and bioengineering applications. J R Soc Interface 6(30):1–10
Jimenez PA, Jimenez SE (2004) Tissue and cellular approaches to wound repair. Am J Surg 187 (5A):56S–64S
Johnson PJ, Parker SR, Sakiyama-Elbert SE (2010) Fibrin-based tissue engineering scaffolds enhance neural fiber sprouting and delay the accumulation of reactive astrocytes at the lesion in a subacute model of spinal cord injury. J Biomed Mater Res A 92((1):152–163
Johnson PJ, Wood MD, Moore AM, Mackinnon SE (2013) Tissue engineered constructs for peripheral nerve surgery. Eur Surg 45(3). https://doi.org/10.1007/s10353-013-0205-0
Koob S, Torio-Padron N, Stark GB, Hannig C, Stankovic Z, Finkenzeller G (2011) Bone formation and neovascularization mediated by mesenchymal stem cells and endothelial cells in critical-sized calvarial defects. Tissue Eng A 17(3–4):311–321
Laurens N, Koolwijk P, de Maat MP (2006a) Fibrin structure and wound healing. J Thromb Haemost 4:932–939
Laurens N, Koolwijk P, de Maat MP (2006b) Fibrin structure and wound healing. J Thromb Haemost 4 (5):932–939
Lee F, Kurisawa M (2013) Formation and stability of interpenetrating polymer network hydrogels consisting of fibrin and hyaluronic acid for tissue engineering. Acta Biomater 9(2):5143–5152
Lee KY, Mooney DJ (2001) Hydrogels for tissue engineering. Chem Rev 101(7):1869–1879
Lee YB, Polio S, Lee W, Dai G, Menon L, Carroll RS et al (2010) Bio-printing of collagen and VEGF-releasing fibrin gel scaffolds for neural stem cell culture. Exp Neurol 223(2):645–652
Lee JC, Lee SY, Min HJ, Han SA, Jang J, Lee S et al (2012) Synovium-derived mesenchymal stem cells encapsulated in a novel injectable gel can repair osteochondral defects in a rabbit model. Tissue Eng A 18(19–20):2173–2186
Li Y, Meng H, Liu Y, Lee BP (2015) Fibrin gel as an injectable biodegradable scaffold and cell carrier for tissue engineering. TheScientificWorldJOURNAL 2015(685690):1
Liu M, Zeng X, Ma C, Yi H, Ali Z, Mou X et al (2017) Injectable hydrogels for cartilage and bone tissue engineering. Bone Res 5:17014
Lorber B, Hsiao WK, Hutchings IM, Martin KR (2014) Adult rat retinal ganglion cells and glia can be printed by piezoelectric inkjet printing. Biofabrication 6 (1):015001
MacNeil S (2008) Biomaterials for tissue engineering of skin. Mater Today 11(5):26–35

Makogonenko E, Tsurupa G, Ingham K, Medved L (2002) Interaction of fibrin(ogen) with fibronectin: further characterization and localization of the fibronectin-binding site. Biochemistry 41:7907–7913

Makris EA, Gomoll AH, Malizos KN, Hu JC, Athanasiou KA (2015) Repair and tissue engineering techniques for articular cartilage. Nat Rev Rheumatol 11(1):21–34

Mano JF, Silva GA, Azevedo HS, Malafaya PB, Sousa RA, Silva SS et al (2007) Natural origin biodegradable systems in tissue engineering and regenerative medicine: present status and some moving trends. J R Soc Interface 4(17):999–1030

Mehdizadeh M, Yang J (2013) Design strategies and applications of tissue bioadhesives. Macromol Biosci 13(3):271–288

Molly L, Quirynen M, Michiels K, van Steenberghe D (2006) Comparison between jaw bone augmentation by means of a stiff occlusive titanium membrane or an autologous hip graft: a retrospective clinical assessment. Clin Oral Implants Res 17(5):481–487

Mosesson MW (2005) Fibrinogen and fibrin structure and functions. J Thromb Haemost 3:1894–1904

Neovius EB, Kratz G (2003) Tissue engineering by cocultivating human elastic chondrocytes and keratinocytes. Tissue Eng 9(2):365–369

Noori A, Ashrafi SJ, Vaez-Ghaemi R, Hatamian-Zaremi A, Webster TJ (2017) A review of fibrin and fibrin composites for bone tissue engineering. Int J Nanomedicine 12:4937–4961

Oh JH, Kim HJ, Kim TI, Baek JH, Ryoo HM, Woo KM (2012) The effects of the modulation of the fibronectin-binding capacity of fibrin by thrombin on osteoblast differentiation. Biomaterials 33:4089–4099

Oh JH, Kim HJ, Kim TI, Woo KM (2014) Comparative evaluation of the biological properties of fibrin for bone regeneration. BMB Rep 47(2):110–114

Park CH, Oh JH, Jung HM, Choi Y, Rahman SU, Kim S et al (2017) Effects of the incorporation of epsilon-aminocaproic acid/chitosan particles to fibrin on cementoblast differentiation and cementum regeneration. Acta Biomater 61:134–143

Passaretti D, Silverman RP, Huang W, Kirchhoff CH, Ashiku S, Randolph MA et al (2001) Cultured chondrocytes produce injectable tissue-engineered cartilage in hydrogel polymer. Tissue Eng 7(6):805–815

Pati F, Ha DH, Jang J, Han HH, Rhie JW, Cho DW (2015) Biomimetic 3D tissue printing for soft tissue regeneration. Biomaterials 62(164–175

Peretti GM, Xu JW, Bonassar LJ, Kirchhoff CH, Yaremchuk MJ, Randolph MA (2006) Review of injectable cartilage engineering using fibrin gel in mice and swine models. Tissue Eng 12(5):1151–1168

Perka C, Schultz O, Spitzer RS, Lindenhayn K, Burmester GR, Sittinger M (2000) Segmental bone repair by tissue-engineered periosteal cell transplants with bioresorbable fleece and fibrin scaffolds in rabbits. Biomaterials 21(11):1145–1153

Pober JS, Tellides G (2012) Participation of blood vessel cells in human adaptive immune responses. Trends Immunol 33(1):49–57

Priya SG, Jungvid H, Kumar A (2008) Skin tissue engineering for tissue repair and regeneration. Tissue Eng Part B Rev 14(1):105–118

Rimann M, Laternser S, Keller H, Leupin O, Graf-Hausner U (2015) 3D bioprinted muscle and tendon tissues for drug development. Chimia 69(1–2):65–67

Rybarczyk BJ, Lawrence SO, Simpson-Haidaris PJ (2003) Matrix-fibrinogen enhances wound closure by increasing both cell proliferation and migration. Blood 102:4035–4043

Sacchi V, Mittermayr R, Hartinger J, Martino MM, Lorentz KM, Wolbank S et al (2014) Long-lasting fibrin matrices ensure stable and functional angiogenesis by highly tunable, sustained delivery of recombinant VEGF164. Proc Natl Acad Sci USA 111 (19):6952–6957

Sakiyama SE, Schense JC, Hubbell JA (1999) Incorporation of heparin-binding peptides into fibrin gels enhances neurite extension: an example of designer matrices in tissue engineering. FASEB J 13 (15):2214–2224

Sakiyama-Elbert SE, Hubbell JA (2000) Development of fibrin derivatives for controlled release of heparin-binding growth factors. J Control Release 65 (3):389–402

Saltz R, Sierra D, Feldman D, Saltz MB, Dimick A, Vasconez LO (1991) Experimental and clinical applications of fibrin glue. Plast Reconstr Surg 88 (6):1005–1015 discussion 1016-1007

Santoro E, Agresta F, Buscaglia F, Mulieri G, Mazzarolo G, Bedin N et al (2007) Preliminary experience using fibrin glue for mesh fixation in 250 patients undergoing minilaparoscopic transabdominal preperitoneal hernia repair. J Laparoendosc Adv Surg Tech A 17(1):12–15

Schek RM, Hollister SJ, Krebsbach PH (2004) Delivery and protection of adenoviruses using biocompatible hydrogels for localized gene therapy. Mol Ther 9 (1):130–138

Schmidt CE, Leach JB (2003) Neural tissue engineering: strategies for repair and regeneration. Annu Rev Biomed Eng 5:293–347

Simonpieri A, Del Corso M, Vervelle A, Jimbo R, Inchingolo F, Sammartino G et al (2012) Current knowledge and perspectives for the use of platelet-rich plasma (PRP) and platelet-rich fibrin (PRF) in oral and maxillofacial surgery part 2: bone graft, implant and reconstructive surgery. Curr Pharm Biotechnol 13(7):1231–1256

Spicer PP, Mikos AG (2010) Fibrin glue as a drug delivery system. J Control Release 148(1):49–55

Stevens MM (2008) Biomaterials for bone tissue engineering. Mater Today 11(5):18–25

Subramanian A, Krishnan UM, Sethuraman S (2009) Development of biomaterial scaffold for nerve tissue engineering: biomaterial mediated neural regeneration. J Biomed Sci 16:108

Tajdaran K, Shoichet MS, Gordon T, Borschel GH (2015) A novel polymeric drug delivery system for localized and sustained release of tacrolimus (FK506). Biotechnol Bioeng 112(9):1948–1953

Tallawi M, Rosellini E, Barbani N, Cascone MG, Rai R, Saint-Pierre G et al (2015) Strategies for the chemical and biological functionalization of scaffolds for cardiac tissue engineering: a review. J R Soc Interface 12 (108):20150254

Tsai EC, Dalton PD, Shoichet MS, Tator CH (2006) Matrix inclusion within synthetic hydrogel guidance channels improves specific supraspinal and local axonal regeneration after complete spinal cord transection. Biomaterials 27(3):519–533

Vinatier C, Bouffi C, Merceron C, Gordeladze J, Brondello JM, Jorgensen C et al (2009) Cartilage tissue engineering: towards a biomaterial-assisted mesenchymal stem cell therapy. Curr Stem Cell Res Ther 4 (4):318–329

Wechselberger G, Russell RC, Neumeister MW, Schoeller T, Piza-Katzer H, Rainer C (2002) Successful transplantation of three tissue-engineered cell types using capsule induction technique and fibrin glue as a delivery vehicle. Plast Reconstr Surg 110(1):123–129

Westreich R, Kaufman M, Gannon P, Lawson W (2004) Validating the subcutaneous model of injectable autologous cartilage using a fibrin glue scaffold. Laryngoscope 114(12):2154–2160

Whelan D, Caplice NM, Clover AJ (2014) Fibrin as a delivery system in wound healing tissue engineering applications. J Control Release 196:1–8

Wolberg AS (2007) Thrombin generation and fibrin clot structure. Blood Rev 21:131–142

Xu T, Gregory CA, Molnar P, Cui X, Jalota S, Bhaduri SB et al (2006) Viability and electrophysiology of neural cell structures generated by the inkjet printing method. Biomaterials 27(19):3580–3588

Ye Q, Zund G, Benedikt P, Jockenhoevel S, Hoerstrup SP, Sakyama S et al (2000) Fibrin gel as a three dimensional matrix in cardiovascular tissue engineering. Eur J Cardiothoracic Surg 17(5):587–591

Yuan Ye K, Sullivan KE, Black LD (2011) Encapsulation of cardiomyocytes in a fibrin hydrogel for cardiac tissue engineering. J Vis Exp 55

Zhang L, Hu J, Athanasiou KA (2009) The role of tissue engineering in articular cartilage repair and regeneration. Crit Rev Biomed Eng 37(1–2):1–57

17 Fabrication of Electrochemical-Based Bioelectronic Device and Biosensor Composed of Biomaterial-Nanomaterial Hybrid

Mohsen Mohammadniaei, Chulhwan Park, Junhong Min, Hiesang Sohn, and Taek Lee

17.1 Introduction

With the rapid advances in biotechnology (BT), nanotechnology (NT) and information & communication technology (ICT), a new technology field called bioelectronics emerged (Christof and Chad 2004; Itamar and Eugenii 2005; Noy 2011). Since 2000, the bioelectronics has led to the development of biochips (Farzadfard and Lu 2014; Michael 2007; Qiu et al. 2013), biosensors (Lee et al. 2007; Sarkar et al. 2014), biomedical devices (Deng et al. 2014) and bioelectronic devices for computation (Nikitin et al. 2014). Specifically, bioelectronic devices have been investigated in several fields, such as electrical engineering, nanobiotechnology, mechanical engineering and chemistry (Offenhäusser and Rinaldi 2009; Ren et al. 2017; Strukov and Kohlstedt 2012). The bioelectronic computation system can be at the center of these advances, as the elements that control information storage (Choi et al. 2007), determination, process (Benenson et al. 2004; de Silva and Uchiyama 2007), and logical behavior (Baron et al. 2006a; Fujibayashi et al. 2008; Win and Smolke 2008) provide appropriate functions to constitute the integrated molecular circuit (IMC). The advantages of bioelectronic devices include miniaturization, new functions, implantable devices that will be able to replace silicon-based (digitalized) systems in the future. Several groups have proposed the biocomputation concept (Adleman 1794; Ausländer et al. 2012; Rinaudo et al. 2007; Weber et al. 2008; Yin et al. 2008).

Bioelectronic devices for computation are usually composed of biomolecules such as metalloprotein (Chen et al. 2012; Lee et al. 2014b), enzyme (Katz and Privman 2010), DNA (Okamoto et al. 2004) and RNA (Win and Smolke 2008). These biomaterials have intriguing properties in nature, and their original properties have been mimicked in order to use computation on to the chip. For the immobilization of those biomolecules onto the inorganic substrate, the self-assembly technique was suitable for this application (Lu and Suo 2002; Schwartz 2001). Various groups have used biomolecules to demonstrate the logic gate (Baron et al. 2006b; Hild et al. 2010; Willner and Katz 2000; Zhang et al. 2013; Zhou et al. 2009), information storage device (Min et al. 2010; Yagati et al. 2009a, b, 2010; Yoon et al.

M. Mohammadniaei
Department of Chemical and Biomolecular Engineering, Sogang University, Seoul, South Korea
e-mail: mniaei@sogang.ac.kr

C. Park · H. Sohn (✉) · T. Lee (✉)
Department of Chemical Engineering, Kwangwoon University, Seoul, South Korea
e-mail: hsohn@kw.ac.kr; tlee@kw.ac.kr

J. Min
School of Integrative Engineering Chung-Ang University, Seoul, South Korea
e-mail: junmin@cau.ac.kr

I. Noh (ed.), *Biomimetic Medical Materials*, Advances in Experimental Medicine and Biology 1064,
https://doi.org/10.1007/978-981-13-0445-3_17

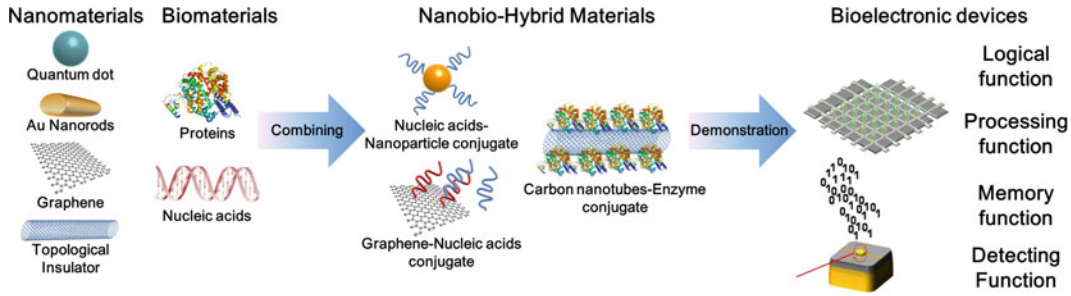

Fig. 17.1 Schematic diagram shows biomaterials and nanomaterials combination allow their integration in nanobio hybrid materials for bioelectronic devices

2014), transistor (Artés et al. 2012; Keren et al. 2003; Meng et al. 2011), computation device (Liu et al. 2000; Xie et al. 2011). Usually, those biomolecules were combined with nanomaterials such as nanoparticle, grapheme and quantum dot that provide the multi-functionality (Luo et al. 2018) (Fig. 17.1).

Willner Group suggested several enzyme-based logic gates (Baron et al. 2006a; Itamar and Eugenii 2005; Katz and Privman 2010). They introduced a pair of enzymes, horseradish peroxidase (HRP) and glucose dehydrogenase (GDH), for gate performance. As an input material, hydrogen peroxide (H_2O_2) and glucose were used to show the AND, XOR Gate functions. Recently, they proposed that the DNA computing circuit comprised libraries of DNAzymes. The system operated the parallel logic gate that depends on input markers. This operation process intends to regulate the anti-sense molecules and aptamer, which inhibit the enzymes. They provided a potential biochemical computer for the therapeutic control of biomedical applications. Furthermore, various enzyme-based logic gates were established (Baron et al. 2006b; Willner and Katz 2000; Zhang et al. 2013; Zhou et al. 2009). Also, Smolke group proposed that the information processing devices consisted of an RNA aptamer and RNA ribozyme (Win and Smolke 2008). The information processor received, processed and transmitted the input materials to express the green fluorescent protein as an output. In this study, the RNA aptamer and ribozyme combination can be used as the activating materials for a biomolecule-based processor. Furthermore, some pioneering groups suggested the RNA or DNA molecule-based biocompuation systems for medical applications or cell system analysis (Liu et al. 2000; Weber et al. 2008; Xie et al. 2011). Huang's group demonstrated the protein-based transistor. For transistor fabrication, Huang developed the antibody-two gold nanoparticle complex immobilized onto the molecular gap that connected to the source and drain electrodes. This protein-based transistor provides a versatile platform for studying single molecule-based electronic devices. The fabricated bioelectronic device has the following advantage (Fig. 17.2).

Biosensors are powerful analytical devices, usually composed of biological sensing materials (bioreceptors) and physiochemical transducers (Fig. 17.3). These devices are employed to recognize and detect the desired target molecules with high specificity, selectivity and sensitivity either at the trace amounts or in the complex environments (Hunt and Armani 2010; Tamayo et al. 2013). Amongst all the sensing devices, electrochemical biosensors have received intensive attention for the detection of clinical biomarkers and analytes due to their fast response, low fabrication cost, high sensitivity and selectivity as well as simplicity and miniaturization capability, which have made them considerable candidates for the point-of-care diagnostics (Liu et al. 2017; Thévenot et al. 2001).

Electrochemical method is fundamentally based on the process of electron transfer between the electrode surface and the electroactive substances in solution (electrolyte). The electrode

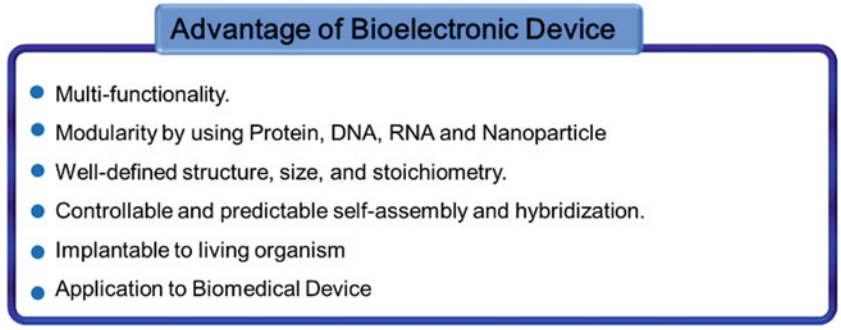

Fig. 17.2 Schematic diagram of main advantage of bioelectronics device

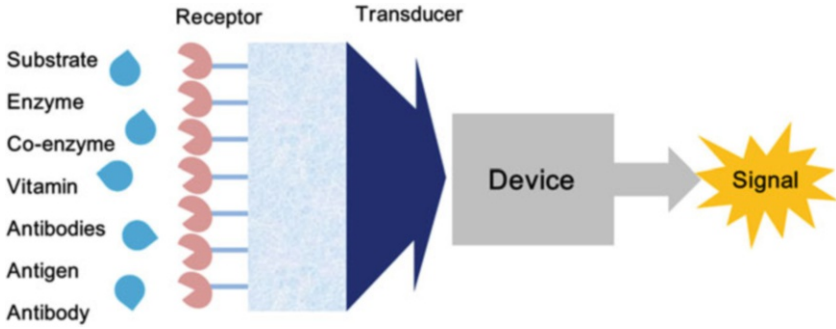

Fig. 17.3 Schematic diagram of working mechanism of biosensor

surface could be composed of metal (such as gold, platinum, etc.), conducting polymers, carbon or composite materials. The electroactive materials which are meant to have redox properties (oxidation/reduction) generally consist of ions, organic/inorganic materials and enzymes (Grieshaber et al. 2008; Pingarrón et al. 2008; Ronkainen et al. 2010; Wang 2002). Electrochemical biosensors are normally set up in a three-electrode electrochemical cell composed of working electrode (Target substrate, where the reaction of studied species occurs), counter electrode (To detect the electrochemical current/signal) and standard electrode, possessing a stable and fixed potential (Usually Ag/AgCl, due to its construction simplicity) (Pumera et al. 2007). The recorded electrochemical signal is directly proportional to the concentration of the electroactive species and is defined as the detection signal. There are mainly two analytical techniques applied for illustrating the experimental data; current vs. potential (i–v) which is called voltammetry, and current vs. time (i–t) that is called chronoamperometry, in which, the working electrode is maintained at a constant potential (Kimmel et al. 2012).

As the major sensing element of biosensors, the biological sensing materials are substances with well immobilization properties to be attached strongly onto the electrode surface and high selectivity features to specifically detect the target analytes. They are mainly categorized in two groups: (1) Proteins and (2) Nucleic acids.

17.2 Protein-Based Electrochemical Bioelectronic Device

The protein-based biomolecular information storage device was proposed to alter the current silicon-based information storage device (Choi et al. 2007). Consequently, there are several types of biomemory devices proposed, for example, the WORM-type biomemory device (Yagati

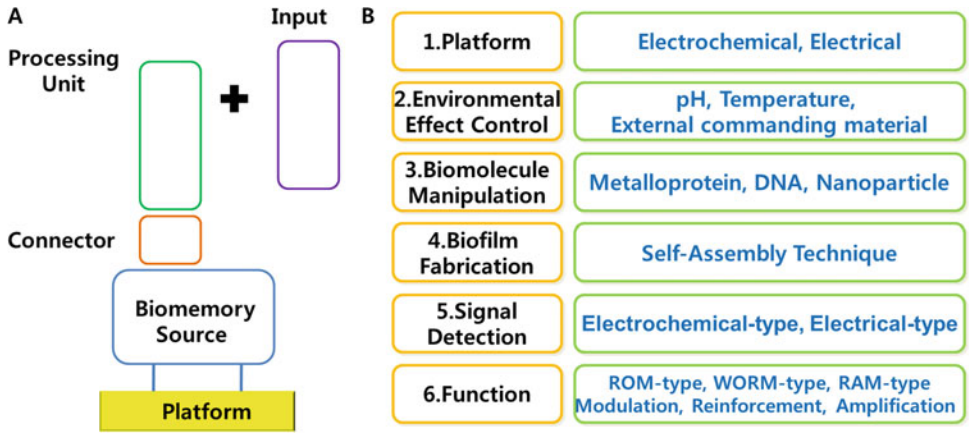

Fig. 17.4 (**a**) Schematic representation shows the expected structure of electrochemical bioelectronic device. (**b**) Classification of bioelectronics device constitution

et al. 2009b), multi-bit biomemory device (Yagati et al. 2009a), multi-level biomemory device (Lee et al. 2010), multi-functional biomemory chip (Lee et al. 2011a), signal-enhanced biomemory device (Yuan et al. 2013), and the bioprocessor (Ko et al. 2011). Such devices could control and modulate the electrochemical signal due to the redox property of metalloprotein in order to achieve the store and release the electron by external potential. Usually, the bioelectronic devices were classified with six categories (Fig. 17.4). This article briefly introduced devise ranging from the basic concept of a biomolecular memory device to the various function validations of multi-functional biomemory devices and bioprocessors.

In previous time, they proposed the bioelectronic device composed of metalloprotein. The purpose of this electronic device was to accomplish electronic functions of the information storage. For this reason, Choi group introduced the redox protein for making biomemory device by self-assembly technique and validating the electrochemical biomemory functions (Choi et al. 2007). Recently, the protein/DNA-based bioprocessor was demonstrated to show the multi-functionality in one defined devices corresponding to input materials (Lee et al. 2014b). Here, we review from the protein-based biomemory device, protein/DNA-based bioprocessor, also briefly survey DNA/RNA biologic gate and device which could be one of alternative standard device format in biocomputation system.

17.2.1 Protein-Based Information Storage Device

In the early stage, the metalloprotein-based biomemory device was proposed to overcome the limitation of inorganic molecule-based information storage device by Choi group (Choi et al. 2007). The metalloprotein contained the metal ion in the protein molecule that can be enabled to store the electron corresponding to input potentials. To fabricate the biomemory device, the immobilization and orientation of biomolecule technique should be required. To immobilize the biomolecule onto the inorganic substrate, a self-assembly (SA) method has been widely used to immobilize biomolecules on the substrate (Mitsumasa et al. 2010). The immobilization of biomolecules on the substrate needs an additional linker which anchors between the biomolecule and the substrate. Chemical linkers like (3-aminopropyl)triethoxysilane (APTES), 2-mercaptoacetic acid (2-MAA) 6-mercaptohexanoic acids (6-MHA) can be used to make connections between the gold substrate and the biomolecule (Chung et al. 2011; Robles-Águila et al. 2014; Yoo et al. 2011). However, direct

immobilization of biomolecules on the substrate without chemical linkers is more effective for the fabricating a well-ordered biomolecular monolayer than the use of chemical linkers. To achieve direct immobilization, a cysteine-modified azurin was introduced as an electron storage element to fabricate a biomolecular memory device. On the basis of this technique, *pseudomonas aeruginosa* azurin was modified to possess cysteine residue for direct immobilization on the gold surface by covalent bonding. This recombinant azurin was immobilized directly on the gold substrate, and its orientation was investigated by atomic force microscopy (AFM) and surface plasmon resonance (SPR). Then, the redox property of azurin was investigated by cyclic voltammetry (CV).

The basic mechanism of the proposed biomolecular memory device is that electrons flow into the recombinant azurin. A reduced copper ion in azurin gives the 'write' state and outflowing of electron from the recombinant azurin, and the oxidized metal ion in azurin gives the 'erase' state. Like this process, based on metalloprotein, electrons can flow in and out of the recombinant azurin by applied voltage. The quantity of the stored charge can be calculated as the memory performance of the fabricated biomolecular memory device using chronoamperometry (CA). Also, the recombinant azurin showed unique redox potential peaks and memory functions. From experimental results, this proposed biomemory device indicates new conceptual approach to bioelectronic application. Furthermore, the biomolecular memory devices have been developed by several groups (Ko et al. 2011; Mitsumasa et al. 2010; Yuan et al. 2013). Yu group suggested the electrochemical based biomemory device based on living bacteria *Shewanella oneidensis* (Yuan et al. 2013). Furthermore, Cho group investigated the electrical bistable property of ferritin to develop a resistive memory device application (Ko et al. 2011). Among those biomolecules, metalloprotein was widely investigated to use a biomemory source due to its bistable redox properties (Choi et al. 2007).

The main advantage of biomemory is functionality compared to inorganic molecule-based memory device. Usually, the biomolecule can be easily tailored and conjugated with other biomolecule or nanoparticle that can provides the additional functionality such as signal-amplified current or dual-level information storage. It is hard to perform the inorganic molecule-based memory device and silicon-based memory device because of simple molecular structure. However, the biomemory can be extended to the various functionalities based on combination of biomolecule and nanoaprticle. The natural property of a biomolecule can be modified and extended by introduction of nanoparticles. Yang's group conjugated the tobacco mosaic virus and quantum dot nanoparticles, and electrical investigation of that virus/nanoparticle conjugates for digital memory application (Tseng et al. 2006). Moreover, the functional benefits of a biomolecule are its original redox property and recombinant technique for feasible formation that can be applied to bioelectronics devices.

The gold nanoparticle on the recombinant azurin monolayer was developed an electrochemical signal enhanced biomemory device (Lee et al. 2011b) (Fig. 17.5). In this study, they introduced various gold nanoparticles to recombinant azurin monolayer (5 nm ~ 60 nm) to optimize the gold nanoparticle size which transfer the maximum electron transfer. For this reason, the recombinant azurin was immobilized directly on the gold substrate by cysteine residue, and 1-Octadecanethiol was used as a connecter between the recombinant azurin and gold nanoparticle. From the electrochemical results acquired by CV, in a small particle range, the electrochemical signal of recombinant azurin/gold nanoparticle decreased, but in a large particle range, the electrochemical signal only originated from a gold nanoparticle without recombinant azurin. Therefore, 5 nm size of gold nanoparticle was determined as the optimal size. After that, biomemory device composed of recombinant azurin and gold nanoparticle was fabricated on the gold substrate. The confirmation of recombinant azurin and gold nanoparticle immobilization was verified by SPR and AFM. Then, the electrochemical investigation of the recombinant azurin/gold nanoparticle was carried out to evaluate the electrochemical signal enhancing effect compared to a recombinant azurin

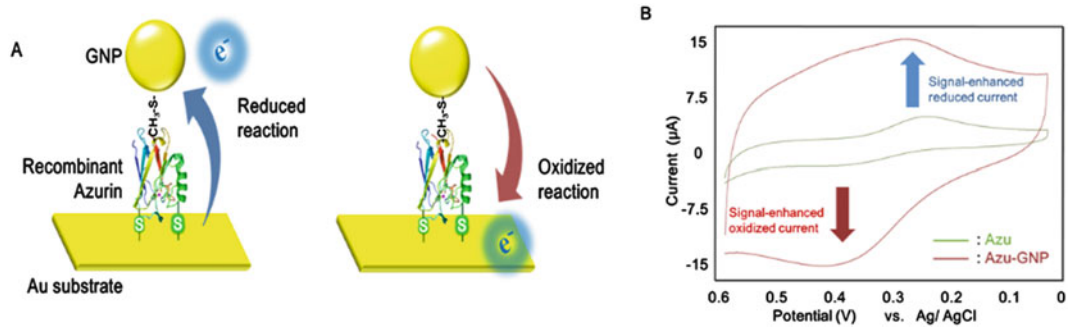

Fig. 17.5 (**a**) Scheme of the proposed signal-enhanced biomemory device composed of recombinant azurin and gold nanoparticle. (**b**) Cyclic voltamogram of recombinant azurin (green plot), recombinant azurin/gold nano particle (red plot). (Figures adapted from Lee et al. (2011b), with permission from © WILEY-VCH Verlag GmbH & Co. KGaA 2011)

monolayer without a gold nanoparticle by CV and CA. The electrochemical signal of the recombinant azurin/gold nanoparticle was five times greater than the recombinant azurin monolayer. Also, the stored charge amount of the recombinant azurin/gold nanoparticle, measured as memory performance, was 4.503 μC, and 1.14 μC in the case of the recombinant azurin monolayer. This signal enhanced biomemory device suggested the possibility of bioelectronic development at a single molecular level with subjugation of a signal detecting limitation. As seen in this research, biomolecules have a huge potential with limitless functional expansion through the combination of various materials (Jensen et al. 2009).

In the conventional field of electronics, researchers have tried to improve memory density and circuit-integration efficiency to develop an advanced computing system. However, as the approach applies a scale of a less than 50 nm for fabricating semiconductor-based chip, economic and technical limitations have been identified. In terms of the field of bioelectronics, a Moreover, the biomemory can be developed to increase the memory density in the defined area. Biomolecular based electronic system might be an alternative option to overcoming this limitation. This combination can be used to realize a biomolecular memory device with improved memory density.

The multi-level biomolecular memory device composed of recombinant azurin and cytochrome c to increase memory density with multiple redox states (Lee et al. 2013) (Fig. 17.6). The heterolayer composed of recombinant azurin and cytochrome c was fabricated through self-assembled layer-by-layer formation on the gold substrate. First, recombinant azurin was immobilized directly on the gold substrate, and then cytochrome c was immobilized on the recombinant azurin layer through electrostatic interaction. At pH 7.0, the isoelectric point of recombinant azurin was 6.03 and that of cytochrome c was 9.59, so recombinant azurin had a negatively-charged surface and cytochrome c had a positively-charged surface. Confirmation of the heterolayer formation was operated by SPR and AFM. After biochip fabrication, the electrochemical properties of the heterolayer were investigated. Using CV, the heterolayer showed that both redox peaks of recombinant azurin and cytochrome c had an obvious shape. The oxidation potential peak and reduction potential peak of recombinant azurin and cytochrome c were 0.062 V, 0.131 V and 0.131 V, 0.294 V, respectively. These redox values coincided with copper ion in recombinant azurin and iron ion in cytochrome c. Two different metal ions in recombinant azurin and cytochrome c played key roles as storage for controlling the various data in defined memory sector. Those acquired redox potential values were used as oxidation potential for the 'write' and reduction potential for 'erase', and open circuit potential was applied as the 'read'

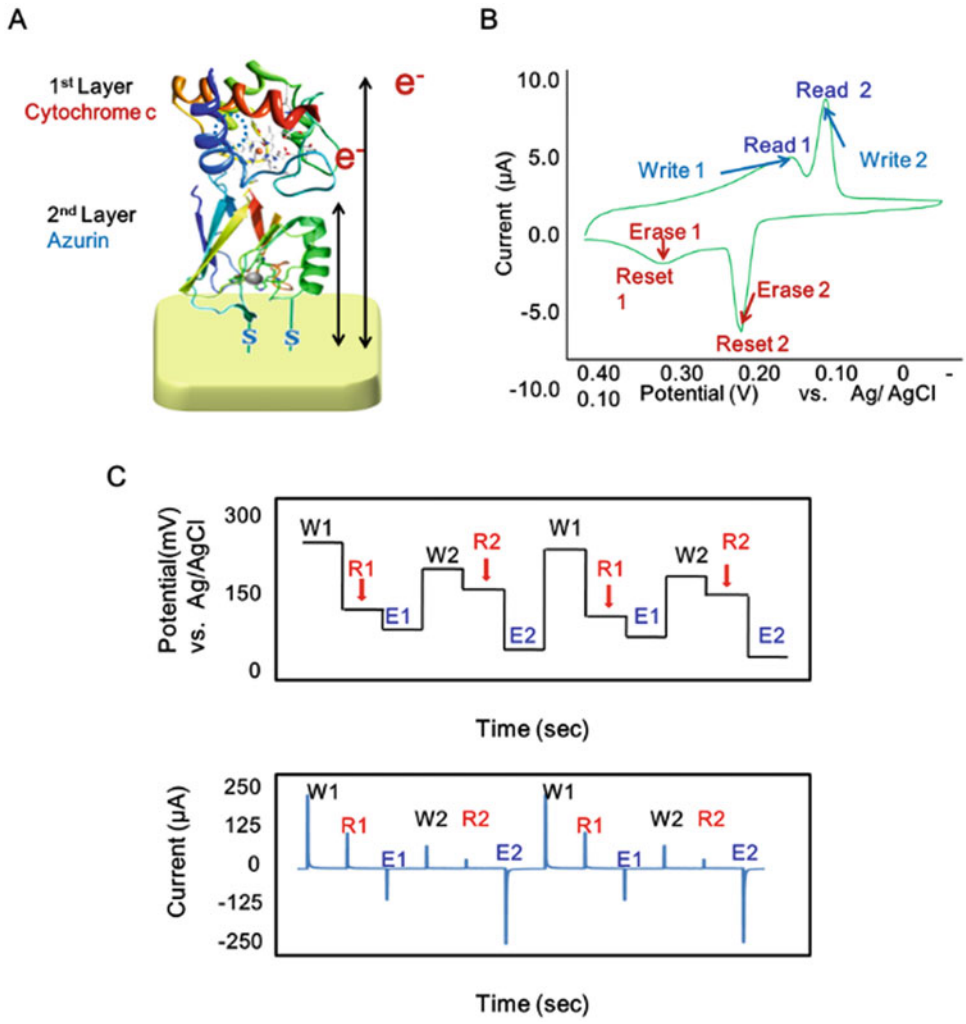

Fig. 17.6 A schmatic diagram reprents (**a**) The electron transfer mechanism of a cytochrome c/recombinant azurin heterolayer on Au surface. (**b**) Cyclic voltammogram of cytochrome c/recombinant azurin heterolayers. (**c**). Multi-level biomemory performance by OCPA. (Figures adapted from Lee et al. (2010), with permission from © WILEY-VCH Verlag GmbH & Co. KGaA 2010)

step. Accordingly, the multi-level memory function was evaluated by open circuit potential amperometry (OCPA). From OCPA results, the fabricated heterolayer showed exceptional multi-level memory performance by applied potentials. This biomolecular memory device offered the potential of a biomolecular based memory device with high memory density. Recently, they proposed a new method to fabricate a multi-level biomolecular memory device (Lee et al. 2014c). As seen in this section, the combination of metalloproteins and nanoparticles can be applied to develop the functional biomemory devices.

17.2.2 Enzyme-Based Logic Gate

As seen in the part of the front section, biomolecules have been widely used for bioelectronic devices including information storage device. Furthermore, those materials also have been introduced to develop the biologic gate. In conventional electronic field, logic gates

have been developed to acts as performing component in electronic device for logical operation such as Boolean function using field-effect transistor (FET), metal–oxide–semiconductor field-effect transistor (MOSFET) (Lee et al. 2015; Tomohiro et al. 2004).

However, with the miniaturization of electronic devices, scale down of logic gate has been researched in electronic researching areas. Thus, molecular-based logic gate or nanomaterial-based logic gate was developed to demonstrate logic function at molecular level (de Ruiter and van der Boom 2011; de Silva and Uchiyama 2007; Huang et al. 2001). Biomolecules also had been researched as a candidate to apply logic gate with miniaturization (Bychkova et al. 2010). However, in recent years, biomolecules have been recognized as a logic component because of the new advantages compared to conventional logic devices. The first advantage is that biomolecules can offer the possibility of homogeneous system fabrication to develop the uniform three-dimensional logic system compared to two-dimensional solid-state device which is widely used (Gdor et al. 2013). Thus, biomolecules-based system can provide the integration of complex reacting process for the development of high-order logic gate (Katz 2015). The second is that biomolecules-based logic gate can be operated by various input signals and output signals including light energy instead of electronic input signal (Prokup et al. 2012). Thus, biomolecules-based logic gate may not be bound to the electronic system for logic operation.

Among various biomolecules, enzyme and DNA have been widely used for biologic gate development. The advantage of enzyme used for logic gate is that various input signals can be used according to the used enzymes and chain reaction by related enzymes can be used for logic function. Thus, the complex logic systems have been demonstrated by enzyme (Baron et al. 2006a). In case of DNA, DNA can be used to build the complicated geometric structures by specific binding and conformational changes of DNA which is able to develop logic gate only using DNA itself (Okamoto et al. 2004; Seelig et al. 2006). In addition to these biomolecules, bacteria also have been investigated for logic gate fabrication (Arugula et al. 2012).

Enzyme has been used in bioelectronics field due to its unique properties like structure-folding and specific interaction with the substrate. Based on the property of enzyme, different output materials and signals can be induced by different input substrate injected into the enzyme. Thus, various combination of enzyme and the substrate have been used to develop logic gates like "AND" or "NAND" logic gate (Zhou et al. 2009). Katz group has been developed various functional enzyme-based logic gates. They developed the Boolean logic gate using enzymes including glucose oxidase, glucose dehydrogenase as input signals for logic operation (Strack et al. 2008b).

They developed the concatenated enzyme-based logic gate by highly specific recognition chain reactions using invertase, glucose oxidase and microperoxidase-11. Figure 17.7 shows the schematic mechanism of this logic gate. Sucrose, glucose and hydrogen peroxide were used as input materials. These input signals were considered "1" when they were existed and "0" when they were absent. To measure the output signal of this logic gate, the absorbance change of ABTS, biocatalytically oxidized dye, was used with defined threshold value (O.D = 0.3). Thus, the output signal with overthreshold was defined as "1", otherwise "0". According to the associated chain reaction of this logic system, only when all three inputs were injected, the output signal overpassed the defined threshold value. So, only (h), defined as "1,1,1", showed the "1" as the output signal (Strack et al. 2008a). This logic system, where individual reactions were interrelating and input materials were compatible, could be used as an alternative solution for assembling complex logic process which is difficult to demonstrate with synthesized chemical molecules due to limitation of synthetic complexity and scale up.

In addition to the logic gate based on interaction of enzyme and input substrate, there exists the other type of logic gate using induced folding and unfolding of polypeptide chain in protein (Deonarine et al. 2003; Muramatsu et al. 2006).

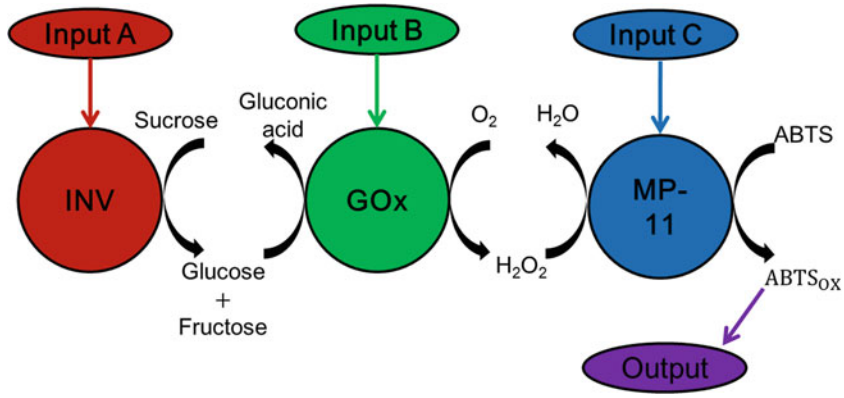

Fig. 17.7 Schematic mechanism of the developed concatenated enzyme-based logic gate by highly specific recognition chain reactions using invertase, glucose oxidase and microperoxidase-11

Looking in detail, structure of genetically and chemically engineered chaperonin azo-GroEL was changed by ATP and light. According to light as input signal, photomechanical gate of GroEL was induced to trans-to-cis isomerization and cis-to-trans isomerization by UV and visible lights, respectively. Also, its geometrical structure was changed by ATP. Using these two inputs, "AND" logic gate was developed.

Besides these logic gates, enzyme-based logic gates using interfacial pH change (Pita et al. 2009a), enzyme-functionalized nanoparticles (Pita et al. 2008) and supramolecular enzyme-hydrogel hybrids (Ikeda et al. 2014) were developed. These enzyme-based logic gates offer a huge potential for application in wide areas including clinical field for drug delivery and physiological conditioning assessment (Mailloux et al. 2014; Pita et al. 2009b; Radhakrishnan et al. 2013).

17.2.3 Protein-DNA-Based Bioprocessor

The conventional information processor is a programmable device that performs the various functions according to input data, then, the proper output produced-based on defined functions. The biomolecule can be applied to construct the bioprocessing device. The protein-DNA hybrid molecule-based information-processing device was developed for mimicking the information process in cellular signal (Lee et al. 2014b). The proposed bioprocessing device performed three functions: 'information regulation', 'information reinforcement', and 'information amplification'. The information process system is based on the biomemory platform consisting of metalloprotein/DNA hybrids, and could be regulated by surrounding commands (metal ions, conducting nanoparticles and semiconducting nanoparticles) (Fig. 17.8). The core material (redox material) in the biomemory platform was re-engineered from a simple metalloprotein into protein/DNA hybrids to receive the surrounding's commands and to store the information based on input.

The azurin was rolled as the memory core and the ssDNA can be used as the processing receptor. When cDNA-nanoparticle or various metal ions are hybridized, the ssDNA can be hybridized or intercalated with metal ions for bioprocessing functions. The information reinforcement and information regulation functions were validated based on input materials by the chronoamperometry (CA) method. The ssDNA arm has a charged backbone that can bind to various heavy metal ions, such as Cu, Zn, Ni, Co, Fe, Mn.

To assess the information amplification function, a scanning tunneling spectroscopy experiment was carried out on the recombinant azurin/DNA hybrid when cDNA-quantum dot (QD: CdSe-ZnS) added to bioprocessor. In the case of

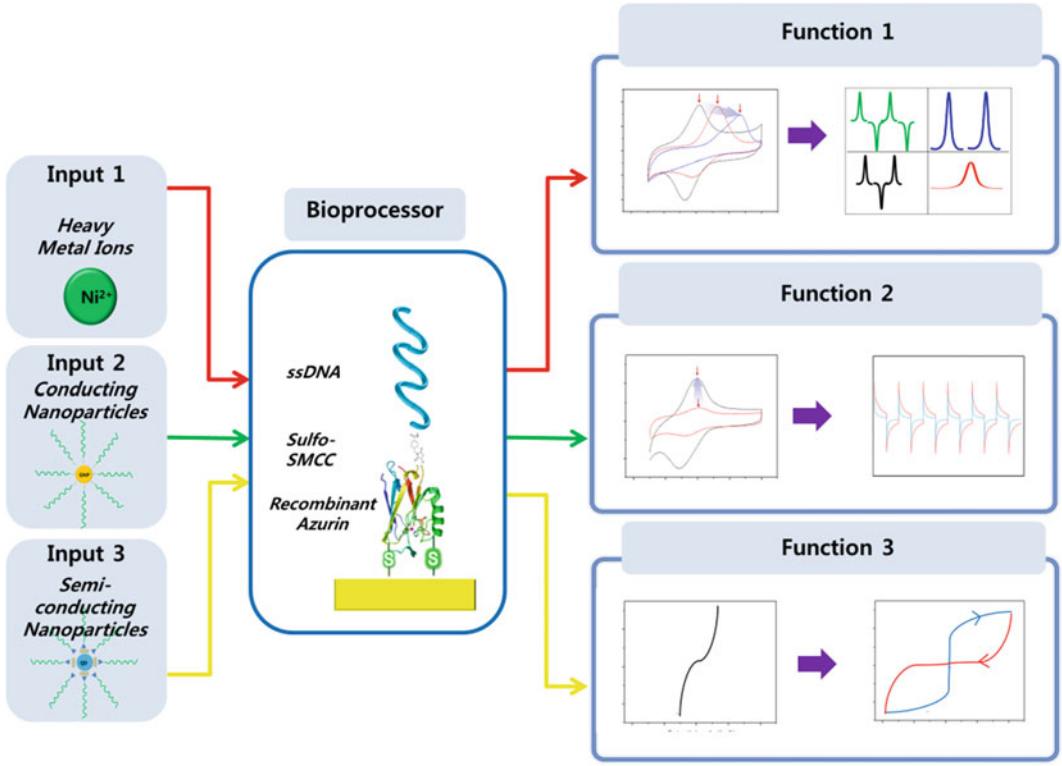

Fig. 17.8 Schematic diagram of bioprocessing device comprised with recombinant protein/DNA hybrid corresponding to input materials. That shows the proper pre-defined functions

the recombinant azurin/DNA hybrid, the I-V result shows the semiconductor behavior, as after 0.2 V of the applied bias, the recombinant azurin/DNA hybrid shows a non-ohmic behavior. However, in the case of the recombinant azurin/DNA-cDNA/QD complex, the result shows that the bi-electrical stability ranges from −2.0 to +2.0 V. In this case, the recombinant azurin/DNA hybrid-biotin-tagged cDNA/streptavidin-coated QD conjugate is initially in a low conducting state until it reaches about 0.8 V. After 0.8 V, the I-V curve drastically changed which indicates a transition of the recombinant azurin/DNA hybrid /biotin-tagged cDNA/streptavidin-coated QD complex conjugate from a low conducting state to a high conducting state. This state change can be defined as 'information amplification'. Thus, the protein/DNA-based bioprocessor has complex functionality with the suggested concept and this functionality can be extended with new input materials such as graphene, nanoparticles, proteins and RNA. This concept provides the possibility for biomolecular-based computing systems; analog style memorizing, fuzzy type determining, and the environment are affected.

17.3 Nucleic Acid-Based Bioelectronic Device

Nucleic acid has been received attention due to its functionality and programmability. By specific recognition and hybridization with complementary nucleic acid sequence, Especially, DNA has become an attractive biomolecule for bioelectronics application including biosensor and biologic gate (Campolongo et al. 2011). Widely studied DNA logic gate is based on the specific-sequence recognizing and binding property of DNA itself. For example, in DNA hybridizing mechanism, longer-specific

complementary DNA can disrupt the hybridized DNAs formed with shorter-specific complementary DNA. Then, longer-specific complementary DNA replaces the shorter-specific sequence and shorter-specific complementary DNA is de-hybridized from interaction. This mechanism is fit to develop logic gate like DNA displacement-based logic gate (Frezza et al. 2007). In the field of DNA logic gate, Willner group and Winfree group have developed various logic gates based on functionality of DNA (Liu et al. 2012b; Seelig et al. 2006).

17.3.1 DNA-Based Logic Gate

Willner group designed and developed the aptamer-based DNA tweezer structure for "SET-RESET" logic demonstration (Elbaz et al. 2009a) (Fig. 17.9). This DNA tweezer, composed of four different nucleic acids, could be trans-shaped its structure, opened shape or closed shape, by insertion of specific materials such as adenosine monophosphate (AMP), adenosine deaminase (AD) and inosine monophosphate. This DNA tweezer possessed fluorescence dye (Cy5) and quencher (Iowa black RQ) located on tweezer frame nucleic acid. Thus, in the case of closed shape, fluorescence intensity was quenched, but in the case of opened shape, high fluorescence intensity was detected. By this mechanism, shape-change of DNA tweezer was verified through fluorescence intensity. Two different but related DNA tweezers which were called "Tweezer A" and "Tweezer B" respectively, possessing two different dyes and quenchers each other, were used to develop "SET-RESET' logic gate in this paper, and these tweezers were trans-shaped in contrast to each other. By addition of AD, the system composed of two different DNA tweezers could become "state1" as defined "RESET", and the system could become "state2" by addition of AMP as "SET". Each state was confirmed by fluorescence intensity. Figure 17.9a, b show the schematic image and process of this logic system and "SET-RESET" logic data with exist of two different states.

In addition to this research, G-quadruplexes, one type of DNA sequence composed of stacks of guanine tetrads by Hoogsteen hydrogen bonding, have been wide used for DNA logic gate due to the easy modulation of DNA structure under benign conditions (He et al. 2013; Wang et al. 2012). For example, G-quadruplex-hemin complex was formed by the insertion of potassium ion and hemin into G-quadruplex, then specific

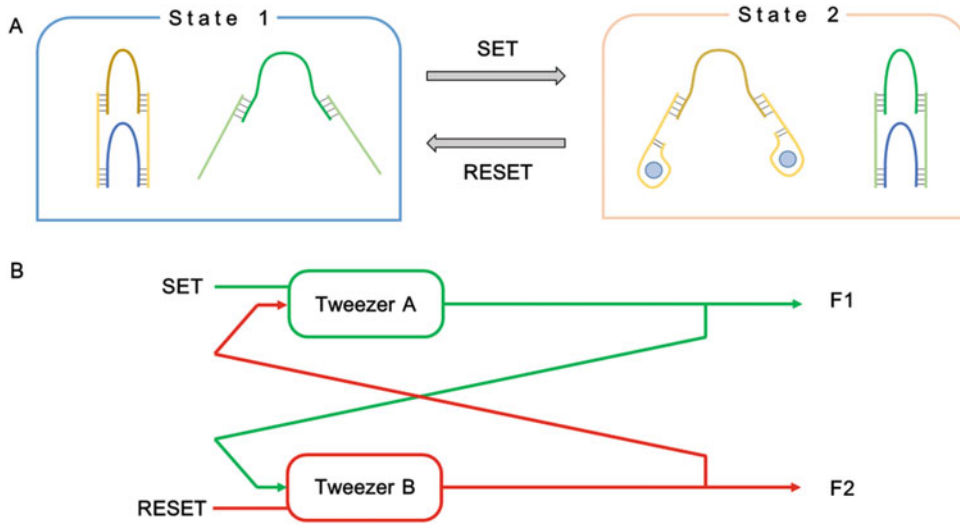

Fig. 17.9 (**a**) Scheme of coherent activating logic gate of two tweezers using adenosine monophosphate and adenosine deaminase as input materials. (**b**) Schematic diagram of the SET-RESET system

structure was formed and hemin used as electrochemical probe was inserted inside that structure. That change could be detected by electrochemical technique. Using this mechanism, "AND" logic was demonstrated. Both potassium and hemin were added to G-quadruplex, then the output signal was passed over the defined threshold value, 1, however, addition of only one of them to G-quadruplex showed the under-threshold value, 0. Also, the output signal was under-threshold value without potassium ion and hemin (Wang et al. 2012).

In addition to these achievements, pH, nanoparticles have also used to fabricate DNA logic gates similar to enzyme-based logic gates (Elbaz et al. 2009b, 2012; Freeman et al. 2009). Also, there exists logic gate using mismatching of hybridized DNA, insertion of mercury ion in thymine–thymine (T–T) mismatch in hybridized DNA and insertion of iron ion in cytosine–cytosine (C–C) mismatch in DNA duplexes, for electrochemical logic outputs (Li et al. 2011).

These developed DNA logic gates can be applied for DNA computing development. Winfree group developed the digital circuit computation with multilayer circuits by DNA displacement cascades within all logical operation (Qian and Winfree 2011). Furthermore, using DNA displacement cascades, they developed the DNA computing system mimicking neural network computation which even showed the property of Hopfield networks associative memory (Qian et al. 2011). As seen in this chapter, biomolecules, especially enzyme and DNA, have been widely investigated for the development of logic gate. There is also the case of programmable DNA-enzyme conjugates fabrication for logic gate (Gianneschi and Ghadiri 2007). These biomolecular logic gates give a chance to develop the effective complex computing functions demonstration for biocomputer system development (Ogihara and Ray 2000), also enrich the life of mankind due to the expanded application of biomolecules in clinical field (Mailloux et al. 2014; Pita et al. 2009b; Radhakrishnan et al. 2013).

17.3.2 RNA-Based Biologic Gate

The RNA molecule is a powerful source for constructing molecular logic gate owing to its intriguing characteristics. Compared to DNA molecule, RNA has various functionality and applications (Haque et al. 2012; Jaeger and Chworos 2006). Those functionalities of RNA molecules were originated from the proper folding and assembly of RNA molecule tertiary structures using the formation of hairpin loops, dove-tail, bulges, and internal loops. Those tertiary structures of RNA give a unique functionality such as aptamers, ribozymes, and riboswitches (Grabow and Jaeger 2014). These functional RNA molecules can be easily designed to constitute the logic gate core for performing specific function such as gene expression, diagnosis, or cell signaling (Benenson et al. 2004; Rinaudo et al. 2007). The RNA-based logic gate is usually activated through the RNA hybridization or displacement that gives conformational change or ligand binding according to input molecule (Benenson 2009; Xie et al. 2010).

Benenson group reported the RNAi-based logic evaluator to perform Boolean logic behavior-based on to input molecules (Rinaudo et al. 2007). The constituted biological circuit was composed of a couple of mRNA species to produce the fluorescent protein in human kidney cell. Those mRNA species were constituted with the different non-coding region to perform the logic behavior. Then, the specific designed DNA contained plasmid was applied to control the gate function in the cell through transfection. The siRNA was used to regulate the mRNA degradation as the gate input. Then, the mRNA produced the fluorescence protein corresponding to input signal and this expression of fluorescence protein level was used to the output signal.

Recently, the field-effect transistor structure-based genetic RNA logic gate was suggested (Bonnet et al. 2012, 2013). The bacteriophage serine integrase was used to regulate the state of double stranded DNA. Interestingly, this study defined the input and output signals are the

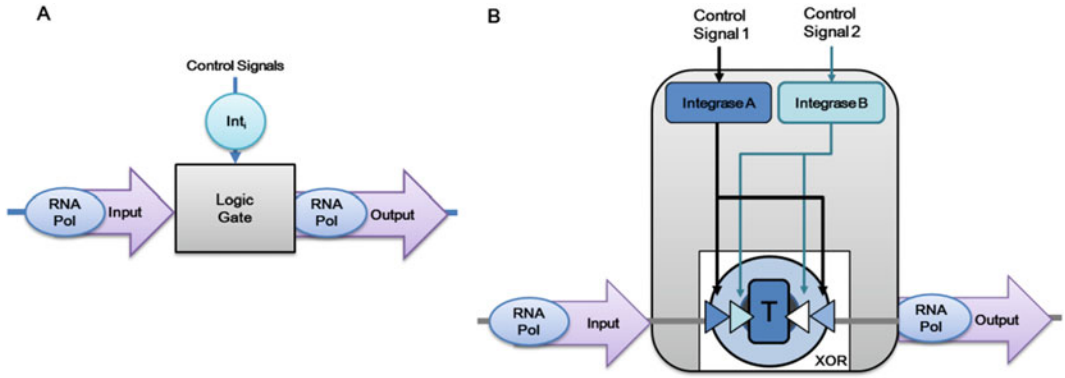

Fig. 17.10 (**a**) Three-terminal transcriptor based gates use integrase (Int) control signals to modulate RNApolymerase (RNA Pol) flow between a separate gate input and output. (**b**) The logic element within a three-terminal Boolean integrase XOR gate such that gate output is high only if control signals are different

transcription rates of the flow of RNA polymerase according to DNA at the logic element boundaries (Fig. 17.10). The integrase-serine control invert or delete the DNA encoding transcription, thus terminating or promoting the transcription rates. With this mechanism, the AND, OR, XOR, NOR and XNOR gates have been fabricated with one/two asymmetric transcriptor. Those results demonstrated RNA molecule can be extended to construct new concept of logic gate which is hard to achieve in molecular logic gate.

17.3.3 RNA-Based Bioprocessor

The RNA has a unique functionality such as catalytic property, recognition, self-folding, self-splicing and etc. (Grabow and Jaeger 2014; Haque et al. 2012; Jaeger and Chworos 2006). Those properties of RNA molecule can be extended to use of bioprocessor unit (Benenson 2009; Win and Smolke 2008). Usually, the bioprocessor composed of RNA molecule can be received the chemicals or RNA sequences and it process the information. The RNA molecule can be used to the molecular information processor operating in living systems with a biological environment (Rinaudo et al. 2007; Win and Smolke 2008), RNA-based biocomputation system would be powerful alternative to solve the current limitation of silicon-based computation, for example, (1) RNA molecule-based computation can be directly used to diagnostic system such as cancer or hereditary disease. (2) The combination of RNA-molecule can be used to detect RNA-related virus sensing system (3) it may provide new type of computation that gives the analogue-based result corresponding to RNA input material. (4) the silicon-based computation system is hard to operate in a living organism (Xie et al. 2010).

The synthetic RNA-based information processing devices was fabricated to perform the logic gates, signal filtering, and cooperativity functions (Win and Smolke 2008). The RNA-based bioprocessor that constituted with ribozymes and RNA aptamers was received the molecular input. Then, the processed input was transmitted to control the expression of the green fluorescent protein as output. The RNA aptamer that rolled as the sensor part was composed of a hammerhead ribozyme for cleaving of the aptamer. Also, the information transmitter part has the complementary RNA sequences for binding to RNA aptamer and ribozymes parts. Like this, RNA molecule can be used to bioprocessor module to perform the multi-functional information processor development (Fig. 17.11).

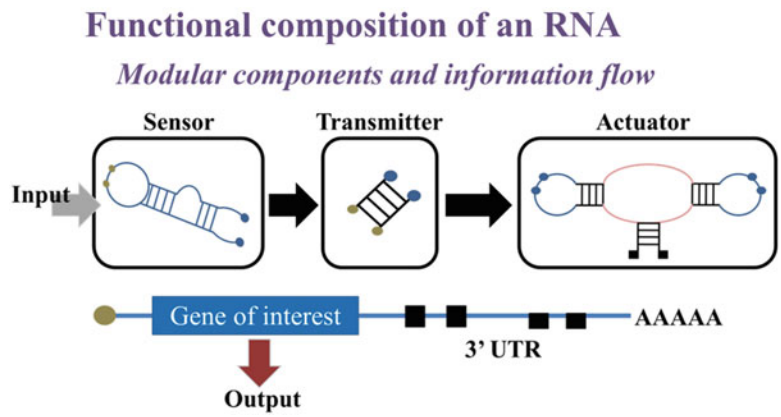

Fig. 17.11 Functional RNA device composition framework. The color scheme for all figures is as follows: brown, aptamer or sensor component; purple, catalytic core of the ribozyme or actuator component; blue, loop regions of the actuator component; green and red, strands within the transmitter component that participate in the competitive hybridization event. A functional composition framework for assembling RNA devices from modular components. Information in the form of a molecular input is received by the sensor and transmitted by the transmitter to a regulated activity of the actuator, which in turn controls the translation of a target transcript as an output

The interesting concept of RNA-based autonomous bioinformation processor was reported to program a biomolecular computing device to work inside a living cell (Ausländer et al. 2012). In this study, the autonomous biomolecular information processor was fabricated to control the disease-related gene expression for small-cell lung cancer and prostate cancer detection system. To operate the autonomous bioinformation processor, the regulation of specific mRNA level and chemicals level should be required to control the point mutation as the input material. Then, the bioprocessor gives a short ssDNA which control the gene expression level for anticancer effect as the output. The automaton bioprocessor regulates 'positive state' and 'negative state' corresponding to specific gene expression level. They demonstrated RNA-based computation system can be directly applied to the gene expression control system for future diagnostic detection. Like this, the advances in RNA-based information processing system demonstrate the promise for biocomputation with new functionality.

17.3.4 RNA-Based Biomemory

In recent years, Choi's group reported the RNA and semiconductor nanoparticle hybrid can be used to the resistive memory device application (Lee et al. 2015). To construct the resistive memory device, the thermodynamically stable pRNA 3WJ from the phi29 DNA packaging motor was used and conjugated with quantum dot nanoparticle (CdSe-ZnS). The pRNA 3WJ was easily conjugated with the quantum dot using Sephadex G100 resin-recognized RNA aptamer-based site-specific conjugation method. The prepared pRNA 3WJ/QD hybrid was immobilized onto Au substrate by self-assembly technique. The pRNA 3WJ was rolled as the connector between QD nanoparticles and Au substrate for the resistive memory performance. Furthermore, the pRNA 3WJ rolled as the insulator between the QD and Au substrate. As a semiconductor, the QD was rolled to storing the electron for memory function. And, the metal Au substrate was rolled to

m. The electrical bi-stability property (I-V curve) of pRNA 3WJ/QD hybrid was confirmed by scanning tunneling spectroscopy (STS). As a result, the pRNA 3WJ/QD hybrid exhibited the resistive memory property. The proposed resistive memory device using a combination of RNA and nanoparticles can be applied to bioinformation storage device.

17.4 Protein-Based Electrochemical Biosensor

Protein-based electrochemical biosensors (ECBs) can be divided into two classes of enzyme-based and antibody-based biosensors (Vestergaard et al. 2007). However, in comparison with immunosensors, enzymatic biosensors have been most regularly used in disease diagnosis and point-of-care applications. They are biological catalysts and can be exploited in the purified forms and be engineered for the particular reactions. Whereas, antibodies (used for immunosensors) are non-catalytic biological elements which are well capable to specifically bind with their corresponding antigens. Although, they have a very high specificity, their applications are limited and their handling needs a considerable experimental proficiency (Li et al. 2009; Ramanavičius et al. 2006; Rocchitta et al. 2016).

Enzymes are large macromolecules, mostly proteins, which usually harbor prosthetic groups (one or more metal ions). These metal ions enable the enzymes to undergo oxidation and reduction upon the reaction with their corresponding analytes. This redox action which is corresponding to the presence of the analyte, can be detected electrochemically as the function of enzymatic ECBs. The basic mechanism for enzyme catalysis is as follows:

$$S + E \underset{k_{-1}}{\overset{k_1}{\rightleftharpoons}} ES \overset{k_2}{\rightarrow} E + P \qquad (17.1)$$

Where, S is substrate, E is enzyme, ES is enzyme/substrate complex, and P is product.

The enzymatic ECBs are highly selective and fast with high sensitivity due to their catalytic activities and they can be effectively immobilized onto the substrate (transducer) due to their 3D structure. However, they are relatively expensive and still suffering from the loss of activity after a prolonged usage, due to the deactivation and/or substrate detachment (Rocchitta et al. 2016).

Basically, analytes can be directly oxidized/reduced at ordinary solid electrodes. However, employment of conventional electrodes have been restricted because of their slow electron transfer kinetics and high overpotentials, which reduce the sensing performance of the biosensors (Pumera et al. 2007). It has been reported that, incorporation of enzymes with nanostructured solid electrodes can enhance the electron-transfer rate between the modified electrode and the solution interface (Wang 2005). Moreover, the size and structure of enzymes can be engineered for the further amplification of sensing performances (Dolatabadi et al. 2011; Malekzad et al. 2017). On the other hand, enzyme immobilization onto the electrode surface is a very important issue to be studied. The successful immobilization normally requires; (i) enzyme stability and specific affinity towards the surface, (ii) surfaces uniformity, (iii) maintenance of the natural enzymes' biological functions, and (iv) controlling the enzyme orientation for the achievement of maximum surface density (Zhang et al. 2009).

There are usually two methods of immobilization: (1) Indirect immobilization; (2) Direct immobilization. The indirect immobilization technique is based on the modification of the electrode surface with suitable linkers for the establishment of functional groups to be further used for the enzyme binding reaction. Whereas, the direct immobilization method does not require extra chemical linkers and involves either physical adsorption or specific interaction between the enzyme and the electrode, such as immobilization by means of Au-thiol (sulfhydryl) interaction (Rao et al. 1798; Singh et al. 2016; Wong et al. 2009). Although, the enzyme-based ECBs have been utilized for the detection of various toxins and analytes, such as glucose (Wang 2008), urea (Chen et al. 2011; Cho and Huang 1798), nitric

oxide (Nagase et al. 1797; Yoon et al. 2017b) and hydrogen peroxide, here we demonstrate some examples of enzyme-based ECBs for the detection of hydrogen peroxide (H_2O_2).

17.4.1 Protein-Based Electrochemical Biosensor for H_2O_2 Detection

Hydrogen peroxide (H_2O_2) is an important biomarker of the major reactive oxygen species (ROS) whose mediated pathways have been related to various bodily disorders such as neurodegenerative diseases, Alzheimer, asthma, cancer and inflammatory arthritis (Andre et al. 2013; Giorgio et al. 2007; Rojkind et al. 2002; Schalkwijk et al. 1786). Therefore, detection of low concentration of H_2O_2 in a rapid and selective fashion is highly demanding. Up until now, many enzymes (redox-active proteins) have been exploited to develop various H_2O_2 ECBs, such as cytochrome c (cyt c), Myoglobin (Mb), Hemoglobin (Hb), Ferredoxin (Fdx) and Horseradish Peroxidase (HRP). Their corresponding electrocatalytic reactions towards H_2O_2 is shown as follows:

$$\begin{aligned} &\mathrm{Mb}\left(\mathrm{Fe}^{3+}\right)+\mathrm{e}^{-} \rightarrow \mathrm{Mb}\left(\mathrm{Fe}^{2+}\right) \\ &2\,\mathrm{Mb}\left(\mathrm{Fe}^{2+}\right)+\mathrm{H_2O_2} \rightarrow 2\,\mathrm{Mb}\left(\mathrm{Fe}^{3+}\right)+2\mathrm{H_2O} \end{aligned} \tag{17.2}$$

$$\begin{aligned} &\text{cyt c}\left(\mathrm{Fe}^{3+}\right)+\mathrm{e}^{-} \rightarrow \text{cyt c}\left(\mathrm{Fe}^{2+}\right) \\ &2\,\text{cyt c}\left(\mathrm{Fe}^{2+}\right)+2\mathrm{H}^{+}+\mathrm{H_2O_2} \rightarrow 2\,\text{cyt c}\left(\mathrm{Fe}^{3+}\right)+2\mathrm{H_2O} \end{aligned} \tag{17.3}$$

$$\begin{aligned} &\mathrm{Hb}\left(\mathrm{Fe}^{3+}\right)+\mathrm{H_2O_2} \rightarrow \text{Compound I}\left(\mathrm{Fe}^{4+}=\mathrm{O}\right)+\mathrm{H_2O} \\ &\text{Compound I}\left(\mathrm{Fe}^{4+}=\mathrm{O}\right)+\mathrm{e}^{-}+\mathrm{H}^{+} \rightarrow \text{Compound II} \\ &\text{Compound II}+\mathrm{e}^{-}+\mathrm{H}^{+} \rightarrow \mathrm{Hb}\left(\mathrm{Fe}^{3+}\right)+\mathrm{H_2O} \end{aligned} \tag{17.4}$$

$$\begin{aligned} &\mathrm{Fdx}\,(2\mathrm{Fe}-2\mathrm{S})^{2+}+\mathrm{e}^{-} \rightarrow \mathrm{Fdx}\,(2\mathrm{Fe}-2\mathrm{S})^{+} \\ &\mathrm{Fdx}\,(2\mathrm{Fe}-2\mathrm{S})^{+}+\mathrm{H_2O_2} \rightarrow \mathrm{Fdx}\,(2\mathrm{Fe}-2\mathrm{S})^{2+}+2\mathrm{OH}^{-} \end{aligned} \tag{17.5}$$

$$\begin{aligned} &\mathrm{HRP}\left(\mathrm{Fe}^{3+}\right)+\mathrm{H_2O_2} \rightarrow \text{Compound I}\left(\mathrm{Fe}^{4+}=\mathrm{O}\right)+\mathrm{H_2O} \\ &\text{Compound I}\left(\mathrm{Fe}^{4+}=\mathrm{O}\right)+\mathrm{e}^{-}+\mathrm{H}^{+} \rightarrow \text{Compound II} \\ &\text{Compound II}+\mathrm{e}^{-}+\mathrm{H}^{+} \rightarrow \mathrm{HRP}\left(\mathrm{Fe}^{3+}\right)+\mathrm{H_2O} \end{aligned} \tag{17.6}$$

A typical experimental setup for the electrochemical detection of H_2O_2 is shown in Fig. 17.12. Basically, amperometric technique (i−t) is employed, from which, the applied voltage is kept constant at the value where all the species are in the reduced states. Then, an identical aliquot of H_2O_2 with various concentrations is injected inside the N_2-saturated buffer solution with the constant time intervals, while the solution is continuously stirring. The current versus time is recorded for further analysis.

The Mb, cyt c, Hb, Fdx and HRP as the class of metalloproteins are hemeproteins containing iron cation(s). Due to the redox capability of hemeproteins, these metalloproteins have been widely incorporated for enzyme-based biosensors, particularly H_2O_2 biosensors. However, as we mentioned earlier, to increase the electron transfer rate of the solid electrodes, the modification of electrode prior to the enzyme immobilization is necessary.

Gold nanoparticle-modified iridium tin oxide (Au NP/ITO) has been reported to enhance the electrochemical properties of the cyt c (Yagati et al. 2012). It was observed that, the Au NP provided not only conduction enhancement but also a very high surface to volume ratio for the effective and dense immobilization of cyt c. This led to a clear quasi-reversible redox current signals resulting from the $Fe^{3+/2+}$ redox center, which showed a good electron exchange between the protein and solid electrode. Later, Cho's group developed new electrode by coupling gold nanoparticles with graphene oxide as the precursor for the immobilization of HRP to be further used for the sensitive detection of H_2O_2 (Yagati et al. 2014). The electrode was fabricated using chronoamperometry method based on electrochemical co-reduction of graphene oxide/nanoparticle (ERGO-NP) composite films onto ITO electrode. The ERGO-NP/ITO electrodes demonstrated a very high conductivity (ca. 5 times higher than the unmodified electrodes) which was attributed to well-distribution of immobilized enzyme onto the surface as well as the high surface area and highly conductivity of the substrate. The sensor showed excellent sensitivity of 1808.9 μA mM^{-1} cm^{-2}

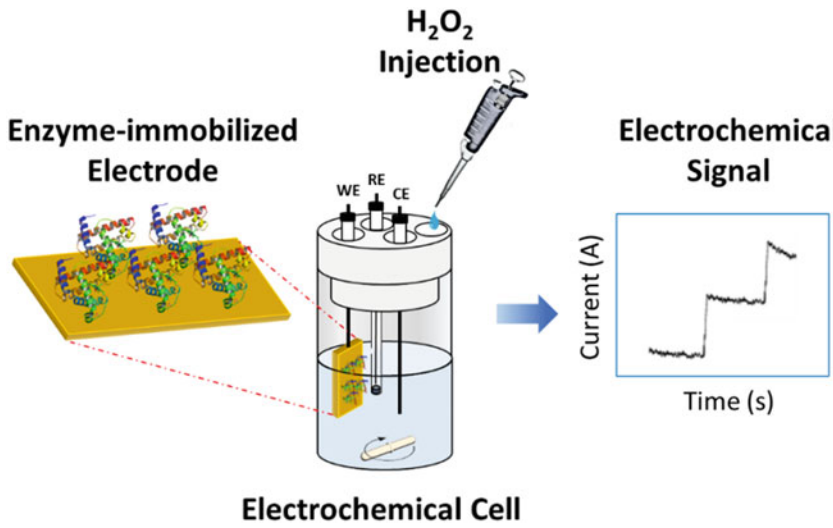

Fig. 17.12 Schematic diagram of the enzyme-based ECB experimental setup. WE, RE and CE stand for working, reference and counter electrode, respectively

and selectivity with a linear dynamic detection range and the detection limit of 0.6 μM.

Another report dealt with the Mb immobilization onto porous cerium dioxide (CeO_2) which was priory electrodeposited onto the ITO glass (Yagati et al. 2013). The developed CeO_2/ITO film offered a nanoporous structure with a large surface area for the direct immobilization of Mb without any chemical linker to hamper the electron transfer between the interfaces. The biosensor represented a good selectivity and a sound current response of 10 s. Recently, a very sensitive enzyme-based H_2O_2 ECB was reported which was based on the MoS_2 nanoparticle encapsulated with graphene oxide (Fig. 17.13) (Yoon et al. 2017a). Owing to the unique electrochemical properties of topological insulator (MoS_2) nanoparticle as well as the graphene oxide, the proposed biosensor exhibited high electrochemical signal which gave rise to the sensitive detection of H_2O_2 at 20 nm. A comprehensive report of different enzyme-based H_2O_2 ECBs is provided in Table 17.1.

17.4.2 Protein/DNA-Based Electrochemical Biosensor for H_2O_2 Detection

The study of interaction between protein and DNA has become a very interesting topic in variety fields of biology, chemistry and biotechnology (Gromiha and Nagarajan 2013). The study on charge transfer between the redox proteins or enzymes and nucleic acids has attracted much attention, since it can provide deeper understandings of the electron transfer mechanism in real biological systems and establish a stepping stone for the fabricating of novel biosensors and biodevices (Gorton et al. 1799; Nowak et al. 2011). Here we review some examples of Protein/DNA-based ECBs for the detection of H_2O_2 and oligonucleotides.

There are mainly two methods for the DNA/protein conjugation: electrostatic bonding and covenant bonding. Taking the advantage of electrostatic bonding, ECBs composed of DNA and hemoglobin (Hb) dropletting onto the gold electrode to detect H_2O_2. The DNA helped the Hb to keep its native structure and to less aggregate giving rise to its reducibility enhancement (Kafi et al. 2006). Another approach was based on HRP/DNA–silver nanohybrids and poly

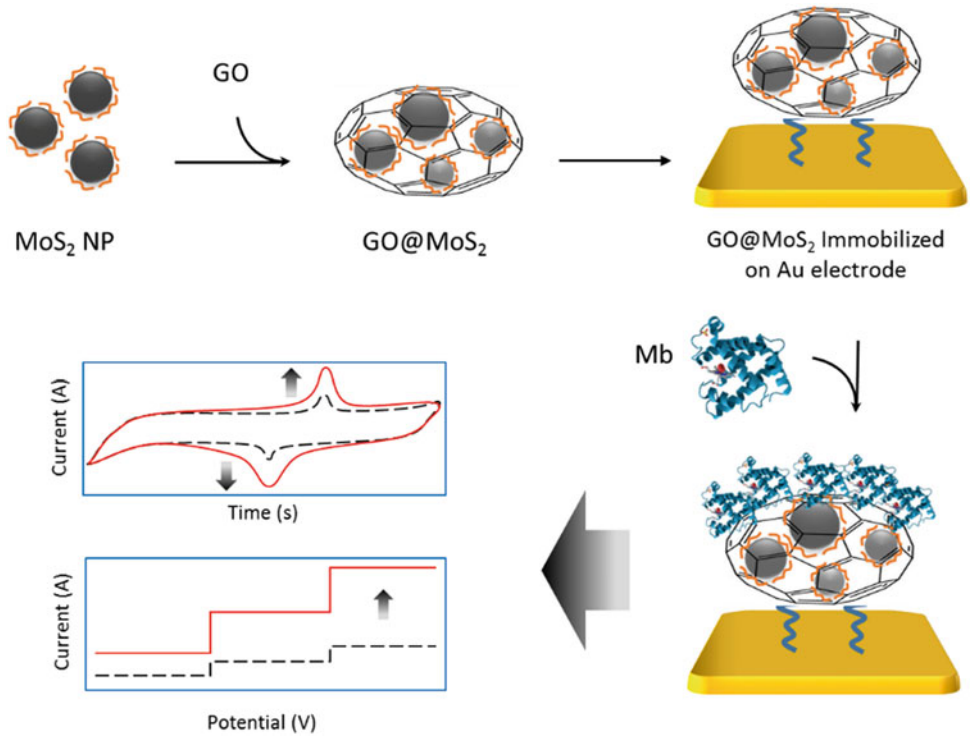

Fig. 17.13 Schematic depicting the synthesis route of the biosensor (Upper panel) and constitution of biosensor towards EC signal enhancement and H_2O_2 detection improvement. (Figure reproduced with permission from Yoon et al. 2017a)

Table 17.1 List of protein-based electrochemical biosensor for H_2O_2 detection

Protein	Modified Electrode	LOD (μM)	Dynamic Range (μM)	References
Cyt c	Au NP/ITO	0.5	–	Yagati et al. (2012)
	MPCE	0.146	0.02–24	Zhang (2008)
	GNPs/RTIL/MWNTs/GCE	3.0	0.05–11.5	Xiang et al. (2008)
	RTIL-PDDA-AuNPs/MUA-MCH/au	5.0	0.04–3.45	Song et al. (2013)
	MPA/au	1.0	0–0.25	Suárez et al. (2013)
Mb	GO@MoS_2	0.02	–	Yoon et al. (2017a)
	CeO_2/ITO	0.6	3.0–3000	Yagati et al. (2013)
	Nafion/IL/GCE	0.14	1.0–180	Safavi and Farjami (2010)
	GNRs@SiO2/RTIL-sol-gel/GCE	0.12	0.2–180	Zhu et al. (2009)
	Clay-IL/GCE	0.73	3.9–259	Dai et al. (2009)
Hb	GNPs/MWNT/GC	0.08	0.21–3000	Jia et al. (2009)
	Graphene/Fe_3O_4/GCE	6.0	0.25–1.7	Wang et al. (2013)
	ZnO/MWCNT/GCE	0.02	–	Palanisamy et al. (2012)
	SDS/TiO_2/GCE	0.087	0.5–70	Wang et al. (2011)
HRP	ERGO-NP	0.6	–	Yagati et al. (2014)
	Composite-3	0.009	0.01–0.22	Umasankar et al. (2012)
	PTMSPA@GNR	0.06	10–1000	Komathi et al. (2013)
	Au NAE	0.42	0.74–15,000	Xu et al. (2010)
	Au NP/MPA/au	0.16	0.48–1200	Wan et al. (2013)

(diallyldimethylammonium chloride) (PDDA)-protected gold nanoparticles (Ma et al. 2009). As shown in Fig. 17.14, at first, DNA–Ag + complex was electrochemically reduced onto the bare gold electrode to obtain negatively charged immobilization matrix (DNA–Ag) for the further immobilization of PDDA–Au particles. Then the process of A and B were repeated to achieve a more conductive bilayer structure. Next, the positively charged HRP (H_2O_2 reducing enzyme) was bond to the negative surface for the subsequent detection of H_2O_2. The reported biosensor represented a linear dynamic range over H_2O_2 concentrations from 7.0 μm to 7.8 mm and the detection limit of 2.0 μm (S/N = 3) with good selectivity and acceptable stability.

Using two different types of proteins (HRP and Cyt c) in conjugation with DNA, Yonghai et al. fabricated an H_2O_2 biosensor to mimic the charge transfer and electrocatalytic mechanism of two proteins in living organisms (Song et al. 2012). According to their results, a faster charge transfer rate was observed for the bi-protein bio-interphase than the single protein biointerphase, demonstrating a synergetic effect to better the electron transfer. The DNA role was to provide a network film as a biocompatible microenvironment for the proteins adsorption and an essential pathway for the charge transfer between the electrode and proteins (Fig. 17.15).

17.4.3 Protein/DNA-Based Electrochemical Biosensor for Oligonucleotide Detection

Interaction between DNA and protein has been also studied to develop various ECBs for the detection of different genomic DNA/RNA strands. One of the well-known protein-ligand covalent conjugation techniques is the streptavidin (STV)-biotin. (Dundas et al. 2013; González et al. 1799) Making use of STV-biotin interaction, Shanlin et al. fabricated a chemical controllable electrode for EC detection of DNA using EIS method (Pan and Rothberg 2005). As depicted in Fig. 17.16, bare gold electrode was firstly modified with the mixed monolayer of 2-mercaptoethanol (ME) and 11-mercaptoundecanoic acid (11-MUA) to provide enough space for the conjugation of STV onto the free carboxyl group of the 11-MUA through amide bonding. A biotin-modified ssDNA was then bound to the STV through the robust STV-biotin chemistry. Using $[Fe(CN)_6]^{4-/3-}$ redox reporter, the EIS measurement was performed. Before the target invasion, the ssDNAs hampered the redox probes to reach the gold electrode surface leading, whereas, after the target hybridization, the formation of the upright dsDNA facilitated approach of the redox probe to the surface. The resistance difference was monitored by EIS method to offer a very sensitive and selective ECB with the detection limit of 10 pm.

The redox active proteins or enzymes have been also implemented for the nucleic acid detection. For instance, using HRP as the redox reporter by reducing the H_2O_2. Gang et al. reported a very sensitive enzyme-based E-DNA sensor consists of a stemloop DNA probe which was labeled with biotin and digoxigenin (DIG) at its each end (Liu et al. 2008). The probe was immobilized onto an avidin-modified electrode through the biotin-avidin conjugation (another strong conjugation technique). In the absence of the target DNA, the DIG was shielded from being approached by bulky AntiDIG-modified HRP because of the steric effect. After the target induction and hybridization, the dsDNA forced the DIG to be detached from the surface and be accessible by the AntiDIG-modified HRP for the enzymatic transduction via H_2O_2 reduction. The proposed biosensor exhibited a high sensitivity down to femtomolar with the ability of mismatch detection.

An alternative approach for the oligonucleotide detection using protein/DNA-based ECB was to make use of metalloproteins in conjugation

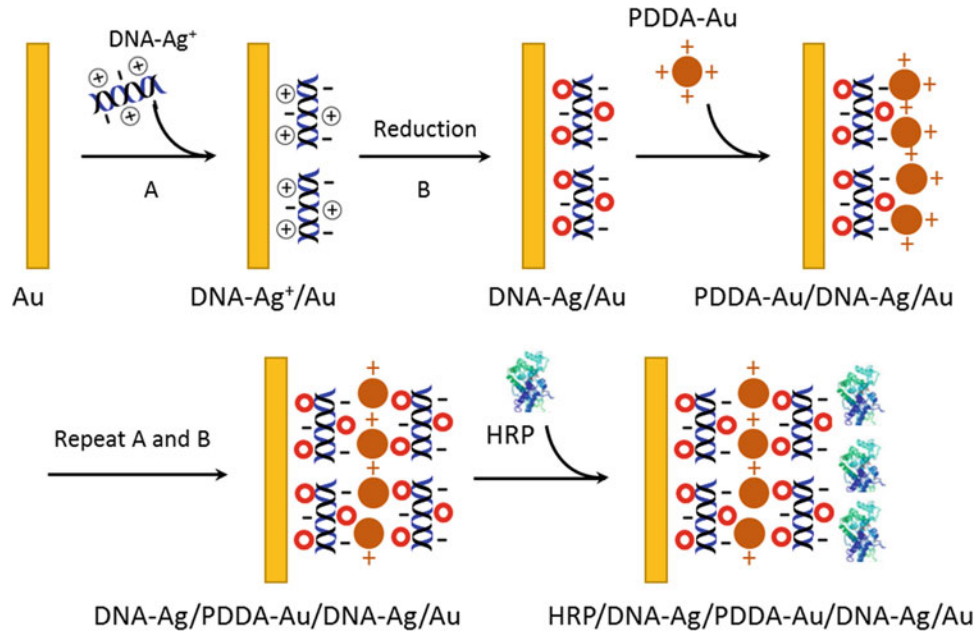

Fig. 17.14 Layer-by-layer formation of the DNA-Ag/PDDA-Au/DNA-Ag/Au

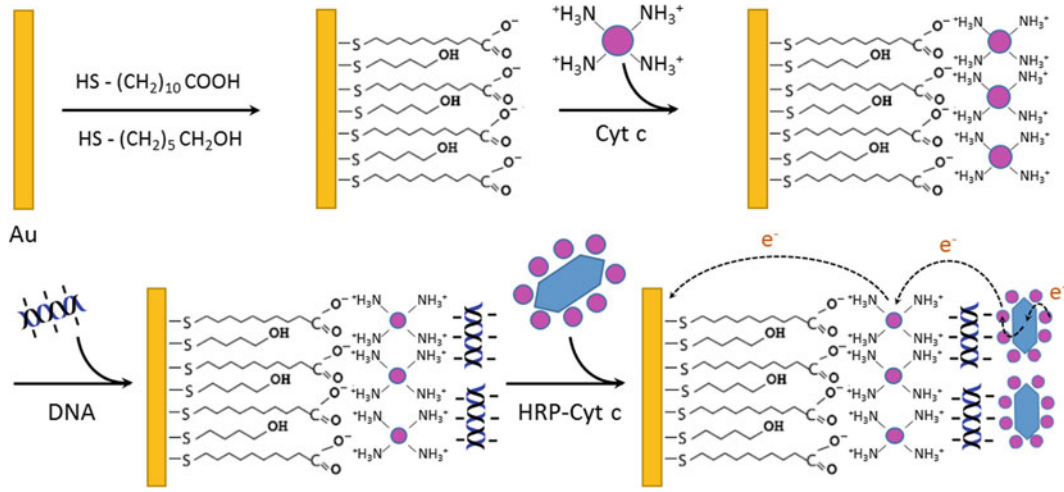

Fig. 17.15 Surface functionalization of the biosensor composed of DNA and HRP-Cyt c

with nucleic acids. Recently, a novel parallel dsDNA and recombinant azurin hybrid was developed to have higher conductance that of the canonical DNA and they conjugated it with recombinant Azurin protein (denoted as PSD/rAzu) for the general detection of various viral DNAs and miRNAs (Mohammadniaei et al. 2017). As depicted in Fig. 17.17, the immobilized rAzu onto the gold electrode provided Cu^{+}/Cu^{2+} redox reaction and a stable anchoring site to remove the requirements of additional chemical linkers and rolled as a selective-arrayed molecule due its appropriate cross-sectional diameter (~5 nm) and capability to receive only one DNA strand at its N-terminus. The EC and scanning tunneling spectroscopy (STS) measurement

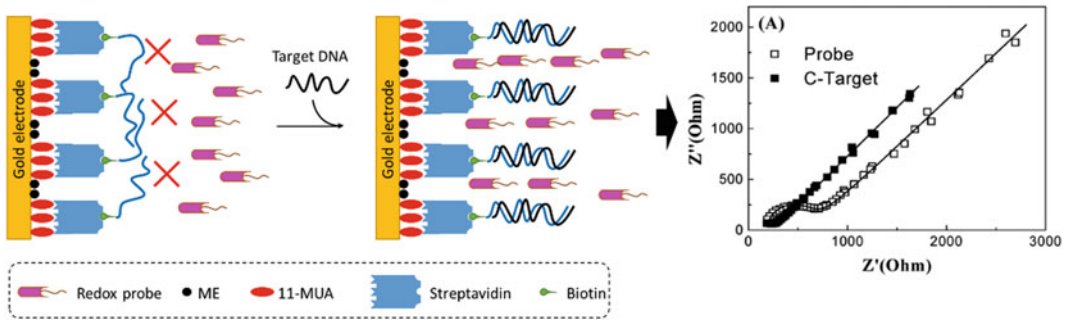

Fig. 17.16 Surface functionalization of the biosensor and further EIS measurement. (Figure reproduced with permission from Pan and Rothberg 2005)

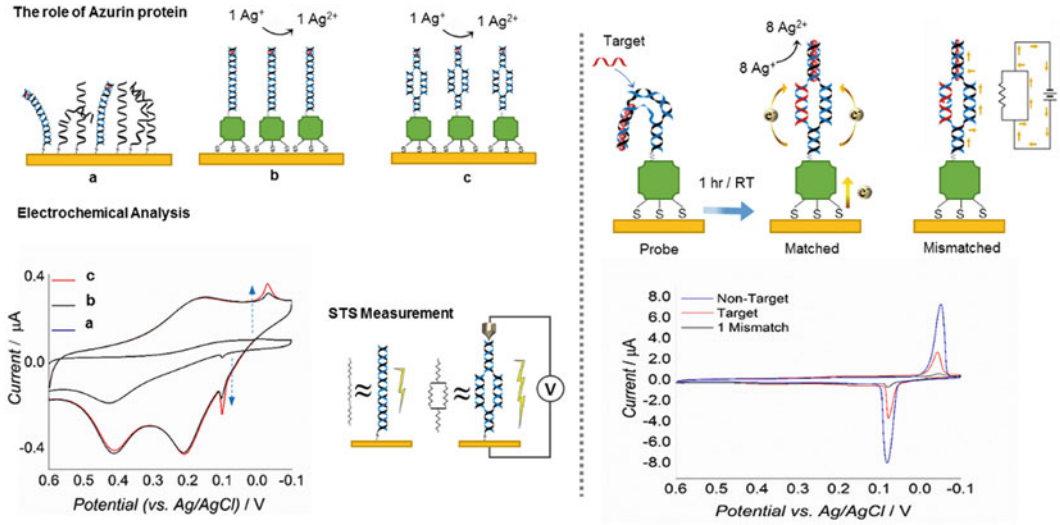

Fig. 17.17 Schematic illustration of PSD/rAzu biosensor

confirmed higher electron conductivity of the PSD (resembling a parallel electrical circuit,) compared to the dsDNA. Silver ion bond between C-C mismatched base pairs on the top of each helix, functioned as the redox signal reporter for EC conductance measurement and sensing application. The single mismatch detection strategy was inspired by the short-circuit law in classical physics which illustrates that, in a parallel electrical circuit possessing two current flow paths, current migrates through the path with no electrical impedance. Therefore, the single mismatched duplex could be considered as the path with higher impedance, resulting a lower electrochemical signal. The developed biosensor could detect miR-155, miR-21, miR-141, miR-143 as well as genomic MERS-CoV and HIV-1.

17.5 DNA-Based Electrochemical Biosensor

DNA-based electrochemical biosensors have been mostly used as the hybridization assays for the genetic analysis, due to the ability of the single stranded DNA (ssDNA), as the sensor probe, to seek out and hybridize with the target gene (Paleček and Jelen 2002; Wang 2002; Zhai et al. 1797). However, DNA has been also incorporated with different organic/inorganic

platforms to form various biosensors (Chowdhury et al. 2014; Gao et al. 2016; Liu et al. 2015a). In this section, we are going to review some examples of DNA-based ECBs towards H_2O_2 detection and oligonucleotide detection.

Conventionally, the nucleic acids possess weak enzymatic properties due to the lack of prosthetic groups, in order to exploit them for the H_2O_2 detection (catalytic reaction) the necessity for the incorporation of this biomolecule with metal ions is demanding.

17.5.1 DNA-Based Electrochemical Biosensor for H_2O_2 Detection

In 2006, researchers developed a dimension-controlled silver–DNA hybrid nanoparticles which was electrodeposited on a glassy carbon electrode based on the reduction of silver with the help of DNA (Wu et al. 2006). The DNA rolled to avoid aggregation of silver nanoparticles and enhanced the catalytic capability of the nanocomplex to further detect H_2O_2 at the low concentration of 0.6 μM and linear detection range of 2.0 μm–2.5 mm.

Another amperometric H_2O_2 biosensor was reported by Yasushi group, composed of DNA-Cu(II) and chitosan polyion (Gu et al. 2009). DNA/chitosan polyion complex membrane was employed as a precursor for entrapment of electrocatalytic copper ions, which could specifically bound to double stranded DNA (dsDNA) and further reduce the H_2O_2 on the glassy carbon electrode (GCE). The sensor exhibited good sensitivity and selectivity towards ascorbic acid with the linear range from 10 μm to 10 mm and the detection limit of 3 μm.

DNA in the form of G-quadruplex DNAzyme has been also integrated with hemin to electrochemically detect H_2O_2 in a very low concentration of 0.16 μm (Wu et al. 2015). Deoxyribozymes (DNAzymes), are ssDNAs with particular catalytic features. G-quadruplex DNA is a self-assembled G-rich DNA sequence, whereas the hemin/G-quadruplex is formed by coordination of hemin inside the G-quadruplex DNA (Li et al. 2016). Owing to the Fe ion of the hemin group, the hemin/G-quadruplex can effectively catalyze H_2O_2. As depicted in Fig. 17.18, the G-quadruplex was firstly self-assembled onto the gold particles modified heated copper disk electrode (Au-HCuDE), then the electrode was back-field with 6-mercapto-1-hexanol (MCH) in order to remove physical bindings of thiol-modified ssDNA to the surface. After that, the hemin was introduced to the structure to form the hemin/G-quadruplex. Enhancement of the electrode temperature to 50 °C, resulted in the amplification of the electrocatalytic activity in the developed biosensor.

Recently, a highly sensitive H_2O_2 ECB with the ability of H_2O_2 detection in the sterilize milk has been reported based on a novel "on-off-on" switch system. The electrode consisted of methylene blue (MB) as the charge mediator, gold nanoparticle as the electrochemical signal enhancer and iridium (III)/G-quadroplex to provide a hydrophobic layer (switch off). After the introduction of H_2O_2, iridium (III)/G-quadroplex was cleaved into DNA fragments. Releasing the DNA fragments from the electrode surface led to the signal recovering (switch on), which enabled H_2O_2 detection.

17.5.2 DNA-Based Electrochemical Biosensor for Oligonucleotide Detection

It has been proved that, nucleic acid (DNA/RNA) detection and analysis is highly essential not only for obtaining genetic information but also for the sake of diagnosis, identification and classification of various diseases and genetic disorders (Abi et al. 2018; Zhai et al. 1797). Nucleic acid ECBs are usually based on the hybridization method. It involves monitoring the electrochemical signal response, resulting from the Watson–Crick base-pairing of the genomic DNA/RNA target with the sensor probe (Jolly et al. 2016).

In 1994, Millan et al. reported an electrochemical DNA sequence-selective biosensor which was a stepping stone for the development of various nucleic acid ECBs (Millan et al. 1794).

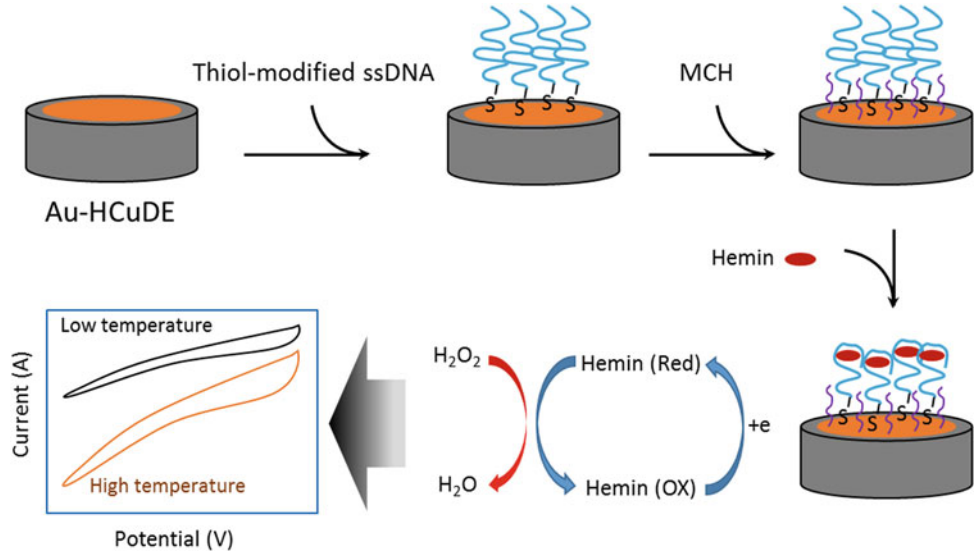

Fig. 17.18 Schematic construction and performance of the biosensing platform for electrocatalytic reduction of H_2O_2 at the elevated electrode temperature

Generally, in the nucleic acid ECBs, sensor probe (recognition platform) consists of ssDNA or ssRNA covalently self-assembled onto the electrode surface, which should be conductive, biocompatible and have a low over potential (Odenthal and Gooding 2007). The probe sensor is then immersed into the solution containing target ssDNA/ssRNA, which is complementary to the probe strand, to form a double stranded nucleic acid helix. Depending on the experimental design and whether the sensor is "signal-off" or "signal-on", the hybridization process results in a notable change in the transduced electrochemical signal and further detection by the signal processor (Liu et al. 2012a). There have been usually two main techniques for the development of electrochemical nucleic acid biosensors: labeled and label-free approaches. In the labeled method, enzyme labels or redox labels are employed to bind to the nucleic acids. This binding can be specific, covalent or electrostatic. Whereas, the label-free approach is commonly based on the difference in the electrical properties of the single stranded and double stranded structures. Schematic diagram in Fig. 17.19 demonstrates the two mentioned approaches.

Several challenges have remained to develop nucleic acid ECBs such as surface immobilization control, single mismatch detection and fast response. Fabrication of a highly reproducible and credible nucleic acid ECB to discover genetic disorders caused by base pair mutation is highly demanding for early-stage diagnosis of different types of cancers and diseases (Baker 2006; Drummond et al. 2003). An acceptable nucleic acid ECB should compete against the standard sensing methods such as quantitative real-time polymerase chain reaction (qRT-PCR) (Maddocks and Jenkins 2017), northern blotting (NB) (Schwarzkopf and Pierce 2016) and microarray (Dastjerdi et al. 2014). However, microarray technique is prone to high cost which makes it less approachable to every user. Also the NB method is restricted due to the requirements for radiolabeling leading to cross contamination and low efficiency. The major limitation of qRT-PCR, regardless to its high cost, would be the detection of short strand nucleic acids such as microRNAs, due to their low melting temperature following by the complicated primer design to causes contamination experimental errors (Lee et al. 2014a; Wu and Qu 2015).

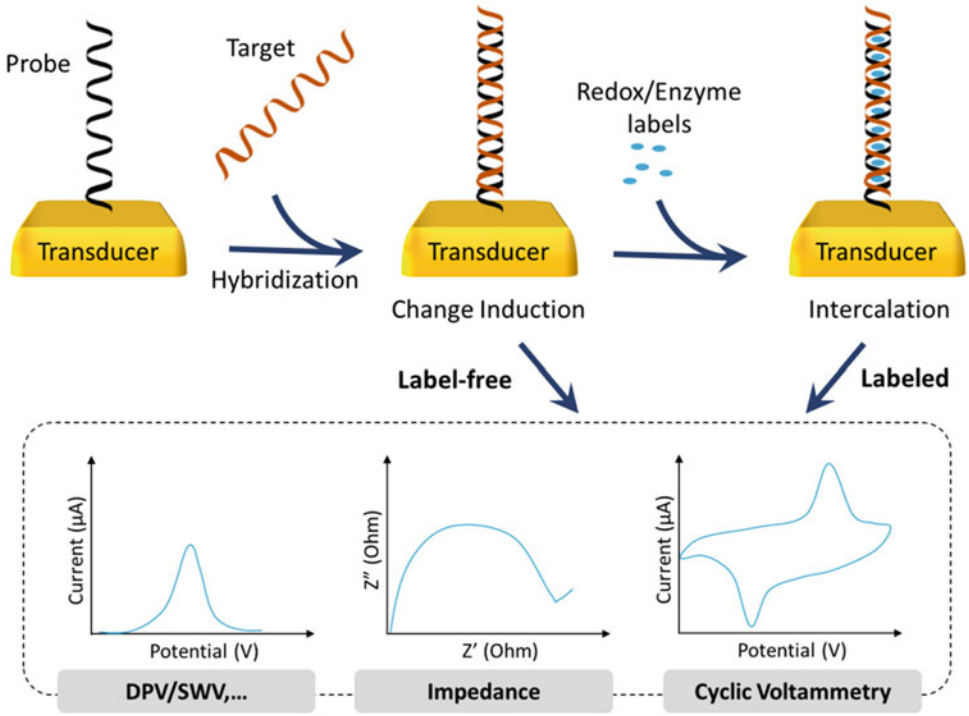

Fig. 17.19 General diagram for the labeled and label-free electrochemical nucleic acid biosensor; DPV and SWV stand for differential phase voltammetry and square wave voltammetry, respectively

In 2005, Masahiko group reported a great capability of DNA ECBs for the detection of single mutation inside the dsDNA (Inouye et al. 2005). The idea was simply based on the defining the dsDNA as an electrical wire whose one end was attached onto the gold electrode and the other end was modified with Ferrocene as the EC redox reporter (Fig. 17.20). The duplex with mismatch base pair resulted in the rupture in π- π orbital loss in the dsDNA to interrupt the charge transfer from the electrode surface to Ferrocene through the double strand helix leading to a significant electrochemical signal drop (SWV technique).

One of the famous methods for sensitive electrochemical detection of nucleic acids is hybridization chain reaction (HCR) (Trifonov et al. 2016). This biosensor was consisted of a gold electrode, fictionalized by thiol-modified ssDNA (1) which is partially complementary to the target oligonucleotide (2). Hybridization of the analyte (2), with the probe leads to the formation of a dsDNA containing a toehold sequence. In the presence of the two hairpins of HA (3) and HB (4), the HCR triggers. The HCR mechanism is as follows: The toehold sequence of stand (2) opens the hairpin (3), exposing a new single-stranded toehold (W) which opens hairpin (4). The results in another free toehold (X) to open the hairpin (3) and the process keeps going until the hairpins supply is exhausted. The electrochemical detection method was EIS that is based on the semicircular diameter of the Nyquist plot from which the higher frequencies explains the higher charge transfer resistance (R_{et}) corresponding to the more negative charge of the electrodes resulting from the layer-by-layer assembly of the electrode surface with oligonucleotides. The HEPES buffer (10 mM, pH = 7.2) was used which contained $Fe(CN)_6^{3-/4-}$ as the negatively charged redox probe to indicate the electrode surface modification based on its repulsion from the surface, associated with the sequential addition of oligonucleotides (negative charge) to the surface. For a fixed incubation

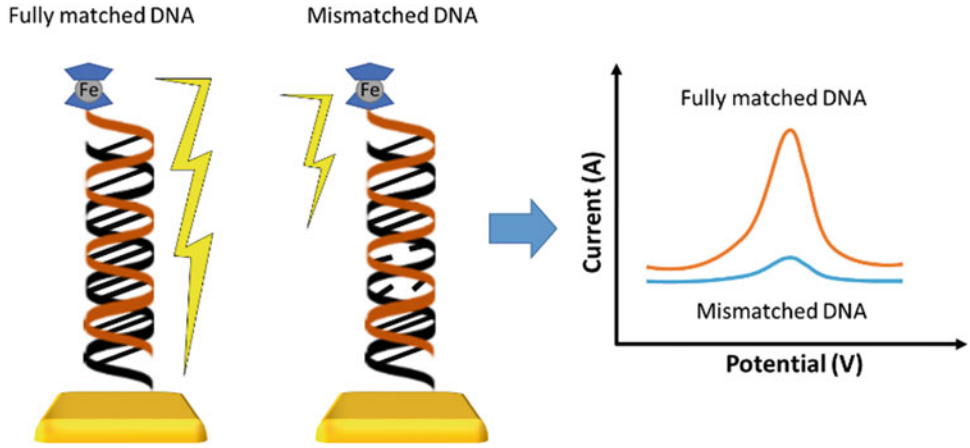

Fig. 17.20 Mechanism of the electrochemical detection of mismatched DNA

time of 45 min, different concentration of the analyte (2) was added to the biosensor to achieve the dynamic detection range. This method offered a detection limit of 1.2 nm of the analyte.

More recently, a simply-designed single-step miRNA biosensor was fabricated using the combination of EC and surface enhanced Raman spectroscopy techniques (SERS) (Fig. 17.21). With the strength of EC method, they removed the weakness of SERS technique for the single-mismatch detection. Also, in a back-to-back supporting situation, the combining method gave rise to the extension dynamic detection range of the biosensor from 10 pM to 450 nM (SERS: 10 pm ~ 5 nm and EC: 5 nm ~ 450 nm) (Mohammadniaei et al. 2018). In this report, a single stranded 3′ methylene blue (MB) and 5′ thiol-modified RNA (MB-ssRNA-SH) was immobilized onto the spectroelectrochemical-active gold nanoparticle-modified ITO (ITO/GNP) to detect the target miR-155. As a signal-off biosensor, upon the addition of target strand, the dsRNA transformed to an upright position resulting in a considerable decrease in SERS and EC signals of the MB.

In this section we tried to give the reader some insights into the different techniques for the detection of oligonucleotides based on nucleic acid-ECBs, although, there have been reported many outstanding DNA-based ECBs such as dichalcogenides based electrochemical biosensors (Wang et al. 2017), rolling cycle amplification-based methods (RCA) (Cheng et al. 2009), isothermal amplification, (Zhang and Zhang 2012) aloe-like gold micro/nanostructures (Shi et al. 2013), three-mode system (Labib et al. 2013), (details of previous reports are provided in Table 17.2).

17.6 Future Prospective

In spite of initial achievement, the investigation of bioelectronic devices and biosensors are still required. The discussed results are intriguing for the electrochemical bioelectronics devices including biomemory device, biologic gate, bioinformation, biosensors and processor for future biocomputer systems. The biomolecule can easily be tailored and modified with other biomolecule or nanoparticles to embody the specific functionality. Not only the biomolecule can combine the original property with various nanoparticles and other biomolecules to the development of various bioelectronics computation platforms, but also the proto-type biocomputer can operate in living organism with hybrid molecule-neural cell connection. Moreover, unlike that of the silicon-based device, the future biomolecular-based computer could easily be integrated with the input module and energy module that give the new concept of output

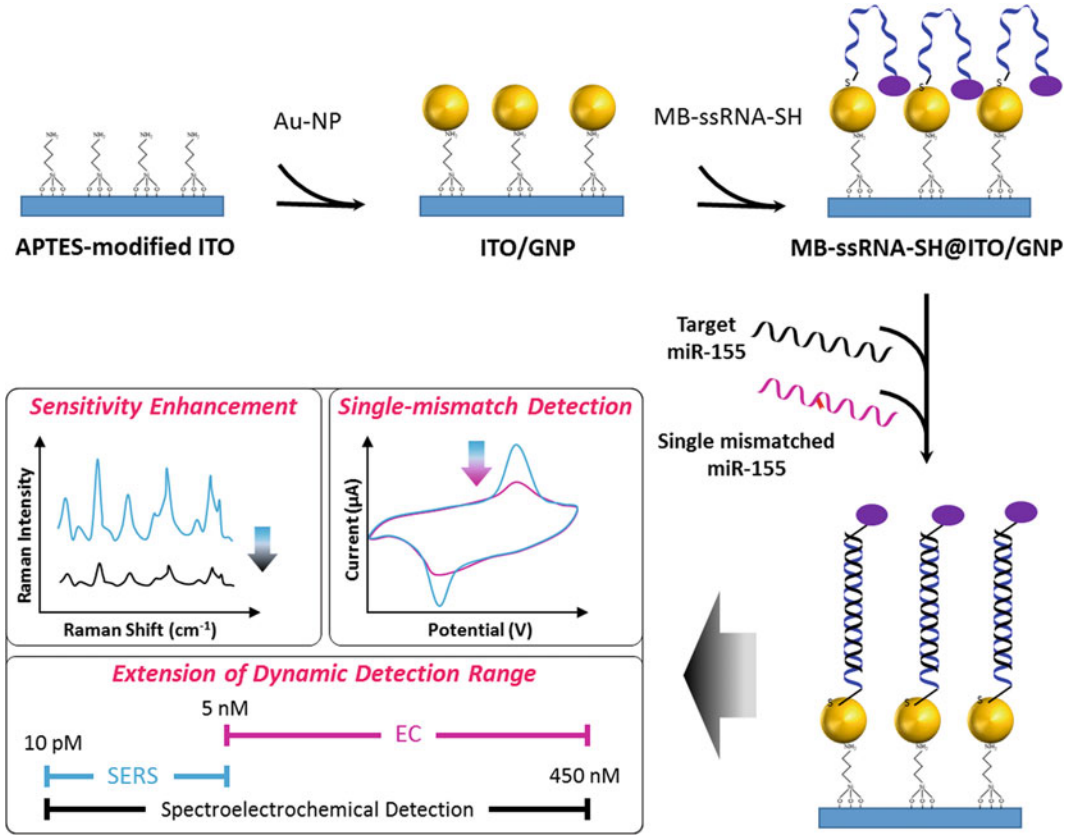

Fig. 17.21 Schematic diagram of the surface modification and microRNA detection of the MB-dsDNA-SH@ITO/GNP biosensor

Table 17.2 Oligonucleotide detection using nucleic acid-based ECBs

Detection method	Detection steps	LOD	Labeling	Detection time	References
Cleavage-based signal amplification	10	69.2 aM	G-quadruplex hemin	> 2 h	Zhao et al. (2013)
Amperometric magnetobiosensor	4	0.4 fM	Biotin–strep-HRP	~ 3 h	Campuzano et al. (2014)
Three-mode electrochemical sensor	2	5 aM	None	~ 2 h	Labib et al. (2013)
Carbon nanotube-bridged field-effect transistor assisted by p19	2	1 aM	None	~ 2 h	Ramnani et al. (2013)
Tandem polymerization and cleavage-mediated cascade system	7	5 fM	None	~ 4 h	Liu et al. (2016)
DNA tetrahedral scaffold	4	10 aM	Biotinylated probe-avidin-HRP, poly-HRP80	~ 8 h	wen et al. (2012)
Oxidized carbon nano tubes and nanodiamonds	2	1.95 fM	DNAzyme based hybrid structure	~ 2 h	Liu et al. (2015b)

combination for the disease diagnostics and cancer cell identifications. That kind of characteristic is quite intriguing and potentially useful as a new concept of computing for bioelectronic medicine devices. On the edge of bioelectronics, biomolecule-based electronic devices can be envisaged as a powerful alternative, once appropriate fabrication technique and integrating circuit are achieved, then, the nano-scale system can be achieved with a biomolecule-nanoparticle hybrid.

Acknowledgements This research was supported by NRF-2018R1D1A1B07049407 and by the Research Grant of Kwangwoon University in 2018.

References

Abi A, Mohammadpour Z, Zuo X, Safavi A (2018) Nucleic acid-based electrochemical nanobiosensors. Biosens Bioelectron 102:479–489. https://doi.org/10.1016/j.bios.2017.11.019

Adleman L (1994) Molecular computation of solutions to combinatorial problems. Science 266:1021–1024. https://doi.org/10.1126/science.7973651

Andre C, Kim SW, Yu X-H, Shanklin J (2013) Fusing catalase to an alkane-producing enzyme maintains enzymatic activity by converting the inhibitory byproduct H_2O_2 to the cosubstrate O_2. Proc Natl Acad Sci 110:3191–3196. https://doi.org/10.1073/pnas.1218769110

Artés JM, Díez-Pérez I, Gorostiza P (2012) Transistor-like behavior of single Metalloprotein junctions. Nano Lett 12:2679–2684. https://doi.org/10.1021/nl2028969

Arugula MA, Shroff N, Katz E, He Z (2012) Molecular AND logic gate based on bacterial anaerobic respiration. Chem Commun 48:10174–10176. https://doi.org/10.1039/C2CC35595G

Ausländer S, Ausländer D, Müller M, Wieland M, Fussenegger M (2012) Programmable single-cell mammalian biocomputers. Nature 487:123. https://doi.org/10.1038/nature11149

Baker M (2006) New-wave diagnostics. Nat Biotechnol 24:931–938

Baron R, Lioubashevski O, Katz E, Niazov T, Willner I (2006a) Elementary arithmetic operations by enzymes: a model for metabolic pathway based computing. Angew Chem Int Ed 45:1572–1576. https://doi.org/10.1002/anie.200503314

Baron R, Lioubashevski O, Katz E, Niazov T, Willner I (2006b) Logic gates and elementary computing by enzymes. Chem A Eur J 110:8548–8553. https://doi.org/10.1021/jp0568327

Benenson Y (2009) RNA-based computation in live cells. Curr Opin Biotechnol 20:471–478. https://doi.org/10.1016/j.copbio.2009.08.002

Benenson Y, Gil B, Ben-Dor U, Adar R, Shapiro E (2004) An autonomous molecular computer for logical control of gene expression. Nature 429:423. https://doi.org/10.1038/nature02551

Bonnet J, Subsoontorn P, Endy D (2012) Rewritable digital data storage in live cells via engineered control of recombination directionality. Proc Natl Acad Sci 109:8884–8889. https://doi.org/10.1073/pnas.1202344109

Bonnet J, Yin P, Ortiz ME, Subsoontorn P, Endy D (2013) Amplifying genetic logic gates. Science 340:599–603. https://doi.org/10.1126/science.1232758

Bychkova V, Shvarev A, Zhou J, Pita M, Katz E (2010) Enzyme logic gate associated with a single responsive microparticle: scaling biocomputing to microsize systems. Chem Commun 46:94–96. https://doi.org/10.1039/B917611J

Campolongo MJ, Kahn JS, Cheng W, Yang D, Gupton-Campolongo T, Luo D (2011) Adaptive DNA-based materials for switching, sensing, and logic devices. J Mater Chem 21:6113–6121. https://doi.org/10.1039/C0JM03854G

Campuzano S, Torrente-Rodríguez RM, López-Hernández E, Conzuelo F, Granados R, Sánchez-Puelles JM, Pingarrón JM (2014) Magnetobiosensors based on viral protein p19 for MicroRNA determination in cancer cells and tissues. Angew Chem Int Ed 53:6168–6171. https://doi.org/10.1002/anie.201403270

Chen Y-P, Liu B, Lian H-T, Sun X-Y (2011) Preparation and application of urea electrochemical sensor based on chitosan molecularly imprinted films. Electroanalysis 23:1454–1461. https://doi.org/10.1002/elan.201000693

Chen Y-S, Hong M-Y, Huang GS (2012) A protein transistor made of an antibody molecule and two gold nanoparticles. Nat Nanotechnol 7:197. https://doi.org/10.1038/nnano.2012.7

Cheng Y, Zhang X, Li Z, Jiao X, Wang Y, Zhang Y (2009) Highly sensitive determination of microRNA using target-primed and branched rolling-circle amplification. Angew Chem Int Ed 48:3268–3272. https://doi.org/10.1002/anie.200805665

Cho W-J, Huang H-J (1998) An Amperometric urea biosensor based on a polyaniline−Perfluorosulfonated ionomer composite electrode. Anal Chem 70:3946–3951. https://doi.org/10.1021/ac980004a

Choi J-W, Oh B-K, Kim YJ, Min J (2007) Protein-based biomemory device consisting of the cysteine-modified azurin. Appl Phys Lett 91:263902. https://doi.org/10.1063/1.2828046

Chowdhury AD, Gangopadhyay R, De A (2014) Highly sensitive electrochemical biosensor for glucose, DNA and protein using gold-polyaniline nanocomposites as a common matrix. Sensors Actuators B Chem 190:348–356. https://doi.org/10.1016/j.snb.2013.08.071

Christof MN, Chad AM (2004) Nanobiotechnology: concepts, applications and perspectives. Wiley-VCH, Weinheim, p 491

Chung Y-H, Lee T, Min J, Choi J-W (2011) Investigation of the redox property of a metalloprotein layer self-

assembled on various chemical linkers. Colloids Surf B Biointerfaces 87:36–41. https://doi.org/10.1016/j.colsurfb.2011.04.034

Dai Z, Xiao Y, Yu X, Mai Z, Zhao X, Zou X (2009) Direct electrochemistry of myoglobin based on ionic liquid–clay composite films. Biosens Bioelectron 24:1629–1634. https://doi.org/10.1016/j.bios.2008.08.032

Dastjerdi A, Fooks AR, Johnson N (2014) Chapter nineteen – oligonucleotide microarray: applications for lyssavirus speciation. Current laboratory techniques in rabies diagnosis, research and prevention. Academic Press, Amsterdam, pp 193–203

de Ruiter G, van der Boom ME (2011) Surface-confined assemblies and polymers for molecular logic. Acc Chem Res 44:563–573. https://doi.org/10.1021/ar200002v

de Silva AP, Uchiyama S (2007) Molecular logic and computing. Nat Nanotechnol 2:399. https://doi.org/10.1038/nnano.2007.188

Deng H, Shen W, Ren Y, Gao Z (2014) A highly sensitive microRNA biosensor based on hybridized microRNA-guided deposition of polyaniline. Biosens Bioelectron 60:195–200. https://doi.org/10.1016/j.bios.2014.04.023

Deonarine AS, Clark SM, Konermann L (2003) Implementation of a multifunctional logic gate based on folding/unfolding transitions of a protein. Futur Gener Comput Syst 19:87–97. https://doi.org/10.1016/S0167-739X(02)00110-3

Dolatabadi JEN, Mashinchian O, Ayoubi B, Jamali AA, Mobed A, Losic D, Omidi Y, de la Guardia M (2011) Optical and electrochemical DNA nanobiosensors. TrAC Trends Anal Chem 30:459–472. https://doi.org/10.1016/j.trac.2010.11.010

Drummond TG, Hill MG, Barton JK (2003) Electrochemical DNA sensors. Nat Biotechnol 21:1192–1199

Dundas CM, Demonte D, Park S (2013) Streptavidin–biotin technology: improvements and innovations in chemical and biological applications. Appl Microbiol Biotechnol 97:9343–9353. https://doi.org/10.1007/s00253-013-5232-z

Elbaz J, Moshe M, Willner I (2009a) Coherent activation of DNA tweezers: a "SET–RESET" logic system. Angew Chem Int Ed 48:3834–3837. https://doi.org/10.1002/anie.200805819

Elbaz J, Wang Z-G, Orbach R, Willner I (2009b) pH-stimulated concurrent mechanical activation of two DNA "tweezers". A "SET−RESET" logic gate system. Nano Lett 9:4510–4514. https://doi.org/10.1021/nl902859m

Elbaz J, Wang F, Remacle F, Willner I (2012) pH-programmable DNA logic arrays powered by modular DNAzyme libraries. Nano Lett 12:6049–6054. https://doi.org/10.1021/nl300051g

Farzadfard F, Lu TK (2014) Genomically encoded analog memory with precise in vivo DNA writing in living cell populations. Science 346:1256272. https://doi.org/10.1126/science.1256272

Freeman R, Finder T, Willner I (2009) Multiplexed analysis of Hg^{2+} and Ag^{+} ions by nucleic acid functionalized CdSe/ZnS quantum dots and their use for logic gate operations. Angew Chem Int Ed 48:7818–7821. https://doi.org/10.1002/anie.200902395

Frezza BM, Cockroft SL, Ghadiri MR (2007) Modular multi-level circuits from immobilized DNA-based logic gates. J Am Chem Soc 129:14875–14879. https://doi.org/10.1021/ja0710149

Fujibayashi K, Hariadi R, Park SH, Winfree E, Murata S (2008) Toward reliable algorithmic self-assembly of DNA tiles: a fixed-width cellular automaton pattern. Nano Lett 8:1791–1797. https://doi.org/10.1021/nl0722830

Gao W, Wei X, Wang X, Cui G, Liu Z, Tang B (2016) A competitive coordination-based CeO2 nanowire-DNA nanosensor: fast and selective detection of hydrogen peroxide in living cells and in vivo. Chem Commun 52:3643–3646. https://doi.org/10.1039/C6CC00112B

Gdor E, Katz E, Mandler D (2013) Biomolecular AND logic gate based on immobilized enzymes with precise spatial separation controlled by scanning electrochemical microscopy. J Phys Chem B 117:16058–16065. https://doi.org/10.1021/jp4095672

Gianneschi NC, Ghadiri MR (2007) Design of Molecular Logic Devices Based on a programmable DNA-regulated semisynthetic enzyme. Angew Chem Int Ed 46:3955–3958. https://doi.org/10.1002/anie.200700047

Giorgio M, Trinei M, Migliaccio E, Pelicci PG (2007) Hydrogen peroxide: a metabolic by-product or a common mediator of ageing signals? Nat Rev Mol Cell Biol 8:722. https://doi.org/10.1038/nrm2240

González M n, Argaraña CE, Fidelio GD (1999) Extremely high thermal stability of streptavidin and avidin upon biotin binding. Biomol Eng 16:67–72. https://doi.org/10.1016/S1050-3862(99)00041-8

Gorton L, Lindgren A, Larsson T, Munteanu FD, Ruzgas T, Gazaryan I (1999) Direct electron transfer between heme-containing enzymes and electrodes as basis for third generation biosensors. Anal Chim Acta 400:91–108. https://doi.org/10.1016/S0003-2670(99)00610-8

Grabow WW, Jaeger L (2014) RNA self-assembly and RNA nanotechnology. Acc Chem Res 47:1871–1880. https://doi.org/10.1021/ar500076k

Grieshaber D, MacKenzie R, Vörös J, Reimhult E (2008) Electrochemical biosensors - sensor principles and architectures. Sensors 8:1400

Gromiha MM, Nagarajan R (2013) Chapter three - computational approaches for predicting the binding sites and understanding the recognition mechanism of protein–DNA complexes. In: Donev R (ed) Advances in Protein Chemistry Structural Biology. Academic Press, New York, pp 65–99

Gu T, Liu Y, Zhang J, Hasebe Y (2009) Amperometric hydrogen peroxide biosensor based on immobilization of DNA-Cu(II) in DNA/chitosan polyion complex

membrane. J Environ Sci 21:S56–S59. https://doi.org/10.1016/S1001-0742(09)60037-1

Haque F, Shu D, Shu Y, Shlyakhtenko LS, Rychahou PG, Mark Evers B, Guo P (2012) Ultrastable synergistic tetravalent RNA nanoparticles for targeting to cancers. Nano Today 7:245–257. https://doi.org/10.1016/j.nantod.2012.06.010

He H-Z, Chan DS-H, Leung C-H, Ma D-L (2013) G-quadruplexes for luminescent sensing and logic gates. Nucleic Acids Res 41:4345–4359. https://doi.org/10.1093/nar/gkt108

Hild W, Pollinger K, Caporale A, Cabrele C, Keller M, Pluym N, Buschauer A, Rachel R, Tessmar J, Breunig M, Goepferich A (2010) G protein-coupled receptors function as logic gates for nanoparticle binding and cell uptake. Proc Natl Acad Sci 107:10667–10672. https://doi.org/10.1073/pnas.0912782107

Huang Y, Duan X, Cui Y, Lauhon LJ, Kim K-H, Lieber CM (2001) Logic gates and computation from assembled nanowire building blocks. Science 294:1313–1317. https://doi.org/10.1126/science.1066192

Hunt HK, Armani AM (2010) Label-free biological and chemical sensors. Nanoscale 2:1544–1559. https://doi.org/10.1039/C0NR00201A

Ikeda M, Tanida T, Yoshii T, Kurotani K, Onogi S, Urayama K, Hamachi I (2014) Installing logic-gate responses to a variety of biological substances in supramolecular hydrogel–enzyme hybrids. Nat Chem 6:511. https://doi.org/10.1038/nchem.1937

Inouye M, Ikeda R, Takase M, Tsuri T, Chiba J (2005) Single-nucleotide polymorphism detection with "wire-like" DNA probes that display quasi "on–off" digital action. Proc Natl Acad Sci USA 102:11606–11610. https://doi.org/10.1073/pnas.0502078102

Itamar W, Eugenii K (2005) Bioelectronics: from theory to applications. Wiley-VCH, Weinheim

Jaeger L, Chworos A (2006) The architectonics of programmable RNA and DNA nanostructures. Curr Opin Struct Biol 16:531–543. https://doi.org/10.1016/j.sbi.2006.07.001

Jensen PS, Chi Q, Zhang J, Ulstrup J (2009) Long-range interfacial electrochemical Electron transfer of Pseudomonas aeruginosa Azurin−gold nanoparticle hybrid systems. J Phys Chem C 113:13993–14000. https://doi.org/10.1021/jp902611x

Jia N, Lian Q, Wang Z, Shen H (2009) A hydrogen peroxide biosensor based on direct electrochemistry of hemoglobin incorporated in PEO–PPO–PEO triblock copolymer film. Sensors Actuators B Chem 137:230–234. https://doi.org/10.1016/j.snb.2008.10.011

Jolly P, Estrela P, Ladomery M (2016) Oligonucleotide-based systems: DNA, microRNAs, DNA/RNA aptamers. Essays Biochem 60:27–35. https://doi.org/10.1042/ebc20150004

Kafi AKM, Fan Y, Shin H-K, Kwon Y-S (2006) Hydrogen peroxide biosensor based on DNA–Hb modified gold electrode. Thin Solid Films 499:420–424. https://doi.org/10.1016/j.tsf.2005.06.073

Katz E (2015) Biocomputing – tools, aims, perspectives. Curr Opin Biotechnol 34:202–208. https://doi.org/10.1016/j.copbio.2015.02.011

Katz E, Privman V (2010) Enzyme-based logic systems for information processing. Chem Soc Rev 39:1835–1857. https://doi.org/10.1039/B806038J

Keren K, Berman RS, Buchstab E, Sivan U, Braun E (2003) DNA-templated carbon nanotube field-effect transistor. Science 302:1380–1382. https://doi.org/10.1126/science.1091022

Kimmel DW, LeBlanc G, Meschievitz ME, Cliffel DE (2012) Electrochemical sensors and biosensors. Anal Chem 84:685–707. https://doi.org/10.1021/ac202878q

Ko Y, Kim Y, Baek H, Cho J (2011) Electrically Bistable properties of layer-by-layer assembled multilayers based on protein nanoparticles. ACS Nano 5:9918–9926. https://doi.org/10.1021/nn2036939

Komathi S, Gopalan AI, Kim S-K, Anand GS, Lee K-P (2013) Fabrication of horseradish peroxidase immobilized poly(N-[3-(trimethoxy silyl)propyl]aniline) gold nanorods film modified electrode and electrochemical hydrogen peroxide sensing. Electrochim Acta 92:71–78. https://doi.org/10.1016/j.electacta.2013.01.032

Labib M, Khan N, Ghobadloo SM, Cheng J, Pezacki JP, Berezovski MV (2013) Three-mode electrochemical sensing of ultralow MicroRNA levels. J Am Chem Soc 135:3027–3038. https://doi.org/10.1021/ja308216z

Lee SW, Chang W-J, Bashir R, Koo Y-M (2007) "Bottom-up" approach for implementing nano/microstructure using biological and chemical interactions. Biotechnol Bioprocess Eng 12:185. https://doi.org/10.1007/bf02931092

Lee T, Kim SU, Min J, Choi JW (2010) Multilevel biomemory device consisting of recombinant Azurin/cytochrome c. Adv Mater 22:510–514. https://doi.org/10.1002/adma.200902288

Lee T, Min J, Kim S-U, Choi J-W (2011a) Multifunctional 4-bit biomemory chip consisting of recombinant azurin variants. Biomaterials 32:3815–3821. https://doi.org/10.1016/j.biomaterials.2011.01.072

Lee T, Yoo SY, Chung YH, Min J, Choi JW (2011b) Signal enhancement of electrochemical biomemory device composed of recombinant Azurin/gold nanoparticle. Electroanalysis 23:2023–2029. https://doi.org/10.1002/elan.201100182

Lee HJ, Oh JH, Oh JM, Park JM, Lee JG, Kim MS, Kim YJ, Kang HJ, Jeong J, Kim SI, Lee SS, Choi JW, Huh N (2013) Efficient isolation and accurate in situ analysis of circulating tumor cells using detachable beads and a high-pore-density filter. Angew Chem Int Ed 52:8337–8340. https://doi.org/10.1002/anie.201302278

Lee H, Park J-E, Nam J-M (2014a) Bio-barcode gel assay for microRNA. Nat Commun 5(5):3367. https://doi.org/10.1038/ncomms4367

Lee T, Yagati AK, Min J, Choi JW (2014b) Bioprocessing device composed of protein/DNA/inorganic material hybrid. Adv Funct Mater 24:1781–1789. https://doi.org/10.1002/adfm.201302397

Lee T, Chung Y-H, Yoon J, Min J, Choi J-W (2014c) Fusion protein-based biofilm fabrication composed of recombinant azurin–myoglobin for dual-level biomemory application. Appl Surf Sci 320:448–454. https://doi.org/10.1016/j.apsusc.2014.09.020

Lee T, Yagati AK, Pi F, Sharma A, Choi J-W, Guo P (2015) Construction of RNA–quantum dot chimera for nanoscale resistive biomemory application. ACS Nano 9:6675–6682. https://doi.org/10.1021/acsnano.5b03269

Li H, Liu S, Dai Z, Bao J, Yang X (2009) Applications of nanomaterials in electrochemical enzyme biosensors. Sensors 9:8547

Li X, Sun L, Ding T (2011) Multiplexed sensing of mercury(II) and silver(I) ions: a new class of DNA electrochemiluminescent-molecular logic gates. Biosens Bioelectron 26:3570–3576. https://doi.org/10.1016/j.bios.2011.02.003

Li W, Li Y, Liu Z, Lin B, Yi H, Xu F, Nie Z, Yao S (2016) Insight into G-quadruplex-hemin DNAzyme/RNAzyme: adjacent adenine as the intramolecular species for remarkable enhancement of enzymatic activity. Nucleic Acids Res 44:7373–7384. https://doi.org/10.1093/nar/gkw634

Liu Q, Wang L, Frutos AG, Condon AE, Corn RM, Smith LM (2000) DNA computing on surfaces. Nature 403:175. https://doi.org/10.1038/35003155

Liu G, Wan Y, Gau V, Zhang J, Wang L, Song S, Fan C (2008) An enzyme-based E-DNA sensor for sequence-specific detection of Femtomolar DNA targets. J Am Chem Soc 130:6820–6825. https://doi.org/10.1021/ja800554t

Liu A, Wang K, Weng S, Lei Y, Lin L, Chen W, Lin X, Chen Y (2012a) Development of electrochemical DNA biosensors. TrAC Trends Anal Chem 37:101–111. https://doi.org/10.1016/j.trac.2012.03.008

Liu X, Aizen R, Freeman R, Yehezkeli O, Willner I (2012b) Multiplexed Aptasensors and amplified DNA sensors using functionalized graphene oxide: application for logic gate operations. ACS Nano 6:3553–3563. https://doi.org/10.1021/nn300598q

Liu B, Sun Z, Huang P-JJ, Liu J (2015a) Hydrogen peroxide displacing DNA from Nanoceria: mechanism and detection of glucose in serum. J Am Chem Soc 137:1290–1295. https://doi.org/10.1021/ja511444e

Liu L, Song C, Zhang Z, Yang J, Zhou L, Zhang X, Xie G (2015b) Ultrasensitive electrochemical detection of microRNA-21 combining layered nanostructure of oxidized single-walled carbon nanotubes and nanodiamonds by hybridization chain reaction. Biosens Bioelectron 70:351–357. https://doi.org/10.1016/j.bios.2015.03.051

Liu S, Gong H, Wang Y, Wang L (2016) Label-free electrochemical nucleic acid biosensing by tandem polymerization and cleavage-mediated cascade target recycling and DNAzyme amplification. Biosens Bioelectron 77:818–823. https://doi.org/10.1016/j.bios.2015.10.056

Liu H, Weng L, Yang C (2017) A review on nanomaterial-based electrochemical sensors for H2O2, H2S and NO inside cells or released by cells. Microchim Acta 184:1267–1283. https://doi.org/10.1007/s00604-017-2179-2

Lu W, Suo Z (2002) Symmetry breaking in self-assembled monolayers on solid surfaces: anisotropic surface stress. Phys Rev B 65:085401

Luo Z, Weiss DE, Liu Q, Tian B (2018) Biomimetic approaches toward smart bio-hybrid systems. Nano Res 11:3009. https://doi.org/10.1007/s12274-018-2004-1

Ma L, Yuan R, Chai Y, Chen S (2009) Amperometric hydrogen peroxide biosensor based on the immobilization of HRP on DNA–silver nanohybrids and PDDA-protected gold nanoparticles. J Mol Catal B Enzym 56:215–220. https://doi.org/10.1016/j.molcatb.2008.05.007

Maddocks S, Jenkins R (2017) Chapter 4 – Quantitative PCR: things to consider. In: Understanding PCR. Academic, Boston, pp 45–52

Mailloux S, Halamek J, Katz E (2014) A model system for targeted drug release triggered by biomolecular signals logically processed through enzyme logic networks. Analyst 139:982–986. https://doi.org/10.1039/C3AN02162A

Malekzad H, Sahandi Zangabad P, Mirshekari H, Karimi M, Hamblin Michael R (2017) Noble metal nanoparticles in biosensors: recent studies and applications. Nanotechnol Rev 6(3):301–329. https://doi.org/10.1515/ntrev-20160014

Meng F, Jiang L, Zheng K, Goh CF, Lim S, Hng HH, Ma J, Boey F, Chen X (2011) Protein-based Memristive Nanodevices. Small 7:3016–3020. https://doi.org/10.1002/smll.201101494

Michael CP (2007) Molecular electronics: from principles to practice. Wiley, West Sussex

Millan KM, Saraullo A, Mikkelsen SR (1994) Voltammetric DNA biosensor for cystic fibrosis based on a modified carbon paste electrode. Anal Chem 66:2943–2948. https://doi.org/10.1021/ac00090a023

Min J, Lee T, Oh S-M, Kim H, Choi J-W (2010) Electrochemical biomemory device consisting of recombinant protein molecules. Biotechnol Bioprocess Eng 15:30–39. https://doi.org/10.1007/s12257-009-3074-4

Mitsumasa I, Young-Soo K, Takhee L (2010) Nanoscale Interface for organic electronics. World Scientific Publisher, Singapore

Mohammadniaei M, Lee T, Yoon J, Lee D, Choi J-W (2017) Electrochemical nucleic acid detection based on parallel structural dsDNA/recombinant azurin hybrid. Biosens Bioelectron 98:292–298. https://doi.org/10.1016/j.bios.2017.07.005

Mohammadniaei M, Lee T, Yoon J, Choi J-W (2018) Spectroelectrochemical detection of microRNA-155 based on functional RNA immobilization onto ITO/GNP Nanopattern. J Biotechnol 274:40

Muramatsu S, Kinbara K, Taguchi H, Ishii N, Aida T (2006) Semibiological molecular machine with an implemented "AND" logic gate for regulation of protein folding. J Am Chem Soc 128:3764–3769. https://doi.org/10.1021/ja057604t

Nagase S, Ohkoshi N, Ueda A, Aoyagi K, Koyama A (1997) Hydrogen peroxide interferes with detection of nitric oxide by an electrochemical method. Clin Chem 43:1246–1246

Nikitin MP, Shipunova VO, Deyev SM, Nikitin PI (2014) Biocomputing based on particle disassembly. Nat Nanotechnol 9:716. https://doi.org/10.1038/nnano.2014.156

Nowak C, Schach D, Gebert J, Grosserueschkamp M, Gennis RB, Ferguson-Miller S, Knoll W, Walz D, Naumann RLC (2011) Oriented immobilization and electron transfer to the cytochrome c oxidase. J Solid State Electrochem 15:105–114. https://doi.org/10.1007/s10008-010-1032-x

Noy A (2011) Bionanoelectronics. Adv Mater 23:807–820. https://doi.org/10.1002/adma.201003751

Odenthal KJ, Gooding JJ (2007) An introduction to electrochemical DNAbiosensors. Analyst 132:603–610. https://doi.org/10.1039/B701816A

Offenhäusser A, Rinaldi R (2009) Nanobioelectronics – for electronics, biology, and medicine. Springer, New York

Ogihara M, Ray A (2000) DNA computing on a chip. Nature 403:143. https://doi.org/10.1038/35003071

Okamoto A, Tanaka K, Saito I (2004) DNA logic gates. J Am Chem Soc 126:9458–9463. https://doi.org/10.1021/ja047628k

Palanisamy S, Cheemalapati S, Chen S-M (2012) Highly sensitive and selective hydrogen peroxide biosensor based on hemoglobin immobilized at multiwalled carbon nanotubes–zinc oxide composite electrode. Anal Biochem 429:108–115. https://doi.org/10.1016/j.ab.2012.07.001

Paleček E, Jelen F (2002) Electrochemistry of nucleic acids and development of DNA sensors. Crit Rev Anal Chem 32:261–270. https://doi.org/10.1080/10408340290765560

Pan S, Rothberg L (2005) Chemical control of electrode functionalization for detection of DNA hybridization by electrochemical impedance spectroscopy. Langmuir 21:1022–1027. https://doi.org/10.1021/la048083a

Pingarrón JM, Yáñez-Sedeño P, González-Cortés A (2008) Gold nanoparticle-based electrochemical biosensors. Electrochim Acta 53:5848–5866. https://doi.org/10.1016/j.electacta.2008.03.005

Pita M, Krämer M, Zhou J, Poghossian A, Schöning MJ, Fernández VM, Katz E (2008) Optoelectronic properties of nanostructured ensembles controlled by biomolecular logic systems. ACS Nano 2:2160–2166. https://doi.org/10.1021/nn8004558

Pita M, Tam TK, Minko S, Katz E (2009a) Dual Magnetobiochemical logic control of electrochemical processes based on local interfacial pH changes. ACS Appl Mater Interfaces 1:1166–1168. https://doi.org/10.1021/am900185c

Pita M, Zhou J, Manesh KM, Halámek J, Katz E, Wang J (2009b) Enzyme logic gates for assessing physiological conditions during an injury: towards digital sensors and actuators. Sensors Actuators B Chem 139:631–636. https://doi.org/10.1016/j.snb.2009.03.001

Prokup A, Hemphill J, Deiters A (2012) DNA computation: a photochemically controlled AND gate. J Am Chem Soc 134:3810–3815. https://doi.org/10.1021/ja210050s

Pumera M, Sánchez S, Ichinose I, Tang J (2007) Electrochemical nanobiosensors. Sensors Actuators B Chem 123:1195–1205. https://doi.org/10.1016/j.snb.2006.11.016

Qian L, Winfree E (2011) Scaling up digital circuit computation with DNA strand displacement cascades. Science 332:1196–1201. https://doi.org/10.1126/science.1200520

Qian L, Winfree E, Bruck J (2011) Neural network computation with DNA strand displacement cascades. Nature 475:368. https://doi.org/10.1038/nature10262

Qiu M, Khisamutdinov E, Zhao Z, Pan C, Choi J-W, Leontis NB, Guo P (2013) RNA nanotechnology for computer design and in vivo computation. Philos Trans R Soc A Math Phys Eng Sci 371:20120310. https://doi.org/10.1098/rsta.2012.0310

Radhakrishnan K, Tripathy J, Raichur AM (2013) Dual enzyme responsive microcapsules simulating an "OR" logic gate for biologically triggered drug delivery applications. Chem Commun 49:5390–5392. https://doi.org/10.1039/C3CC42017E

Ramanavičius A, Ramanavičienė A, Malinauskas A (2006) Electrochemical sensors based on conducting polymer—polypyrrole. Electrochim Acta 51:6025–6037. https://doi.org/10.1016/j.electacta.2005.11.052

Ramnani P, Gao Y, Ozsoz M, Mulchandani A (2013) Electronic detection of MicroRNA at Attomolar level with high specificity. Anal Chem 85:8061–8064. https://doi.org/10.1021/ac4018346

Rao SV, Anderson KW, Bachas LG (1998) Oriented immobilization of proteins. Microchim Acta 128:127–143. https://doi.org/10.1007/bf01243043

Ren X, Yan J, Wu D, Wei Q, Wan Y (2017) Nanobody-based apolipoprotein E Immunosensor for point-of-care testing. ACS Sensors 2:1267–1271. https://doi.org/10.1021/acssensors.7b00495

Rinaudo K, Bleris L, Maddamsetti R, Subramanian S, Weiss R, Benenson Y (2007) A universal RNAi-based logic evaluator that operates in mammalian cells. Nat Biotechnol 25:795. https://doi.org/10.1038/nbt1307

Robles-Águila MJ, Pérez KS, Stojanoff V, Juárez-Santiesteban H, Silva-González R, Moreno A (2014) Design of molecular devices based on metalloproteins: a new approach. J Mater Sci Mater Electron 25:1354–1360. https://doi.org/10.1007/s10854-014-1734-4

Rocchitta G, Spanu A, Babudieri S, Latte G, Madeddu G, Galleri G, Nuvoli S, Bagella P, Demartis M, Fiore V, Manetti R, Serra P (2016) Enzyme biosensors for biomedical applications: strategies for safeguarding analytical performances in biological fluids. Sensors 16:780

Rojkind M, Domínguez-Rosales J-A, Nieto N, Greenwel P (2002) Role of hydrogen peroxide and oxidative stress in healing responses. Cell Mol Life Sci 59:1872–1891. https://doi.org/10.1007/pl00012511

Ronkainen NJ, Halsall HB, Heineman WR (2010) Electrochemical biosensors. Chem Soc Rev 39:1747–1763. https://doi.org/10.1039/B714449K

Safavi A, Farjami F (2010) Hydrogen peroxide biosensor based on a myoglobin/hydrophilic room temperature ionic liquid film. Anal Biochem 402:20–25. https://doi.org/10.1016/j.ab.2010.03.013

Sarkar D, Liu W, Xie X, Anselmo AC, Mitragotri S, Banerjee K (2014) MoS2 field-effect transistor for next-generation label-free biosensors. ACS Nano 8:3992–4003. https://doi.org/10.1021/nn5009148

Schalkwijk J, van den Berg WB, van de Putte LBA, Joosten LAB (1986) An experimental model for hydrogen peroxide–induced tissue damage. Effects of a single inflammatory mediator on (peri)articular tissues. Arthritis Rheum 29:532–538. https://doi.org/10.1002/art.1780290411

Schwartz DK (2001) Mechanisms and kinetics of self-assembled monolayer formation. Annu Rev Phys Chem 52:107–137. https://doi.org/10.1146/annurev.physchem.52.1.107

Schwarzkopf M, Pierce NA (2016) Multiplexed miRNA northern blots via hybridization chain reaction. Nucleic Acids Res 44:e129. https://doi.org/10.1093/nar/gkw503

Seelig G, Soloveichik D, Zhang DY, Winfree E (2006) Enzyme-free nucleic acid logic circuits. Science 314:1585–1588. https://doi.org/10.1126/science.1132493

Shi L, Chu Z, Liu Y, Jin W, Chen X (2013) Facile synthesis of hierarchically aloe-like gold micro/nanostructures for ultrasensitive DNA recognition. Biosens Bioelectron 49:184–191. https://doi.org/10.1016/j.bios.2013.05.012

Singh P, Pandey SK, Singh J, Srivastava S, Sachan S, Singh SK (2016) Biomedical perspective of electrochemical Nanobiosensor. Nano-Micro Lett 8:193–203. https://doi.org/10.1007/s40820-015-0077-x

Song Y, Wan L, Wang Y, Zhao S, Hou H, Wang L (2012) Electron transfer and electrocatalytics of cytochrome c and horseradish peroxidase on DNA modified electrode. Bioelectrochemistry 85:29–35. https://doi.org/10.1016/j.bioelechem.2011.11.007

Song Y, Liu H, Wan L, Wang Y, Hou H, Wang L (2013) Direct electrochemistry of cytochrome c based on poly (diallyldimethylammonium chloride)- graphene Nanosheets/gold nanoparticles hybrid nanocomposites and its biosensing. Electroanalysis 25:1400–1409. https://doi.org/10.1002/elan.201200524

Strack G, Ornatska M, Pita M, Katz E (2008a) Biocomputing security system: concatenated enzyme-based logic gates operating as a biomolecular keypad lock. J Am Chem Soc 130:4234–4235. https://doi.org/10.1021/ja7114713

Strack G, Pita M, Ornatska M, Katz E (2008b) Boolean logic gates that use enzymes as input signals. Chembiochem 9:1260–1266. https://doi.org/10.1002/cbic.200700762

Strukov DB, Kohlstedt H (2012) Resistive switching phenomena in thin films: materials, devices, and applications. MRS Bull 37:108–114. https://doi.org/10.1557/mrs.2012.2

Suárez G, Santschi C, Martin OJF, Slaveykova VI (2013) Biosensor based on chemically-designed anchorable cytochrome c for the detection of H2O2 released by aquaticcells. Biosens Bioelectron 42:385–390. https://doi.org/10.1016/j.bios.2012.10.083

Tamayo J, Kosaka PM, Ruz JJ, San Paulo A, Calleja M (2013) Biosensors based on nanomechanical systems. Chem Soc Rev 42:1287–1311. https://doi.org/10.1039/C2CS35293A

Thévenot DR, Toth K, Durst RA, Wilson GS (2001) Electrochemical Biosensors: recommended definitions and classification. Biosensors Bioelectron 16:121–131. https://doi.org/10.1016/S0956-5663(01)00115-4

Tomohiro M, Satoshi S, Masaaki T (2004) Novel reconfigurable logic gates using spin metal–oxide–semiconductor field-effect transistors. Jpn J Appl Phys 43:6032

Trifonov A, Sharon E, Tel-Vered R, Kahn JS, Willner I (2016) Application of the hybridization chain reaction on electrodes for the amplified and parallel electrochemical analysis of DNA. J Phys Chem C 120:15743–15752. https://doi.org/10.1021/acs.jpcc.5b11308

Tseng RJ, Tsai C, Ma L, Ouyang J, Ozkan CS, Yang Y (2006) Digital memory device based on tobacco mosaic virus conjugated with nanoparticles. Nat Nanotechnol 1:72. https://doi.org/10.1038/nnano.2006.55

Umasankar Y, Unnikrishnan B, Chen S-M, Ting T-W (2012) Graphene impregnated with horseradish peroxidase multimer for the determination of hydrogen peroxide. Anal Methods 4:3653–3660. https://doi.org/10.1039/C2AY25276G

Vestergaard M, Kerman K, Tamiya E (2007) An overview of label-free electrochemical protein sensors. Sensors 7:3442

Wan Q, Song H, Shu H, Wang Z, Zou J, Yang N (2013) In situ synthesized gold nanoparticles for direct electrochemistry of horseradish peroxidase. Colloids Surf B Biointerfaces 104:181–185. https://doi.org/10.1016/j.colsurfb.2012.12.009

Wang J (2002) Electrochemical nucleic acid biosensors. Anal Chim Acta 469:63–71. https://doi.org/10.1016/S0003-2670(01)01399-X

Wang J (2005) Carbon-nanotube based electrochemical biosensors: a review. Electroanalysis 17:7–14. https://doi.org/10.1002/elan.200403113

Wang J (2008) Electrochemical glucose biosensors. Chem Rev 108:814–825. https://doi.org/10.1021/cr068123a

Wang R, Zhang J, Hu Y (2011) Liquid phase deposition of hemoglobin/SDS/TiO2 hybrid film preserving photoelectrochemical activity. Bioelectrochemistry 81:34–38. https://doi.org/10.1016/j.bioelechem.2011.01.003

Wang Z, Ning L, Duan A, Zhu X, Wang H, Li G (2012) A set of logic gates fabricated with G-quadruplex assembled at an electrode surface. Chem Commun 48:7507–7509. https://doi.org/10.1039/C2CC33088A

Wang Y, Zhang H, Yao D, Pu J, Zhang Y, Gao X, Sun Y (2013) Direct electrochemistry of hemoglobin on graphene/Fe3O4 nanocomposite-modified glass carbon electrode and its sensitive detection for hydrogen peroxide. J Solid State Electrochem 17:881–887. https://doi.org/10.1007/s10008-012-1939-5

Wang Y-H, Huang K-J, Wu X (2017) Recent advances in transition-metal dichalcogenides based electrochemical biosensors: a review. Biosens Bioelectron 97:305–316. https://doi.org/10.1016/j.bios.2017.06.011

Weber W, Schoenmakers R, Keller B, Gitzinger M, Grau T, Daoud-El Baba M, Sander P, Fussenegger M (2008) A synthetic mammalian gene circuit reveals antituberculosis compounds. Proc Natl Acad Sci 105:9994–9998. https://doi.org/10.1073/pnas.0800663105

Wen Y, Pei H, Shen Y, Xi J, Lin M, Lu N, Shen X, Li J, Fan C (2012) DNA nanostructure-based interfacial engineering for PCR-free ultrasensitive electrochemical analysis of microRNA. Sci Rep 2(2):867. https://doi.org/10.1038/srep00867

Willner I, Katz E (2000) Integration of layered redox proteins and conductive supports for bioelectronic applications. Angew Chem Int Ed 39:1180–1218. https://doi.org/10.1002/(SICI)1521-3773(20000403)39:7<1180::AID-ANIE1180>3.0.CO;2-E

Win MN, Smolke CD (2008) Higher-order cellular information processing with synthetic RNA devices. Science 322:456–460. https://doi.org/10.1126/science.1160311

Wong LS, Khan F, Micklefield J (2009) Selective covalent protein immobilization: strategies and applications. Chem Rev 109:4025–4053. https://doi.org/10.1021/cr8004668

Wu L, Qu X (2015) Cancer biomarker detection: recent achievements and challenges. Chem Soc Rev 44:2963–2997. https://doi.org/10.1039/C4CS00370E

Wu S, Zhao H, Ju H, Shi C, Zhao J (2006) Electrodeposition of silver–DNA hybrid nanoparticles for electrochemical sensing of hydrogen peroxide and glucose. Electrochem Commun 8:1197–1203. https://doi.org/10.1016/j.elecom.2006.05.013

Wu S-H, Tang Y, Chen L, Ma X-G, Tian S-M, Sun J-J (2015) Amplified electrochemical hydrogen peroxide reduction based on hemin/G-quadruplex DNAzyme as electrocatalyst at gold particles modified heated copper disk electrode. Biosens Bioelectron 73:41–46. https://doi.org/10.1016/j.bios.2015.05.039

Xiang C, Zou Y, Sun L-X, Xu F (2008) Direct electron transfer of cytochrome c and its biosensor based on gold nanoparticles/room temperature ionic liquid/carbon nanotubes composite film. Electrochem Commun 10:38–41. https://doi.org/10.1016/j.elecom.2007.10.030

Xie Z, Liu SJ, Bleris L, Benenson Y (2010) Logic integration of mRNA signals by an RNAi-based molecular computer. Nucleic Acids Res 38:2692–2701. https://doi.org/10.1093/nar/gkq117

Xie Z, Wroblewska L, Prochazka L, Weiss R, Benenson Y (2011) Multi-input RNAi-based logic circuit for identification of specific Cancer cells. Science 333:1307–1311. https://doi.org/10.1126/science.1205527

Xu J, Shang F, Luong JHT, Razeeb KM, Glennon JD (2010) Direct electrochemistry of horseradish peroxidase immobilized on a monolayer modified nanowire array electrode. Biosens Bioelectron 25:1313–1318. https://doi.org/10.1016/j.bios.2009.10.018

Yagati AK, Kim S-U, Min J, Choi J-W (2009a) Multi-bit biomemory consisting of recombinant protein variants, azurin. Biosens Bioelectron 24:1503–1507. https://doi.org/10.1016/j.bios.2008.07.080

Yagati AK, Kim S-U, Min J, Choi J-W (2009b) Write-once–read-many-times (WORM) biomemory device consisting of cysteine modified ferredoxin. Electrochem Commun 11:854–858. https://doi.org/10.1016/j.elecom.2009.02.014

Yagati AK, Kim S-U, Min J, Choi J-W (2010) Ferredoxin molecular thin film with intrinsic switching mechanism for biomemory application. J Nanosci Nanotechnol 10:3220–3223. https://doi.org/10.1166/jnn.2010.2229

Yagati AK, Lee T, Min J, Choi J-W (2012) Electrochemical performance of gold nanoparticle–cytochrome c hybrid interface for H2O2 detection. Colloids Surf B Biointerfaces 92:161–167. https://doi.org/10.1016/j.colsurfb.2011.11.035

Yagati AK, Lee T, Min J, Choi J-W (2013) An enzymatic biosensor for hydrogen peroxide based on CeO2 nanostructure electrodeposited on ITO surface. Biosens Bioelectron 47:385–390. https://doi.org/10.1016/j.bios.2013.03.035

Yagati AK, Min J, Cho S (2014) Electrosynthesis of ERGO-NP nanocomposite films for Bioelectrocatalysis of horseradish peroxidase towards H2O2. J Electrochem Soc 161:G133–G140. https://doi.org/10.1149/2.1001414jes

Yin P, Choi HMT, Calvert CR, Pierce NA (2008) Programming biomolecular self-assembly pathways. Nature 451:318. https://doi.org/10.1038/nature06451

Yoo S-Y, Lee T, Chung Y-H, Min J, Choi J-W (2011) Fabrication of biofilm in nanoscale consisting of cytochrome f/2-MAA bilayer on Au surface for bioelectronic devices by self-assembly technique. J

Nanosci Nanotechnol 11:7069–7072. https://doi.org/10.1166/jnn.2011.4845

Yoon J, Chung Y-H, Yoo S-Y, Min J, Choi J-W (2014) Electrochemical-signal enhanced information storage device composed of cytochrome c/SNP bilayer. J Nanosci Nanotechnol 14:2466–2471. https://doi.org/10.1166/jnn.2014.8542

Yoon J, Lee T, Bapurao GB, Jo J, Oh B-K, Choi J-W (2017a) Electrochemical H2O2 biosensor composed of myoglobin on MoS2 nanoparticle-graphene oxide hybrid structure. Biosens Bioelectron 93:14–20. https://doi.org/10.1016/j.bios.2016.11.064

Yoon J, Shin J-W, Lim J, Mohammadniaei M, Bharate Bapurao G, Lee T, Choi J-W (2017b) Electrochemical nitric oxide biosensor based on amine-modified MoS2/graphene oxide/myoglobin hybrid. Colloids Surf B Biointerfaces 159:729–736. https://doi.org/10.1016/j.colsurfb.2017.08.033

Yuan Y, Zhou S, Yang G, Yu Z (2013) Electrochemical biomemory devices based on self-assembled graphene-Shewanella oneidensis composite biofilms. RSC Adv 3:18844–18848. https://doi.org/10.1039/C3RA42850H

Zhai J, Cui H, Yang R (1997) DNA based biosensors. Biotechnol Adv 15:43–58. https://doi.org/10.1016/S0734-9750(97)00003-7

Zhang L (2008) Direct electrochemistry of cytochrome c at ordered macroporous active carbon electrode. Biosens Bioelectron 23:1610–1615. https://doi.org/10.1016/j.bios.2008.01.022

Zhang Y, Zhang C-y (2012) Sensitive detection of microRNA with isothermal amplification and a single-quantum-dot-based Nanosensor. Anal Chem 84:224–231. https://doi.org/10.1021/ac202405q

Zhang J, Dong S, Lu J, Turner APF, Fan Q, Jia S, Yang H, Qiao C, Zhou H, He G (2009) A label free electrochemical Nanobiosensor study. Anal Lett 42:2905–2913. https://doi.org/10.1080/00032710903201941

Zhang YM, Zhang L, Liang RP, Qiu JD (2013) DNA electronic logic gates based on metal-ion-dependent induction of oligonucleotide structural motifs. Chem Eur J 19:6961–6965. https://doi.org/10.1002/chem.201300625

Zhao Y, Zhou L, Tang Z (2013) Cleavage-based signal amplification of RNA. Nat Commun 4:1493. https://doi.org/10.1038/ncomms2492 http://www.nature.com/articles/ncomms2492#supplementary-information

Zhou J, Arugula MA, Halámek J, Pita M, Katz E (2009) Enzyme-based NAND and NOR logic gates with modular design. J Phys Chem B 113:16065–16070. https://doi.org/10.1021/jp9079052

Zhu W-L, Zhou Y, Zhang J-R (2009) Direct electrochemistry and electrocatalysis of myoglobin based on silica-coated gold nanorods/room temperature ionic liquid/silica sol–gel composite film. Talanta 80:224–230. https://doi.org/10.1016/j.talanta.2009.06.056

18 Biomimetic Self-Assembling Peptide Hydrogels for Tissue Engineering Applications

Jiaju Lu and Xiumei Wang

18.1 Introduction

Tissue engineering is an exciting research field that aims to replace/repair tissue or organ that has been damaged because of disease, injury or trauma (Khademhosseini and Langer 2016; Langer and Vacanti 1993; Vacanti and Langer 1999). There are three main components in tissue engineering: Cells, scaffolds and signaling biomolecules (or growth factors), which are generally referred to as the tissue engineering triad. Among them, scaffolds play a pivotal role in providing the beneficial microenvironment for regenerative cells survival, proliferation and differentiation, as well as carrying signaling biomolecules for mediating cellular response. Therefore, a three dimensions (3D), porous biomimetic scaffold that could mimic the natural extracellular matrix (ECM) is critical (Ma 2008; Shin et al. 2003).

Molecular self-assembly offers a powerful bottom-up fabrication technology to construct a stable and well-organized structure at nano- and/or micro- scales (Palmer and Stupp 2008; Whitesides and Grzybowski 2002; Zhang 2003). It is a spontaneous and prevalent process in living systems, such as protein folding and DNA double-helix formation (Whitesides et al. 1991; Zhang 2003). Scientists are inspired by these complex and elegant phenomenon to prepare functional materials by using the mechanisms of self-assembly. The process of peptide self-assembly is mainly mediated by noncovalent interactions, such as hydrogen bonding, hydrophobic interaction, van der Waals, electrostatic interaction, and π-π stacking interactions (Whitesides and Grzybowski 2002). Compared with covalent bonding, these noncovalent forces show several advantages of reversible property, high synthetic convergence and precise design (Sun et al. 2017).

Although a number of building blocks like cholesteryl group (Xu et al. 2013), sugar-based molecules (Ogawa et al. 2012) have been explored for applications in molecular self-assembly, peptides derived from natural or synthetic amino acids possess unique properties. Firstly, beyond the advantages include biocompatibility and biodegradability, they are also easily obtained by solid-phase synthesis methods and designed by adding diverse functional motifs in native protein (Pérez et al. 2015). In addition, they could self-assemble into different kinds of supramolecular structures, such as nanotubes, nanosphere, vesicles, and micelles (Mandal et al. 2014). Most importantly, peptides are the most promising candidates for regenerative scaffolds, because the main "cell signaling language" in the ECM is mediated through peptide epitopes (Habibi et al. 2016; Pérez et al. 2015).

J. Lu · X. Wang (✉)
State Key Laboratory of New Ceramics and Fine Processing, School of Materials Science and Engineering, Tsinghua University, Beijing, China
e-mail: lujj13@mails.tsinghua.edu.cn; wxm@mail.tsinghua.edu.cn

I. Noh (ed.), *Biomimetic Medical Materials*, Advances in Experimental Medicine and Biology 1064,
https://doi.org/10.1007/978-981-13-0445-3_18

Various bioactive motifs derived from naturally occurring proteins have been widely designed and introduced to the pure self-assembling peptides. The functionalized peptides hydrogel scaffolds could provide a beneficial environment that is permissive for regeneration of damaged tissues and allows for cell survival, proliferation and differentiation. In this chapter, we summarize the most widely used classes (α-helical coiled-coil peptide, β-sheet peptides, and peptide amphiphiles) and hydrogel formation of self-assembling peptides, as well as their recent and promising applications in tissue engineering.

18.2 Self-Assembling Peptide Design and Hydrogel Formation

Although only 20 natural amino acids exist in the live systems, the combinations of 20 natural amino acids are highly diversified. Recently, non-natural amino acids and their derivatives are also utilized for making up the self-assembling peptide (Orbach et al. 2009). A number of self-assembled peptide systems have been designed and developed via tuning the basic conformational units of peptides (Table 18.1). The typical molecular structures naturally occurred in proteins including β-sheets, α-helices and coiled coils, which could be designed to direct the self-assembling processes of peptides (Ulijn and Smith 2008).

18.2.1 α-Helical Coiled-Coil Peptide

The α-helical structures are main secondary structures of peptides and commonly seen in the cytoskeleton and extracellular matrix in biological systems (Beck and Brodsky 1998; Robson Marsden and Kros 2010; Woolfson 2001). Like the majority of self-assembling peptides, the non-covalent hydrophobic interactions is main driven force of peptide folding, which are between the side chains of different α-helices. In theory, the α-helical has 3.6 residues per turn, so hydrophobic amino acids are usually designed to space three to four amino acids to meet the requirements of α-helical geometry (Pauling et al. 1951; Woolfson 2010). However, stabilizing an α-helices conformation result from hydrogen bonds is often difficult because of its inherent thermodynamic instability in solution (García and Sanbonmatsu 2002; Ziv et al. 2005).

An α-helical coiled-coil structure could be formed through the assembly of two or more α-helicals into superhelical structures, which are highly ordered and stable. Pioneering work was done by Petka et al. in 1998, they designed a

Table 18.1 Some examples of biomimetic self-assembling peptides

Name	Peptide sequence	Secondary structure	Gelation conditions	References
hSAFAAA	p1(IAALKAK-IAALKAE-IAALEAE-NAALEA)	α-Helix	Temperature	Banwell et al. (2009)
	p2(IAALKAK-NAALKAE-IAALEAE-IAALEA)			
EAK16-II	$(AEAEAKAK)_2$	β-Sheet	Ionic strength	Zhang et al. (1993)
RADA16-I	$(RADA)_4$	β-Sheet	pH, ionic strength	Zhang and Altman (1999)
K24	KLEALYVLGFFGFFTLGIMLSYIR	β-Sheet	Polar solvents	Aggeli et al. (1996)
P11-I	QQRQQQQQEQQ	β-Sheet	Polar solvents	Aggeli et al. (1997b)
MAX1	VKVKVKVKVDPPTKVKVKVKV	β-Turn	pH, shear-thinning	Schneider et al. (2002)
PA	1: $C_{16}H_{31}O$-NH-AAAAGGGEIKVAV	β-Sheet	pH	Niece et al. (2003)
	2: $C_{16}H_{31}O$-NH-AAAAGGGKYIGSR			

synthetic coiled-coil peptide that could reversibly self-assembled into a hydrogel (Petka et al. 1998). The typical α-helical coiled-coil peptide consists of a heptad repeat pattern $(abcdefg)_n$, where a and d are usually hydrophobic amino acid and the remaining residues tend to be polar (Kumar et al. 2016; Lupas and Gruber 2005; Walshaw and Woolfson 2001). These repeating heptad could self-assemble into the amphipathic helices under hydrophobic interactions, and further into coiled-coil dimers, promoting aggregation and subsequent gelation.

Most notably, various α-helical coiled-coil systems have been designed and developed by Woolfson's group (Banwell et al. 2009; Mehrban et al. 2014; Moutevelis and Woolfson 2009). These so-called hydrogelating self-assembling fibers (hSAFs) comprise two-component α-helical peptides (SAF-p1 and SAF-p2), coassembling into an offset α-helical heterodimer with complementary "sticky ends". The end promoted lengthwise extension of fibrils. And the hydrogel was formed by multiple weak interactions between the fibers (Pandya et al. 2000; Smith et al. 2006). Dong et al. demonstrate that α-helical coiled-coil nanofibers can be formed via an alternative mechanism without designed "sticky ends". By increased peptide concentration, the blunt-ended dimers could form nanofibers (Dong et al. 2008).

18.2.2 β-Sheet Peptides

In 1993, Zhang et al. found a 16-residue peptide fragment in the yeast protein Zuotin, EAK16-II (Ac-AEAEAKAKAEAEAKAK-$CONH_2$). The alanine (A) has a neutral hydrophobic residue, while the glutamic acid (E) and lysine (K) have negatively and positively charged hydrophilic residues, respectively. In the high ionic strength environment, the ionic self-complementary oligopeptide EAK16-II with β-sheet secondary structures could spontaneously self-assembled into β-sheet secondary structures and further form a macroscopic membrane (Zhang et al. 1993, 1994). Since then, there's increasing study and focus on self-assembling motifs based on the β-sheet.

The feature of the ionic self-complementary peptides is their periodic repeats of alternating ionic hydrophilic and hydrophobic amino acids that contain 50% charged residues (Zhang et al. 2005). According to the charge distribution of hydrophilic surface, the ionic self-complementary peptides can generally be divided into four categories: modulus I (− + − + − + − +), modulus II (− − + + − − + +), modulus III (− − − + + +), and modulus IV (− − − − + + + +) (Zhang et al. 2005). With strong hydrophobic and electrostatic interactions, these amphiphilic oligopeptides could form stable β-sheet nanofibers by molecular self-assembly (Yanlian et al. 2009). Furthermore the scaffold hydrogel could be fabricated from nanofibers with great than 99% water content (Chen 2005).

RADA16-I is another well-known member of the ionic-complementary peptide family discovered by Zhang et al. (Zhang and Altman 1999; Zhang et al. 1994). Different from EAK16-II, this peptide is designed by replacing lysine and glutamate with arginine and aspartate residues. In an aqueous media, the self-assembling peptide RADA16-I forms a β-sheet structure and self-assembles into nanofibers. And the self-assembled nanofibers could undergo reproducibly dynamic reassembly after sonication, which breaks the ionic bonds and hydrophobic interactions (Yokoi et al. 2005). By changing to neutral pH or adding physiological concentrations of salt solutions, the gelation process of RADA16-I is accelerated and 3D scaffold hydrogel finally formed contains over 99% (w/v) water with 10 nm fiber diameter and 5–200 nm pore size, similar to nanostructure of the natural ECM (Meng et al. 2014; Ye et al. 2008). Due to its excellent biocompatibility for promoting cell growth and tissue regeneration, RADA16-I has been commercialized available as a product named PuraMatrix (McGrath et al. 2010; Moradi et al. 2012; Zhang et al. 1995).

Aggeli et al. discover a 24-residue peptide (K24, NH_2-Lys-Leu-Glu-Ala-Leu-Tyr-Val-Leu-Gly-Phe-Phe-Gly-Phe-Phe-Thr-Leu-Gly-Ile-Met-Leu-Ser-Tyr-Ile-Arg-COOH) derived from the

single transmembrane domain of the IsK protein, and K24 could form β-sheet nanotapes in non-aqueous solvents such as methanol (Takumi 1993; Takumi et al. 1988). And K27, its longer 27-residue version, has a predominantly β-strand secondary structure in lipid bilayers (Aggeli et al. 1996, 1997a). Subsequently, Aggeli and coworkers designed a novel class of self-assembling peptides with a high content of glutamate, such as P_{11}-I (CH_3CO-QQRQQQQQEQQ-NH_2) and P_{11}-II (CH_3CO-QQRFQWQFEQQ-NH_2) (Aggeli et al. 1997b; Fishwick et al. 2003). Following the initial design, Collier and Messersmith also developed a variation that called Q11 (Ac-QQKFQFQFEQQ-Am) (Collier and Messersmith 2003; Jung et al. 2008). These glutamate-rich peptides were designed by using aromatic residues as the hydrophobic component of the β-sheet motif, which helped drive β-strand assembly additionally via π-π stacking interactions (Davies and Aggeli 2011). And they could transform to a macroscopic hydrogel at low pH conditions (Aggeli et al. 2003).

The hairpin peptides including two antiparallel β-strands and a β-turn were also found to self-assemble into fibrillar macromolecular scaffolds. In 2002, Schneider and Pochan et al. described a series of short amphiphilic peptides composed of a tetrapeptide β-turn (-V^DPPT-) with alternating valine (hydrophobic) and lysine (hydrophilic) residues flanking regions (Pochan et al. 2003; Schneider et al. 2002). These peptides firstly intramolecularly fold into an amphiphilic β-hairpin along their hydrophobic faces, and subsequently undergo self-assembly via both intermolecular hydrogen bonding and van der Waals forces. For example, MAX1 (VKVKVKVKVDPPTKVKVKVKV-NH_2) adopted a hairpin conformation and exhibited pH-triggered self-assembly into a hydrogel in basic aqueous medium (Schneider et al. 2002). Responsive hydrogels from the variations of MAX1 have been prepared and their hydrogelation could be precisely controlled by changing conditions such as ionic strength (Micklitsch et al. 2011; Ozbas et al. 2007), light (Haines et al. 2005), pH (Rajagopal et al. 2009) and temperature (Pochan et al. 2003).

18.2.3 Peptide Amphiphiles (PAs)

The representative PAs are a class of molecules with hydrophilic peptide sequences linked to a hydrophobic alkyl chain. In 1995, Berndt et al. reported one of the first PAs (Berndt et al. 1995). They introduced a dialkyl chain to a peptide sequence derived from collagen, which could form stable monolayers at the air-water interface. Most notably, various PA molecules have been extensively studied and developed by Stupp group (Bull et al. 2005; Hartgerink et al. 2001; Niece et al. 2003). The chemical structure of PAs is composed of four regions (Cui et al. 2010; Perez et al. 2015): (1) a long hydrophobic alkyl tail; (2) hydrophilic β-sheet peptide sequences; (3) charged amino acids as a linker; (4) bioactive epitope. When dissolved in water, both hydrophobic interactions of the alkyl tails and hydrogen bonding among the amino acids in β-sheet structure drive the self-assembly process of PAs, which is similar to spontaneous protein folding. Various types of structures such as nanofibers (Matson et al. 2011; Silva et al. 2004), nanotubes (Arnold et al. 2005), micelles and vesicles (Greenfield et al. 2009), and ribbons (Pashuck and Stupp 2010; Sone et al. 2002) could be constructed by this self-assembly process.

In 2011, Shao'group developed a novel PA (C_{12}-GAGAGAGY) based on silk fibroin (Zhang et al. 2011). They found that this amphiphile peptide assembled into nanostructures from cylindrical nanofibers to nanoribbons with the decreasing of pH value from 11 to 8. And a hierarchically structured hydrogel was formed with a high modulus following further decrease of pH value (Guo et al. 2013). Another major class of PA is aromatic PA, which contains a short peptide sequence and usually utilizes the fluorenyl-9-methoxycarbonyl (Fmoc) group as an N-terminal capping group (Fleming et al. 2013). For example, the Fmoc-dipeptide (Fmoc-FF) could spontaneous assembly into fibrous hydrogels under physiological conditions (Jayawarna et al. 2006). And the π-stacking between the aromatic fluorenyl rings was used

as a driving force for the self-assembly of short peptides (Smith et al. 2008).

18.3 Applications in Tissue Engineering

Recently, biomimetic self-assembling peptide hydrogel have been increasingly exploited as artificial scaffolds for tissue regeneration (Loo et al. 2012; Pugliese and Gelain 2017). Compared with micro-scale size of conventional polymeric materials, the nanofibrous microarchitecture of self-assembled peptide hydrogels is biomimetic, which is more similar to an ECM-like environment (Gelain et al. 2006). The nanofiber scaffolds made from self-assembling peptide could provide cells in a true 3D microenvironment. Furthermore, the modification of self-assembling peptide nanofiber scaffolds could be produced by incorporating various functional peptide sequence motifs (Table 18.2). These appended functional motifs are derived from naturally occurring proteins, giving superior biological activities such as promote cell adhesion (Bellis 2011), promote neurite outgrowth (Tashiro et al. 1989), enhance osteoblast proliferation, differentiation and migration (Horii et al. 2007), and so on so forth. In the latter part of this review, we will highlight recent progress made in applying biomimetic self-assembling peptide hydrogels as biological scaffolds in tissue engineering.

18.3.1 Angiogenesis

Angiogenesis refers to the process of sprouting of new blood vessels from the pre-existing ones, which involves complex and highly dynamic interactions between associated supporting cells and growth factors (Eilken and Adams 2010; Risau 1997). The regrowth of damage cells and tissues depends on the establishment of an adequate blood supply, hence angiogenesis is essential during tissue repair, especially of ischemic disease (Li et al. 2005). In 2005, Narmoneva et al. established a 3D angiogenic environment for human microvascular endothelial cells by using the unmodified self-assembling short oligopeptide RAD16-II (AcN-RARADA-DARARADADA-$CONH_2$) (Narmoneva et al. 2005). Without adding extra angiogenic factors, the peptide hydrogel could not only inhibit

Table 18.2 Some examples of functional peptide motifs/epitopes

Bioactive motifs/ epitopes	Origin	Application	References
ALKRQGRTLYGF	Osteogenic growth peptide	Osteobast proliferation and differentiation	Horii et al. (2007)
DGRGDSVAYG	Osteopontin cell adhesion domain		
KLTWQELYQLKYKGI	Vascular endothelial growth factor	Angiogenesis; Myocardial regeneration	Wang et al. (2008), Liu et al. (2012) and Li et al. (2017)
PRGDSGYRGDS	2-unit RGD binding peptide		
SVVYGLR	Osteopontin	Angiogenesis; Nerve regeneration	Wang et al. (2017)
PDSGR	Laminin	Neural cells survival; Nerve regeneration;	Gelain et al. (2006)
SDPGYIGSR			
FPGERGVEGPGP	Collagen I		
SKPPGTSS	Bone marrow homing peptide-1		
PFSSTKT	Bone marrow homing peptide-2		
IKVAV	Laminin	Nerve regeneration	Silva et al. (2004) and Sun et al. (2016)

endothelial cell apoptosis, but also increase the gene expression of vascular endothelial growth factor (VEGF). Their results showed that the scaffolds facilitated capillary-like network formation and long-time cell survival. Subsequently, this injectable peptide scaffold was applied for myocardial regeneration (Davis et al. 2005). The self-assembling peptide nanofiber microenvironments augmented the recruitment of endogenous endothelial cells and smooth muscle cells, and the survive of the transplanted cells.

In 2008, Wang et al. reported two functionalized self-assembling peptide RAD-KLT (Ac-$(RADA)_4G_4$KLTWQELYQLKYKGI-$CONH_2$) and RAD-PRG (Ac-$(RADA)_4$GPRGDSGYRGDS-$CONH_2$), which were designed by directly introducing VEGF-mimicking peptide motif KLT (KLTWQELYQLKYKGI) and 2-unit RGD motif PRG (PRGDSGYRGDS) to pure RADA16-I, respectively (Fig. 18.1) (Wang et al. 2008, 2011). The study showed proangiogenic potential of these two nanofiber scaffolds, which significantly promoted endothelial cell growth, migration and tubulogenesis *in vitro*. And then the angiogenic activity of RAD-KLT and RAD-PRG was evaluated *in vivo* using the chicken embryo chorioallantoic membrane (CAM) assay (Liu et al. 2012). The results demonstrated that the functionalized peptide mixture RAD/KLT showed a significantly better performance on inducing CAM tissue invasion and new capillary vessel formation, without the help of exogenous VEGF (Fig. 18.2). Recently they tested these peptide mixture RAD/PRG and RAD/KLT with bone marrow mesenchymal stem cells (BMSCs) for the treatment of acute myocardial infarction in a mouse model

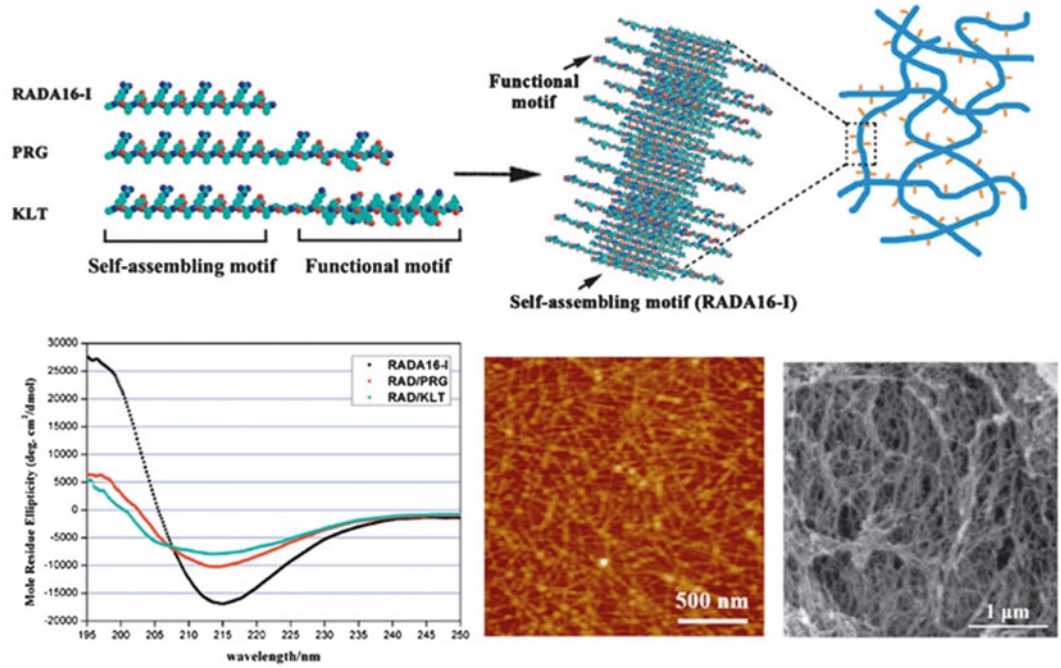

Fig. 18.1 Molecular models of designer self-assembling peptide RADA16-I, PRG and KLT. After mixing RADA16-I, the nanofibers scaffolds of self-assembling peptide are formed, which are representing a β-sheet second structure. The alternating positive (arginine) and negative (aspartic acid) charges are present on one side and the other side is aggregated by hydrophobic alanine side groups. And the functional motifs extrude from the nanofiber backbone. The typical CD spectrum, AFM morphology and SEM morphology of the functionalized peptide nanofiber scaffold are presented. (Reproduced from Wang et al. (2008) with permission from The Royal Society of Chemistry)

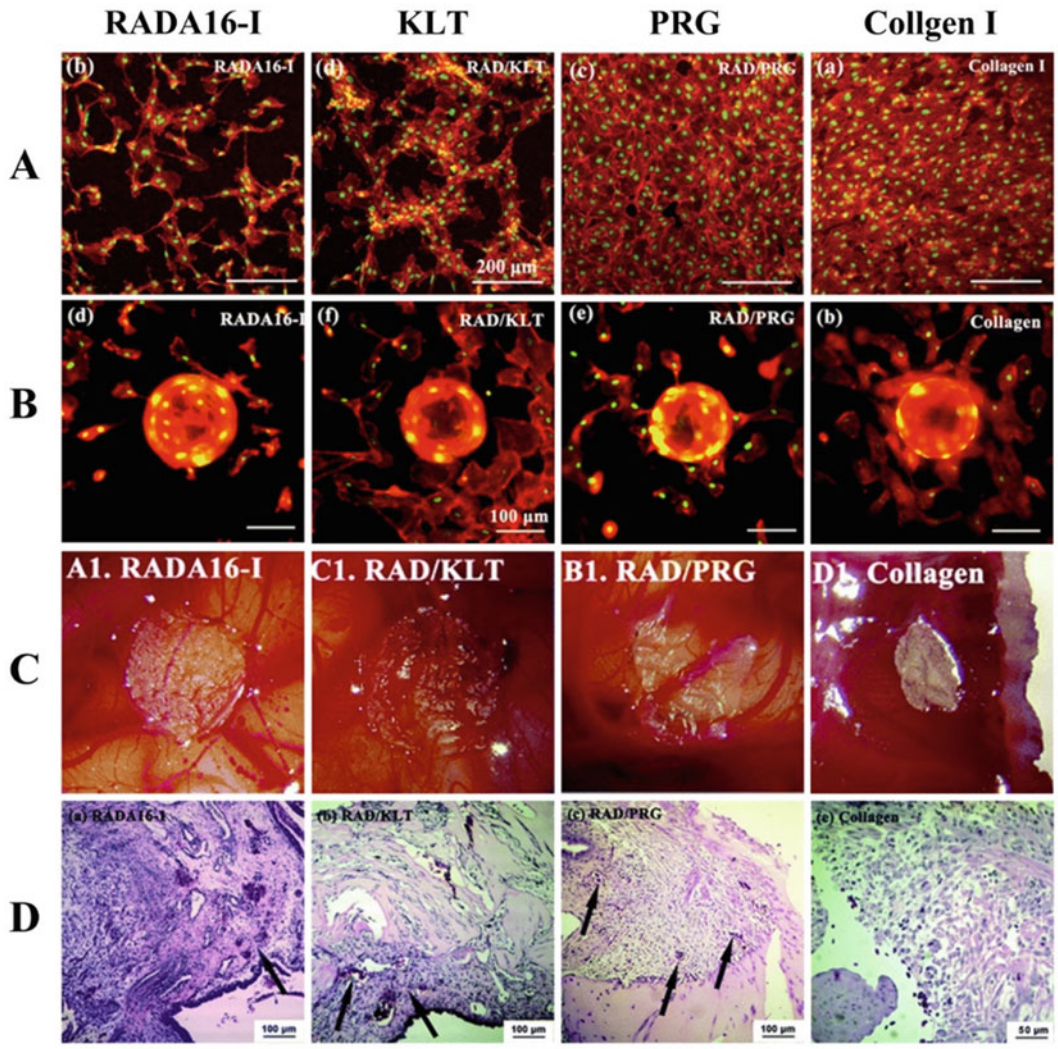

Fig. 18.2 (**a**) Fluorescence microscopy images of HUVECs morphology on different peptide scaffolds after 2-day culture. The collagen-I gel was used as a positive control. Fluorescent staining with Rhodamin phalloidin for F-actin (red) and SYTOX Green for nuclei (green) showed the cell attachments and viabilities. Bar = 200 μm. (**b**) HUVECs migration to different surrounding scaffold hydrogels after 1 day culture without adding extra VEGF. Bar = 100 μm. (**c**) Gross morphology of CAM with different scaffold hydrogels at day 4 after implantation. (**d**) HE staining of CAM with VEGF in the peptide scaffold hydrogels at day 4 after implantation. Black arrows indicate new capillary vessels. (Reproduced from Wang et al. (2008) and Liu et al. (2012) with permission from The Royal Society of Chemistry)

(Li et al. 2017). And the localization and survival of GFP/Fluc- BMSCs in the infarcted myocardium were enhanced by co-transplantation with RAD/PRG. Stupp's group also used the aforementioned VEGF-mimetic motif KLT to modify PA molecule, where the VEGF-mimetic epitope was in α-helical conformation (Webber et al. 2011). They demonstrated that the VEGF-PA promoted proangiogenic behavior in endothelial cells by specifically activating VEGF receptors *in vitro*. And the nanofiber gels formed from VEGF-PA were evaluated in a mouse hind-limb ischemia model, which showed the nanofibers

increased the density of microcirculation and functional recovery *in vivo*.

In addition, self-assembling peptide was applied as delivery system for therapeutic agents including growth factors and small molecule drugs (Eskandari et al. 2017). Aim at improving performance of islet transplantation for the treatment of type 1 diabetes, Stupp's group used heparin-binding PAs (HBPAs) to deliver VEGF and fibroblast growth factor-2 (FGF-2) to extrahepatic islet isografts in diabetic mice (Stendahl et al. 2008). Their outcomes indicated that the scaffold HBPAs provided a suitable microenvironment for islet engraftment and increased blood vessel density in the mouse omentum with the help of angiogenic growth factors. Hsieh et al. investigated the controlled delivery of platelet-derived growth factor (PDGF)-BB using injectable self-assembling peptide nanofibers RAD-II for myocardial protection (Hsieh et al. 2006). Their study showed that the RAD-II with PDGF-BB promoted cardiomyocyte survival and maintained systolic function after myocardial infarction.

18.3.2 Bone Regeneration

For decades, autogenous bone has been considered as the "gold standard", although many kinds of scaffolds including ceramics, metals and alloys were developed for reconstructing bone tissue. However, the application of autograft is limited due to the donor site morbidity and graft availability. This is a challenge for researchers to seek suitable scaffolds substitutes with osteoinductive or osteogenic properties (Giannoudis et al. 2005; Pape et al. 2010). Garreta et al. reported that the 3D-culture systems made from pure self-assembling peptide RADA16-I promoted the differentiation of mouse embryonic stem cells (mESCs) and mouse embryonic fibroblasts (MEFs) into osteoblast-like cells, as well as elevated collagen I synthesis and alkaline phosphatase (ALP) activity (Garreta et al. 2006). And they found that primary MEFs could maintain their "stem cell-like" phenotype and proliferation capacity in 3D environment but not in 2D. Similar results were reported by Hamada et al. and the osteogenic differentiation of mesenchymal stem cells (MSCs) was enhanced in 3D culture of RADA16-I scaffold (Hamada et al. 2008). In 2007, Horii et al. designed three peptide nanofiber scaffolds for osteoblasts through coupling the bioactive motifs to the pure RADA16-I (Horii et al. 2007). The selected motifs were derived from osteogenic growth peptide (ALK, ALKRQGRTLYGF), cell adhesion domain of osteopontin (DGR, DGRGDSVAYG) and 2-unit RGD motifs (PRG, PRGDSGYRGDS). The results showed that these designer peptide scaffolds promoted cell proliferation, differentiation and migration of mouse pre-osteoblast MC3T3-E1 cell.

However, the biomimetic self-assembling peptide hydrogel scaffolds are not satisfying *in vivo*, on account of their poor mechanical properties (Koutsopoulos 2016). In 2001, Stupp and coworkers designed the PA molecules with a single phosphorylated serine residue region, which could allow the PA nanofibers to direct mineralization of hydroxyapatite (Hartgerink et al. 2001). They then obtained a nanostructured composite material by self-assembly and mineralization of this PA molecules. Surprisingly, the structural alignment of composite material with preferred orientation of hydroxyapatite on the fibers was the same as that observed between collagen and hydroxyapatite in bone. Subsequently, they made the surface nucleation grow and 3D networks of PA nanofibers were formed by promoting mineralization (Spoerke et al. 2009). These 3D biomimetic systems were then examined in an orthotopic 5-mm wide critical-sized rat femoral defect model (Mata et al. 2010). The *in vivo* study demonstrated that the biomimetic matrices promote bone regeneration.

In 2015, Wu et al. used RADA16-I scaffold hydrogels for 3D culture of peripheral blood mesenchymal stem cells (PBMSCs), and they found that the peptide gels promoted PBMSCs survival and osteogenic differentiation *in vitro* (Wu et al. 2015). To meet the requirement for reconstructing large scale calvarial bone defect, the RADA16-I scaffold seeded with PBMSCs was splinted by two membranes of poly(lactic-glycolic acid)

(PLGA). Hence, the obtained composite scaffold could be transplanted to repair an 8 mm cranial defect in rats and contribute to new bone formation. In another study, Hayashi et al. reported increased bone regeneration from transplanted induced pluripotent stem cells (iPSCs) within RADA16-I scaffold in rat calvarial bone defect (Hayashi et al. 2016).

18.3.3 Cartilage Regeneration

The chondral and osteochondral lesions is frequently caused by aging, trauma and degenerative joint diseases. Unfortunately, articular cartilage can hardly repair itself after injury, because of the absence of vascular, neural and lymphatic networks and progenitor cells, which attributes to further degeneration of articular cartilage and even causes disability (Gomoll and Minas 2014; Huey et al. 2012). In 2002, Kisiday et al. developed a self-assembling peptide KLD-12 (AcN-KLDLKLDLKLDL-CNH_2) hydrogel scaffolds for cartilage repair and used it as a 3D scaffold to encapsulate chondrocytes (Kisiday et al. 2002). Their results demonstrated that the chondrocytes in a 3D cell culture of KLD-12 peptide gels maintained a stable chondrocyte phenotype, and the cartilage-like ECM was rich in proteoglycans and type II collagen during the culture period *in vitro*. Over time, the material stiffness of ECM was increasing, which showed mechanically functional cartilage tissue. Then the peptide scaffolds KLD-12 were applied to explore the chondrogenic potentials of other cell types, such as bone marrow mesenchymal stem cells (BM-MSCs) and adipose-derived progenitor cells (ADPCs) (Kisiday et al. 2008). After 3 weeks culture in the presence transforming growth factor-β1 (TGF-β1), the ECM synthesis and accumulation was significant increased in KLD-12 gels but not in agarose hydrogels. The classical self-assembling peptide RAD16-I was also tested to encapsulate BMSCs, which provided the appropriate cell microenvironment for their chondrogenic differentiation (Kopesky et al. 2009).

In another study, self-assembling peptide KLD-12 hydrogels were modified to deliver TGF-β1 to encapsulate BMSCs in two different ways: tethered TGF-β1 (Teth-TGF) or adsorbed TGF-β1 (Ads-TGF), respectively (Kopesky et al. 2010). Kopesky and coworkers found that the Ads-TGF peptide hydrogels could stimulate chondrogenesis of BMSCs inducing cell proliferation and producing a cartilage-like ECM, whereas Teth-TGF could not. In 2010, Miller et al reported the in *vivo study* of KLD-12 peptide gels with or without chondrogenic factors (CF) and BMSCs for cartilage repair in a full-thickness, critically-sized, rabbit cartilage defect model (Miller et al. 2010). And their results showed that the KLD-12 scaffold hydrogel alone could fill full-thickness osteochondral defects in situ and improve the quality of repair, as well as increased osteophyte formation. In 2014, Miller et al. evaluated the performance of KLD-12 scaffold to fill a 15 mm cartilage defect with or without microfracture in an equine model (Miller et al. 2014). And their results demonstrated that only KLD-12-treated defect or treatment with only microfracture contributed to an improvement in clinical symptoms compared with no treatment, but the improvement were varied depending on the treatment.

Stupp's group designed a self-assembling PA molecule (HSNGLPLGGGSEEEAAAVVV(K)-$CO(CH_2)_{10}CH_3$) containing a binding sequence (HSNGLPL), which had a binding affinity to TGF-β1 (Shah et al. 2010). They proved that the PA scaffolds could support the cell viability and chondrogenic differentiation of MSCs *in vitro*. And the *in vivo* studies showed that the PA gels presenting TGF-β1 promoted hyaline cartilage regeneration in chondral defect microfracture rabbit model. Recently, Zhou et al. reported that both L-and D-form peptide hydrogels RADA16-I could afford the slow and sustained release of TGF-β1 (Zhou et al. 2016). These hydrogels promoted the proliferation of BMSCs.

18.3.4 Nerve Regeneration

The nervous system is the most important system of human body, which consists of central nervous system (CNS) and peripheral nervous system

(PNS). The damage to the nervous system may even lead to permanent severe neurological deficits and death. It is a challenging problem for doctors and scientists to repair the injured nervous system completely because of its limited capability of regeneration (Ai et al. 2013). The development of cellular therapies offer new therapeutic options for nerve regeneration and biomimetic self-assembling peptide hydrogels provide a beneficial microenvironment that both enhance the function of the transplanted cells and accelerate the regeneration of damage tissues (He et al. 2014; Koss and Unsworth 2016).

The encapsulation of various nerve cells in self-assembling peptide nanofiber scaffolds *in vitro* has been extensively investigated. In 2000, Holmes et al. demonstrated that RADA16-I and RADA16-II scaffolds could support extensive neurite outgrowth from several types of neuronal cells, including rat PC12 cells and freshly isolated primary cells (Holmes et al. 2000). In addition, they found that the SAP scaffolds did not cause detectable toxic effects *in vivo* when injected into the leg muscles of Fisher 344 rats. Subsequently, Semino et al. developed a 3D culture method to entrap hippocampal tissue slices in RADA16-I peptide nanofiber scaffolds (Semino et al. 2004). In 2004, Stupp' group reported neural progenitor cells differentiated selectively into neurons *in vitro* within a 3D PA scaffold, which was designed to present the neurite-promoting laminin epitope IKVAV to cells (Silva et al. 2004). In 2006, Gelain et al. designed a class of functionalized peptides for 3D culture of mouse adult neural stem cells (NSCs) by linking different bioactive motifs to RADA16-I (Gelain et al. 2006). In these designer scaffolds, they found that the RADA16-I containing bone marrow homing motifs BMHP1 (SKPPGTSS) and BMHP2 (PFSSTKT) could significantly promote the neural cell survival without the help of extra soluble growth factors. In another study, Gelain et al. developed several biotinylated self-assembling peptides derived from BMHP1 sequence with self-healing propensity and these scaffolds were verified to enhance the adhesion, differentiation, and proliferation of human NSCs (Gelain et al. 2011).

The application of biomimetic self-assembling peptide hydrogel for CNS injury has been reviewed previously (Liu et al. 2015). Here, we will focus on recent works of self-assembling peptide scaffolds for brain injuries, and acute or chronic spinal cord injuries. In 3D cell cultures or cell transplantation *in vivo*, the low pH of RADA16-I solutions could damage cells and even host tissues by injection. To overcome this problem, Sun et al. synthesized two oppositely charged peptides RADA16-RGD (Ac-$(RADA)_4$-DGDRGDS) and RADA16-IKVAV (Ac-$(RADA)_4$-RIKVAV), so that the hydrogel scaffold (-IKVAV/-RGD) could be formed when these two peptides solutions were mixed at neutral pH (Sun et al. 2016). *In vitro* study showed that NPCs/NSCs showed good survival and viability when directly mixed into -IKVAV/-RGD solutions before gelation. In addition, the -IKVAV/-RGD hydrogel scaffolds promoted the neuron and astrocyte differentiation of NPCs/NSCs without adding extra growth factors. And this hydrogel provided a suitable environment for Schwann cell recruitment and nerve regeneration in the spinal cord transection model. In 2017, Wang et al. designed a functionalized self-assembling peptide RADA16-SVVYGLR (AcN-$(RADA)_4$SVVYGLR-$CONH_2$), and its functional motif SVVYGLR was derived from osteopontin, which could promoted the adhesion, migration and tube formation of endothelial cells (Wang et al. 2017). This peptide hydrogel was proved to promote both angiogenesis and neurogenesis in an *in vivo* zebrafish brain injury model, as well as the functional recovery of the severed optic tectum.

Unlike CNS, PNS has certain ability to regenerate after injury. However, it cannot regenerate when the nerve lesion has a long distance. Recently, artificial nerve guidance conduits (NGCs) have been developed for the treatment of severe injuries with a long gap (Gu et al. 2014). Zhan et al. firstly reported that RADA16-I

hydrogel as a intraluminal filling was filled into an empty blood vessel conduit and implanted to repair a 10 mm nerve gap after sciatic nerve transection (Zhan et al. 2013). The results demonstrated that RADA16-I hydrogel scaffold accelerated axonal regeneration and remyelination, as well as functional recovery. Based on this experience, more studies using RADA16-I peptide and its derivative filled with different types of conducts have been done (Nune et al. 2017; Wang et al. 2014; Lu et al. 2018). In 2011, Angeloni et al. reported that sonic hedgehog (SHH) was delivered to the cavernous nerve by novel PA nanofibers (C_{16}-$V_2A_2E_2$-NH_2) (Angeloni et al. 2011). The *in vivo* study showed that SHH treatment via aligned PA promoted nerve regeneration, inhibited penile apoptosis and caused a 58% improvement in erectile function.

18.4 Conclusion and Perspectives

This chapter has reviewed most of the published work on biomimetic peptides as the building block to fabricate nanofiber hydrogel scaffolds for the application in tissue engineering. By molecular self-assembly, the 3D biomimetic hydrogel scaffolds could be constructed to mimic the native ECM. Numerous bioactive amino acid sequences derive from naturally occurring proteins have been designed and introduced to biomimetic self-assembling peptides, so that the functionalized peptide scaffold could regulate cell fate and cell function. In past two decades, the exciting findings of self-assembling peptide in *in vitro* culture systems and *in vivo* animal models show its great potential use in tissue repair for human being. Several products based on self-assembling peptide have been tested in clinical trials for different diseases, such as P_{11}−4 (CH_3CO-QQRFEWEFEQQ-$CONH_2$) (Brunton et al. 2013) and RADA16-I peptides (Yoshida et al. 2014). Although many advances on tissue engineering by biomimetic peptides have been achieved, there are still unresolved issues ahead with self-assembling peptides hydrogel. For example, it is difficult to control accurately the size and morphology of nanofibers in the process of peptide self-assembly, therefore these nanofibers are heterogeneous to some extent (Yu et al. 2016). In addition, the application of biomimetic peptide hydrogel scaffold for hard tissue engineering is limited because of its poor mechanical performance. The effort to improve the robustness of self-assembling peptides should be considered.

References

Aggeli A, Boden N, Cheng YL, Findlay JB, Knowles PF, Kovatchev P, Turnbull PJ (1996) Peptides modeled on the transmembrane region of the slow voltage-gated IsK potassium channel: structural characterization of peptide assemblies in the beta-strand conformation. Biochemistry 35(50):16213. https://doi.org/10.1021/bi960891g

Aggeli A, Bell M, Boden N, Keen JN, Knowles PF, McLeish TCB, Pitkeathly M, Radford SE (1997a) Responsive gels formed by the spontaneous self-assembly of peptides into polymeric β-sheet tapes. Nature 386:259. https://doi.org/10.1038/386259a0

Aggeli A, Bell M, Boden N, Keen JN, McLeish TCB, Nyrkova I, Radford SE, Semenov A (1997b) Engineering of peptide [small beta]-sheet nanotapes. J Mater Chem 7(7):1135–1145. https://doi.org/10.1039/A701088E

Aggeli A, Bell M, Carrick L, Fishwick C, Harding R, Mawer P, Radford S, Strong A, Boden N (2003) pH as a trigger of peptide beta-sheet self-assembly and reversible switching between nematic and isotropic phases. J Am Chem Soc 125(32):9619. https://doi.org/10.1021/ja021047i

Ai J, Kiasatdolatabadi A, Ebrahimibarough S, Lotfibakhshaiesh N (2013) Polymeric scaffolds in neural tissue engineering: a review. Arch Neurosci 1 (1):15–20. https://doi.org/10.5812/archneurosci.9144

Angeloni NL, Bond CW, Tang Y, Harrington DA, Zhang S, Stupp SI, McKenna KE, Podlasek CA (2011) Regeneration of the cavernous nerve by Sonic hedgehog using aligned peptide amphiphile nanofibers. Biomaterials 32(4):1091–1101. https://doi.org/10.1016/j.biomaterials.2010.10.003

Arnold MS, Guler MO, Hersam MC, Stupp SI (2005) Encapsulation of carbon nanotubes by self-assembling peptide amphiphiles. Langmuir 21(10):4705–4709. https://doi.org/10.1021/la0469452

Banwell EF, Abelardo ES, Adams DJ, Birchall MA, Corrigan A, Donald AM, Kirkland M, Serpell LC, Butler MF, Woolfson DN (2009) Rational design and application of responsive alpha-helical peptide hydrogels. Nat Mater 8(7):596–600. https://doi.org/10.1038/nmat2479

Beck K, Brodsky B (1998) Supercoiled protein motifs: the collagen triple-helix and the alpha-helical coiled coil. J Struct Biol 122(1–2):17. https://doi.org/10.1006/jsbi.1998.3965

Bellis SL (2011) Advantages of RGD peptides for directing cell association with biomaterials. Biomaterials 32(18):4205–4210. https://doi.org/10.1016/j.biomaterials.2011.02.029

Berndt P, Fields GB, Tirrell M (1995) Synthetic lipidation of peptides and amino acids: monolayer structure and properties. J Am Chem Soc 117(37):9515–9522. https://doi.org/10.1021/ja00142a019

Brunton PA, Davies RPW, Burke JL, Smith A, Aggeli A, Brookes SJ, Kirkham J (2013) Treatment of early caries lesions using biomimetic self-assembling peptides – a clinical safety trial. Bdj 215:E6. https://doi.org/10.1038/sj.bdj.2013.741

Bull SR, Guler MO, Bras RE, Meade TJ, Stupp SI (2005) Self-assembled peptide amphiphile nanofibers conjugated to MRI contrast agents. Nano Lett 5(1):1–4. https://doi.org/10.1021/nl0484898

Chen P (2005) Self-assembly of ionic-complementary peptides: a physicochemical viewpoint. Colloid Surf A 261(1–3):3–24. https://doi.org/10.1016/j.colsurfa.2004.12.048

Collier JH, Messersmith PB (2003) Enzymatic modification of self-assembled peptide structures with tissue transglutaminase. Bioconjug Chem 14(4):748–755. https://doi.org/10.1021/bc034017t

Cui HG, Webber MJ, Stupp SI (2010) Self-assembly of peptide amphiphiles: from molecules to nanostructures to biomaterials. Biopolymers 94(1):1–18. https://doi.org/10.1002/bip.21328

Davies RPW, Aggeli A (2011) Self-assembly of amphiphilic β-sheet peptide tapes based on aliphatic side chains. J Pept Sci 17(2):107–114. https://doi.org/10.1002/psc.1335

Davis ME, Motion JPM, Narmoneva DA, Takahashi T, Hakuno D, Kamm RD, Zhang S, Lee RT (2005) Injectable Self-Assembling Peptide Nanofibers Create Intramyocardial Microenvironments for Endothelial Cells. Circulation 111(4):442–450. https://doi.org/10.1161/01.cir.0000153847.47301.80

Dong H, Paramonov SE, Hartgerink JD (2008) Self-assembly of α-helical coiled coil nanofibers. J Am Chem Soc 130(41):13691–13695. https://doi.org/10.1021/ja8037323

Eilken HM, Adams RH (2010) Dynamics of endothelial cell behavior in sprouting angiogenesis. Curr Opin Cell Biol 22(5):617–625. https://doi.org/10.1016/j.ceb.2010.08.010

Eskandari S, Guerin T, Toth I, Stephenson RJ (2017) Recent advances in self-assembled peptides: implications for targeted drug delivery and vaccine engineering. Adv Drug Deliv Rev 110:169–187. https://doi.org/10.1016/j.addr.2016.06.013

Fishwick CWG, Beevers AJ, Carrick LM, Whitehouse CD, Aggeli A, Boden N (2003) Structures of helical β-tapes and twisted ribbons: the role of side-chain interactions on twist and bend behavior. Nano Lett 3(11):1475–1479. https://doi.org/10.1021/nl034095p

Fleming S, Debnath S, Frederix PWJM, Tuttle T, Ulijn RV (2013) Aromatic peptide amphiphiles: significance of the Fmoc moiety. Chem Commun 49(90):10587–10589. https://doi.org/10.1039/c3cc45822a

García AE, Sanbonmatsu KY (2002) α-Helical stabilization by side chain shielding of backbone hydrogen bonds. Proc Natl Acad Sci 99(5):2782–2787. https://doi.org/10.1089/ten.2006.12.2215

Garreta E, Genové E, Borrós S, Semino CE (2006) Osteogenic differentiation of mouse embryonic stem cells and mouse embryonic fibroblasts in a three-dimensional self-assembling peptide scaffold. Tissue Eng 12(8):2215–2227

Gelain F, Bottai D, Vescovi A, Zhang S (2006) Designer self-assembling peptide nanofiber scaffolds for adult mouse neural stem cell 3-dimensional cultures. Plos One 1(1):e119. https://doi.org/10.1371/journal.pone.0000119

Gelain F, Silva D, Caprini A, Taraballi F, Natalello A, Villa O, Nam KT, Zuckermann RN, Doglia SM, Vescovi A (2011) BMHP1-derived self-assembling peptides: hierarchically assembled structures with self-healing propensity and potential for tissue engineering applications. ACS Nano 5(3):1845–1859. https://doi.org/10.1021/nn102663a

Giannoudis PV, Dinopoulos H, Tsiridis E (2005) Bone substitutes: an update. Injury 36(3, Supplement):S20–S27. https://doi.org/10.1016/j.injury.2005.07.029

Gomoll AH, Minas T (2014) The quality of healing: articular cartilage. Wound Repair Regen 22:30–38. https://doi.org/10.1111/wrr.12166

Greenfield MA, Palmer LC, Vernizzi G, de la Cruz MO, Stupp SI (2009) Buckled membranes in mixed-valence ionic amphiphile vesicles. J Am Chem Soc 131(34):12030–12031

Gu X, Ding F, Williams DF (2014) Neural tissue engineering options for peripheral nerve regeneration. Biomaterials 35(24):6143–6156. https://doi.org/10.1016/j.biomaterials.2014.04.064

Guo H, Zhang JM, Xu T, Zhang ZD, Yao JR, Shao ZZ (2013) The robust hydrogel hierarchically assembled from a pH sensitive peptide amphiphile based on silk fibroin. Biomacromolecules 14(8):2733–2738. https://doi.org/10.1021/bm4005645

Habibi N, Kamaly N, Memic A, Shafiee H (2016) Self-assembled peptide-based nanostructures: smart nanomaterials toward targeted drug delivery. Nano Today 11(1):41–60. https://doi.org/10.1016/j.nantod.2016.02.004

Haines LA, Rajagopal K, Ozbas B, Salick DA, Pochan DJ, Schneider JP (2005) Light-activated hydrogel formation via the triggered folding and self-assembly of a designed peptide. J Am Chem Soc 127(48):17025–17029. https://doi.org/10.1021/ja054719o

Hamada K, Hirose M, Yamashita T, Ohgushi H (2008) Spatial distribution of mineralized bone matrix produced by marrow mesenchymal stem cells in self-

assembling peptide hydrogel scaffold. J Biomed Mater Res Part A 84A(1):128–136. https://doi.org/10.1002/jbm.a.31439

Hartgerink JD, Beniash E, Stupp SI (2001) Self-assembly and mineralization of peptide-amphiphile nanofibers. Science 294(5547):1684–1688. https://doi.org/10.1126/science.1063187

Hayashi K, Ochiaishino H, Shiga T, Onodera S, Saito A, Shibahara T, Azuma T (2016) Transplantation of human-induced pluripotent stem cells carried by self-assembling peptide nanofiber hydrogel improves bone regeneration in rat calvarial bone defects. BDJ Open 2:15007. https://doi.org/10.1038/bdjopen.2015.7

He B, Yuan X, Jiang D (2014) Molecular self-assembly guides the fabrication of peptide nanofiber scaffolds for nerve repair. RSC Adv 4(45):23610–23621. https://doi.org/10.1039/C4RA01826E

Holmes TC, de Lacalle S, Su X, Liu G, Rich A, Zhang S (2000) Extensive neurite outgrowth and active synapse formation on self-assembling peptide scaffolds. Proc Natl Acad Sci 97(12):6728–6733. https://doi.org/10.1073/pnas.97.12.6728

Horii A, Wang X, Gelain F, Zhang S (2007) Biological designer self-assembling peptide nanofiber scaffolds significantly enhance osteoblast proliferation, differentiation and 3-D migration. PloS One 2(2):e190. https://doi.org/10.1371/journal.pone.0000190

Hsieh PCH, Davis ME, Gannon J, MacGillivray C, Lee RT (2006) Controlled delivery of PDGF-BB for myocardial protection using injectable self-assembling peptide nanofibers. J Clin Invest 116(1):237–248. https://doi.org/10.1172/JCI25878

Huey DJ, Hu JC, Athanasiou KA (2012) Unlike bone, cartilage regeneration remains elusive. Science 338 (6109):917–921. https://doi.org/10.1126/science.1222454

Jayawarna V, Ali M, Jowitt TA, Miller AF, Saiani A, Gough JE, Ulijn RV (2006) Nanostructured hydrogels for three-dimensional cell culture through self-assembly of fluorenylmethoxycarbonyl–dipeptides. Adv Mater 18(5):611–614. https://doi.org/10.1002/adma.200501522

Jung JP, Jones JL, Cronier SA, Collier JH (2008) Modulating the mechanical properties of self-assembled peptide hydrogels via native chemical ligation. Biomaterials 29(13):2143–2151. https://doi.org/10.1016/j.biomaterials.2008.01.008

Khademhosseini A, Langer R (2016) A decade of progress in tissue engineering. Nat Protoc 11(10):1775–1781. https://doi.org/10.1038/nprot.2016.123

Kisiday J, Jin M, Kurz B, Hung H, Semino C, Zhang S, Grodzinsky A (2002) Self-assembling peptide hydrogel fosters chondrocyte extracellular matrix production and cell division: implications for cartilage tissue repair. Proc Natl Acad Sci 99(15):9996–10001. https://doi.org/10.1073/pnas.142309999

Kisiday JD, Kopesky PW, Evans CH, Grodzinsky AJ, McIlwraith CW, Frisbie DD (2008) Evaluation of adult equine bone marrow- and adipose-derived progenitor cell chondrogenesis in hydrogel cultures. J Orthop Res 26(3):322–331. https://doi.org/10.1002/jor.20508

Kopesky PW, Vanderploeg EJ, Sandy JS, Kurz B, Grodzinsky AJ (2009) Self-assembling peptide hydrogels modulate in vitro chondrogenesis of bovine bone marrow stromal cells. Tissue Eng Part A 16 (2):465–477. https://doi.org/10.1089/ten.TEA.2009.0158

Kopesky PW, Vanderploeg EJ, Kisiday JD, Frisbie DD, Sandy JD, Grodzinsky AJ (2010) Controlled delivery of transforming growth factor β1 by self-assembling peptide hydrogels induces chondrogenesis of bone marrow stromal cells and modulates Smad2/3 signaling. Tissue Eng Part A 17(1–2):83–92. https://doi.org/10.1089/ten.tea.2010.0198

Koss KM, Unsworth LD (2016) Neural tissue engineering: bioresponsive nanoscaffolds using engineered self-assembling peptides. Acta Biomater 44:2–15. https://doi.org/10.1016/j.actbio.2016.08.026

Koutsopoulos S (2016) Self-assembling peptide nanofiber hydrogels in tissue engineering and regenerative medicine: progress, design guidelines, and applications. J Biomed Mater Res Part A 104(4):1002–1016. https://doi.org/10.1002/jbm.a.35638

Kumar VA, Wang BK, Kanahara SM (2016) Rational design of fiber forming supramolecular structures. Exp Biol Med 241(9):899–908. https://doi.org/10.1177/1535370216640941

Langer R, Vacanti JP (1993) Tissue Eng Sci 260 (5110):920–926. https://doi.org/10.1126/science.8493529

Li WW, Talcott KE, Zhai AW, Kruger EA, Li VW (2005) The role of therapeutic angiogenesis in tissue repair and regeneration. Adv Skin Wound Care 18 (9):491–500

Li X, Chen YY, Wang XM, Gao K, Gao YZ, Cao J, Zhang ZL, Lei J, Jin ZY, Wang YN (2017) Image-guided stem cells with functionalized self-assembling peptide nanofibers for treatment of acute myocardial infarction in a mouse model. Am J Transl Res 9(8):3723–3731

Liu X, Wang X, Horii A, Wang X, Qiao L, Zhang S, Cui FZ (2012) In vivo studies on angiogenic activity of two designer self-assembling peptide scaffold hydrogels in the chicken embryo chorioallantoic membrane. Nanoscale 4(8):2720–2727. https://doi.org/10.1039/C2NR00001F

Liu X, Pi B, Wang H, Wang XM (2015) Self-assembling peptide nanofiber hydrogels for central nervous system regeneration. Front Mater Sci 9(1):1–13. https://doi.org/10.1007/s11706-015-0274-z

Loo Y, Zhang S, Hauser CA (2012) From short peptides to nanofibers to macromolecular assemblies in biomedicine. Biotechnol Adv 30(3):593–603. https://doi.org/10.1016/j.biotechadv.2011.10.004

Lu JJ, Sun X, Yin HY, Shen XZ, Yang SH, Wang Y, Jiang WL, Sun Y, Zhao LY, Sun XD, Lu SB, Mikos AG, Peng J, Wang XM (2018) A neurotrophic peptide-functionalized selfassembling peptide nanofiber

hydrogel enhances rat sciatic nerve regeneration. Nano Res. https://doi.org/10.1007/s12274-018-2041-9
Lupas AN, Gruber M (2005) The structure of α-helical coiled coils. Adv Protein Chem 70:37–38
Ma PX (2008) Biomimetic materials for tissue engineering. Adv Drug Deliv Rev 60(2):184–198. https://doi.org/10.1016/j.addr.2007.08.041
Mandal D, Nasrolahi SA, Parang K (2014) Self-assembly of peptides to nanostructures. Org Biomol Chem 12 (22):3544–3561. https://doi.org/10.1039/C4OB00447G
Mata A, Geng Y, Henrikson KJ, Aparicio C, Stock SR, Satcher RL, Stupp SI (2010) Bone regeneration mediated by biomimetic mineralization of a nanofiber matrix. Biomaterials 31(23):6004–6012. https://doi.org/10.1016/j.biomaterials.2010.04.013
Matson JB, Zha RH, Stupp SI (2011) Peptide self-assembly for crafting functional biological materials. Curr Opin Solid State Mater Sci 15(6):225–235. https://doi.org/10.1016/j.brainresbull.2010.07.001
McGrath AM, Novikova LN, Novikov LN, Wiberg M (2010) BD™ PuraMatrix™ peptide hydrogel seeded with Schwann cells for peripheral nerve regeneration. Brain Res Bull 83(5):207–213
Mehrban N, Abelardo E, Wasmuth A, Hudson KL, Mullen LM, Thomson AR, Birchall MA, Woolfson DN (2014) Assessing cellular response to functionalized alpha-helical peptide hydrogels. Adv Healthc Mater 3 (9):1387–1391. https://doi.org/10.1002/adhm.201400065
Meng Q, Yao S, Wang X, Chen Y (2014) RADA16: a self-assembly peptide hydrogel for the application in tissue regeneration. J Biomater Tissue Eng 4(12):1019–1029. https://doi.org/10.2106/JBJS.M.01408
Micklitsch CM, Knerr PJ, Branco MC, Nagarkar R, Pochan DJ, Schneider JP (2011) Zinc-triggered hydrogelation of a self-assembling β-hairpin peptide. Angew Chem 50(7):1577–1579. https://doi.org/10.1002/ange.201006652
Miller RE, Grodzinsky AJ, Vanderploeg EJ, Lee C, Ferris DJ, Barrett MF, Kisiday JD, Frisbie DD (2010) Effect of self-assembling peptide, chondrogenic factors, and bone marrow-derived stromal cells on osteochondral repair. Osteoarthr Cartil 18(12):1608–1619. https://doi.org/10.1016/j.joca.2010.09.004
Miller RE, Grodzinsky AJ, Barrett MF, Hung HH, Frank EH, Werpy NM, Mcilwraith CW, Frisbie DD (2014) Effects of the combination of microfracture and self-assembling peptide filling on the repair of a clinically relevant trochlear defect in an equine model. J Bone Joint Surg Am 96(19):1601
Moradi F, Bahktiari M, Joghataei MT, Nobakht M, Soleimani M, Hasanzadeh G, Fallah A, Zarbakhsh S, Hejazian LB, Shirmohammadi M (2012) BD PuraMatrix peptide hydrogel as a culture system for human fetal Schwann cells in spinal cord regeneration. J Neurosci Res 90(12):2335–2348. https://doi.org/10.1002/jnr.23120
Moutevelis E, Woolfson DN (2009) A periodic table of coiled-coil protein structures. J Mol Biol 385 (3):726–732. https://doi.org/10.1016/j.jmb.2008.11.028
Narmoneva DA, Oni O, Sieminski AL, Zhang S, Gertler JP, Kamm RD, Lee RT (2005) Self-assembling short oligopeptides and the promotion of angiogenesis. Biomaterials 26(23):4837–4846. https://doi.org/10.1021/ja028215r
Niece KL, Hartgerink JD, Donners JJ, Stupp SI (2003) Self-assembly combining two bioactive peptide-amphiphile molecules into nanofibers by electrostatic attraction. J Am Chem Soc 125(24):7146–7147
Nune M, Subramanian A, Krishnan UM, Kaimal SS, Sethuraman S (2017) Self-assembling peptide nanostructures on aligned poly (lactide-co-glycolide) nanofibers for the functional regeneration of sciatic nerve. Nanomed Nanotechnol Biol Med 12 (3):219–235. https://doi.org/10.2217/nnm-2016-0323
Ogawa Y, Yoshiyama C, Kitaoka T (2012) Helical assembly of azobenzene-conjugated carbohydrate hydrogelators with specific affinity for lectins. Langmuir 28(9):4404–4412. https://doi.org/10.1021/jp075117p
Orbach R, Adler-Abramovich L, Zigerson S, Mironi-Harpaz I, Seliktar D, Gazit E (2009) Self-assembled Fmoc-peptides as a platform for the formation of nanostructures and hydrogels. Biomacromolecules 10 (9):2646–2651. https://doi.org/10.1021/bm900584m
Ozbas B, Rajagopal K, Hainesbutterick L, Schneider JP, Pochan DJ (2007) Reversible stiffening transition in β-hairpin hydrogels induced by ion complexation. J Phys Chem B 111(50):13901
Palmer LC, Stupp SI (2008) Molecular self-assembly into one-dimensional nanostructures. Acc Chem Res 41 (12):1674–1684. https://doi.org/10.1021/ar8000926
Pandya MJ, Spooner GM, Sunde M, Thorpe JR, Rodger A, Woolfson DN (2000) Sticky-end assembly of a designed peptide fiber provides insight into protein fibrillogenesis. Biochemistry 39(30):8728–8734. https://doi.org/10.1021/bi000246g
Pape HC, Evans A, Kobbe P (2010) Autologous bone graft: properties and techniques. J Orthop Trauma 24:S36–S40. https://doi.org/10.1097/BOT.0b013e3181cec4a1
Pashuck ET, Stupp SI (2010) Direct observation of morphological tranformation from twisted ribbons into helical ribbons. J Am Chem Soc 132(26):8819–8821. https://doi.org/10.1021/ja100613w
Pauling L, Corey RB, Branson HR (1951) The structure of proteins; two hydrogen-bonded helical configurations of the polypeptide chain. P Natl Acad Sci USA 37 (4):205–211. https://doi.org/10.1073/pnas.37.4.205
Pérez CMR, Stephanopoulos N, Sur S, Lee SS, Newcomb C, Stupp SI (2015) The powerful functions of peptide-based bioactive matrices for regenerative medicine. Ann Biomed Eng 43(3):501–514. https://doi.org/10.1007/s10439-014-1166-6
Petka WA, Harden JL, McGrath KP, Wirtz D, Tirrell DA (1998) Reversible hydrogels from self-assembling artificial proteins. Science 281(5375):389–392. https://doi.org/10.1126/science.281.5375.389

Pochan DJ, Schneider JP, Kretsinger J, Ozbas B, Rajagopal K, Haines L (2003) Thermally reversible hydrogels via intramolecular folding and consequent self-assembly of a de novo designed peptide. J Am Chem Soc 125(39):11802. https://doi.org/10.1021/ja0353154

Pugliese R, Gelain F (2017) Peptidic biomaterials: from self-assembling to regenerative medicine. Trends Biotechnol 35(2):145. https://doi.org/10.1016/j.tibtech.2016.09.004

Rajagopal K, Lamm MS, Hainesbutterick LA, Pochan DJ, Schneider JP (2009) Tuning the pH responsiveness of beta-hairpin peptide folding, self-assembly, and hydrogel material formation. Biomacromolecules 10 (9):2619

Risau W (1997) Mechanisms of angiogenesis. Nature 386 (6626):671–674. https://doi.org/10.1021/bm900544e

Robson Marsden H, Kros A (2010) Self-assembly of coiled coils in synthetic biology: inspiration and progress. Angew Chem Int Ed 49(17):2988–3005. https://doi.org/10.1002/anie.200904943

Schneider ‡ DJP, Ozbas B, Rajagopal K, Lisa Pakstis A, Kretsinger J (2002) Responsive hydrogels from the intramolecular folding and self-assembly of a designed peptide. J Am Chem Soc 124(50):15030. https://doi.org/10.1089/107632704323061997

Semino CE, Kasahara J, Hayashi Y, Zhang S (2004) Entrapment of migrating hippocampal neural cells in three-dimensional peptide nanofiber scaffold. Tissue Eng 10(3-4):643–655

Shah RN, Shah NA, Lim MMDR, Hsieh C, Nuber G, Stupp SI (2010) Supramolecular design of self-assembling nanofibers for cartilage regeneration. Proc Natl Acad Sci 107(8):3293–3298

Shin H, Jo S, Mikos AG (2003) Biomimetic materials for tissue engineering. Biomaterials 24(24):4353–4364. https://doi.org/10.1016/S0142-9612(03)00339-9

Silva GA, Czeisler C, Niece KL, Beniash E, Harrington DA, Kessler JA, Stupp SI (2004) Selective differentiation of neural progenitor cells by high-epitope density nanofibers. Science 303(5662):1352–1355. https://doi.org/10.1126/science.1093783

Smith AM, Banwell EF, Edwards WR, Pandya MJ, Woolfson DN (2006) Engineering increased stability into self-assembled protein fibers. Adv Funct Mater 16 (8):1022–1030. https://doi.org/10.1002/adfm.200500568

Smith AM, Williams RJ, Tang C, Coppo P, Collins RF, Turner ML, Saiani A, Ulijn RV (2008) Fmoc-Diphenylalanine self assembles to a hydrogel via a novel architecture based on pi-pi interlocked beta-sheets. Adv Mater 20(1):37–41. https://doi.org/10.1002/adma.200701221

Sone ED, Zubarev ER, Stupp SI (2002) Semiconductor nanohelices templated by supramolecular ribbons. Angew Chem Int Ed 41(10):1705–1709. https://doi.org/10.1097/TP.0b013e3181806d9d

Spoerke ED, Anthony SG, Stupp SI (2009) Enzyme directed templating of artificial bone mineral. Adv Mater 21(4):425–430. https://doi.org/10.1002/adma.200802242

Stendahl JC, Wang L-J, Chow LW, Kaufman DB, Stupp SI (2008) Growth factor delivery from self-assembling nanofibers to facilitate islet transplantation. Transplantation 86(3):478

Sun Y, Li W, Wu X, Zhang N, Zhang Y, Ouyang S, Song X, Fang X, Seeram R, Xue W (2016) Functional self-assembling peptide nanofiber hydrogels designed for nerve degeneration. ACS Appl Mater Interfaces 8 (3):2348–2359. https://doi.org/10.1021/acsami.5b11473

Sun L, Zheng C, Webster TJ (2017) Self-assembled peptide nanomaterials for biomedical applications: promises and pitfalls. Int J Nanomed 12:73. https://doi.org/10.2147/IJN.S117501

Takumi T (1993) A protein with a single transmembrane domain forms an ion channel. Physiology 8 (4):175–178

Takumi T, Ohkubo H, Nakanishi S (1988) Cloning of a membrane protein that induces a slow voltage-gated potassium current. Science 242(4881):1042

Tashiro K-i, Sephel GC, Weeks B, Sasaki M, Martin GR, Kleinman HK, Yamada Y (1989) A synthetic peptide containing the IKVAV sequence from the A chain of laminin mediates cell attachment, migration, and neurite outgrowth. J Biol Chem 264(27):16174–16182

Ulijn RV, Smith AM (2008) Designing peptide based nanomaterials. Chem Soc Rev 37(4):664–675. https://doi.org/10.1039/B609047H

Vacanti JP, Langer R (1999) Tissue engineering: the design and fabrication of living replacement devices for surgical reconstruction and transplantation. Lancet 354:Si32–Si34. https://doi.org/10.1016/S0140-6736(99)90247-7

Walshaw J, Woolfson DN (2001) Socket: a program for identifying and analysing coiled-coil motifs within protein structures. J Mol Biol 307(5):1427–1450. https://doi.org/10.1006/jmbi.2001.4545

Wang X, Horii A, Zhang S (2008) Designer functionalized self-assembling peptide nanofiber scaffolds for growth, migration, and tubulogenesis of human umbilical vein endothelial cells. Soft Matter 4(12):2388–2395

Wang XM, Lin Q, Horii A (2011) Screening of functionalized self-assembling peptide nanofiber scaffolds with angiogenic activity for endothelial cell growth. Prog Nat Sci Mater Int 21(2):111–116. https://doi.org/10.1039/B807155A

Wang X, Pan M, Wen J, Tang Y, Hamilton AD, Li Y, Qian C, Liu Z, Wu W, Guo J (2014) A novel artificial nerve graft for repairing long-distance sciatic nerve defects: a self-assembling peptide nanofiber scaffold-containing poly (lactic-co-glycolic acid) conduit. Neural Regen Res 9(24):2132. https://doi.org/10.4103/1673-5374.147944

Wang TW, Chang KC, Chen LH, Liao SY, Yeh CW, Chuang YJ (2017) Effects of an injectable functionalized self-assembling nanopeptide hydrogel on angiogenesis and neurogenesis for regeneration of the central nervous system. Nanoscale 9(42):16281–16292. https://doi.org/10.1039/C7NR06528K

Webber MJ, Tongers J, Newcomb CJ, Marquardt K-T, Bauersachs J, Losordo DW, Stupp SI (2011) Supramolecular nanostructures that mimic VEGF as a strategy for ischemic tissue repair. Proc Natl Acad Sci 108 (33):13438–13443. https://doi.org/10.1073/pnas.1016546108

Whitesides GM, Grzybowski B (2002) Self-assembly at all scales. Science 295(5564):2418–2421. https://doi.org/10.1126/science.1070821

Whitesides GM, Mathias JP, Seto CT (1991) Molecular self-assembly and nanochemistry – a chemical strategy for the synthesis of nanostructures. Science 254 (5036):1312–1319. https://doi.org/10.1126/science.1962191

Woolfson DN (2001) Core-directed protein design. Curr Opin Struct Biol 11(4):464–471. https://doi.org/10.1016/S0959-440X(00)00234-7

Woolfson DN (2010) Building fibrous biomaterials from alpha-helical and collagen-like coiled-coil peptides. Pept Sci 94(1):118. https://doi.org/10.1002/bip.21345

Wu G, Pan M, Wang X, Wen J, Cao S, Li Z, Li Y, Qian C, Liu Z, Wu W (2015) Osteogenesis of peripheral blood mesenchymal stem cells in self assembling peptide nanofiber for healing critical size calvarial bony defect. Sci Rep 5. https://doi.org/10.1038/srep16681

Xu FM, Wang HB, Zhao J, Liu XS, Li DD, Chen CJ, Ji J (2013) Chiral packing of cholesteryl group as an effective strategy to get low molecular weight supramolecular hydrogels in the absence of intermolecular hydrogen bond. Macromolecules 46(11):4235–4246. https://doi.org/10.1021/ma400276u

Yanlian Y, Ulung K, Xiumei W, Horii A, Yokoi H, Shuguang Z (2009) Designer self-assembling peptide nanomaterials. Nano Today 4(2):193–210. https://doi.org/10.1016/j.nantod.2009.02.009

Ye Z, Zhang H, Luo H, Wang S, Zhou Q, Du X, Tang C, Chen L, Liu J, Shi YK (2008) Temperature and pH effects on biophysical and morphological properties of self-assembling peptide RADA16-I. J Pept Sci 14 (2):152–162. https://doi.org/10.1002/psc.988

Yokoi H, Kinoshita T, Zhang S (2005) Dynamic reassembly of peptide RADA16 nanofiber scaffold. Proc Natl Acad Sci U S A 102(24):8414–8419. https://doi.org/10.1073/pnas.0407843102

Yoshida M, Goto N, Kawaguchi M, Koyama H, Kuroda J, Kitahora T, Iwasaki H, Suzuki S, Kataoka M, Takashi F, Kitajima M (2014) Initial clinical trial of a novel hemostat, TDM-621, in the endoscopic treatments of the gastric tumors. J Gastroenterol Hepatol 29:77–79. https://doi.org/10.1111/jgh.12798

Yu Z, Cai Z, Chen Q, Liu M, Ye L, Ren J, Liao W, Liu S (2016) Engineering [small beta]-sheet peptide assemblies for biomedical applications. Biomater Sci 4(3):365–374. https://doi.org/10.1039/C5BM00472A

Zhan X, Gao M, Jiang Y, Zhang W, Wong WM, Yuan Q, Su H, Kang X, Dai X, Zhang W (2013) Nanofiber scaffolds facilitate functional regeneration of peripheral nerve injury. Nanomed Nanotechnol Biol Med 9 (3):305–315. https://doi.org/10.1016/j.nano.2012.08.009

Zhang SG (2003) Fabrication of novel biomaterials through molecular self-assembly. Nat Biotechnol 21 (10):1171–1178. https://doi.org/10.1038/nbt874

Zhang SG, Altman M (1999) Peptide self-assembly in functional polymer science and engineering. React Funct Polym 41(1-3):91–102. https://doi.org/10.1016/S1381-5148(99)00031-0

Zhang SG, Holmes T, Lockshin C, Rich A (1993) Spontaneous assembly of a self-complementary oligopeptide to form a stable macroscopic membrane. P Natl Acad Sci USA 90(8):3334–3338. https://doi.org/10.1073/pnas.90.8.3334

Zhang SG, Lockshin C, Cook R, Rich A (1994) Unusually stable beta-sheet formation in an ionic self-complementary oligopeptide. Biopolymers 34 (5):663–672. https://doi.org/10.1002/bip.360340508

Zhang S, Holmes TC, DiPersio CM, Hynes RO, Su X, Rich A (1995) Self-complementary oligopeptide matrices support mammalian cell attachment. Biomaterials 16(18):1385–1393. https://doi.org/10.1016/0142-9612(95)96874-Y

Zhang SG, Gelain F, Zhao XJ (2005) Designer self-assembling peptide nanofiber scaffolds for 3D tissue cell cultures. Semin Cancer Biol 15(5):413–420. https://doi.org/10.1016/j.semcancer.2005.05.007

Zhang JM, Hao RW, Huang L, Yao JR, Chen X, Shao ZZ (2011) Self-assembly of a peptide amphiphile based on hydrolysed Bombyx mori silk fibroin. Chem Commun 47 (37):10296–10298. https://doi.org/10.1039/c1cc12633d

Zhou A, Chen S, He B, Zhao W, Chen X, Jiang D (2016) Controlled release of TGF-beta 1 from RADA self-assembling peptide hydrogel scaffolds. Drug Des Devel Ther 10:3043–3051. https://doi.org/10.2147/DDDT.S109545

Ziv G, Haran G, Thirumalai D (2005) Ribosome exit tunnel can entropically stabilize α-helices. P Natl Acad Sci USA 102(52):18956–18961. https://doi.org/10.1073/pnas.0508234102

Bioartificial Esophagus: Where Are We Now?

19

Eun-Jae Chung

19.1 Introduction

The response to tissue injury in adult mammals is well documented in the literature (Diegelmann and Evans 2004; Metz 2003). However, the potential of functional regeneration is expressed only in selected tissues, such as the skin (Adolphe and Wainwright 2005), bone marrow (Lewis and Trobraughfe 1964), intestinal epithelium (Potten et al. 1984), and liver (Michalopoulos 2007). Tissues that do not possess functional regenerative potential after injury can lead to serious morbidity, aesthetic deformity, and mortality. To minimize morbidity, the current treatment options for tissue loss include replacement therapies, medical devices, and reconstructive surgery (Sweet et al. 2006; Saxena 2014).

Treating esophageal disorders such as esophageal cancer requires the surgical removal of the affected area, but the esophagus is a complicated organ made of non-redundant tissue that does not have regenerative capacity. Hence, the only feasible treatment option for extensive structural loss is the surgical replacement of the damaged esophagus. Several options have been described for treating this condition, and the most common procedure is the gastric pull-up technique, which substitutes tissue conduits harvested from the colon or jejunum (Poghosyan et al. 2011; Shen et al. 2013). However, the use of gastrointestinal segments can cause various surgical morbidities and mortality because additional abdominal surgery is required at the expense of other anatomic structures (Tan et al. 2012). Therefore, tissue engineering and regenerative medicine have emerged as promising approaches to mimic the native esophageal tissue that could be implanted as an artificial graft.

This article presents a review of the progress made in the field of regenerative medicine for esophageal reconstruction from bench to bedside.

19.2 The Human Esophagus

The esophagus is a long, continuous muscular tube that connects the pharynx and the stomach. The adult human esophagus is an 18 ~ 25 cm long, and it transverses the neck, thorax, and abdomen. It has two muscular rings or sphincters that regulate the content of esophagus, with one at the top (upper esophageal sphincter) and one at the bottom (lower esophageal sphincter) (Saxena 2014).

Histologically, there are four concentric layers in the esophagus: mucosa, submucosa, muscularis externa, and adventitia. The mucosa, which is composed of stratified squamous epithelium, plays a major role in the barrier or protective function of the digestive system. The submucosa

E.-J. Chung (✉)
Department of Otorhinolaryngology-Head and Neck Surgery, College of Medicine, Seoul National University, Seoul, South Korea
e-mail: voicechung@snu.ac.kr

I. Noh (ed.), *Biomimetic Medical Materials*, Advances in Experimental Medicine and Biology 1064,
https://doi.org/10.1007/978-981-13-0445-3_19

is a loose connective tissue that consists of blood vessels, nerves, and small glands, and it secretes mucous to aid food passage. The muscularis externa consists of two layers of smooth muscle that are arranged in inner circular and outer longitudinal directions and generate the coordinated contractions known as peristalsis. Once the swallowing (deglutition) process is started as a voluntary process, esophageal peristalsis is initiated through parasympathetic and sympathetic innervation by a well-orchestrated series of muscle contractions, including that of the sphincters (Londono and Badylak 2015; Skandalakis and Ellis 2000). The longitudinal muscle layer distal to the bolus contracts to expand the esophagus, and the circular muscle layer proximal to the bolus contracts to pump the bolus towards the stomach (Saxena 2014).

To achieve more functional properties for a tissue-engineered construct, the scaffold should mimic the architecture of the native esophagus. Optimally, the tissue-engineered scaffold should be integrated into the native tissue without leakage (early post-implantation) and stenosis (late post-implantation). To enable food transfer in an artificial esophagus without early or late complication, having the adequate mechanical characteristics is extremely important. The esophagus is constantly exposed to repeated cycles of stretching and should have a considerable degree of compliance. Hence, the viscoelasticity and dilatation/burst strength of the scaffold should have similar characteristics to the native esophagus (Kuppan et al. 2012). The scaffolds being too flaccid can lead to rupture or leakage and cause serious complications, such as mediastinitis. In contrast, a scaffold that has little compliance may obstruct the esophageal lumen and prevent food passage.

The ideal esophageal substitute should have biocompatibility, biodegradation and resistance to gastric acid reflux. In addition, the substitute should have the properties of cell adhesion, infiltration and proliferation, and it should not cause inflammation or infection. The suture retention strength also should be adequate to resist the pressure of the food bolus.

19.3 The Esophagus and Regenerative Medicine

An engineered esophageal tissue, which can be used to create a functional esophagus, avoids the necessity of esophagectomy and preserves the integrity of the esophagus. However, although tissue engineering potentially offers an alternative to the current treatments of esophageal defects, there are high barriers for its clinical application. There are serious clinical problems and significant heterogeneities among studies. Leakage of the anastomosis site, life-threatening infections and inflammation, and stenotic changes related to poor re-epithelization and poor muscle regeneration likely remain significant challenges to address. To overcome these limitations by using a tissue engineering approach, an optimal scaffold and the cell sources must be addressed (Maghsoudlou et al. 2014).

The pathologies affecting the esophagus are diverse, and the involved anatomic extents also differ case by case. For example, whereas the purpose of regenerative medicine strategies for esophageal mucosal injury and superficial esophageal cancer is the mucosal regeneration of congenital abnormalities, transmural esophageal injury and deep invasive esophageal cancer both require reconstructing an entire layer of the esophagus (Fig. 19.1).

Endoscopic resection for superficial esophageal cancer or premalignant lesion (endoscopic submucosal dissection) is a minimally invasive surgical procedure that has low morbidity. However, the incidence of stenosis leading to dysphagia is still high in endoscopic submucosal dissection (Chian et al. 2015). Even after a successful procedure, repeated postsurgical dilation should be considered in more than 50% of such cases (Londono and Badylak 2015). A tissue-engineered patch construct could be an attractive solution to prevent recurrent stenosis (Chian et al. 2015). Transmural defects are divided into partial and circumferential defects. Among the transmural defects, circumferential defects (360 degree, transmural) are a more significant challenge (Londono and Badylak 2015).

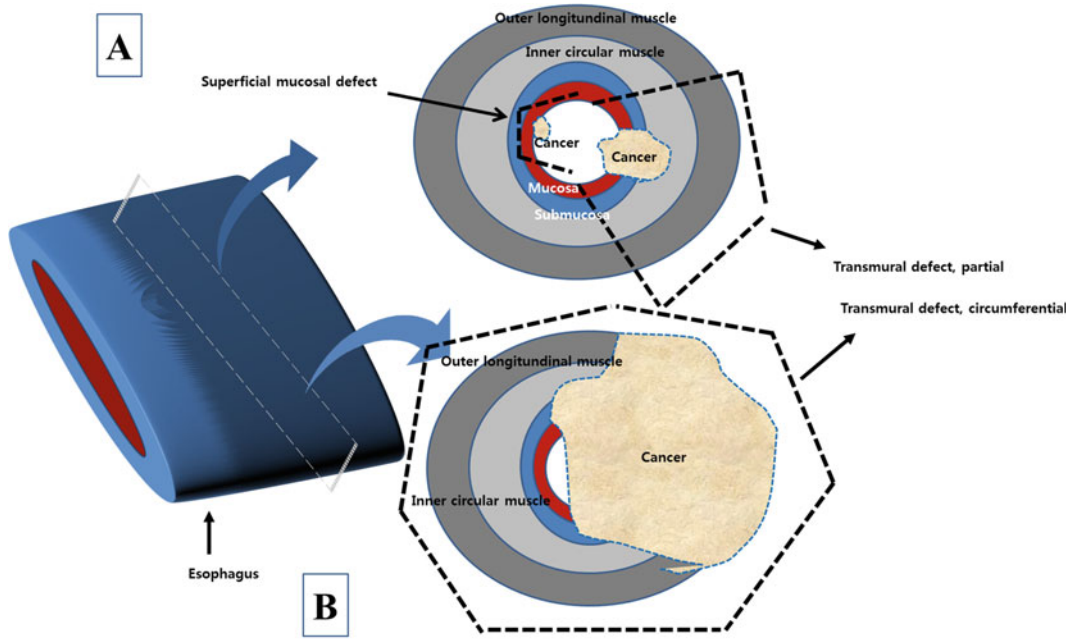

Fig. 19.1 Classification of esophageal defects according to tumor extent. (**a**) Superficial mucosa/submucosa defect (endoscopic mucosal resection). (**b**) Transmural partial esophageal defect (mucosa/submucosa/muscle). andtransmural circumferential esophageal defect for advanced tumor

19.4 Animal Models for Esophageal Reconstruction

Different types of animal models can be used, according to the extent of the defect, in tissue engineering strategies for esophageal reconstruction (Londono and Badylak 2015). An animal model for esophageal mucosal resection has been realized in rodents (Nieponice et al. 2013), dog (Badylak et al. 2005; Nieponice et al. 2009), and pig (Farrell et al. 2001). These are important models for treating early-stage esophageal cancer that preserve the remaining layers of the esophagus. The primary objectives of this animal model are aimed toward mucosal regeneration to prevent stricture.

Full-thickness transmural defects can include part of or the full circumference of the esophagus. Post-operative wound care should be carefully considered in a full-thickness defect model, especially for a circumferential defect (360 degree, transmural). A full-thickness partial defect model has been described in the pig (Jönsson et al. 2014), dog (Badylak et al. 2000), and rat (Sjöqvist et al. 2014). A significant portion of the normal esophageal tissue was preserved in these partial full-thickness models. Therefore, in most cases, an oral diet is possible starting in the immediate post-operative period. However, full-thickness circumferential defects are technically challenging, and surgical techniques such as micro-suture are required to achieve successful transplantation, especially in the murine esophagus (Londono and Badylak 2015; Kuppan et al. 2012). Anastomosis site leakage and necrosis of the implanted artificial esophagus inevitably lead to contamination of the surrounding space and mortality because the leakage site is anatomically close to the aseptic space (e.g., mediastinum and neck compartments) (Zhang et al. 2006). Therefore, it is extremely important to prevent food or saliva accumulation in the wound (Fig. 19.2), and a nasogastric tube, gastrostomy or intravenous nutrition is often required in cases of transplantation to minimize morbidity and mortality in the transplanted animals. Further, non-oral feeding should be considered until the primary wound

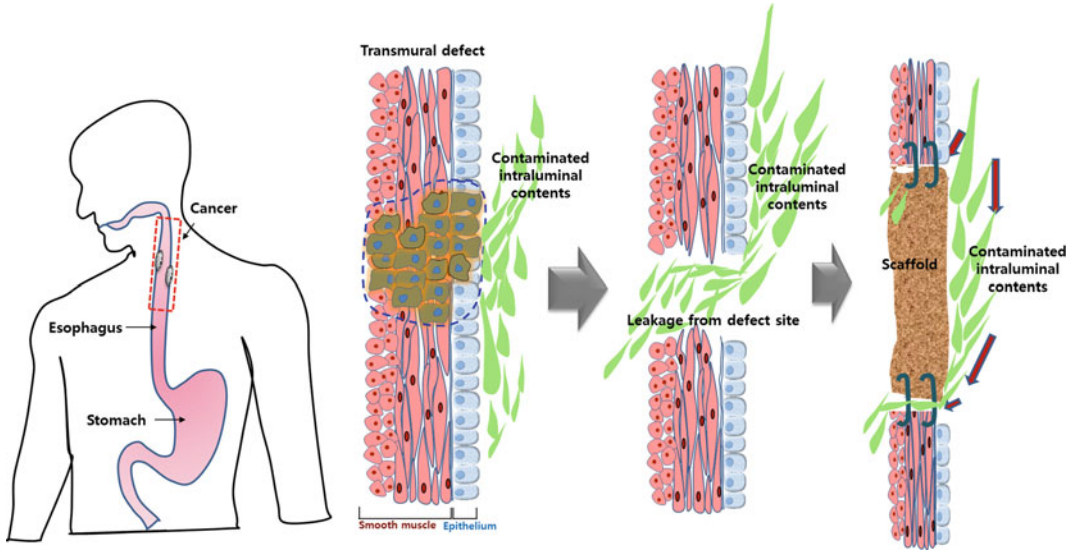

Fig. 19.2 The concept of anastomosis site leakage and contamination from the intraluminal contents. To achieve optimal graft survival for esophageal reconstruction, it is essential to minimize the inflammation at the implant site from the contaminated intraluminal contents

healing is completed (post-operative 1 or 2 weeks). Large animal models (i.e., dogs) undergoing circumferential esophageal defect reconstruction are technically easier to consider in the transmural defect model. The size of their esophagus is bigger, which allows easier surgical implantation and continuous food passage, even without local peristalsis. Moreover, large animals can be fed only by intravenous hyperalimentation for 2–4 weeks after implanting the prosthesis (Londono and Badylak 2015). However, such a non-oral feeding model has not been established in a murine model. A nasogastric tube is impossible for most animals, and a gastrostomy model is unavailable for the adult rat because the device is often damaged by self-biting. Several intragastric infusion techniques have been reported over the past 20 years in infant rodent models. For instance, Zhang et al. reported that tube-inserted gastrostomy was attempted to investigate the use of probiotics to regulate intestinal inflammation in an infant rat model (Zhang et al. 2006). Li et al. also examined the effects of glutamine and glutamate on the developing rat small intestine using a gastrostomy-fed "pup-in-a-cup" rat model (Li et al. 2004). Most gastrostomy studies have been performed on neonatal rats or mice, but none have been successful in adult rats. Researchers have been unable to maintain the feeding tube in the adult rat for a long time because rats are extremely active and uncontrollable.

19.5 Biomaterials for Esophageal Reconstruction

The general essential properties of scaffolds are to be non-toxic to host cells, have a matched degradation rate of the scaffold with the tissue remodeling rate, attract host esophageal epithelial-smooth muscle cells into the scaffold, and avoid the default inflammatory/scar tissue response (Chian et al. 2015). Moreover, the special environment of the esophagus should be considered: (1) continuously contacting contaminated saliva, bacteria, and food material; (2) closed with breathing and open with swallowing; (3) peristalsis; and (4) exposure to gastric acid.

There have been reports of using biologic and synthetic materials for esophageal reconstruction. Synthetic biomaterials can typically be manufactured with precision, and the mechanical characteristics can be finely tuned for various applications. However, synthetic materials can easily cause a foreign body reaction. In contrast, biologic scaffolds can promote a friendlier host response and remodeling, but they tend to have inferior mechanical and tunable properties (Londono and Badylak 2015). To reduce the complications after the implantation of acellular scaffolds, cellular grafts have shown better early tissue remodeling, adequate inflammatory responses, and prevention of stricture in esophageal reconstruction (Chian et al. 2015).

For esophageal tissue engineering, esophageal epithelial cell (EEC) regeneration is a prerequisite to prevent the leakage of contaminated saliva, bacteria or food material from the inside of the tissue. Saxena et al. (2009) investigated in vitro esophageal epithelium generation, survivability on a collagen scaffold and oriented smooth muscle cell regeneration on unidirectional basement membrane matrix (BMM)-coated collagen scaffolds for up to 8 weeks. REEC differentiation to the mature esophageal epithelium was complete after 14 days, and oriented smooth muscle strands were identified on the scaffold. Another study analyzed the growth of REECs in 3-dimensional collagen scaffolds. The REECs organized after 48 h and formed clusters after 72–96 h. The organization of the EEC was complete after 7 days in culture, and the characteristics of the mature esophageal epithelium were identified after 14 days of culture. Ovine esophageal epithelial cells (OEECs) seeded on three-dimensional scaffolds were viable for 6 weeks but did not form an epithelial sheet (Saxena et al. 2010a, b). However, when the same cells were seeded on two-dimensional collagen scaffolds, a single-layer epithelium formed; it was identified after 3 weeks of in vitro culture and remained viable up to 6 weeks. The same group also investigated the feasibility of vascularizing the EEC scaffold construct via stent tubularization and omental culture in the sheep model (Saxena et al. 2010a, b). Omental wrapping (not orthostatic transplantation) resulted in vascular growth both within and around the constructs. Following stent removal, the cultured scaffold revealed a structure similar to that of the native esophagus. Koffler et al. demonstrated that the positive selection of the ovine PCK-26-positive EEC seeded on collagen scaffolds for a week increased the proliferative capacity (Kofler et al. 2010). PCK-26-negative OECC had a low proliferative capability of 13%, which compared poorly to the 80% of the PCK-26-positive subpopulation. Miki et al. found that the degree of epithelial layers was correlated with the number of co-seeded with fibroblasts (Miki et al. 1999).

19.5.1 Natural Biologic Materials for Esophageal Reconstruction

Naturally derived biomaterials can be classified into the following groups: (1) protein-based materials (collagen, silk, gelatin), (2) polysaccharide-based materials (chitosan, cellulose) and (3) decellularized extracellular matrix (ECM). There are significantly more reports of esophageal reconstruction with naturally derived biomaterials than there are of synthetic biomaterials (Tables 19.1 and 19.2). Among these substitutes, a wide range of tissue-derived ECM, such as decellularized esophagus, small intestinal submucosa (SIS), urinary bladder submucosa (UBS), acellular dermal grafts, and the gastric acellular matrix (GAM), has been investigated for the application of esophagus reconstruction (Shen et al. 2013).

The extracellular matrix (ECM) is an intricate network composed of various proteins, proteoglycans, and polysaccharides released by the host cell. The ECM is one of the most important regulators of signal transportation, mechanical support, and tissue adherence. Decellularized ECM scaffolds preserve the native ECM, biomechanical properties, and surface topography of the native tissue**.** Theoretically, these ECM scaffolds are believed to promote cellular growth, orientation and proliferation. Furthermore, the decellularized ECM maintains the tissue

Table 19.1 Biological materials for esophageal reconstruction

Article	Cell	Animal	Material	Analysis point (post implant)	Epithelium	Inflammation	Vessel/nerve/gland
	Oral diet	Complication/final survival	Surgical method	Analysis methods	Smooth muscle	Stenosis	Scaffold degradation
Urita et al. (2007)	–	Rat (n = 21)	Gastric acellular matrix (GAM)	1, 2, 4 weeks/2, 4, 6, 8, 12, 18 months	1 week: partial regeneration	No gross inflammation	No comment
					2 weeks: complete regeneration	Inflammatory mononuclear cells into the GAM graft (2 months)	
						Inflammation subsided by 4 months	
	No restriction	Anastomosis site leakage (n = 1)	Abdominal esophagus 5 × 3 mm partial defect with omentum coverage	H&E, MT, Desmin, α-SMA, proliferation assay	No regeneration (until 18 months)	No stenosis	No comment
		No complication until the end of study (n = 20)					
Badylak et al. (2000)	–	Dog (n = 11)	SIS (n = 12) UBS (n = 3)	4 days ~ 15 months (partial defect only)	Complete regeneration	Mononuclear cell 4, 7, 15, and 35 days	Abundant neovascularization first 50 days
		Partial defect, 5 cm × 3 cm, 40–50% Circumferential defect, 5 cm				Neomatrix consisting of amorphous collagenous connective tissues 7 ~ 50 days	
	No oral feeding for 2 days (IV hydration)	Partial defect: no problem	Cervical esophagus 5 cm × 3 cm partial defect (n = 7)	H&E	Immature regeneration	Circumferential defect, all stricture within 45 days	Patch identified until 50 days (Histological)
	Normal diet from 14 days	Circumferential defect: all stricture	Circumferential defect 5 cm (n = 4)	Smooth muscle actin Immunoperoxidase stain			

Badylak et al. (2005)	–	Dog (n = 22)	Porcine UBM	2 weeks	Complete regeneration: Group 3,4 only at 3 months	No comment	Abundant neovascularization group 3,4
	Soft diet 1 week after surgery	Group 1. Mucosa + muscle resection with ECM reconstruction (n = 5): longest survival 19 days after surgery	Cervical esophagus 5 cm whole mucosa with or without muscle resection	Endoscopic exam group 1,2: Impossible (stenosis) group 3,4: Normal at s weeks after surgery	Complete regeneration: group 3, 4	Group 1. Mucosa + muscle resection with ECM reconstruction (n = 5): all stricture	No comment
	Solid diet after 2~3 week after surgery	Group 2. Mucosa resection without ECM (n = 5): Longest survival 27 days				Group 2. Mucosa resection without ECM reconstruction (n = 5): all stricture	
		Group 3. Mucosa +70% muscle resection with ECM (n = 5): longest survival 104 days				Group 3. Mucosa +70% muscle resection with ECM reconstruction (n = 5): 1 stricture	
				Esophagography		Group 4. Mucosa resection with ECM (n=7): 1 stricture	
		Group 4. Mucosa resection with ECM (n = 7): longest survival 230 days		Group 1,2: very limited passage (2 weeks)			
				Group 3,4: normal, motility+ from 2 mo			
Nieponice et al. (2013)	Bone marrow derived	Mice (n = 10)	UBM (n = 5)	8 weeks	Complete	No comment	No comment
	Cells (BMCs)	Expressing green fluorescent protein (GFP) in all BMCs	Control (n = 5)				
	No restriction	8 weeks after surgery scheduled to sacrifice	Cervical esophagus mucosa only, 5 mm partial resection	Esophagography	No comment	No stenosis	No comment
		No problem		Visualization of GFP protein: GFP positive cells populated in the ECM remodeling site			

(continued)

Table 19.1 (continued)

Article	Cell Oral diet	Animal Complication/final survival	Material Surgical method	Analysis point (post implant) Analysis methods	Epithelium Smooth muscle	Inflammation Stenosis	Vessel/nerve/gland Scaffold degradation
Lopes et al. (2006)	–	Rat (n = 58)	Porcine SIS	Esophagography 2 weeks	Complete regeneration (Partial defect only)	Initially Invasion by mononuclear inflammatory cells	Nerve regeneration (partial defect)
	Balanced liquid diet immediate after surgery	Partial defect: Survived 1 ~ 150 months without problem	Cervical esophagus partial defect (50% mucosa, 1 cm) (n = 34)	Esophagography	Partial regeneration after 5 months (partial group)	No stenosis (partial defect group)	No comment
		Circumferential defect: all anastomosis site leakage within 1 week, died within 17 days	Cervical esophagus circumferential defect (5 mm) (n = 24)	Partial defect: all normal			
				Circumferential defect: esophagography was possible in only 2, and all died during esophagography			
				Hemoglobin, hematocrit, total protein, albumin, sodium, potassium and chloride: circumferential: serious malnutrition			
				H&E, muscle actin, HHF35, S-100 (nerve)			

Isch et al. (2001)	–	Dog (n = 12)	Artificial dermis	1, 2, 3 months	Complete regeneration after 2 months	Grossly no inflammation reactive giant cell positive	Vessel regeneration increased until 2 months
							Elastin positive in 2 months
	Intravenous nutrition for 2 days after surgery Gastrostomy feeding between 3th and 14th days after surgery	No complication	Cervical esophagus 2 cm × 1 cm partial defect	Esophagography normal	No comment	No stenosis	No comment
	Oral diet from 15 days after surgery	No mortality		H&E			
				Elastin			
				Intact epithelium 2 months after surgery			
Saito et al. (2000)	–	Rabbit (n = 13)	Artificial dermis		Complete regeneration	Macrophages, lymphocytes, plasma cells, multinuclear giant cells were found, predominantly around the grafted collagen	No comment
	Intravenous nutrition only	Less than 50% (n = 5) survived more than 5 days	Cervical esophagus 2 cm circumferential defect reconstructed by latissimus dorsi muscle tuing with inner stent	Esophagography	No comment	No comment	No comment
		Longest survival 16 days					
Yamamoto et al. (2000)	–	Dog (n = 14)	Collagen with silicone tube	1, 2, 3, 6, 12, 24 months	Complete regeneration (3 months)	No comment	Vessel regeneration 12 months
	Intravenous nutrition during 1 ~ 2 months after surgery	Survival in no omental wrapping group: 3	Thoracic esophagus 5 cm circumferential defect (n = 9)	H&E	Distal margin partial only (12 months)	Stenosis 47%	No comment
		Survival in omental wrapping group: 7	Anastomosis site omental wrapping (n = 5)	Streptavidin	No further regeneration until 24 months		
				Biotin			

(continued)

Table 19.1 (continued)

Article	Cell Oral diet	Animal Complication/final survival	Material Surgical method	Analysis point (post implant) Analysis methods	Epithelium Smooth muscle	Inflammation Stenosis	Vessel/nerve/gland Scaffold degradation
				α-smooth muscle actin			
Wei et al. (2009)	Oral mucosa cell (OMEC)	Dog (n = 12)	Porcine SIS with oral OMEC	Esophagography at 2 weeks after surgery	OMEC- group: partial regeneration only at 4 weeks	No gross inflammation	No comment
				Histology analysis at 1~2 months after surgery	OMEC+ group: complete regeneration at 4 weeks		
	Intravenous nutrition for 3 days after surgery	OMEC+ group (n = 6): no complication	Cervical esophagus 5 cm × 2.5 cm partial defect	Esophagography	OMEC- group: only short bundle cell+OMEC+ group: many clusters of the muscle	No stenosis	Identified 4 weeks
	Soft diet until 1 week after surgery	OMEC- group (n = 6): no complication		H&E	Cells, not organized		Not identified 8 weeks
	Normal diet from 1 week after surgery			MT			
Marzaro et al. (2006)	Porcine pig esophageal smooth muscle cell	Pig (n = 6)	Porcine esophagus	3 weeks	Cell+ group: complete regeneration	Lower granulocyte and macrophage infiltration in cell+ group (3 weeks)	No comment
					Cell- group: partial regeneration		
	1 day	Cell+ group (n = 3): no mortality	Thoracic esophagus 2 cm partial defect	α-smooth muscle actin	Cell+ group: partial regeneration, no organization	No stenosis	No comment
		Cell- group (n = 3): no mortality		CAM assay	Cell- group: no regeneration		

Poghosyan et al. (2015)	Porcine skeletal Myoblasts (PSM) Porcine Oral epithelial cells (OEC)	Mini pig (n = 18)	Porcine Small intestinal submucosa Wrapped polyester silicone stent	12 months	Complete regeneration (scaffold+stent group, 3 months)	No comment	Partial regeneration in scaffold+stent group
	Two days after surgery	Scafflod with stent (n = 6): no complication until more than 6 months after surgery (n = 3)	Cervical esophagus 5 cm circumferential defect at cervical esophagus	Endoscope Esophagography anti-CD56, Desmin, flow cytometer, α-smooth muscle actin	Partial regeneration: Scaffold+stent group, Desmin-positive cells, not organized, 7 months	Scaffold only group, stent only group: all stenosis	No comments
		Scaffold only (n = 6): all died within 2 months due to stenosis	Omentum culture during 2 weeks		Complete regeneration: Scaffold+stent group, 12 months	Scaffold+stent group: 1 stenosis	
		Stent only (n = 6): All died within 2 months due to stenosis, leakage					

Abbreviations: *H&E* hematoxylin eosin staining, *MT* Mmasson's trichrome staining

Table 19.2 Synthetic materials for esophageal reconstruction

Article	Cell	Animal	Material	Analysis point (post implant)	Epithelium	Inflammation	Vessel/nerve/gland
	Oral diet	Complication/final survival	Surgical method	Analysis methods	Smooth muscle	Stenosis	Scaffold degradation
Lynen et al. (2004)	–	Rabbit (n = 10)	Poly(vinylidene fluoride) (PVDF, n = 5)	Esophagoscopy: every 1 month	Complete regeneration	PVDF group: no inflammatory change	Neovascularization +
			Polyglactin (n = 5)	Histology: 12 weeks		Polyglactin group: diffse, deep foreign body reaction & granuloma	
	No comment	PVDF group: no complication (n = 4)	Abdominal esophagus 1 cm × 0.5 cm partial defect	Esophagoscopy Ki67, desmin	Muscle cell regeneration, not organized, partial	PVDF group: No stenosis Polyglactin group: 1 stenosis	No comments
		Polyglactin group: 3 anastomosis site leakage and death within 1st week					
Diemer et al. (2015)	–	Rabbit (n = 15)	Poly-(ε-caprolactone)	1 month	Complete regeneration	All contain macrophage foreign body giant cell (n = 4)	Neovascularization +
	No comment	Survival (n = 15) no complication (n = 6)	Abdominal esophagus 1 cm × 0.6 cm partial defect	H&E, α-SMA, desmin	Regeneration+	Stenosis (n = 2)	No comment
Aikawa et al. (2013)	–	Pig (n = 9)	50:50 copolymer of polylactic acid and polycaprolactone and reinforced with poly(glycolic acid) fibers	1, 2, 3 months	Complete regeneration: 1 month	No comment	No comment
	Liquid diet for 5 days	No complication	Thoracic esophagus 4 cm × 2 cm partial defect	Endoscopy: 2, 4, 8, 12 weeks	Hardly regeneration: 1 month	No stenosis	No comment
					Partial regeneration: 2 months complete		

					regeneration: 3mo		
Grikscheit et al. (2003)	Green fluorescent protein (GFP) labeled esophageal organoid unit	Rat (n = 8)	Poly(glycolic acid) coated with 1:100 collagen type 1	42 days	Complete regeneration	No comment	No comment
	Oral diet from 4 days	1 death in partial defect 1 death in circumferential defect	Abdominal esophagus 2.5 cm × 1 cm Partial defect (n = 3) Circumferencial 2 cm defect (n = 3) Omentum culture (n = 2)	Esophagography, H&E, green fluorescent, protein (GFP)–labeled OUs	Partial regeneration, not organized	Partial defect: no stenosis Circumferential defect: upper stenosis+	No comment
Nakase et al. (2008)	Oral keratinocytes and fibroblasts (KF)	Dog (n = 12)	Poly(glcycolic acid) mesh with smooth muscle tissue	10, 20, 50, 70 weeks	KF + group: complete regeneration KF – group: partial regeneration only	Grossly no inflammatory change	No comment
	Gastrostomy for 1 week	KF + group (n = 6):	Thoracic esophagus 3 cm circumferential defect	Esophagography, H&E α-SMA, cytokeratin MNF116	KF + group: muscle like structure, not organized	KF + group: mild stenosis at junction (n = 2)	No comment
		KF – group (N = 6):	Oral mucosal epithelial sheet –> polyglycolic acid mesh –> omentum culture –> implantation		KF – group: not regenerated	KF – group: all stenosis, almost obstruction (2–3 weeks)	
Jensen et al. (2015)	Rat esophageal epithelial cell, rat esophageal smooth muscle cell	Rat	PLGA and PLGA/PCL	14 days	Regeneration+	No comment	Regeneration+
	Soft diet for 5 days normal diet from 6 days		Rat cervical esophagus 1 cm partial, bioreactor 2 weeks	E-cadherin, α-SMA, glial cell marker S100β	Regeneration+, not organized	No comment	No comment

Abbreviations: *H&E* hematoxylin eosin staining, *MT* Mmasson's trichrome staining, *PCL* polycaprolactone, *PLGA* poly(lactic-co-glycolic) acid

components and contains various components of growth factors, collagen, elastin, laminin, and fibronectin (Maghsoudlou et al. 2014). Additionally, it has hypothetical advantages over synthetic materials because it does not produce potentially toxic degradation products or induce inflammatory reactions, which are among the most important issues in the regeneration process of esophageal defects (Jensen et al. 2015). However, natural biologic materials have problems such as low mechanical strength, a lack of sources, and rapid degradation (Shen et al. 2013).

Urita et al. used a decellularized stomach to repair partial esophageal defects in the rat model (Urita et al. 2007). In this study, rats were sacrificed sequentially until 18 months after surgery, and the results showed that the keratinized stratified squamous epithelium had regenerated completely in the entire construct by 2 weeks after implantation. However, no muscle regeneration was observed by the end of the study. Badylak et al. used the small intestinal submucosa (SIS, n = 12) and urinary bladder submucosa (UBS, n = 3) for esophageal reconstruction in a canine model (Badylak et al. 2000). Partial defects (5 cm × 3 cm, n = 7) or circumferential defects (length 5 cm) were created in the cervical esophagus, and ECM scaffolds were implanted. The animals were allowed to eat an oral diet starting at 48 h post-operation. Hydration was maintained via the intravenous route during this period. The animals then followed a normal diet starting on day 14. The animals were kept alive for 15 months (partial defect). The defect areas were replaced by complete squamous epithelium and immature muscle, which were oriented appropriately. However, the scaffolds for the circumferential defects showed stricture formation within 45 days following implantation.

Badylak et al. reported the necessity of a native muscle component for adequate esophageal reconstruction to prevent stenosis. In these experiments, esophageal reconstruction was performed using UBM in a dog model (n = 22) according to the different portions of the esophageal tissue resection (Badylak et al. 2005). The treatment groups included circumferential resection including muscle with (n = 7) and without (n = 5) UBM reconstruction, circumferential mucosal defect resections (muscle preservation) with UBM, and circumferential mucosal resections with 30% intact muscularis externa (n = 5). This study concluded that UBM bioscaffolds plus autologous muscle tissue, but not UBM scaffolds or muscle tissue alone, can facilitate the tissue remodeling of the esophageal defect. In a mouse model of esophageal reconstruction with UBS, Nieponice et al. evaluated the role of bone marrow-derived stem cells (BMCs) in esophageal repair (Nieponice et al. 2013). In that study, mice were subjected to mucosal resection (without muscle resection) followed by UBS scaffold implantation. The authors found that GFP-labeled BMCs were present at the treatment site and concluded that stem cells originating from the bone marrow participate in the ECM remodeling process during the esophageal wound healing process.

Lopes et al. performed partial (n = 34) and circumferential esophageal defect (n = 24) reconstructions using porcine SIS in a rat model (Lopes et al. 2006), and their results were similar to those obtained by Chung et al. (Chung et al. 2015). All of the animals in the circumferential defect group died within 17 days after surgery. All animals in the partial defect group survived until the scheduled date, and there were no signs of esophageal dysfunction or malnutrition and no significant stenosis, fistula, or diverticula. The epithelium and muscle were completely regenerated in the partial defect group, but muscle regeneration took 5 months. Isch et al. performed partial esophageal defect reconstruction with a commercial decellularized skin, AlloDerm® (LifeCell™), in canine cervical esophagus (2 cm × 1 cm) (Isch et al. 2001). Complete epithelialization and neovascularization were achieved by 2 months post-operation, but there were no reports of muscle regeneration. Saito et al. demonstrated the feasibility of using a collagen sponge wrapped with a latissimus dorsi muscle flap (Saito et al. 2000). They investigated whether the use of collagen prevented the contraction of grafted skin and the effect of muscle wrapping on the extensibility of the neoesophagus in a rabbit mode (n = 12). The new esophagus made by the collagen and

latissimus dorsi muscle flap group had better extensibility than did that of control group. However, most of the animals died within 5 days, and the longest survival period of any of the rabbits was 16 days. A series of experiments was performed using collagen scaffolds with silicone stents to reconstruct circumferential esophageal defects (5 cm) in a dog model (Yamamoto et al. 2000). The silicone tube was used as a stent to support the scaffold until the tissue regenerated, and this stent was removed 1 or 2 months after surgery. They reported that the mucosa regenerated fully within 3 months but noted that the muscle regeneration developed as islets of smooth muscle within 12 months and did not extend to the middle of the regenerated esophagus, even after 24 months (Yamamoto et al. 1999, 2000).

The cellular grafts that were undertaken with epithelial cells, smooth muscle cells, stem cells or the co-seeding of multiple cells were expected to regenerate esophageal tissue that more closely resembled a native human esophagus. There have been trials of esophageal grafts that used luminal epithelial cells and abluminal layers with smooth muscle or other types of cells combined with a latissimus dorsi (Hayashi et al. 2004) or omentum (Grikscheit et al. 2003) flap to vascularize this cellular graft. Wei et al. investigated the feasibility and effectiveness of the obtained mucosal epithelial cells from oral biopsy (OMEC) that were seeded onto small intestinal submucosa (SIS) scaffolds for esophageal reconstruction (Wei et al. 2009). They implanted scaffolds for partial esophageal defects (5×2.5 cm) in 12 dogs. Complete epithelialization was observed in the SIS-OMEC group, but only partial epithelialization developed in the SIS group 4 weeks after surgery. Eight weeks after surgery, partial muscle regeneration was observed only in the SIS-OMEC animals. Marzaro et al. evaluated the possibility of obtaining an implantable tissue-engineered esophagus composed of decellularized esophageal ECM and seeded porcine esophageal smooth muscle cells (SMCs) in vitro (Marzaro et al. 2006). The ECM matrix showed angiogenic activity in vivo on the chick embryo chorioallantoic membrane (CAM), and the scaffold appeared to be completely covered by SMCs in vitro. They implanted this scaffold in the partial esophageal defect model in pig ($n = 6$). At 3 weeks after surgery, earlier tissue remodeling and a lower inflammatory response were observed than would be expected with non-seeded constructs. Poghosyan et al. performed circumferential cervical esophageal defect reconstruction (mini pig, $n = 18$, 5 cm) using small intestinal submucosa that was cellularized with autologous skeletal myoblasts and covered by a human amniotic membrane seeded with autologous oral epithelial cells (Poghosyan et al. 2015). They cultured a substitute in the omentum for 2 weeks before implantation. The epithelium regeneration was complete at 3 months, and the organized muscle regeneration was complete at 12 months after implantation.

19.5.2 Synthetic Materials for Esophageal Reconstruction

Synthetic scaffolds have been widely used due to their inherent advantages of being reproducible, readily available, xeno-free and low-cost. Despite the failures of many trials that used synthetic polymers, pioneering attempts to overcome challenges such as anastomosis site leakage, graft failure, infection and optimal biodegradation are currently ongoing.

Theoretically, the use of synthetic materials is a more feasible approach to treat esophageal reconstruction because the artificial material can be sized for each individual (Jensen et al. 2015). Although the hydrophobic and biologically inert surfaces of synthetic biomaterials lead to inferior reactions with the host cells, a coating of common ECM proteins (e.g., fibronectin, laminin and collagen) can create a bioactive surface to attract and enhance cell attachment (Chian et al. 2015; Shen et al. 2013). Zhu et al. reported that fibronectin (Fn) grafted on a poly(L-lactide-co-caprolactone) (PLLC) scaffold greatly promotes porcine esophageal epithelium regeneration in vitro (Zhu et al. 2007). Hou et al. synthesized tubular PLLC incorporated with fibrin. The biocompatibility was improved in an in vitro primary epithelial

cell culture and an in vivo partial scaffold implantation model (Hou et al. 2015).

Many of these polymers, such as the biodegradable foam of poly(glycolic acid) (PGA), poly(L-lactic acid) (PLLA), and polycaprolactone (PCL), have been adopted specifically for esophageal tissue engineering, and their copolymers have received regulatory approval by the U.S. Food and Drug Administration (FDA). As an initial step towards a synthetically derived artificial esophagus, Beckstead et al. (Beckstead et al. 2005) characterized the epithelial identity and in vitro interaction between rat esophageal epithelial cells (REEC) and AlloDerm, PLLA, poly(lactic-co-glycolic) acid (75:25) (PLGA75), poly(lactic-co-glycolic) acid (50:50) (PLGA50), and PCL/PLLA (50:50). When a matrix composed of AlloDerm (decellularized human skin) was compared to synthetically derived scaffolds in vitro, the AlloDerm scaffold showed a better proliferating basal cell layer, six layers of stratification, and a thick keratin layer.

When porous patches in the form of surgical meshes composed of poly(vinylidene fluoride) (PVDF) and polyglastin-910 (Vicryl) were compared for use in the regeneration of partial defects in rabbits, PVDF was shown to lead to improved results in terms of neo-epithelialization, minimal inflammation reaction, and an absence of strictures after 3 months in a partial defect of rabbit (Lynen et al. 2004). Diemer et al. reported that both epithelial and smooth muscle cell regeneration was identified 1 month after treating a partial abdominal esophageal defect (0.6 cm × 1 cm) in a rabbit model with poly-ε-caprolactone mesh (Diemer et al. 2015). Aikawa et al. used porous surgical meshes made from a biodegradable polymer (50:50 copolymer of polylactic acid and polycaprolactone, reinforced with poly(glycolic acid) fibers to treat partial esophageal defects (4 cm × 2 cm) in pigs (Aikawa et al. 2013). At 12 weeks after surgery, epithelium and muscle tissues resembling the native esophagus were shown on the replacement graft.

Grikscheit et al. isolated esophageal organoid units (OU, mesenchymal cores surrounded by epithelial cells from neonatal or adult rats) and paratopically seeded them on biodegradable synthetic poly(glycolic acid) scaffold (Grikscheit et al. 2003). After 4 weeks of omentum culture, the construct was used to cover a partial and circumferential defect. The tissue-engineered esophagus architecture was maintained after a partial or circumferential defect, and the animals had no functional deficit. Nakase et al. used an oral mucosal epithelial sheet (keratinocytes and fibroblasts cultured on the human amniotic membrane) wrapped with a poly(glycolic acid) mesh on which autologous smooth muscle tissues were seeded (Nakase et al. 2008). The investigators implanted the tubular construct in the omentum for 3 weeks to establish a squamous epithelium and vascularized thick muscle tissue. Next, they used the implanted cellular construct to cover a 3-cm intra-thoracic circumferential esophageal defect in the same dog. In the control group (without keratinocytes and fibroblasts), strictures developed after the esophageal replacement with almost complete obstruction within 2–3 weeks. In contrast, in the KF (with keratinocyte and fibroblast) group, the in-situ tissue-engineered esophagus showed good distensibility, and the animals survived without feeding problems for more than 1 year. Jensen et al. isolated rat epithelial and smooth muscle cells and seeded them on PLGA and PCL/PLGA scaffolds (Jensen et al. 2015). They orthotopically transplanted cellular grafts after 2 weeks of in vitro culture in a bioreactor. Epithelial, smooth muscle, and glial cellular phenotypes were identified 2 weeks after orthotopic implantation.

19.6 Clinical Trials

Since 2011, there have been two clinical trials and two clinical studies to reconstruct esophageal tissues using commercial decellularized matrices, such as porcine SIS (Badylak et al. 2011; Hoppo et al. 2012) and urinary bladder matrix (Nieponice et al. 2014). Badylak et al. (56) applied porcine SIS to the raw surface of the esophagus following circumferential endoscopic submucosal resection (8 cm–13 cm) in superficial cancers (Badylak et al. 2011) and used a follow-up of

4–24 months (n = 5). The restoration of a normal mature epithelial layer without any problem for a normal diet and return to a normal diet without significant dysphagia were reported for all patients. This was the first clinical trial of a tissue-engineered esophageal scaffold in the human body. This study provided evidence that a biomaterial-based regenerative medicine strategy may enable a noninvasive endoscopic resection for selected esophageal cancers, thereby avoiding the traditional approaches, which have serious potential complications. Nieponice et al. performed partial esophageal defect reconstruction with ECM in 4 patients (Nieponice et al. 2014). The full-thickness defects were replaced by a porcine UBM, similar to the patch angioplasty in vascular surgery. All patients showed a favorable outcome, and both esophagography and EGD showed complete tissue regeneration that was indistinguishable from near-normal tissue. Although one patient presented an anastomosis site leakage, it closed spontaneously after drainage. Two patients presented stenosis, and they underwent a dilatation procedure (Nieponice et al. 2014).

In addition to a full-thickness esophageal defect, cell sheets have been used to repair superficial esophageal defects above the muscle layers to prevent stricture after endoscopic submucosal dissection both in dogs and in human clinical studies (Ohki et al. 2006, 2012; Kanai et al. 2012; Takagi et al. 2010). This procedure might be used to prevent stricture formation following endoscopic submucosal dissection (ESD) and improve the patients' quality of life. Takagi et al. reported the reproducibility and efficacy of a human oral mucosal epithelial cell (hOMEC) sheet in 7 healthy volunteers (Takagi et al. 2010). Cultured autologous oral mucosal epithelial cell sheets implanted on the canine esophageal partial superficial defect after ESD promoted re-epithelialization. Yamato et al. used an oral mucosal epithelial cell sheet harvested from dogs to repair an esophageal defect after EMR (Ohki et al. 2006). The transplanted cell sheets integrated on the underlying muscle layers in ESD sites, and complete wound healing with no observable stenosis was seen at 4 weeks after surgery. OHKI et al. applied Sutureless, the endoscopic transplantation of cell sheets cultured from autologous oral mucosal epithelial cells for ESD defects, in 9 patients (Ohki et al. 2012). The cell sheets were successfully transplanted in all cases, and complete epithelialization was achieved within 3 weeks.

19.7 Conclusion

Although esophageal tissue engineering is a promising option for esophageal reconstruction, there is currently no verified strategy for recreating a functional esophagus. A thorough understanding of the anatomic and functional issues of the native esophagus, such as the environment contaminated with saliva, bacteria, food material, and gastric acid with serious complications from a minor leakage; a collapsed organ that opens with the entrance of food material; and peristaltic movement, is essential for safe and functional esophageal reconstruction. Some key problems, such as organized smooth muscle regeneration, angiogenesis, nerve regeneration, and stricture prevention, should be resolved prior to clinical application. In the near future, an artificial esophagus may be a valid treatment alternative for congenital or acquired esophageal disease.

Acknowledgments This research was supported by the Korea Health Technology R&D Project through the Korea Health Industry Development Institute (KHIDI), funded by the Ministry of Health & Welfare, Republic of Korea (grant number: HI16C0362).

References

Adolphe C, Wainwright B (2005) Pathways to improving skin regeneration. Expert Rev Mol Med 7(20):1–14. https://doi.org/10.1017/S1462399405009890

Aikawa M, Miyazawa M, Okamoto K, Okada K, Akimoto N, Sato H, Koyama I, Yamaguchi S, Ikada Y (2013) A bioabsorbable polymer patch for the treatment of esophageal defect in a porcine model. J Gastroenterol 48(7):822–829. https://doi.org/10.1007/s00535-012-0716-7

Badylak S, Meurling S, Chen M, Spievack A, Simmons-Byrd A (2000) Resorbable bioscaffold for esophageal

repair in a dog model. J Pediatr Surg 35(7):1097–1103. https://doi.org/10.1053/jpsu.2000.7834

Badylak SF, Vorp DA, Spievack AR, Simmons-Byrd A, Hanke J, Freytes DO, Thapa A, Gilbert TW, Nieponice A (2005) Esophageal reconstruction with ECM and muscle tissue in a dog model. J Surg Res 128 (1):87–97. https://doi.org/10.1016/j.jss.2005.03.002

Badylak SF, Hoppo T, Nieponice A, Gilbert TW, Davison JM, Jobe BA (2011) Esophageal preservation in five male patients after endoscopic inner-layer circumferential resection in the setting of superficial cancer: a regenerative medicine approach with a biologic scaffold. Tissue Eng Part A 17(11–12):1643–1650. https://doi.org/10.1089/ten.TEA.2010.0739

Beckstead BL, Pan S, Bhrany AD, Bratt-Leal AM, Ratner BD, Giachelli CM (2005) Esophageal epithelial cell interaction with synthetic and natural scaffolds for tissue engineering. Biomaterials 26(31):6217–6228. https://doi.org/10.1016/j.biomaterials.2005.04.010

Chian KS, Leong MF, Kono K (2015) Regenerative medicine for oesophageal reconstruction after cancer treatment. Lancet Oncol 16(2):e84–e92. https://doi.org/10.1016/S1470-2045(14)70410-3

Chung EJ, Ju HW, Park HJ, Park CH (2015) Three-layered scaffolds for artificial esophagus using poly(?--caprolactone) nanofibers and silk fibroin: an experimental study in a rat model. J Biomed Mater Res A 103 (6):2057–2065. https://doi.org/10.1002/jbm.a.35347

Diegelmann RF, Evans MC (2004) Wound healing: an overview of acute, fibrotic and delayed healing. Front Biosci 9:283–289

Diemer P, Markoew S, Le DQ, Qvist N (2015) Poly-ε-caprolactone mesh as a scaffold for in vivo tissue engineering in rabbit esophagus. Dis Esophagus 28(3):240–245. https://doi.org/10.1111/dote.12172

Farrell TM, Archer SB, Metreveli RE, Smith CD, Hunter JG (2001) Resection and advancement of esophageal mucosa. A potential therapy for Barrett's esophagus. Surg Endosc 15(9):937–941. https://doi.org/10.1007/s004640080057

Grikscheit T, Ochoa ER, Srinivasan A, Gaissert H, Vacanti JP (2003) Tissue-engineered esophagus: experimental substitution by onlay patch or interposition. J Thorac Cardiovasc Surg 126(2):537–544

Hayashi K, Ando N, Ozawa S, Kitagawa Y, Miki H, Sato M, Kitajima M (2004) A neo-esophagus reconstructed by cultured human esophageal epithelial cells, smooth muscle cells, fibroblasts, and collagen. ASAIO J 50(3):261–266

Hoppo T, Badylak SF, Jobe BA (2012) A novel esophageal-preserving approach to treat high-grade dysplasia and superficial adenocarcinoma in the presence of chronic gastroesophageal reflux disease. World J Surg 36(10):2390–2393. https://doi.org/10.1007/s00268-012-1698-6

Hou L, Jin J, Lv J, Chen L, Zhu Y, Liu X (2015) Constitution and in vivo test of micro-porous tubular scaffold for esophageal tissue engineering. J Biomater Appl 30 (5):568–578. https://doi.org/10.1177/0885328215596285

Isch JA, Engum SA, Ruble CA, Davis MM, Grosfeld JL (2001) Patch esophagoplasty using AlloDerm as a tissue scaffold. J Pediatr Surg 36(2):266–268. https://doi.org/10.1053/jpsu.2001.20685

Jensen T, Blanchette A, Vadasz S, Dave A, Canfarotta M, Sayej WN, Finck C (2015) Biomimetic and synthetic esophageal tissue engineering. Biomaterials 57:133–141. https://doi.org/10.1016/j.biomaterials.2015.04.004

Jönsson L, Friberg LG, Gatzinsky V, Jennische E, Sandin A, Abrahamsson K (2014) Early regenerative response in the intrathoracic porcine esophagus-the impact of the inflammation. Artif Organs 38 (6):439–446. https://doi.org/10.1111/aor.12216

Kanai N, Yamato M, Ohki T, Yamamoto M, Okano T (2012) Fabricated autologous epidermal cell sheets for the prevention of esophageal stricture after circumferential ESD in a porcine model. Gastrointest Endosc 76 (4):873–881. https://doi.org/10.1016/j.gie.2012.06.017

Kofler K, Ainoedhofer H, Höllwarth ME, Saxena AK (2010) Fluorescence-activated cell sorting of PCK-26 antigen-positive cells enables selection of ovine esophageal epithelial cells with improved viability on scaffolds for esophagus tissue engineering. Pediatr Surg Int 26(1):97–104. https://doi.org/10.1007/s00383-009-2512-x

Kuppan P, Sethuraman S, Krishnan UM (2012) Tissue engineering interventions for esophageal disorders–promises and challenges. Biotechnol Adv 30 (6):1481–1492. https://doi.org/10.1016/j.biotechadv.2012.03.005

Lewis JP, Trobraughfe JR (1964) Haematopoietic stem cells. Nature 204:589–590

Li N, Lassman BJ, Liu Z, Liboni K, Neu J (2004) Effects of protein deprivation on growth and small intestine morphology are not improved by glutamine or glutamate in gastrostomy-fed rat pups. J Pediatr Gastroenterol Nutr 39(1):28–33

Londono R, Badylak SF (2015) Regenerative medicine strategies for esophageal repair. Tissue Eng Part B Rev 21(4):393–410. https://doi.org/10.1089/ten.TEB.2015.0014

Lopes MF, Cabrita A, Ilharco J, Pessa P, Paiva-Carvalho J, Pires A, Patrício J (2006) Esophageal replacement in rat using porcine intestinal submucosa as a patch or a tube-shaped graft. Dis Esophagus 19(4):254–259. https://doi.org/10.1111/j.1442-2050.2006.00574.x

Lynen Jansen P, Klinge U, Anurov M, Titkova S, Mertens PR, Jansen M (2004) Surgical mesh as a scaffold for tissue regeneration in the esophagus. Eur Surg Res 36 (2):104–111. https://doi.org/10.1159/000076650

Maghsoudlou P, Eaton S, De Coppi P (2014) Tissue engineering of the esophagus. Semin Pediatr Surg 23 (3):127–134. https://doi.org/10.1053/j.sempedsurg

Marzaro M, Vigolo S, Oselladore B, Conconi MT, Ribatti D, Giuliani S, Nico B, Perrino G, Nussdorfer

GG, Parnigotto PP (2006) In vitro and in vivo proposal of an artificial esophagus. J Biomed Mater Res A 77 ((4):795–801. https://doi.org/10.1002/jbm.a.30666

Metz CN (2003) Fibrocytes: a unique cell population implicated in wound healing. Cell Mol Life Sci 60 (7):1342–1350. https://doi.org/10.1007/s00018-003-2328-0

Michalopoulos GK (2007) Liver regeneration. J Cell Physiol 213(2):286–300. https://doi.org/10.1002/jcp.21172

Miki H, Ando N, Ozawa S, Sato M, Hayashi K, Kitajima M (1999) An artificial esophagus constructed of cultured human esophageal epithelial cells, fibroblasts, polyglycolic acid mesh, and collagen. ASAIO J 45 (5):502–508

Nakase Y, Nakamura T, Kin S, Nakashima S, Yoshikawa T, Kuriu Y, Sakakura C, Yamagishi H, Hamuro J, Ikada Y, Otsuji E, Hagiwara A (2008) Intrathoracic esophageal replacement by in situ tissue-engineered esophagus. J Thorac Cardiovasc Surg 136(4):850–859. https://doi.org/10.1016/j.jtcvs.2008.05.027

Nieponice A, McGrath K, Qureshi I, Beckman EJ, Luketich JD, Gilbert TW, Badylak SF (2009) An extracellular matrix scaffold for esophageal stricture prevention after circumferential EMR. Gastrointest Endosc 69(2):289–296. https://doi.org/10.1016/j.gie

Nieponice A, Gilbert TW, Johnson SA, Turner NJ, Badylak SF (2013) Bone marrow-derived cells participate in the long-term remodeling in a mouse model of esophageal reconstruction. J Surg Res 182(1):e1–e7. https://doi.org/10.1016/j.jss.2012.09.029

Nieponice A, Ciotola FF, Nachman F, Jobe BA, Hoppo T, Londono R, Badylak S, Badaloni AE (2014) Patch esophagoplasty: esophageal reconstruction using biologic scaffolds. Ann Thorac Surg 97(1):283–288. https://doi.org/10.1016/j.athoracsur.2013.08.011

Ohki T, Yamato M, Murakami D, Takagi R, Yang J, Namiki H, Okano T, Takasaki K (2006) Treatment of oesophageal ulcerations using endoscopic transplantation of tissue-engineered autologous oral mucosal epithelial cell sheets in a canine model. Gut 55 (12):1704–1710. https://doi.org/10.1136/gut.2005.088518

Ohki T, Yamato M, Ota M, Takagi R, Murakami D, Kondo M, Sasaki R, Namiki H, Okano T, Yamamoto M (2012) Prevention of esophageal stricture after endoscopic submucosal dissection using tissue-engineered cell sheets. Gastroenterology 143 (3):582–588. https://doi.org/10.1053/j.gastro.2012.04.050

Poghosyan T, Gaujoux S, Sfeir R, Larghero J, Cattan P (2011) Bioartificial oesophagus in the era of tissue engineering. J Pediatr Gastroenterol Nutr 52(1):S16–S17. https://doi.org/10.1097/MPG.0b013e3182105964

Poghosyan T, Sfeir R, Michaud L, Bruneval P, Domet T, Vanneaux V, Luong-Nguyen M, Gaujoux S, Gottrand F, Larghero J, Cattan P (2015) Circumferential esophageal replacement using a tube-shaped tissue-engineered substitute: an experimental study in minipigs. Surgery 158(1):266–277. https://doi.org/10.1016/j.surg.2015.01.020

Potten CS, Chadwick C, Ijiri K, Tsubouchi S, Hanson WR (1984) The recruitability and cell-cycle state of intestinal stem cells. Int J Cell Cloning 2(2):126–140. https://doi.org/10.1002/stem.5530020206

Saito M, Sakamoto T, Fujimaki M, Tsukada K, Honda T, Nozaki M (2000) Experimental study of an artificial esophagus using a collagen sponge, a latissimus dorsi muscle flap, and split-thickness skin. Surg Today 30 (7):606–613. https://doi.org/10.1007/s005950070100

Saxena AK (2014) Esophagus tissue engineering: designing and crafting the components for the "hybrid construct" approach. Eur J Pediatr Surg 24(3):246–262. https://doi.org/10.1055/s-0034-1382261

Saxena AK, Kofler K, Ainödhofer H, Höllwarth ME (2009) Esophagus tissue engineering: hybrid approach with esophageal epithelium and unidirectional smooth muscle tissue component generation in vitro. J Gastrointest Surg 13(6):1037–1043. https://doi.org/10.1007/s11605-009-0836-4

Saxena AK, Ainoedhofer H, Höllwarth ME (2010a) Culture of ovine esophageal epithelial cells and in vitro esophagus tissue engineering. Tissue Eng Part C Methods 16(1):109–114. https://doi.org/10.1089/ten.TEC.2009.0145

Saxena AK, Baumgart H, Komann C, Ainoedhofer H, Soltysiak P, Kofler K, Höllwarth ME (2010b) Esophagus tissue engineering: in situ generation of rudimentary tubular vascularized esophageal conduit using the ovine model. J Pediatr Surg 45(5):859–864. https://doi.org/10.1016/j.jpedsurg.2010.02.005

Shen Q, Shi P, Gao M, Yu X, Liu Y, Luo L, Zhu Y (2013) Progress on materials and scaffold fabrications applied to esophageal tissue engineering. Mater Sci Eng C Mater Biol Appl 33(4):1860–1866. https://doi.org/10.1016/j.msec.2013.01.064

Sjöqvist S, Jungebluth P, Lim ML, Haag JC, Gustafsson Y, Lemon G, Baiguera S, Burguillos MA, Del Gaudio C, Rodríguez AB, Sotnichenko A, Kublickiene K, Ullman H, Kielstein H, Damberg P, Bianco A, Heuchel R, Zhao Y, Ribatti D, Ibarra C, Joseph B, Taylor DA, Macchiarini P (2014) Experimental orthotopic transplantation of a tissue-engineered oesophagus in rats. Nat Commun 5:3562. https://doi.org/10.1038/ncomms4562

Skandalakis JE, Ellis H (2000) Embryologic and anatomic basis of esophageal surgery. Surg Clin North Am 80 (1):85–155

Sweet SC, Wong HH, Webber SA, Horslen S, Guidinger MK, Fine RN, Magee JC (2006) Pediatric transplantation in the United States, 1995–2004. Am J Transplant 6(5 Pt 2):1132–1152. https://doi.org/10.1111/j.1600-6143.2006.01271.x

Takagi R, Murakami D, Kondo M, Ohki T, Sasaki R, Mizutani M, Yamato M, Nishida K, Namiki H, Yamamoto M, Okano T (2010) Fabrication of human

oral mucosal epithelial cell sheets for treatment of esophageal ulceration by endoscopic submucosal dissection. Gastrointest Endosc 72(6):1253–1259. https://doi.org/10.1016/j.gie.2010.08.007

Tan JY, Chua CK, Leong KF, Chian KS, Leong WS, Tan LP (2012) Esophageal tissue engineering: an in-depth review on scaffold design. Biotechnol Bioeng 109 (1):1–15. https://doi.org/10.1002/bit.23323

Urita Y, Komuro H, Chen G, Shinya M, Kaneko S, Kaneko M, Ushida T (2007) Regeneration of the esophagus using gastric acellular matrix: an experimental study in a rat model. Pediatr Surg Int 23 (1):21–26. https://doi.org/10.1007/s00383-006-1799-0

Wei RQ, Tan B, Tan MY, Luo JC, Deng L, Chen XH, Li XQ, Zuo X, Zhi W, Yang P, Xie HQ, Yang ZM (2009) Grafts of porcine small intestinal submucosa with cultured autologous oral mucosal epithelial cells for esophageal repair in a canine model. Exp Biol Med (Maywood) 234(4):453–461. https://doi.org/10.3181/0901-RM-5

Yamamoto Y, Nakamura T, Shimizu Y, Matsumoto K, Takimoto Y, Kiyotani T, Sekine T, Ueda H, Liu Y, Tamura N (1999) Intrathoracic esophageal replacement in the dog with the use of an artificial esophagus composed of a collagen sponge with a double-layered silicone tube. J Thorac Cardiovasc Surg 118 (2):276–286. https://doi.org/10.1016/S0022-5223(99)70218-7

Yamamoto Y, Nakamura T, Shimizu Y, Matsumoto K, Takimoto Y, Liu Y, Ueda H, Sekine T, Tamura N (2000) Intrathoracic esophageal replacement with a collagen sponge--silicone double layer tube: evaluation of omental-pedicle wrapping and prolonged placement of an inner stent. ASAIO J 46(6):734–739

Zhang L, Li N, des Robert C, Fang M, Liboni K, McMahon R, Caicedo RA, Neu J (2006) Lactobacillus rhamnosus GG decreases lipopolysaccharide-induced systemic inflammation in a gastrostomy-fed infant rat model. J Pediatr Gastroenterol Nutr 42(5):545–552

Zhu Y, Leong MF, Ong WF, Chan-Park MB, Chian KS (2007) Esophageal epithelium regeneration on fibronectin grafted poly(L-lactide-co-caprolactone) (PLLC) nanofiber scaffold. Biomaterials 28(5):861–868. https://doi.org/10.1016/j.biomaterials.2006.09.051

Part VII

3-D Bioprinting Biomaterials

ECM Based Bioink for Tissue Mimetic 3D Bioprinting

20

Seung Yun Nam and Sang-Hyug Park

20.1 Trends in Tissue Engineering and Regenerative Medicine

20.1.1 3D Bioprinting for Tissue/Organ Fabrication

The increasing need for organ and tissue regeneration in patients is being challenged by a scarcity of donors as well as biocompatibility or immune rejection issues encountered during transplantation. To address this, the development of implantable tissue and compatible organ transplantation has rapidly evolved to satisfy unmet clinical needs (Langer and Vacanti 2016). Regenerative medicine requires the combination of engineering and biology to generate functional tissue constructs (Arealis and Nikolaou 2015; Amini et al. 2012). Tissue engineering strategies commonly require a combination of cells and biomaterial scaffolds to form implantable engineered tissues and organs capable of regeneration and performing physiological functions. Despite some initial successes in engineering relatively simple tissues, many challenges remain in developing tissues and organs suitable for clinical transplantation (Mandrycky et al. 2016; Atala et al. 2012; Mikos et al. 2006).

S. Y. Nam · S.-H. Park (✉)
Department of Biomedical Engineering, Pukyong National University, Busan, South Korea
e-mail: synam@pknu.ac.kr; shpark1@pknu.ac.kr

The main goal of tissue engineering is to generate 3D constructs that mimic natural tissue in order to achieve functional and structural tissue formation once implanted (Temenoff and Mikos 2000). One of the important components is the functional scaffold, which must have adequate physical and mechanical properties in addition to being biocompatible and biodegradable (Esposito et al. 2009). A variety of scaffold fabrication techniques have been developed to successfully regenerate complex and functional tissues. Popular methods include: gas foaming, phase separation, salt leaching, and freeze drying (Oberpenning et al. 1999). Conventional tissue engineering has demonstrated success in generating bone and cartilage, but achieving reproducible results has proved challenging. One of the major limitations of such conventional scaffold-based approaches include the intrinsic inability to mimic the complex architectures that are required for clinical use (Mandrycky et al. 2016; Langer and Vacanti 2016).

The recently developed three-dimensional (3D) printing technology is an additive manufacturing method that promises to bridge the difference between artificially-engineered tissues and native tissues. Such 3D printing is rapidly emerging as a key scaffold fabrication strategy for mimicking native tissue complexity (Fedorovich et al. 2011). The combined use of anatomical 3D image analysis and computed tomography techniques can achieve tailored treatment for tissue defects (Mironov et al. 2011) Scaffolds generated by 3D printing layer-by-layer can have complex

I. Noh (ed.), *Biomimetic Medical Materials*, Advances in Experimental Medicine and Biology 1064,
https://doi.org/10.1007/978-981-13-0445-3_20

geometries such as undercuts, curvatures, and interconnecting channels, while maintaining a relatively high-throughput fabrication process (Lee and Wu 2012). In practice, a layer-by-layer stratification of 3D printing can precisely deliver different cells or mechanical cures in the designed 3D architecture than what can be achieved via conventional fabrication methods (Zhang et al. 2016; Sears et al. 2016). Organ/tissue printing now enables accurate 3D organization of components such as cells, biomaterials, and biomolecules in a way that mimics the structure of native tissues (Kim et al. 2016; Mallikarjunaiah; Sobral et al. 2011).

The ultimate goal of 3D printing technology based on a layer-by-layer stratification is to create tissue substitutes with qualities similar to human tissues that can be implanted to quickly repair tissue loss. Although the development of printed grafts that match the shape, size, and type of defect is challenging, 3D printing offers enormous potential for advanced regenerative therapy (Gu et al. 2015). It is important to understand the biological environment prior to fabricating the tissues and organs using 3D printing as cells interact with the substrate matrix in printed 3D spaces. The cell response, stability of the structure, and ECM deposition are important attributes in tissue printing (Do et al. 2015). In the past decade, researchers have demonstrated the potential of 3D bioprinting technologies for the fabrication of functional tissue constructs (Xu et al. 2013; Longo et al. 2012; Atala et al. 2012; Amini et al. 2012). We believe that 3D printed tissues will overcome many of the shortcomings of tranditional tissue engineering. However, advancement of bioprinting technology is limited by the viability of materials that facilitate both, bioprinting logistics as well as support cell viability and function by providing tissue-specific cues.

20.1.2 3D Scaffolds Using Tissue-Derived Extracellular Matrix (ECM)

Regenerative processes depend heavily on interactions between the cells that participate in regeneration and the substrate on which they function. Tissue engineering involves the development of a new generation of materials or devices capable of specific interactions with biological tissues. Biomaterials with the ability to live are a key ingredient in tissue engineering applications. Development of these biomaterials is an ongoing process; the challenge is to replace old materials with new ones that allow better exploitation of advances in a number of technologies.

Extracellular matrix (ECM) provides structural and biochemical support for cell growth and is composed of several types of proteins and glycans. Alterations to ECM influences the cell state and function (Yue 2014). The ECM represents nature's scaffold for tissue development and repair. The use of decellularized extracellular matrix (dECM) scaffolds for regenerative medicine approaches is rapidly expanding (Chan and Leong 2008). Numerous tissues and organs have now been decellularized for practical applications of the ECM, and the latter has been successfully used clinically for regeneration of various tissues (Scarritt et al. 2015). Preservation of the dECM ultrastructure and composition induces favorable tissue organization and remodeling. The dECM modulates cell behavior – attachment, migration, and differentiation (Song and Ott 2011; Ott et al. 2008). The advantage of dECM organ specificity potentially ensures the maintenance of selected cell functions and phenotypes (Jung et al. 2016).

Over the last few years, different research groups following similar approaches have been able to derive full scale dECM scaffolds from different organs including skin, vascular tissue, heart valves and bladder, with promising results, particularly for the generation of biological scaffolds for biomedical applications (Schultheiss et al. 2005; Chen et al. 2004; Schmidt and Baier 2000). For instance, cartilage ECM is a structurally complex 3D environment composed of various types of collagens and proteoglycans carrying various bioactive factors such as growth factors, integrins, and functional peptides (Benders et al. 2013). In one study, a cartilage acellular matrix was shown to provide a 3D environment suitable for attachment, proliferation, and chondrogenic differentiation of bone marrow-derived mesenchymal stem cells (Yang et al. 2008). Intact acellular small intestinal submucosa matrices have

been used as a biomaterial by the Badylak research team after mechanically removing all mesenteric tissues (Gilbert et al. 2006).

20.1.3 Role of ECM Components

Tissue formation by cells is influenced by chemical and physical stimulation of the surrounding environment. Significantly different behaviors including migration, attachment, and differentiation are found in 2D and 3D cell culture systems (Stanton et al. 2015). Tissues in the body have complex compositions, and various subpopulations of cells secrete signaling molecules like growth factors and cytokines that aid in maintaining viability and function of cells in tissues. ECM microenvironments including growth and differentiation factors, cell adhesion molecules, and components of the ECM itself are essential to regulate cell differentiation. The development and normal functioning of all cell types in an organism depends on its interactions with the molecules in their environments. Furthermore, proteins and polymers that makeup the ECM provide structure to the tissue apart from interacting with cell receptors and serve as another type of signaling. ECM contributes to the mechanical integrity, rigidity and elasticity of skin, the vasculature, tendons, lungs, and other organs (Rosso et al. 2004).

The specific composition and distribution of the ECM constituents vary depending on the tissue source. In this section the role of each of the major ECM components is reviewed for a better understanding of ECM biomaterial. Glycosaminoglycans (GAGs) in the ECM are important for regulating the size and properties of the extracellular spaces in organs. Major constituents identified initially in ECM included collagen, non-collagenous glycoproteins, and proteoglycans.

Collagen constitutes a superfamily of ECM proteins with structural role being the primary function. All collagen proteins have domains with a triple helical conformation; such domains are formed by three subunits α -chains, each containing a $(Gly\text{-}X\text{-}Y)_n$ repetitive sequence motif (Lazarev et al. 1978). It represents about 25% of the entire protein mass of connective tissues present in mammals.

Proteoglycans are a group of ubiquitous proteins found on cell surfaces, within intracellular vesicles, and incorporated into the ECM. Unlike other proteins that are grouped into families on the basis of amino acid similarities, the proteoglycans are commonly defined by the type of post-translational modification: the glycosaminoglycan moiety. GAGs are polysaccharides that are structurally very different from the N- and O- linked oligosaccharides found on most cell surfaces and secreted proteins (Jacobsson and Lindahl 1987).

Aggrecan, a core protein of the large aggregating keratan-sulfate/chondroitin-sulfate proteoglycan is found in the cartilaginous tissues. As an ECM structural molecule, aggrecan localizes in the cartilage by virtue of high affinity binding to the hyaluronan-linked protein complex. This provides a strongly hydrated space filling gel resulting from the large number of polyanionic GAG chains covalently attached to the protein core (Wong et al. 1992).

Biglycan is a small proteoglycan, whose primary gene product is found associated with the cell surface or pericellular matrix in a variety of cells including specific subsets of developing mesenchymal, endothelial, and epithelial tissues (Nastase et al. 2012).

Fibromodulin is a keratosulfate proteoglycan present in many types of connective tissues, e.g. cartilage, tendon, and skin. Fibromodulin is structurally related to the dermatan sulfate/chondroitin sulfate, proteoglycans decorin, and biglycan. Fibromodulin binds to collagen and affects the collagen fibrillogenesis *in vitro* (Petri et al. 1999).

Fibronectins are high molecular weight glycoproteins found in many ECMs. They promote cell adhesion, affect cell morphology, migration and differentiation, in addition to cytoskeletal organization (Karasaki 1980).

Hyaluronan (HA) is a high molecular weight highly anionic polysaccharide composed of repeating disaccharides. HA is found in ECMs, where it plays a structural role; while on the cell surfaces it is believed to influence cell behavior. Important to both types of function are its unique

physicochemical properties and its interactions with HA-binding proteins. HA-binding proteoglycans and link proteins contribute to the structure of ECM via interactions with HA; cell surface-associated HA-binding proteoglycans are thought to act as HA receptors, which mediate the effects of HA on cell behavior (Delpech et al. 1993).

Tenascin is a large disulfide-linked hexameric ECM glycoprotein. The proposed biological functions include some effects on cell adhesion and cell morphology, and consequently effecting cell differentiation (Jones and Jones 2000).

Syndecan is an integral membrane proteoglycan, containing both heparin sulfate and chondroitin sulfate GAG chains that associate extracellularly with a variety of matrix molecules, and intracellularly with the actin cytoskeleton (Gopal et al. 2017; Bernfield and Sanderson 1990).

20.2 ECM Based Bioinks

20.2.1 Bioink Biomaterials

For 3D printing of a specific tissue shape a high resolution compatible bioink that can modulate the internal structure and external shape must be used. These properties facilitate the nutrient supply and metabolic activity of the cells after formation of the tissue. To date, numerous biomaterials have been explored for efficient 3D bioprinting. Printing using available biomaterials is a key success factor in 3D bioprinting; each printing hydrogel (bioink) offers different properties and thus the different bioprinting requirements (Hospodiuk et al. 2017). Some of the representable bioink materials are described in following sections.

Agarose is one of the typical polysaccharide molecules with gelation properties (Xiong et al. 2005). However, agarose cannot provide a compatible environment for the cell (Fedorovich et al. 2008), even though it has superior mechanical stability. Therefore, recent work had focused on the utilization of tailored hydrogel blends made of agarose-type I collagen and agarose-fibrinogen for 3D printing (Kreimendahl et al. 2017).

Alginate is a preferred polysaccharide natural biomaterial used in 3D bioprinting due its biocompatibility, various crosslinking properties, and good rheology for 3D plotting (Ozbolat and Hospodiuk 2016). Ionic crosslinking in alginate can be achieved by treatment with calcium chloride solution (Sahiner et al. 2015). However, chemical modifications are often required to induce the desirable cellular functions and maintain the 3D printed structure.

Collagen is a very popular and major ECM protein obtained from natural sources. It has been extensively used in 3D bioprinting due to ease of crosslinking using temperature and pH (Mandrycky et al. 2016; Ren et al. 2016). Crosslinking begins with the conversion to peptide-bound aldehydes of specific lysine and hydroxylysine residues in collagen. Cross-linking renders the collagen fibers stable and provides them with an adequate degree of tensile strength and visco-elasticity to perform their structural roles. However, collagen requires a gelation time of at least 30 min at 37 °C, which is considered slow, and is a major barrier for use in 3D printing. In addition, the low mechanical property must be overcome to achieve stable stratification. Single-layered construct samples have been printed using collagen bioink under extrusion-based bioprinting (Smith et al. 2004).

Fibrin, the blood clotting protein is a hydrogel formed by the enzymatic reaction of thrombin and fibrinogen. Notable features of fibrin include biocompatibility, biodegradability, and the fibronectin-rich natural matrix. The rapid degradation of fibrin makes it unsuitable for long-term tissue culture. Moreover, the weak mechanical properties in addition to the early degradation of fibrin must be addressed for allowing stable stratification using printing technology (Cui and Boland 2009). Despite these challenges, fibrin has been used in 3D printing (Gruene et al. 2011). Quasi-three-dimensional models have been printed with parallel biocompatible alginate/gelatin/fibrin composite bioink (Xu and Wang 2015).

Hyaluronic acid (HA), a linear non-sulfated glycosaminoglycan, is ubiquitous in almost all connective tissues, and is a major ECM component of cartilage (Park et al. 2005). Photo-crosslinked HA is used as a bioink through chemical modifications, which are performed to enhance the rheological properties of HA as a bioink. Like other natural biomaterials, HA also

has a slow gelation rate along with poor mechanical properties (Highley et al. 2016).

Silk proteins have found substantial applications in biomedicine owing to their high biocompatibility, tunable biodegradability, and good mechanical features (Floren et al. 2016). Other study highlight the potential of silk based bioink to mimic the tissue shape for fabrication (Park et al. 2016). Cell laden silk-gelatin bioink has been developed by the same research group for application in extrusion printing systems (Das et al. 2015).

Although natural biomaterials have led to the development of engineered tissues, these cannot reproduce the complex architecture and arrangement of native tissues composed of multiple cells and ECMs (Kim et al. 2017; Bajaj et al. 2014).

20.2.2 Tissue-Derived ECM Bioink

One of main purposes of 3D printed scaffolds is the imitation of biological and physical properties to mimic native ECM microenvironments (Hoshiba et al. 2016). As new printing bioinks are developed and improved printing methods are being discovered, and the use of 3D printed scaffolds in tissue engineering continues to become favorable (Ozbolat and Hospodiuk 2016). Recent advances in functional bioinks, and tissue-decellularized ECM (dECM) has been considered a new source for 3D tissue printing. Previous studies have evaluated the potential of prepared and characterized multiple tissue-derived dECM-based biomaterials that contain complex combinations of growth factors, collagens, glycosaminoglycans, and elastin. These biomaterials can be incorporated into bioinks to provide the important biochemical cues of different tissue types (Skardal et al. 2015). dECM components provide a highly biomimetic environment for cell proliferation and differentiation as they are comprised of matrix proteins essential for cellular activities (Pati et al. 2014) (Fig. 20.1).

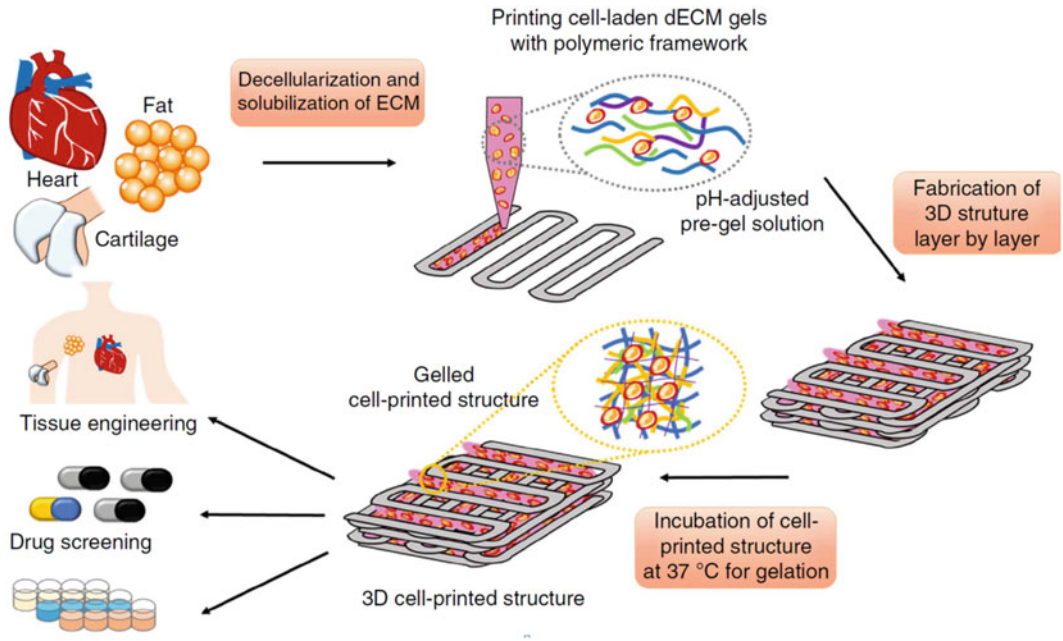

Fig. 20.1 Schematic elucidating the tissue printing process using dECM bioink. Respective tissues were decellularized after harvesting with a combination of physical, chemical and enzymatic processes. (Reprinted by permission from Macmillan Publishers Limited: Nat Commun. (Pati et al. 2014), Copyright 2014)

The possibility of 3D printing for manufacturing complex tissue constructs using cartilage tissue-derived ECM bioink has been demonstrated (Song et al. 2015). The plotting method was successfully developed for high viscous ECM-based bioink and 3D plotted scaffolds, which show highly interconnected pores as well as a complex shape. However, ECM bioprinting has not yet been well-established, the main hurdle being the very weak mechanical properties of dECM. Therefore, a frame printed using hard materials is necessary to maintain the dECM structure. To handle higher mechanical loads, ceramic materials or composite scaffolds are usually required to improve the mechanical properties of the scaffold (Xavier et al. 2015). A carrier polymer could be used to increase the solubility, to tune the viscosity, or to induce/enhance post crosslinking of the bioink (Ji and Guvendiren 2017). Pati et al. used dECM components to print tissue analogs, and achieved high cell survival rate and functionality from dECM-based 3D printed structures that were supported by a PCL frame (Pati et al. 2014). Other recent work by Jang et al. (2016) used a pig heart dECM to prepare cardiac-specific hydrogels that in combination with human cardiac progenitor cells were used to fabricate 3D bioprinted cardiac constructs (Jang et al. 2016). dECM bioink was used to fabricate a stem cell patch for cardiac function improvement. Highly bioactive ink was created consisting of collagen/ECM and alginate, which was used to print 3D porous cell blocks. Lee et al. demonstrated that the 3D cell-laden structure fabricated using collagen/ECM-based bioinks provide a novel platform for various tissue engineering applications (Lee et al. 2015). An innovative method for 3D printing and bioprinting alginate and ECM analogs based bioinks allows for high-resolution 3D printing (≈100 μm) of intricate solid geometries with exceptional shape fidelity (Costantini et al. 2016).

The 3D printed scaffolds using dECM bioinks support differentiation and maturation of the three tissue-specific cells. The dECM bioinks reported previously are an attractive option for *in vitro* and *in vivo* tissue development, and an alternative to chemically-crosslinked bioinks (Pati et al. 2014).

20.2.3 Bioink Requirements for Extrusion 3D Printing

Tissue-derived ECMs provide a unique tissue-specific microenvironment for tissue formation. The organization and structure of the unique ECM of each tissue affects cell attachment, migration, and proliferation. Due to these physical and biochemical properties, an ECM can replicate the biochemical and mechanical properties of each organ, such as tensile and compressive strength, and elasticity. To better represent the complexity of ECM *in vivo*, the dECM can be used for tissue friendly bioink formation. Multiple dECM bioinks have been investigated for various tissues, including adipose, cartilage, and heart tissues. ECM-based bioinks possess some of the most challenging characteristics in terms of 3D printing for tissue engineering (Pati et al. 2014).

Developments in the printing process, and the availability of new materials are needed to solve the issues of printing large-sized and uniform tissue substitutes for clinical applications. Among the printing methods, extrusion printing is the most suitable method for rapidly and precisely fabricating 3D structures of tissue and organ shapes (Yeong et al. 2004). Therefore, the physical and mechanical properties of bioinks should be reproduced in the plotting process (Murphy and Atala 2014). ECM bioinks are particularly difficult to plot, and a printed ECM often has inadequate mechanical properties (Combellack et al. 2016). For 3D printing of an ECM without a framework, a natural polymer is suitable as a composite, given that natural biomaterials are functionally superior to synthetic polymers as they are biocompatible and biodegradable. In particular, printed scaffolds made of a constant extrusion material have well-interconnected pores (Trachtenberg et al. 2017). Tissue ECM based 3D printing will be highly beneficial for biomimetic tissue and organ printing if mechanically-enhanced dECM bioink composites can be printed without supporting material.

However, current 3D bioprinting has some limitations, such as low resolution and limited material selection. Thus, this section will discuss the

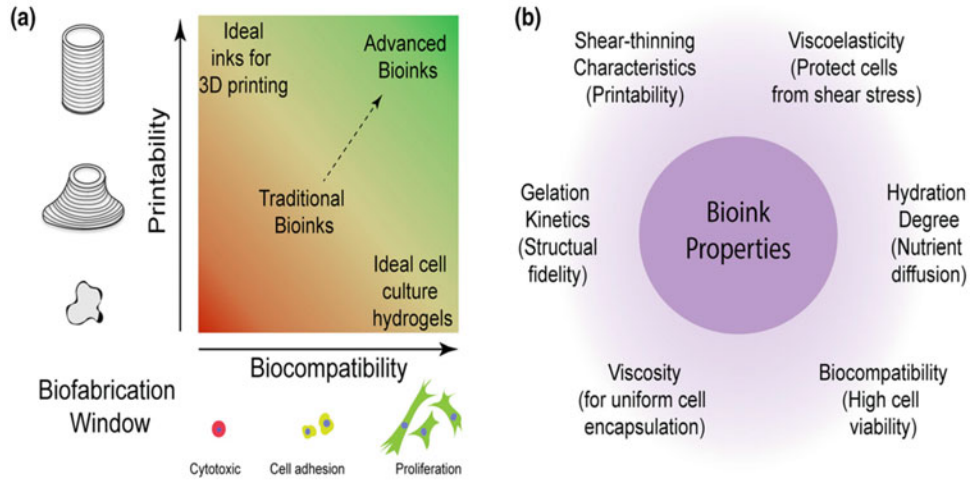

Fig. 20.2 Advanced bioinks for 3D printing. (**a**) Biofabrication window for rational design of bioinks requires compromise between printability and biocompatibility. (**b**) Ideal bioink characteristics require interplay between different materials properties. (Reprinted by permission from Springer: Annals of Biomedical Engineering, (Chimene et al. 2016), Copyright 2016)

requirements for bioink development. Figure 20.2 shows the requirement considerations for an optimized ECM bioink including resolution, viscoelasticity, and printability.

Mechanical and Structural Integrity

Bioinks must provide sufficient strength and structural maintenance for tissue formation. The mechanical and structural properties of bioink depend on the type and concentration of the bioink. These properties of bioink should be carefully selected according to the application needs. Skardal et al. suggested the use of modular hyaluronic acid and gelatin-based hydrogels supplemented with tissue dECM. Printable bioinks with different stiffness ranging from 100 Pa to 20 kPa have been achieved, thus enabling mimicking the mechanical characteristics of different tissues in the body (Skardal et al. 2015).

Degradability

The composition of ECM scaffold consists of a complex mixture of molecules that mediate structural and biological properties. Typically, scaffold materials are biodegradable unless processed in such a manner that irreversible crosslinks are formed between the resident molecules. The composite structure and degradability of these ECM molecules can regulate tissue remodeling for the ultimate clinical outcome. Degradability of bioink material depends on the selected biomaterials or combination, concentration, temperature, physiological conditions, and the presence of external additives. The degradation rate of the bioink should be matched to the pace of ECM tissue synthesis. However, this is a major challenge as the appropriate functional and mechanical properties of bioink for a specific tissue are difficult to match the ability of the cellular components to replace the bioink along the degradation process. Therefore, the degradability of bioink should be carefully manipulated after considering the target tissue characteristics.

Crosslinking

Biomaterial type and concentration, degree of cross linking, as well as post-printing crosslinking can be tailored to control the material properties of the bioinks and 3D-printed structures (Rutz et al. 2015). Many proteins and natural polymers have low viscosities and poor mechanical

properties, while some are water soluble at room temperature. Thus, the proteins or natural polymers should be chemically cross-linked with carbodiimide crosslinker or glutaraldehyde.

Chemically-crosslinked biomaterials are characterized by covalent bonding of polymer chains, which often provide better mechanical stability compared to physically-crosslinked ones. The use of a crosslinker could induce undesirable reactions with the hydrogel surface or result in cytotoxicity (Hennink and van Nostrum 2002).

Physical crosslinking methods have been a growing interest in biomaterials, which can be effectively crosslinked without the use of any exogenous agents, thus minimizing the risk of chemical contamination or chemically-induced toxicity (Chen et al. 2013). Due to the inability of a bioink to be self-supporting for layer-by-layer stratification, the bioink must either be made very viscous or gelled rapidly after extrusion (Rutz et al. 2015).

Viscosity

Bioink for use in 3D printing must possess adequate and injectable viscosity to allow for structural stratification. Bioinks with lower than the appropriate viscosity may be injectable, but multi-layer stacking is not possible. On the other hand, bioink of a higher viscosity can be stacked into a 3D structure, but continuous linear printing is difficult. Resolution of bioprinting processes depends on the bioprinting modality as well as the bioink viscosity. Other reports mention the increase in the viscosity of natural bioink using nanoparticles that was successful in printing without crosslink agents (Buyukhatipoglu et al. 2009). The increased viscosity of alginate by nanoparticles could plot the fine line of printed material and influence the stability of the printed structure (Buyukhatipoglu et al. 2010).

Printability

Extrusion-based bioprinting employs a pneumatic or mechanical printing process. Precise deposition of natural material begins with the method of dispensing (Vozzi et al. 2002). Bioink printability is affected by their viscosities and the crosslinking mechanism (Park et al. 2016; Song et al. 2015). For instance, the concentrated cartilage-derived ECM bioink was not able to plot the 3D structure due to low viscosity. Thus, the authors focused on designing an ECM-based ink with tailored rheological properties for printing 3D scaffolds with controlled architectures. Powder based plotting approach was adapted in order to print the stable 3D construct using cartilage-derived ECM bioink. Identification of the optimal ECM-hydrogel blending ratio for stable printability of ECM-based bioink revealed the interconnected pore structures had no significant difference from those of PCL scaffolds, thus proving outstanding 3D printability (Song et al. 2015). The extrusion range in 3D bioprinting is approximately 50 μm (Ozbolat and Yu 2013). With high resolution, 3D printing could be used to print scaffolds that mimic *in vivo* structure and environment of tissues (Mandrycky et al. 2016). Therefore, we needed to use high resolution compatible bioink that can modulate the specific tissue shape. These properties can facilitate the nutrient supply and metabolic activity of the cells after formation of the tissue. However, low viscosity still remains a problem when using dECM hydrogels as bioinks, which could compromise shape fidelity of the bioprinted 3D construct.

In the next section, optimizing methods for improving the printability will be discussed in detail.

20.3 Printability Characterization of ECM-Based Bioink

20.3.1 Rheological Characterization

Rheological properties of bioprinting materials are vital to printing resolution and shape fidelity (Atala and Yoo 2015; Kyle et al. 2017; Ozbolat 2016). Low viscosity materials provide favorable environments for cell growth and proliferation. However, bioprinting materials also need to be sufficiently viscous to maintain the three-dimensional printed structure (Kyle et al. 2017; Jia et al. 2014). Moreover, the viscosity of the bioprinting materials is not constant but varies as a function of shear rate, which mostly presents

non-Newtonian shear-thinning behaviors (Malkin and Isayev 2017; Morrison 2001). The non-Newtonian rheological properties are generally measured using rotational rheometers in oscillatory mode.

For the rheological measurement of viscoelastic printing materials, an oscillatory shear strain is applied:

$$\gamma(t) = \gamma_0 e^{i\omega t}$$

where, γ is the shear strain, γ_0 is the amplitude of oscillatory shear strain, t is the time, and ω is the angular frequency. The shear strain leads to shear stress in the viscoelastic material:

$$\tau(t) = \tau_0 e^{i(\omega t+\delta)}$$

where, τ is the shear strain, τ_0 is the amplitude of changing stress and δ is the phase shift between the applied strain and the stress response. The complex shear modulus G^* can be obtained using shear strain and shear stress as follows:

$$G^* = \frac{\tau(t)}{\gamma(t)} = \frac{\tau_0}{\gamma_0} e^{i\delta} = \frac{\tau_0}{\gamma_0}\cos\delta + i\frac{\tau_0}{\gamma_0}\sin\delta$$

The real and imaginary components of the complex shear modulus can be defined as storage modulus $G^{'}$ and loss modulus $G^{"}$, respectively, and they can be written as follows:

$$G^* = G' + iG''$$

$$G' = \frac{\tau_0}{\gamma_0}\cos\delta$$

$$G'' = \frac{\tau_0}{\gamma_0}\sin\delta$$

As shown in the equations, $G^{'}$ is in phase with the applied strain and related to storage of elastic energy by the material. $G^{"}$ is out of phase with the strain and related to the viscous response of the material. Hence, loss tangent can be expressed as:

$$\tan\delta = \frac{G''}{G'}$$

which is 0 for ideal elastic solid ($G^{"} = 0$, $\delta = 0$) and infinite for an ideal viscous fluid ($G^{'} = 0$, $\delta = 90^{\circ}$). Additionally, $\tan\delta = 1$ is known as the sol-gel transition point, which is an essential criterion for gelation. Complex viscosity η^* is defined using shear rate $\dot{\gamma}$ instead of shear strain γ as follows:

$$\eta^* = \frac{\tau(t)}{\dot{\gamma}(t)} = \frac{\tau(t)}{i\omega\gamma(t)} = \frac{G^*}{i\omega}$$

The complex viscosity can be rearranged with its real and imaginary components expressed as:

$$\eta^* = \eta' - i\eta''$$

$$\eta' = \frac{\tau_0}{\gamma_0\omega}\sin\delta = \frac{G''}{\omega}$$

$$\eta'' = \frac{\tau_0}{\gamma_0\omega}\cos\delta = \frac{G'}{\omega}$$

The magnitude of complex modulus and viscosity can be written as follows:

$$|G^*| = \sqrt{(G')^2 + (G'')^2}$$

$$|\eta^*| = \sqrt{(\eta')^2 + (\eta'')^2}$$

Numerous bioprinting studies with natural and synthetic hydrogels, including alginate, collagen, gelatin, hyaluronic acid, silk, GelMA, Pluronic F-127, PEG, and their composites have used rheological characteristics to enhance biocompatibility as well as printability (Atala and Yoo 2015; Jia et al. 2014; Ozbolat 2016; Duan et al. 2013). Despite decent optimization of rheological properties, hydrogel-based bioink often suffers from intrinsic low viscosity resulting in poor printing resolution and low structural fidelity (Kyle et al. 2017). Therefore, various other materials have been incorporated with hydrogel-based bioink to increase shear viscosity and enhance shape fidelity. Markstedt et al. incorporated nanocellulose to improve the rheological properties of alginate and enhanced the shear viscosity at low shear rate, thus providing better resolution and higher shear modulus ($G^{'}$ >10 kPa) (Markstedt et al. 2015). Li et al. also used rheological characteristics to show that

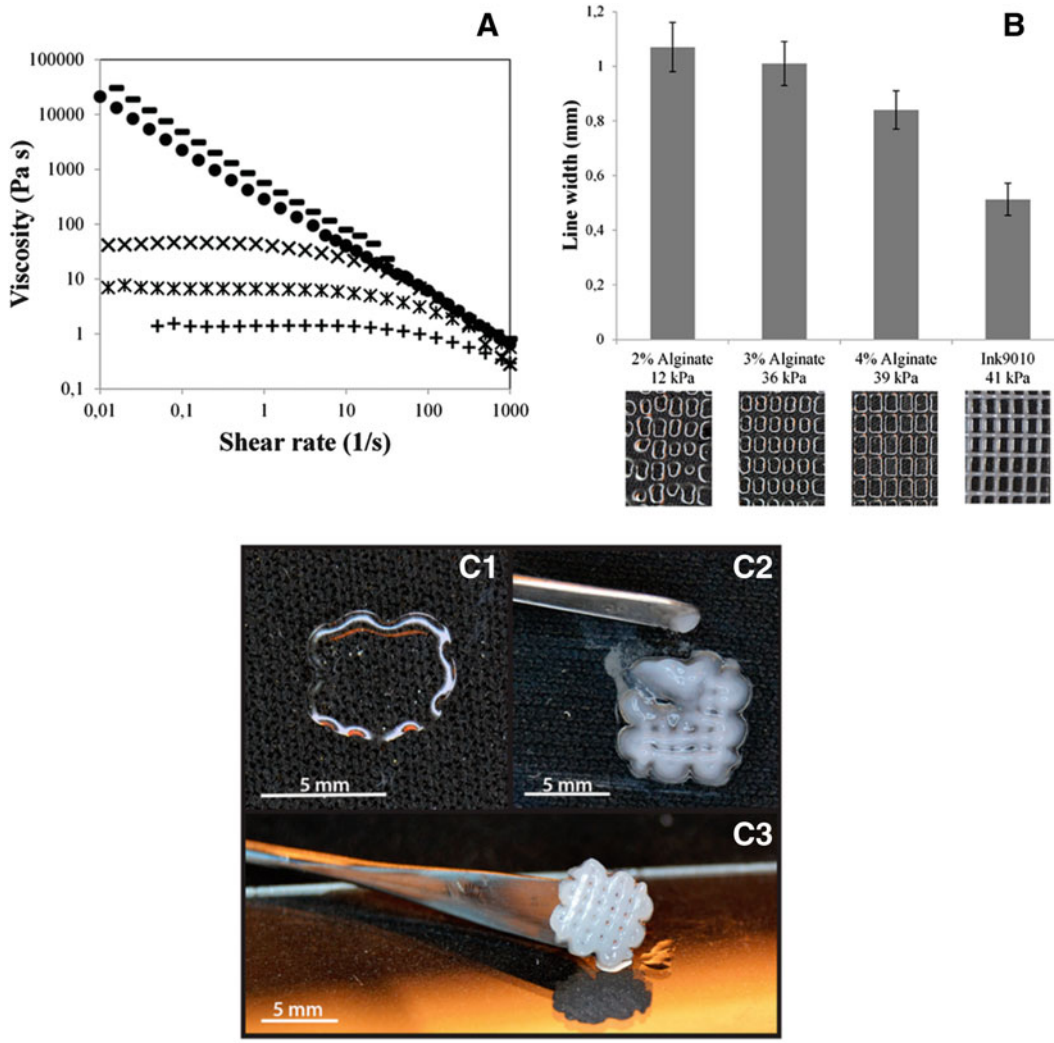

Fig. 20.3 (**a**) Flow curves of 2.5% nanofibrillated cellulose (NFC, −), NFC/alginate (90:10, NFC 2.25%, alginate 0.25%, •), 4% alginate (×), 3% alginate (∗), and 2% alginate (+). (**b**) Printed diameters of bioprinted struts with alginate solutions compared to NFC/alginate. The photos below the graph show the printed grids and their different line resolutions. (**c**) Small grid printed with (C1) 3% alginate and (C2) 2.5% NFC. (C3) Printed and cross-linked structure of NFC/alginate. (Reprinted with permission from American Chemical Society (Markstedt et al. 2015), Copyright 2015)

incorporation of graphene oxide enhances printability of alginate (Li et al. 2016) (Fig. 20.3).

dECM bioink is composed of various macromolecules such as collagen, laminin, elastin, fibronectin, and GAGs, whose structure and composition are affected by the decellularization process (Wolf et al. 2012). Hence, rheological characteristics plays a more significant role for dECM-based bioink. Rheological properties of dECM, including shear viscosity and shear modulus, are strongly dependent on the protein composition of dECM (Freytes et al. 2008; Lee et al. 2017; Pati et al. 2014). Therefore, the rheological properties of dECM are significantly related to the tissue source in decellularization. Three different tissues – adipose, cartilage, and heart tissue were

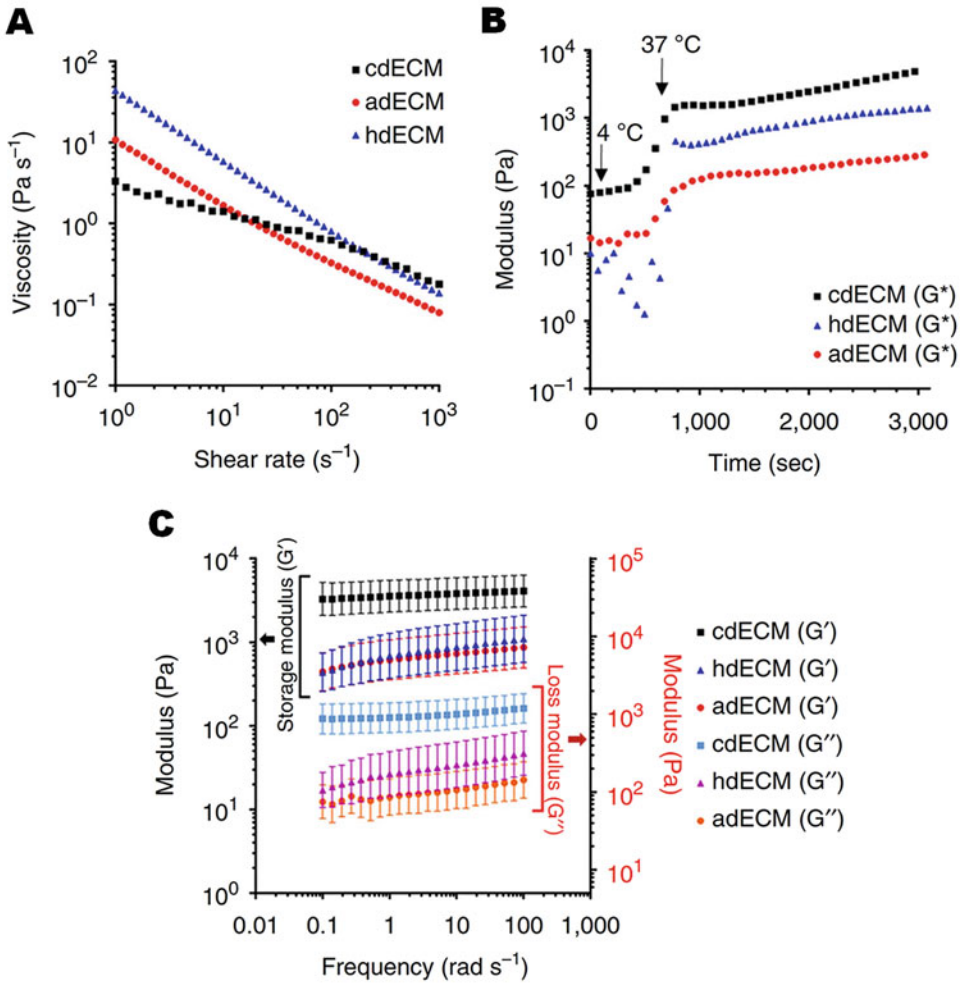

Fig. 20.4 Rheological properties of the dECM pre-gels (**a**) viscosity at 15 °C, (**b**) gelation kinetics from 4 to 37 °C., and (**c**) storage and loss modulus at varying frequency at 37 °C. (Reprinted by permission from Macmillan Publishers Limited: Nat Commun. (Pati et al. 2014), Copyright 2014)

decellularized and prepared as bioink for extrusion-based bioprinting by Pati et al. (2014). All the dECM bioinks from the three tissue sources had shear-thinning properties within the measured shear rate range. Also, dECM bioink of cartilage tissue had a much larger storage modulus (>1 kPa) than the others, possibly due to strong mechanical properties of the native tissue. Wolf et al. also compared storage moduli and viscosity of dECM from different sources – dermal ECM and urinary bladder matrix. They concluded that dECM of dermal tissue had a higher maximum storage modulus (> 0.4 kPa) compared to collagen, and lesser GAG content compared to dECM from urinary bladder tissue (Wolf et al. 2012). Lee et al. successfully decellularized liver tissue and bioprinted it in 3D without structural support of other polymers such as PCL (Lee et al. 2017). In their study, the dECM bioink of liver tissue showed shear-thinning behaviors for both dECM concentrations (1.5% and 3%). In addition, they reported that the storage moduli of dECM of liver tissue were between 1.5- and 2-fold higher than those of collagen hydrogel for 1.5% and 3% dECM concentrations, respectively (Fig. 20.4).

20.3.2 Mathematical Modeling of Pneumatic Extrusion-Based Bioprinting

In bioprinting, three types of bioprinters, mainly inkjet-based, laser-based, and extrusion-based bioprinters have been used for various tissue engineering and regenerative medicine applications (Ozbolat 2016). Among these, extrusion-based bioprinting is considered to be the most versatile method to print using a wide viscosity range for various types of bioink. dECM bioinks must be viscous enough for three-dimensional deposition, as such most bioprinting studies related to dECM bioink have used the extrusion-based bioprinting technology (Fig. 20.5).

Rheological properties of bioink, and printing parameters including nozzle size, pressure, and printing speed are closely related to each other. Therefore, printing resolution can be predicted using a mathematical model of pneumatic extrusion-based bioprinting (Attalla et al. 2016; Kyle et al. 2017; Li et al. 2016; Suntornnond et al. 2016). Using the mathematical modeling, time-consuming and expensive failures to optimize the printing parameters can be avoided.

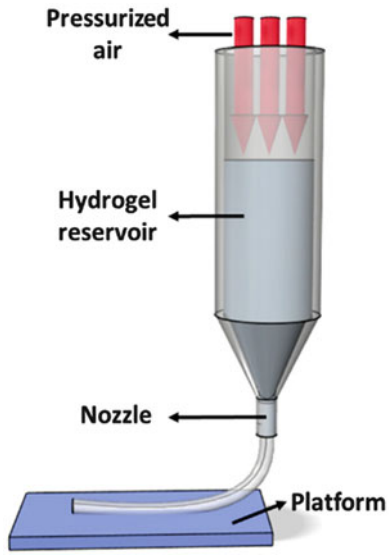

Fig. 20.5 Schematic of pneumatic extrusion-based bioprinting. (Reprinted from an open access article distributed under the Creative Commons Attribution License which permits unrestricted use (Suntornnond et al. 2016))

For the mathematical calculation, acquired experimental rheological data must be simplified and fitted to the rheological models. Among many rheological models, the power law model has been widely used for shear thinning materials without a Newtonian plateau at low shear rates (Morrison 2001; Malkin and Isayev 2017). The power law model describes that the shear stress is proportional to the power of the shear rate:

$$\tau = \tau_0 \left(\frac{\dot{\gamma}}{\dot{\gamma}_0} \right)^n$$

Where, τ is shear stress, $\dot{\gamma}$ is shear rate, τ_0 is shear stress at the reference state, and n is the power law index, which is less than 1 for shear-thinning materials. Using the relation of shear stress, shear viscosity, and shear rate, it can be written as:

$$\frac{\tau}{\tau_0} = \frac{\eta}{\eta_0} \frac{\dot{\gamma}}{\dot{\gamma}_0}$$

and the shear viscosity can be expressed as follows:

$$\eta = \eta_0 \left(\frac{\dot{\gamma}}{\dot{\gamma}_0} \right)^{n-1}$$

Where, η is shear viscosity, $\dot{\gamma}$ is shear rate, $\dot{\gamma}_0$ is the reference shear rate, and η_0 is the viscosity at the reference shear rate called zero viscosity. The reference shear rate is often taken as $\dot{\gamma}_0 = 1\,\mathrm{s}^{-1}$ so that the power law equation for shear viscosity can be written as:

$$\eta = \eta_0 \dot{\gamma}^{n-1}$$

For a steady and laminar flow of an incompressible and time-independent fluid in the pneumatic extrusion system, the following equations are available:

$$\tau = \frac{r}{2} \left(\frac{\partial P}{\partial z} \right)$$

$$\tau = \eta \dot{\gamma} = \eta \left(\frac{\partial v}{\partial r} \right)$$

Where, r is radius, z is parallel distance to the direction of extrusion, v is flow velocity, and P is pressure. Using the equations above, the equation

for the flow velocity in the extrusion system with a radius R can be derived as follows:

$$v = \left(\frac{n}{n+1}\right)\left(\frac{\partial P/\partial z}{2\eta_0}\right)^{\frac{1}{n}}\left(r^{\frac{n+1}{n}} - R^{\frac{n+1}{n}}\right)$$

At $r = 0$ and $v = v_0$,

$$v_0 = \left(\frac{n}{n+1}\right)\left(\frac{\partial P/\partial z}{2\eta_0}\right)^{\frac{1}{n}} R^{\frac{n+1}{n}}$$

Therefore, the flow velocity can be rearranged as:

$$v = v_0\left(1 - \left(\frac{r}{R}\right)^{\frac{n+1}{n}}\right)$$

A flow rate Q in the extrusion system is determined using the flow velocity at radius r as follows:

$$Q = \int_0^R 2\pi r v\, dr = \left(\frac{\pi n}{3n+1}\right)\left(\frac{\partial P/\partial z}{2\eta_0}\right)^{\frac{1}{n}} R^{\frac{3n+1}{n}}$$

For the extrusion system with a nozzle diameter D and the pressure drop ΔP within the nozzle length L, the flow rate is expressed as:

$$Q = \left(\frac{\pi n}{3n+1}\right)\left(\frac{\Delta P}{2\eta_0 L}\right)^{\frac{1}{n}}\left(\frac{D}{2}\right)^{\frac{3n+1}{n}}$$

Although the flow rate is determined for a given condition, the nozzle velocity is also significantly related to printing resolution. If we assume that the material is deposited in a perfectly cylindrical form, the flow rate also can be expressed using the nozzle velocity and the printed diameter as follows:

$$Q = \frac{V}{t} = \left(\pi\left(\frac{D_p}{2}\right)^2 l\right)\frac{1}{t} = \frac{\pi {D_p}^2 v_n}{4}$$

where V is the printed volume, t is the printed time, D_p is the printed diameter, l is the printed length, and v_n is the nozzle velocity. Since the flow rates for both equations are the same, the printed diameter can be determined based on printing parameters acquired from the rheological characteristics and extrusion conditions:

$$D_p = \sqrt{\frac{4Q}{\pi v_n}}$$

$$D_p = \sqrt{\frac{4n}{3n+1}}\sqrt{\frac{1}{v_n}}\left(\frac{\Delta P}{2\eta_0 L}\right)^{\frac{1}{2n}}\left(\frac{D}{2}\right)^{\frac{3n+1}{2n}}$$

Therefore, the printing resolution can be predicted with the power law index and zero viscosity calculated from the rheological measurements, pressure applied to the nozzle, nozzle diameter, nozzle length, and nozzle velocity, which can be expressed as:

$$D_p = f(n, \eta_0, D, L, \Delta P, v_n)$$

$$D_p \propto {v_n}^{-0.5}$$

$$D_p \propto \Delta P^{\frac{1}{2n}}$$

$$D_p \propto D^{\frac{3n+1}{2n}}$$

Theoretically, if the nozzle velocity is high and the applied pressure is low enough, the printed diameter D_p can be extremely small. However, it is practically difficult to print using a bioink with a diameter smaller than the nozzle diameter. Due to intrinsic viscosity and surface tension, the discontinuous strut can occur at small D_p. Also, the printing quality deteriorates at a higher nozzle velocity. Furthermore, in many practical cases, the cross-sectional shape of the printed strut is close to elliptical or semi-elliptical shape due to gravity and surface tension. If the shape is elliptical with a strut thickness D, the printed diameter can be calculated as $4Q/\pi D v_n$. As a result, if the printed cross-sectional shape becomes more elliptical, the printed diameter is proportionally related more closely to ${v_n}^{-1}$ instead of ${v_n}^{-0.5}$ (Fig. 20.6).

There have been several reports highlighting the rheological properties of bioink that have been used for prediction and optimization of bioprinting. Khalil et al. predicted the flow rate and the printed diameter of bioprinted alginate

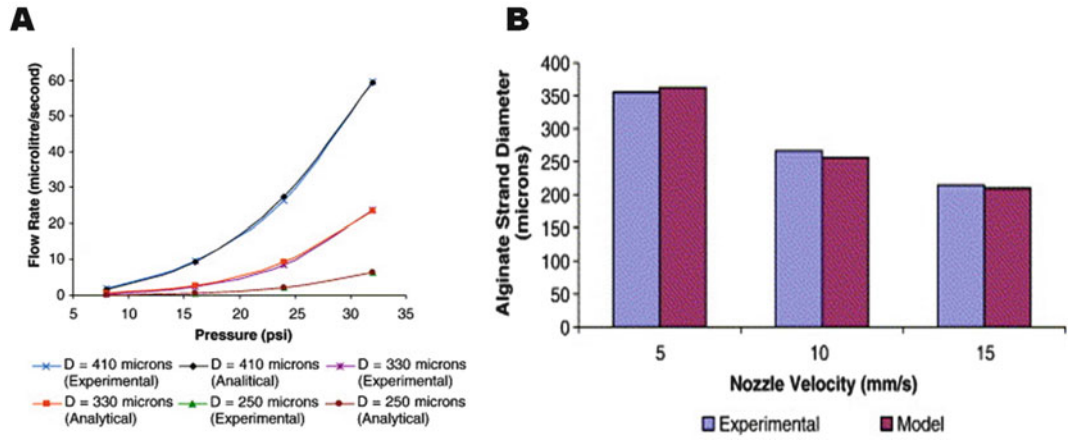

Fig. 20.6 (**a**) Comparison of the experimental and analytical flow rate versus pressure for 3% (w/v) sodium alginate solution with nozzle diameters of 250 μm, 330 μm, and 410 μm. (**b**) Comparison of alginate strut diameters at nozzle velocities of 5 mm/s, 10 mm/s, and 15 mm/s with a constant flow rate of 0.51 μl/s for the mathematical model and experiments. (Reprinted with permission from Elsevier: The Materials Science and Engineering: C (Khalil and Sun 2007), Copyright 2007)

solution using rheological measurements and the mathematical modeling of a pneumatic microvalve (Khalil and Sun 2007). The analytical and experimental results revealed agreement at multiple nozzle velocities (5, 10, and 15 mm/s) and pressures (up to 32 psi). Suntornnond et al. also applied a mathematical model to predict the resolution of bioprinting (Suntornnond et al. 2016). Pluronic F-127 at two different concentrations (24.5 and 30 wt%) was printed using the extrusion-based bioprinter at various operational conditions (nozzle velocities: 10, 20, and 30 mm/s, and nozzle diameters: 210, 260, and 512 μm). The experimental data of printing resolution matched well with the theoretical data.

Given that a variety of dECM based bioinks have different shear-thinning properties, the mathematical modeling incorporating the power law model can be easily used to optimize printing parameters and verify the printability of novel materials. Recently, Lee et al. evaluated the printability of liver dECM bioink based on the measurement of the printed diameter at various nozzle velocities (200–2000 mm/min) and multiple pressures (30, 40, 60 kPa) (Lee et al. 2017). Although the mathematical model was not applied to the experimental data, the study highlights the feasibility of accurate optimization of bioprinting parameters, and prediction of printing resolution and deposition (Fig. 20.7).

20.4 Summary

3D bioprinting for implantable tissue is gaining popularity and advancing technologically. It has become a valuable method for the fabrication of complex biostructures. In the meantime, tremendous progress has been made in the natural biomaterial development for tissue engineering. In particular, ECM derived natural biomaterials have become popular candidates and promising sources of bioink. Several studies have demonstrated the exceptional characteristics of dECM-based bioinks in comparison to the ones existing today. dECM-based bioink development is critical for bioprinting and to fabricate implantable tissue-mimicked constructs. In order to develop such printable dECM bioink, compatible bioprinting processes should be first identified as each bioprinting modality possesses different requirements depending on the dECM bioink material. Especially, rheological properties of bioink have significant influence on printing

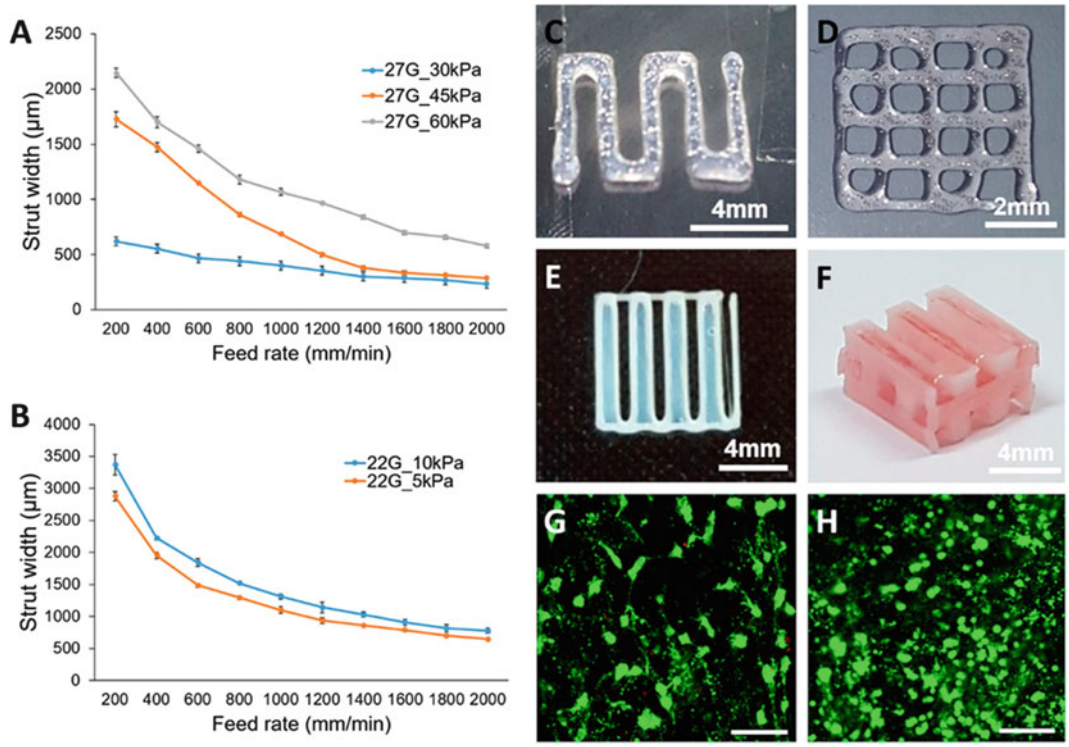

Fig. 20.7 Evaluation of strut width of bioprinted liver dECM bioink with (**a**) a 27 gauge (inner diameter of 200 μm) nozzle and (**b**) a 22 gauge (inner diameter of 400 μm) nozzle in relation to 3D cell printing conditions. Results of (**c** and **d**) 2D printing patterns and (**e** and **f**) 3D hybrid structures with the polymer. Cell viability of the cell-printed hybrid structure using the live/dead assay on day 7: (**g**) BMMSCs and (**h**) HepG2 cell line (green for live cells, red for dead cells, scale bar of 200 μm). (Reprinted with permission from American Chemical Society (Lee et al. 2017), Copyright 2017)

resolution and shape fidelity. Introduction of rotational rheometers in oscillatory mode, and the mathematical power law modeling of this chapter will serve as valuable tools for measuring the non-Newtonian rheological properties. A new field of study on the design and development of novel bioink materials is likely to emerge in the near future. We propose that future efforts should be devoted to engineering of new bioinks, as we expect fully differentiated 3D printed tissues to be developed with adequate strength to endure implantation. In addition, advancement of bioink in the area of printing speed and layer resolution will allow *in situ* printing to augment tissue regeneration endeavors with a short recovery time.

Acknowledgement This work was funded by a Marine Biotechnology Program grant (20150220) in the Ministry of Oceans and Fisheries, Korea and supported by the Pukyong National University Research Fund in 2016 (CD20161157).

References

Amini AR, Laurencin CT, Nukavarapu SP (2012) Bone tissue engineering: recent advances and challenges. Crit Rev Biomed Eng 40(5):363–408

Arealis G, Nikolaou VS (2015) Bone printing: new frontiers in the treatment of bone defects. Injury 46 (Suppl 8):S20–S22. https://doi.org/10.1016/S0020-1383(15)30050-4

Atala A, Yoo JJ (2015) Essentials of 3D biofabrication and translation. Academic Press, London

Atala A, Kasper FK, Mikos AG (2012) Engineering complex tissues. Sci Transl Med 4(160):160rv112. https://doi.org/10.1126/scitranslmed.3004890

Attalla R, Ling C, Selvaganapathy P (2016) Fabrication and characterization of gels with integrated channels using 3D printing with microfluidic nozzle for tissue engineering applications. Biomed Microdevices 18 (1):17. https://doi.org/10.1007/s10544-016-0042-6

Bajaj P, Schweller RM, Khademhosseini A, West JL, Bashir R (2014) 3D biofabrication strategies for tissue engineering and regenerative medicine. Annu Rev Biomed Eng 16:247–276. https://doi.org/10.1146/annurev-bioeng-071813-105155

Benders KE, van Weeren PR, Badylak SF, Saris DB, Dhert WJ, Malda J (2013) Extracellular matrix scaffolds for cartilage and bone regeneration. Trends Biotechnol 31(3):169–176

Bernfield M, Sanderson RD (1990) Syndecan, a developmentally regulated cell surface proteoglycan that binds extracellular matrix and growth factors. Philos Trans R Soc Lond Ser B Biol Sci 327(1239):171–186

Buyukhatipoglu K, Jo W, Sun W, Clyne AM (2009) The role of printing parameters and scaffold biopolymer properties in the efficacy of a new hybrid nanobioprinting system. Biofabrication 1(3):035003

Buyukhatipoglu K, Chang R, Sun W, Clyne AM (2010) Bioprinted nanoparticles for tissue engineering applications. Tissue Eng Part C Methods 16 (4):631–642. https://doi.org/10.1089/ten.TEC.2009.0280

Chan B, Leong K (2008) Scaffolding in tissue engineering: general approaches and tissue-specific considerations. Eur Spine J 17(4):467–479

Chen RN, Ho HO, Tsai YT, Sheu MT (2004) Process development of an acellular dermal matrix (ADM) for biomedical applications. Biomaterials 25 (13):2679–2686

Chen C, Wang L, Deng L, Hu R, Dong A (2013) Performance optimization of injectable chitosan hydrogel by combining physical and chemical triple crosslinking structure. J Biomed Mater Res A 101(3):684–693. https://doi.org/10.1002/jbm.a.34364

Chimene D, Lennox KK, Kaunas RR, Gaharwar AK (2016) Advanced Bioinks for 3D Printing: A Materials Science Perspective. Ann Biomed Eng 44(6):2090–2102. https://doi.org/10.1007/s10439-016-1638-y

Combellack EJ, Jessop ZM, Naderi N, Griffin M, Dobbs T, Ibrahim A, Evans S, Burnell S, Doak SH, Whitaker IS (2016) Adipose regeneration and implications for breast reconstruction: update and the future. Gland Surg 5(2):227

Costantini M, Idaszek J, Szoke K, Jaroszewicz J, Dentini M, Barbetta A, Brinchmann JE, Swieszkowski W (2016) 3D bioprinting of BM-MSCs-loaded ECM biomimetic hydrogels for in vitro neocartilage formation. Biofabrication 8(3):035002. https://doi.org/10.1088/1758-5090/8/3/035002

Cui X, Boland T (2009) Human microvasculature fabrication using thermal inkjet printing technology. Biomaterials 30(31):6221–6227. https://doi.org/10.1016/j.biomaterials.2009.07.056

Das S, Pati F, Choi YJ, Rijal G, Shim JH, Kim SW, Ray AR, Cho DW, Ghosh S (2015) Bioprintable, cell-laden silk fibroin-gelatin hydrogel supporting multilineage differentiation of stem cells for fabrication of three-dimensional tissue constructs. Acta Biomater 11:233–246. https://doi.org/10.1016/j.actbio.2014.09.023

Delpech B, Vannier JP, Girard N, Bizet M, Delpech A, Lenormand B, Tilly H, Piguet H (1993) Expression of the hyaluronan-binding glycoprotein hyaluronectin in leukemias. Leukemia 7(2):172–176

Do AV, Khorsand B, Geary SM, Salem AK (2015) 3D printing of scaffolds for tissue regeneration applications. Adv Healthc Mater 4(12):1742–1762. https://doi.org/10.1002/adhm.201500168

Duan B, Hockaday LA, Kang KH, Butcher JT (2013) 3D bioprinting of heterogeneous aortic valve conduits with alginate/gelatin hydrogels. J Biomed Mater Res A 101 (5):1255–1264. https://doi.org/10.1002/jbm.a.34420

Esposito M, Grusovin MG, Felice P, Karatzopoulos G, Worthington HV, Coulthard P (2009) The efficacy of horizontal and vertical bone augmentation procedures for dental implants – a Cochrane systematic review. Eur J Oral Implantol 2(3):167–184

Fedorovich NE, De Wijn JR, Verbout AJ, Alblas J, Dhert WJ (2008) Three-dimensional fiber deposition of cell-laden, viable, patterned constructs for bone tissue printing. Tissue Eng Part A 14(1):127–133. https://doi.org/10.1089/ten.a.2007.0158

Fedorovich NE, Alblas J, Hennink WE, Oner FC, Dhert WJ (2011) Organ printing: the future of bone regeneration? Trends Biotechnol 29(12):601–606. https://doi.org/10.1016/j.tibtech.2011.07.001

Floren M, Migliaresi C, Motta A (2016) Processing techniques and applications of silk hydrogels in bioengineering. J Funct Biomater 7(3):26

Freytes DO, Martin J, Velankar SS, Lee AS, Badylak SF (2008) Preparation and rheological characterization of a gel form of the porcine urinary bladder matrix. Biomaterials 29(11):1630–1637. https://doi.org/10.1016/j.biomaterials.2007.12.014

Gilbert TW, Sellaro TL, Badylak SF (2006) Decellularization of tissues and organs. Biomaterials 27(19):3675–3683. https://doi.org/10.1016/j.biomaterials.2006.02.014

Gopal S, Multhaupt HAB, Pocock R, Couchman JR (2017) Cell-extracellular matrix and cell-cell adhesion are linked by syndecan-4. Matrix Biol 60-61:57–69. https://doi.org/10.1016/j.matbio.2016.10.006

Gruene M, Pflaum M, Hess C, Diamantouros S, Schlie S, Deiwick A, Koch L, Wilhelmi M, Jockenhoevel S, Haverich A, Chichkov B (2011) Laser printing of three-dimensional multicellular arrays for studies of cell-cell and cell-environment interactions. Tissue Eng Part C Methods 17(10):973–982. https://doi.org/10.1089/ten.TEC.2011.0185

Gu Q, Hao J, Lu Y, Wang L, Wallace GG, Zhou Q (2015) Three-dimensional bio-printing. Sci China Life Sci 58 (5):411–419. https://doi.org/10.1007/s11427-015-4850-3

Hennink WE, van Nostrum CF (2002) Novel crosslinking methods to design hydrogels. Adv Drug Deliv Rev 54 (1):13–36

Highley CB, Prestwich GD, Burdick JA (2016) Recent advances in hyaluronic acid hydrogels for biomedical applications. Curr Opin Biotechnol 40:35–40. https://doi.org/10.1016/j.copbio.2016.02.008

Hoshiba T, Chen G, Endo C, Maruyama H, Wakui M, Nemoto E, Kawazoe N, Tanaka M (2016) Decellularized extracellular matrix as an in vitro model to study the comprehensive roles of the ECM in stem cell differentiation. Stem Cells Int 2016:6397820. https://doi.org/10.1155/2016/6397820

Hospodiuk M, Dey M, Sosnoski D, Ozbolat IT (2017) The bioink: a comprehensive review on bioprintable materials. Biotechnol Adv 35(2):217–239. https://doi.org/10.1016/j.biotechadv.2016.12.006

Jacobsson KG, Lindahl U (1987) Degradation of heparin proteoglycan in cultured mouse mastocytoma cells. Biochem J 246(2):409–415

Jang J, Kim TG, Kim BS, Kim SW, Kwon SM, Cho DW (2016) Tailoring mechanical properties of decellularized extracellular matrix bioink by vitamin B2-induced photo-crosslinking. Acta Biomater 33:88–95. https://doi.org/10.1016/j.actbio.2016.01.013

Ji S, Guvendiren M (2017) Recent advances in bioink design for 3D bioprinting of tissues and organs. Front Bioeng Biotechnol 5:23. https://doi.org/10.3389/fbioe.2017.00023

Jia J, Richards DJ, Pollard S, Tan Y, Rodriguez J, Visconti RP, Trusk TC, Yost MJ, Yao H, Markwald RR, Mei Y (2014) Engineering alginate as bioink for bioprinting. Acta Biomater 10(10):4323–4331. https://doi.org/10.1016/j.actbio.2014.06.034

Jones FS, Jones PL (2000) The tenascin family of ECM glycoproteins: structure, function, and regulation during embryonic development and tissue remodeling. Dev Dyn 218(2):235–259. https://doi.org/10.1002/(SICI)1097-0177(200006)218:2<235::AID-DVDY2>3.0.CO;2-G

Jung JP, Bhuiyan DB, Ogle BM (2016) Solid organ fabrication: comparison of decellularization to 3D bioprinting. Biomater Res 20(1):27. https://doi.org/10.1186/s40824-016-0074-2

Karasaki S (1980) [An adhesive glycoprotein polymer on cell surface: fibronectin (author's transl)]. Tanpakushitsu Kakusan Koso 25(9):890–905

Khalil S, Sun W (2007) Biopolymer deposition for freeform fabrication of hydrogel tissue constructs. Mater Sci Eng C 27(3):469–478. https://doi.org/10.1016/j.msec.2006.05.023

Kim JH, Yoo JJ, Lee SJ (2016) Three-dimensional cell-based bioprinting for soft tissue regeneration. Tissue Eng Regen Med 6(13):647–662

Kim BS, Kim H, Gao G, Jang J, Cho DW (2017) Decellularized extracellular matrix: a step towards the next generation source for bioink manufacturing. Biofabrication 9(3):034104. https://doi.org/10.1088/1758-5090/aa7e98

Kreimendahl F, Kopf M, Thiebes AL, Duarte Campos DF, Blaeser A, Schmitz-Rode T, Apel C, Jockenhoevel S, Fischer H (2017) Three-dimensional printing and angiogenesis: tailored agarose-type I collagen blends comprise three-dimensional printability and angiogenesis potential for tissue-engineered substitutes. Tissue Eng Part C Methods 23(10):604–615. https://doi.org/10.1089/ten.TEC.2017.0234

Kyle S, Jessop ZM, Al-Sabah A, Whitaker IS (2017) 'Printability' of candidate biomaterials for extrusion based 3D printing: state-of-the-art. Adv Healthc Mater 6(16). https://doi.org/10.1002/adhm.201700264

Langer R, Vacanti J (2016) Advances in tissue engineering. J Pediatr Surg 51(1):8–12. https://doi.org/10.1016/j.jpedsurg.2015.10.022

Lazarev YA, Lobachov VM, Grishkovski BA, Shibnev VA, Grechishko VS, Finogenova MP, Esipova NG, Rogulenkova VN (1978) Formation of the collagen-like triple-helical structure in oligopeptides during elongation of the molecular chain. Biopolymers 17(5):1215–1233. https://doi.org/10.1002/bip.1978.360170509

Lee M, Wu BM (2012) Recent advances in 3D printing of tissue engineering scaffolds. Methods Mol Biol 868:257–267. https://doi.org/10.1007/978-1-61779-764-4_15

Lee HJ, Kim YB, Ahn SH, Lee JS, Jang CH, Yoon H, Chun W, Kim GH (2015) A new approach for fabricating collagen/ECM-based bioinks using Preosteoblasts and human adipose stem cells. Adv Healthc Mater 4(9):1359–1368. https://doi.org/10.1002/adhm.201500193

Lee H, Han W, Kim H, Ha DH, Jang J, Kim BS, Cho DW (2017) Development of liver Decellularized extracellular matrix bioink for three-dimensional cell printing-based liver tissue engineering. Biomacromolecules 18 (4):1229–1237. https://doi.org/10.1021/acs.biomac.6b01908

Li H, Liu S, Lin L (2016) Rheological study on 3D printability of alginate hydrogel and effect of graphene oxide. Int J Bioprinting 2(2):54–66. https://doi.org/10.18063/ijb.2016.02.007

Longo UG, Loppini M, Forriol F, Romeo G, Maffulli N, Denaro V (2012) Advances in meniscal tissue engineering. Stem Cells Int 2012:420346. https://doi.org/10.1155/2012/420346

Malkin AY, Isayev AI (2017) Rheology: concepts, methods, and applications. Elsevier, Toronto

Mallikarjunaiah CA. A method to fabricate solid free form scaffolds for liver tissue engineering by using 3D printing: Kaunas University of Technology

Mandrycky C, Wang Z, Kim K, Kim DH (2016) 3D bioprinting for engineering complex tissues. Biotechnol Adv 34(4):422–434. https://doi.org/10.1016/j.biotechadv.2015.12.011

Markstedt K, Mantas A, Tournier I, Martinez Avila H, Hagg D, Gatenholm P (2015) 3D bioprinting human

chondrocytes with Nanocellulose-alginate bioink for cartilage tissue engineering applications. Biomacromolecules 16(5):1489–1496. https://doi.org/10.1021/acs.biomac.5b00188

Mikos AG, Herring SW, Ochareon P, Elisseeff J, Lu HH, Kandel R, Schoen FJ, Toner M, Mooney D, Atala A, Van Dyke ME, Kaplan D, Vunjak-Novakovic G (2006) Engineering complex tissues. Tissue Eng 12 (12):3307–3339. https://doi.org/10.1089/ten.2006.12.3307

Mironov V, Kasyanov V, Markwald RR (2011) Organ printing: from bioprinter to organ biofabrication line. Curr Opin Biotechnol 22(5):667–673. https://doi.org/10.1016/j.copbio.2011.02.006

Morrison FA (2001) Understanding rheology. Topics in chemical engineering. Oxford University Press, Oxford

Murphy SV, Atala A (2014) 3D bioprinting of tissues and organs. Nat Biotechnol 32(8):773–785

Nastase MV, Young MF, Schaefer L (2012) Biglycan: a multivalent proteoglycan providing structure and signals. J Histochem Cytochem 60(12):963–975. https://doi.org/10.1369/0022155412456380

Oberpenning F, Meng J, Yoo JJ, Atala A (1999) De novo reconstitution of a functional mammalian urinary bladder by tissue engineering. Nat Biotechnol 17 (2):149–155. https://doi.org/10.1038/6146

Ott HC, Matthiesen TS, Goh SK, Black LD, Kren SM, Netoff TI, Taylor DA (2008) Perfusion-decellularized matrix: using nature's platform to engineer a bioartificial heart. Nat Med 14(2):213–221. https://doi.org/10.1038/nm1684

Ozbolat IT (2016) 3D bioprinting: fundamentals, principles and applications. Academic Press, London

Ozbolat IT, Hospodiuk M (2016) Current advances and future perspectives in extrusion-based bioprinting. Biomaterials 76:321–343. https://doi.org/10.1016/j.biomaterials.2015.10.076

Ozbolat IT, Yu Y (2013) Bioprinting toward organ fabrication: challenges and future trends. IEEE Trans Biomed Eng 60(3):691–699. https://doi.org/10.1109/TBME.2013.2243912

Park SH, Park SR, Chung SI, Pai KS, Min BH (2005) Tissue-engineered cartilage using fibrin/hyaluronan composite gel and its in vivo implantation. Artif Organs 29(10):838–845. https://doi.org/10.1111/j.1525-1594.2005.00137.x

Park S-H, Jung CS, Min B-H (2016) Advances in three-dimensional bioprinting for hard tissue engineering. Tissue Eng Regen Med 13(6):622–635

Pati F, Jang J, Ha DH, Won Kim S, Rhie JW, Shim JH, Kim DH, Cho DW (2014) Printing three-dimensional tissue analogues with decellularized extracellular matrix bioink. Nat Commun 5:3935. https://doi.org/10.1038/ncomms4935

Petri JB, Rott O, Wetzig T, Herrmann K, Haustein UF (1999) The small proteoglycan fibromodulin is expressed in mitotic, but not in postmitotic fibroblasts. Mol Cell Biol Res Commun 1(1):59–65. https://doi.org/10.1006/mcbr.1999.0113

Ren X, Wang F, Chen C, Gong X, Yin L, Yang L (2016) Engineering zonal cartilage through bioprinting collagen type II hydrogel constructs with biomimetic chondrocyte density gradient. BMC Musculoskelet Disord 17:301. https://doi.org/10.1186/s12891-016-1130-8

Rosso F, Giordano A, Barbarisi M, Barbarisi A (2004) From cell-ECM interactions to tissue engineering. J Cell Physiol 199(2):174–180. https://doi.org/10.1002/jcp.10471

Rutz AL, Hyland KE, Jakus AE, Burghardt WR, Shah RN (2015) A multimaterial bioink method for 3D printing tunable, cell-compatible hydrogels. Adv Mater 27 (9):1607–1614. https://doi.org/10.1002/adma.201405076

Sahiner N, Sagbas S, Aktas N (2015) Single step natural poly(tannic acid) particle preparation as multitalented biomaterial. Mater Sci Eng C Mater Biol Appl 49:824–834. https://doi.org/10.1016/j.msec.2015.01.076

Scarritt ME, Pashos NC, Bunnell BA (2015) A review of cellularization strategies for tissue engineering of whole organs. Front Bioeng Biotechnol 3:43. https://doi.org/10.3389/fbioe.2015.00043

Schmidt CE, Baier JM (2000) Acellular vascular tissues: natural biomaterials for tissue repair and tissue engineering. Biomaterials 21(22):2215–2231

Schultheiss D, Gabouev AI, Cebotari S, Tudorache I, Walles T, Schlote N, Wefer J, Kaufmann PM, Haverich A, Jonas U, Stief CG, Mertsching H (2005) Biological vascularized matrix for bladder tissue engineering: matrix preparation, reseeding technique and short-term implantation in a porcine model. J Urol 173 (1):276–280. https://doi.org/10.1097/01.ju.0000145882.80339.18

Sears NA, Seshadri DR, Dhavalikar PS, Cosgriff-Hernandez E (2016) A review of three-dimensional printing in tissue engineering. Tissue Eng Part B Rev 22(4):298–310. https://doi.org/10.1089/ten.TEB.2015.0464

Skardal A, Devarasetty M, Kang HW, Mead I, Bishop C, Shupe T, Lee SJ, Jackson J, Yoo J, Soker S, Atala A (2015) A hydrogel bioink toolkit for mimicking native tissue biochemical and mechanical properties in bioprinted tissue constructs. Acta Biomater 25:24–34. https://doi.org/10.1016/j.actbio.2015.07.030

Smith CM, Stone AL, Parkhill RL, Stewart RL, Simpkins MW, Kachurin AM, Warren WL, Williams SK (2004) Three-dimensional bioassembly tool for generating viable tissue-engineered constructs. Tissue Eng 10 (9–10):1566–1576. https://doi.org/10.1089/ten.2004.10.1566

Sobral JM, Caridade SG, Sousa RA, Mano JF, Reis RL (2011) Three-dimensional plotted scaffolds with controlled pore size gradients: effect of scaffold geometry on mechanical performance and cell seeding efficiency. Acta Biomater 7(3):1009–1018

Song JJ, Ott HC (2011) Organ engineering based on decellularized matrix scaffolds. Trends Mol Med 17

(8):424–432. https://doi.org/10.1016/j.molmed.2011.03.005

Song BR, Yang SS, Jin H, Lee SH, Park DY, Lee J, Park SR, Park SH, Min BH (2015) Three dimensional plotted extracellular matrix scaffolds using a rapid prototyping for tissue engineering application. Tissue Eng Regen Med 12(3):172–180

Stanton MM, Samitier J, Sanchez S (2015) Bioprinting of 3D hydrogels. Lab Chip 15(15):3111–3115. https://doi.org/10.1039/c5lc90069g

Suntornnond R, Tan EYS, An J, Chua CK (2016) A mathematical model on the resolution of extrusion bioprinting for the development of new bioinks. Materials (Basel) 9(9):756. https://doi.org/10.3390/ma9090756

Temenoff JS, Mikos AG (2000) Review: tissue engineering for regeneration of articular cartilage. Biomaterials 21(5):431–440

Trachtenberg JE, Placone JK, Smith BT, Fisher JP, Mikos AG (2017) Extrusion-based 3D printing of poly(propylene fumarate) scaffolds with hydroxyapatite gradients. J Biomater Sci Polym Ed 28(6):532–554. https://doi.org/10.1080/09205063.2017.1286184

Vozzi G, Previti A, De Rossi D, Ahluwalia A (2002) Microsyringe-based deposition of two-dimensional and three-dimensional polymer scaffolds with a well-defined geometry for application to tissue engineering. Tissue Eng 8(6):1089–1098

Wolf MT, Daly KA, Brennan-Pierce EP, Johnson SA, Carruthers CA, D'Amore A, Nagarkar SP, Velankar SS, Badylak SF (2012) A hydrogel derived from decellularized dermal extracellular matrix. Biomaterials 33(29):7028–7038. https://doi.org/10.1016/j.biomaterials.2012.06.051

Wong M, Lawton T, Goetinck PF, Kuhn JL, Goldstein SA, Bonadio J (1992) Aggrecan core protein is expressed in membranous bone of the chick embryo. Molecular and biomechanical studies of normal and nanomelia embryos. J Biol Chem 267(8):5592–5598

Xavier JR, Thakur T, Desai P, Jaiswal MK, Sears N, Cosgriff-Hernandez E, Kaunas R, Gaharwar AK (2015) Bioactive nanoengineered hydrogels for bone tissue engineering: a growth-factor-free approach. ACS Nano 9(3):3109–3118. https://doi.org/10.1021/nn507488s

Xiong JY, Narayanan J, Liu XY, Chong TK, Chen SB, Chung TS (2005) Topology evolution and gelation mechanism of agarose gel. J Phys Chem B 109 (12):5638–5643. https://doi.org/10.1021/jp044473u

Xu Y, Wang X (2015) Fluid and cell behaviors along a 3D printed alginate/gelatin/fibrin channel. Biotechnol Bioeng 112(8):1683–1695. https://doi.org/10.1002/bit.25579

Xu T, Binder KW, Albanna MZ, Dice D, Zhao W, Yoo JJ, Atala A (2013) Hybrid printing of mechanically and biologically improved constructs for cartilage tissue engineering applications. Biofabrication 5(1):015001. https://doi.org/10.1088/1758-5082/5/1/015001

Yang Q, Peng J, Guo Q, Huang J, Zhang L, Yao J, Yang F, Wang S, Xu W, Wang A (2008) A cartilage ECM-derived 3-D porous acellular matrix scaffold for in vivo cartilage tissue engineering with PKH26-labeled chondrogenic bone marrow-derived mesenchymal stem cells. Biomaterials 29(15):2378–2387

Yeong WY, Chua CK, Leong KF, Chandrasekaran M (2004) Rapid prototyping in tissue engineering: challenges and potential. Trends Biotechnol 22 (12):643–652. https://doi.org/10.1016/j.tibtech.2004.10.004

Yue B (2014) Biology of the extracellular matrix: an overview. J Glaucoma 23(8 Suppl 1):S20–S23. https://doi.org/10.1097/IJG.0000000000000108

Zhang YS, Yue K, Aleman J, Mollazadeh-Moghaddam K, Bakht SM, Yang J, Jia W, Dell'Erba V, Assawes P, Shin SR, Dokmeci MR, Oklu R, Khademhosseini A (2016) 3D bioprinting for tissue and organ fabrication. Ann Biomed Eng 45:148. https://doi.org/10.1007/s10439-016-1612-8

3D Bioprinting for Artificial Pancreas Organ

21

Seon Jae Lee, Jae Bin Lee, Young-Woo Park, and Dong Yun Lee

21.1 Introduction

Type 1 diabetes mellitus (T1DM) results from autoimmune destruction of insulin-producing beta cell in the islet of the endocrine pancreas. The disease constitutes 5–10% of the diagnosed diabetes that corresponds to approximately 23 million worldwide. Currently, the most common method is injection of insulin directly. However, the intensive insulin therapy cannot tightly control the blood glucose levels in the diabetic patients due to fluctuation of blood glucose. Alternatively insulin pump is also used to control the blood glucose with continuous blood glucose monitoring (CBGM). Still it is necessary to develop insulin delivery system according to the fluctuation of blood glucose level.

The promising ideal strategy is transplantation of isolated insulin-secreting pancreatic islets. Flame of islet transplantation was initially ignited at the University of Alberta in Canada carrying out human islet transplants. Seven patients were transplanted more than 800,000 human islets isolated from recipients two or three through intrahepatic injection (Shapiro et al. 2000). These patients maintained blood glucose control for approximately 1 year when accompanied with 'Edmonton protocol' that is administration of several kinds of immunosuppressive medications. Then the global and multicenter clinical of the Edmonton protocol performed by the immune Tolerance Network showed that 16 of 44 islet transplants recipients (44%) had no insulin independence for 1 year and 10 experienced complete transplanted islet defects (Shapiro et al. 2006). Finally, the proportion of short-term grafts was up to approximately 80%, but less than 20% of grated recipients remained insulin independent until 5 years (Desai and Shea 2017). Thus, although islet transplantation is actually applied in clinical practice, still it has not been a perfect treatment. So, there are many challenges remained. Main issues are donor islet shortage and immune reaction after islet transplantation. As mentioned above, two to three donors per patient are needed. Hence, the efficiency of islet transplantation is drastically reduced due to the shortage of donors. Therefore, xenotransplantation of pancreatic islet has been proposed as a solution to settle the shortage of donors. In this case, the xenotransplanted islets are dramatically rejected due to xenogeneic immune rejection. Therefore, immunosuppressive medications

S. J. Lee · J. B. Lee · Y.-W. Park
Department of Bioengineering, College of Engineering, BK21 PLUS Future Biopharmaceutical Human Resource Training and Research Team, Hanyang University, Seoul, South Korea

D. Y. Lee (✉)
Department of Bioengineering, College of Engineering, BK21 PLUS Future Biopharmaceutical Human Resource Training and Research Team, Hanyang University, Seoul, South Korea

Institute of Nano Science & Technology (INST), Hanyang University, Seoul, South Korea
e-mail: dongyunlee@hanyang.ac.kr

I. Noh (ed.), *Biomimetic Medical Materials*, Advances in Experimental Medicine and Biology 1064,
https://doi.org/10.1007/978-981-13-0445-3_21

should be administered into the body to immunologically protect allogeneic or xenogeneic islets.

The need for lifelong immunosuppressants greatly limits the broad availability of this islet transplantation therapy. However, when immunosuppressive medications are administered for a long time, they show severe adverse effect such as nephrotoxicity, hepatotoxicity, and other abnormalities. Therefore, to attenuate the dose of immunosuppressive medications, pancreatic islet encapsulation with biocompatible polymers is developed (Borg and Bonifacio 2011). The biocompatible polymers are used as an immunoprotective barrier to protect the transplanted pancreatic islets. However, the conventional encapsulation strategies have several disadvantages such as hypoxia issue, degradability, reproducibility and retrievability. Recently, 3D bioprinting technology is considered as alternative tissue engineering. It can manufacture capsules capable of accommodating cells for a transplantable level and inhibit hypoxia by promoting vascularization through structure and releasing molecules.

In this chapter, therefore, we discuss about the islet encapsulation technologies with limitation issues and how the proposed 3D bioprinting technologies to overcome the limitations of encapsulation strategies can be applied. In addition, we address research perspectives for making commercially available artificial pancreas complementary to 3D bioprinting technology.

21.2 Necessity for Manufacturing of Artificial Pancreas

21.2.1 Encapsulation of Islet

To attenuate the dose of immunosuppressive medications, encapsulation of islets with biocompatible polymers has been developed, which provides physical barriers to the transplanted islets and inhibits the immune response from their recipients (Desai and Shea 2017). Various microencapsulation and macroencapsulation methods have been developed over the past several decades with the goal of creating immune-protected beta cells (Scharp and Marchetti 2014). The principle of encapsulation is that the cells to be implanted are contained in compartments separated by semi-permeable membranes. The capsule should protect the islets from damage caused by immune response. Therefore, the capsule is an "immune-isolation capsule". In addition to the protective mechanisms provided by the capsules, islets in the capsule can also regulate blood glucose levels by releasing insulin, while small molecules (glucose, oxygen and nutrients) and external (metabolic waste) can pass through this membrane. The encapsulation system is, therefore, also considered a "biological artificial pancreas". Immune-isolation capsule or biological artificial pancreas are generally divided into two categories: macroencapsulation and microencapsulation (Qi 2014).

Microcapsules and macrocapsules are classified by their size (Fig. 21.1). Microencapsulation use many microscales (100 μm–1 mm) capsules, containing single cells or islets that maximize surface-to-volume ratio and promote optimized nutrient and oxygen exchange (Elliott et al. 2007; Tuch et al. 2009; Desai et al. 2004). However, this technique has limited control over membrane thickness and pore size, and limits the number of capsules required for implantation. On the other hand, macroencapsulation capsules (3–8 cm) contain many cells or islets (Tarantal et al. 2009). These larger capsules provide better control of membrane parameters such as pore size and porosity and neovascularization by their rough surface, but limit nutrient and oxygen diffusion and cell response due to capsule thickness and large reservoirs (Cornolti et al. 2009; Desai and Shea 2017; Lembert et al. 2005).

21.2.2 Microencapsulation

As mentioned earlier, microencapsulation is a method of encapsulating cells on a micro scale using biocompatible materials. For successful microencapsulation, studies have been conducted using a variety of materials and these studies have now reached the clinical trial stage. Some of the fundamental limitations of microencapsulation

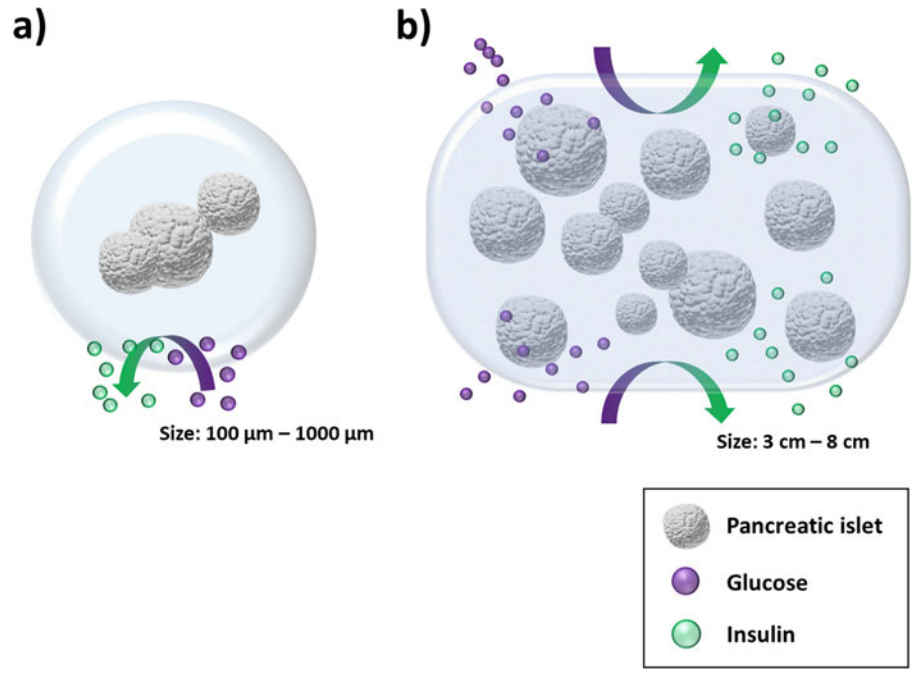

Fig. 21.1 Structure and function of microcapsule and macrocapsule. Microcapsule and macrocapsule are classified according to their sizes. (**a**) Microcapsule is typically prepared in the size of 100 µm–1 mm and contains one or several cells. (**b**) Macrocapsule is usually made in 3–8 cm size and contains multiple cells. Each capsule forms a semipermeable membrane through biocompetable material to protect the inner cells from the immune cell and the antibody, while relatively small glucose and insulin are freely diffused

prevent this from becoming a complete technology. From now on, we will discuss the process by which microencapsulation has been developed and the limitations of that strategy.

In 1964, cell microencapsulation technology was first described Chang (1964), and in 1980, microcapsules were used to treat diabetes, demonstrating prolonged survival of isograft islets using alginate-polylysine-polyethyleneimine microcapsules (Lim and Sun 1980). Non-encapsulated islets without post-transplant immunosuppression survived for 8 days whereas encapsulated islets survived to 3 weeks (Lim and Sun 1980). Thereafter, studies on the materials were conducted, so microcapsule material was improved in 1984. The previously used polyethylene imine component was disappeared and alginate was designed as the outer layer of the microcapsule (O'Shea et al. 1984). The use of alginate has considerably improved the microencapsulation technology because it can be produced under physiological conditions and don't affect to islet function and non-toxic (Menard et al. 2010). In this experiment, the microencapsulated islets survived for the 365 day in 1 of 5 animals. The alginate as material of microcapsule microcapsules was increased the strength of microcapsules. And decreasing the impurities and increasing the guluronic acid to mannuronic acid ratio further improved the biocompatibility of alginate microcapsules (Klock et al. 1994; Otterlei et al. 1991). After this study, studies on microencapsulation using alginate have been actively conducted, but in addition to alginate many other polymers such as chitosan, agarose, methacrylic acid, polyethylene glycol (PEG), methyl methacrylate and 2-hydroxyethyl methacrylate (HEMA) have been used successfully in islet encapsulation studies with limited success (de Vos et al. 2010).

Over the next few decades, research has been conducted to develop microcapsules with sufficient durability and biocompatibility. The experiments was conducted on small animals and many were successful (Klock et al. 1994; O'Shea et al. 1984; Sawhney et al. 1993). To improve the microcapsule, more than 1000 combinations of polyanions and polycations have been evaluated for relevance to cell encapsulation. A polyelectrolyte complex formation process was identified through the experiments with five different polymers, which enabled independent control over capsule size, wall thickness, mechanical strength and permeability (Wang et al. 1997).

And since then, microencapsulation technology has proven effective in many experiments on rodents. Between 2000 and 2010, more than 60 studies of microencapsulation strategies studies were performed on rodents and the viability of islets encapsulated with alginate without immunosuppression was the best for 100 days (Desai and Shea 2017; Souza et al. 2011). And encapsulated islet allotransplantation clinical trial, since its inception in 1994, Several clinical trials were conducted (Soon-Shiong et al. 1994). These experiments were performed by allo/xenotransplantation of the encapsulated islets in T1DM patients who did not receive immunosuppressants and then controlled blood glucose level normal in the long term. Despite other numerous clinical trials were conducted by academia and biotechnology companies, complete encapsulated islets were not have not been developed (Basta et al. 2011; Calafiore et al. 2006; Jacobs-Tulleneers-Thevissen et al. 2013; Valdes-Gonzalez et al. 2005, 2010). Each trials was shown to temporarily inhibit diabetes, but in the long term the therapy failed due to islet apoptosis and necrosis (Buder et al. 2013).

So, what is the limit of microencapsulation that causes the failure of these clinical trials? Process systems that are not standardized due to the diversity of raw materials in the manufacturing process and experiments that have been mainly done on the rodent model are also one cause, but the major reason is fibrotic overgrowth by micro-scale of capsules. In the case of microcapsules, the smaller size, the more fibrotic overgrowth due to the foreign body response, which leads to immune rejection in the transplanted cells, resulting in the failure of transplantation (Veiseh et al. 2015).

To overcome this problem, we need to increase the size of the capsule, but it which can make the capsule layer thicker, inhibiting oxygen, nutrient transport and inducing hypoxia. Therefore, there is a dilemma between improving the microencapsulation strategy and suppressing fibrotic overgrowth. So, when these problems are solved, can microencapsulation be commercialized? One of the biggest challenges faced by the microencapsulation technique is the scale up of the capsulation process. In the case of conventional microencapsulation, the process is usually carried out on a laboratory scale and we need to scale up these fabrication processes to an industrial level. However, in microencapsulation, controlling the formed diameter is important for proper operation and perturbation of the capsule and in order to form a micro-level bead, the flow rate at which the material is injected must be controlled.

So, there is a significant limitation in scaling up the microencapsulation process at the laboratory level to the industrial level.

21.2.3 Macroencapsulation

As mentioned earlier, islet encapsulation is classified into two types, depending on their size: macrocapsule and microcapsule. Moreover, macrocapsule is also divided in two types, extravascular intravascular types (Fig. 21.2). Although extravascular and intravascular macroencapsulation has been developed with individual advantages, these strategies also have some problems that prevent these strategies from becoming complete biological artificial pancreas. From now on, we will discuss the process by which each extravascular and intravascular macroencapsulation has been developed to the preclinical stage and limitations of them.

The extravascular macrocapsule has a diffusion chamber structure and is not connected to

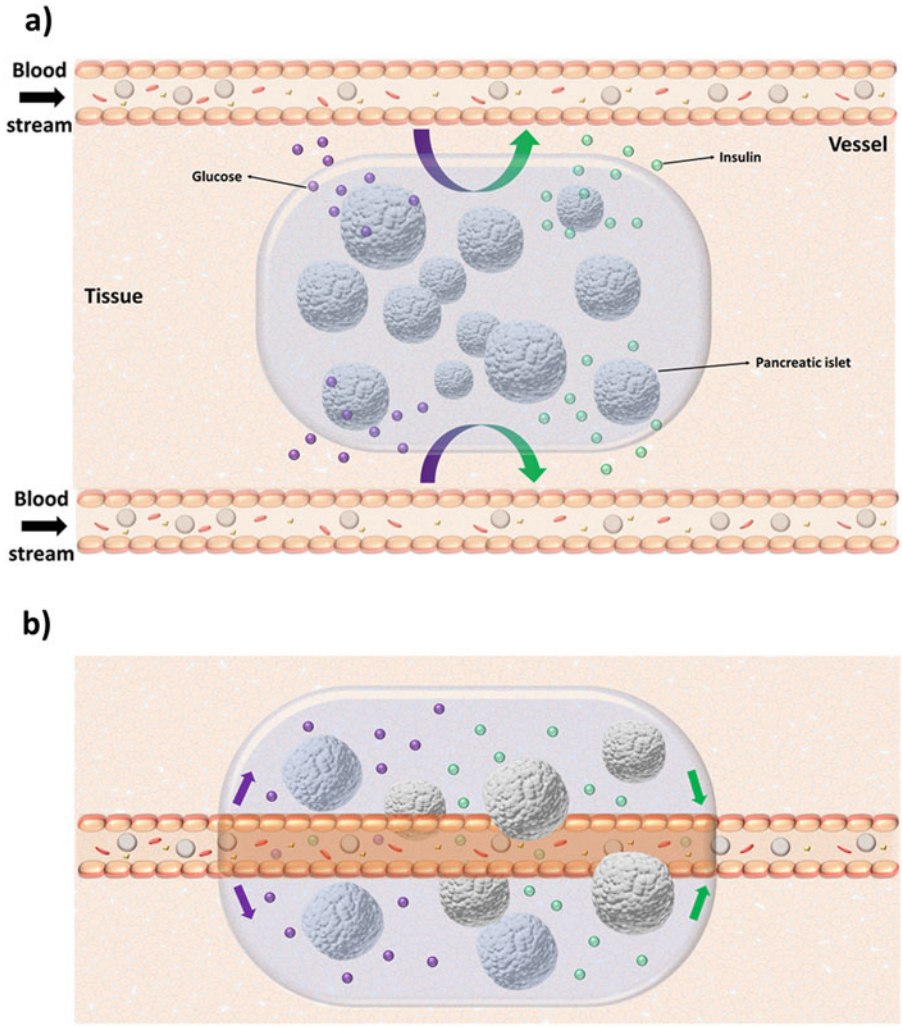

Fig. 21.2 Two types of macroencapsulation; Extravascular (**a**) and Intravascular (**b**). (**a**) The cell-laden macrocapsule is located on an external blood vessel where it is implanted intraperitonally or subcutaneously. (**b**) Arteries and veins are besieged with the macrocapsule, which directly borders the vessels

blood vessels, etc. Therefore, it can be implanted intraperitonally or subcutaneously, which has advantage in that the process of implantation and removal is somewhat simple (Sakata et al. 2012; Schweicher et al. 2014).

The first macroencapsulation used this extravascular macrocapsule developed in the 1950s (Algire et al. 1954; Prehn et al. 1954). During the 1970s, Millipore Corporation developed and produced commercially available extravascular macrocapsules for implantation (Scharp and Marchetti 2014). Their macrocapsules had a pore size of about 450 nm and could inhibit direct cell-cell immunity, which enabled immunoprotection at allotransplantation available level. A series of studies at the time demonstrated that encapsulation through these macrocapsules can improve cell viability (Algire and Legallais 1949; Gates et al. 1972; Strautz 1970).

Although many studies at this time were performed through syngenic cells, transplantation failure occurred because of the fibrotic

overgrowth caused by the lack of proper biocompetability of the materials used (Desai and Shea 2017). And it was also due to the limitations of extravascular microencapsulation that nutrient and oxygen transport depend only on diffusion through thick layers. This restriction induces hypoxia and apoptosis/necrosis in the encapsulated cells, leading to graft failure (Schweicher et al. 2014).

To overcome these limitations, intravascular macrocapsulation has been studied since the 1970s (Chick et al. 1975). The intravascular macrocapsule has a perfusion chamber structure and is directly connected to the arteries and veins of the host (Monaco et al. 1991). The islets are supplied nutrients and oxygen through the blood flowing through the hollow fibers inside the chamber and releases the insulin. Because there is a semi-permeable membrane between the chamber and the hollow fibers, the islets are immunoprotected.

The islet containing intravascular microcapsules chamber made from diverse materials whereas tested on a diabetic rat, monkey model, which could be expected to replace the previously advanced extravascular capsulation (Chick et al. 1977; Orsetti et al. 1978; Sun et al. 1977; Tze et al. 1976, 1980; Sun et al. 1980). However, blood coagulation and hemorrhage occurred in these experiments to confirm the possibility of intravascular microcapsule (Sun et al. 1980; Tze et al. 1980). This is because thrombosis is induced by the blood flow somewhat suppressed at the interface between the blood vessel and the capsule, and blood coagulation is caused by the limited biocompetibility of macrocapsule itself. Unfortunately, systemic anticoagulation agents cannot be used for T1DM patients, and therefore a method to replace intravascular macrocapsules is needed.

Studies have been conducted to overcome these limitations, and several studies have been carried out showing that the induction of host neovascularization can solve the problem of extravascular capsules have been carried out. These attempts to allow blood vessels to form inside the capsule have allowed the host cell to penetrate into the capsule through pore size control. One study in the 1990s (Brauker et al. 1995, 1996) compared the extent of host neovascularization with membrane pore size differences and found that about 100 times more neovascularization was formed in the membrane with the appropriate pore size (Brauker et al. 1995, 1996). And the vascularization was further accelerated when large pore layers were laminated to capsules carrying immune protection through a small pore, confirming that this significantly higher level of vascularization was retained for 1 year. However, the subcutaneous tissue is a low blood-flow tissue, and more research was needed to confirm whether accelerated vascularization is adequate for islet survival. However, the subcutaneous tissue originally had a low blood flow, resulting in a somewhat exaggerated vascularization effect, so more research was needed to confirm whether vascularization is sufficiently accelerated in other tissues and it can improve the survival of islets (Clark et al. 2000; Fumimoto et al. 2009; Ryan et al. 2001).

Another study showed that allograft transplantation of macroencapsulated islets into the epididymal fat pad of streptozotocin-induced diabetic mice yielded normal glucose tolerance for 12 weeks (Suzuki et al. 1998). However, in this experiment too, there was a problem caused by hypoxia caused by the encapsulation of large mass of islets into one capsule. In addition, failure of transplantation due to fibrotic overgrowth around the capsule was also observed. Since then, the biocompetability of the material has gradually improved and macroencapsulation capsules have demonstrated some success in large animals, although the results have not been consistent. In nonhuman primates (NHPs), porcine islets placed within an alginate macrocapsule transplanted subcutaneously were found to provide normoglycaemia for up to 6 months (Dufrane et al. 2006).

And other macrocapsule studies using alginate sheet structures showed significant results in preclinical trials, but at the same time showed limitations in maintaining sheet planarity (Storrs et al. 2001). The thickness of the sheet was determined by considering the maximum distance of oxygen and nutrient diffusion (250 μm). The

prepared islet containing alginate sheet was implanted to the omentum of pancreas resected dog. As a result of the experiment, fasting euglycemia was confirmed for 84 days. After that, the islet in macrocapule was collected again and it was confirmed that it was alive. This confirms that fasting blood glucose lowering is due to macroencapsulation-induced immunoprotection.

However, despite the success of this large animal, macroencapsulation capsules have yet to enter the human clinical trial (Scharp and Marchetti 2014). For xenotransplantation in humans, about 5000–20,000 IEq/kg is needed (Ekser et al. 2016), There is not yet a way to overcome the increased threat of core hypoxia as these islet masses are encapsulated in one capsule. In addition, currently used macrocapsule production techniques are limited in that there is little way to induce vascularization other than controlling pore size. So, if these hypoxia problems cannot be solved, macroencapsulation cannot be presented as a treatment for T1DM.

So if macroencapsules are improved to solve the core hypoxia problem, is it likely to be successfully commercialized? So, if the problem of hypoxia after transplantation is solved, can macroencapsulation capsules be commercialized? In macroencapsulation, the capsule is formed in a single mass, so hypoxia can occur in the cells of the inner core during manufacturing process too. Also, because it is made of a single mass, it is difficult to distribute the cells properly in capsule. These points limit the scale up of the macrocapsule capsule manufacturing process and bring it up to the industrial level.

21.3 3D Bioprinting

21.3.1 Introduction of 3D Bioprinting

3D bioprinting is a technique for positioning biochemical materials and alive cells in a stacking layer by layer at a desired location. Using this techique, a 3D structure can be fabricated by controlling the space of the positioned components (Murphy and Atala 2014). Therefore, 3D bioprinting is emerging as a new technology for encapsulation of cell due to positioning alive cells in a specific location (Billiet et al. 2012; Wust et al. 2011). Furthermore, depending on the applied biochemical materials and types of cells being encapsulated, a variety of functional tissue or organs can be created (Murphy and Atala 2014; Zadpoor and Malda 2017). In this respect, organ transplantation is focused on 3D bioprinting as a solution to manufacture an alternative organ. Consequently, the desired organs are manufactured that what kinds of materials or cells are applied to 3D bioprinting.

Therefore, in the field of 3D bioprinting, it is essential to find suitable cells and materials for finally fabricated organs. Additionally, the materials have sufficient mechanical properties to allow 3D structures to manufacture through the stacking layer by layer method.

Generally, the 3D bioprinting can be classified into two systems depending on the materials, the first is a scaffolding system. A synthetic polymer is mainly applied to the system. It is liquefied through a thermal process and the molten polymer is extruded. Then, the extruded polymer is cooled to produce the scaffold. In general, polylacitc acid (PLA), poly(Lactide-co-glycolic acid) (PLGA), and polycaprolactone (PCL) approved by FDA are mainly used as synthetic polymers applied in 3D bioprinting due to a superior biocompatibility and biodegradability to regenerate tissues and organs (Gunatillake and Adhikari 2003; Shim et al. 2011). Herein, the scaffold composed of the synthetic polymer is mainly used for scaffoling purpose. In addition, cells are seeded in these scaffolds. Finally, the 3D structure containing the cells is completed. Pati et al. (2016). In fact, the scaffold composed of blending PLA and PLGA was made by 3D bioprinting (Shim et al. 2011). Then, rat primary hepatocytes and a mouse pre-osteoblast MC3T3-E1 cell encapsulated hydrogels were injected in the printed scaffold. After 7 days of injection, the encapsulated cells were observed to be proliferated felicitously. Furthermore, a viability was also maintained until 10 days. Additionally, dual cell laden 3D structure composed of PLA

containing both osteoblast and chondrocyte was successfully constructed (Shim et al. 2012). This dual cell laden system maintained a viability and proliferation of cells for 1 week appropriately. In addition, the surface of a scaffold made of PCL may be modified to improve the affinity with cells (Domingos et al. 2013). The second is a scaffolding free system. A hydrogel is mostly used for this system. The hydrogel contains a large amount of water and can provide the optimal environment for cells (Melchels et al. 2012). Unlike the scaffolding system previously described, the hydrogel containing alive cells is positioned in a specific location directly; this hydrogel is called a bio-ink. The bio-ink is applied not only to cells but also to various drugs or biomolecules together (Kaigler et al. 2013; Wust et al. 2014). Additionally, the hydrogel is solidified by physical or chemical crosslinking to stack layer by layer to complete the 3D structure (Nichol et al. 2010; Pescosolido et al. 2011; Wang et al. 2006; Yan et al. 2005). In fact, gelatin metacrylamide containing alive cells was printed and crosslinked by a photo-initator to solidify immediately after printing. The viability of printed cells right after printing was maintained at over 97%. Consequently, cell-laden hydrogel was successfully manufactured (Billiet et al. 2014). In addition, an Extra-cellular matrix (ECM) based hydrogel was used to increase the viability and bio-functionality of encapsulated cells (Yeo et al. 2016). To protect cells encapsulated in the ECM based hydrogel, a shell of alginate was formed on the outside to form a core-sheath structure. Later, the core-sheath 3D structure containing human adipose stem cells (hASCs) maintained viability for approximately 1 weeks. It also effectively differentiated in hepatogenic cultures. Likewise 3D bioprinting is an innovative field that can mimic human tissues or organs by selecting appropriate materials and cells according to a function of the finally fabricated 3D structure.

The development of an artificial pancreas containing pancreatic islets using 3D bioprinting is still an introductory stage. Nowdays, as the shortage of islet donors, the production of biological artificial pancreas is urgent. Fortunately, 3D bioprinting is a revolutionary system that can be mass-produced through a rapid automated system (Bak 2003). However, conventional micro/macroencapsulation is difficult for mass production of artificial pancreas. The process of conventional encapsulation is usually carried out on a laboratory scale. In fact, in the case of microencapsulation, controlling the formed diameter is important for proper stability and durability of the capsule. The flow rate through which the material is injected must be adjusted to produce an appropriate size of bead. However, that is a significant limitation in scaling up the microencapsulation process at the laboratory level to the industrial level. In macroencapsulation, the cell enclosed form is a single mass. In other words unlike the case of microencapsulation, hypoxia can occur in the cells of the inner core. This hypoxia can also occur when macrocapsule is implanted (O'Sullivan et al. 2010). Also, proper cell distribution in the macroencapsulation becomes difficult. As a result, that is also a limit to scale up to the industrial level. However, 3D bioprinting can overcome the limitations of these conventional encapsulation technology. As mentioned earlier, 3D bioprinting can position biochemical materials and alive cells where desired. Therefore, the printed cells are properly distributed in the 3D structure. In addition, 3D bioprinting has the potential to improve the hypoxia of cells in the 3D structure by vascularization and locally distribution of the printed cells (Novosel et al. 2011). The 3D structure with a special shape can also be regarded as a building block. Then, the building blocks can be made into a larger structure. And 3D bioprinting can create complex shaped artificial structures. Therefore, the disadvantages of conventional encapsulation could overcome the limitation of scaling up (Ozbolat 2015; Ozbolat and Yu 2013; Pati et al. 2016). In the next sections, we will look at the development of the current artificial pancreas through 3D bioprinting, and discuss possibiliy of improvement in scaling up and hypoxia aspects in the artificial pancreas.

21.3.2 Scalling Up of Artificial Pancreas

The artificial pancreas developed so far was produced through the scaffolding system. Various cells from primary cells to beta cell like stem cells were planted in a framework based on FDA approved biocompatible synthesis polymers. These approaches have introduced the production of artificial pancreas. Initially developed artificial pancreas was scaffolded with PLGA (Daoud et al. 2011). The final 3D structure was constructed by seeding the ECM based hydrogel containing human pancreatic islet into the PLGA scaffold. Generally, ECM components are critical factors for participations in cellular adhesion, matrix for supporting cells, and various signaling pathways with cells (Hamamoto et al. 2003; Jiang et al. 2002; Kaido et al. 2004). Furthermore, pancreatic islets also showed better survival when cultured in a matrix containing ECM components (Thomas et al. 1999). Thus, human pancreatic islets were encapsulated via an ECM supplemented gels composed of collagen I, fibronectin and collagen IV. In addition, the porosity and pore size of the scaffold were controlled by varying the shape of the PLGA scaffold. Therefore, it had a synergism to seeded cells in the ECM based hydrogel. Therefore, human pancreatic islets in the 3D structure were 1.8-fold more effective insulin release than islets in normal suspension culture. Additionally, an expression of insulin secreting genes in the 3D structure was increased by 50-fold compared to a normal culture. That is because the PLGA scaffold provided a proper environment through an improved oxygen and mass transfer. In conclusion, 3D bioprinting has informed a start of the artificial pancreas development through the proper combination of the scaffold and ECM based hydrogel.

Mesenchymal stem cells (MSCs) differentiated into islet like cell aggregates (ILCA) applied to the manufacture of the artificial pancreas using 3D bioprinting instead of a primary cell (Sabek et al. 2016). Indeed, MSCs were used as a cell source for islet transplantation to T1DM (Chao et al. 2008). It also induced engraftment and vascularization of transplanted islets through co-transplantation with pancreatic islets (Figliuzzi et al. 2009; Ito et al. 2010). Thus, MSCs are applied to islet transplantation directly and also involved in differentiation to islet like cells (Chen et al. 2004). To apply ILCA to 3D bioprinting, a PLA scaffold was prepared. The scaffold was discoidal shape and had a diameter of 13 mm and thickness of 4.5 mm. Additionally, the scaffold was obtained to the surface charge and hydrophilicity to improve suitability with the encapsulated cells. A poly-L-lysine (PLL) coated on the surface of the PLA to give a charge. Additionally, the surface of the PLA was etched through argon (Ar) or oxygen (O_2) plasma to improve hydrophilicity. In addition, an endothelial cell attachment factor (ECAF) was coated on the surface of the PLA to promote vascularization around the scaffold. Indeed, a surface modification of a material changed a cell behavior and gene expression of adjacent cells (Mrksich 2000; Stevens and George 2005). Therefore, the surface modification of the PLA scaffold expected a synergism with the seeded cells In addition, a platelet lysate (PL) gel was used to encapsulate the ILCA into PLA scaffold. In general, the PL gel was an ECM component obtained from animal platelet. It was often used to encapsulate an endothelial cell for vascular capillary formation (Fortunato et al. 2016). In this way, the ILCA was encapsulated in PL gel. Then, the PL was seeded into the PLA scaffold which is only modified surface by etching N_2 or O_2 plasma. Interestingly, the duration of insulin secretion maintained in ILCA in the PLA scaffold longer than in ILCA that was in a normal suspension culture. That resulted in the accumulation of insulin secreted from ILCA in the PL gel. In addition, a larger PLA disk (diameter 20 mm, thickness 1 mm) treated with Ar plasma, PLL, and ECAF. A cytotoxicity of human unbilical vein endothelial cells (HUVECs) with the PLA disk were observed. Certainly, in the case of the PLA disk treated with Ar and PLL, a toxicity of

HUVECs was observed. In conclusion, although the cytotoxicity of PLA scaffold occurred, the approach of modifying a surface of the scaffold may assist on the development of a new artificial pancreas.

With the introduction of this scaffolding system, the size of the scaffold can be adjusted according to the size and design of the scaffold to be printed. In other word, the scaffold can be made in sizes that are possible to apply to real human organs. In fact, there was a case that the scaffolding system using 3D bioprinting. It was used to manufacture a size similar to an actual human ear (Lee et al. 2014a, b). The main part of the scaffold was composed of PCL. Then, the cell-laden hydrogel was seeded in the PCL scaffold. Furthermore, the final human scale ear was printed by using polyethyleneglycol (PEG) with a sacrificial part. The sacrificial part additionally supports the main PCL scaffold with a complex shape during the process of 3D bioprinting. It is widely applied to print complex shapes in the 3D bioprinting (King and Tansey 2003). In the printing process, PEG could support the main part of PCL, but it was easily removed through aqueous solution or culture medium. In order to create an element similar to the human ear, chondrocytes and adipocytes that were differentiated from adipose derived stromal cells (ASCs) were encapsulated in alginate hydrogel. Chondrogenic and adipogenic expression was higher when the cells were co-encapsulated than enclosed separately. Indeed, because of a synergism associated with an treatment of fat tissue for cartilage formation, an injection of the fat tissue may be used to regenerate a septal cartilage formation (Nakakita et al. 1999). Unfortunately, the alginate hydrogel containing these cells was applied to the artificial ear shaped scaffold. However, the ability of these cells to differentiate properly could be demonstrated by using another shape of a scaffold composed of PCL. In conclusion, it was suggested that the ear-shaped structure containing with multi-cells could be sufficiently possible for regeneration of the auricular cartilage.

Unfortunately, there has been no report on the production of human scale pancreas as using 3D bioprinting. However, in order to perform pancreatic cancer surgery, a patient-specific pancreas and peripancreatic region were manufactured by using 3D printing technology. Then, a plan of the surgery was made based on the printed anatomical pancreas. Therefore, it has not reported that the human scale pancreas was not used to treat T1DM. Indeed, for performance of islet transplantation in the clinical trial, the number of transplanted islets was 5000–20,000 IEq/kg, which was a very large amount (Ekser et al. 2016). A capsule containing cells must have a sufficient volume. In conclusion, the new approach of developing the artificial pancreas indicates that the scaffolding system of 3D bioprinting can be used to make a large size of the main scaffold, and the hydrogel containing various cell types as well as pancreatic islets can be seeded into the scaffold.

A case of developing the artificial pancreas with the scaffolding free system has been reported (Marchioli et al. 2015). To make the artificial pancreas composed solely of a hydrogel, composite hydrogels were prepared by alginate hydrogel. Additionally, various materials such as gelatin, hyaluronic acid or Matrigel were mixed with alginate. To make the artificial pancreas through these various hydrogel mixtures, the main material, alginate, was pre-crosslinked by a low concentration of calcium ion. Because of the pre-crosslinked alginate, the viscosity of the alginate hydrogel was increased. Therefore, lamination was possible to make the 3D structure temporarily. In addition, when the temporary 3D structure was printed completely, a post-crosslinking was performed by a high concentration of calcium ion to strengthen the mechanical properties. There is a lack of mechanical properties to stack layer by layer if a hydrogel precusor is only used to print the 3D structure. Therefore, the mechanical properties must be sufficiently strengthened through physical or chemical crosslinking. In fact, using pre-crosslinked alginate could improve the resolution of the printed 3D structure if complex structures are printed (Tabriz et al. 2015). In addition, INS1E-beta cell that derived from rat insulinoma was encapsulated in various hydrogel mixtures to make the artificial pancreas. Then, a viability of

the cell was monitored depending on the components of the hydrogel mixtures. As a result, the viability of the cells in the alginate/gelatin mixture was maintained at 95% to 21 days after printing. The structure was also preserved soundly. Using the only hydrogel to make the artificial pancreas has indicated that a new approach can create an environment similar to the mechanical properties of the real pancreas. Indeed, the pancreas has a significantly lower modulus than other organs, skin, muscles and skeletons (Liu et al. 2015). In conclusion, the development of the artificial pancreas as using the scaffolding free system can be an approach to mimic the proper environment of the actual pancreas.

The scaffolding system produces the based scaffold composed of synthetic polymers non containing cells to print human scale organs. On the other hands, the scaffolding free system requires only the use of the cell-laden hydrogel to make human scale organs. However, because of the prolonged printing process in order to produce the large scale structure, a viability of the cells encapsulated in the hydrogel may be drastically reduced (Ozbolat and Yu 2013). Instead of printing tissues or organs of the human scale at once, there is a new approach to assemble building blocks or mini-tissues composed of only hydrogels to complete the final human scale organs (Ozbolat 2015; Ozbolat and Yu 2013). In fact, to construct a vascular tissue through the scaffolding free system, agarose rods were prepared by 3D bioprinting to use as building blocks to assemble a desired shape of molding template (Norotte et al. 2009). Then, uniform multicellular spheroids were printed into patterns designed at the template. Thereafter, the printed spheroids were self-assembled to a large vascular tissue depending on the patterns in the template. Additionally, the formed large vascular tissues could be assembled together to make one new larger vascular tissue. Thus, building blocks can be used to create a new large-scale structure consisting entirely of hydrogel without scaffolds. In conclusion, in order to create the original environment of pancreas, it is also necessary to produce the artificial pancreas with only hydrogel without the scaffold. For introduction the artificial pancreas through introducing the concept of advanced assembly system, it is possible to develop a new human scale pancreas capable of proper vascularization.

21.3.3 Prevention of Hypoxia through Vascularization

Hypoxia is the most decisive factor of the efficiency of islet transplantation (Pedraza et al. 2012). And this is a big problem in the case of the technique of forming immunoprotective layer, such as encapsulation. In the 3D bioprinting, mainly macro scale capsules are manufactured and therefore, the problem of extravascular macroencapsulation mentioned above such as core hypoxia is maintained. Macro scale capsules are mainly implanted in subcutaneous tissue, and the viability of the transplanted islets in the subcutaneous site is drastically reduced because the cells isolated from the surrounding blood vessels. As has been mentioned, islets have highly rate of consumption of oxygen and nutrients relative to their proportion in the pancreas because insulin secretion in islets requires a lot of mitochondrial respiration (Sato et al. 2011). Therefore, the oxygen supply to the transplanted islets is tremendously critical.

So, how do we solve this hypoxia problem? Currently, 3D bioprinting based technologies use vascularization to solve these hypoxia problems (Lee et al. 2014a, b). A blood vessel system is formed to form a homogeneous blood flow inside the 3d bioprinting based transplantation capsule. This technique is also being studied in the above-mentioned macroencapsulation, so it may question whether 3D bioprinting is necessary to solve hypoxia. As mentioned above, because this technique is also being studied in the macro encapsulation, 3D bio-printing can be asked if it is a necessary technique to solve hypoxia. However, the development of 3D bioprinting based transplantation capsules offers a variety of strategies to promote vascularization and therefore, 3D bioprinting has utility value as a tool to solve the problems of existing technique.

Currently, there are two types of vascularization techniques applied in the field of 3D bioprinting: cell based strategy and hydrogel/scaffold based strategy (Novosel et al. 2011). In cell based strategy, activation of endothelial cells through growth factors, adhesion peptides, and co-culture with other cells leads to neovascularization in the capsule and this method proceeds through prevascularization of the capsule followed by transplantation or by inducing neoangiogenesis after transplantation.

21.3.3.1 Cell Based Prevascularization

Prevascularization is a method of forming a vascular network through vasculogenesis or angiogenesis using endothelial cells in the capsule, and this method proceeds either in vitro prevascularization or in vivo prevascularization.

In 'in vitro prevascularization', endothelial cells with other cells such as myoblast or fibroblast are seeded to capsule and they are. The structure is cultured in vitro for the purpose of constructing a three dimensional (3D) prevascularized structure (Rivron et al. 2008). This method has the advantage that the manufacturing process of the capsule is simpler, but it takes time to connect the vascular network of the host to the network of which the manufactured capsule to be implanted to the network of the manufactured. Oxygen and nutrient diffusion is possible only from 100 to 200 μm from the blood vessel (Rouwkema et al. 2008), Therefore, to survive transplanted cells, the vascular network in the capsule must be activated immediately after transplantation, so whether or not these drawbacks can be overcome will determine the success or failure of transplantation.

In contrast to the method of vascularization through a pre – seeded capsule, 'in vivo prevascularization' uses a nonvascularized construct. During the preliminary implantation, the de novo vascularization of the construct proceeds at the recipient's implant site. First, when a macroporous capsule is implanted, blood vessels infiltrate and vascular networks are formed. Since then, several studies have demonstrated that host cells can establish a perfusion network of vessels in appropriate artificial capsules (Chen et al. 2009; Laschke et al. 2008; Tremblay et al. 2005). The main disadvantage of this method is that at least three operations are required during the procedure: the implantation for vascularization, the removal of the prevascularized capsule and secondary implantation (Rouwkema et al. 2008). Vascular networks produced in an in vivo environment allow oxygen and nutrient delivery to transplanted cells immediately when the capsule is implanted, but the complex manufacturing process of this method lowers the commercial applicability of this method.

21.3.3.2 Cell Based Neoangiogenesis

So, how about the recipient host makes vascularization by himself? So, how about letting vascularization take the capsule to the recipient host? If host-induced vascularization can occurs in the implanted capsule quickly and appropriately, the process of manufacturing the capsule will be much simpler since the process of vascularization in the capsule is omitted. If host-induced vascularization occurs in the implanted capsule, the process of manufacturing the capsule will be much simpler since the process of vascularization in the capsule is omitted. However, the vascularization naturally occurred by the implant is slow and transplanted cells in the capsules are exposed to damage by hypoxia during vascularization. To prevent it, vascularization should be promoted as much as possible. In current researches, various methods of seeding endothelial cells in the capsule and promoting vascularization through angiogenic growth factors or immobilized molecules are used.

Angiogenic growth factors activate endothelial (progenitor) cells and induce migration by gradient to promote neovascularization. In addition, they stimulate blood vessel formation and maturation by inducing cell assembly (Nomi et al. 2006). The major growth factors that promote the angiogenesis process are the basic fibroblast growth factor (bFGF), the vascular endothelial growth factor (VEGF) and the hepatocyte growth

factor (HGF). In addition, the interaction of cytokines such as platelet-derived growth factor (PDGF), angiopoietin and transforming growth factor beta (TGF beta) act as an indirect angiogenic factor and promote the regeneration of endothelial tubes. These growth factors and cytokines promote the vascularization process of endothelial cells seeded in the capsule, which increases the feasibility of host-induced vascularization.

However, this method of using growth factors needs to solve one big problem in order to produce successful results. The rapid degradation rate of the growth factor can prevent the vascular network from being formed sufficiently, which can lead to hypoxia in transplanted cells, resulting in failure of transplantation. To solve this problem, the growth factor must be continuously controlled released around the capsule (Santos and Reis 2010). For controlled release of these growth factors, studies on capsules degradable or containing preencapsulated microspheres have been made. For controlled release of these growth factors, studies have been made on capsules degradable or contain preencapsulated microspheres (Borselli et al. 2010; Demirdogen et al. 2010; Ko et al. 1995). In conclusion, in order for cell-based neoangiogenesis to be successful, an appropriate controlled release of the growth factors and thus rapid vascularization are important.

So, we have discussed how to perform cell-based vascularization through each *in vitro*/*in vivo* prevascularization and neoangiogenesis. Although these methods have advantages and disadvantages, they are efficient methods for vascularization of capsules based on 3D bioprinting technology.

However, it is necessary to think again whether the methods discussed above are efficient for islet transplantation. To manufacture artificial pancreas, we need a capsule to immunoprotect the transplanted islets from the immune response of the host. However, it is difficult to fabricate biological artificial pancreas because of the hypoxia induced by the capsule manufactured for this purpose. To overcome this limitation, research using 3D bioprinting has been conducted on a capsule that does not induce hypoxia. Therefore, it is important to solve the hypoxia problem through vascularization, but it suppresses the immunoprotection function, which is originally intended for the capsule. In the case of cell-based vascularization, a vascular network is formed in the capsule, which means that transplanted islets may become more vulnerable to the host immune response. Then, can vascularization-based methods be applied to islet transplantation? Fortunately, we can do cell distribution properly within the capsule via 3D bioprinting. Therefore, we can manufacture a capsule suitable for artificial pancreas by controlling the density of the formed vascular network to such an extent that immune protection can be sustained without causing cell hypoxia.

21.3.3.3 Hydrogel/Scaffold – Based Strategy

So how can we control the density of these vascular networks? Of course, it can regulate itself and it is more efficient. The proper 3D design of the capsule has the effect of promoting proper vascularization (Liu and Chen 2005). And this means that the degree of vascularization can be controlled according to how we fabricate the 3D design of capsule is done. We can manufacture capsules suitable for islet transplantation by controlling vascularization through capsule material, porosity, pore size, capsule material and channel designing.

Then, how are these factors considered and determined when designing a real capsule? First, the porosity and pore size of the capsule, which is one of the most important factors in determining vascularization, capsule is determined by the density of the material and the length of the polymer chain, which is one of the most important factors in determining vascularization (Keskar et al. 2009). And we can consider a variety of materials that we will use to make 3D printing based capsules, using scaffolds and hydrogels made primarily from synthetic peeolymers (Novosel et al. 2011). Since the polymer chain length of each material is different from biocompatibility

and stability, it is important to select the appropriate material for capsule design.

And In addition, the 3D bioplotting method using hydrogel is mainly used for manufacturing artificial pancreas compared to other organs and pancreas because porosity can be controlled by the density of network formed during bioplotting. Of course, creating a capillary network in the capsule more directly through 3D bioprinting can also be considered. However, forming a complete capillary network is difficult because there is a problem of maximum resolution and production time on current 3D bioprinting technology. Therefore, in the current 3D bioprinting field, researchers we use microchannel in capsule to induce formation of vascular network (Lee et al. 2014a, b). A study conducted until 2014 has shown that 3D bioprinting produces a fluidic vascular channel, and that the angiogenic channel that extends from this vascular channel andis is connected to the vascular network that is separately formed in the capsule. In this channeled capsule made by 3D bioprinting, the capsule entry of endothelial cells and other supporting cells and soluble factors is much easier, which promotes the vascularization process. Through this vascular channel, we can induce vascularization at the desired position, thereby inducing oxygen and nutrient transport efficiently while immunoprotecting the cell (Lee et al. 2014a, b).

21.3.3.4 Conclusion

So far, we have discussed cell-based and hydrogel/scaffold-based vascularization techniques that can be used to produce artificial pancreas via 3D bioprinting. Although each method has been described separately, proper vascularization through 3D bioprinting is more effective when using the above methods together. If we resolve hypoxia, one of the biggest problems of artificial pancreas, through vascularization, we will be able to step closer to commercialization of artificial pancreas.

21.4 Vision of the Artificial Pancreas Future Research

As previously mentioned, islets require a lot of oxygen, so when islets are isolated, they can get hypoxic damage. Especially, because size of islets is large (50~350 μm), so the core region of them can get this hypoxia damage easily (Ramachandran et al. 2015). And vascularization takes a few days. To solve this problem, forming islet cell spheroid (ICS) can be is another strategy to prevent hypoxia because of smaller size than intact islet. Islet spheroids can be obtained by clustering single cells obtained by breaking down intact islet cells or β-cell lines. And it is efficient to use the spheroids because they maintain the function despite the small size compared to the intact islet. Moreover, smaller size of islets is more suitable than larger when transplanted (MacGregor et al. 2005).

There are several spheroid formation methods; hanging drop, centrifugation, non-adherent surfaces, etc. (Mehta et al. 2012; Sutherland et al. 1981). For example, hanging drop method is using the cell suspended droplets and allows cell aggregation at the bottom of the droplets by gravity Foty (2011). Centrifugation can also form spheroids, centrifugal force improves cell aggregation (Handschel et al. 2007). Non-adherent surface is using molecules such as chitosan to avoid from cells adhering to culture dish, so cells can aggregate easily (Huang et al. 2011).

Since the islet spheroids produced by the above methods are highly resistant to hypoxia and have high functional efficiency, they can reduce the size of the capsules produced when used in a 3D bioprinting based transplantation capsule and as a result, it is possible to scale up the manufacture process. Also, they can make the manufacturing process more efficient by reducing the possibility of core hypoxia that can occur during 3D printing. In addition, the small size of the islet spheroid improves resolution by allowing smaller nozzles to be used in 3D printing. This allows the making of more detailed vascularization induction structures.

These advantages of spheroids increase the likelihood that 3D bioprinting based artificial pancreas can be commercialized.

21.5 Conclusion

The ideal strategy for treating T1DM is islet transplantation. However, transplanted islets are rejected from host immune cells. To protect the immune response, islets are encapsulated with a biocompatible polymer for an immune-barrier. The thickness and pore size of polymer membrane surrounding islets can be controlled. Therefore, it protects attack from the immune cells and provide interchange of small molecules; oxygen, nutrients, insulin, metabolic wastes, etc.

However, the conventional encapsulation technology has a significant limitation. First, the hypoxia occurs in islets encapsulated at the core of capsule. That reduces viability of islets. Consequently, the efficiency of the transplantation is dramatically decreased. Second, it is difficult to scale up the capsule. In order to be applied to clinical trial, capsule must be possible to contain a large amount of islets. Therefore, scaling up the capsule is essential.

In this chapter, 3D bioprinting is suggested that a new approach can overcome the conventional limitation in islet encapsulation. The printed cells are properly distributed in the 3D structure by the desired positioning system. Additionally, forming the vascularization through 3D bioprinting can overcome the hypoxia. In addition, scaling up of the 3D structures can be possible for two systems depending on the used materials; scaffolding system, scaffolding free system. However, the development of the artificial pancreas via 3D bioprinting is actually initial stage. As donors of islets are shortage, development of the artificial pancreas is urgently required.

Acknowledgements This study was supported by Basic Science Research Program (NRF-2015R1A2A1A05001832) and partially by the Bio & Medical Technology Development Program (NRF-2015M3A9E2030125) through the National Research Foundation (NRF) funded by the Korean Government (MSIP & MOHW). Also, this study was partially supported by a grant of the Korea Health Technology R&D project through the Korea Health Industry Development Institute (KHIDI), funded by the Ministry of Health & Welfare, Republic of Korea (grant number: HI14C2099).

Reference

Algire GH, Legallais FY (1949) Recent developments in the transparent-chamber technique as adapted to the mouse. J Natl Cancer Inst 10(2):225–253

Algire GH, Weaver JM, Prehn RT (1954) Growth of cells in vivo in diffusion chambers. I. Survival of homografts in immunized mice. J Natl Cancer Inst 15 (3):493–507

Bak D (2003) Rapid prototyping or rapid production? 3D printing processes move industry towards the latter. Assembly Autom 23(4):340–345. https://doi.org/10.1108/01445150310501190

Basta G, Montanucci P, Luca G, Boselli C, Noya G, Barbaro B, Qi M, Kinzer KP, Oberholzer J, Calafiore R (2011) Long-term metabolic and immunological follow-up of nonimmunosuppressed patients with type 1 diabetes treated with microencapsulated islet allografts: four cases. Diabetes Care 34 (11):2406–2409. https://doi.org/10.2337/dc11-0731

Billiet T, Vandenhaute M, Schelfhout J, Van Vlierberghe S, Dubruel P (2012) A review of trends and limitations in hydrogel-rapid prototyping for tissue engineering. Biomaterials 33(26):6020–6041. https://doi.org/10.1016/j.biomaterials.2012.04.050

Billiet T, Gevaert E, De Schryver T, Cornelissen M, Dubruel P (2014) The 3D printing of gelatin methacrylamide cell-laden tissue-engineered constructs with high cell viability. Biomaterials 35 (1):49–62. https://doi.org/10.1016/j.biomaterials.2013.09.078

Borg DJ, Bonifacio E (2011) The use of biomaterials in islet transplantation. Curr Diab Rep 11(5):434–444. https://doi.org/10.1007/s11892-011-0210-2

Borselli C, Ungaro F, Oliviero O, d'Angelo I, Quaglia F, La Rotonda MI, Netti PA (2010) Bioactivation of collagen matrices through sustained VEGF release from PLGA microspheres. J Biomed Mater Res A 92a(1):94–102. https://doi.org/10.1002/jbm.a.32332

Brauker JH, Carrbrendel VE, Martinson LA, Crudele J, Johnston WD, Johnson RC (1995) Neovascularization of synthetic membranes directed by membrane microarchitecture. J Biomed Mater Res 29 (12):1517–1524. https://doi.org/10.1002/jbm.820291208

Brauker J, Martinson LA, Young SK, Johnson RC (1996) Local inflammatory response around diffusion chambers containing xenografts – nonspecific destruction of tissues and decreased local vascularization.

Transplantation 61(12):1671–1677. https://doi.org/10.1097/00007890-199606270-00002
Buder B, Alexander M, Krishnan R, Chapman DW, Lakey JR (2013) Encapsulated islet transplantation: strategies and clinical trials. Immune Netw 13(6):235–239. https://doi.org/10.4110/in.2013.13.6.235
Calafiore R, Basta G, Luca G, Lemmi A, Montanucci MP, Calabrese G, Racanicchi L, Mancuso F, Brunetti P (2006) Microencapsulated pancreatic islet allografts into nonimmunosuppressed patients with type 1 diabetes: first two cases. Diabetes Care 29(1):137–138
Chang TM (1964) Semipermeable Microcapsules. Science 146(3643):524–525
Chao KC, Chao KF, Fu YS, Liu SH (2008) Islet-like clusters derived from mesenchymal stem cells in Wharton's jelly of the human umbilical cord for transplantation to control type 1 diabetes. PLoS One 3(1):e1451. https://doi.org/10.1371/journal.pone.0001451
Chen LB, Jiang XB, Yang L (2004) Differentiation of rat marrow mesenchymal stem cells into pancreatic islet beta-cells. World J Gastroenterol 10(20):3016–3020
Chen XF, Aledia AS, Ghajar CM, Griffith CK, Putnam AJ, Hughes CCW, George SC (2009) Prevascularization of a fibrin-based tissue construct accelerates the formation of functional anastomosis with host vasculature. Tissue Eng Pt A 15(6):1363–1371. https://doi.org/10.1089/ten.tea.2008.0314
Chick WL, Like AA, Lauris V (1975) Beta cell culture on synthetic capillaries: an artificial endocrine pancreas. Science 187(4179):847–849
Chick WL, Perna JJ, Lauris V, Low D, Galletti PM, Panol G, Whittemore AD, Like AA, Colton CK, Lysaght MJ (1977) Artificial pancreas using living Beta cells – effects on glucose homeostasis in diabetic rats. Science 197(4305):780–782. https://doi.org/10.1126/science.407649
Clark H, Barbari TA, Stump K, Rao G (2000) Histologic evaluation of the inflammatory response around implanted hollow fiber membranes. J Biomed Mater Res 52(1):183–192
Cornolti R, Figliuzzi M, Remuzzi A (2009) Effect of micro- and macroencapsulation on oxygen consumption by pancreatic islets. Cell Transplant 18(2):195–201
Daoud JT, Petropavlovskaia MS, Patapas JM, Degrandpre CE, Diraddo RW, Rosenberg L, Tabrizian M (2011) Long-term in vitro human pancreatic islet culture using three-dimensional microfabricated scaffolds. Biomaterials 32(6):1536–1542. https://doi.org/10.1016/j.biomaterials.2010.10.036
de Vos P, Spasojevic M, Faas MM (2010) Treatment of diabetes with encapsulated islets. Adv Exp Med Biol 670:38–53
Demirdogen B, Elcin AE, Elcin YM (2010) Neovascularization by bFGF releasing hyaluronic acid-gelatin microspheres: in vitro and in vivo studies. Growth Factors 28(6):426–436. https://doi.org/10.3109/08977194.2010.508456
Desai T, Shea LD (2017) Advances in islet encapsulation technologies. Nat Rev Drug Discov 16(5):338–350. https://doi.org/10.1038/nrd.2016.232
Desai TA, West T, Cohen M, Boiarski T, Rampersaud A (2004) Nanoporous microsystems for islet cell replacement. Adv Drug Deliv Rev 56(11):1661–1673. https://doi.org/10.1016/j.addr.2003.11.006
Domingos M, Intranuovo F, Gloria A, Gristina R, Ambrosio L, Bartolo PJ, Favia P (2013) Improved osteoblast cell affinity on plasma-modified 3-D extruded PCL scaffolds. Acta Biomater 9(4):5997–6005. https://doi.org/10.1016/j.actbio.2012.12.031
Dufrane D, Goebbels RM, Saliez A, Guiot Y, Gianello P (2006) Six-month survival of microencapsulated pig islets and alginate biocompatibility in primates: proof of concept. Transplantation 81(9):1345–1353. https://doi.org/10.1097/01.tp.0000208610.75997.20
Ekser B, Bottino R, Cooper DKC (2016) Clinical islet xenotransplantation: a step forward. EBioMedicine 12:22–23. https://doi.org/10.1016/j.ebiom.2016.09.023
Elliott RB, Escobar L, Tan PL, Muzina M, Zwain S, Buchanan C (2007) Live encapsulated porcine islets from a type 1 diabetic patient 9.5 yr after xenotransplantation. Xenotransplantation 14(2):157–161. https://doi.org/10.1111/j.1399-3089.2007.00384.x
Figliuzzi M, Cornolti R, Perico N, Rota C, Morigi M, Remuzzi G, Remuzzi A, Benigni A (2009) Bone marrow-derived mesenchymal stem cells improve islet graft function in diabetic rats. Transplant Proc 41(5):1797–1800. https://doi.org/10.1016/j.transproceed.2008.11.015
Fortunato TM, Beltrami C, Emanueli C, De Bank PA, Pula G (2016) Platelet lysate gel and endothelial progenitors stimulate microvascular network formation in vitro: tissue engineering implications. Sci Rep 6:25326. https://doi.org/10.1038/srep25326
Foty R (2011) A simple hanging drop cell culture protocol for generation of 3D spheroids. J Vis Exp 51. https://doi.org/10.3791/2720
Fumimoto Y, Matsuyama A, Komoda H, Okura H, Lee CM, Nagao A, Nishida T, Ito T, Sawa Y (2009) Creation of a rich subcutaneous vascular network with implanted adipose tissue-derived stromal cells and adipose tissue enhances subcutaneous grafting of islets in diabetic mice. Tissue Eng Part C Methods 15(3):437–444. https://doi.org/10.1089/ten.tec.2008.0555
Gates RJ, Smith R, Lazarus NR, Hunt MI (1972) Return to normal of blood-glucose, plasma-insulin, and weight-gain in New Zealand obese mice after implantation of islets of langerhans. Lancet 2(7777):567–570
Gunatillake PA, Adhikari R (2003) Biodegradable synthetic polymers for tissue engineering. Eur Cell Mater 5:1–16 discussion 16
Hamamoto Y, Fujimoto S, Inada A, Takehiro M, Nabe K, Shimono D, Kajikawa M, Fujita J, Yamada Y, Seino Y

(2003) Beneficial effect of pretreatment of islets with fibronectin on glucose tolerance after islet transplantation. Horm Metab Res 35(8):460–465. https://doi.org/10.1055/s-2003-41802

Handschel JG, Depprich RA, Kubler NR, Wiesmann HP, Ommerborn M, Meyer U (2007) Prospects of micromass culture technology in tissue engineering. Head Face Med 3:4. https://doi.org/10.1186/1746-160X-3-4

Huang GS, Dai LG, Yen BL, Hsu SH (2011) Spheroid formation of mesenchymal stem cells on chitosan and chitosan-hyaluronan membranes. Biomaterials 32 (29):6929–6945. https://doi.org/10.1016/j.biomaterials.2011.05.092

Ito T, Itakura S, Todorov I, Rawson J, Asari S, Shintaku J, Nair I, Ferreri K, Kandeel F, Mullen Y (2010) Mesenchymal stem cell and islet co-transplantation promotes graft revascularization and function. Transplantation 89(12):1438–1445

Jacobs-Tulleneers-Thevissen D, Chintinne M, Ling Z, Gillard P, Schoonjans L, Delvaux G, Strand BL, Gorus F, Keymeulen B, Pipeleers D, Beta Cell Therapy Consortium E-F (2013) Sustained function of alginate-encapsulated human islet cell implants in the peritoneal cavity of mice leading to a pilot study in a type 1 diabetic patient. Diabetologia 56(7):1605–1614. https://doi.org/10.1007/s00125-013-2906-0

Jiang FX, Naselli G, Harrison LC (2002) Distinct distribution of laminin and its integrin receptors in the pancreas. J Histochem Cytochem 50(12):1625–1632. https://doi.org/10.1177/002215540205001206

Kaido T, Yebra M, Cirulli V, Montgomery AM (2004) Regulation of human beta-cell adhesion, motility, and insulin secretion by collagen IV and its receptor alpha1beta1. J Biol Chem 279(51):53762–53769. https://doi.org/10.1074/jbc.M411202200

Kaigler D, Silva EA, Mooney DJ (2013) Guided bone regeneration using injectable vascular endothelial growth factor delivery gel. J Periodontol 84 (2):230–238. https://doi.org/10.1902/jop.2012.110684

Keskar V, Gandhi M, Gemeinhart EJ, Gemeinhart RA (2009) Initial evaluation of vascular ingrowth into superporous hydrogels. J Tissue Eng Regen M 3 (6):486–490. https://doi.org/10.1002/term.183

King D, Tansey T (2003) Rapid tooling: selective laser sintering injection tooling. J Mater Process Tech 132 (1–3):42–48. Pii S0924-0136(02)00257-1. doi: https://doi.org/10.1016/S0924-0136(02)00257-1

Klock G, Frank H, Houben R, Zekorn T, Horcher A, Siebers U, Wohrle M, Federlin K, Zimmermann U (1994) Production of purified alginates suitable for use in immunoisolated transplantation. Appl Microbiol Biotechnol 40(5):638–643

Ko C, Dixit V, Shaw W, Gitnick G (1995) In-vitro slow-release profile of endothelial-cell growth-factor immobilized within calcium alginate microbeads. Artif Cell Blood Sub 23(2):143–151. https://doi.org/10.3109/10731199509117934

Laschke MW, Rucker M, Jensen G, Carvalho C, Mulhaupt R, Gellrich NC, Menger MD (2008) Improvement of vascularization of PLGA scaffolds by inosculation of in situ-preformed functional blood vessels with the host microvasculature. Ann Surg 248(6):939–948. https://doi.org/10.1097/SLA.0b013e31818fa52f

Lee JS, Hong JM, Jung JW, Shim JH, Oh JH, Cho DW (2014a) 3D printing of composite tissue with complex shape applied to ear regeneration. Biofabrication 6 (2):024103. https://doi.org/10.1088/1758-5082/6/2/024103

Lee VK, Lanzi AM, Ngo H, Yoo SS, Vincent PA, Dai GH (2014b) Generation of multi-scale vascular network system within 3D hydrogel using 3D bio-printing technology. Cell Mol Bioeng 7(3):460–472. https://doi.org/10.1007/s12195-014-0340-0

Lembert N, Wesche J, Petersen P, Doser M, Zschocke P, Becker HD, Ammon HP (2005) Encapsulation of islets in rough surface, hydroxymethylated polysulfone capillaries stimulates VEGF release and promotes vascularization after transplantation. Cell Transplant 14 (2–3):97–108

Lim F, Sun AM (1980) Microencapsulated islets as bioartificial endocrine pancreas. Science 210 (4472):908–910

Liu WF, Chen CS (2005) Engineering biomaterials to control cell function. Mater Today 8(12):28–35. https://doi.org/10.1016/S1369-7021(05)71222-0

Liu J, Zheng HY, Poh PSP, Machens HG, Schilling AF (2015) Hydrogels for engineering of Perfusable vascular networks. Int J Mol Sci 16(7):15997–16016

MacGregor RR, Williams SJ, Tong PY, Kover K, Moore WV, Stehno-Bittel L (2005) Small rat islets are superior to large islets in in vitro function and in transplantation outcomes. Am J Physiol Endocrinol Metab 290 (5):771–779

Marchioli G, van Gurp L, van Krieken PP, Stamatialis D, Engelse M, van Blitterswijk CA, Karperien MBJ, de Koning E, Alblas J, Moroni L, van Apeldoorn AA (2015) Fabrication of three-dimensional bioplotted hydrogel scaffolds for islets of Langerhans transplantation. Biofabrication 7(2):025009

Mehta G, Hsiao AY, Ingram M, Luker GD, Takayama S (2012) Opportunities and challenges for use of tumor spheroids as models to test drug delivery and efficacy. J Control Release 164:192–204

Melchels FPW, Domingos MAN, Klein TJ, Malda J, Bartolo PJ, Hutmacher DW (2012) Additive manufacturing of tissues and organs. Prog Polym Sci 37(8):1079–1104. https://doi.org/10.1016/j.progpolymsci.2011.11.007

Menard M, Dusseault J, Langlois G, Baille WE, Tam SK, Yahia L, Zhu XX, Halle JP (2010) Role of protein contaminants in the immunogenicity of alginates. J Biomed Mater Res B Appl Biomater 93(2):333–340. https://doi.org/10.1002/jbm.b.31570

Monaco AP, Maki T, Ozato H, Carretta M, Sullivan SJ, Borland KM, Mahoney MD, Chick WL, Muller TE, Wolfrum J et al (1991) Transplantation of islet allografts and xenografts in totally

pancreatectomized diabetic dogs using the hybrid artificial pancreas. Ann Surg 214(3):339–360 discussion 361–332

Mrksich M (2000) A surface chemistry approach to studying cell adhesion. Chem Soc Rev 29(4):267–273. https://doi.org/10.1039/a705397e

Murphy SV, Atala A (2014) 3D bioprinting of tissues and organs. Nat Biotechnol 32(8):773–785. https://doi.org/10.1038/nbt.2958

Nakakita N, Sezaki K, Yamazaki Y, Uchinuma E (1999) Augmentation rhinoplasty using an L-shaped auricular cartilage framework combined with dermal fat graft for cleft lip nose. Aesthet Plast Surg 23(2):107–112. https://doi.org/10.1007/s002669900251

Nichol JW, Koshy ST, Bae H, Hwang CM, Yamanlar S, Khademhosseini A (2010) Cell-laden microengineered gelatin methacrylate hydrogels. Biomaterials 31 (21):5536–5544. https://doi.org/10.1016/j.biomaterials.2010.03.064

Nomi M, Miyake H, Sugita Y, Fujisawa M, Soker S (2006) Role of growth factors and endothelial cells in therapeutic angiogenesis and tissue engineering. Curr Stem Cell Res Ther 1(3):333–343

Norotte C, Marga FS, Niklason LE, Forgacs G (2009) Scaffold-free vascular tissue engineering using bioprinting. Biomaterials 30(30):5910–5917

Novosel EC, Kleinhans C, Kluger PJ (2011) Vascularization is the key challenge in tissue engineering. Adv Drug Deliver Rev 63(4–5):300–311. https://doi.org/10.1016/j.addr.2011.03.004

O'Shea GM, Goosen MF, Sun AM (1984) Prolonged survival of transplanted islets of Langerhans encapsulated in a biocompatible membrane. Biochim Biophys Acta 804(1):133–136

O'Sullivan ES, Johnson AS, Omer A, Hollister-Lock J, Bonner-Weir S, Colton CK, Weir GC (2010) Rat islet cell aggregates are superior to islets for transplantation in microcapsules. Diabetologia 53(5):937–945. https://doi.org/10.1007/s00125-009-1653-8

Orsetti A, Guy C, Zouari N, Deffay R (1978) Implantation of a bio-artificial insulin distributor in dog, using islets of Langerhans from different animal species. Cr Soc Biol 172(1):144–150

Otterlei M, Ostgaard K, Skjak-Braek G, Smidsrod O, Soon-Shiong P, Espevik T (1991) Induction of cytokine production from human monocytes stimulated with alginate. J Immunother 10(4):286–291

Ozbolat IT (2015) Bioprinting scale-up tissue and organ constructs for transplantation. Trends Biotechnol 33 (7):395–400. https://doi.org/10.1016/j.tibtech.2015.04.005

Ozbolat IT, Yu Y (2013) Bioprinting toward organ fabrication: challenges and future trends. IEEE Trans Biomed Eng 60(3):691–699. https://doi.org/10.1109/TBME.2013.2243912

Pati F, Gantelius J, Svahn HA (2016) 3D bioprinting of tissue/organ models. Angew Chem Int Ed Engl 55 (15):4650–4665. https://doi.org/10.1002/anie.201505062

Pedraza E, Coronel MM, Fraker CA, Ricordi C, Stabler CL (2012) Preventing hypoxia-induced cell death in beta cells and islets via hydrolytically activated, oxygen-generating biomaterials. P Natl Acad Sci USA 109(11):4245–4250

Pescosolido L, Schuurman W, Malda J, Matricardi P, Alhaique F, Coviello T, van Weeren PR, Dhert WJA, Hennink WE, Vermonden T (2011) Hyaluronic acid and dextran-based semi-IPN hydrogels as. Biomater Bioprinting Biomacromolecules 12(5):1831–1838. https://doi.org/10.1021/bm200178w

Prehn RT, Weaver JM, Algire GH (1954) The diffusion-chamber technique applied to a study of the nature of homograft resistance. J Natl Cancer Inst 15 (3):509–517

Qi M (2014) Transplantation of encapsulated pancreatic islets as a treatment for patients with type 1 diabetes mellitus. Adv Med 2014:429710. https://doi.org/10.1155/2014/429710

Ramachandran K, Huang H-H, Stehno-Bittel L (2015) A simple method to replace islet equivalents for volume quantification of human islets. Cell Transplant 24:1183–1194

Rivron NC, Liu J, Rouwkema J, de Boer J, van Blitterswijk CA (2008) Engineering vascularised tissues in vitro. Eur Cells Mater 15:27–40

Rouwkema J, Rivron NC, van Blitterswijk CA (2008) Vascularization in tissue engineering. Trends Biotechnol 26(8):434–441. https://doi.org/10.1016/j.tibtech.2008.04.009

Ryan EA, Lakey JR, Rajotte RV, Korbutt GS, Kin T, Imes S, Rabinovitch A, Elliott JF, Bigam D, Kneteman NM, Warnock GL, Larsen I, Shapiro AM (2001) Clinical outcomes and insulin secretion after islet transplantation with the Edmonton protocol. Diabetes 50 (4):710–719

Sabek OM, Farina M, Fraga DW, Afshar S, Ballerini A, Filgueira CS, Thekkedath UR, Grattoni A and Gaber AO (2016) Three-dimensional printed polymeric system to encapsulate human mesenchymal stem cells differentiated into islet-like insulin-producing aggregates for diabetes treatment. J Tissue Eng 7 2041731416638198. https://doi.org/10.1177/2041731416638198

Sakata N, Sumi S, Yoshimatsu G, Goto M, Egawa S, Unno M (2012) Encapsulated islets transplantation: past, present and future. World J Gastrointest Pathophysiol 3(1):19–26. https://doi.org/10.4291/wjgp.v3.i1.19

Santos MI, Reis RL (2010) Vascularization in bone tissue engineering: physiology, current strategies, major hurdles and future challenges. Macromol Biosci 10 (1):12–27. https://doi.org/10.1002/mabi.200900107

Sato Y, Endo H, Okuyama H, Takeda T, Iwahashi H, Imagawa A, Yamagata K, Shimomura I, Inoue M (2011) Cellular hypoxia of pancreatic beta-cells due to high levels of oxygen consumption for insulin secretion in vitro. J Biol Chem 286(14). https://doi.org/10.1074/jbc.M110.194738

Sawhney AS, Pathak CP, Hubbell JA (1993) Interfacial photopolymerization of poly(ethylene glycol)-based hydrogels upon alginate-poly(l-lysine) microcapsules for enhanced biocompatibility. Biomaterials 14 (13):1008–1016

Scharp DW, Marchetti P (2014) Encapsulated islets for diabetes therapy: history, current progress, and critical issues requiring solution. Adv Drug Deliver Rev 67–68:35–73. https://doi.org/10.1016/j.addr.2013.07.018

Schweicher J, Nyitray C, Desai TA (2014) Membranes to achieve immunoprotection of transplanted islets. Front Biosci (Landmark Ed) 19:49–76

Shapiro AM, Lakey JR, Ryan EA, Korbutt GS, Toth E, Warnock GL, Kneteman NM, Rajotte RV (2000) Islet transplantation in seven patients with type 1 diabetes mellitus using a glucocorticoid-free immunosuppressive regimen. N Engl J Med 343(4):230–238. https://doi.org/10.1056/NEJM200007273430401

Shapiro AM, Ricordi C, Hering BJ, Auchincloss H, Lindblad R, Robertson RP, Secchi A, Brendel MD, Berney T, Brennan DC, Cagliero E, Alejandro R, Ryan EA, DiMercurio B, Morel P, Polonsky KS, Reems JA, Bretzel RG, Bertuzzi F, Froud T, Kandaswamy R, Sutherland DE, Eisenbarth G, Segal M, Preiksaitis J, Korbutt GS, Barton FB, Viviano L, Seyfert-Margolis V, Bluestone J, Lakey JR (2006) International trial of the Edmonton protocol for islet transplantation. N Engl J Med 355(13):1318–1330. https://doi.org/10.1056/NEJMoa061267

Shim JH, Kim JY, Park M, Park J, Cho DW (2011) Development of a hybrid scaffold with synthetic biomaterials and hydrogel using solid freeform fabrication technology. Biofabrication 3(3):034102. https://doi.org/10.1088/1758-5082/3/3/034102

Shim JH, Lee JS, Kim JY, Cho DW (2012) Bioprinting of a mechanically enhanced three-dimensional dual cell-laden construct for osteochondral tissue engineering using a multi-head tissue/organ building system. J Micromech Microeng 22(8):085014. https://doi.org/10.1088/0960-1317/22/8/085014

Soon-Shiong P, Heintz RE, Merideth N, Yao QX, Yao Z, Zheng T, Murphy M, Moloney MK, Schmehl M, Harris M et al (1994) Insulin independence in a type 1 diabetic patient after encapsulated islet transplantation. Lancet 343(8903):950–951

Souza YE, Chaib E, Lacerda PG, Crescenzi A, Bernal-Filho A, D'Albuquerque LA (2011) Islet transplantation in rodents. Do encapsulated islets really work? Arq Gastroenterol 48(2):146–152

Stevens MM, George JH (2005) Exploring and engineering the cell surface interface. Science 310 (5751):1135–1138. https://doi.org/10.1126/science.1106587

Storrs R, Dorian R, King SR, Lakey J, Rilo H (2001) Preclinical development of the islet sheet. Ann N Y Acad Sci 944:252–266

Strautz RL (1970) Studies of hereditary-obese mice (Obob) after implantation of pancreatic islets in Millipore filter capsules. Diabetologia 6(3):306–312. https://doi.org/10.1007/Bf01212243

Sun AM, Parisius W, Healy GM, Vacek I, Macmorine HG (1977) Use, in diabetic rats and monkeys, of artificial capillary units containing cultured islets of Langerhans (artificial endocrine pancreas). Diabetes 26 (12):1136–1139. https://doi.org/10.2337/diabetes.26.12.1136

Sun A, Parisius W, Macmorine H, Sefton M, Stone R (1980) An artificial endocrine pancreas containing cultured islets of Langerhans. Artif Organs 4 (4):275–278

Sutherland RM, Carlsson J, Durand R (1981) Spheroids in cancer research. Cancer Res 41:2980–2984

Suzuki K, Bonner-Weir S, Trivedi N, Yoon KH, Hollister-Lock J, Colton CK, Weir GC (1998) Function and survival of macroencapsulated syngeneic islets transplanted into streptozocin-diabetic mice. Transplantation 66(1):21–28. https://doi.org/10.1097/00007890-199807150-00004

Tabriz AG, Hermida MA, Leslie NR, Shu WM (2015) Three-dimensional bioprinting of complex cell laden alginate hydrogel structures. Biofabrication 7(4)

Tarantal AF, Lee CC, Itkin-Ansari P (2009) Real-time bioluminescence imaging of macroencapsulated fibroblasts reveals allograft protection in rhesus monkeys (Macaca mulatta). Transplantation 88(1):38–41. https://doi.org/10.1097/TP.0b013e3181a9ee6c

Thomas FT, Contreras JL, Bilbao G, Ricordi C, Curiel D, Thomas JM (1999) Anoikis, extracellular matrix, and apoptosis factors in isolated cell transplantation. Surgery 126(2):299–304

Tremblay PL, Hudon V, Berthod F, Germain L, Auger FA (2005) Inosculation of tissue-engineered capillaries with the host's vasculature in a reconstructed skin transplanted on mice. Am J Transplant 5 (5):1002–1010. https://doi.org/10.1111/j.1600-6143.2005.00790.x

Tuch BE, Keogh GW, Williams LJ, Wu W, Foster JL, Vaithilingam V, Philips R (2009) Safety and viability of microencapsulated human islets transplanted into diabetic humans. Diabetes Care 32(10):1887–1889. https://doi.org/10.2337/dc09-0744

Tze WJ, Wong FC, Chen LM, Oyoung S (1976) Implantable artificial endocrine pancreas unit used to restore Normoglycaemia in diabetic rat. Nature 264 (5585):466–467. https://doi.org/10.1038/264466a0

Tze WJ, Tai J, Wong FC, Davis HR (1980) Studies with implantable artificial capillary units containing rat islets on diabetic dogs. Diabetologia 19(6):541–545

Valdes-Gonzalez RA, Dorantes LM, Garibay GN, Bracho-Blanchet E, Mendez AJ, Davila-Perez R, Elliott RB, Teran L, White DJ (2005) Xenotransplantation of porcine neonatal islets of Langerhans and Sertoli cells: a 4-year study. Eur J Endocrinol 153(3):419–427. https://doi.org/10.1530/eje.1.01982

Valdes-Gonzalez R, Rodriguez-Ventura AL, White DJ, Bracho-Blanchet E, Castillo A, Ramirez-Gonzalez B, Lopez-Santos MG, Leon-Mancilla BH, Dorantes LM

(2010) Long-term follow-up of patients with type 1 diabetes transplanted with neonatal pig islets. Clin Exp Immunol 162(3):537–542. https://doi.org/10.1111/j.1365-2249.2010.04273.x

Veiseh O, Doloff JC, Ma M, Vegas AJ, Tam HH, Bader AR, Li J, Langan E, Wyckoff J, Loo WS, Jhunjhunwala S, Chiu A, Siebert S, Tang K, Hollister-Lock J, Aresta-Dasilva S, Bochenek M, Mendoza-Elias J, Wang Y, Qi M, Lavin DM, Chen M, Dholakia N, Thakrar R, Lacik I, Weir GC, Oberholzer J, Greiner DL, Langer R, Anderson DG (2015) Size- and shape-dependent foreign body immune response to materials implanted in rodents and non-human primates. Nat Mater 14(6):643–651. https://doi.org/10.1038/nmat4290

Wang T, Lacik I, Brissova M, Anilkumar AV, Prokop A, Hunkeler D, Green R, Shahrokhi K, Powers AC (1997) An encapsulation system for the immunoisolation of pancreatic islets. Nat Biotechnol 15(4):358–362. https://doi.org/10.1038/nbt0497-358

Wang XH, Yan YN, Pan YQ, Xiong Z, Liu HX, Cheng B, Liu F, Lin F, Wu RD, Zhang RJ, Lu QP (2006) Generation of three-dimensional hepatocyte/gelatin structures with rapid prototyping system. Tissue Eng 12(1):83–90. https://doi.org/10.1089/ten.2006.12.83

Wust S, Muller R, Hofmann S (2011) Controlled positioning of cells in biomaterials-approaches towards 3D tissue printing. J Funct Biomater 2(3):119–154. https://doi.org/10.3390/jfb2030119

Wust S, Godla ME, Muller R, Hofmann S (2014) Tunable hydrogel composite with two-step processing in combination with innovative hardware upgrade for cell-based three-dimensional bioprinting. Acta Biomater 10(2):630–640. https://doi.org/10.1016/j.actbio.2013.10.016

Yan YN, Wang XH, Xiong Z, Liu HX, Liu F, Lin F, Wu RD, Zhang RJ, Lu QP (2005) Direct construction of a three-dimensional structure with cells and hydrogel. J Bioact Compat Pol 20(3):259–269. https://doi.org/10.1177/0883911505053658

Yeo M, Lee JS, Chun W, Kim GH (2016) An innovative collagen-based cell-printing method for obtaining human adipose stem cell-laden structures consisting of Core sheath structures for tissue engineering. Biomacromolecules 17(4):1365–1375. https://doi.org/10.1021/acs.biomac.5b01764

Zadpoor AA, Malda J (2017) Additive manufacturing of biomaterials, tissues, and organs. Ann Biomed Eng 45(1):1–11. https://doi.org/10.1007/s10439-016-1719-y

Part VIII

Intellectual Properties in Applications of Biomimetic Medical Materials

Current Status of Development and Intellectual Properties of Biomimetic Medical Materials

22

Janarthanan Gopinathan and Insup Noh

22.1 Biomimetic Medical Materials

22.1.1 Introduction

Biomimetic medical materials are the materials which mimic the important characteristic features of natural material structures or architectures either physically, chemically or biologically and which are mainly used in biomedical applications (Chen et al. 2016). As our knowledge related to cell biology, tissue pathology and homeostasis increases by technical support of accumulated experiences and information technology, the importance of developing such biomimetic medical materials is evolving to a new level. These materials may be prepared from natural sources such as either naturally obtained polysaccharides, proteins, nucleic acids or certain kinds of natural monomers/oligomers/polymers or may be entirely synthetic materials (Patterson et al. 2010). As the chosen materials have many similarities with the native biological structures either at the physical, chemical or structural level, these biomimetic medical materials are predicted to possibly outclass many presently existing biomaterials. The chemical similarities of the biomimetic medical materials with the naturally available materials contribute in developing materials with high biochemical and biomechanical specificities, tunable biodegradation, with superior cell adhesion sites, cell differentiations and diminished cytotoxicity (Park et al. 2016a, b, c). Further modifications at the chemical level resulted in various self-assembled structures like liposomes which mimic the naturally available cytoplasmic membranes, polymeric nanofibrous mats and hydrogels with tunable x-linking which mimics our extracellular matrix (ECM) (Walters and Gentleman 2015), *etc*. Such hydrogels biomaterials have been produced to mimic the biological and physiological features of ECM which includes the presentation of adhesion sites with engineered proteins (Yang et al. 2017), peptides (Hauser and Seow 2017), morphological patterns (Bang et al. 2017; Sari et al. 2016), or polysaccharides and growth factors (Yayon et al. 2017). These kinds of biomimetic medical materials show immense potentials to produce numerous tissue engineering products for the future. Apart from the understanding and mimicking the structural properties of the native tissues, it is important to focus on the other aspects like biochemistry, molecular biology of the tissues and organs to create more advanced biomimetic materials for tissue engineering applications. Likewise, looking at the tissues

J. Gopinathan · I. Noh (✉)
Department of Chemical & Biomolecular Engineering, Seoul National University of Science and Technology (Seoul Tech), Seoul, South Korea

Convergence Institute of Biomedical Engineering & Biomaterials, Seoul National University of Science and Technology (Seoul Tech), Seoul, South Korea
e-mail: drgopinathan@seoultech.ac.kr; insup@seoultech.ac.kr

I. Noh (ed.), *Biomimetic Medical Materials*, Advances in Experimental Medicine and Biology 1064,
https://doi.org/10.1007/978-981-13-0445-3_22

and organs at the nano- and micro-scale level will further improve the understanding of the tissues and will aid us in developing better biomaterials with more precise and functional properties. Even though recent knowledge related to biomaterial and microstructure of the tissue scaffolds has increased considerably, however, more in-depth understanding and comprehensive approaches are required to meet the precise and functional requirements to develop such biomimetic medical materials for the tissue engineering applications (Jonelle et al. 2017). Furthermore, scientists are looking to inculcate multidisciplinary and convergence approaches to develop such biomimetic medical materials by utilizing new technologies, e.g. information technology, 3D bioprinting and nanobiotechnology. This can be evidently observed from the number of papers and patents filed recently in this area of research. The novel materials, methods, different development strategies and the intellectual property rights related to biomimetic medical materials are discussed in this chapter.

22.2 Fabrications of Biomimetic Medical Materials

Figure 22.1 shows divers factors and processing for synthesizing the bioinspired materials such as material source, physical and chemical properties, biochemistry, molecular biology, nano/micro technological cues. Also, the different methods and its various applications have been applied in the biomedical fields. Different forms of biomimetic medical materials have been fabricated by various scientists such as membranes, meshes, nanoparticle, modified hydrogels, 3D (bio)printing products and other novel structures which may serve as a tissue model for drug testing and studies, as well as tissue engineering scaffolds or which may act as templates for regenerative medicine. (Pina et al. 2016; Islam et al. 2015; Demirel et al. 2015; Naleway et al. 2015). Levy reported an interpenetrating network of poly(ethylene glycol) (PEG) and poly(acrylic acid) (PAA) which has the similar ability to swell like human tissues, as well as it has the ability to resist both protein adsorption and inflammation, as examples (Levy 2006). Duoptix, a hydrogel like material for developing artificial cornea, was prepared using a patterned structure with the ability to permit nutrient intrusion and waste removal showed increased corneal epithelial and fibroblast cell growth in a designed keratoprothesis model (Jabbari et al. 2014). Bioinspiration was obtained by coating of biological materials on medical devices. As an example, antimicrobial coatings on biomedical devices based on furanone are inspired from the *Delisea pulchra*, a marine alga. This macro alga produces a biofilm with natural furanones which helps in self-defense against bacterial infections (Busetti et al. 2017).

Another naturally inspired biomimetic medical device is miniaturized directional microphone which has the ability to detect sounds and exclude background noises. This fly-ear mimetic design and engineering of the microphone is being developed by the scientists of the University of Strathclyde and the MRC/CSO Institute for Hearing Research (IHR)-Scottish Section at the Glasgow Royal Infirmary (Whitmer et al. 2014). In robotics, to develop high performance devices, natural manipulators (snakes, octopus arms, elephant trunks, squid tentacles, *etc*) are seen as model materials for locomotion and grasping. One such robotic material is the flexible manipulator designed for minimal invasive surgery, which has the ability to reach surgical site as well as can interact with biological structures at the same time (Ranzani et al. 2015). Nanocomposites based on poly(dimethyl siloxane)-graphene have been demonstrated to have the ability to be used in implantable surgery robotics which is soft, light driven and has quick response (Jiang et al. 2014). Different biological elements such as proteins and DNAs are tested as bio-nanorobots for employing them as nanomotors, nanosensors, joints, *etc*. These bio-nanorobots are capable of performing various activities at nanoscales with precise control over the actions. Many such biomimetic sensors are being developed for biomedical applications (Yan et al. 2016). These kinds of biomimetic devices and materials are highly investigated by many key research institutes and companies like Biomimicry Guild (USA), BIONIS (UK),

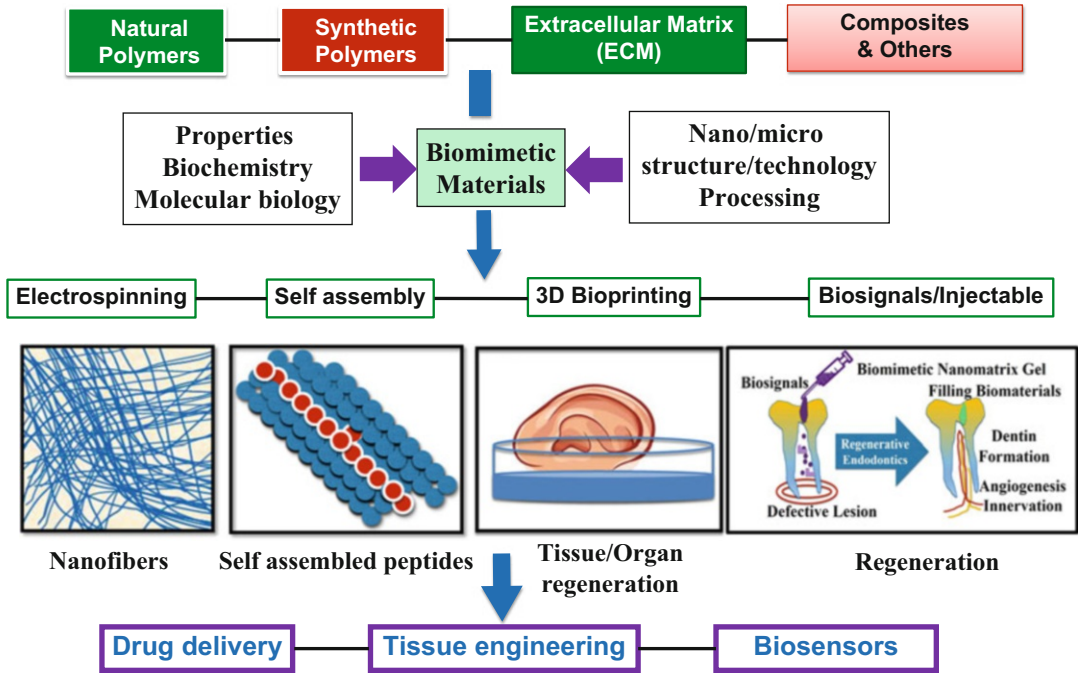

Fig. 22.1 Syntheses and applications of biomimetic medical materials

Biomimicry Institute, BIOKON (Germany), the Century Centre of Excellence (Japan), *etc*, which show the increasing significance of these biomimetic materials in various biomedical applications (Matsumoto et al. 2012).

The current biomimetic medical materials research related to tissue engineering and regeneration shows promising results in solving many serious challenges that are associated with human diseases. Tissue engineering approaches also deal with biologically mimicking the native structures chemically or physically or morphologically (Green and Elisseeff 2016). For structurally mimicking native materials, shape-changing polymers are investigated more, considering their numerous advantages than other polymers (Chan et al. 2016). Predominantly, thermo- and pH-responsive polymers attract more attention mainly due to their ability to control surface cell attachment and detachment in cell culture (Gandhi et al. 2015; Das et al. 2017a, b). This cell culture substrate allows the polymers to be reused for subsequent cell cultures (Higashi et al. 2017). These thermo-responsive polymers are also used *in situ* as injectable gels for cell adhesion and proliferation (Sala et al. 2017). By using such advantages of thermos-responsive polymers, several micro and nano fabrication methods have been developed for various tissue engineering applications (Mandrycky et al. 2016; Laing et al. 2016). One of the important areas where these cell substrates are highly preferred is cell sheet engineering, which has the ability to produce functional tissues without using scaffolding materials. This method also reduces the immune responses like inflammation and rejection (Uhlig et al. 2016; da Silva et al. 2007). A number of tissue types were developed using this technology, which includes cardiac tissues (Akintewe et al. 2017; Roshanbinfar et al. 2017; Kawamura et al. 2017; Tekin et al. 2011), bone tissues (Pirraco et al. 2011; Long et al. 2014), kidney tissues (Matsuura et al. 2014), skin (Frueh et al. 2017), nerve tissues (Hsu et al. 2017), hepatic tissues (Kobayashi et al. 2016; Fujii et al. 2017) and corneal tissues (Syed-Picard et al. 2016; Teichmann et al. 2015). One more important application of thermo-responsive polymers includes the use of live cells along with

the polymers for tissue regeneration. In this method, known quantity of live cells is mixed with polymer solutions at room temperature and injected *in vivo*, where it changes the conformation to form physical gels having live cells entrapped in it. This conformational change primarily occurs when the temperature of the body increases above the lower critical solution temperature (LCST) of the thermo-responsive polymer (Xue et al. 2017). Among different thermo-responsive materials used in tissue engineering applications, hydrogels are the most attractive and smart materials considering their advantages and as it can be easily injected *in vivo*. These injectable hydrogels are reported for various tissue repairs such as vascular tissue (Wang et al. 2014), nerve tissue (Tonda-Turo et al. 2017; Rose et al. 2017), corneal tissue (Soiberman et al. 2017), adipose tissue (Jaikumar et al. 2015; Bidarra et al. 2014), muscle (Kwee and Mooney 2017), bone (Vo et al. 2017; Seo et al. 2017), and cardiac tissue (Bao et al. 2017; Saludas et al. 2017).

The other important material used in biomimetic medical devices development and application includes the piezoelectric materials. The piezoelectric materials are promising candidates for tissue engineering, mainly because of its ability to conduct electrical signals to the live cells (Marino et al. 2017). The signals are applied to cells *via* mechano-electrical transduction method. This approach is vastly used in neural (Uz and Mallapragada 2017; Delaviz et al. 2011), bone (Gorodzha et al. 2017; Bodhak et al. 2016), and muscle regeneration (Sahara et al. 2016; Ribeiro et al. 2015; Martins et al. 2013). Also, different electrically conducting nanocomposite polymers are used to culture cartilage, nerve, and bone cells *in vitro* (Gopinathan et al. 2016a, b, 2017). Furthermore, these different materials are used in various forms for tissue engineering applications such as films (Gopinathan et al. 2016a, b), fibers (Damaraju et al. 2017; Mota et al. 2017; Gopinathan et al. 2015), porous membranes (Correia et al. 2016; Nunes-Pereira et al. 2015; Cardoso et al. 2015), spheres (Correia et al. 2014), and 3D scaffolds (Correia et al. 2016; Das et al. 2017a, b). These polymers with different properties like piezoelectric, thermo-responsive, pH-sensitive, electrically conductive, thiol-ene reaction, Michael type reaction and time-dependent may be used to address the various drawbacks associated in mimicking the biological tissues.

22.3 Techniques and Methods for Developing Biomimetic Medical Materials

Various techniques have been used to develop biomimetic medical materials for tissue engineering application. Electrospinning technique is used for producing different nanofibrous membranes, which mimics the structural sizes of extracellular matrices in tissues (Fu et al. 2016; Gopinathan et al. 2015). Self-assembly techniques are used to develop biomimetic scaffolds for various tissue engineering approaches using interactive peptides (Li et al. 2017b; Halperin-Sternfeld et al. 2017), liposomes (Wagle and Arce 2017), *etc*. 3D (bio) printing of polymers using additive manufacturing or direct inkjet, or laser-based printing have also been used to develop biomimetic medical materials and devices (He et al. 2016). Recently, a new type of 3D printing was reported by Gao et al. (2017), where they have used multiphoton-excited 3D printing to produce ECM scaffolds. They achieved submicron resolution for the printing of these materials, demonstrating the ability of the printed materials by seeding three different cells together to form a functional cardiac muscle patch using induced pluripotent stem cells (iPSCs) differentiation in a murine model.

Bioinks with polymeric biomaterials and live cells are used to develop spatially controlled specific patterns, subsequently leading to the formation of living tissues (Rutz et al. 2015). The bioink is the raw biomaterial for the 3D bioprinting which consists of soft biomaterials and live cells or live cell aggregates alone without any polymer (Hospodiuk et al. 2017; Kim et al. 2016; Park et al. 2016a, b, c). The desired 3D structure can be created using computer aided design (CAD) software from the images obtained from computed tomography (CT) scanning, magnetic resonance imaging (MRI), and various other techniques (Ratheesh et al. 2017; Zhang et al.

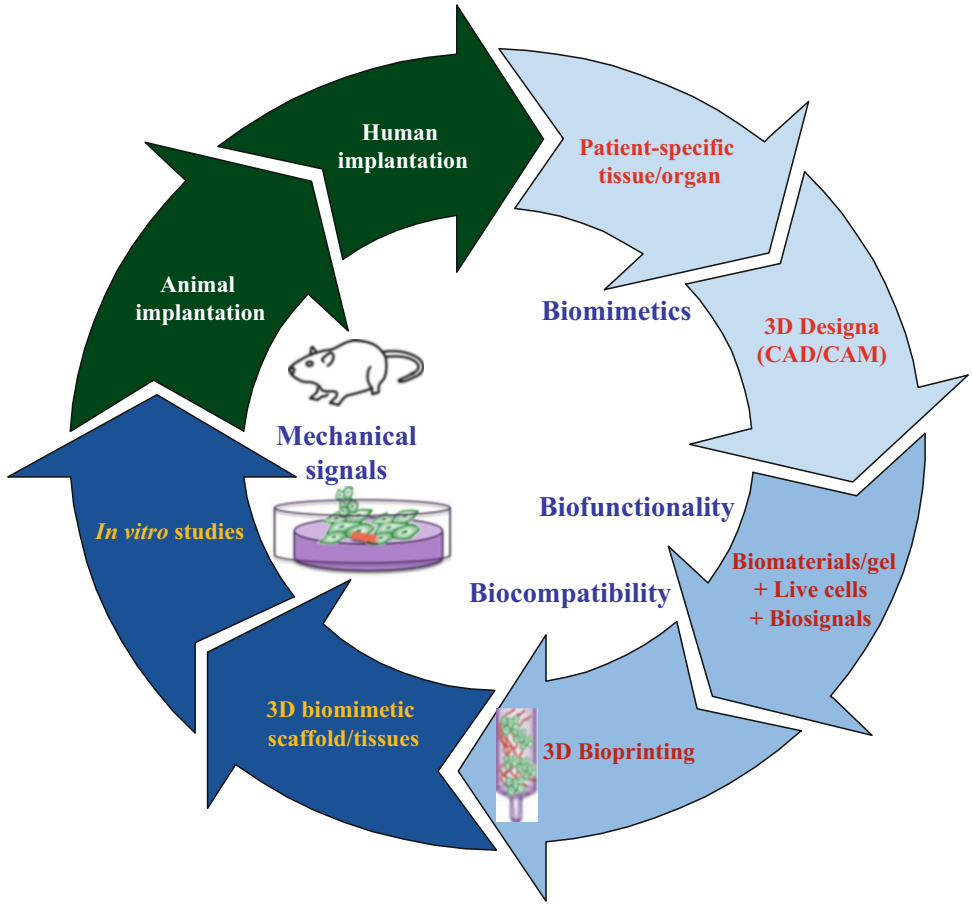

Fig. 22.2 Hydrogels/biomaterials in 3D bioprinting technology for tissue engineering

2017a, b). Among the different approaches reported for developing such biomaterials, 3D bioprinting is more promising and it has the ability to create the most difficult and complexest structures with various morphologies and also with live cells (Atala and Richardson 2016; Jung et al. 2017). Also, it has high repeatability and accuracy compared to other methods for developing biomimetic materials (Walker et al. 2017). The Fig. 22.2 depicts the steps and important factors involved in developing 3D printed biomimetic medical materials and its tissue engineering application, among many other techniques.

A recent review on 3D bioprinting using key structural proteins such as collagen, silk, fibrin explains the growing importance of mimicking natural structures using such proteins and their various applications in tissue engineering (Włodarczyk-Biegun and Campo 2017). They suggest that these proteins can mimic the compositions of biochemical and biophysical properties and their hierarchical structures more efficiently than synthetic materials. The usage of such different materials for biomimetic medical material application also extends to dental and medical tissue engineering through 3D bioprinting (Bertassoni 2017; Yang et al. 2015).

Self-supporting hydrogels were developed using laponite nanoclay as additive in 3D bioprinting technology (Jin et al. 2017; Zhai et al. 2017; Gladman et al. 2016; DeVolder et al. 2017). The authors have demonstrated that the self-supporting hydrogels can be used to develop structures with better mechanical properties and can retain their printed structure even before crosslinking procedure. Two

different hydrogels were tested in the experiment, namely alginate and gelatin. The distinct crystal structure of the laponite having positive and negative charges makes it an ideal internal biomaterial to be used in different hydrogel structures (Jin et al. 2017; Zhai et al. 2017). Li et al reported a combination of alginate and methylcellulose as a 3D bioprinted material with superior printability and high stackability, mainly by increasing the adhesion between the printed layers. They demonstrated the ability of these materials to form stable structures with high cell viability above 95% (Li et al. 2017a).

Lee et al. used 3D bioprinting technique for the regeneration of *in vivo* human skin tissues. They used collagen as dermal matrix; whereas keratinocytes and fibroblasts were used as the epidermis and dermis layer of the skin, respectively. Thus, the developed 3D bioprinted tissues were morphologically and biologically similar to that of *in vivo* skin of humans (Lee et al. 2013). The additional advantage of using this bioprinting technique is the ability to regenerate functional skin tissue *in vivo*. Hence, for the treatment of full thickness wounds of mice, this bioprinting technique was preferred by Skardal et al. (2012). These researchers printed the wound site directly with fibrin-collagen gel alone and also, with a gel containing cells suspension of mesenchymal stem cells (MSC) isolated from amniotic fluids and bone, separately. The results from the treated wound site showed that the gels containing MSC cells were significantly better in terms of wound closure and reepithelialization than the gels without cells. Further, the gels containing cells induced more angiogenesis with higher microvessel thicknesses and capillaries on the wound site than the gels without cells.

These studies clearly indicate that the 3D bioprinting techniques give advancement in producing vast materials with various different combinations for *in vivo* skin regeneration. Their combinations include polymers, live cells, and biological elements which show a massive potential in creating new strategies to mimic *in vivo* skin with respect to angiogenesis, cell colonization and differentiation (Pourchet et al. 2017). Especially for this skin regeneration application, many new methods can be inculcated to develop such type of materials with the help of different biofunctional polymers which have remarkable properties related this application (Mondschein et al. 2017). One such biomaterial is the bacterial cellulose synthesized by various bacterial strains and these produced materials have high purity, desired shapes and by using less expensive methods (Henriksson et al. 2017; Lin and Dufresne 2014). The bacterial cellulose with nanofibrous structures possess more advantages like hydrophilicity, large surface to volume ratio and with the ability to retain more amount of water which warrants to act as a hydrogel having superior mechanical properties also (Abitbol et al. 2016). Additional properties of bacterial cellulose include hemocompatibility and non-genotoxicity with any gene mutation induction such as chromosome variation or nucleic acid changes (Anil et al. 2016; Andrade et al. 2010, 2011). Also, it can be combined with various biological or synthetic materials to develop numerous scaffolds required for different 3D bioprinting applications (Favi et al. 2016; Goncalves et al. 2016).

Several scaffolds such as polymeric random nanofibrous matrices (Wang et al. 2017), aligned nanofibrous matrices (Wu et al. 2017; Kharaziha et al. 2013), decellulairized cell matrices (Perea-Gil et al. 2015), ECM derived hydrogel matrices (Saldin et al. 2017) and polymeric scaffolds with cells (Liu et al. 2017) were reported by various researchers to address the problems in mimicking the architecture of cardiac tissues. Even though these methods showed promising results, they failed to completely regenerate functional cardiac tissue mimicking its native structure. The 3D bioprinting technique is a promising method for the regeneration of cardiac tissue, especially considering its ability to mimic the architecture, geometry and heterogeneous structures of myocardium, heart valves and coronary arteries with desired material properties (Duan 2017; Mosadegh et al. 2015). Human microvascular endothelial cells were bioprinted with fibrin gel to form microvasculature formation by Cui and Boland 2009. This simultaneous production of the printed structures with both cells and gel induced the cells to self-align and proliferate

inside the channels resulting in confluent linings (Cui and Boland 2009). In another study, two different cells, namely aortic root sinus smooth muscle cells (SMCs) in the root and aortic valve leaflet interstitial cells (VICs) in leaflet were used for 3D bioprinting of the heart valve. The cell viabilities were retained even after 7 days of culture and also, hydrogel with cells maintained the required tensile properties (Duan et al. 2013). Further, in a related work, Duan et al. used methacrylate-gelatin and methacrylate-hyaluronic acid based hydrogels to bioprint the human trileaflet valve. They demonstrated higher human aortic valvular interstitial cell viability and ECM secretion in the 3D bioprinted valves (Duan et al. 2014). Many such heart valves, vascularized constructs and myocardium are printed using 3D printing technology (Duan 2017; Dasi et al. 2017). Among the different techniques reported for developing biomimetic medical materials, 3D bioprinting technique stands out as an ideal method for producing such high-quality materials with high precision and resolution for tissue engineering applications.

The three main strategies for development of biomimetic medical materials in terms of ECMs are (1) material patterning at nano- to macroscales, (2) integration and release of active biomolecules and (3) modification of biomaterial surfaces using either ECM macromolecules or specific binding motifs. These strategies are used either in combination or alone to obtain the desired properties (Cha et al. 2017; Yuan et al. 2017; Theocharis et al. 2016). ECM is highly tissue-specific and heterogeneous in nature (Yuan et al. 2017). Many soluble factors regulate the cell behavior during cell-cell and cell-ECM interactions. There are other insoluble macromolecules that are used for such applications include structural proteins (collagen, elastin, *etc*.), fibrous glycoproteins (vitronectin, fibronectin, *etc*.) and glycosaminoglycans (GAGs) (chondroitin sulfate, hyaluronic acid, *etc*.) (Theocharis et al. 2016). Each of these proteins and macromolecules are capable of producing a viable environment for the specific cells by providing binding, attachment and signaling factors to form the functional tissue structures (Frantz et al. 2010). But recently, scientists are focusing on physical cues at nanoscale level to regulate cell behaviors. Cells usually respond to similar cellular nanoscale features on the biomaterials. These features are also shown to have the ability to influence the cellular characteristics such as morphology, gene expression, *etc*. These modifications at nanoscale level using nanofabrication methods are a massively growing area of research (Donnelly et al. 2017). To mimic the structure of the original tissue at the nano- and micro-level, Minardi et al. (2014) developed a multi-compartment collagen scaffolds. The prepared scaffolds had different types of nanostructured composite microspheres with the proteins inside. They reported that the scaffolds were able to preserve the structural cues at the nano and micro level without affecting its macroscopic features. Also, the spatially arranged microspheres allowed the reporter proteins to be released at different layers of the scaffolds. This approach shows the versatility of the methods to yield better mimicking biomaterials at the nano and micro level and capable of releasing active biomolecules for tissue engineering applications.

The mimicking of ECM macromolecules is one of the promising approaches among the three methods. The biomaterials with specific proteins on their surface can improve the cell adhesion, signaling and differentiations (Alas et al. 2017). The unavailability of similar host proteins or macromolecules on the surface of the biomaterial may initiate foreign body response and may lead to faster rejection of the biomaterial when implanted (Morris et al. 2017). The initial foreign body reaction can be avoided by using ECM peptides or macromolecules on the surface of the biomaterials (Morris et al. 2017). Highly ordered ECM structures provide the vital physical and chemical clues to the normal cells and usually act as a template for biomineralization and thus helping in controlling the formation of soft and hard tissues (Corradetti et al. 2016). Chung et al. (2011) developed structurally highly ordered biomaterials and tested their ability to guide directions of cell growth. They initially modified the phages to present either cell adhesive Arg-Gly-Asp(RGD) tripeptide domain or

glutamine (E) EEEE tetrapeptides. Integrin facilitated cell adhesion was promoted by RGD peptides and the bone mineral formation can be further improved by the other negatively charged motifs. They reported the ability of the cells to recognize the microstructures on the self-templated film surface and align themselves according to the surface either longitudinally or perpendicularly. The films, also guided the cells in multiple directions in an ordered way, according to the microstructures clues. Furthermore, they demonstrated the biomineralization of calcium phosphate on the developed films.

Growth factors are another vital biological signals which can control the cell attachment, proliferation and stem cell differentiation (Mitchell et al. 2016). In regenerative medicine, they play major roles by coordinating the cell differentiation and tissue organization in developmental biology. Thus, many researchers developed biomimetic materials with the combination of ECM, growth factors and cell nanointerface as seen in native cells. Also, scientists tried incorporating the growth factors in cell culture medium and in other possible ways to improve the biofunctions of biomaterials. However, growth factors which are covalently bonded or attached were more effective than their soluble administration in regulating the cell behavior at nanoscale interface. Researchers also reported the dual approach where they used both integrins and growth factors for such applications to mimic the native ECM (Llopis-Hernández et al. 2016; Ngandu Mpoyi et al. 2016).

Other approaches include the incorporation of different physical responsive characteristics in the biomaterials for the development of biomimetic materials. Tam et al. (2017) developed biomimetic photo- and enzymatically responsive 3D hydrogels. These hydrogels were made of photosensitive agarose and hyaluronic acid, which can be activated using irradiation. They also x-linked the hydrogels with biodegradable peptides from matrix metalloproteinases (MMPs). These hydrogels with peptides starts degrading when in contact with the targeted cells which releases matrix metalloproteinases. This process allows the cells to remodel the local environment and protrudes inside the hydrogels containing the peptides. Meng et al. (2017) reported a dual-responsive biomimetic materials with poly(L-glutamate)s copolymerized with both the oligo(ethylene glycol) (OEG) moiety and glutamic acid residues. They demonstrated the ability of these materials to respond for pH and temperature simultaneously, using different experiments. These kinds of physical or chemical responsive biomimetic medical materials may be potential contenders for the future development of such smart biomimetic materials for different tissue engineering applications.

Table 22.1 shows the representative biomimetic medical materials reported recently for tissue engineering applications. The table also explains the various key points, limitations of the biomaterials and methods used and their specific applications in tissue engineering. The diverse biomaterials used includes the ECM-derived hydrogels, alginate and gelatin composite, gelatins with different synthetic polymers, gellan, cellulose-based biomaterials and other synthetic biomaterials like PLGA, PCL, etc. The different 3D printing machines used for the development of such biomimetic medical materials are described in the table also. The various applications of these biomimetic medical materials includes tissue engineering of blood vessels, nerve, patient cartilages, bone and skins, etc.

22.4 Intellectual Properties (IP) Related to Biomimetic Medical Materials: Perspectives and Area of Scope

Among the different technologies used to produce biomimetic medical materials, the 3D bioprinting technology has been recently considered as most promising and widely researched in the area of tissue engineering, regenerative medicine and drug delivery. The scientists are collaborating with different pharma companies, to develop functional 3D tissue models which may help in testing the new drugs and formulations in advance, instead of testing it in a human body

Table 22.1 Recent biomimetic medical materials and its application

S. no	Biomaterials	Method & machine	Key points	Application	References
1	ECM-derived gelatin-MA	Direct-write printing. NovoGen MMX bioprinter TM (Organovo) modified	Different concentrations of gel and cells, complex structures with hepatocyte- (HepG2) and fibroblast (NIH3T3) cells separately.	3D microarchitectures of pre-polymerized cell-laden gels while preserving high cell viability.	Bertassoni et al. (2014).
			Limitations: Dispensing of continuous fibers may not be possible for longer time		
2	Alginate-gelatin gel composite	Filament-based deposition, Fab@Home printer Model 2 (2-syringe) (The Nextfab)	Complex channel systems (horizontal and vertical) with human mesenchymal stem cells.	Nerve generation or vasculature in 3D constructs	Wüst et al. (2015).
			Limitation: Slight material accumulation, shape deformation at intersections such as the S and X-shape		
3	Gelatin, gelatin methacrylate, fibrinogen, PEG-amine, homo-bifunctional PEG succinimidyl valerate	Direct-write printing. EnvisionTEC 3D-bioplotter with EnvisionTEC printer cartridges.	Bioink with soft, printable gels obtained from amine-containing polymers and polymer blends. Mixed with human dermal fibroblasts and human umbilical vein endothelial cells. Human mesenchymal stem cells after printing. Rheological studies of the bioink were performed.	Customized and biomimetic 3D-printed constructs and study in cell–cell signaling and tissue morphogenesis in 3D.	Rutz et al. (2015).
			Limitation: Gel cohesiveness needs further quantification.		

(continued)

Table 22.1 (continued)

S. no	Biomaterials	Method & machine	Key points	Application	References
4	Gellan, alginate and BioCartilage (cartilage ECM particles)/hydroxy apatite particles	Extrusion printer biofactory (RegenHu, Switzerland). Dual extruder.	Cartilaginous grafts like nose, meniscus and intervertebral disks were made. Bovine chondrocytes from articular cartilage. Good cell viability and production of ECM. Rheological studies of the bioink were performed. High swelling properties. **Limitation:** Reduced mechanical properties (tensile).	Patient-specific cartilage grafts, tissue-specific and bioactive scaffolds	Kesti et al. (2015).
5	PLGA-PEG-PLGA triblock copolymer, carboxymethyl cellulose (CMC)	Direct-write printing. Fab@Home platform (Model 2) with 16 G tapered dispensing tips	Protein activity up to 9 days and sustained release up to 15 days. Improved mechanical properties. Immortalized human MSCs. **Limitations:** Significant reduction in cell viability	Patterning biological constituents with various architectures, and prevention of issues related to post-fabrication cell seeding and other factors. Bone tissue engineering	Sawkins et al. (2015).
6	Poly (ε-caprolactone) (PCL), poly (lactide-co-caprolactone) (PLCL), fibrinogen, gelatin and hyaluronic acid	Integrated organ printing (IOP) system (custom-made 3D bioprinter). Multiple nozzle system	Rabbit bladder urothelial cells and smooth muscle cells were separately printed. PCL and PLCL helped to improve mechanical properties, whereas fibrin, gelatin, HA to improve the biological activity of the cells. **Limitation:** Difficult to achieve the spatial arrangements of multiple cell types when using hybrid polymers. Reduced cell viability after 7 days of culture	3D bioprinting for development of urethral constructs	Zhang et al. (2017a).

(continued)

Table 22.1 (continued)

S. no	Biomaterials	Method & machine	Key points	Application	References
7	Gelatin/alginate/ collagen hydrogel with sodium citrate/ sodium alginate	Extrusion-based 3D cell-printing machine (built in house)	Degradation controllable hydrogels with human corneal epithelial cells. Collagen was incorporated and printed via extruder which mimics ECM. **Limitation**: Due to the presence of alginate in bioprinted hydrogels, cell-cell or cell-matrix interactions may not be achieved completely	3D-printed hydrogel system with interconnected channels and a macroporous structure with relatively high cell viability for tissue engineering applications.	Wu et al. (2016).
8	Gelatin methacrylamide (GelMA) and bioactive graphene nanoplatelets	Stereolithography based 3D bioprinter	Neural stem cells were encapsulated, and cell viability was tested. Increased compressive modulus with increase in GelMA. **Limitation**: Neural stem cells encapsulated in hydrogels resulted in lower proliferation compared to 2D surface culture	Developing complex structures with a neural cell laden scaffold for neural tissue engineering	Zhu et al. (2016).
9	Nanofibrillated cellulose (NFC) composite with alginate (NFC/A) or hyaluronic acid (NFC/HA)	3D discovery (regenHu, Switzerland) 3D bioprinter (300-μm nozzle)	Human-derived induced pluripotent stem cells (iPSCs) were differentiated using various growth factors and modified medium. **Limitation:** When the concentration of the NFC was increased, cell viability decreased; whereas higher alginate resulted in less stable and inhomogeneous structures.	Stable structures with high NFC content in alginate based bioink. iPSCs cells differentiated into chondrocyte cells. Cartilage tissue engineering.	Nguyen et al. (2017).
10	Gelatin methacrylate (GelMa)	Computer-aided photopolymerization-based 3D bioprinting system using (DLP)	Human umbilical vein endothelial cells and mesenchymal stem cells were cultured. **Limitation**: Advanced instrumentation is needed	Complex 3D microarchitectures using a rapid DLP bioprinting method vascular tissue engineering	Zhu et al. (2017).

directly. Because of such multidisciplinary approaches and enormous investments towards the 3D bioprinting, it has allowed this technology to reach a new level. Mainly, the innovations related to 3D bioprinting machines, their software and different methods, as well as the novel materials combining nanotechnology are speeding up such modern technologies to grow faster. Such enhancements and inventions by the researchers and inventors will surely benefit the human society in the near future. However, the companies and investors who spend their valuable time and funds in developing such technologies, may perhaps also get benefited from the successful inventions by protecting their intellectual properties. This might help them to invest more in the future research and innovations technologies. Further, their claims are secured and protected by the IP law services (Minssen and Mimler 2017). This IP is generally defined as "creations of the mind, such as inventions; literary and artistic works; designs; and symbols, names and images used in commerce (World IP Organization 2017)". Even though, IP rights provide the assurance of not exploiting the patents, copyrights, trademarks, or trade secrets, there should be an even balance between the life enrichment of the common people and inventors' individual benefits. Both the people and the inventors should get benefitted equally, as the invented product should be affordable by the common people and at the same time, it should be rewarding to the actual inventors. This section mainly discusses about the different IP rights related to 3D bioprinting technology and its applications.

The inventors and researchers around the world are mostly relying on the patents to protect their innovations from the risks and exploitations. This is evident from the elevation in the number of applications filed each year in this area of 3D bioprinting research and development (Yoo 2015). In another study conducted by Hornick and Rajan, also indicated the worldwide increase in the patent applications related to 3D bioprinting (Hornick and Rajan 2015). During the period from April 2015 to June 2016, it has increased from 700 to 900 respectively, including pending applications. Their study also indicated that more than 100 organizations around the world are currently involved in the 3D bioprinting patent activity and filing (Hornick and Rajan 2016).

Organovo is the leading organization which tops the Hornick and Rajan's list of 3D bioprinting companies among the group and followed by Wake Forest University and Philips (Hornick and Rajan 2016). Although, more applications are received from different parts of the world, US tops the list with the most number of patents filed, as per a study conducted by Robert W. Esmond (Esmond 2016).

Even though, 3D bioprinting technologies show tremendous potential to create biomimetic devices and materials, still the IP rights related to 3D bioprinting are not clearly defined. However, as per the previous reports, there are three stages of patent claims available related to 3D bioprinting (Pashkov and Harkusha 2017). Namely, they are design, production and post printing stage. The design stage includes the machines, different techniques, methods used during the initial designing of the material or the device using bioimaging and computer aided design (CAD), mainly related to research and development (Pashkov and Harkusha 2017). For example, in a US patent No. 8579620 filed by Andy Wu, claims the methods for developing the 3D models from 3D image sets. This method involves the conversion of digital images to geometrical dimensions which can be used directly in commercially available 3D printers. This technology can represent complex geometries and data conversion methods which enables the user to develop 3D models faster and easier (Wu 2014). In another patent, which was filed by Vellinger et al. (2016), claimed the system, method and an apparatus for 3D bioprinting of tissues under reduced gravity. This method can be used for manufacturing complex structures with different cell lines and materials. Similarly, many such patents are filed related to the designing of the 3D bioprinting.

The production stages include the actual preparation of different source biomaterials such as bioink, hydrogels, *etc*, and conditions used to

develop such source materials or bioink (US patent No. 8143055). The patent claims the development of structures and methods for patterning a number of multicellular bodies comprising living cells to create an engineered tissue construct. The assembly includes filler bodies like biocompatible materials which do not allow cells to migrate or adhere from the site. In this method, 3D tissue constructs can be arranged either by printing or generally stacking the multicellular and filler bodies to such an extent, that there is immediate contact between adjacent multicellular bodies; reasonably with a contact zone that has a considerable length. This direct contact between the multicellular bodies will promote more efficient and stable fusions among them. Various methods for developing multicellular bodies with features that can assist in the formation of 3D tissue construct were also demonstrated (Forgacs et al. 2017). The same patent was filed in different places such as Europe, Australia, Canada, China, Japan and Republic of Korea. But it was initially assigned to The Curators of the university of Missouri which expires on 2029. However, the University had signed an MOU with the 3D bioprinting pioneer company Organovo and it now has the license for the patents filed related to the same application (Press release 2012).

The different patents related to the second category i.e. production stages are given as follows. A method for preparing a self-assembling hydrogel, comprising of hydrophobic peptide and/or peptidomimetic in an aqueous solution was filed by Hauser and Loo (2014). This patent appealed to have applications in regenerative medicine and tissue engineering and can act as 2D and 3D synthetic cell culture substrate, biofunctionalized surfaces and also, can be used in biofabrication such as bio-printing. Isolation of cellulose (composition) from different sources and methods for fabrication of 2D or 3D conductive materials was filed by Abidi and Hu (2016). Cellulose biomaterial obtained from various sources were printed in different forms with conductive nanofillers like CNT, GO and which were stabilized by any enhancers such as alginate, gelatin, poly(vinyl alcohol), or polylactide. The applications of this technology may include photovoltaic, biomedical sensors, biological signal delivery, electrical paper, conductive fabrics, *etc.* In a patent filed titled "Ready-to-print cells and integrated devices" by Rowley and Lock (2015), development of cartridge for 3D bioprinting with live cells was demonstrated. This patent was related to the stem cell-based technologies and medical devices, tissue engineering, biomedical research and development. hMSCs were printed with alginate and tested for various secretions and activity. Cartridges with preserved MSC for direct 3D printing was introduced and they demonstrated the ability of the method to maintain the viability of the biopreserved cells. Chavarria and Aguilar filed a patent which reported a new method for developing the biomimetic 3D scaffolds which uses the electric field and insulating biomaterials to create patterns with different molecules on 3D hydrogels which were polymerized earlier. This invention allows the molecules/macromolecules to be positioned on the surface of a 3D matrix with high accuracy and reproducibility. Ideal cells that can be employed are the ECM forming cells like fibroblasts, chondrocytes and osteoblasts; however, any cell may be used. This technique has the potential to be used in various tissue engineering applications where as to create 3D biomimetic framework or environments to guide cells and make tissues *in vitro* (Chavarria and Aguilar 2017). Varanasi et al. (2016) filed a patent titled "*In vivo* live 3D printing of regenerative bone healing scaffolds for rapid fracture healing". They used gelatin-MA or chitosan-MA, a silicate-based nanoparticles and sucrose particles to develop the bioink. They demonstrated the direct printing of biodegradable biomaterial (bioink) in the defect site of an animal using a 3D printer extruder and they used UV light for crosslinking. After 4 weeks, the scaffolds seeded with periosteum derived progenitor cells regenerated tissue. In another patent which is initially filed to British patent GB2478801 related to "Multilayered Vascular Tubes" have an expiry date up to March 16, 2031. The same patent was also filed in different other countries (Khatiwala et al. 2011a). This patent also is owned by the Organovo Inc.

This patent is related to the development of engineered multilayered vascular tube consisting of fibroblast, smooth muscle cells and adult endothelial cells in different layers with appropriate features as claimed by them in the patent using a 3D bioprinter (Khatiwala et al. 2011b).

The third category, i.e. final post printing stages include the different methods or techniques used to enhance the maturation of the developed tissue either using biochemical or biophysical principles or related to organ production (US patent No. 8747880). It may be a bioreactor, or other technologies which can provide essential nutrients and oxygen to the cells to survive and grow to form tissues (da Silva Bartolo 2011; Ozbolat 2016). Device and method for 3D bioprinting of tissue/organ avoiding direct exposure to UV radiation with high printing resolution was reported by Mironov et al. (2015). This comprised of different units, namely printing unit with bioink printing module, gel forming composition, printing module, displacing the nozzles relative to the platform and a control unit with operating panel. 3D printing of biological tissues and whole organs can be possible. Another example, which explains the post production stage IP related to 3D printing is the "Engineered biological nerve graft, fabrication and application thereof". This patent claims the development of 3D nerve graft material printed using a 3D bioprinter (Forgacs et al. 2014). There are different patents which cover the claims related to the development of fully grown organs or which enhances the maturation of the cells to form tissues (Kupecz et al. 2015).

22.4.1 The Method Claims vs Product Claims Related to 3D Bioprinting

The success of the patent application will be possibly higher when the claim is related to the novel 3D bioprinting processes, rather than the actual products. Further, the process claims may not depend merely on the bioprinted products or the ineligible products that are not stated in the explanation of the process claim (Tran 2015). Recently, the United States Supreme court issued a notice in a case related to different eligibility criteria for method claims related to 3D bioprinting technology. The judges said that the "laws of nature, natural phenomena, and abstract ideas" are exceptions and cannot be claimed for patent eligibility in any manner (Minssen and Mimler 2017). Also, related to the 3D bioprinting software and its patent eligibility, there are two step processes for accessing it. First step is to check the claim reliability of the abstract idea related to the process. In that case, whether the ability of the process claim appears to transform into an eligible patent innovation is also considered. Further, they added that more than a mere abstract idea, it should contribute "significantly more" as an "inventive concept". In the second step, they made it clear that the "the mere recitation of a generic computer cannot transform a patent-ineligible abstract idea into a patent-eligible invention." Similarly, the claims related to well established, regular and traditional features may not be appropriate to be claimed as an "inventive concept" (Minssen and Mimler 2017). However, there are possibilities to file patents related to 3D bioprinting software as they mainly work with the help of electronic blue prints (CAD files) of the organs or tissues. Because, these 3D bioprinting still requires more advanced software technologies and tools to develop biomimetic medical materials for the tissue engineering applications (Pashkov and Harkusha 2017; Leckart 2013). Remarkably, in Europe the patent eligible criteria are more flexible than in the US, related to 3D bioprinting. Except the claims of products, diagnostic and few others, many patent eligibility criteria related to bioinformatic programs/software are more easily fileable in Europe than in the US. However, the software and related claims should be promising and novel, as well as it should be an inventive step to create better products and it should have industrial applications.

The steps involved in the biomimetic research to the commercialization of the biomimetic medical products are shown in Fig. 22.3. Most scientists used 3D bioprinting technique for developing the biomimetic medical materials or

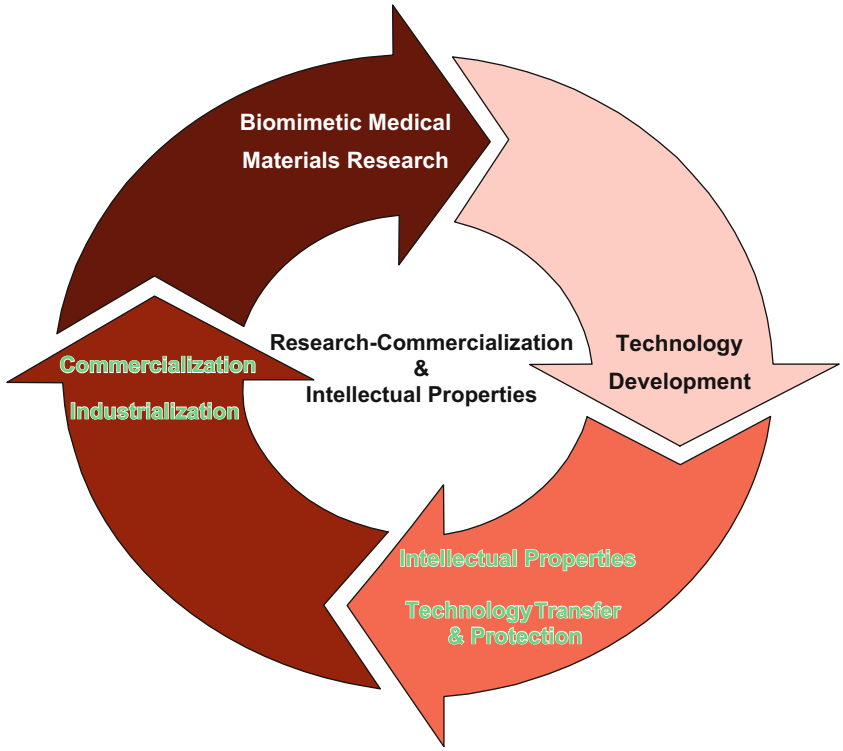

Fig. 22.3 Steps involved in research to commercialization of biomimetic medical materials

devices as it is evident from the recent patents. Among these materials reported, hydrogels showed more promising results. High cell viability, mechanical properties and structural integrity of the hydrogels are the most important parameters considered in the different patents filed. Even though each reported biomaterial had its limitations, these biomaterials or medical devices are promising considering the currently available biomaterials. Most of the researchers used their own custom built 3D bioprinters (Lee et al. 2017) or modified version of the commercial 3D printers for developing such novel biomimetic materials or devices. Either, they have used live cells during printing or after printing the biomaterial. Alginate hydrogel has been the most predominant material preferred by many of the scientists for 3D bioprinting. Apart from alginate, various other biomaterials also showed promising results such as gelatin-MA or chitosan-MA, cellulose, peptides, collagen gel, *etc.* The major applications of these biomimetic medical materials include tissue regeneration, drug delivery, medical devices and surgery, *etc*. The actual applications of this technology may increase the life span and even avoid mortality; however, the ethical aspects of the technology should be clearly regulated (Varkey and Atala 2015). Also, the transparencies in regulation and societal awareness should be taken care to make the 3D bioprinted tissue/organ products acceptable by all religions and cultures around the world (Mimler and Minssen 2017). As discussed earlier, it should be affordable and easily accessible. This modern technology shows promising results which may deliver personalized medicine with more benefits to the mankind in the near future (Varkey and Atala 2015).

22.5 Conclusions and Future Scope

The biomimetic medical materials have been investigated for their applications mainly in tissue

engineering, drug delivery systems, medical devices, sensors and various other biomedical applications. These materials mimicked native biological structures and morphology in detailed and controlled ways, thus showing much more biofunctional capabilities. These biomimetic medical materials can be precisely controlled either physiologically or using different stimuli, and transformed into functional medical products and biomaterials. Among them, functional hydrogels seems to have an edge considering all other polymeric biomaterials in the research area such as nanotechnology, 3D bioprinting, tissue engineering. Also, the 3D bioprinting technology and products with live cells have been considered as very promising and was evidently judged by the recent patents and research papers. Further improvements in production of modern biomimetic medical materials will surely enhance the success rate of the clinical application of such biomaterials through development of advanced biomaterials and technologies, as well as a multidisciplinary approach by the scientists. Integration of new approaches from nanotechnology and tissue engineering through synthesis and development of biomimetic medical materials will further increase the safeness and effectiveness of these biomaterials in clinical applications. These biomimetic medical materials are foreseen as future materials for biomedical applications. Their patents and intellectual propety rights with academic advancement will lead the solid way to the future biomedical industry in the aging society.

Acknowledgement This work was supported by the National Research Foundation of Korea (NRF) Grant (2015R1A2A1A10054592).

References

Abidi N, Hu Y, Texas Tech University System (2016) Cotton fiber dissolution and regeneration and 3D printing of cellulose based conductive composites. U.S. Patent Application 15/355,480

Abitbol T, Rivkin A, Cao Y, Nevo Y, Abraham E, Ben-Shalom T, Lapidot S, Shoseyov O (2016) Nanocellulose, a tiny fiber with huge applications. Curr Opin Biotechnol 39:76–88

Akintewe OO, Roberts EG, Rim NG, Ferguson MA, Wong JY (2017) Design approaches to myocardial and vascular tissue engineering. Annu Rev Biomed Eng 19(0):389

Alas GR, Agarwal R, Collard DM, García AJ (2017) Peptide-functionalized poly [oligo (ethylene glycol) methacrylate] brushes on dopamine-coated stainless steel for controlled cell adhesion. Acta Biomater 59:108–116

Andrade FK, Costa R, Domingues L, Soares R, Gama M (2010) Improving bacterial cellulose for blood vessel replacement: functionalization with a chimeric protein containing a cellulose-binding module and an adhesion peptide. Acta Biomater 6(10):4034–4041

Andrade FK, Silva JP, Carvalho M, Castanheira E, Soares R, Gama M (2011) Studies on the hemocompatibility of bacterial cellulose. J Biomed Mater Res A 98((4):554–566

Anil M, Ayyildiz-Tamis D, Tasdemir S, Sendemir-Urkmez A, Gulce-Iz S (2016) Bioinspired materials and biocompatibility. In: Emerging research on bioinspired materials engineering. IGI Global, Hershey, pp 296–324

Atala A, Richardson K (2016) The quest to 3D print body parts. http://www.biochemist.org/bio/03804/0024/038040024.pdf. Accessed on 10 Oct 2017

Bang SM, Das D, Yun J, Noh I (2017) Evaluation of MC3T3 cells proliferation and drug release study from sodium hyaluronate-BDDGE patterned gel. Nanomaterials 7(10):328–346

Bao R, Tan B, Liang S, Zhang N, Wang W, Liu W (2017) A π-π conjugation-containing soft and conductive injectable polymer hydrogel highly efficiently rebuilds cardiac function after myocardial infarction. Biomaterials 122:63–71

Bertassoni LE (2017) Dentin on the nanoscale: hierarchical organization, mechanical behavior and bioinspired engineering. Dent Mater 33:637

Bertassoni LE, Cardoso JC, Manoharan V, Cristino AL, Bhise NS, Araujo WA, Zorlutuna P, Vrana NE, Ghaemmaghami AM, Dokmeci MR, Khademhosseini A (2014) Direct-write bioprinting of cell-laden methacrylated gelatin hydrogels. Biofabrication 6 (2):024105

Bidarra SJ, Barrias CC, Granja PL (2014) Injectable alginate hydrogels for cell delivery in tissue engineering. Acta Biomater 10(4):1646–1662

Bodhak S, Bose S, Bandyopadhyay A (2016) Surface modification and electro-thermal polarisation for bone tissue engineering. In: Electrically active materials for medical devices. World Scientific, Hackensack, pp 103–114

Busetti A, Maggs CA, Gilmore BF (2017) Marine macroalgae and their associated microbiomes as a source of antimicrobial chemical diversity. Eur J Phycol 52(4):452–465

Cardoso VF, Lopes AC, Botelho G, Lanceros-Méndez S (2015) Poly (vinylidene fluoride-trifluoroethylene) porous films: tailoring microstructure and physical

properties by solvent casting strategies. Soft Mater 13 (4):243–253
Cha SH, Lee JJ, Koh WG (2017) Study of myoblast differentiation using multi-dimensional scaffolds consisting of nano and micropatterns. Biomater Res 21:1
Chan BQY, Low ZWK, Heng SJW, Chan SY, Owh C, Loh XJ (2016) Recent advances in shape memory soft materials for biomedical applications. ACS Appl Mater Interfaces 8(16):10070–10087
Chavarria AM, Aguilar JP, Queen Mary University of London (2017) Method for manufacturing a three-dimensional biomimetic scaffold and uses thereof. U.S. Patent 9,631,172
Chen C, Bang S, Cho Y, Lee S, Lee I, Zhang S, Noh I (2016) Research trends in biomimetic medical materials for tissue engineering: 3D bioprinting, surface modification, nano/micro-technology and clinical aspects in tissue engineering of cartilage and bone. Biomater Res 20(1):10
Chung WJ, Oh JW, Kwak K, Lee BY, Meyer J, Wang E, Hexemer A, Lee SW (2011) Biomimetic self-templating supramolecular structures. Nature 478 (7369):364–368
Corradetti B, Weiner BK, Tasciottia E (2016) Biomimetic nanostructured platforms for biologically inspired medicine. In: Bio-inspired regenerative medicine: materials, processes, and clinical applications, vol 21. Pan Stanford Publishing, Singapore
Correia DM, Gonçalves R, Ribeiro C, Sencadas V, Botelho G, Ribelles JG, Lanceros-Méndez S (2014) Electrosprayed poly (vinylidene fluoride) microparticles for tissue engineering applications. RSC Adv 4(62):33013–33021
Correia DM, Ribeiro C, Sencadas V, Vikingsson L, Gasch MO, Ribelles JG, Botelho G, Lanceros-Méndez S (2016) Strategies for the development of three dimensional scaffolds from piezoelectric poly (vinylidene fluoride). Mater Des 92:674–681
Cui X, Boland T (2009) Human microvasculature fabrication using thermal inkjet printing. Biomaterials 30 (31):6221–6227
da Silva Bartolo PJ (ed) (2011) Innovative developments in virtual and physical prototyping: proceedings of the 5th international conference on advanced research in virtual and rapid prototyping, Leiria, Portugal, CRC Press
Da Silva RM, Mano JF, Reis RL (2007) Smart thermoresponsive coatings and surfaces for tissue engineering: switching cell-material boundaries. Trends Biotechnol 25(12):577–583
Damaraju SM, Shen Y, Elele E, Khusid B, Eshghinejad A, Li J, Jaffe M, Arinzeh TL (2017) Three-dimensional piezoelectric fibrous scaffolds selectively promote mesenchymal stem cell differentiation. Biomaterials 149:51–62
Das D, Bang SM, Zhang SM, Noh I (2017a) Biomolecules release and cell responses of alginate-α-tricalcium phosphate hybrid gel. Nanomaterials 7:389. https://doi.org/10.3390/nano7110389,2017-11-13
Das D, Zhang SM, Noh I (2017b) Synthesis and characterizations of alginate-α-tricalcium phosphate microparticle hybrid film with flexibility and high mechanical property as biomaterials. Biomed Mater. Online
Dasi LP, Grande-Allen J, Kunzelman K, Kuhl E (2017) The pursuit of engineering the ideal heart valve replacement or repair: a special issue of the annals of biomedical engineering. Ann Biomed Eng 45 (2):307–309
Delaviz H, Faghihi A, Delshad AA, Hadi Bahadori M, Mohamadi J, Roozbehi A (2011) Repair of peripheral nerve defects using a polyvinylidene fluoride channel containing nerve growth factor and collagen gel in adult rats. Cell J 13(3):137
Demirel MC, Cetinkaya M, Pena-Francesch A, Jung H (2015) Recent advances in nanoscale bioinspired materials. Macromol Biosci 15(3):300–311
DeVolder RJ, Seo YB, Kong HJ (2017) Proangiogenic alginate-g-pyrrole hydrogel with decoupled control of mechanical rigidity and electrically conductivity. Biomater Res 21:24
Donnelly H, Dalby MJ, Salmeron-Sanchez M, Sweeten PE (2017) Current approaches for modulation of the nanoscale interface in the regulation of cell behaviour. Nanomed Nanotechnol Biol Med. In Press
Duan B (2017) State-of-the-art review of 3D bioprinting for cardiovascular tissue engineering. Ann Biomed Eng 45(1):195–209
Duan B, Hockaday LA, Kang KH, Butcher JT (2013) 3D bioprinting of heterogeneous aortic valve conduits with alginate/gelatin hydrogels. J Biomed Mater Res A 101 (5):1255–1264
Duan B, Kapetanovic E, Hockaday LA, Butcher JT (2014) Three-dimensional printed trileaflet valve conduits using biological hydrogels and human valve interstitial cells. Acta Biomater 10(5):1836–1846
Esmond RW (2016) Bioprinting: the patent landscape, available from: https://www.pharmafocusasia.com/strategy/bioprinting. Accessed on 01 Nov 2017
Favi PM, Ospina SP, Kachole M, Gao M, Atehortua L, Webster TJ (2016) Preparation and characterization of biodegradable nano hydroxyapatite–bacterial cellulose composites with well-defined honeycomb pore arrays for bone tissue engineering applications. Cellulose 23 (2):1263–1282
Forgacs G, Colbert SH, Hubbard BA, Marga F, Christiansen D, The Curators of The University of Missouri (2014) Engineered biological nerve graft, fabrication and application thereof. U.S. Patent 8,747,880
Forgacs G, Marga FS, Norotte C, The Curators of The University of Missouri (2017) Self-assembling multicellular bodies and methods of producing a three-dimensional biological structure using the same. U.S. Patent 9,556,415

Frantz C, Stewart KM, Weaver VM (2010) The extracellular matrix at a glance. J Cell Sci 123(24):4195–4200

Frueh FS, Menger MD, Lindenblatt N, Giovanoli P, Laschke MW (2017) Current and emerging vascularization strategies in skin tissue engineering. Crit Rev Biotechnol 37(5):613–625

Fu X, Xu M, Jia C, Xie W, Wang L, Kong D, Wang H (2016) Differential regulation of skin fibroblasts for their TGF-β1-dependent wound healing activities by biomimetic nanofibers. J Mater Chem B 4 (31):5246–5255

Fujii M, Yamanouchi K, Sakai Y, Baimakhanov Z, Yamaguchi I, Soyama A, Hidaka M, Takatsuki M, Kuroki T, Eguchi S (2017) In vivo construction of liver tissue by implantation of a hepatic non-parenchymal/adipose-derived stem cell sheet. J Tissue Eng Regen Med 12:e287. https://doi.org/10.1002/term.2424

Gandhi A, Paul A, Sen SO, Sen KK (2015) Studies on thermoresponsive polymers: phase behaviour, drug delivery and biomedical applications. Asian J Pharm Sci 10(2):99–107

Gao L, Kupfer M, Jung J, Yang L, Zhang P, Sie Y, Tran Q, Ajeti V, Freeman B, Fast V, Campagnola P (2017) Myocardial tissue engineering with cells derived from human induced-pluripotent stem cells and a native-like, high-resolution, 3-dimensionally printed scaffold. Circ Res, CIRCRESAHA-116 120:1318. https://doi.org/10.1161/CIRCRESAHA.116.310277

Gladman AS, Matsumoto EA, Nuzzo RG, Mahadevan L, Lewis JA (2016) Biomimetic 4D printing. Nat Mater 15(4):413–418

Goncalves S, Rodrigues IP, Padrão J, Silva JP, Sencadas V, Lanceros-Mendez S, Girão H, Gama FM, Dourado F, Rodrigues LR (2016) Acetylated bacterial cellulose coated with urinary bladder matrix as a substrate for retinal pigment epithelium. Colloids Surf B Biointerfaces 139:1–9

Gopinathan J, Mano S, Elakkiya V, Pillai MM, Sahanand KS, Rai BD, Selvakumar R, Bhattacharyya A (2015) Biomolecule incorporated poly-ε-caprolactone nanofibrous scaffolds for enhanced human meniscal cell attachment and proliferation. RSC Adv 5 (90):73552–73561

Gopinathan J, Pillai MM, Elakkiya V, Selvakumar R, Bhattacharyya A (2016a) Carbon nanofillers incorporated electrically conducting poly ε-caprolactone nanocomposite films and their biocompatibility studies using MG-63 cell line. Poly Bull 73 (4):1037–1053

Gopinathan J, Quigley AF, Bhattacharyya A, Padhye R, Kapsa RM, Nayak R, Shanks RA, Houshyar S (2016b) Preparation, characterisation, and in vitro evaluation of electrically conducting poly (□-caprolactone)-based nanocomposite scaffolds using PC12 cells. J Biomed Mater Res A 104(4):853–865

Gopinathan J, Pillai MM, Sahanand KS, Rai BD, Selvakumar R, Bhattacharyya A (2017) Synergistic effect of electrical conductivity and biomolecules on human meniscal cell attachment, growth, and proliferation in poly-ε-caprolactone nanocomposite scaffolds. Biomed Mater 12(6):065001

Gorodzha SN, Muslimov AR, Syromotina DS, Timin AS, Tcvetkov NY, Lepik KV, Petrova AV, Surmeneva MA, Gorin DA, Sukhorukov GB, Surmenev RA (2017) A comparison study between electrospun polycaprolactone and piezoelectric poly (3-hydroxybutyrate-co-3-hydroxyvalerate) scaffolds for bone tissue engineering. Colloids Surf B Biointerfaces 160:48–59

Green JJ, Elisseeff JH (2016) Mimicking biological functionality with polymers for biomedical applications. Nature 540(7633):386–394

Halperin-Sternfeld M, Ghosh M, Adler-Abramovich L (2017) Advantages of self-assembled supramolecular polymers toward biological applications. In: Supramolecular chemistry of biomimetic systems. Springer, Singapore, pp 9–35

Hauser C, Loo Y, Agency for Science (2014) Novel ultrashort hydrophobic peptides that self-assemble into nanofibrous hydrogels and their uses. U.S. Patent Application 15/039,922

Hauser C, Seow WY, Agency for Science (2017) Building stratified biomimetic tissues and organs using crosslinked ultrashort peptide hydrogel membranes. U.S. Patent 9,687,591

He Y, Yang F, Zhao H, Gao Q, Xia B, Fu J (2016) Research on the printability of hydrogels in 3D bioprinting. Sci Rep 6:29977

Henriksson I, Gatenholm P, Hägg DA (2017) Increased lipid accumulation and adipogenic gene expression of adipocytes in 3D bioprinted nanocellulose scaffolds. Biofabrication 9(1):015022

Higashi N, Hirata A, Nishimura SN, Koga T (2017) Thermo-responsive polymer brushes on glass plate prepared from a new class of amino acid-derived vinyl monomers and their applications in cell-sheet engineering. Colloids Surf B Biointerfaces 159:39–46

Hornick JF, Rajan K (2015) Chapter 16: intellectual property in 3D printing and nanotechnology. In: Zhang LG, Fisher JP, Leong K (eds) 3D Bioprinting and nanotechnology in tissue engineering and regenerative medicine. Academic Press, Amsterdam, pp 349–364 ISBN: 978-0-12-800547-7

Hornick JF, Rajan K (2016) The 3D bioprinting patent landscape takes shape as IP leaders emerge available from: https://3dprintingindustry.com/news/3d-bioprinting-patent-landscape-takes-shape-ip-leaders-emerge-84541

Hospodiuk M, Dey M, Sosnoski D, Ozbolat IT (2017) The bioink: a comprehensive review on bioprintable materials. Biotechnol Adv 35(2):217–239

Hsu MN, Liao HT, Li KC, Chen HH, Yen TC, Makarevich P, Parfyonova Y, Hu YC (2017) Adipose-derived stem cell sheets functionalized by hybrid baculovirus for prolonged GDNF expression

and improved nerve regeneration. Biomaterials 140:189–200

Islam MM, Cėpla V, He C, Edin J, Rakickas T, Kobuch K, Ruželė Ž, Jackson WB, Rafat M, Lohmann CP, Valiokas R (2015) Functional fabrication of recombinant human collagen–phosphorylcholine hydrogels for regenerative medicine applications. Acta Biomater 12:70–80

Jabbari E, Kim DH, Lee LP (eds) (2014) Handbook of biomimetics and bioinspiration: biologically-driven engineering of materials, processes, devices, and systems. World Scientific, Hackensack

Jaikumar D, Sajesh KM, Soumya S, Nimal TR, Chennazhi KP, Nair SV, Jayakumar R (2015) Injectable alginate-O-carboxymethyl chitosan/nano fibrin composite hydrogels for adipose tissue engineering. Int J Biol Macromol 74:318–326

Jiang W, Niu D, Liu H, Wang C, Zhao T, Yin L, Shi Y, Chen B, Ding Y, Lu B (2014) Photoresponsive soft-robotic platform: biomimetic fabrication and remote actuation. Adv Funct Mater 24(48):7598–7604

Jin Y, Liu C, Chai W, Compaan AM, Huang Y (2017) Self-supporting Nanoclay as internal scaffold material for direct printing of soft hydrogel composite structures in air. ACS Appl Mater Interfaces 9(20):17456–17465

Jonelle ZY, Korkmaz E, Berg MI, LeDuc PR, Ozdoganlar OB (2017) Biomimetic scaffolds with three-dimensional undulated microtopographies. Biomaterials 128:109–120

Jung CS, Kim BK, Lee J, Min BH, Park SH (2018) Development of printable natural cartilage matrix bioink for 3D printing of irregular tissue shape. Tissue Eng Regen Med 15(2):155–162

Kawamura M, Miyagawa S, Fukushima S, Saito A, Miki K, Funakoshi S, Yoshida Y, Yamanaka S, Shimizu T, Okano T, Daimon T (2017) Enhanced therapeutic effects of human iPS cell derived-cardiomyocyte by combined cell-sheets with omental flap technique in porcine ischemic cardiomyopathy model. Sci Rep 7:8824

Kesti M, Eberhardt C, Pagliccia G, Kenkel D, Grande D, Boss A, Zenobi-Wong M (2015) Bioprinting complex cartilaginous structures with clinically compliant biomaterials. Adv Funct Mater 25(48):7406–7417

Kharaziha M, Nikkhah M, Shin SR, Annabi N, Masoumi N, Gaharwar AK, Camci-Unal G, Khademhosseini A (2013) PGS: gelatin nanofibrous scaffolds with tunable mechanical and structural properties for engineering cardiac tissues. Biomaterials 34(27):6355–6366

Khatiwala C, Murphy K, Shepherd B, Organovo, Inc. (2011a) Multilayered vascular tubes, GB 2478801 B, https://search.wellspringsoftware.net/patent/GB2478801B, referring also published as: AU2011227282B2, CA2793205C, CN102883680B, CN105749349A, EP02547288A2, GB2489081B, HK1159682A1, mJP2016052527A

Khatiwala C, Murphy K, Shepherd B, Organovo, Inc. (2011b) Multilayered vascular tubes. U.S. Patent Application 13/634,863

Kim JE, Kim SH, Jung Y (2016) Current status of three-dimensional printing inks for soft tissue regeneration. Tissue Eng Regen Med 13(6):636–646

Kobayashi J, Akiyama Y, Yamato M, Okano T (2016) November. ECM-mimicking thermoresponsive surface for manipulating hepatocyte sheets with maintenance of hepatic functions. In micro-Nanomechatronics and human science (MHS), 2016 international symposium on IEEE, pp 1–4

Kupecz A, Roox K, Dekoninck C, Schertenleib D, Stief M, Sanna F, Orsingher M, Miralles S, Molina E, Crosse T, Gilbert M (2015) Safe harbors in Europe: an update on the research and Bolar exemptions to patent infringement. Nat Biotech 33(7):710–715

Kwee BJ, Mooney DJ (2017) Biomaterials for skeletal muscle tissue engineering. Curr Opin Biotechnol 47:16–22

Laing S, Suriano R, Lamprou DA, Smith CA, Dalby MJ, Mabbott S, Faulds K, Graham D (2016) Thermoresponsive polymer micropatterns fabricated by dip-pen nanolithography for a highly controllable substrate with potential cellular applications. ACS Appl Mater Interfaces 8(37):24844–24852

Leckart S (2013) How 3-D printing body parts will revolutionize medicine, popular science, available from: https://www.popsci.com/science/article/2013-07/how-3-d-printing-body-parts-will-revolutionize-medicine. Accessed on 01 Nov 2017

Lee V, Singh G, Trasatti JP, Bjornsson C, Xu X, Tran TN, Yoo SS, Dai G, Karande P (2013) Design and fabrication of human skin by three-dimensional bioprinting. Tis Eng Part C: Methods 20(6):473–484

Lee J, Kim KE, Bang B, Noh I, Lee C (2017) A desktop multi-material 3D bio-printing system with open-source hardware and software. Int J Precis Eng Manuf 18(4):605–612

Levy D (2006) An artificial cornea is in sight, thanks to biomimetic hydrogels. Stanford report. http://news.stanford.edu/news/2006/september13/cornea-091306.html

Li H, Tan YJ, Leong KF, Li L (2017a) 3D bioprinting of highly thixotropic alginate/methylcellulose hydrogel with strong interface bonding. ACS Appl Mater Interfaces 9(23):20086–20097

Li R, Xu J, Wong DSH, Li J, Zhao P, Bian L (2017b) Self-assembled N-cadherin mimetic peptide hydrogels promote the chondrogenesis of mesenchymal stem cells through inhibition of canonical Wnt/β-catenin signaling. Biomaterials 145:33–43

Lin N, Dufresne A (2014) Nanocellulose in biomedicine: current status and future prospect. Eur Polym J 59:302–325

Liu Y, Wang S, Zhang R (2017) Composite poly (lactic acid)/chitosan nanofibrous scaffolds for cardiac tissue engineering. Int J Biol Macromol 103:1130–1137

Llopis-Hernández V, Cantini M, González-García C, Cheng ZA, Yang J, Tsimbouri PM, García AJ, Dalby MJ, Salmerón-Sánchez M (2016) Material-driven fibronectin assembly for high-efficiency presentation of growth factors. Sci Adv 2(8):e1600188

Long T, Zhu Z, Awad HA, Schwarz EM, Hilton MJ, Dong Y (2014) The effect of mesenchymal stem cell sheets on structural allograft healing of critical sized femoral defects in mice. Biomaterials 35(9):2752–2759

Mandrycky C, Wang Z, Kim K, Kim DH (2016) 3D bioprinting for engineering complex tissues. Biotech Adv 34(4):422–434

Marino A, Genchi GG, Mattoli V, Ciofani G (2017) Piezoelectric nanotransducers: the future of neural stimulation. Nano Today 14:9–12

Martins PM, Ribeiro S, Ribeiro C, Sencadas V, Gomes AC, Gama FM, Lanceros-Méndez S (2013) Effect of poling state and morphology of piezoelectric poly (vinylidene fluoride) membranes for skeletal muscle tissue engineering. RSC Adv 3(39):17938–17944

Matsumoto M, Umeda Y, Masui K, Fukushige S (eds) (2012) Design for innovative value towards a sustainable society: proceedings of ecodesign 2011: 7th international symposium on environmentally conscious design and inverse manufacturing. Springer Science & Business Media

Matsuura K, Utoh R, Nagase K, Okano T (2014) Cell sheet approach for tissue engineering and regenerative medicine. J Control Release 190:228–239

Meng F, Fu X, Ni Y, Sun J, Li Z (2017) Biomimetic polypeptides with reversible pH-dependent thermal responsive property. Polymer 118:173–179

Minardi S, Sandri M, Martinez JO, Yazdi IK, Liu X, Ferrari M, Weiner BK, Tampieri A, Tasciotti E (2014) Multiscale patterning of a biomimetic scaffold integrated with composite microspheres. Small 10 (19):3943–3953

Minssen T, Mimler M (2017) Patenting bioprinting-technologies in the US and Europe–the 5th element in the 3rd dimension. Chapter 7. Available from: https://papers.ssrn.com/sol3/papers.cfm?abstract_id=2946209

Mironov VA, Khesuani YD, Mitryashkin AN, Gladkaya IS, Ostrovsky AY, Novoselov SV, Private Institution Lab For Biotechnological Research 3D Bioprinting Solutions (2015) Device and methods for printing biological tissues and organs. U.S. Patent Application 15/311,242

Mitchell AC, Briquez PS, Hubbell JA, Cochran JR (2016) Engineering growth factors for regenerative medicine applications. Acta Biomater 30:1–2

Mondschein RJ, Kanitkar A, Williams CB, Verbridge SS, Long TE (2017) Polymer structure-property requirements for stereolithographic 3D printing of soft tissue engineering scaffolds. Biomaterials 140:170–188

Morris AH, Stamer DK, Kyriakides TR (2017) The host response to naturally-derived extracellular matrix biomaterials. In: Seminars in immunology, vol 29. Academic Press, London, p 72

Mosadegh B, Xiong G, Dunham S, Min JK (2015) Current progress in 3D printing for cardiovascular tissue engineering. Biomed Mater 10(3):034002

Mota C, Labardi M, Trombi L, Astolfi L, D'Acunto M, Puppi D, Gallone G, Chiellini F, Berrettini S, Bruschini L, Danti S (2017) Design, fabrication and characterization of composite piezoelectric ultrafine fibers for cochlear stimulation. Mater Des 122:206–219

Naleway SE, Porter MM, McKittrick J, Meyers MA (2015) Structural design elements in biological materials: application to bioinspiration. Adv Mater 27 (37):5455–5476

Ngandu Mpoyi E, Cantini M, Reynolds PM, Gadegaard N, Dalby MJ, Salmerón-Sánchez M (2016) Protein adsorption as a key mediator in the nanotopographical control of cell behavior. ACS Nano 10(7):6638–6647

Nguyen D, Hägg DA, Forsman A, Ekholm J, Nimkingratana P, Brantsing C, Kalogeropoulos T, Zaunz S, Concaro S, Brittberg M, Lindahl A (2017) Cartilage tissue engineering by the 3D bioprinting of iPS cells in a nanocellulose/alginate bioink. Sci Rep 7 (1):658

Nunes-Pereira J, Ribeiro S, Ribeiro C, Gombek CJ, Gama FM, Gomes AC, Patterson DA, Lanceros-Méndez S (2015) Poly (vinylidene fluoride) and copolymers as porous membranes for tissue engineering applications. Poly Testing 44:234–241

Ozbolat IT (2016) 3D bioprinting: fundamentals, principles and applications. Academic Press, London

Park JH, Jang J, Lee JS, Cho DW (2016a) Current advances in three-dimensional tissue/organ printing. Tissue Eng Regen Med 13(6):612–621

Park KD, Wang X, Lee JY, Park KM, Zhang S, Noh I (2016b) Research trends in biomimetic medical materials for tissue engineering: commentary. Biomater Res 20(1):8

Park SH, Jung CS, Min BH (2016c) Advances in three-dimensional bioprinting for hard tissue engineering. Tissue Eng Regen Med 13(6):622–635

Pashkov V, Harkusha A (2017) 3-D bioprinting law regulation perspectives. Wiadomosci lekarskie (Warsaw, Poland: 1960), 70, 480. Available from http://pli.nlu.edu.ua/wp-content/uploads/2017/10/5.pdf. Accessed on 01 Nov 2017

Patterson J, Martino MM, Hubbell JA (2010) Biomimetic materials in tissue engineering. Mater Today 13 (1):14–22

Perea-Gil I, Uriarte JJ, Prat-Vidal C, Gálvez-Montón C, Roura S, Llucià-Valldeperas A, Soler-Botija C, Farré R, Navajas D, Bayes-Genis A (2015) *In vitro* comparative study of two decellularization protocols in

search of an optimal myocardial scaffold for recellularization. Am J Transl Res 7(3):558
Pina S, Oliveira JM, Reis RL (2016) Biomimetic strategies to engineer mineralized human tissues. In: Handbook of bioceramics and biocomposites. Springer, Cham, pp 503–519
Pirraco RP, Obokata H, Iwata T, Marques AP, Tsuneda S, Yamato M, Reis RL, Okano T (2011) Development of osteogenic cell sheets for bone tissue engineering applications. Tissue Eng Part A 17(11–12):1507–1515
Pourchet LJ, Thepot A, Albouy M, Courtial EJ, Boher A, Blum LJ, Marquette CA (2017) Human skin 3D bioprinting using scaffold-free approach. Adv Healthc Mater 6(4):1601101
Press Release (2012) Organovo announces two issued patents, first company patent and key founder patent, https://www.sec.gov/Archives/edgar/data/1497253/000119312512297696/d379308dex992.htm. Accessed on 01 Nov 2017
Ranzani T, Gerboni G, Cianchetti M, Menciassi A (2015) A bioinspired soft manipulator for minimally invasive surgery. Bioinspir Biomim 10(3):035008
Ratheesh G, Venugopal JR, Chinappan A, Ezhilarasu H, Sadiq A, Ramakrishna S (2017) 3D fabrication of polymeric scaffolds for regenerative therapy. ACS Biomater Sci Eng 3:1175
Ribeiro C, Correia DM, Ribeiro S, Sencadas V, Botelho G, Lanceros-Méndez S (2015) Piezoelectric poly (vinylidene fluoride) microstructure and poling state in active tissue engineering. Eng Life Sci 15(4):351–356
Rose JC, Cámara-Torres M, Rahimi K, Köhler J, Möller M, De Laporte L (2017) Nerve cells decide to orient inside an injectable hydrogel with minimal structural guidance. Nano Lett 17(6):3782
Roshanbinfar K, Hilborn J, Varghese OP, Oommen OP (2017) Injectable and thermoresponsive pericardial matrix derived conductive scaffold for cardiac tissue engineering. RSC Adv 7(51):31980–31988
Rowley JA, Lock LT, Roosterbio, Inc. (2015) Ready-to-print cells and integrated devices. U.S. Patent Application 15/311,018
Rutz AL, Hyland KE, Jakus AE, Burghardt WR, Shah RN (2015) A multimaterial bioink method for 3D printing tunable, cell-compatible hydrogels. Adv Mater 27 (9):1607–1614
Sahara G, Hijikata W, Tomioka K, Shinshi T (2016) Implantable power generation system utilizing muscle contractions excited by electrical stimulation. Proc Inst Mech Eng Part H: J Eng Med 230(6):569–578
Sala RL, Kwon MY, Kim M, Gullbrand SE, Henning EA, Mauck RL, Camargo ER, Burdick JA (2017) Thermosensitive poly (N-vinylcaprolactam) injectable hydrogels for cartilage tissue engineering. Tissue Eng Part A 23(17–18):935–945
Saldin LT, Cramer MC, Velankar SS, White LJ, Badylak SF (2017) Extracellular matrix hydrogels from decellularized tissues: structure and function. Acta Biomater 49:1–15
Saludas L, Pascual-Gil S, Prósper F, Garbayo E, Blanco-Prieto M (2017) Hydrogel based approaches for cardiac tissue engineering. Int J Pharm 523(2):454–475
Sari DP, Bang SM, Nguyen LT, Cho Y, Park KD, Lee SH, Lee IS, Zhang SM, Noh I (2016) Micro/Nano surface topography and 3D bioprinting of biomaterials in tissue engineering. J Nanosci Nanotechnol 16:8909–8922
Sawkins MJ, Mistry P, Brown BN, Shakesheff KM, Bonassar LJ, Yang J (2015) Cell and protein compatible 3D bioprinting of mechanically strong constructs for bone repair. Biofabrication 7(3):035004
Seo BB, Koh JT, Song SC (2017) Tuning physical properties and BMP-2 release rates of injectable hydrogel systems for an optimal bone regeneration effect. Biomaterials 122:91–104
Skardal A, Mack D, Kapetanovic E, Atala A, Jackson JD, Yoo J, Soker S (2012) Bioprinted amniotic fluid-derived stem cells accelerate healing of large skin wounds. Stem Cells Transl Med 1(11):792–802
Soiberman U, Kambhampati SP, Wu T, Mishra MK, Oh Y, Sharma R, Wang J, Al Towerki AE, Yiu S, Stark WJ, Kannan RM (2017) Subconjunctival injectable dendrimer-dexamethasone gel for the treatment of corneal inflammation. Biomaterials 125:38–53
Syed-Picard FN, Du Y, Hertsenberg AJ, Palchesko R, Funderburgh ML, Feinberg AW, Funderburgh JL (2016) Scaffold-free tissue engineering of functional corneal stromal tissue. J Tissue Eng Regen Med 12:59. https://doi.org/10.1002/term.2363
Tam RY, Smith LJ, Shoichet MS (2017) Engineering cellular microenvironments with photo-and enzymatically responsive hydrogels: toward biomimetic 3D cell culture models. Acc Chem Res 50(4):703–713
Teichmann J, Nitschke M, Pette D, Valtink M, Gramm S, Härtel FV, Noll T, Funk RH, Engelmann K, Werner C (2015) Thermo-responsive cell culture carriers based on poly (vinyl methyl ether) – the effect of biomolecular ligands to balance cell adhesion and stimulated detachment. Sci Technol Adv Mater 16(4):045003
Tekin H, Sanchez JG, Tsinman T, Langer R, Khademhosseini A (2011) Thermoresponsive platforms for tissue engineering and regenerative medicine. AICHE J 57(12):3249–3258
Theocharis AD, Skandalis SS, Gialeli C, Karamanos NK (2016) Extracellular matrix structure. Adv Drug Deliv Rev 97:4–27
Tonda-Turo C, Gnavi S, Ruini F, Gambarotta G, Gioffredi E, Chiono V, Perroteau I, Ciardelli G (2017) Development and characterization of novel agar and gelatin injectable hydrogel as filler for peripheral nerve guidance channels. J Tissue Eng Regen Med 11(1):197–208
Tran JL (2015) Patenting bioprinting Harvard journal of law and technology digest, 2015 symposium, 2, Available from https://papers.ssrn.com/sol3/papers.cfm?abstract_id=2603693. Accessed on 01 Nov 2017)

Uhlig K, Wegener T, He J, Zeiser M, Bookhold J, Dewald I, Godino N, Jaeger M, Hellweg T, Fery A, Duschl C (2016) Patterned thermoresponsive microgel coatings for noninvasive processing of adherent cells. Biomacromolecules 17(3):1110–1116

Uz M, Mallapragada SK (2017) Smart materials for nerve regeneration and neural tissue engineering. In: Smart materials for tissue engineering. RSC, Cambridge, pp 382–408

Varanasi VG, Ilyas A, Kramer PR, Azimaie T, The Texas A&M University System (2016) In vivo live 3D printing of regenerative bone healing scaffolds for rapid fracture healing. U.S. Patent Application 15/360,788

Varkey M, Atala A (2015) Organ bioprinting: a closer look at ethics and policies. Wake Forest JL & Pol'y 5:275

Vellinger JC, Boland E, Kurk MA, Milliner K, Logan NS, Inventors; Techshot, Inc., assignee (2016) Biomanufacturing system, method, and 3D bioprinting hardware in a reduced gravity environment. U.S. Patent Application 15/225,547

Vo TN, Tatara AM, Santoro M, van den Beucken JJ, Leeuwenburgh SC, Jansen JA, Mikos AG (2017) Acellular mineral deposition within injectable, dual-gelling hydrogels for bone tissue engineering. J Biomed Mater Res A 105(1):110–117

Wagle D, Arce P (2017) Liposome-nanotemplated agarose-gel for tissue engineering scaffold: preliminary synthesis & transport characterization. In: Proceedings of student research and creative inquiry day, 1. https://publish.tntech.edu/index.php/PSRCI/article/view/161. Accessed on 10 Oct 2017

Walker JM, Bodamer E, Krebs O, Luo Y, Kleinfehn A, Becker ML, Dean D (2017) Effect of chemical and physical properties on the in vitro degradation of 3D printed high resolution poly (propylene fumarate) scaffolds. Biomacromolecules 18(4):1419–1425

Walters NJ, Gentleman E (2015) Evolving insights in cell–matrix interactions: elucidating how non-soluble properties of the extracellular niche direct stem cell fate. Acta Biomater 11:3–16

Wang LS, Lee F, Lim J, Du C, Wan AC, Lee SS, Kurisawa M (2014) Enzymatic conjugation of a bioactive peptide into an injectable hyaluronic acid–tyramine hydrogel system to promote the formation of functional vasculature. Acta Biomater 10(6):2539–2550

Wang L, Wu Y, Hu T, Guo B, Ma PX (2017) Electrospun conductive nanofibrous scaffolds for engineering cardiac tissue and 3D bioactuators. Acta Biomater 59:68–81

Whitmer WM, Seeber BU, Akeroyd MA (2014) The perception of apparent auditory source width in hearing-impaired adults. The J Acoust Soc Am 135 (6):3548–3559

Włodarczyk-Biegun MK, del Campo A (2017) 3D bioprinting of structural proteins. Biomaterials 134:180–201

World Intellectual Property Organization (2017) What is intellectual property? Available from: www.wipo.int/about-ip/en/. Accessed on 01 Nov 2017

Wu A (2014) Single-action three-dimensional model printing methods. US Patent 8,817,332

Wu Z, Su X, Xu Y, Kong B, Sun W, Mi S (2016) Bioprinting three-dimensional cell-laden tissue constructs with controllable degradation. Sci Rep 6:24474

Wu Y, Wang L, Guo B, Ma PX (2017) Interwoven aligned conductive nanofiber yarn/hydrogel composite scaffolds for engineered 3D cardiac anisotropy. ACS Nano 11(6):5646–5659

Wüst S, Müller R, Hofmann S (2015) 3D bioprinting of complex channels – effects of material, orientation, geometry, and cell embedding. J Biomed Mater Res A 103(8):2558–2570

Xue X, Thiagarajan L, Braim S, Saunders BR, Shakesheff KM, Alexander C (2017) Upper critical solution temperature thermo-responsive polymer brushes and a mechanism for controlled cell attachment. J Mater Chem B 5:4926–4933

Yan H, Chang G, Sun T, Xu Y, Ma Z, Zhou T, Lin L (2016) Molecular communication in nanonetworks. Nano Biomed Eng 8(4):274–287

Yang M, Lelkes PI, Gangolli RA, Gerstenhaber JA, Devlin SM, Temple University-Of The Commonwealth System of Higher Education (2015) Biomimetic scaffold for regenerative dentistry. U.S. Patent Application 15/326,189

Yang YJ, Holmberg AL, Olsen BD (2017) Artificially engineered protein polymers. Annu Rev Chem Biomol Eng 8(1):549

Yayon A, Sirkis R, Amit B, Wortzel A, Hepacore Ltd. (2017) Conjugates of carboxy polysaccharides with fibroblast growth factors and variants thereof. U.S. Patent 9,610,357

Yoo SS (2015) 3D-printed biological organs: medical potential and patenting opportunity. Expert Opin Ther Pat 25:507–511

Yuan X, Wei Y, Villasante A, Ng JJ, Arkonac DE, Chao PH, Vunjak-Novakovic G (2017) Stem cell delivery in tissue-specific hydrogel enabled meniscal repair in an orthotopic rat model. Biomaterials 132:59–71

Zhai X, Ma Y, Hou C, Gao F, Zhang Y, Ruan C, Pan H, Lu WW, Liu W (2017) 3D-printed high strength bioactive supramolecular polymer/clay nanocomposite hydrogel scaffold for bone regeneration. ACS Biomater Sci Eng 3(6):1109–1118

Zhang K, Fu Q, Yoo J, Chen X, Chandra P, Mo X, Song L, Atala A, Zhao W (2017a) 3D bioprinting of urethra with PCL/PLCL blend and dual autologous cells in fibrin hydrogel: an in vitro evaluation of biomimetic mechanical property and cell growth environment. Acta Biomater 50:154–164

Zhang YS, Yue K, Aleman J, Mollazadeh-Moghaddam K, Bakht SM, Yang J, Jia W, Dell'Erba V, Assawes P, Shin SR, Dokmeci MR (2017b) 3D bioprinting for tissue and organ fabrication. Ann Biomed Eng 45 (1):148–163

Zhu W, Harris BT, Zhang LG (2016) Gelatin methacrylamide hydrogel with graphene nanoplatelets for neural cell-laden 3D bioprinting. In: Engineering in Medicine and Biology Society (EMBC), 2016 I.E. 38th annual international conference of the IEEE, pp 4185–4188

Zhu W, Qu X, Zhu J, Ma X, Patel S, Liu J, Wang P, Lai CS, Gou M, Xu Y, Zhang K (2017) Direct 3D bioprinting of prevascularized tissue constructs with complex microarchitecture. Biomaterials 124:106–115